

Wesley

NASA SP-5030

SYMPOSIUM ON
TECHNOLOGY STATUS AND TRENDS

HUNTSVILLE, ALABAMA

APRIL 21 - 23, 1965



NATIONAL AERONAUTICS AND SPACE ADMINISTRATION

1966000 8417 IR

SYMPOSIUM ON
TECHNOLOGY STATUS AND TRENDS

HUNTSVILLE, ALABAMA

APRIL 21 - 23, 1965

Sponsored by the Technology Utilization Office
Marshall Space Flight Center



Scientific and Technical Information Division

NATIONAL AERONAUTICS AND SPACE ADMINISTRATION

Washington, D.C.

1966

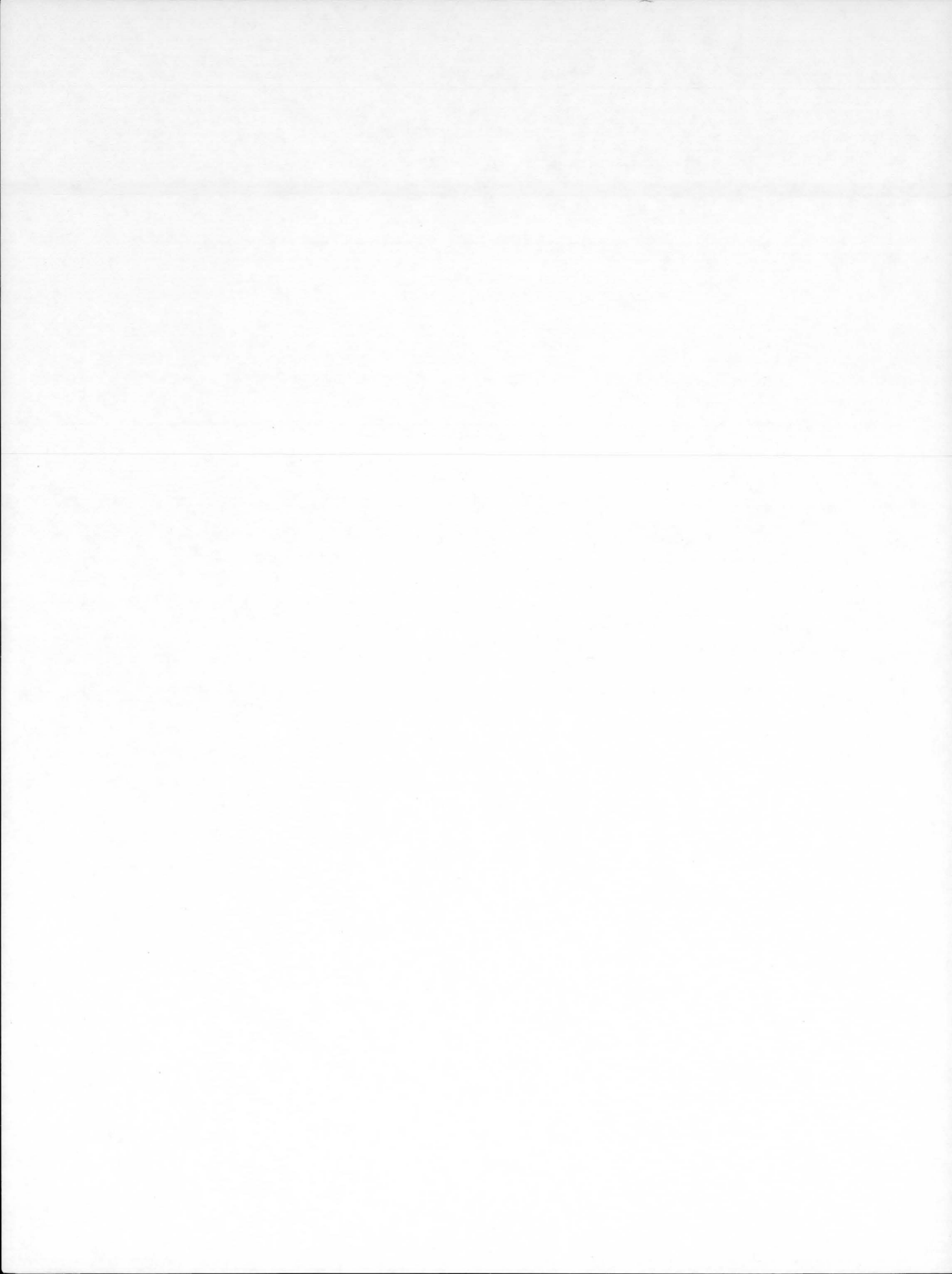
FOR SALE BY THE SUPERINTENDENT OF DOCUMENTS, U.S. GOVERNMENT PRINTING OFFICE
WASHINGTON, D.C., 20402 - PRICE \$1.50

FOREWORD

The objective of the National Aeronautics and Space Administration's Technology Utilization Program is to identify, document, and transfer to the national economy the technical advances resulting from our space and research programs. These innovations, when properly applied in industry and business, hold great promise for improving our everyday life and contributing to the prosperity of the nation.

We believe that the knowledge, progress, and advances associated with aerospace technology contain major potential for industrial applications. The content and method of presenting symposium papers by Marshall and selected contractor personnel have been designed to transfer an awareness of at least some new technology to attendees in nonaerospace fields.

WERNHER VON BRAUN
DIRECTOR, *George C. Marshall Space Flight Center*



CONTENTS

	Page
1. Nonspace Technology Resulting From the NASA Fluid Connector Programs..... <i>F. O. Rathburn, Jr., and L. G. Gitzendanner</i>	1
2. Development of High Pressure Gas Systems..... <i>John Gear</i>	15
3. Commercial Application of Rocket Engine Turbopump Technology..... <i>W. P. Luscher</i>	21
4. Monitoring of Impurities in Fluids and Gases..... <i>W. A. Riehl</i>	37
5. Special Tooling for Joining Tubing in Place..... <i>R. Meredith</i>	43
6. Some Unique Applications of Intense Magnetic Fields..... <i>R. J. Schwinghamer</i>	55
7. Sculpturing, Forming, and Spinning of Large Components for Launch Vehicles..... <i>Etric L. Stone</i>	65
8. Orbital Tube Flare for Tubing Connectors..... <i>James R. Williams</i>	75
9. Tooling Concepts for Assembly of Large Structures..... <i>R. Hoppes</i>	87
10. Sliding Electrical Contact Materials..... <i>J. C. Horton</i>	95
11. Dry Film Lubricants..... <i>J. E. Kingsbury and E. C. McKannan</i>	101
12. Insulation Materials..... <i>R. E. Shannon</i>	105
13. New Polymers for High Temperature Applications..... <i>Robert E. Burks, James D. Byrd, and James E. Curry</i>	115
14. New Lightweight Alloys..... <i>C. E. Cataldo</i>	123
15. Effects of Aerospace Technology on Civilian Life Through Scientific Instrumentation..... <i>John G. Atwood</i>	137
16. Computer-Aided Design for Civil Engineering Structures..... <i>L. A. Harris, J. C. Mitchell, and G. W. Morgan</i>	147
17. Lenticular Stereoscopic Television..... <i>Charles White</i>	161
18. Use of Space Vehicle Television Developments for Commercial and Industrial Use..... <i>C. T. Huggins</i>	167

	Page
19. Commercial Applications of NASA Research in Semiconductors and Microelectronics <i>A. M. Holladay</i>	179
20. The Parametric Amplification of DC Currents..... <i>Thomas L. Greenwood</i>	193
21. Flat Conductor Wiring Systems for Federal and Commercial Applications..... <i>Wilhelm Angele</i>	199
22. Nondestructive Testing—The Road to Quality..... <i>J. E. Kingsbury and W. N. Clotfelter</i>	215
23. An Improved Wind Sensor for Measuring Vertical Wind Velocity Profiles and Some Possible Commercial Uses..... <i>James R. Scoggins</i>	223
24. Digital Events Evaluator..... <i>E. F. Bullington</i>	229
25. The New Micro-Flowmeter..... <i>Fred Wells</i>	235
26. Bellows Joints, Gimbals, and Clamps..... <i>C. M. Daniels</i>	239

1. Nonspace Technology Resulting From the NASA Fluid Connector Programs

F. O. RATHBURN, JR., AND L. G. GITZENDANNER

Advanced Technology Laboratories, General Electric Company

Leakage at static seals is a problem common to both NASA and industry. The subject of an intensive investigation has been the establishing of design criteria for reliable, low-weight, leak-tight fluid connectors. The problem has been broken into areas of investigation: the structure which supports the actual seal and the seal itself.

A Separable Connector Design Handbook has been written to direct designers' efforts toward the optimum connector design for a given purpose. Included in this paper is a brief discussion of the topics covered in the Handbook, notable flanged connector design, threaded connector design, pressure energized seal design, leakage measurement techniques, and a catalog of current satisfactory seal configurations.

Also included in this paper is a discussion of the principles of sealing, including the uses and characteristics of elastomers, plastics, and metals. The load-leakage characteristics of seals, the effect of internal pressure, the effect of surface finish on the leakage rate, the mode of material deformation under load, and the advantages of various seal configurations are discussed.

In nearly all industrial applications where fluids, either liquid or gas, are transported, the problem of leaks exists to some degree. Whether the equipment is a steam turbine, where the tolerable leakage between flanges may be of the order of pounds per hour, or a supersonic aircraft, where tolerable hydraulic fluid leakage is less than 10^{-2} cc/sec, or in space vehicle application, where the tolerable leakage limit may be as low as 10^{-6} atm cc/sec, the problem of reducing leakage from fluid systems persists. Few areas of industry have totally conquered the problem. Where the problem has been conquered, extreme reliability of the equipment has resulted, as in the case of cold controls for home refrigerators, where any measurable leakage would cause drift in calibration and too short a life to be acceptable. The effects of leakage in some systems may be only a slightly reduced efficiency of the overall equipment and may, because of that, be overlooked. In other cases, the loss of some fluid may create unsafe

conditions for personnel, as in the case of some chemical plant applications. In still other cases, a leak, because of its velocity in exiting from the system, or because of its chemistry, may result in catastrophic destruction of equipment, as is the case in some combustion gas leaks. In still other cases, such as deep space vehicle operation, the major problem may be merely the retention of virtually all of the working fluid, because loss of fluid would jeopardize completion of the mission.

NASA, through its headquarters in Washington and the George C. Marshall Space Flight Center, has sponsored two programs with the goal of reducing the leakage problem in aerospace applications. One program had as its goal the establishment of the fundamentals of separable fluid connector designs; the other program had as its goal the development of new (and improvement of old) methods for the fabrication, testing, and inspection of separable, semi-permanent, and permanent fluid connec-

tors for aerospace application. Although the programs have been directed primarily toward applications wherein lightness of weight of the connector and leakages of extremely low levels are involved, the goals also include extreme reliability, best utilization of equipment and material, and reduction in cost. The latter three goals are applicable to all industrial and commercial applications; the first two may also be applicable in some circumstances.

While the investigations under the two programs have not been completed, the efforts have yielded a great deal of useful information and new design concept.

The overall problem of fluid connector design can be broken down into two separate investigations which, although allowing efficient means of study, are coupled strongly together in the overall hardware. It is the purpose of this paper to outline, in both of these areas of investigation, those aspects and results which should prove most helpful to industry at large. The scope of investigation and the results presented here constitute but a small part of the overall investigation. Results published to date are available in the documents cited in the appendix.

The two subareas of investigation are those of (1) the attainment of the seal, and (2) the substructure which supports and maintains the seal. In any separable fluid connector, the barrier to fluid leakage is effected by the maintenance of two surfaces in contact. The surfaces may have varied configurations, be constructed of many different materials, may vary in number, and may require different loads or stresses to hold them in place. The investigation of the relative value of different materials, the effects of internal pressure on the leakage, the effects of the surface finish, and the stress and load requirements (both initially and thereafter during the operational life of the connector) constitute the seal study.

Since it is generally possible for a given sealing system to reduce the leakage flow under an arbitrary pressure to a prescribed tolerable limit if enough load is initially available, the problem of the development of that load and the maintenance of that load comprise the second study—

that of the substructure. Since the capacity of the seal to limit leakage is sensitive, to a certain extent, to reduction of sealing load (and a hostile environment would usually promote reduction in load), the structural problem becomes acute with regard to maintenance of load. Further complicated by the problems of lightness of weight and extreme temperature and vibration environments, the structural problem requires great sophistication of analysis and synthesis.

To facilitate the design of separable connectors for arbitrary applications, a Handbook for Separable Connector Design has been written. In it, both the sealing problem and the structural problem are considered. The goal of the Handbook is to reduce all available information and design techniques to the stage where, given a set of conditions to be met, a designer can effect a configuration and combination of materials so that his requirements will be fulfilled.

TENTATIVE HANDBOOK FOR SEPARABLE CONNECTOR DESIGN

The Handbook is organized into seven chapters, the titles of which are listed below:

- | | |
|-------------|---|
| Chapter I | Fundamental Consideration
of Separable Connector
Design |
| Chapter II | Flange Connector Design |
| Chapter III | Threaded Connector Design |
| Chapter IV | Pressure Energized Cantilever
Seals and Hollow
Metallic O-Rings |
| Chapter V | Leakage Measurement
Techniques |
| Chapter VI | Material Properties and
Compatibility |
| Chapter VII | Catalogue of Seals |

With regard to the two basic problems of sealing and structural integrity, Chapters I, V, and VII deal largely with the sealing problem, and Chapters II, III, V, and VI deal with the structural problems, although for the complete connector design, both groups of chapters must be called upon.

Through the use of sample pages and diagrams from the Handbook, the structural aspects of the problem and their proposed solu-

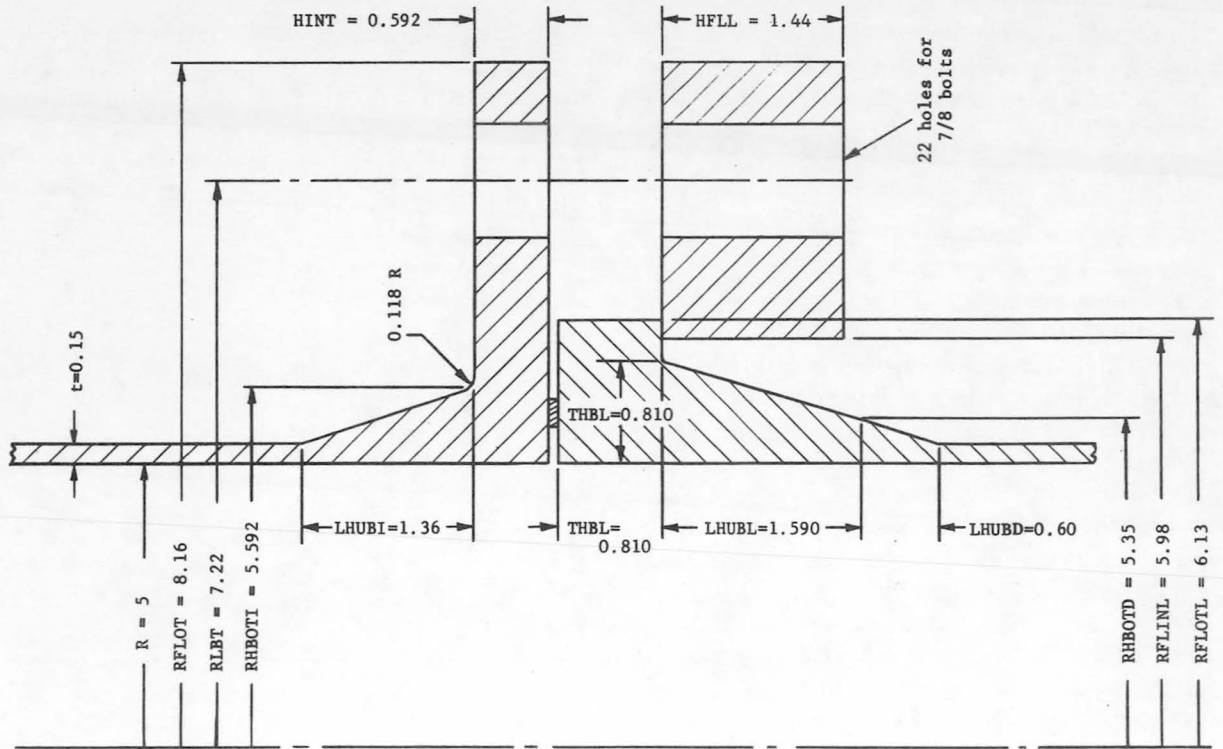


FIGURE 3.—One loose flange, single load path.

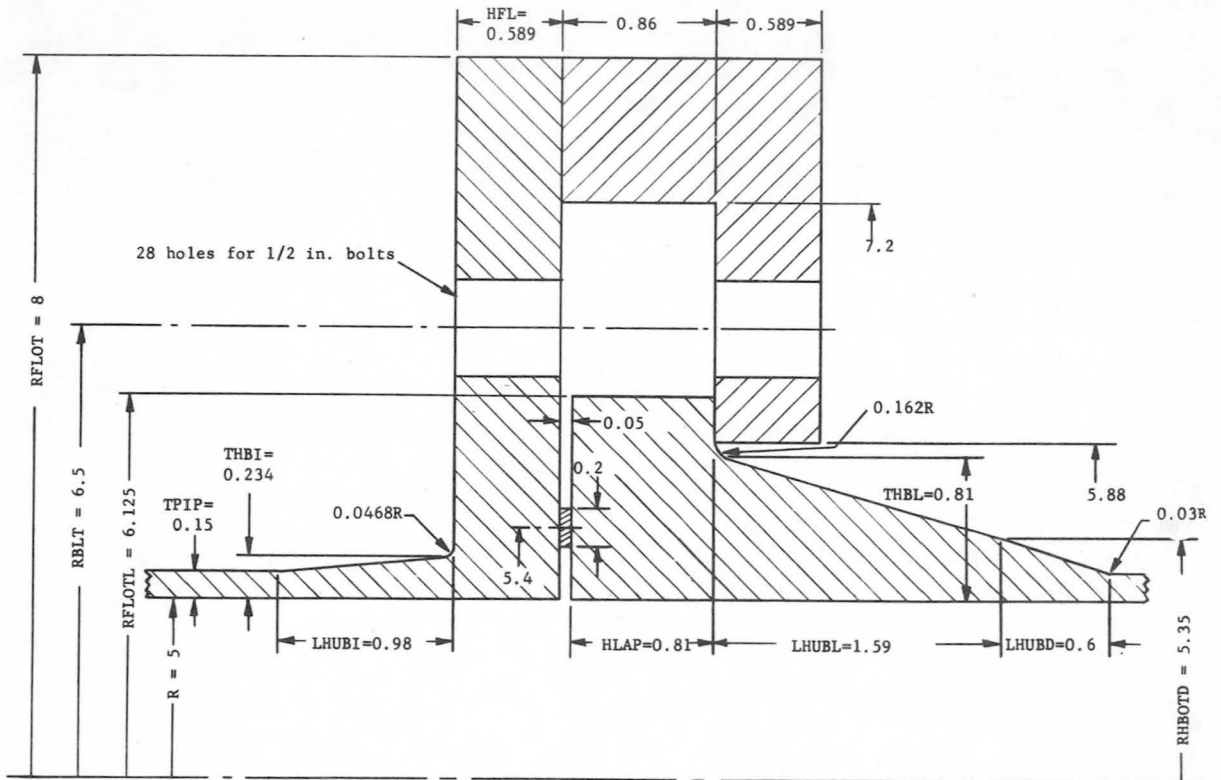


FIGURE 4.—One integral flange, alternate load path.

connector. Evaluation of the stress levels, with regard to their acceptability, provides a criterion for perturbations on the original design. Again, based on specified rules, the initial design is altered, and a second stress analysis is accomplished. After a few iterations, the design of the flange can be optimized. While the details of the analysis and the total number of manipulations required for establishing the initial design would not be of direct interest here, the simplicity of establishing the initial design can be shown by a display of a sample page from the Handbook, shown in figure 5.

Threaded Connector Design

Because of the sophistication required in an analysis of a threaded connector, the same technique of establishment of initial design is used, followed by analysis of the design, and then per-

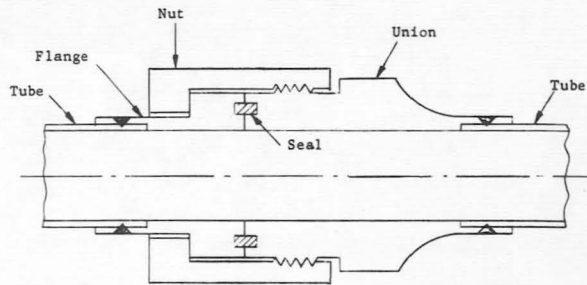


FIGURE 6.—Typical threaded-connector configuration.

turbation of the design parameters to optimize the configuration. A threaded connector, which has many more possible variations in configuration due to the large number of seal configurations available, is assumed to be made up of three basic concepts, namely union, nut, and flange (fig. 6). Each component, although varying in dimension, will have essentially a given shape. The seal, which may vary from connector to connector, will require certain loads to be administered to it by the structural components. The coupling between seal and connector is one of load development and retention. Figure 6 shows the basic configuration considered with regard to the threaded connector.

While the details of the preliminary design and the analysis of that design are not covered in this paper, a feeling for the complexity of the problem can be gained from the following list of those parameters which must be determined before formulation of the design:

- a. Tubing
 - Material
 - Outside diameter, D_t
 - Inside diameter, d_i
- b. Fluid contained in the tubing
 - Name and chemical composition
 - Operating pressure, P_o
 - Constant pressure, P_k
 - Cyclical pressure, P_c
 - Number of cycles of pressure, N_p
 - Temperature, T_g
- c. Environmental conditions
 - Surrounding fluid
 - Ambient pressure, P_a
 - Ambient temperature, T_a

(c) Estimate of bolt circle radius (RBLT) is 6.5 in.

$$\frac{AMIN}{RBLT} = \frac{4.12}{6.5} = .633$$

Entering Table 2.1, Column (1) under Fine Threads, the next larger number is .748, indicating a bolt size of 1/2 in. in Column (2).

$$\text{number of bolts } n = \frac{4.12}{.7486} \text{ (Column 3)} = \boxed{28 \text{ bolts}}$$

Multiplying this number by the minimum bolt spacing (Col. 4)

$$28 \times 1.25 = 35 \text{ in.}$$

Comparing this with the bolt circle circumference

$$2\pi(RBOLT) = 2\pi(6.5) = 40.8 \text{ in.}$$

one sees that the spacing will be adequate with a 6.5 in. bolt circle radius.

(d) The flange thickness (HFL) is

$$(HFL) = (\text{Col. 7}) \sqrt{3(SB)/(SF)}$$

$$(HFL) = .340 \sqrt{3 \frac{100,000}{100,000}}$$

$$(HFL) = \boxed{.589 \text{ in.}}$$

(e) The flange outer radius (RFLOT) is given by (RFLOT) = 2 (RBLT) - R according to paragraph (e) p. 2-34.

$$RFLOT = 2 \times 6.5 - 5 = \boxed{8 \text{ in.}}$$

The radial width of the raised bearing surface at the outer edge is

$$RFLOTB = 0.1 [\text{Col. (1)}]$$

$$RFLOTB = 0.1 [.748] = \boxed{.0748}$$

The height of this surface is

$$HBRC \geq .002 \text{ Col. (1)}$$

$$HBRC \geq .001496$$

(f) The hub thickness is

$$(THBI) = \frac{2.5 R P_{\text{max. oper.}}}{\sigma_{\text{allow.}}}$$

FIGURE 5.—Sample preliminary flange design calculations.

- d. External loads
 Constant force, F_k
 Cyclical force, F_c
 Number of cycles of force, N_f
 Constant transverse moment, m_k
 Cyclical transverse moment, m_c
 Number of cycles of moment, N_m
- e. Allowable leakage level

Pressure Energized Cantilever Seals

One concept used to maintain sealing load during the operational life of the connector is that of designing the seals to use the internal pressure to an advantage. Should the seal, resting between two integral connector components, be shaped as shown in figure 7, then the internal pressure acting on the inside of the seal will tend to push the legs of the "U" apart and thus into firm contact with the mating surfaces, regardless of the external load applied. While such a concept is useful only in certain ranges of pressure, sealing loads, and sizes, it is important to establish procedures for optimum seal design.

Because of the relative simplicity of such a design as compared to that of the flanged or threaded connectors, the procedures for design do not require analysis and iteration, but rather a direct synthesis of the seal configuration is possible. In the Handbook, this synthesis has been reduced to a series of simple design rules, supplemented by nomographs where the use of a detail equation is required. While

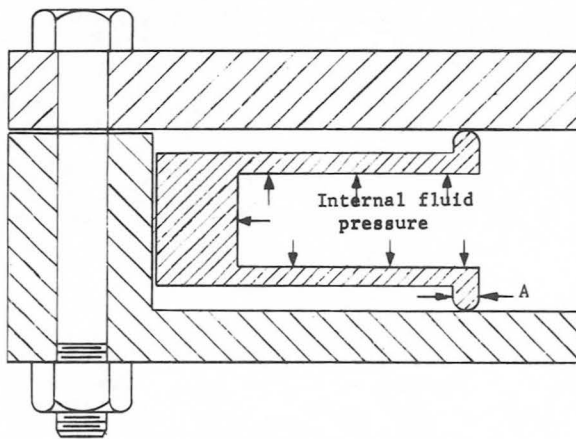


FIGURE 7.—Typical pressure-energized seal configuration.

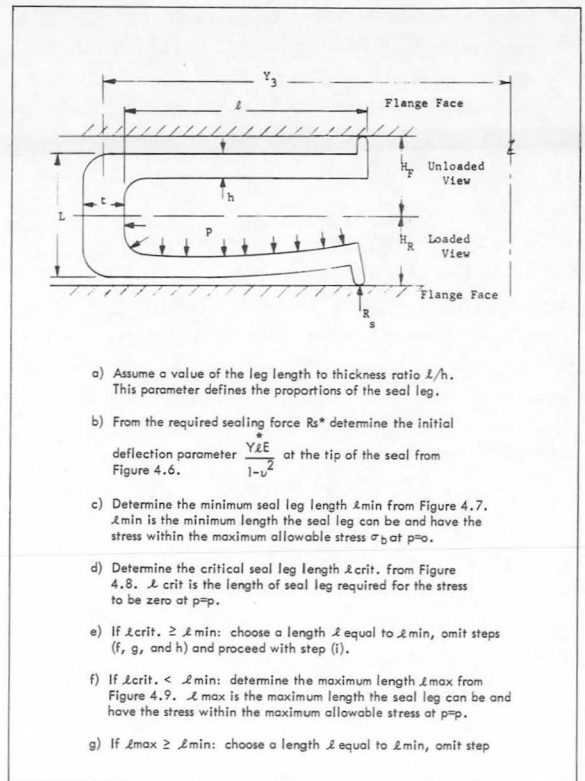


FIGURE 8.—Sample pressure-energized seal calculations.

it is not the purpose here to illustrate the use of the Handbook, it is of value to inspect two sample procedure sheets from the Handbook, shown in figures 8 and 9. The simplicity added by the use of a nomograph over the possible use of the rather complicated equation shown can easily be appreciated.

Cantilever type pressure energized seals of the straight leg type, taper leg type, and those having legs constructed at an angle to the flange faces are all included in the design procedures (fig. 7).

Material Selection

Unfortunately, no one structural material exists as a panacea for all possible problems. The requirements of fluid compatibility, lightness of weight, high strength, and stability of properties at cryogenic temperatures and/or extremely high temperatures make necessary the selection of specific materials for different ap-

plications. A manual outlining all the applicable material properties of all candidate structural metals could not be written for many reasons, such as the enormous number of materials available, the lack of adequate data on many of the materials, and the various heat-treatment conditions of the candidate materials. A possible solution to this dilemma is to make available to the designer a short compendium of some materials, with many of the properties listed, to show the compatibility of those materials with the fluids which might be used, and to suggest further references. A short chapter on this subject is included in the Handbook.

THE SEALING PROBLEM

Since an effective seal is formed when the contact between two surfaces is of such intimacy that molecules of fluid can no longer pass between the voids at the interface, the question of which materials, what type of surfaces, and what necessary loads are best to produce such a contact arises. If these were the only criteria, and if temperature dependence properties, compatibility with the fluid, and the susceptibility of material to vacuum and vibration deformation were not to be considered, then certain generalizations could be made. Even with these associated problems, certain statements can be made.

Whenever possible, elastomeric gasketing material should be used, mated between two metal sealing surfaces. When this can be done, then the surface characteristics of the gasket material and of the metals are of small importance, and near-zero leakage can be affected. Where a certain level of leakage can be tolerated, near the permeation rate through plastics, several different plastics can be used between two metal surfaces. In this instance, the surface characteristics of the metal surfaces are relatively unimportant with regard to the leakage characteristics of the system. However, the problem of cold flow of the plastics must be faced and can complicate the problem greatly.

Where metal-to-metal contact is desired, two alternatives are present, that of using a metal gasket between two integral sealing surfaces of

the connector, and that of mating the two integral surfaces directly. For surfaces other than superfinished surfaces, it can be concluded, that in order to effect a seal with a leakage rate of below 10^{-6} atm cc/sec (with 1500 psi or greater internal pressure) plastic yielding must take place, at least locally, at the sealing interface. The degree of plastic deformation necessary depends upon the level of internal pressure, the material at hand, and to a great extent the surface finish of the stronger material in contact. For example, should a soft metal gasket such as copper, aluminum, indium, or lead be used between stainless steel sealing surfaces, the original surface finish on the gasketing material is relatively unimportant. However, the magnitude and the direction of the asperities on the stainless steel are of great importance. As a general rule, should one desire to discount the surface finish on the stronger material, then it would be necessary to plan on the imposition of a stress of approximately 2.75 times the yield strength of the weaker material in order to effect the satisfactory seal. Should prescribed surfaces such as machined surfaces be made and maintained through the life of the connector,

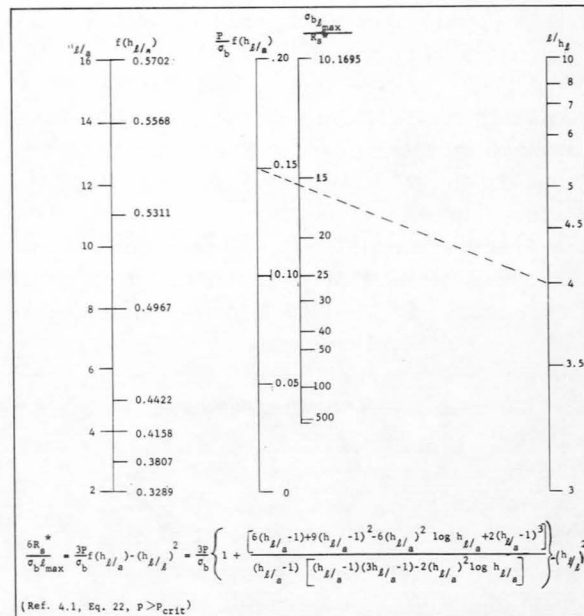


FIGURE 9.—Nomograph for pressure-energized seal calculations.

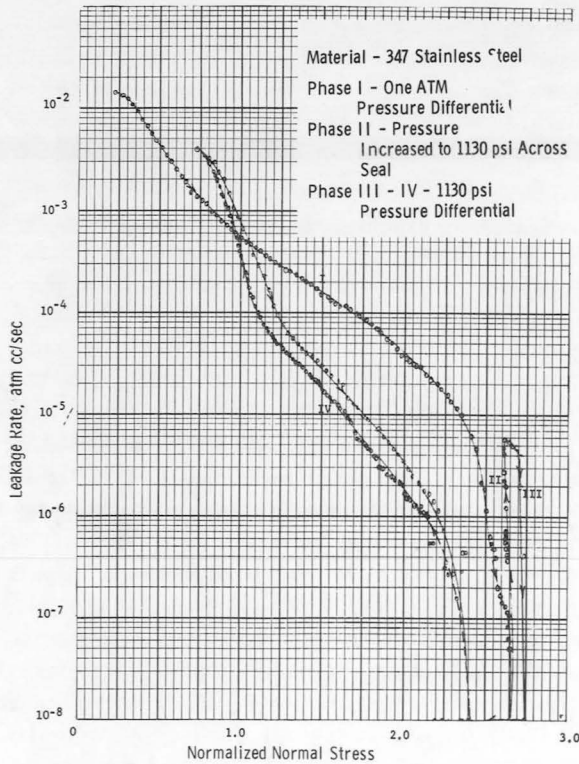


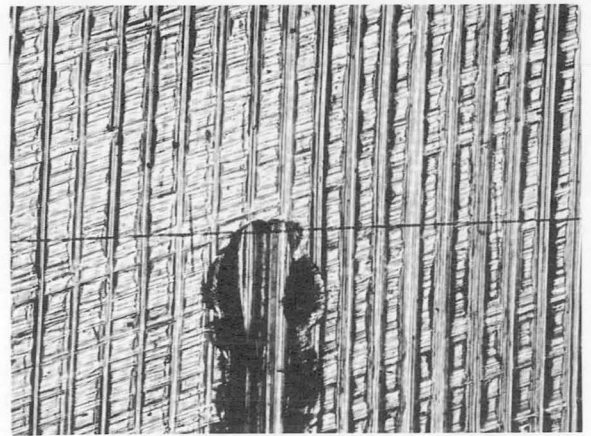
FIGURE 10.—Leakage vs. stress response for a typical system (metal-to-metal).

the planned stress level could be reduced. A typical leakage response to the imposition of stress for a metal-to-metal sealing system is shown in figure 10, where the stress necessary for sealing with one atmosphere internal pressure, the increase in leakage with pressure, the increase in stress necessary for sealing with 2000 psi internal pressure, and the sensitivity of the system to the reduction of stress are shown. With regard to sensitivity to the reduction of stress, the general rule is that: the greater the plastic deformation of the materials involved the less sensitive to stress removal the system will be.

A further complication in the establishment of required stress level for a given sealing system is the lack of uniformity of mating across the width of any seal. The degree of mating is much greater at the outside than at the center, as is shown in figure 11(a) and 11(b) for a typical gasket mated in between sealing surfaces which have been radially ground for

experimental investigation only. Other tests have shown that the capacity to seal is not solely dependent on the true area of contact but also on the direction of the original surface asperities and the continuity of the resulting true areas of contact. While this could be expected, it complicates the problem from an analytical and experimental point of view.

While the use of an intermediate soft material is feasible in many applications and allows the system to be reused without degradation of the integral components of the connector, in some applications such a secondary component is undesirable. In that case, the integral components of the connector must be mated to-



(a) Central area.

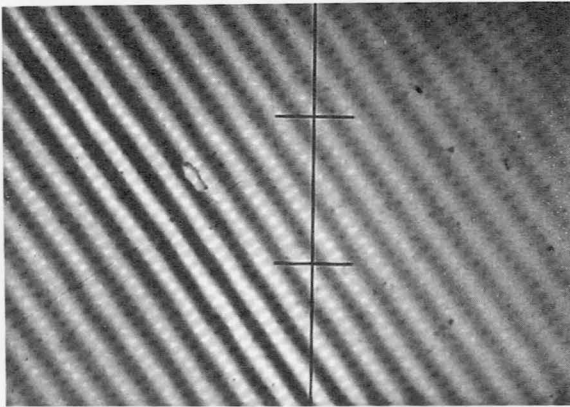


(b) At edge.

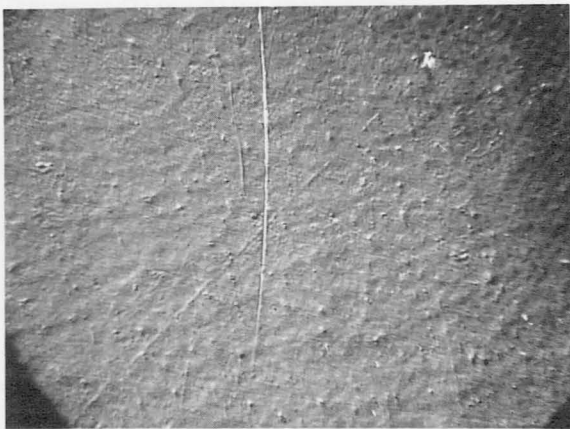
FIGURE 11.—Mating of a flat gasket seal. Vertical lines are original asperities, horizontal lines impressed onto surface by mating. Magnification: 0.00482 inch between scale marks.

gether directly. The added problem reusability of the connector presents itself. Since it has been concluded that some plastic deformation is necessary in order to effect the seal, this is tantamount to saying that the shape of the surfaces, and sometimes the overall configuration of the components, changes after its initial assembly. Should the sealing load have been established based on the original surface finishes, the same sealing load could not be counted upon for the second sealing operation, since the surface finishes are no longer the same. This problem is quite severe in aerospace applications, since extremely low leakages can be tolerated, and reusability must be assured.

A technique which may provide a solution



(a) *Interference photograph. Scale: 0.00194 in. between scale marks.*



(b) *Nomarski photograph. Magnification=168.*

FIGURE 12.—*Superfinished sealing surfaces.*

for this difficulty is the use of a superfinished surface being manufactured on the integral connector components. While this technique has not been fully exploited or insured successful, studies to date have shown that finishes can be manufactured which allow stresses less than the yield strength of the material to be applied and effect leak-type joints for repetitive assemblies. The surface finishes are at the present time expensive but, due to the possible payoff in connector improvement, are still under consideration. Photographs of such a surface made by high magnification microcopy are shown in figure 12. The stress level required for sealing is shown in figure 13 for three successive tests made on such a surface finish. To date, it has been shown that up to 11 successful reassemblies can be made. Accumulation of surface damage due to the foreign particles present when the surfaces are brought together prevents further use of the surfaces.

In this discussion, the leakage rates measured in fractions of atm cc/sec have been used. Leakage levels that small are extremely difficult to measure or even detect. The means most acceptable for experimental work is that of a mass spectrometer detector which utilizes helium as the tracer gas. For other gases in other applications and other leak rates, simpler methods are possible such as water tests and bubble tests. Comparisons of the various leak testing methods and relative leakage rates are shown in table I. One means, quite universal in the number of gases which can be detected and the range of sensitivities which can be gained in the Condensate Nuclei Detector, the capabilities of which are outlined in table II.

Handbook Coverage of Sealing

Chapter I of the Handbook delineates the various modes of leakage that can exist in a connector, notably those of molecular flow and viscous flow of a fluid through an interface, and also establishes the possibility of the permeation and diffusion processes of leakage. Chapter V establishes in detail what are considered to be minimum standards for the leak detection and measurement facility suitable for evaluating fluid connectors. Chapter VII is a catalog of

TABLE I.—Sensitivities of Leak-Measuring Methods

[Mass spectrometer detects flow of helium. In laminar flow, volume flow of helium=volume flow of air for the same leak under the same pressure and temperature conditions, since viscosities of air and helium are approximately the same. In molecular flow, volume flow of helium \approx 3 times volume flow of air for the same leak under the same pressure and temperature conditions.]

Type of Measurement	Application	Volume of Helium or Air			Mass Flow (Air), lb, hr
		Micron-ft ³ , hr	Atm-cc, sec	Atm-ft ³ , hr	
A. Bubble test (immerse fully pressurized connector in fluid and look for bubbles).	Component test.				
1. Using water at room temperature and atmospheric pressure.					
a. No bubbles in 5 to 15 min.	-----	20	2.08×10^{-4}	2.64×10^{-5}	2.02×10^{-6}
b. No bubbles in 30 min (estimated).	-----	10	1.04×10^{-4}	1.32×10^{-5}	1.01×10^{-6}
2. Using water at room temperature with pressure above bath reduced to 2 in. Hg (=above 0.07 atmosphere).	-----	3	3.12×10^{-5}	3.96×10^{-6}	3.03×10^{-7}
3. Using silicone oil					
a. At 150° C and atmospheric pressure.	-----	0.45	4.61×10^{-6}	5.85×10^{-7}	4.49×10^{-8}
b. At room temperature with pressure above bath reduced to 1.5 in. Hg (=about 0.05 atmosphere).	-----	0.056	5.85×10^{-7}	7.43×10^{-8}	5.69×10^{-9}
B. Displacement of water in burette by leaking gas.	Component test.	1.6	1.67×10^{-5}	2.12×10^{-6}	1.62×10^{-7}
C. Soap-bubble test (apply soap solution around connector and look for bubbles).	Field assembly test.	5	5.2×10^{-5}	6.6×10^{-6}	5.0×10^{-7}
D. Mass spectrometer leak detector.	Laboratory test.				
1. With maximum sensitivity-----	-----	0.96×10^{-6}	1×10^{-10}	1.27×10^{-11}	0.97×10^{-12}
2. With lower sensitivity-----	-----	0.96×10^{-5}	1×10^{-9}	1.27×10^{-10}	0.97×10^{-11}

seals which have proven satisfactory in certain applications. This chapter, which can be updated upon the acquisition of new information, lists those characteristics of seals which are of interest to the connector designer. Sample entries are given in figures 14 (a) and (b) which show the characteristics of a metal triangle seal suitable for high temperature low leakage application.

CONCLUDING REMARKS

The fluid connector design problem is present not only in NASA aerospace applications but in nearly all industrial endeavors. Its importance varies from industry to industry. The complexity of its solution varies from requirement to requirement. The efforts of NASA to solve its own problems bear fruit for the nonaerospace

TABLE II.—*Condensate Nuclei Detection Techniques*[1 ppm sensitivity would allow for detection of a leak of 2×10^{-5} cc/sec if direct access to the leak were possible]

Material	Detectable	Not detectable	Limits of detection, ppm
Petroleum fractions.....	x		0.1
Hydrogen.....		x	-----
Hydrazine.....	x		~0.1
Unsymmetrical Dimethylhydrazine.....	x		0.1
Aerozine.....	x		~0.1
Hydyne.....	x		~0.1
Ammonia.....	x		0.005
Diborane.....	x		?
Pentaborane.....	x		?
Aluminum Borohydride.....	-----	x	-----
Beryllium Borohydride.....	-----	x	-----
Lithium Borohydride.....	-----	x	-----
Hydrazine Hydrate.....	x		~0.1
Alcohols and Ethers.....	x		5.0
Ethylene Oxide.....	x		?
Mixed Amines.....	x		~0.01-1.0
Nitromethane.....	x		?
Aluminum.....	-----	x	-----
Beryllium.....	-----	x	-----
Beryllium Hydride.....	-----	x	-----
Lithium.....	-----	x	-----
Lithium Hydride.....	-----	x	-----
Oxygen.....	-----	x	-----
Ozone.....	x		~5.0
Hydrogen Peroxide.....	x		~0.1
Nitrogen Textroxide.....	x		~0.5
Nitric Oxide.....	x		~0.5
Nitrogen Dioxide.....	x		~0.5
Nitrous Oxide.....	x		~0.5
Nitric Acid.....	x		0.5
Tetranitromethane.....	x		?
Fluorine.....	x		~1.0
Oxygen Difluoride.....	x		~1.0
Chlorine Trifluoride.....	x		~1.0
Bromine Pentafluoride.....	x		~1.0
Perchloryl Fluoride.....	x		~0.1
Nitrogen Trifluoride.....	x		?
Tetrafluorohydrazine.....	x		?
Ozone Fluoride.....	x		~1.0

industry. All the information, in much more detail than has been presented herein, is or will shortly be available in NASA publications. The Handbook mentioned frequently throughout this discussion will shortly be available.

The fundamentals supporting that document have been reported in seven volumes cited in the appendix. Two further volumes on the subject are presently being written and will be available from the same sources.

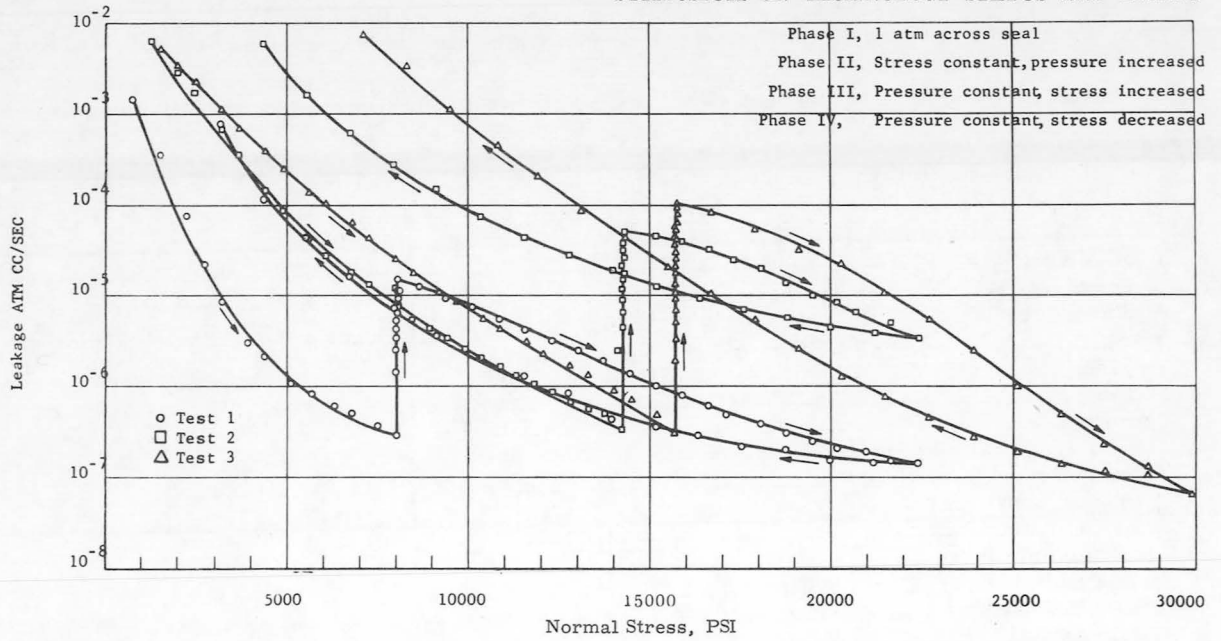


FIGURE 13.—Leakage—normal stress response for superfinished stainless steel surfaces.

CLASSIFICATION: Triangle Seal

MATERIAL: Gasket - 25 aluminum (copper, nickel, etc.). Knife edges constructed from connector structural material.

CONFIGURATION: Initial Configuration Sealed Configuration

TEMPERATURE LIMITATIONS: Determined by creep properties of gasket material.

LOAD DEFLECTION CHARACTERISTICS: (25 aluminum, room temperature): See Figure 7.7.

SEALING CHARACTERISTICS: (25 aluminum, room temperature): After 950 pounds per inch has been applied to the seal (thus causing a dual load path to exist) at an internal pressure of 1800 psi, the load can be reduced to 300 pounds per inch before leakage is evident. At this load, leakage increases drastically.

ADVANTAGES:

1. Shear deformation of the gasket is utilized.
2. Since the internal pressure pushes the gasket radially outward into the knife edges, the gasket is pressure energized.
3. Desired amount of gasket deformation can be specified due to the dual load paths called for in the design.
4. Knife edges, being at an angle to the seal centerline, make the seal insensitive to axial movement of the flange faces.
5. Gasket flanges are positively positioned during assembly.
6. Knife edges are protected from damage and they do not protrude above the flange faces.
7. Gasket is contained by the flanges.

DISADVANTAGES: 1. Each reassembly requires a new gasket.

COMMENTS: Data based on a sealing system having a nominal diameter of one inch.

FIGURE 14(a).—Seal configuration data from separable connector design handbook.

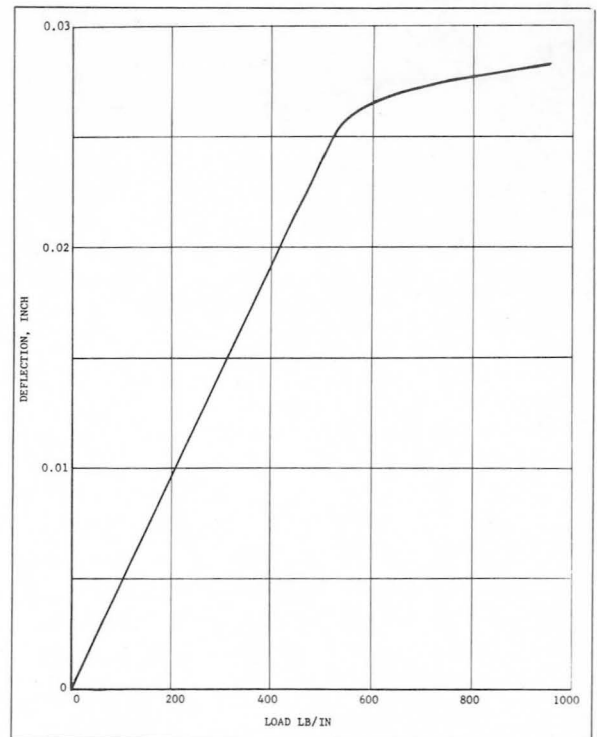


FIGURE 14(b).—Seal configuration data from separable connector design handbook.

APPENDIX—FINAL REPORTS—DESIGN CRITERIA FOR ZERO LEAKAGE CONNECTORS FOR LAUNCH VEHICLES

First Contract Period

VOLUME I—Summary, Conclusions, and Design Examples, edited by T. P. Goodman, N63-18390, NASA-CR-50557 (63GL41), March 15, 1963.

VOLUME II—Leakage Flow, edited by T. P. Goodman, N63-18493, NASA-CR-50558 (63GL42), March 15, 1963.

VOLUME III—Sealing Action at the Seal Interface, edited by F. O. Rathburn, Jr., N63-18159, NASA-CR-50559 (63GL43), March 15, 1963.

VOLUME IV—Design of Connectors, edited by S. Levy, N63-18494, NASA-CR-50560 (63GL44), March 15, 1963.

VOLUME V—Pressure Energized Seals, edited by B. T. Fang, N63-18391, NASA-CR-50561 (63GL45), March 15, 1963.

VOLUME VI—Environmental Effects, edited by S. Levy, N63-18323, NASA-CR-50562 (63GL46), March 15, 1964.

The six volumes are listed in Scientific and Technical Aerospace Reports, Volume 1, No. 17, September 8, 1963, and Volume 1, No. 20, October 23, 1963.

Second Contract Period

Fundamental Seal Interface Studies and Design and Testing of Tube and Duct Separable Connectors, edited by F. O. Rathburn, Jr., N64-27305, NASA-CR-56571 (64GL97), June 1, 1964.

This volume is listed in Scientific and Technical Aerospace Reports, Volume 2, No. 19, October 8, 1964.

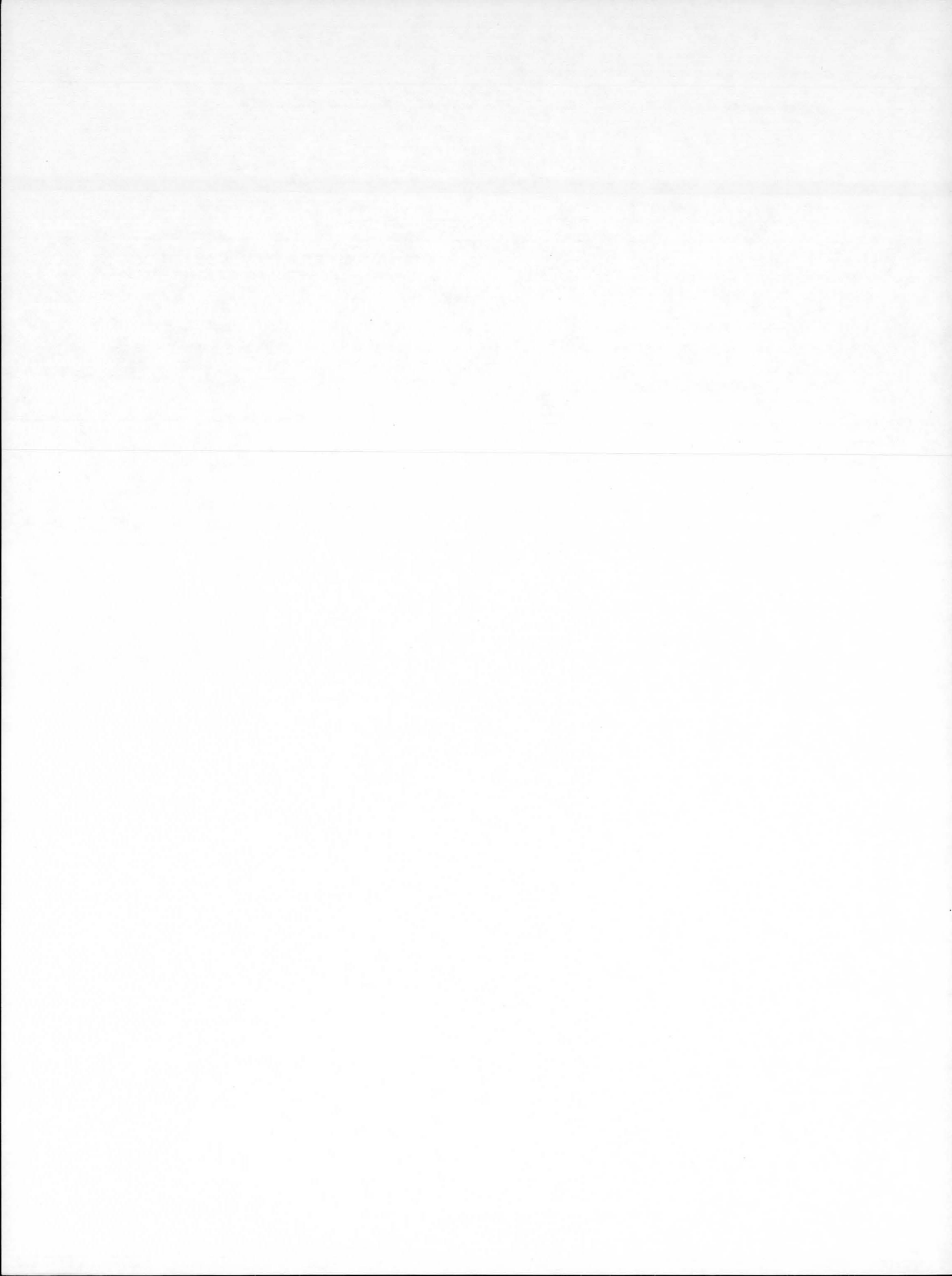
These reports may be purchased from the Defense Documentation Center, or the NASA representative, Code CRT, Scientific and Technical Information Facility, P.O. Box 5700, Bethesda, Maryland.

Third Contract Period

Handbook for Separable Connector Design, edited by F. O. Rathburn, Jr., December 1, 1964.

Sealing Interface Statistical Analysis and Superfinished Surfaces Sealing Study, edited by L. G. Gitzendanner and F. O. Rathburn, Jr., March 1, 1965.

Both volumes are available from the previously mentioned sources.



2. Development of High Pressure Gas Systems

JOHN GEAR

Hayes International Corporation, Birmingham, Alabama

This paper presents a report on the latest advances and technology in the design, construction, testing, and operation of high pressure gas bimetallic pipe systems and high pressure gas tube fittings facilitating greater alignment and manufacturing tolerances, and the supercleaning of high pressure gas systems under field conditions. The following specific topics are discussed:

- Analysis of noncorrosive steels versus bimetallic, high strength steels
- Analysis of various protective finishes versus bimetallic piping
- Testing of high pressure systems
- Pipe liner adhesion properties under varying operating conditions
- Modified flared tube fittings taking into account pressure ranges, materials, costs involved in manufacture, various methods employed to permit sealing of the fitting while meeting cleanliness requirements
- Cleaning requirements appertaining to high pressure gas systems and a discussion of investigations on the effects of velocity and temperature as related to various cleaning chemicals.

The presentation concludes with a discussion on the possible applications of materials and methods in commercial industry.

High pressure gas systems, as described in this paper, are those representing the present state-of-the-art in the missile ground support equipment field. These systems have been developed for two prime reasons: (1) the attainment of maximum power within the smallest envelope dimensions, and (2) the storage and transmission of gas at high pressure and large volumes to facilitate its distribution to and around the large missile complexes. The use of high pressures in gas distribution systems may be compared to the use of high voltage in electrical distribution, each being transformed or regulated at the usage point. High pressure gas distribution and storage systems have been developed to obtain the maximum efficiency from an engineering and cost standpoint. Factors in the development work undertaken have been varied, time consuming, and expensive, a trend which now aims at standardization and reevaluation.

First, let us define what we mean by high pressure gas. The word "high" is purely rela-

tive to the prevailing state-of-the-art; for instance, pressures of 3000 psi were considered high in the early days of the missile effort. By the early 1960's 3000 psi was considered relatively low pressure, for the state-of-the-art had progressed to the 6000 psi system. However, with the use of high strength steels and the advancement of the state-of-the-art, large gas systems are now operated and controlled safely at 10 000 psi. Small bore systems up to $\frac{3}{8}$ -inch internal diameter have been employed in these high pressure ranges for some years; however, the large volume requirements of today have necessitated advances in the technology of design, construction, testing, and operation of high pressure gas systems. Development of system components, tubing, and piping necessitates extensive test programs, but in order to test these components, the test laboratory must store and control gas to pressures as high as 15 000 psi to control effectively the test specimens and also provide adequate flow by storing large volumes of gas above 10 000 psi.

Further complicating the task of the high pressure gas design engineer and his value analysis team is the fact that to fabricate, clean, and maintain cleanliness of high pressure gas systems under field conditions requires careful study of materials in contact with the gas, relative costs of materials, and the strength-to-cost ratio of suitable metals. Manufacturing tolerances have become more critical, and costs have consequently risen in the fabrication of high pressure gas systems which has called for careful economic studies. Consequently systems now on the drawing boards are nearing perfection and are becoming standard.

Corrosion resistant steel pipes and fittings offer the user the best answer to the cleaning and contamination problems; however, with pipe sizes up to 6 inch diameter, the relatively low strength of the corrosion resistant steels requires massive fittings and volume of material, which in turn increases the initial costs to a prohibitive level. It has become standard practice to use bimetallic pipe which consists of a base pipe made from high strength steel and lined with thin wall tubing of a suitable corrosion resistant material, facilitating cleaning and imparting noncontaminating properties. The three most widely employed lining materials are copper, nickel, and stainless steel. These metals are chosen not only for their corrosion resistant properties, but also for their similar coefficients of thermal expansion to the pipe base metal.

The lining of pipes is by no means recent, and in fact dates back to the 1800's. Cold drawn bimetallic tubing in condenser and heat exchanger service is used extensively today. Requirements for high pressure gas bimetallic pipe differ because of pressures and smaller temperature differentials. Pipe base material is of 4320 grade steel lined with various alloys of copper and nickel or stainless steel tubing, type 304 or 316 in wall thickness up to 0.050 inch. Bimetallic pipe is manufactured by hydraulically expanding the thin lining into the base pipe. With the correct selection of internal diameters of the base lining materials and by proper application of pressure, the lining expands with a uniform yield point until it just contacts the base pipe; pressure beyond this ini-

tial level elastically expands the base pipe and continues the plastic expansion of the liner. After final pressure is released, the elastic contraction of the base material actually exceeds that of the contraction of the lining material, thus holding the lining in place by applying a compressive force. (See fig. 1.)

Due to the relatively small temperature differential in the operating temperature range of the gas systems under discussion, the differential in the thermal expansion between the liner and the base material has almost negligible effect on the adhesion between the two; for instance: between copper and steel, the thermal expansion represents approximately 0.000002 inch per inch per degree fahrenheit. Presently, it is only practical to fabricate lined pipe sections in 20 to 40 foot random lengths. These lengths are then joined in the field either by welding or by pre-hubbing and then clamping together. Experience has shown that field welding of lined pipe calls for extremely close control of welding procedures and techniques. The pipe ends have to be prepared by machining a weld angle on the end of the pipe. Then the liners are welded together followed by a carefully controlled first-weld pass on the base material taking care not to burn the liner. Some of the gases used, such as helium and hydrogen, have in the past found their way through the

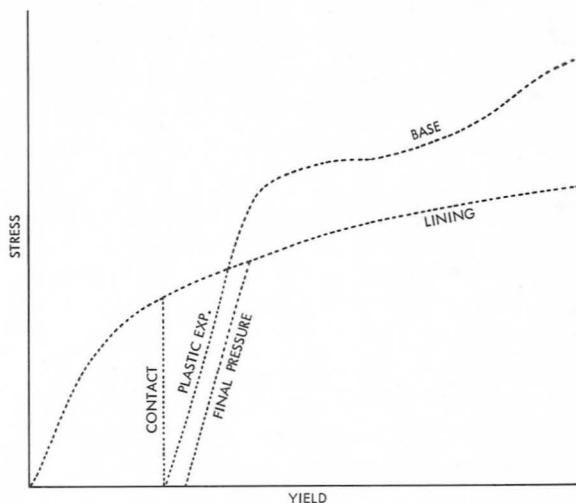


FIGURE 1.—Elastic contraction of base material and living material.

porous welds and have seeped between the base metal and the liner; as a consequence, the pressures inside the pipe and in the annular space between the liner and the base material have been equalized. When the main pipe is vented suddenly, the pressure still existing in the annular space crushes the liner and causes total blockage of the line. Many methods have been tried to circumvent these conditions, but for positive solution of this problem, the utilization of commercial hubbed joints, as used in the oil industry, has proved to be the answer. These hubs may be welded to the base material, after which the liner can be inserted, expanded and flared into the hub sealing surface (see fig. 2) thus insuring 100% sealing capability of the joint with no possible collapse of the liner due to gas seepage in the annular space between it and the base material.

The costs of fabricating bimetallic pipe has proved to be less than that of a pipe with similar pressure capabilities constructed from 100% corrosion resistant steels, when the bore size is above 2 inches. These findings cannot be applied as a rigid definition, and each case must be considered on its own merit. Certain other protective finishes have been tried to compete economically with bimetallic piping. These finishes are produced by phosphating or electrically nickel plating the interior surfaces of the pipe or by chemical nickel coating. Nickel plating has proved to be successful; however, the cost of electrical plating is high unless a large quantity of pipe is plated at one time. The main problem arises in depositing a uni-

form coating inside the pipe, because an electrode must be inserted in the exact center of the pipe and kept there during the electroplating process.

Testing of high pressure gas systems is expensive, but of paramount importance if operation and safety requirements are to be met. The knowledge gained in testing, fabricating, and operating these systems has permitted the selection of the optimum materials to meet cost and fabricating requirements. Tests have included pressurization of piping to 15 000 psi and sudden venting of the line to cause or attempt to cause collapse of the liner. The attainment of such test conditions on a routine basis has called for great ingenuity on the part of the test engineers, as did another test involving pressurization from 0 to 25 000 psi in less than $\frac{1}{10}$ second.

Pipe liner adhesion depends upon surface roughness of the two contacting metals. Should both surface finishes measure 15 microns or less, surface contact will be good, but 100% contact can never be achieved. This does not cause any particular inconvenience to high pressure gas systems since no heat transfer problems are experienced with ambient temperature systems. However, pumping cold fluids or hot gases and fluids might require better adhesion properties due to the thermal transfer characteristics of bimetallic piping. The most popular materials for lining are alloys of copper and nickel ranging from pure copper to pure nickel. These materials do not have all of the corrosion resistant properties desired in some cases, so that the austenitic steels and stainless steels are next in order of demand. Experimental work is being carried out with titanium, zirconium, and tantalum. Each metal holds considerable promise for future needs. The use of the least amount of expensive material practical is the second objective in saving money. Extremely thin liners cannot be used in many cases, and the cost of the lining material per foot is by no means proportional to its thickness. Pipe sizes of 2 to 6 inches, and linings of 0.035 inch now represent a combination of an economical and practical minimum offering adequate corrosion protection and sufficient mechanical

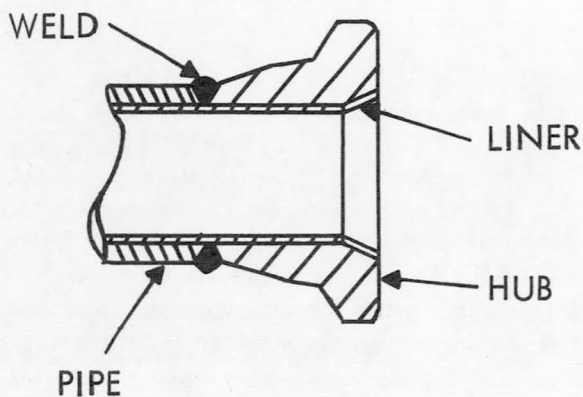


FIGURE 2.—Hub sealing surface.

TABLE I.—Levels of Permissible Contamination

(a) Cleanliness Requirements

Maximum particle population	Cleanliness levels					
	I	I	III	IV	V	VI
	Particle size (microns)					
No limit.....	0-20	0-20	0-50	0-50	0-100	0-175
40.....	21-40	21-45	36-60	51-140	101-280	175-540
10.....	-----	46-70	61-95	141-230	281-460	541-950
3.....	41-80	71-95	96-135	231-410	461-640	951-1270
2.....	-----	96-125	136-170	321-410	641-820	1271-1635
1.....	81-100	126-150	171-350	411-500	321-1000	1636-2000
0.....	101+	151+	351+	501+	1001+	2001+
Condensable hydrocarbon, ppm/weight.....	0.2	1.0	2.0	3.0	3.0	5.0
	Nonvolatile residue in grams/sq ft					
Surface area one square foot and over.....	0.001	0.001	0.001	0.002	0.002	0.003

(b) Fiber* Length and Population Limits

Maximum population	Fiber length limits by cleanliness level (microns)					
	I	II	III	IV	V	VI
No limit.....	0-20	0-20	0-35	0-50	0-100	0-175
10.....	21-40	21-150	36-350	51-500	101-1000	176-2000
1.....	41-100	151-300	351-700	501-1000	1001-2000	2001-4000
0.....	101+	301+	701+	1001+	2001+	4001+

*Fiber is defined as a particle having a length to width ratio of 10 to 1 or greater.

strength for most conditions. One problem area connected with lined pipe for high pressure gas transmission, is a change in direction of the system, and presently it is impractical to line an elbow or a tee effectively; therefore, a substitution for these fittings is made in 100% corrosion resistant steel. The use of bimetallic piping finds its greatest advantage when (a) pressures are high, (b) sizes are large, and (c) the alloy is not expensive.

Regarding small bore, high-pressure gas systems of tube sizes with an internal diameter of

less than $\frac{3}{4}$ inch, the standard AN- and MS-type flared tube fittings have been employed in high pressure gas systems, and if adequate protection is maintained for operating personnel, this type of joint offers many advantages in the 600 to 10 000 psi range. When factors of safety are added to this operating range, it becomes impractical for a design engineer to utilize flared tube fittings above 10 000 psi. Although they will withstand hydrostatic proof pressures, a gas failure cannot be tolerated when personnel have to be in the vicinity of the system. For

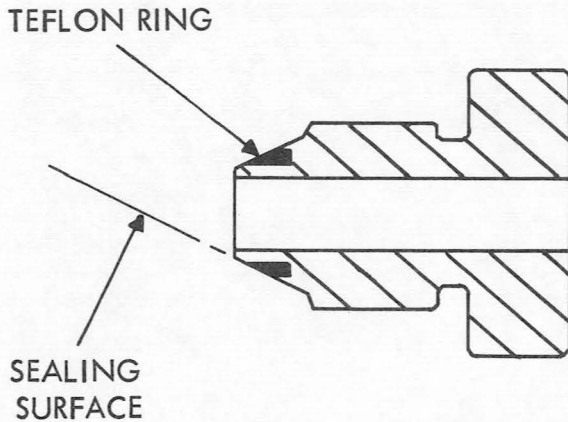


FIGURE 3.—Insertion of Teflon sealing ring in cone sealing ring.

these higher pressures, super-pressure tubing and fittings have been employed, and are commercially available in small bore sizes.

Between $\frac{1}{4}$ inch to 1 inch size stainless steel tubing in a hardened condition may be used in the 6000 to 10 000 psi operating range. However, flared tube fittings above $\frac{3}{8}$ inch require considerable manufacturing care to obtain the polish and the angle on the flares to obtain good sealing characteristics. For this reason, several companies have pioneered modifications to the standard flared tube fittings. The most successful of these modifications has been the insertion of a Teflon sealing ring in the cone sealing surface of the fitting (see fig. 3). This Teflon ring compresses when the system is torqued up, and as a consequence, seals the minor imperfections on the sealing surface, permitting an easier final assembly process. These fittings withstand much abuse and greatly alleviate service problems in the field. The larger flared tube fittings without Teflon seals take 4 hours per joint to seal effectively, even when meeting the precise manufacturing and assembly specifications. When inserts are employed, these problems are eliminated, permitting sealing of the fittings while meeting cleanliness requirements eliminating precise manufacturing tolerances and decreasing costs.

The rigid cleanliness requirements of present gas supply systems have resulted in the expenditure of much effort to obtain the optimum metal-

media combination. Table I is condensed from a Government cleaning specification and illustrates the levels of contamination permissible. An intensive program is now under way to evaluate the effects of velocity and temperature related to various cleaning chemicals on all sizes of pipe and tubing. The whole cleaning spectrum is being reanalyzed to establish the validity of flow rates and cleaning media as specified. Nitric acid, trichloroethylene, Freon, trisodium phosphate, and triton are among those chemicals being used for evaluation and comparison. These fluids will be checked for their detergent capacity, and samples will be analyzed for particle population, critical hydrocarbon saturation level, and nonvolatile residue.

Development of high pressure gas systems embraces all facets of the engineering arts; chemical, metallurgical, thermodynamics, structural, and test. Large volumes of ultraclean gas at very high pressures can be stored and distributed safely. The limitations imposed by economic and physical conditions have been defined within various operating spectra. Further definition is required and results are forthcoming. Many component manufacturers have developed highly reliable gas control equipment. However, the state-of-the-art has advanced so rapidly to keep abreast of requirements, that there is now a trend to standardize on proven design, increase reliability, and reinvestigate the basic concepts to enhance the economic and physical feasibility. Examples of high pressure gas systems are shown in figures 4 to 9.

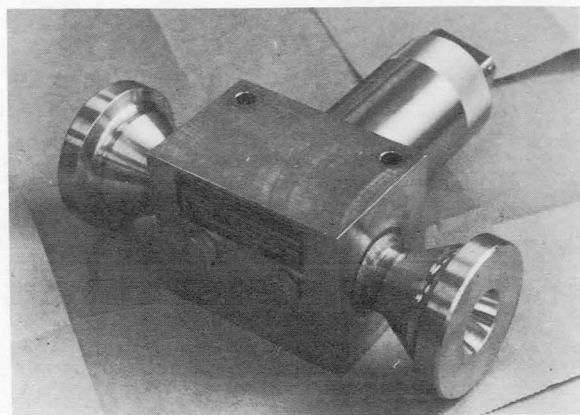


FIGURE 4.—6000 psi regulator.

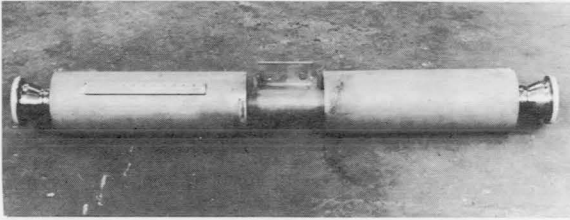


FIGURE 5.—6000 psi expansion joint.

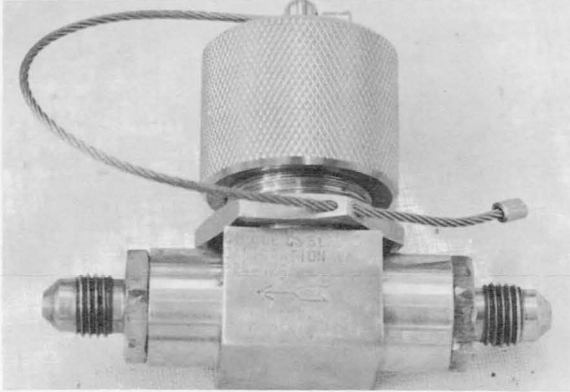


FIGURE 6.—Calibration valve.

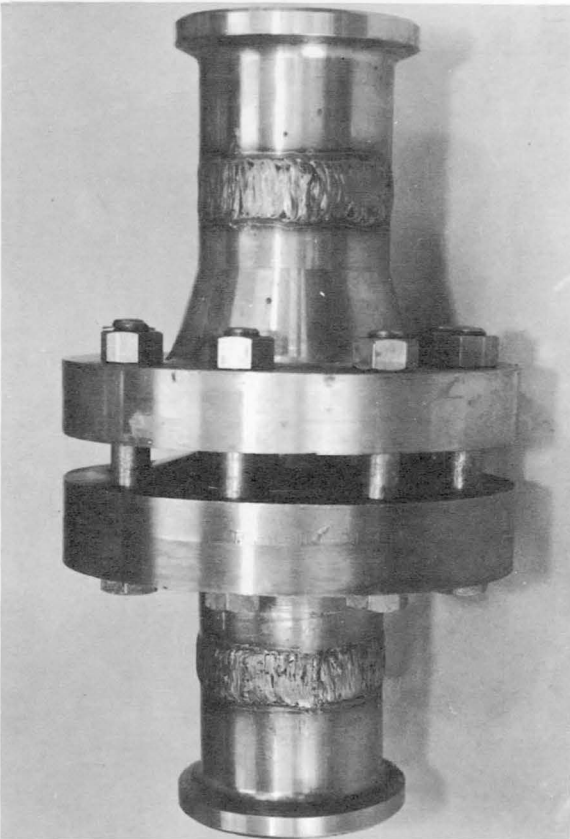


FIGURE 7.—6000 psi gimbal joint.

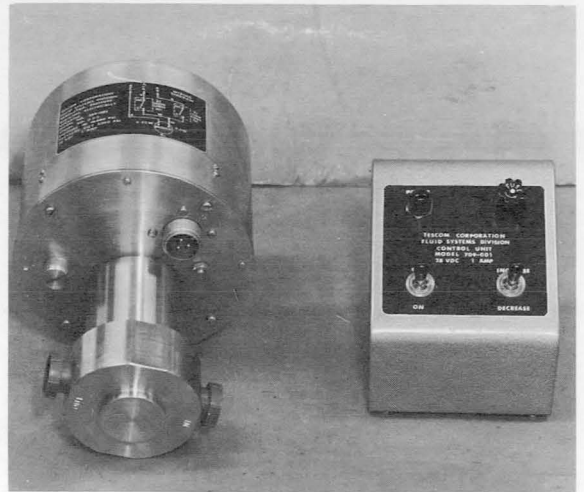


FIGURE 8.—10 000 psi remote regulator.

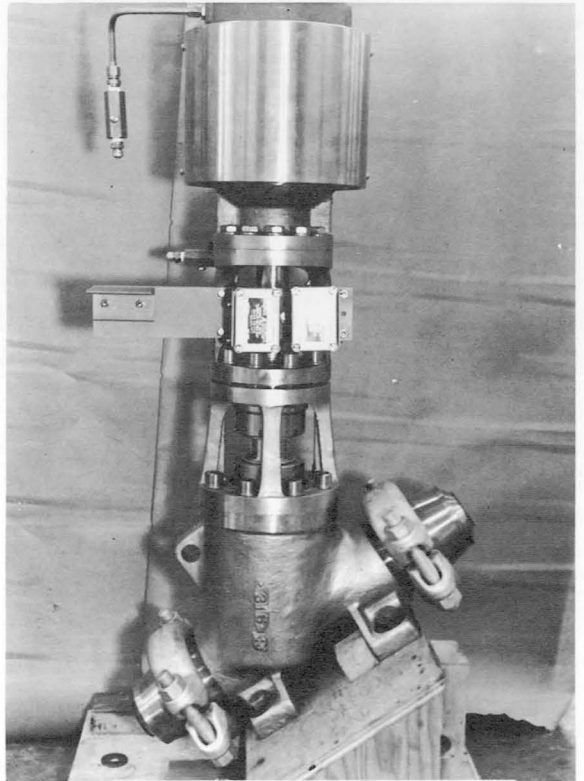


FIGURE 9.—6000-10 000 psi valve (3 in. bore).

3. Commercial Application of Rocket Engine Turbopump Technology

W. P. LUSCHER

Aerojet-General Corporation, Sacramento, California

This paper describes how commercial pump technology was modified for rocket engine application by trading long life for low weight. The component life of typical turbopump components is presented, and the modes of failure will be discussed. A comparison of the basic commercial and rocket engine pump requirements such as flow, pressure, etc. is made. It is concluded that rocket engine pump technology can be applied directly only if similar basic requirements exist in emergency or stand-by equipment.

The specific design requirements for rocket engine turbopumps are presented and the need for high speeds is explained by the weight-speed relationship and the optimum NPSH of the tank and pump system. The trend of required rocket engine pump discharge pressure and future operational requirements is predicted.

The need for inducers and boost pumps in rocket engines is explained, and the results of the flat-plate-inducer cavitation therein are briefly presented.

Design solutions and material selections for high-pressure pump housings, ultra-high tip speed impellers, and pump packaging are demonstrated.

As a typical example of utilizing rocket engine technology for commercial application, a helicopter stand-by engine is shown. This standby engine is designed from existing rocket engine components, using JATO rockets as the prime energy source.

Within the rocket engine system, the turbopump is one of the few components which was originally derived from commercial technology and adapted to the specific requirement of rocket engine propulsion. In order to reverse this situation and apply rocket engine technology to the commercial market, it is necessary to find applications where rocket technology opens new fields or allows existing jobs to be performed more profitably.

It was only a few years ago that the aircraft engine industry began to search for applications where its technology could be profitably applied in the commercial market. A short review of the aircraft industry's experience may be useful for demonstrating the difficulties the rocket engine industry faces in a similar task.

The aircraft engine is, for all practical purposes, a prime mover, and thus it is logical that the industry should have a close look for opportunities in this field. The two promising

areas appear to be in the fields of electrical power generation and pipeline pumping applications, and it is interesting to see why the aircraft engine is competitive in these fields.

The first costs of aircraft engine prime movers are competitive due to the large production quantities of these engines when compared to the diesel engine or commercial land gas turbine. In the past, commercial users of generating equipment always paid a premium for long life since they chiefly feared the long overhaul down-time and the resultant loss of revenue, as well as the long delivery of spare parts. The aircraft engine has now demonstrated a remarkable record of operating hours between overhaul which goes into tens of thousands of hours; due to its light weight it opened a new opportunity for overhaul procedures, as the overhaul is no longer done on site but rather at the engine manufacturer's plant. The prime movers have become so light that they can be trucked or

flown as a complete unit from the site to the plant where they are overhauled by experienced personnel. The overhaul plant is stocked with all spare parts, and thus overhaul time is dramatically reduced from weeks to hours.

Conditions are not so favorable to the rocket engine turbopump, since for commercial application the air-breathing prime mover will be preferred over the propellant-driven one, because of obvious operating cost reasons. Therefore, the application of the technology appears to be restricted to pump technology, and only in very special applications do rocket fuel driven prime movers warrant consideration. It is the purpose of this paper to review and discuss the major contributions which have been made in the development of the pump technology rather than list potential commercial applications.

The functions of the turbopump within the rocket engine system are defined in figure 1.

At the left-hand side, the conventional gas generator cycle is presented. At the right-hand side, the modern staged combustion cycle is presented. The turbopump consists of a turbine, which receives its energy from the gas generator, and a pump, which takes the propellant from the tank, compresses it, and delivers it to the thrust chamber. The turbopump and gas generator form a "bootstrap" system, and all power generated is stored in the propellant, and no direct output horsepower is obtained.

The staged combustion cycle is a direct analog to the jet engine cycle where the fuel pump has the identical function and the oxidizer pump replaces the air compressor of the jet engine cycle.

The environmental conditions in which these turbopumps operate are very severe, especially for cryogenic engines, since the pump will pass a medium at -420°F . next to a turbine of a $+1600^{\circ}\text{F}$. The flow medium is usually toxic

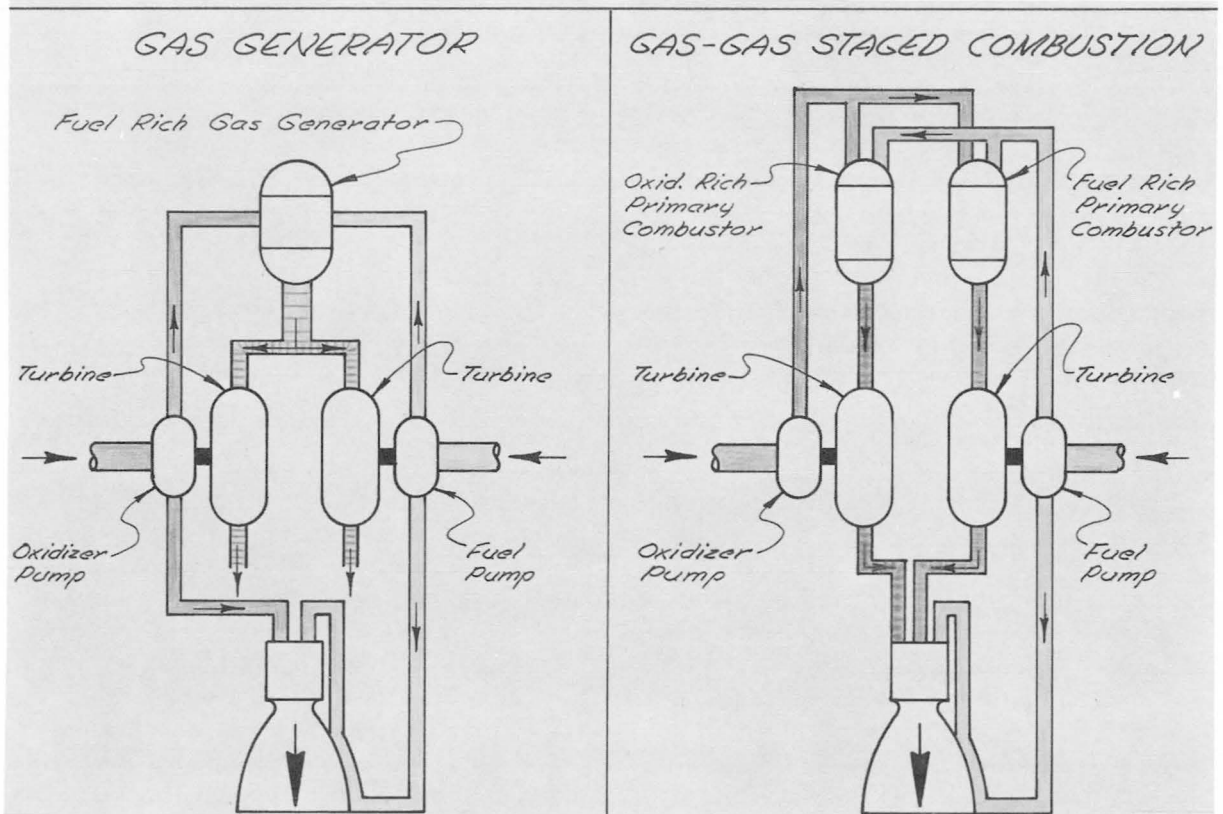


FIGURE 1.—Engine cycles.

and explosive, and no leakage can be tolerated. The materials used have to be compatible with the propellant used.

PUMP TECHNOLOGY

The rocket engine pump requirement is characterized by high pressures up to one order of magnitude above those found in the aircraft gas turbine technology. Extreme compactness and light weight are required to obtain the maximum payload. This in turn is achieved by designing for very high rotational speed and an extremely short life of several thousand seconds. Commercial applications with similar requirements are practically nonexistent, and the application of rocket engine technology is only considered practical through extensive modification, particularly in the areas of cost and operational life. The application which may have similar requirements is airborne emergency equipment for clearing operations after flood disaster or forest fire fighting equipment.

It is the purpose of this paper to present the severe requirements of the rocket engine turbopump technology and the solutions used for overcoming the problems, rather than to present readymade commercial applications of its technology. The rocket engine turbopump technology, however, is very valuable for commercial application since it demonstrates just how far the lightweight pump design can go and what price there is to pay on operational life. The rocket engine industry has built pumps in various sizes, and flow ranges vary from a small auxiliary unit of 60 gpm for the Titan II to a planned advanced large rocket engine fuel pump of 60 000 gpm (fig. 2). These pumps cover a large part of the spectrum of the commercial requirement with the possible exception of large hydroelectric applications (fig. 3).

The lightweight design is achieved by designing for as high an operational shaft speed as possible. The practical speed limit is set by the suction pressure of the pump which in turn is dictated by the tank pressure of the rocket engine. Since the tanks are of formidable size, it is of the utmost importance that

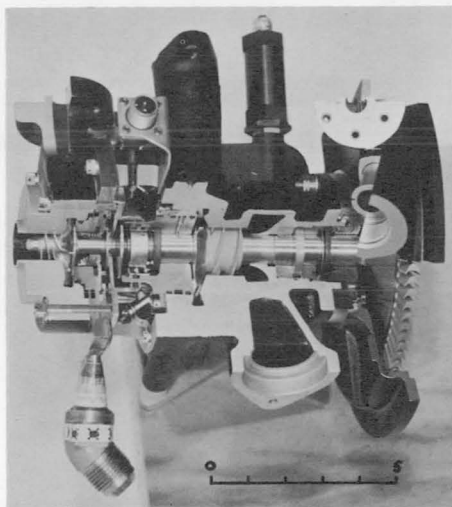
the tank walls be as thin as possible, which in turn, requires low tank pressures. The net positive suction pressure, which is defined as the pressure over the vapor pressure of the medium, is assumed as a compromise between the pump weight and the tank weight as shown in figure 4 for a large rocket engine.

The discharge pressure requirements have increased with time as shown in figure 5. The discharge pressure requirements are dictated by the engine cycle and are projected to go as high as 5000 psi for the modern staged-combustion cycles. This, in turn, will require an improvement of the state-of-the-art in the bearing, seal, thrust balancing, and housing design. A typical mechanical design concept of such a pump is shown in figure 6.

A comparison between achievable rocket turbopump efficiencies and commercial low-speed efficiencies (fig. 7) indicates that the rocket turbopump designer traded pump efficiency for low weight. The reduction in overall efficiency by about 10% is due to the low efficiencies of the inducers which are mandatory for high-suction specific speed pumps. The emphasis on light weight also indicates that rocket turbopumps should be designed for as high a specific speed as possible within the allowable constraints of suction pressure and mechanical limitations such as bearing DN, seal-rubbing velocities, and critical speed requirements. High pump efficiency was not of prime importance for the current gas-generator engine cycles. The coming of new high-pressure staged-combustion cycles, which bear great similarity to the aircraft jet engine cycle, places greater importance on pump efficiency.

The greatest differences between the rocket engine turbopumps and commercial pumps are the component life requirements. In order to illustrate this fact, the life of a typical TPA component and the mode of failures are discussed.

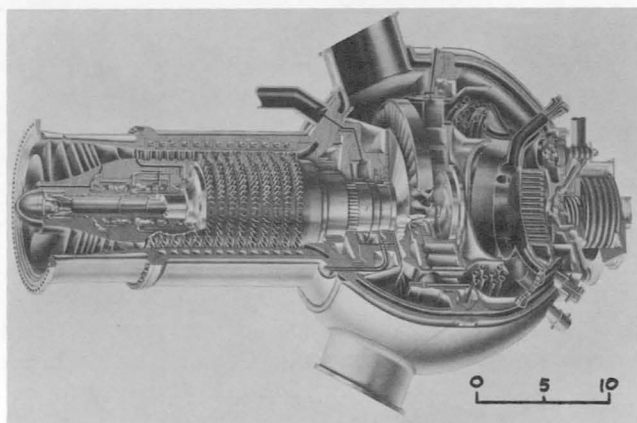
The impeller spends most of its operational life under severe cavitation conditions. The cavity is formed on the leading edge of the impeller and extends far back into the inducer passage where it finally collapses due to the increased pressure. The collapse of this cavi-



Rocket Engine Pumps

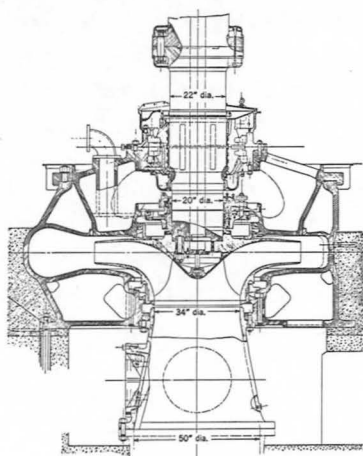
Auxiliary turbopump assembly
for Titan-1 rocket engine

	Propellants	
	LO ₂	RPI
Q, gpm	13.0	49.0
N, rpm	35 600	35 600
Δ H, ft	18 000	2902
Δ P, psi	875	983
S _{max}	23 000	26 000



Fuel turbopump assembly
for LH₂/LO₂ rocket engine

	LH ₂
Q, gpm	60 000
N, rpm	14 000
Δ H, ft	150 000
Δ P, psi	5 000
S _{max}	45 000



Commercial Pumps

Fractional to 1 000 000
gallons per minute for
large hydroelectric
applications

Worthington 42 inch pump:
90 000 gallons per minute at
444 ft head

FIGURE 2.—Comparison of rocket and commercial pumps by flowrate.

tation bubble is so violent that material particles of the blade are broken away. The resulting surface pitting will undermine the rigidity of the impeller in a very short time (fig. 8). The useful life of a typical impeller is approximately 3000 seconds. The collapse of the cavity also induces pressure oscillations on the impeller vane which has a tendency to fatigue the leading edge of the inducer.

In order to improve the life of the impeller to approximate commercial pump require-

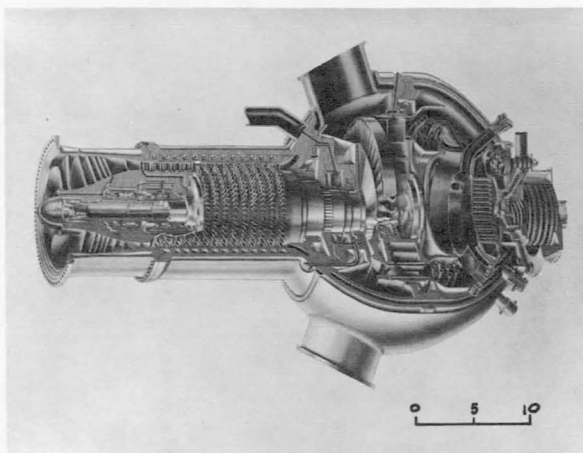
ments, it appears necessary to lower the suction specific speed and thus reduce both the cavitation damage and stress levels.

The machining of an impeller, illustrated in figure 8, is a formidable undertaking, and full use of tape-controlled machine tools is made. Computer programs based on the hydraulic requirements have been developed which design the impeller and result in automatic punching of the tape for machining. Thus no drawings are required, and human errors are reduced to a minimum. Turnaround time for experimental impeller design is greatly reduced. This technique is one area of rocket engine turbopump technology which is directly applicable to commercial pumps.

The impeller design and machining computer program receives as input in tabular form the vane angle distribution and vane thickness distortions for two stream tubes (tip and hub). In addition, vane cant, trim sweep, and leading-edge thickness is specified. The program (suction and pressure) produces surface coordinates θ , R, Z along the inspection stream tubes and trim coordinates θ , R, Z is printed form and/or magnetic tape. The results are then input to a cutter selection program where the maximum cutter on hand is selected for hogging out of passage, scrubbing of hub, and finishing of vane track. Once the cutter is selected coupled with cutter holder (omnimil), the cutter coordinates are computed (compatibility with cam machines also) and translated into axis position coordinates for the five axis numerical control omnimil. The above program is a continuous program; that is, design and machine axis coordinates are given in one pass on the IBM 7094 computer with a present estimated execution time of 15 minutes for all punched tapes (finishing, roughing, hub scrubbing, and trim for all passages of a main vane and two partial-vaned impellers).

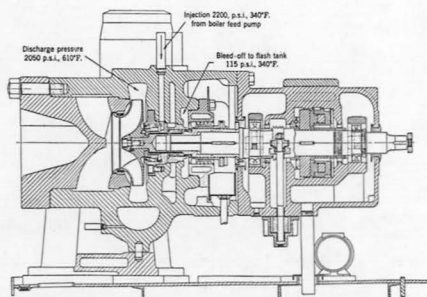
The pump housing (see fig. 8) is a rigid component necessitated by the high-pressure levels under which it operates. Most of the housings are castings of high-strength material and are known to have considerable residual stresses built in. Also, the separating force due to the pressure load is mostly taken by the splitter

Rocket Engine Pumps
A Few Pounds for Small Units to 8000
Pounds for High Thrust Engines



Fuel turbopump (wt = 8000 lb) for 1.5 million pound thrust liquid hydrogen & liquid oxygen rocket

Commercial Pumps
Fractional to Many Tons for Large Hydroelectric
Project Pumps



Pump design characteristics for commercial applications; weight is of little concern here

FIGURE 3.—Comparison of rocket and commercial pumps by weight.

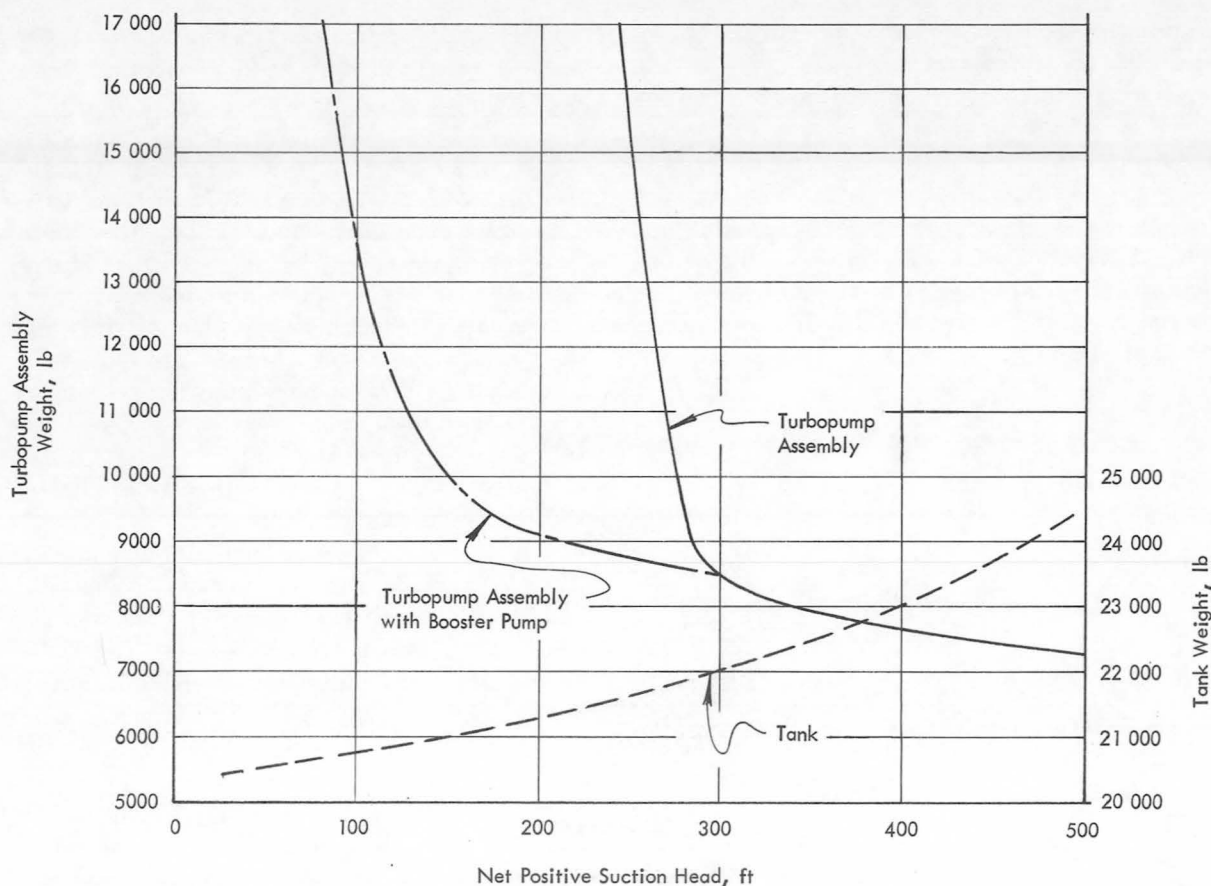


FIGURE 4.—Weight versus net positive suction head. Fuel pump for a 1.5 million pound thrust LO_2/LH_2 rocket engine.

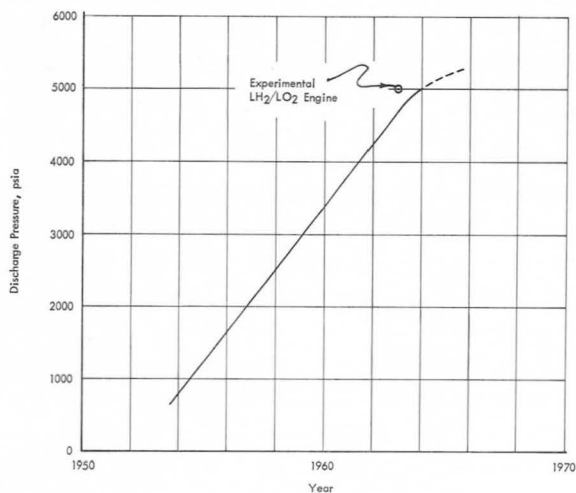


FIGURE 5.—Trend of future pump discharge pressures.

vanes which constitute the critical members of the pump housing. The splitters are also exposed to high frequency oscillating loads due to the aerodynamic forces, and thus the typical mode of failure is fatigue of the splitter vanes.

Improvements in housing life can be achieved by using fabrication methods rather than castings and thus reduce the problems of residual stress. Improved design of splitter vanes to provide greater flexibility and better load sharing will also improve housing life.

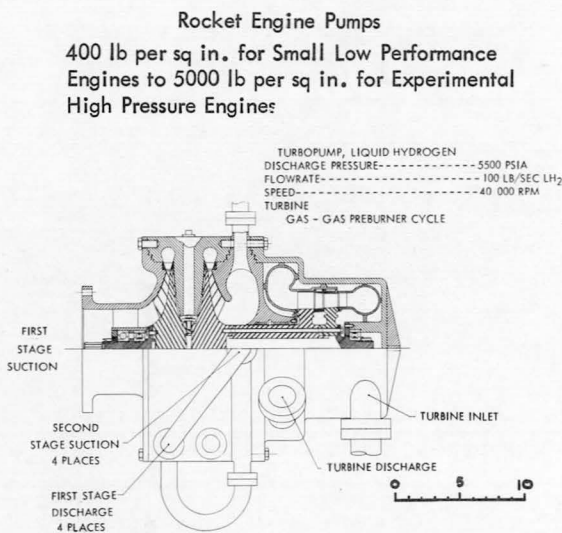
The life of rubbing seals is dependent on the particular application and on the surface velocity and the seal pressure requirements. Seals are the most troublesome components within the rocket engine turbopump. A list of typical seal materials used is shown in table I.

For lower pressure and temperature require-

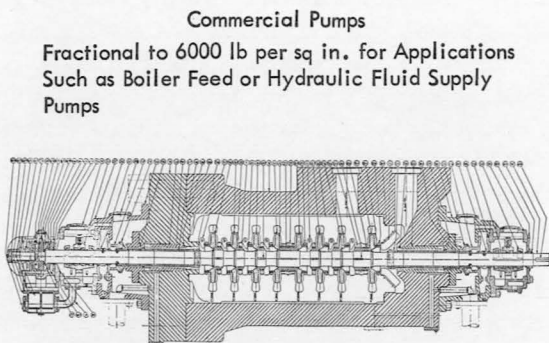
ments of the earlier rocket engine, commercially available bellows-type face seals and shaft-riding seals have been used satisfactorily due to the short life requirements (see fig. 9). With the steady increase of pump discharge pressure and increasing turbing temperatures, the requirements for shaft seals become more exacting. These trends require continued technology improvement in the areas of materials, lubrication, design, and new seal concepts and analysis, including vibration, heat transfer, and thermo-

dynamics. In figure 10, values of sealing pressure and sliding velocity for conventional bellows-type face seals are given. The solid line represents the values which are limited by current technology in the areas referred to above. This limit line has been improved by the aerospace industry in the past few years largely through the development of scuff-resistant tungsten carbide coatings, nonabrasive carbon rubbing materials, vibration dampeners for bellows, seal designs providing uniformity of cross section (distortion), and optimized face loads to prevent excessive heat generation. Methods of bonding and holding face carbons at both high and low temperatures have also been developed. Improved bellows designs for high pressures to minimize fatigue and other static seal concepts have been developed. Future advancements are expected to expand the usefulness of face seals to the material limit shown by the dashed line in figure 10. Values on this curve are achieved through improvements in design to minimize heat and are limited by the melting point or thermal stability of the rubbing materials.

Rotating shaft seals for applications exceeding the dashed line of figure 10 are currently under development. One promising type is a controlled-leakage seal which rides on a fluid



High pressure (500 psi) fuel turbopump for a 300 000 lb thrust liquid hydrogen/liquid oxygen rocket engine



Hydraulic fluid feed pump (1800 psi discharge or 5400 psi when in series operation)

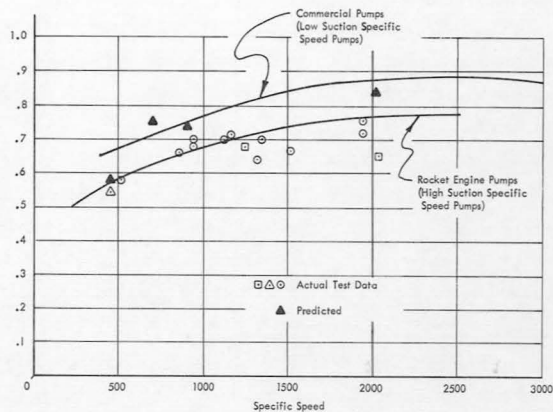


FIGURE 7.—Comparison of rocket and commercial pumps by efficiency.

FIGURE 6.—Comparison of rocket and commercial pumps by discharge pressure.

TABLE I.—*Seal Materials Developed for High Speed Dry Friction Conditions*

Life expectancy	Application	Materials
Face riding seals		
Greater than 30 minutes life at 125 ft/sec and 450 psi.	Running rings.....	Tungsten-chromium carbide (LW-5) coating on Inconel X. Stress relieved hard chrome plate on 304 stainless steel.
	Nose piece.....	Barium fluoride impregnated graphite (P03N). Barium fluoride impregnated into mixture of ground carbon and graphite (P5N).
Shaft riding seals		
Greater than 3 hours life at 325 ft/sec and 200 psi.	Sleeve.....	Tungsten-chromium carbide (LW-5) coating on A286 steel.
	Bearing.....	Mixture of ground carbon and graphite (CDJ83).

film. This is accomplished by a hydrostatic or hydrodynamic action between the seal faces. Theoretically, there is no limit to the life speed or pressure capacities of this type of seal. Metal parts also provide great resistance in a high temperature environment. The main disadvantage of this seal is that a controlled amount of leakage is required. This seal offers a solution in some high temperature nuclear applications.

Another type of noncontacting seal is the visco seal (fig. 11). This seal offers zero leakage and is particularly suited for sealing against a vacuum. In many applications, a buffing fluid compatible with the propellants which must not be mixed can be pumped against the propellants. This seal has successfully maintained virtually zero leakage of oil and mercury into a vacuum at speeds exceeding 10 000 rpm.

The earlier rocket engine turbopump used commercially available rolling contact oil bearings which created a design and operating problem due to the incompatibility of the lubricant with the propellants used. The aerospace industry therefore initiated a new technology of

propellant-cooled rolling contact bearings. The cryogenically cooled bearings have been very successful. Encouraged by these successes, operation of bearings in noncryogenic propellants is now being considered as a practical design solution.

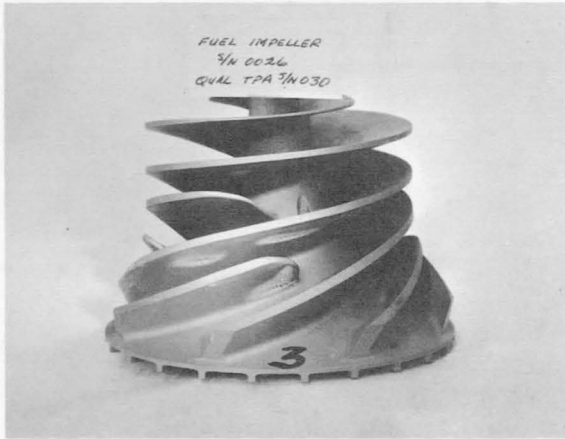
In conventional oil-lubricated bearings, friction, asperity welding, and wear are minimized by the presence of an oil film. In cryogenic bearings, friction, asperity welding, and wear are minimized by an abundance of cooling and the formation of surface films commonly known as dry film lubricants. In oxidizing environments the formation of surface oxides of the bearing material acts synergistically with most dry films. Molydisulfide in a sodium silicate binder sprayed on the races and cages has been successfully used for LH₂ service. Teflon initially burnished on the race surfaces and partially replenished by teflon-glass cage materials has been successfully used in LH₂ and lox service.

Aerojet-General has found that the cooling of the rolling elements is the most important design criteria, provided the clearances are cor-

rect. To this end, special low profile cages (fig. 12) are used which allow maximum exposure of rolling element surfaces to the cryogenic fluid, and also allow maximum cooling at the rolling element—cage pocket sliding surfaces.

The use of these low profile cages has increased bearing life threefold or more.

The ultimate mode of surface failure of properly designed and installed cryogenic bearings relating to rolling contact is not clearly



Pump Housing
Life:
More Than 3000 Sec

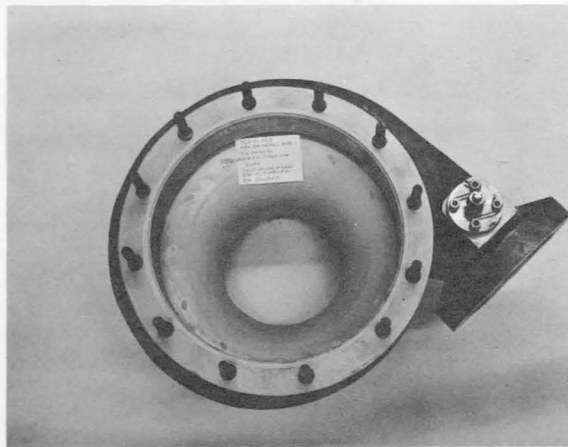
Typical Mode of Failure:
Fatigue of Splitters Due
To Vibration



Pump Seals

Life:
Hot Gas Exposure - 600 Sec
Propellant Exposure - 3000 Sec

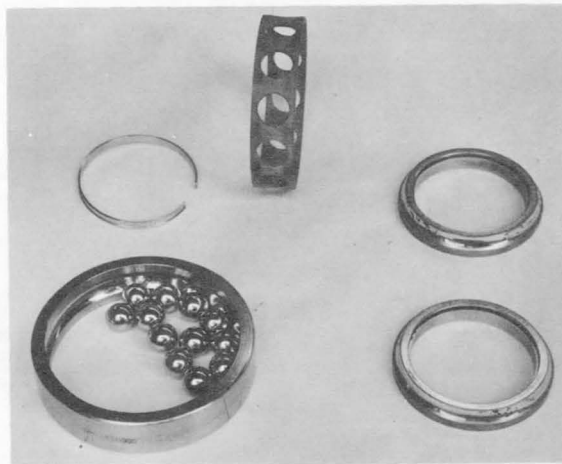
Typical Mode of Failure:
Wear and Excessive Friction
Causes Thermal Distortion



Pump Impeller

Life:
Approximately 3000 Sec

Typical Mode of Failure:
Cavitation Damage



Pump Bearings
(Oil Lubricated)

Life: 6000 Sec
Typical Mode of Failure: Cage Disintegration

FIGURE 8.—Typical turbopump component life.

FIGURE 9.—Typical turbopump component life.

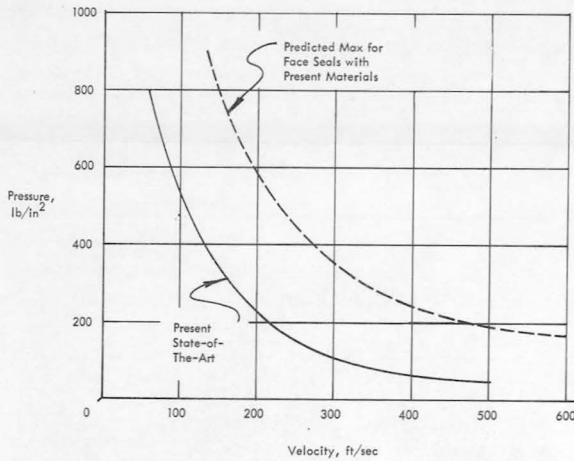


FIGURE 10.—Predicted face seal P versus V values.

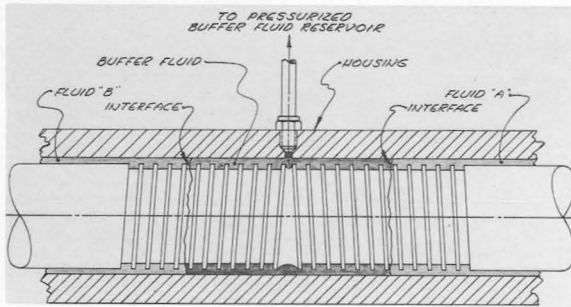


FIGURE 11.—Buffered visco-seal system.

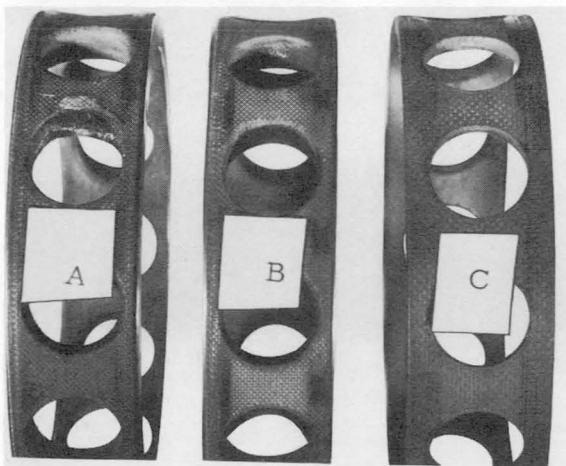


FIGURE 12.—Low profile cages.

defined. Failure can be caused by mechanical fatigue or thermal effects. Thermal effects include: minute surface annealing, minute asperity welding, or thermal fatigue (fig. 13). When surface temperature cycles and gradients are considered, thermal fatigue appears to be very significant. Future long duration (10 to 100 hours) testing of a large number of bearings will be required to define the mode of fail-

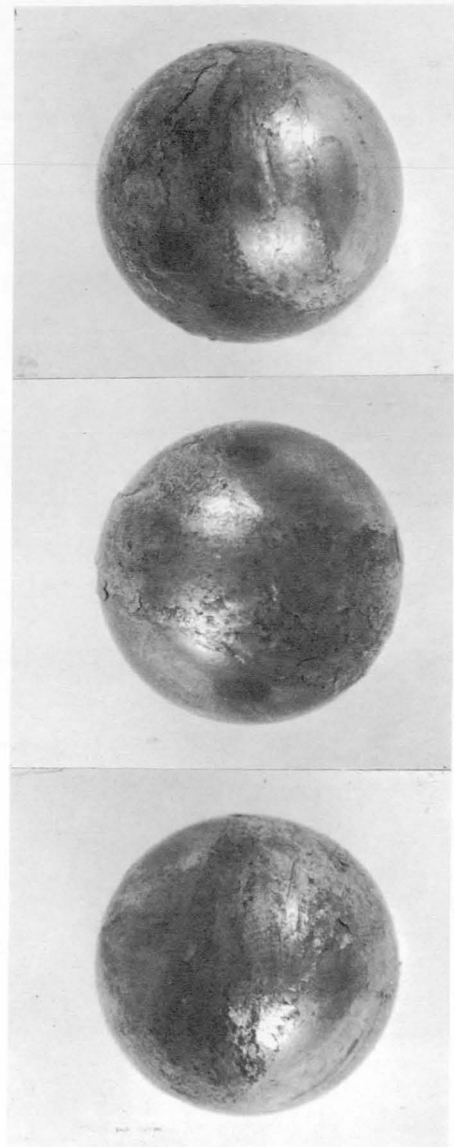


FIGURE 13.—Failure effects.

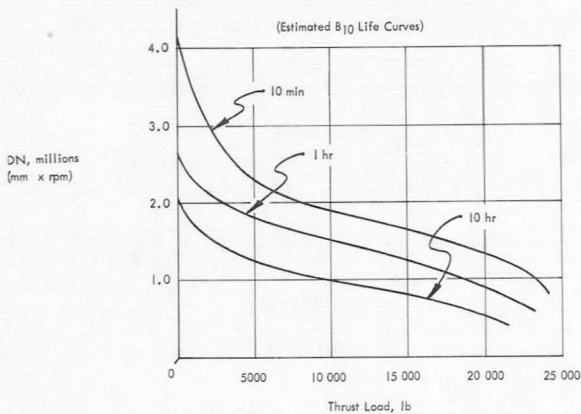


FIGURE 14.—Typical turbopump component. Life of LH_2 cooled rolling contact bearings (optimum selection of bearing size for required thrust).

ure related to rolling contact conditions. The life expectancy of rolling contact bearings as a function of DN and load is shown in figure 14.

In contrast to ultimate modes of failure relating to rolling contact conditions, problems of sliding friction and wear are associated with intermediate modes of failure. These intermediate modes are: loss of clearance due to cage wear debris, excessive roller skewing, and roller skidding due to rapid acceleration (fig. 15). Cage wear debris problems are solved by the selection of cage materials which provide both low friction and low wear. In cases where cage wear debris are used to provide replenishment

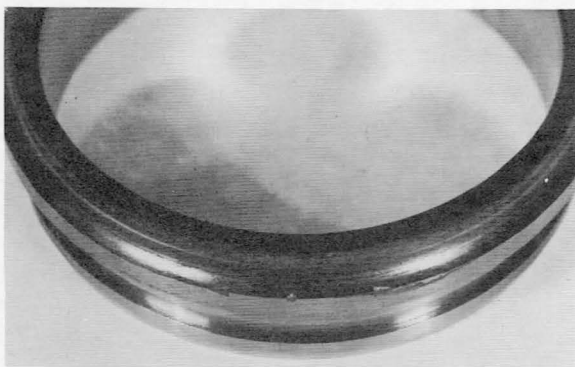


FIGURE 15.—Intermediate modes of failure.

of the dry film lubricant (such as Teflon-containing materials), an optimum wear balance must be determined between adequate lubrication and excessive deposition.

Development programs have passed through successful phases of feasibility testing under a wide range of operating conditions. Life expectancies of several hours are reasonable for most applications before failures due to sliding friction occur.

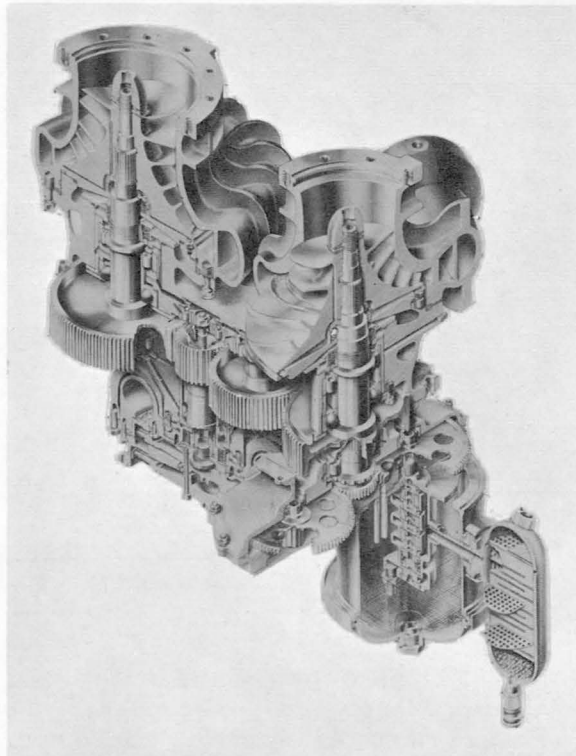


FIGURE 16.—High performance oil lubricated gearbox. Turbine: power=5141 hp, speed=2373 rpm; fuel pump: power=2599 hp, speed=9137 rpm; oxidizer pump: power=2464 hp, speed=8315 rpm.

GEARS

In the earlier versions of rocket engines, it was decided to couple the fuel and oxidizer pump mechanically in order to simplify the control system problem. This was achieved by means of a gear train as shown in figure 16. These gears are oil lubricated and are of ex-

TABLE II.—*Pertinent Gear Box Specification*

	Model 87	Model 91
Horsepower (nominal).....	5141	2300
Input speed, rpm.....	23 873	23 850
Output speed, rpm.....	8315	8480
	9137	23 850
Acceleration, spec to full rpm.....	0. 8/1. 2	0. 8/1. 2
Gear pitchline velocity, fpm.....	17 600	17 200
Tooth loading:		
Compressive stress, psi.....	165 000	157 000
Bending stress, psi.....	87 000	82 000
PVT (scoring factor).....	2 900 000	2 700 000
Required total life, sec.....	3370	4280
Duration, sec.....	198	252
G loading:		
Acceleration.....	5	9
Vibration.....	-----	-----
Oil flow, gpm.....	3. 3	1. 2
Heat exchanger, btu/sec.....	-----	-----
Bulk oil temp., °F.....	250	270
Lubricant MIL-L-7808 (capacity, qt).....	4	2. 1
Weight-dry, lb.....	228	113

treme light weight for the large amount of horsepower transmitted and have unusual operating requirements. The gear box specifications are shown in table II.

These gear trains have to withstand an engine start where the engine is accelerated to full speed and power in a fraction of a second. The mission is so short that the gearbox does not reach a temperature equilibrium and thus has to withstand transient temperature distortions and stresses. Since the gearbox has to be able to operate in vacuum, it is completely sealed and pressurized. The cooling of the gear teeth is achieved by oil jets at the out-of-mesh side of the teeth. Another unusual requirement of this box is the relatively long storage time, and thus the lubricants used have to be compatible with gearbox parts to prevent corrosion during storage.

Corrosion resistant materials are used where gearbox parts come into direct contact with the propellants. AM350 is used for both output shafts. The turbine shaft coupling is made from 17-4 Ph. Interior gearbox parts are fabricated from more conventional materials such

as 52100 bearings, 4620 and 9310 gears, and so forth.

The lubricant used in this gearbox has to meet specific requirements. The viscosity has to be very low to prevent excessive heat generation. The lubricant must prevent air entrainment to carry away the heat from the heavily loaded gears and bearings. The lubricant should be compatible with the propellants and prevent the formation of harmful solids which tend to form in the seals at the propellant interface.

To meet these requirements, a special lubricant has been studied. This study resulted in the formulation of an oil containing additives which are of interest in commercial applications that require a low-viscosity, high-load, high-speed lubricant. Experimental loads carrying phosphorous additives have been synthesized which are active enough to provide a high-load capacity in low-viscosity (low-load capacity) base oils. These additives offer promise in high-speed commercial gearboxes and for gearboxes of commercial aircraft engines. Previous to this development a high concentration of

less active additives has been used which cause cleanliness problems in high-temperature areas.

A new soluble polymeric additive which replaces previously dispersed silicons has proven effective. In many commercial high-speed boxes, lack of cooling due to air entrainment is a primary factor governing premature wear and failure.

INDUCERS

In the state-of-the-art of hydraulic design, the aerospace industry has made its contribution mainly in the field of inducer design. Inducers were developed to operate at very low suction pressure and high speed. Since both of these parameters affect the cavitation performance, they are combined in a characteristic suction—specific speed number which is defined as:

$$S = \frac{n\sqrt{Q}}{\text{NPSH}^{3/4}}$$

when n is measured in rpm, Q in gpm, and NPSH in ft. Under cavitation operation, a vapor bubble is formed on the leading edge of the inducer and extends far back into the flow passage. If cavitation reaches such a level that the passages are about half filled with vapor, the pump head breaks down completely.

It is therefore the objective of the inducer design to keep the thickness of the cavity to a minimum, and this is done by keeping the blade thickness thinner than the thickness of the vapor bubble. Extensive efforts (ref. 1) have been made to define the shape and the thickness of the bubble, analytically (fig. 17). It was found that the parameters affecting the cavity shape the most are the blade angles, the fluid angle, and the NPSH. As a rule of thumb, it can be said that the ratio of fluid angle to blade angle should be 1:2.

Based on the cavity theory, the leading edges of these inducers are very thin and structurally weak. In order to take the heavy pressure loadings, the leading edge is trimmed back so that the tip leading edge is located where the hub has the full vane thickness. The fairing of the inducer is usually linear to simplify the fabrication (fig. 17).

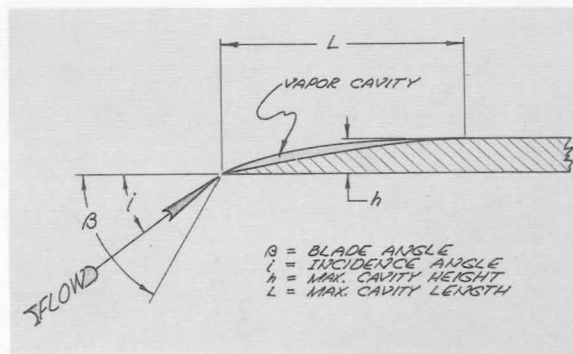


FIGURE 17.—Flat plate inducer blade design.

The blade angle setting of the inducer is dependent on the suction specific speed (fig. 18) and is decreasing with S . The optimizing angles in this figure are such that the static pressure difference to the vapor pressure is optimum. For very high suction specific speeds, the eye diameter is only a function of NPSH.

In figure 18 the design solutions for the various specific speed regions are presented up to 7000 S ; for the low specific speed region, no inducer is needed. The region between 7000 to 50 000 is the region where most rocket engine turbopumps operate and requires an inducer which can be either integrated with the main impeller or separate.

For extreme high suction specific speeds, the pump needs a second inducer which operates at low speed. This second inducer can be driven hydraulically by tapping off from the main pump stage or by gear train if the pumping medium permits.

TURBOROCKET PUMP TECHNOLOGY FOR PRIME MOVERS

As prime movers, for commercial application, it appears at a first glance that the turbopump technology has no chance to compete against the air-breathing engines, in particular, against the aircraft turbopump engine which uses relatively inexpensive fuel and readily available air oxygen and has a long life capability.

However, there appears to be a special application such as short duration emergency power generators where light weight is a

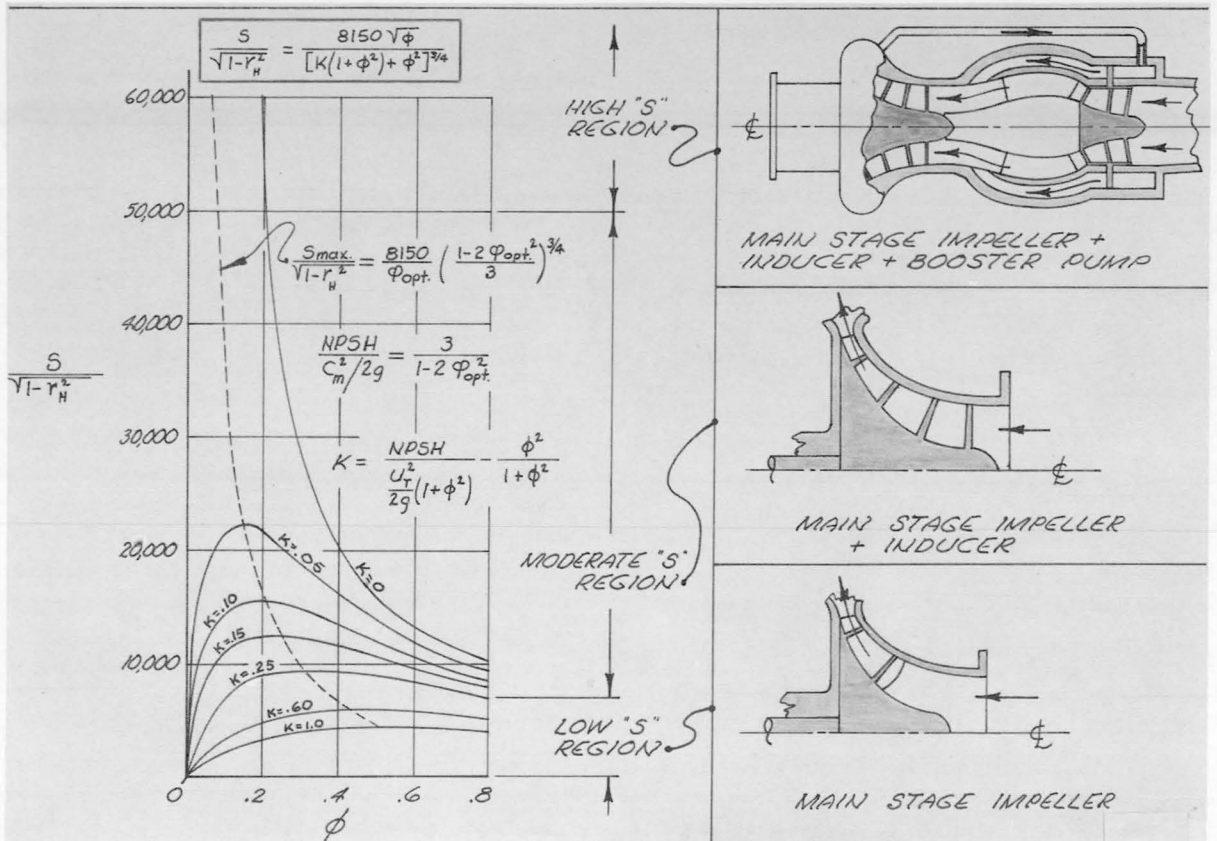


FIGURE 18.—Pump cavitation performance.

necessity and short operational life does not matter. Such a special requirement is believed to exist in an emergency standby unit for helicopters.

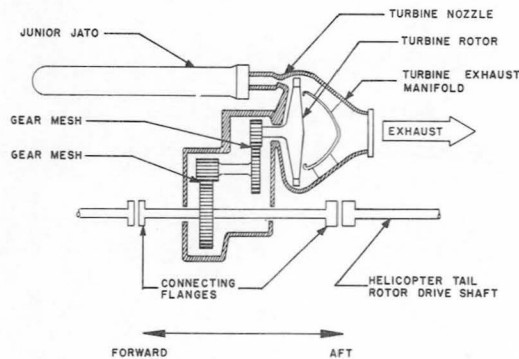


FIGURE 19.—Helicopter standby engine schematic.

The power pack, which is described in figure 19, utilizes a solid propellant power source which is an adaptation of the Aerojet Model 15NS-250 aircraft rocket engine developed as an assist-takoff engine for aircraft of less than 10 000 lb gross weight. This rocket unit, widely known as the Junior JATO, is ideal for use with a turbine drive to provide sufficient power for a helicopter standby engine. It is inexpensive, readily available, and reliable; it provides power instantly and is completely self-sufficient; it is one of only two rocket engines having FAA certification, both of which are manufactured by Aerojet-General Corporation. The 15NS-250 rocket engine is safe to handle, easy to replace, and has a history of increasing payload and safety on many fixed-wing aircraft (fig. 20).

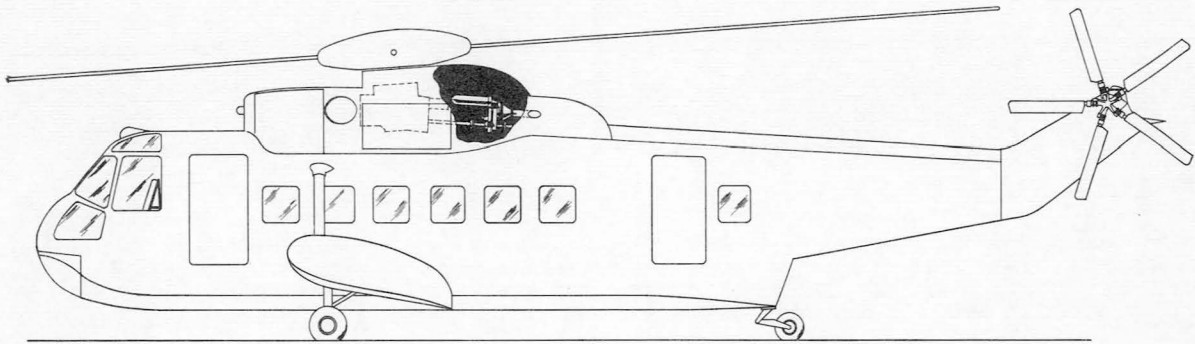


FIGURE 20.—Helicopter standby engine installation.

From one to six 15NS-250 units may be mounted to the standby engine. Helicopter

TABLE III.—Helicopter Standby Engine—
Weight Summary

[15NS-250 weight, 42 lb; Support structure weight per 15NS-250 unit, 2 lb.]

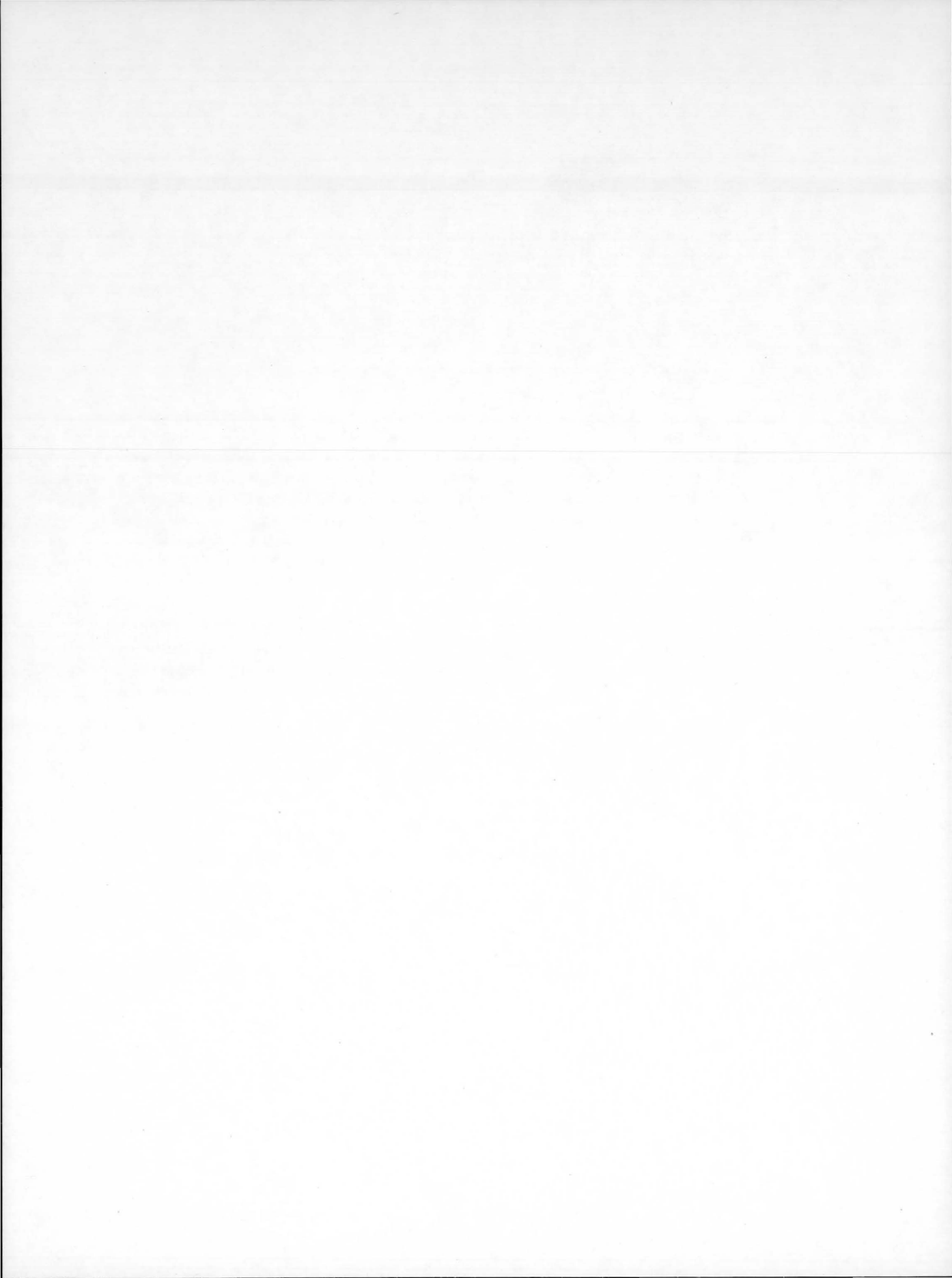
Number of Model 15NS-250 units	Direct drive standby engine weight, lb	Clutch drive standby engine weight, lb
0	95	117
1	139	161
2	183	205
3	227	249
4	271	293
5	315	337
6	359	381

standby engine weight versus number of rocket units is shown in table III. The rocket units may be fired singly, giving a nominal 500 shaft horsepower for 15 seconds per firing; or they may be fired in pairs, giving 1000 shaft horsepower for 15 seconds per firing.

The helicopter standby engine employs a rotating assembly because it is much more efficient to obtain thrust from rotor shaft power than from rocket jet power. For example, the 15NS-250 unit, which produces 250 lb of thrust as a rocket engine, will produce 5000 lb of hovering thrust when its jet power is converted to shaft power by a turbine and transmitted through gearing to the helicopter rotor shaft.

REFERENCE

1. STRIPLING, L. B.; and ACOSTA, A. J.: Cavitation in Turbopumps. Pt. I. ASME paper 61-WA-112.



4. Monitoring of Impurities in Fluids and Gases

W. A. RIEHL

George C. Marshall Space Flight Center, NASA

Aerospace requirements have engendered the need for instruments for automatic determination of trace impurities in liquid and gaseous systems by in-line continuous operation. These include devices for the automatic sizing and counting of minute particles (below 0.1 mm) in closed liquid and gaseous systems, and the automatic determination of nonvolatile residue in solvents and traces of hydrocarbons dissolved or dispersed in gaseous systems.

The principle of operation, and characteristics of instruments, as well as results of experimental testing, are briefly described. Potential industrial applications are also suggested.

The development of aerospace systems has spawned numerous requirements for monitoring impurities in fluids and gases. Generally, these may be classed as methods for monitoring both solid or particulate impurities in liquids and gases, and soluble or dissolved impurities in solvents and gases.

SOLID IMPURITIES IN LIQUIDS

Because of the extremely high fuel consumption rates in space flight, practically no drift can be tolerated in the trajectory. For example, in the Saturn V vehicle, a drift off-course and correction in less than one second would unnecessarily consume tons of propellants and could result in loss of the mission. All of the Saturn vehicles (and currently all large space craft) are guided by swiveling or gimbaling of the engines. This swiveling is accomplished by use of hydraulic fluid power systems. To provide ultra-high speed of response and extremely low-drift, the valves controlling the fluid flow must have extremely close tolerances. Minute particles entrained in the hydraulic fluid may cause blocking of small orifices, drag in response, and other undesirable results such as a "hard-over freeze." Therefore, it is essential to provide extremely clean fluid.

Until the aerospace industry developed, it was common to specify that liquids, gages, hardware, and other systems must be "absolutely clean." This was usually interpreted to infer freedom from spurious particles when viewed with the naked eye.

Because it was found that such "absolutely clean" systems still produced malfunctions in aerospace hydraulic systems, microscopic examination for foreign particles was undertaken. Observation of myriads of particles too small and/or too few for resolution by the human eye led to the recognition that no surfaces are "absolutely clean". Absolute cleanliness is similar to absolute vacuum; it can be approached but never reached. Thus, cleanliness must be defined in quantitative terms; that is, the number of particles in various size ranges per unit volume or surface.

The need for quantitative definition of cleanliness for fluids and surfaces has resulted in rapid advances in methods for in-line monitoring of particulate contamination in gaseous and liquid systems. Initially, microscopic methods previously developed for monitoring air pollution were adapted to aerospace needs, and acceptable quantitative levels of contamination were established. This method was time consuming and tedious, frequently curtailing pro-

duction or fabrication schedules. Furthermore, it was necessary to extract a sample of the fluid from the system. Thus, the need arose for an instrument capable of automatically sizing and counting particles in a closed system; i.e., in-line operation.

Three instruments have recently become available for continuous in-line monitoring of particulate contamination in liquid systems; one is based on ultrasonic methods and two on light phenomena.

In its simplest form, any automatic particle counter consists of two systems: (1) an aerosol or fluid-handling system to transport the gas or liquid sample with its load of particulate material through the counter, and (2) a counting system to generate and record signals which must equal the number of particles and must be proportional to some function of their size.

The ultrasonic particle counter (fig. 1), designed and fabricated by the Sperry Corporation under contract to this center, is based on the phenomenon that solid particles in a fluid will reflect the ultrasonic beam back to the source, the amplitude of the reflection being dependent upon the size of the particle (fig. 2). Experimental tests by this center have shown that once the instrument is calibrated, results can be correlated with those obtained with the standard filtration and microscopic counting procedure. The instrument provides a single output signal, if desired, which is proportional to the contamination and can be fed into a strip-chart recorder. However, there are several drawbacks to this instrument. Skilled effort is required to calibrate and maintain the electronic components, and reliable quantitative counts can be made only with particles over 25 microns in size. The results are also non-linearly related to the microscopic counts.

To utilize light scattering phenomenon for particle monitoring, the sample is passed through the counting cell, which is illuminated by a beam of light. Particulate material in the sample medium scatters the light in all directions. By mounting a photomultiplier tube at 90° to the incident beam of light and connecting the output to appropriate electronic circuitry, a series of pulses is obtained. These

pulses are discriminated into discrete categories corresponding to selected particle size ranges and tallied by means of electronic counters. Tests made at this center on one such instrument gave generally unsatisfactory results in that the automatic counts bore little relation to counts obtained microscopically. Further development is needed before data obtained from instruments based on this principle can be accepted as reliable.

In response to aerospace needs, a small company on the west coast designed on its own initiative, and put into production a line of automatic particle monitors based on the photo extinction, or light blocking principle. In operation, the sample of fluid passes through a counting cell in which the flow characteristics are such that each solid particle passes the window in single file. Light is collimated into a parallel beam and directed through the fluid stream so as to impinge on a photo-tube on the opposite side. Whenever a particle in the fluid stream passes the window, a portion of the light beam is interrupted. This creates a change in the output signal from the photo-tube which is proportional to the size of the particle. The change in signal is amplified and sent to counter circuits that have been adjusted to vari-

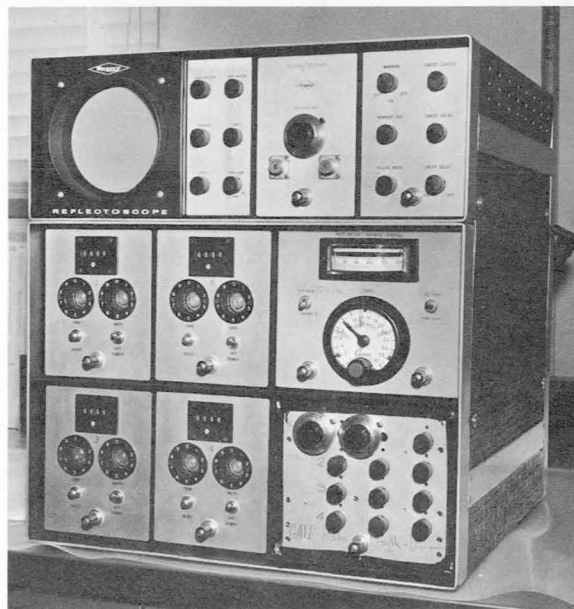


FIGURE 1.—Ultrasonic particle counter.

ous sensitivities for simultaneous counting of individual size ranges. Then, the particle is tallied according to its size. After passing through the cell, the sample is collected in a graduated container so that the results can be recorded as number of particles per given volume of fluid. Alternately, the sample can be returned to the hydraulic system by means of a small pump which is incorporated in the counter. Tests at this center have demonstrated that this counter gives results which are substantially identical to those obtained microscopically for both in-line and laboratory sampling operations.

SOLID IMPURITIES IN GASES

The heart of the guidance system for all Saturn space vehicles consists of a gyroscope. To provide as nearly frictionless rotation as possible, it is supported by air-lubricated bearings; these bearings are machined to within several hundred-thousandths of an inch and separated by only seven ten-thousandths of an inch (17 microns). Low pressure air (approximately 2–10 psi), or nitrogen, flows through this channel to float the rotating shaft. Naturally, the slightest particulate contamination in the air entering the bearing could cause excessive friction, wear, freezing, or at least unequal support. Therefore, it is essential to provide air as free of particulate contamination as possible.

In addition, as the requirements of space vehicle and missile hardware systems became more sophisticated, and subsequently required improved monitoring equipment for the various systems, another area of considerable importance has evolved. In this connection, the more

stringent reliability requirements have necessitated more stringent manufacturing and assembly operations. Consequently, new concepts and apparatus have been developed to permit manufacture and assembly of components in environments sufficiently free of solid impurities so that these operations are no longer appreciably detrimental to the overall problem of furnishing a clean component for the critical system. The air filters for the aid conditioning systems and methods of construction necessary to achieve the required clean environmental areas are sufficient to preclude the major source of solid impurities in these operations. These environmental areas are so designed that solid impurities, including the smallest of bacteria (0.3 micron), are also removed in the air handling system.

Initial efforts to determine cleanliness in pneumatic systems consisted of adapting the microscopic method for the size ranges and contamination levels of interest. This undertaking was only partly successful since the extreme cleanliness requirements for such systems make it desirable to monitor particles smaller than those which can be optically resolved by common microscopic methods. This situation has resulted in considerable emphasis being placed on development of an automatic particle counter for gaseous systems and, particularly, on a counter suitable for in-line operation.

The most widely publicized commercial instrument for this application uses the light-scattering principle and is similar to the light-scattering instrument referred to previously for liquid systems. In this instrument, the gas sample passes through the counting cell which is illuminated by a beam of light; particulate material in the gas stream scatters the light, which is monitored by a photomultiplier tube. The resulting series of pulses is discriminated into discrete categories which correspond to selected particle size ranges and are tallied by means of electronic counters. Tests at this center have indicated that this counter is generally unsatisfactory for the most aerospace applications. The particle counts indicated on the instrument are not normally proportional to those obtained microscopically.

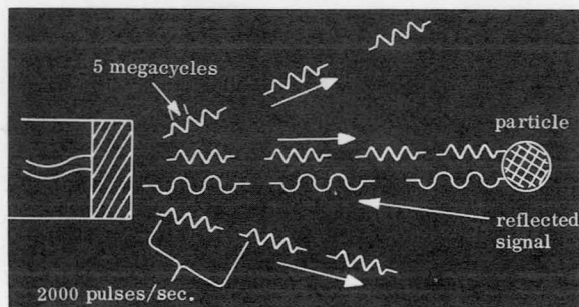


FIGURE 2.—Principle of ultrasonic detection.

INDUSTRIAL APPLICATIONS

Each of the automatic particle counters may have certain advantages over the others due to greater flexibility or counting accuracy for specific applications. Although it has not been developed for particulate monitoring in gases at this time, the instrument based on detection by light blocking appears to have the broader capability. The calibration of this system can be accomplished for all liquid monitoring, if light can be transmitted through the fluid, and if the physical characteristics of the fluids remain stable when used with the counter's optical system. Some fluids which probably cannot be analyzed with any of the currently available counters include cryogenics and certain corrosive fluids. Current and potential uses of automatic particle counters for liquids include determination of the size and distribution of abrasives, catalysts, metals, minerals, phosphors, pigments, cement, ceramics, etc., by dispersion in an inert carrier fluid, as well as determination of the inherent cleanliness of fuels, chemical solutions, and other liquids.

Automatic particle counters for gaseous systems should be valuable, not only for monitoring clean production environment, but also for investigation of air pollution or dust areas and monitoring radioactive materials and sterile or medically clean areas.

SOLUBLE CONTAMINATION IN SOLVENTS

Liquid oxygen is the most widely used oxidizer in space vehicles; over 2000 tons will be used in the first three stages of the Saturn V. Pure liquid oxygen (LOX) is stable and not subject to detonation, but mixtures of LOX with most organic materials will explode under conditions of impact. Aluminum valves and lines transporting LOX have been observed to explode and burn like wicks, with the only explanation being greasy fingerprints left during assembly. During the testing of spacecraft and ground support equipment, explosions which jeopardized the whole system have resulted from contact between LOX and incompatible lubricants.

For these reasons, exceptional measures are taken to insure removal of incompatible organic

materials and traces of grease from all LOX systems. After scrupulous cleaning and degreasing, tanks and other components are inspected by a final rinse with highly purified trichloroethylene or Freon, and the rinsings are examined for any traces of particulate and dissolved contamination. In the standard laboratory method of analysis, particulate contamination is removed by filtration, and the residual solvent is evaporated just to dryness and then weighed to determine the nonvolatile soluble residue (NVR). Because this method is tedious and time consuming, an instrument has been developed for automatic determination of NVR in solvents. The instrument is based upon light-scattering characteristics of an aerosol spray of the solvent and was designed and built by the IIT Research Institute under contract to this center (fig. 3). A sample of solvent is continuously fed to a nebulizer, where it is atomized with a large volume of air to produce micron-sized liquid particles of solvent and soluble contaminant. The large volume of air evaporates the volatile solvent, and the NVR is left behind as an aerosol in trichloroethylene vapor and air. The aerosol size is dependent on the contaminant level. The aerosol, surrounded by a clean air sheath, is fed to a photometer, and the scattered light from a defined field of view is measured. The amount of scattered light is a measure of the contamination level.

The NVR nephelometer is designed to function in two modes of operation: the comparison

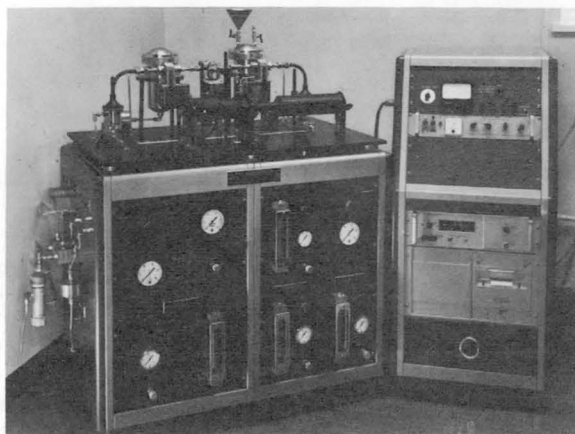


FIGURE 3.—NVR nephelometer (monitoring of oil in solvents).

test and the relative test. The comparison test operation uses two nebulizers; one uses a contaminated solvent and the other a pure or reference solvent. The photometer observes the aerosols from both nebulizers for a fixed period of time, and subsequently provides visual display of signal difference, which is printed out in digital form. The relative cleanliness level is determined by comparison of differences from the noncontaminated (or reference solvent) and the contaminated solvent.

The relative test operation uses one nebulizer. The photometer observes the aerosol for the same fixed period of time as in the comparison tests, stores the information, gives visual display of signal level, and then prints the information. This operation allows determination of NVR in small samples which are obtained from batch-type operations.

Experimental evaluation of this instrument at MSFC has been made by analyzing numerous contaminated and pure solvents both instrumentally and with the standard evaporation and weighing method. Results show that, once calibrated, the instrument provides accurate analysis of the NVR in chlorinated solvents within 40 seconds (per sample) and will detect down to 0.1 to 0.5 milligram per liter of NVR (dependent upon the particular solvent).

Potential industrial applications of this instrument include monitoring of the NVR of solvents and the effectiveness of solvent degreasing processes.

SOLUBLE CONTAMINATION IN GASES

Considerable quantities of air, nitrogen, and helium are used in the Saturn, as well as in all current space vehicles. It is essential that these gases be supplied exceptionally clean and free of oil (either as vapor or aerosol mists) to minimize the possibility of contamination of oxygen systems (which would introduce chemical reaction hazards). Traces of oil dispersed or dissolved in the gas supply to air bearing could condense and increase friction (as compared to air lubrication) and result in mechanical malfunction of the guidance system.

The standard method for the determination of trace quantities of oil in gases is by bubbling

through a long path of solvent (scrubbing train), evaporating to five cubic centimeters, and analyzing by infrared spectrophotometric methods. Limited sampling ability and the time required for this analysis has engendered development of automatic instrumentation. A device for this purpose based upon chromatographic separation and determination by flame ionization phenomena has also been designed and built by the IIT Research Institute under contract to this center. Based upon preliminary evaluation here at MSFC, several improvements have been made, and the modified instrument is currently being tested (fig. 4), and is expected to function as desired.

In general, the instrument is designed to sample gas automatically at a variety of pressures. A specially packed short chromatographic column has been developed to separate all hydrocarbon constituents above and below C_{14} . These are introduced into a flame ionization detector whose output is integrated and monitored by digital methods. Each analysis requires 60 to 80 seconds. Calibration of the instrument by a mixture of known hydrocarbons above C_{14} and by hexane (reference standard for light hydrocarbons) is used to determine the hydrocarbon constituents in the gas stream. The lower limit of detection appears to be 0.05

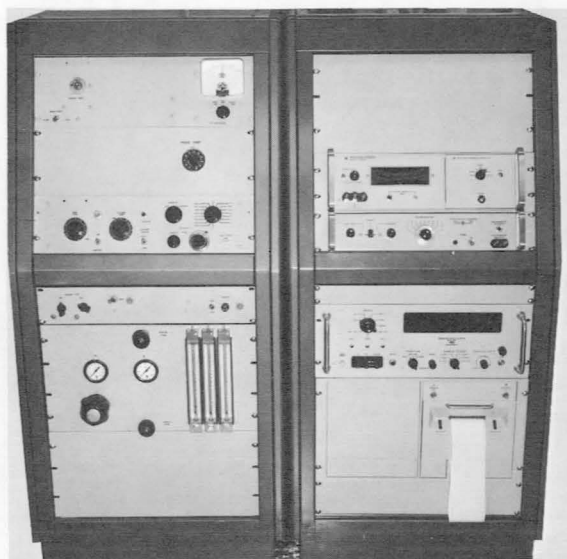


FIGURE 4.—Gaseous hydrocarbon monitor.

part per million (by weight) of hydrocarbons in gaseous systems.

This instrument will probably be useful wherever it is necessary to monitor air, oxygen,

or other gases for hydrocarbon contamination. Some possible applications include assurance of the purity of gases in chemical processes, air breathing oxygen, and sterile rooms.

5. Special Tooling for Joining Tubing in Place

R. MEREDITH

Engineering Development Laboratory, North American Aviation, Inc.

The Saturn S-II stage and the Apollo spacecraft will include in their design and construction various pressurized tubing systems that will encounter service temperatures of 280° F to -423° F. Design engineering and reliability requirements and weight restrictions have dictated new concepts to assure leak-tight joints for rocket engine fuel lines, pressurization systems, utility systems, and hydraulic systems.

An investigation was initiated at North American Aviation, Inc., Space and Information Systems Division, utilizing the in-place automatically controlled miniaturized fusion-welding equipment originally developed by the Los Angeles Division of NAA and modified to meet the needs of Apollo and Saturn welded tubular systems. The objective was to make circumferential flanged weld joints in any position in 304L stainless for Saturn S-II and sleeve-type joints in 304L for Apollo. Inconel X, commercially pure titanium, 5052-0 aluminum, and 6061 T6 aluminum were also tested experimentally.

Extensive environmental, static, and dynamic testing programs were conducted to determine the as-welded mechanical properties, design allowables, and reliability for the tube joints. This paper discusses both the experimental and production phases. Subsequently, the new tube welding process was approved and incorporated into manufacturing fabrication methods for tube joining.

EXPERIMENTAL PHASE

North American Aviation's Space and Information System Division, Downey, California, is principal contractor to NASA's Manned Spacecraft Center, Houston, Texas, for the Apollo command and service modules. Under a separate contract the Space and Information Systems Division is designing and building the Saturn S-II, the second stage of the Saturn V launch vehicle, for NASA's Marshall Space Flight Center, Huntsville, Alabama.

The S-II design and construction will include pressurized tubing systems that will encounter service temperatures of 280° F to -423° F. Reliability and weight restrictions have dictated new concepts (as compared to mechanical fittings) to assure zero-leak, lightweight joints in tubular fuel systems.

A program was initiated at the Space and Information Systems Division utilizing a modified Los Angeles Division-developed, in-place automatic miniaturized fusion-welding tool for making leak-tight joints in the tubing systems. Environmental, static, and dynamic testing programs were required to determine the as-welded mechanical properties and design allowables for welded tubing. An engineering process specification was required for manufacturing and quality control of the new tube-joining process. Because of the high reliability required, an extensive development and testing program was necessary.

OBJECT AND SCOPE

The object of the program was to determine if this equipment could be developed to operate

successfully in small areas and make reliable leak-proof welds in all positions.

Plan of action steps:

1. Development of an optimum joint design.
2. Determination of the radiographic standards for the welded joints.
3. Determination of the hydrogen and helium leak rate of the welded joints.
4. Determination of uniaxial tensile and burst strength.
5. Determination of flexure and impulse-fatigue life.
6. Determination of space requirements for in-place tube welded joints.
7. Preparation of an engineering process specification.

MATERIALS

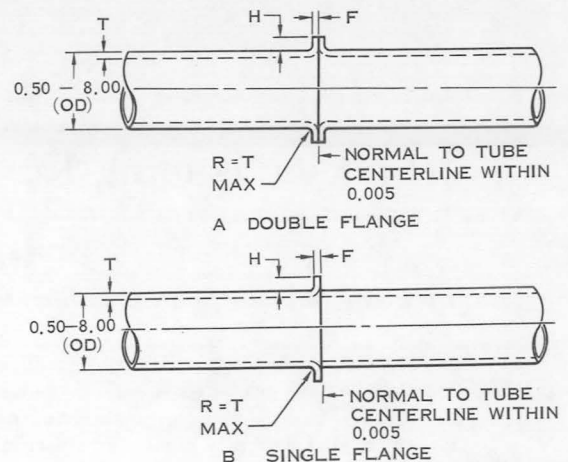
Tubing materials investigated in the development program:

1. 304L stainless steel 1.0-in. o.d. by 0.049-in. wall, 2.0-in. o.d. by 0.040-in. wall, 3.0-in. o.d. by 0.080-in. wall, 8.0-in. o.d. by 0.040-in. wall, 0.75-in. o.d. by 0.028-in. wall
2. 0.75-in. o.d. by 0.028-in. wall Inconel X tubing
3. 0.75-in. o.d. by 0.035-in. wall commercially pure titanium tubing
4. 0.250-in. o.d. by 0.032-in. wall, 0.50-in. o.d. by 0.040-in. wall 5052 condition O aluminum, and 0.375-in. o.d. by 0.032-in. wall 6061 T6 aluminum.

EXPERIMENTAL EQUIPMENT

Flanging

For the experimental phase of the program before obtaining a flanging machine, the tube ends were flanged on a lathe in a two-step spin-form operation. The dimensions of the flanges on various wall-thickness tubing are shown in figure 1. The 1.0-, 2.0-, and 8.0-in. diameter tube specimens were prepared by flanging both joint component ends. Some of the tube specimens were prepared by flanging only one of the tube ends as shown in B of figure 1. Figure 2 shows a manually operated flanging tool designed and fabricated for in-place flanging. Figure 3



NOMINAL TUBE WALL THICKNESS, T	FLANGE THICKNESS* F		FLANGE HEIGHT* —H, INCH, MINIMUM	
	DOUBLE FLANGE JOINTS	SINGLE FLANGE JOINTS	DOUBLE FLANGE JOINTS	SINGLE FLANGE JOINTS
0,020	0,017	0,020	0,015	0,035
0,028	0,025	0,028	0,018	0,035
0,035	0,025	0,035	0,018	0,040
0,049	0,025	0,035	0,020	0,040
0,060	0,025	0,035	0,020	0,040
0,083	0,030	0,040	0,040	0,040
0,125	0,035	0,040	0,050	0,050

* TOLERANCE ± 0.003 INCH

FIGURE 1.—Recommended dimensions for tube flange-joint preparation.

shows the minimum envelope space required for the in-place tube welding tool and is the drawing used by design engineers to establish minimum clearance needed for the tool. Figure 4 shows the production flanging tool for use on all joints except for in-place repairs where a

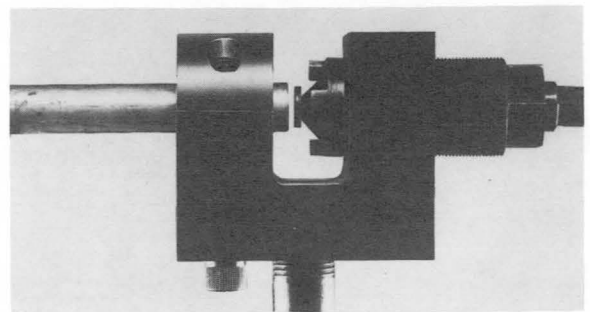


FIGURE 2.—Manual in-place tubing flanging tool.

TUBE OD (INCHES)	A (INCHES)	B (INCHES)
1/4	1.7	1.5
3/8	2.0	1.6
1/2	2.2	1.7
5/8	2.5	1.9
3/4	2.6	2.0
1	2.8	3.0
1-1/4	3.0	3.2
1-1/2	3.1	3.5
2	3.4	4.0
2-1/2	3.6	4.5
3	3.9	5.0
4	4.0	6.5
7	5.0	9.5
8	5.0	10.5

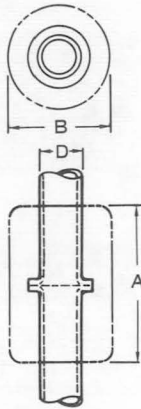


FIGURE 3.—Space required for welding equipment.

joint is cut apart and a section is removed and replaced by a new section.

Welding

Figure 5 shows the experimental welding set-up including power supply, controls, aligning

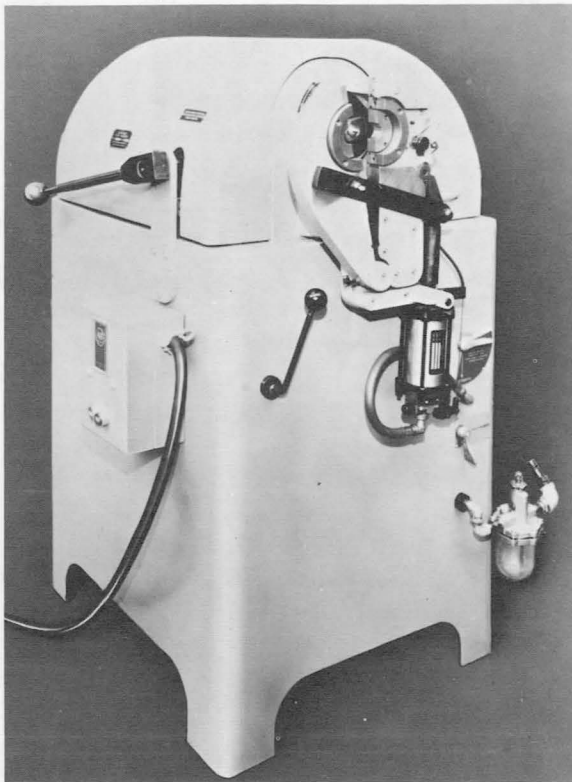


FIGURE 4.—Production flanging tool.

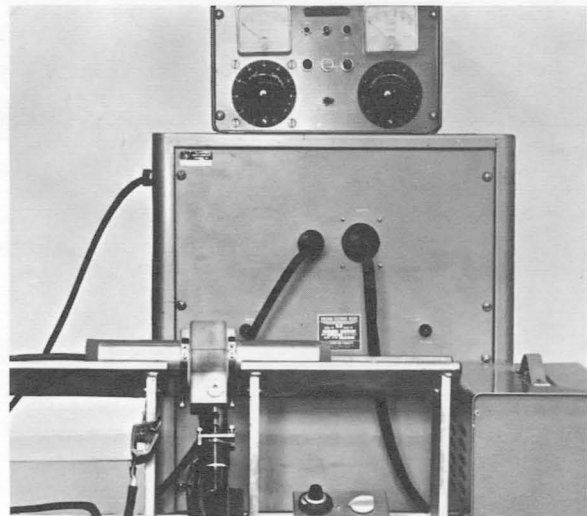


FIGURE 5.—Miniature welder and welding power supply.

jig, and tube-welding head clamped in place ready for welding. Figure 6 shows the experimental in-place welding tool that was used for the welding of 1.0-in. o.d. and 2.0-in. o.d. specimens. The photograph shows a 2.0-in. diameter tube; adapters were used for welding the 1.0-in. diameter tubes. Figure 7 shows an experimental welding head that was designed and constructed to weld 8.0-in. o.d. tubing. Adapters were used as shown for the welding of the 3.0-in. o.d. tubes. Figure 8 shows an-



FIGURE 6.—Welding tool being clamped around tube.

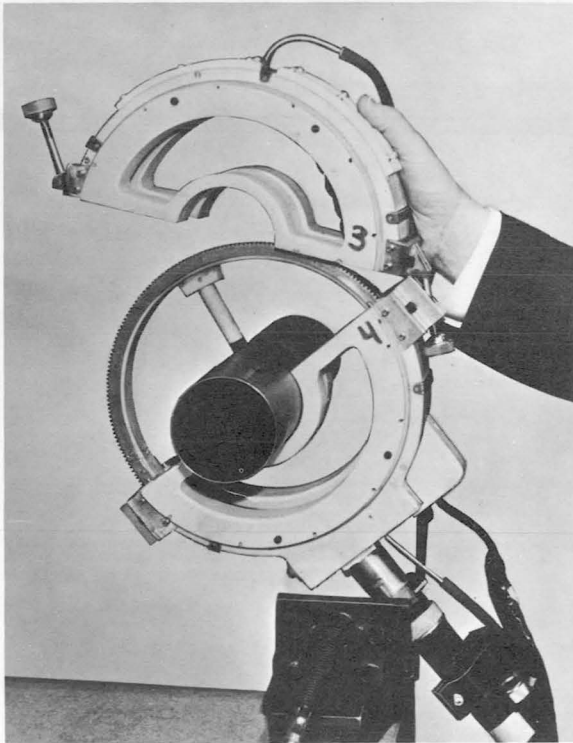


FIGURE 7.—8-in. o.d. welding tool with 3-in. adapter.

other experimental welding head with an exposed arc. This type has the advantage of being used very close to a flange.

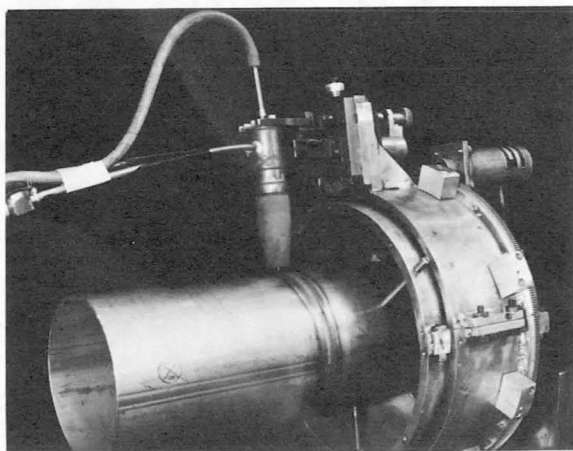


FIGURE 8.—Experimental welding head with an exposed arc.

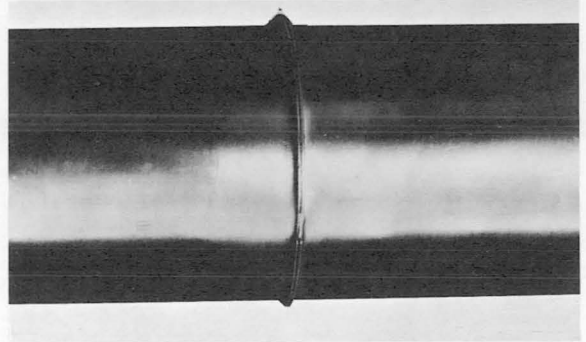


FIGURE 9.—Tube joint tack welded together.

TUBE WELDING

Figure 9 shows a flanged tube tack welded together with a manual TIG welding torch. After aligning and tacking, the welding head was assembled on the circumference of the flanged joint.

Figure 10 shows a 2-in.-diameter tube after welding. The internal inert-gas purging prevented any internal oxidation, and a smooth clean melt-through was obtained.

Figure 11 illustrates the operational sequence, which is performed as follows:

1. The half ring gear segment containing the tungsten electrode is placed around the tack-welded tube joint and locked to the other half of the ring gear to complete the ring gear assembly.
2. The gear and gas housing segments are assembled and locked around the ring gear.
3. Prior to welding, the interior of the enclosed welding head (housing the ring

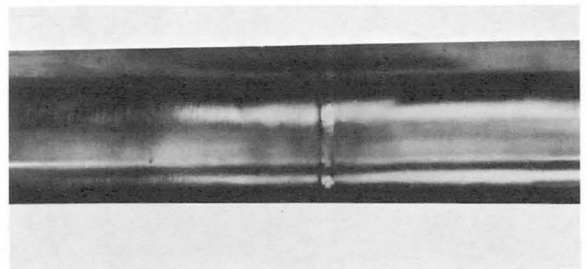
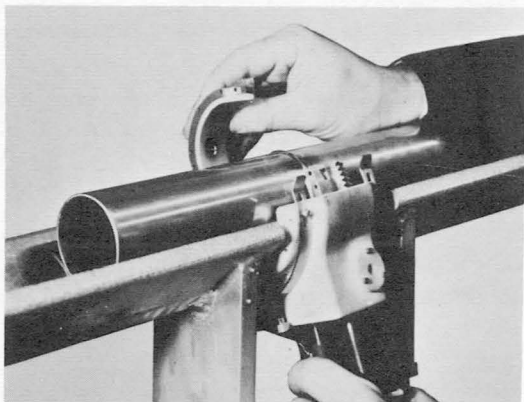
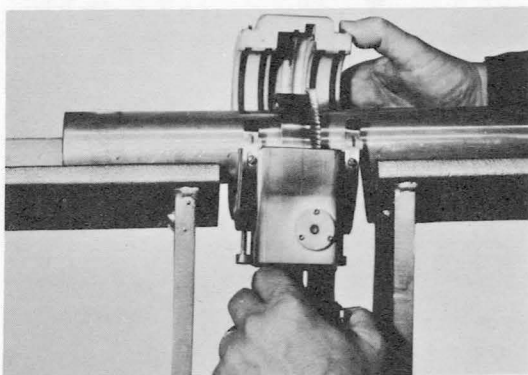


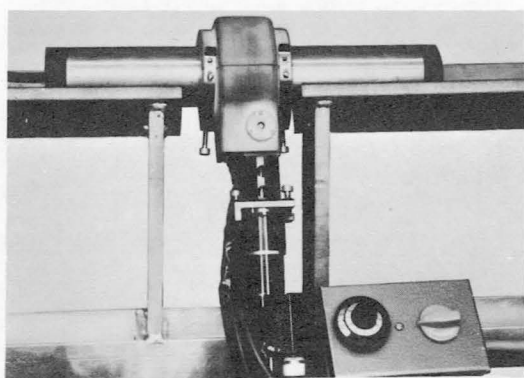
FIGURE 10.—Completed 2-in. o.d. tube weld.



ASSEMBLY OF RING GEAR



ASSEMBLY OF GAS HOUSING



ASSEMBLED TUBE WELDER

FIGURE 11.—*Miniature tube welder operational sequence.*

gear and electrode) is purged with 10 CFH argon, and the interior of the tube is purged with 7 CFH argon for 3 minutes.

4. The welding operation parameters are selected using vernier dials on the control panels, for example, 35 amperes, 10 volts, $4\frac{1}{2}$ in./min travel.
5. The miniature electric motor shown below the ring gear housing and welding head propels the ring gear with the tungsten arc rotated around the flanged joint and fuses the flange as filler-metal, resulting in complete penetration of the joint.

The welding equipment performed satisfactorily in all welding positions.

INSPECTION

Because of the high reliability required, the welds were subjected to visual, radiographic, and helium-leak nondestructive tests.

Visual Test

Approximately 200 tube-joint test specimens have been fusion welded with this equipment. The relatively few visual discrepancies noted were: (1) oxidized underbead due to lack of adequate purging gas, (2) lack of penetration due to improper welding parameters, and (3) lack of penetration due to off-center mislocation of welding arc in relation to flange joint.

The lack of penetration of tube welds is overcome by making a refusion weld pass over the affected area with slightly higher current settings.

Radiographic Test

Radiographic inspection of the welded tube joints met the specification requirements of ABMA-PD R-27A Class II, which is satisfactory for the systems involved.

Helium Leak Test

All the welded and X-rayed tube specimens were helium-leak tested with a Veeco leak detector. None of the leak-tested specimens exceeded the specified maximum rate of 1×10^{-6} Std cc He

sec

MECHANICAL PROPERTIES

Tables I through IV give the results of the uniaxial tensile test of subsize specimens machined from TIG-welded 304L joints in 1.0-in. o.d., 2.0-in. o.d., 3.0-in. o.d. and 8.0-in. o.d. tube. The tests were conducted at room temperature, 280° F, and -423° F.

Internal Pressure Tests

Table V presents test data on a number of welded tube specimens that were pressurized to failure at room temperature, 280° F, and -423° F. The test fluid used for pressurizing specimens tested at room temperature and at 280° F was hydraulic oil per MIL-H-5606. The test

TABLE I.—*Uniaxial Tensile Test Data—1.0-In. o.d., 0.048-In. Wall, 304L Tube*

Test	Test temp., °F	F_{tu} , ksi	Elongation, % ½ in.
Weldment...	280	74.7	26
Weldment...	280	73.6	30
Weldment...	280	77.6	20
Weldment...	280	73.3	30
		74.8 av	26 av
Base metal...	280	93.5	22
Base metal...	280	94.2	18
		93.8 av	20 av
Weldment...	-423	250.0	28
Weldment...	-423	240.2	38
Weldment...	-423	226.4	40
Weldment...	-423	251.3	30
		242.2 av	36 av
Base metal...	-423	289.0	34
Base metal...	-423	290.6	34
Base metal...	-423	291.1	36
		290.2 av	34.4 av
Weldment...	RT	94.4	32
Weldment...	RT	96.0	38
Weldment...	RT	95.4	34
Weldment...	RT	92.2	34
Weldment...	RT	96.6	30
		95.4 av	
Base metal...	RT	116.1	48
Base metal...	RT	114.1	46
		115.1 av	47 av

medium used for pressurizing specimens tested at -423° F was liquid hydrogen. Figure 12 shows the typical burst pattern of flange-type welded points when tested at room temperature.

Figure 13 shows the typical burst pattern of the 8-in. diameter by 0.040-in. wall welded tubes when burst tested at room temperature and at 280° F. Tests were also made at -423° F. The reinforcement rings, shown at the bottom of the photograph, were clamped around the bulkhead welds to force the failure into the center area of the specimen. Figure 14 shows two 4-in. o.d. by 0.060-in. wall and one 8-in. o.d. by 0.040-in. wall welded 304L tube burst test specimens. The tests were conducted at room temperature. Note that neither the girth or longitudinal welds failed.

Figure 15 shows the typical burst pattern and strength of the 1-in. o.d. by 0.49-in. wall

TABLE II.—*Uniaxial Tensile Test Data—2.0-In. o.d., 0.04-In. Wall, 304L Tube*

Test	Test temp., °F	F_{tu} , ksi	Elongation, % ½ in.
Weldment...	280	71.1	32
Weldment...	280	68.7	24
Weldment...	280	75.6	24
Weldment...	280	69.5	20
Weldment...	280	71.9	24
		71.3 av	24 av
Base metal...	280	92.6	18
Base metal...	280	95.8	18
		94.2 av	18 av
Weldment...	-423	276.3	34
Weldment...	-423	223.4	34
Weldment...	-423	273.4	36
Weldment...	-423	255.6	28
		257.0 av	32 av
Base metal...	-423	288.2	32
Base metal...	-423	280.7	30
Base metal...	-423	281.6	28
		283.5 av	30 av
Base metal...	RT	112.3	33
Base metal...	RT	112.0	30
Base metal...	RT	111.2	32
		111.8 av	31 av

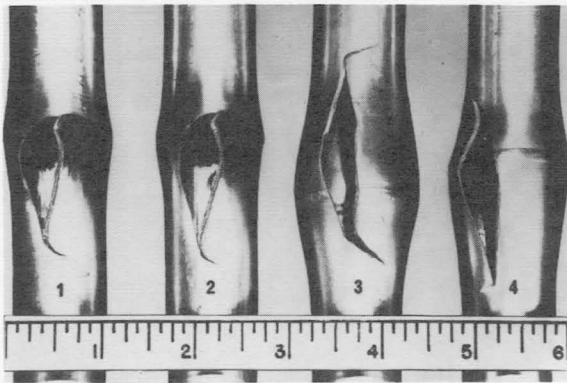


FIGURE 12.—1 in. o.d. tube weld burst test specimens.



FIGURE 13.—Welded 8 in. o.d. 304L burst test specimen.

TABLE III.—Uniaxial Tensile Test Data—2.0 In. o.d., 0.08-In. Wall, 304L Tube

Test	Test temp., °F	F_{tu} , ksi	Elongation, % ½ in.
Weldment...	280	67.4	20
Weldment...	280	67.2	28
Weldment...	280	69.7	22
Weldment...	280	67.4	20
		68.0 av	22 av
Base metal...	280	66.9	50
Base metal...	280	66.3	45
		66.6 av	47.5 av
Weldment...	-423	264.6	68
Weldment...	-423	196.1	24
Weldment...	-423	259.5	26
Weldment...	-423	216.7	22
		234.2 av	35 av
Base metal...	-423	221.1	28
Base metal...	-423	269.1	34
		245.1 av	31 av
Base metal...	RT	88.7	75
Base metal...	RT	87.1	74
		87.9 av	74.5 av

TABLE IV.—Uniaxial Tensile Test Data—8.0 In. o.d., 0.038-In. Wall, 304L Tube

Test	Test temp., °F	F_{tu} , ksi	Elongation, % ½ in.
Weldment...	280	67.7	22
Weldment...	280	64.0	22
Weldment...	280	65.9	20
Weldment...	280	64.5	22
		65.5 av	21.5 av
Base metal...	280	95.4	9
Base metal...	280	90.5	11
Base metal...	280	94.4	10
		93.4 av	10 av
Weldment...	-423	234.7	30
Weldment...	-423	236.0	32
Weldment...	-423	226.0	30
Weldment...	-423	233.2	38
Weldment...	-423	239.3	32
		233.8 av	32 av
Base metal...	-423	236.1	38
Base metal...	-423	234.6	32
Base metal...	-423	252.3	38
		244.3 av	35 av
Base metal...	RT	111.0	36
Base metal...	RT	113.7	31
Base metal...	RT	111.5	41
		112.0 av	36 av

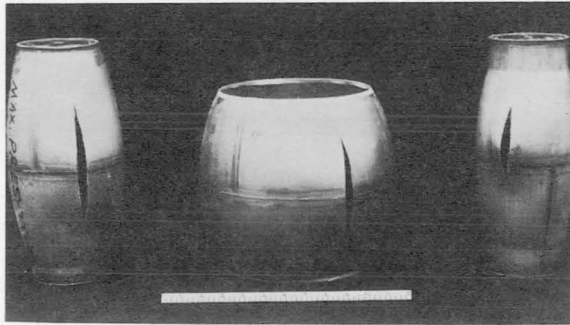


FIGURE 14.—Burst test specimens of two 4 in. o.d. by 0.060 in. wall and one 8 in. o.d. by 0.040 in. wall welded tubes.

sleeve-type joints. The sleeve-type joint has two advantages: it will withstand higher internal burst pressure and will maintain joint alignment without tack welding, but it also has some disadvantages. It cannot be used inside of lox tanks due to lox cleaning problems and adds to the vehicle weight.

Figure 16 shows the failure mode and mechanical properties of uniaxial room temperature tensile tests of sleeve-type welded tubing.

Flexure Fatigue Tests

A few welded tube specimens were flexure-fatigue tested. The setup is shown in figure 17.

TABLE V.—Internal Pressure Test Data, TIG-Weld Joint, 304L Tube

Tube (o.d.), in.	Wall, in.	Number	Test temp., °F	Yield pressure, psig	Maximum design pressure, psig	Operating pressure, psig	Burst pressure, psig
1.0	0.048	1F-1	280	-----	-----	3000	9000
1.0	0.048	1F-2	280	-----	-----	3000	8800
1.0	0.048	1F-3	280	-----	-----	3000	8800
1.0	0.048	1F-25	RT	-----	-----	3000	9600
1.0	0.048	1F-21	-420	-----	-----	3000	*3988
1.0	0.048	1F-20	-420	-----	-----	3000	*4738
2.0	0.038	2F-1	280	-----	2750	700	3940
2.0	0.038	2F-2	280	-----	2750	700	3970
2.0	0.038	2F-3	280	-----	2750	700	3960
2.0	0.038	2F-25	RT	-----	2750	700	4650
2.0	0.038	2F-13	-420	-----	2750	1100	*3100
2.0	0.038	2F-14	-420	-----	2750	1100	*4925
2.0	0.038	2F-15	-420	-----	2750	1100	*4150
3.0	0.080	3F-1	280	1800	2750	700	3250
3.0	0.080	3F-2	280	1700	2750	700	3250
3.0	0.080	3F-3	280	1750	2750	700	3280
3.0	0.080	3F-14	-420	-----	2750	1100	*4150
3.0	0.080	3F-15	-420	-----	2750	1100	*3800
3.0	0.080	3F-13	-420	-----	2750	1100	3900
3.0	0.080	3F-9	-420	-----	2750	1100	*4280
3.0	0.080	3F-7	-420	-----	2750	1100	*4450
3.0	0.080	3F-8	-420	-----	2750	1100	*4500
8.0	0.038	8F-1	280	280	185	132	680
8.0	0.038	8F-2	280	350	185	132	690
8.0	0.038	8F-3	280	308	185	132	705
8.0	0.038	8F-13	-420	-----	185	132	1838
8.0	0.038	8F-14	**—363	-----	185	132	1940
8.0	0.038	8F-15	**—400	-----	185	132	1750
8.0	0.038	8F-20	**—375	-----	185	132	1874
8.0	0.038	8F-21	**—420	-----	185	132	*1738

*Maximum pressure, no actual failure.

**Variation in cryogenic test temperatures resulted from test facility functions beyond control.

The test was performed at 280° F with MIL-H-5606 hydraulic oil as the test-fluid. This test was discontinued because of the inability to establish parameters until a more firm design on the type and location of mounting brackets was completed.

Impulse Fatigue Tests

No leakage or deformation was observed during or after completion of impulse test cycling. Table VI shows the number of impulse cycles, working pressures, impulse pressures, and test temperature. All proof-impulse tested tube joint specimens were subsequently helium-leak tested, and none exceeded the required maximum of $1 \times 10^{-6} \frac{\text{Std cc He.}}{\text{sec}}$.

LOX CLEANING

Figure 18 shows the test setup used to determine if welding after lox cleaning would con-

taminate the tubing beyond the acceptable limits permitted for lox systems. Welding increased the particle count but did not exceed the maximum allowable per MSFC—Spec-164.

PRODUCTION PHASE

Materials

Though other materials were tested experimentally, only the type 304L stainless tubing was used in production. However, some research is continuing on aluminum tubing. Aluminum alloys are much more difficult to weld than either stainless or titanium.

Equipment

After proving the feasibility of welding tubing in a range of wall thicknesses and diameters experimentally, production welding equipment had to be developed. Figure 19 shows the power supply and controls developed for production by Navan Products, Inc. Figure 20 shows the

TABLE VI.—Internal Impulse-Pressure Fatigue Test Data, TIG-Weld Joint, 304L Tube

Tube (o.d.), in.	Wall, in.	Number	Test temp., ° F	Working pressure, psig	Impulse pressure, psig	Number cycles
1.0	0.048	1F-10	280	3000	4500	1000
1.0	0.048	1F-11	280	3000	4500	1000
1.0	0.048	1F-12	280	3000	4500	1000
1.0	0.048	1F-17	-420	3000		1000
2.0	0.039	2F-10	280	700	1050	1000
2.0	0.039	2F-11	280	700	1050	1000
2.0	0.039	2F-12	280	700	1050	1000
2.0	0.039	2F-18	*-405	1100	1050	1000
3.0	0.080	3F-10	280	1100	1650	1000
3.0	0.080	3F-11	280	1100	1650	1000
3.0	0.080	3F-12	280	1100	1650	1000
3.0	0.080	3F-17	*-405	1100	1650	1000
3.0	0.080	3F-18	-420	1100	1680	1000
8.0	0.037	8F-10	280	132	200	1000
8.0	0.037	8F-11	280	132	200	1000
8.0	0.037	8F-12	280	132	200	1000
8.0	0.037	8F-16	-420	132		1000
8.0	0.037	8F-17	-420	132	140	1000
8.0	0.037	8F-18	-420	132	115	1000
8.0	0.037	8F-19	-420	132	124	1000

*Variation in cryogenic test temperatures resulted from test facility functions beyond control.

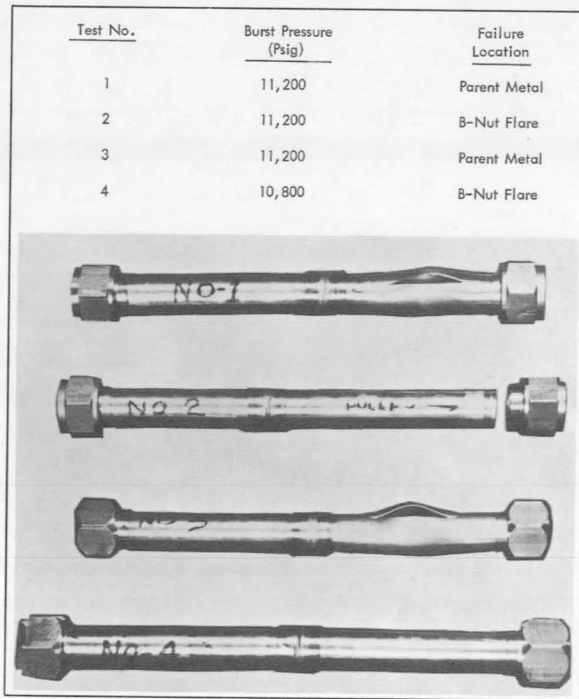


FIGURE 15.—1 in. o.d. by 0.049 in wall sleeve-type burst tests at room temperature.

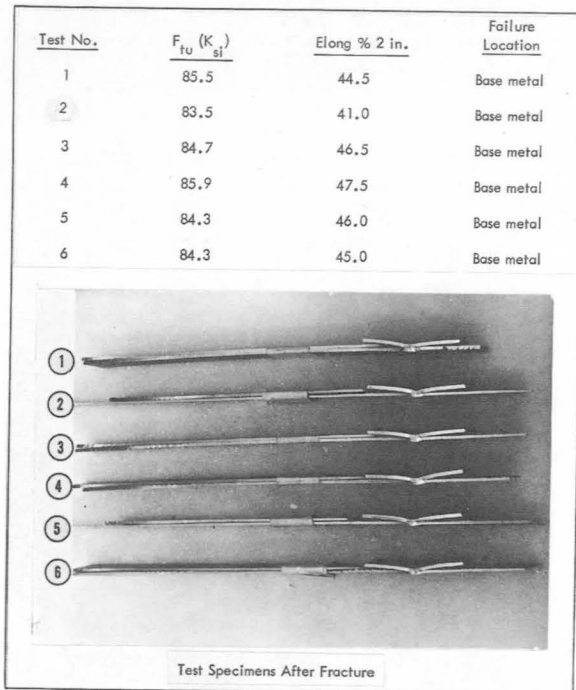


FIGURE 16.—Mechanical properties of sleeve-type welded joints in 3 in. o.d. by 0.034 in. wall 304L tubing tested at room temperature.

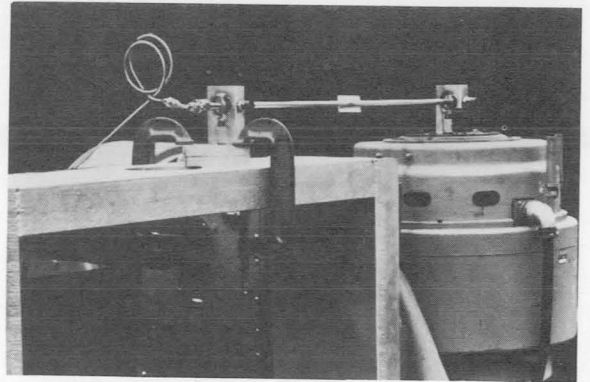


FIGURE 17.—Flexure-fatigue test setup.

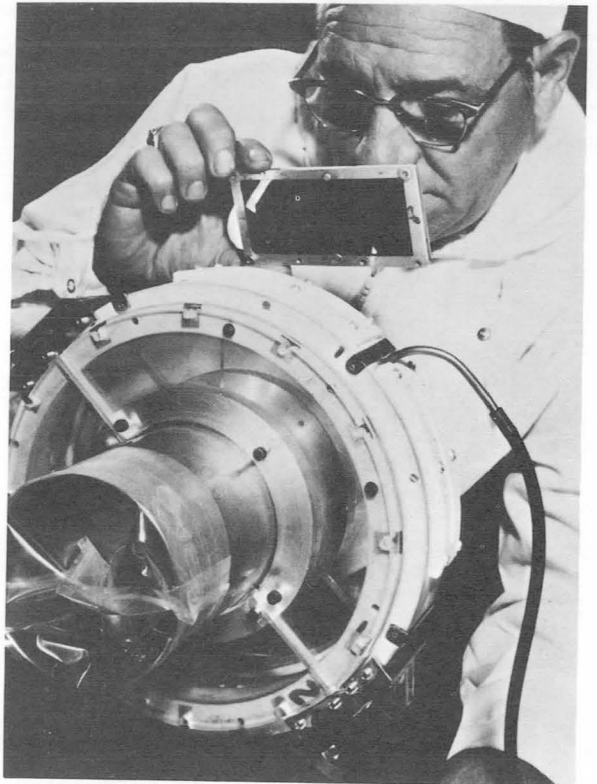


FIGURE 18.—Welding low-cleaned tubing.



FIGURE 19.—Navan welding power supply.



FIGURE 20.—Orbit arc automatic welding head developed by Navan Products, Inc.

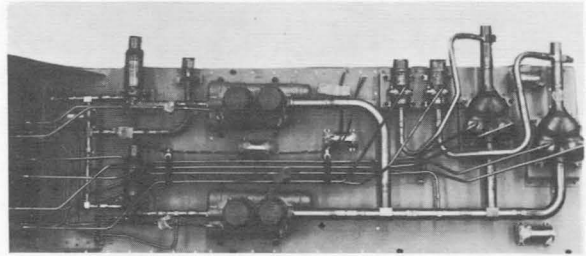


FIGURE 21.—Helium-pressurization system.

welding head, which has approximately the same basic design as the experimental model, except that the production head is built more ruggedly. The head was developed by the Los Angeles Division of NAA for Navan.

PRODUCTION WELDED ASSEMBLY

Figure 21 shows a production assembly helium-pressurization system for the Apollo service module. Some joints were induction brazed and others welded using the sleeve-type joint. Originally, all joints were to be brazed; however, in production it was found that the close tolerances required for brazing could not be held on the larger diameter tubing. Thus, a decision was made to weld all lines 1.00-in. diameter and greater. Using the sleeve-type joint instead of the flanged type made an easy transition from brazing to welding. Figure 22 shows the Saturn Stage-II gaseous helium and nitrogen fuel pressurization lines. Both single- and double-flanged joints were used on this assembly.

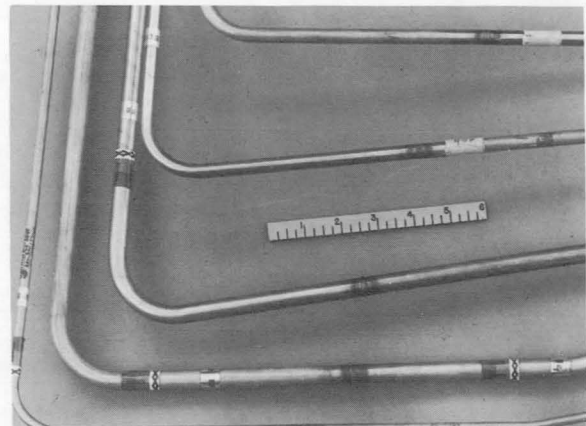
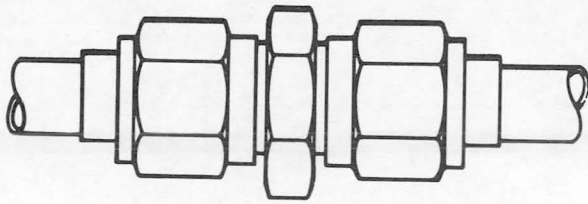
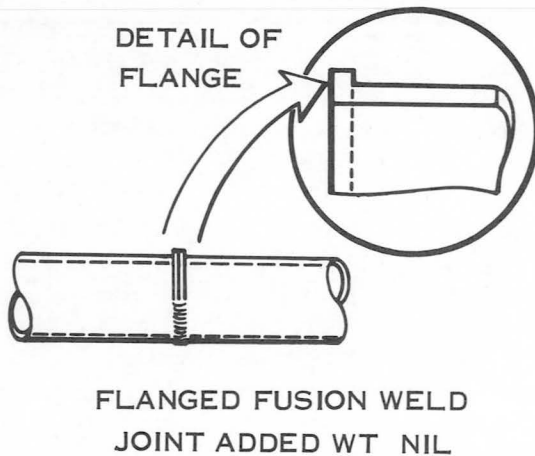


FIGURE 22.—Saturn Stage-II gaseous nitrogen and helium fuel pressurization lines.



MECHANICAL JOINT
APPROX WT (1 INCH DIA)
.96 LBS



FLANGED FUSION WELD
JOINT ADDED WT NIL

FIGURE 23.—Joint weight comparison, 304L stainless.

Advantages

Figure 23 shows the tremendous weight savings of the flanged welded joint as compared with the mechanical fitting. The welded joint is also more reliable than the mechanical fitting, which will leak when subjected to thermal and vibration cycling for extended periods of time.

CONCLUSIONS

1. The double-flanged joint is superior to other types of welded tube joints.
2. Successful automatic miniaturized TIG-welding equipment has been developed for making reliable in-place welded joints in tubing systems.
3. Radiographic inspection of in-place TIG-welded tube joints revealed excellent weld quality.
4. Helium-leak detector tests revealed no adverse leakage rate in the weld joints.
5. Uniaxial tensile, burst, flexure-fatigue, and impulse-fatigue tests of TIG-welded tube joints tested at room temperature, at 280° F, and at -423° F met the engineering design requirements.
6. Welding of tube joints was performed satisfactorily after lox cleaning without exceeding the maximum permissible particle count.
7. Welded tube joints are lighter in weight and more leak proof than tube joints made using mechanical fittings.

6. Some Unique Applications of Intense Magnetic Fields

R. J. SCHWINGHAMER

George C. Marshall Space Flight Center, NASA

A brief history of our knowledge of ordinary magnetism and electromagnetism is given, from the time of the Roman poet, Lucretius Carus, to the present. Practical examples of magnetic field strength associated with objects familiar to all are discussed, and a frame of reference regarding magnetic field strength is thereby established. The earliest known investigators of intense transient magnetic field manipulation of solid conductor materials are mentioned, and the phenomena described. Systems, apparatus, and basic theory of operation are detailed. The importance of adequate diagnostics is discussed, and some techniques employed are illustrated. The "magnetic sawing" phenomenon is described, and implications explained. Typical applications are shown, including swaging, sizing, sealing, clamping, forming, and other unique neoterisms. A particularly successful application, the magnetomotive sizer, is described in detail, and beneficial application in the Saturn V program is described. Potential industrial applications are prognosticated, and developmental trends are indicated.

"I have seen those Samothracian iron rings leap up, and iron filings in the brazen bowls seethe furiously when underneath was the magnet stone." So spoke the famous Roman poet Lucretius Carus (98-55 B.C.) in his epic poem on the nature of things, *De Rerum Natura*. In general, it appears that this interesting phenomenon, magnetism, has been known to mankind for several thousand years. Even centuries before the Christian era, the Greeks knew that the mineral lodestone (a magnetic oxide of iron) had the ability to attract iron and other pieces of the same mineral. Thales of Miletus mentioned this in the sixth century B.C., as did Socrates somewhat later. The magnetic compass dates back to about 1090 A.D., when the Moslems are said to have guided their ships in this manner in plying their trade between Canton and Sumatra. However, the first detailed description of the compass as an instrument of navigation was provided in 1269 by Petrus Peregrinus de Maricourt, a French Crusader. In 1600 William Gilbert, court physician to Queen Elizabeth, published his "De Magnete," which summarized the available

knowledge of magnetism at that time. The English unit of magnetomotive force was named for this same William Gilbert.

After this, Isaac Newton and Robert Boyle held sway with their laws of gravitation and gases, and little more was developed in the field of magnetism until about 1820 when Hans Christian Oersted discovered electromagnetism—the fact that electric currents can also produce a magnetic field. From then to the present, the field is studded with illustrious names such as Ampere, Faraday, Henry, Maxwell, and, more recently, Kapitsa, Tesla, Heisenberg, and Bohr. The quantum theory we hear so much about today in connection with nuclear work and lasers has also provided considerable impetus in the magnetic field area and, indeed, has even prompted many of the new developments in high magnetic field techniques. Magnetic fields can be created today which cause even the hardest steel to flow like water and sometimes to explode like a bomb.

To depart somewhat from the historical aspect, and to give a few practical facts, the field of an ordinary garden-variety bar magnet

amounts to 2 or 3 thousand gauss. On the other hand, the Earth's magnetic field is something less than a single gauss. (The gauss is the unit of magnetic field strength, and is named for the great German mathematician Karl Friedrich Gauss.) For comparison purposes, an electromagnet using a core of metal to amplify the field generated by the electric current in the coil can reach perhaps 60 000 gauss, at the very most. Superconducting coils have recently attained field strengths in excess of 100 000 gauss. But, to go much higher, one must eliminate the core and produce the magnetic field in air or in a vacuum.

While the importance of magnetic fields is obvious in such mundane devices as electric motors, relays, and the like, a pair of plasma physicists, Furth and Waniek, discovered a newer and less obvious magnetic field phenomena at the Harvard Cyclotron Laboratory in 1955. They found that with sufficiently high mag-

netic fields, they could push tough metal around as if it were merely soft plastic. They discovered this during their attempts to create high magnetic fields for the purpose of determining the charge and momentum of particles by their deflection in a high magnetic field region. The practical results of their work and the work of several others, such as Colgate, a group at General Atomics, and the work at Marshall Space Flight Center (MSFC), have certainly been utilitarian, and an entirely new tooling concept has been developed.

MAGNETIC FORMING TECHNIQUES

Let us consider how solid conductors can be manipulated or formed electromagnetically with a pulse power system. A magnetomotive pulse power system, the type of system required to generate high intensity pulsed fields, is shown in figure 1. Static magnetic fields are not effective in forming metals while pulsed or

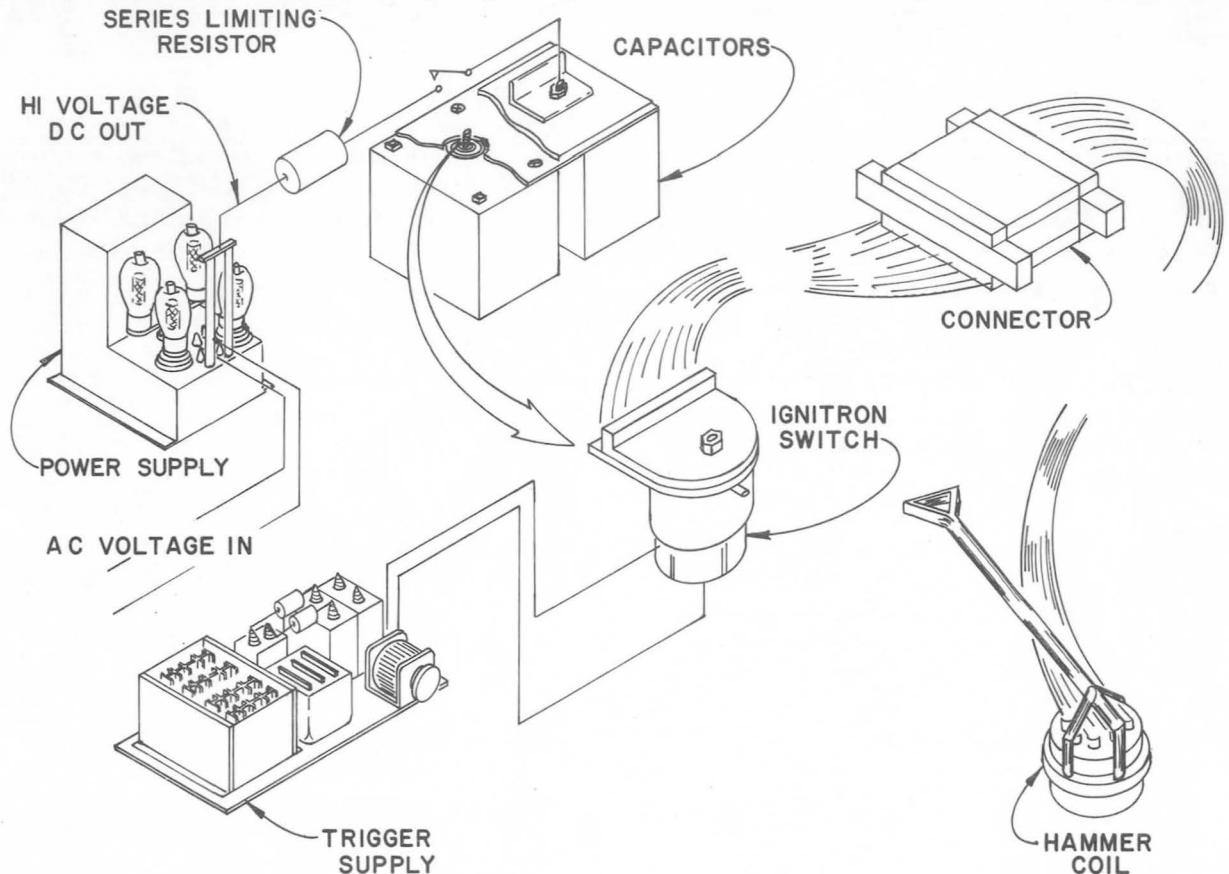


FIGURE 1.—Magnetomotive pulse power system.

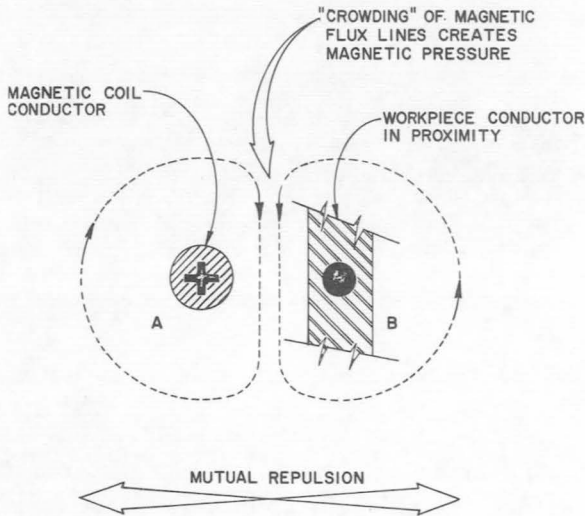


FIGURE 2.—Magnetomotive coil and workpiece: (a) indicates current flow into plane of illustration; (b) indicates current flow out of plane of illustration.

transient fields are. Figure 2, magnetomotive coil and workpiece, shows why. This figure is a pictorial representation of what takes place when a heavy transient current pulse is discharged through a coil, with an electrically conductive workpiece inside. The coil current creates a magnetic field, causing an eddy current to flow in the workpiece in proximity to the coil. The eddy current then provides an induced field which interacts with the primary coil to create high magnetic pressure between

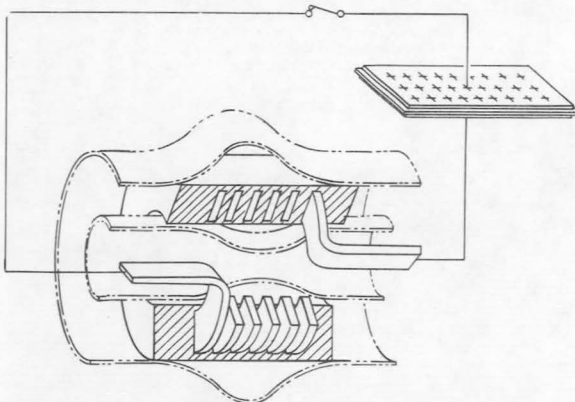


FIGURE 3.—Magnetomotive energy relationships. Stored energy:

$$\frac{1}{2} CV^2 \rightarrow \frac{1}{2} LI^2 \rightarrow \frac{1}{8\pi} \int H^2 dv$$

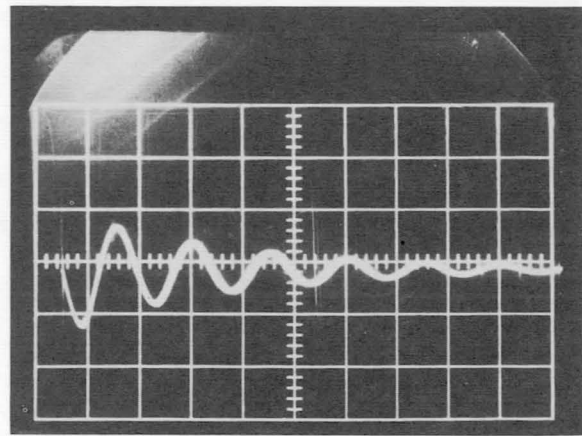


FIGURE 4.—Characteristic current discharge trace.

the coil and the workpiece. If the coil is physically of inertially stronger than the workpiece, the workpiece yields and is formed. The pertinent magnetomotive energy relationships associated with this operation are shown in figure 3, where we see that the stored energy in the capacitors is converted to magnetic field energy in the coil, which, in turn, creates magnetic pressure proportional to the field strength squared over the volume v .

Figure 4 shows the fluctuation of the current and magnetic field. This damped oscillatory type current discharge is frequently used in magnetomotive forming coils. This rate can be recognized as a typical result in an R-L-C circuit operating in the damped oscillatory mode. The application of this theory can be seen in figure 5, which shows the precision forming of stiffening convolutes in a thin-walled aluminum cylinder, a strictly experimental structural development which was at one time considered for application on the Saturn V lox tunnels. Although this idea was not adopted the converse technique is now being applied. That is, we are sizing oversized tunnels down to the proper diameter by a coil on the outside. The arrangement is shown in figure 6. The tunnel, which is 25 inches in diameter with a wall thickness of 0.224 inch, can be seen to the left, while the magnetomotive coil and the sizing mandrel can be seen at center and to the right.

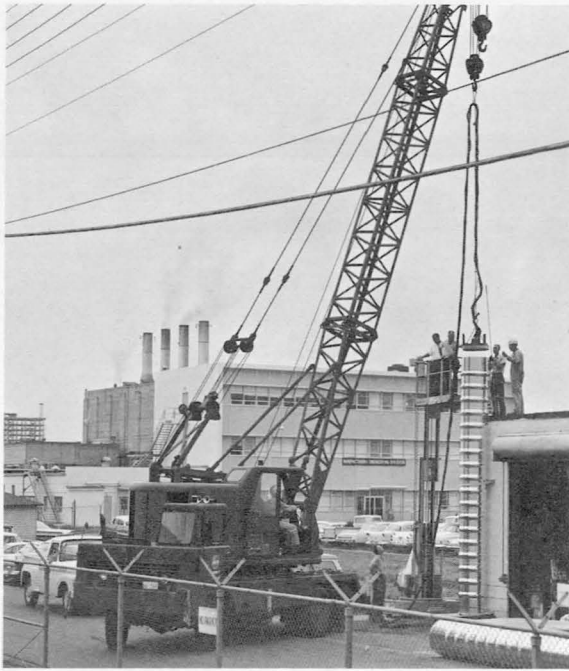


FIGURE 5.—Precision convolute forming using crane.

The components used for stainless steel tube bulging experiments presently underway are shown in figure 7. The special coil design can be seen at the left. The entire assembly is inserted in the tube at the right. Sealing of stainless steel tubes into titanium by magnetic pressure is also being investigated.

Figure 8 shows a group of mechanical fasteners which utilize the power inherent in an

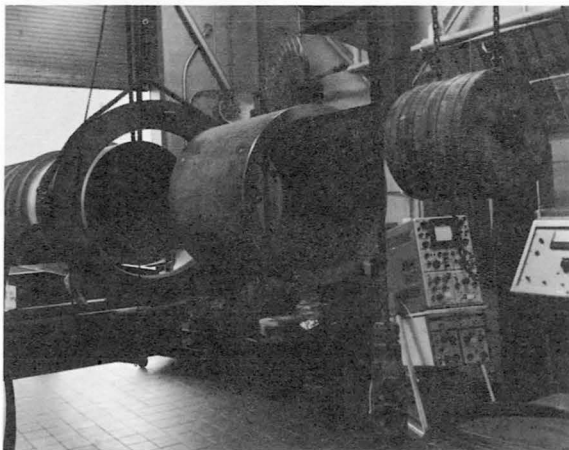


FIGURE 6.—Magnetic sizing Saturn V S-1C lox tunnel.

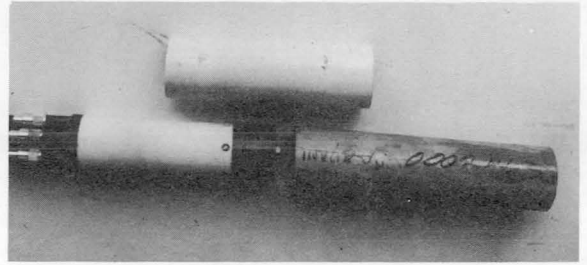


FIGURE 7.—Stainless steel tube bulging.

intense transient magnetic field in order to clamp materials tightly together by swaging a metal sleeve on a specially designed bolt. It is, for the most part, a torqueless, momentless operation, but although promising, is not completely perfected as yet.

Apparatus used in experiments on magneto-motive forming fasteners is shown in figure 9. The process has been termed *Magnelok*. Adequate diagnostics apparatus is essential in developing new systems. Another promising new magnetic field tool is shown in figure 10. One of the attractive applications of this remarkable new tooling concept involves the forming of flared outlets with a single impulse. Because the impulse is so rapid, strain rates of thousands of inches per inch are generated, and these flares can be made with the material in the hardened condition. The assembly clamps together as a sandwich, with the material to be formed between coil and die, as seen on the left.

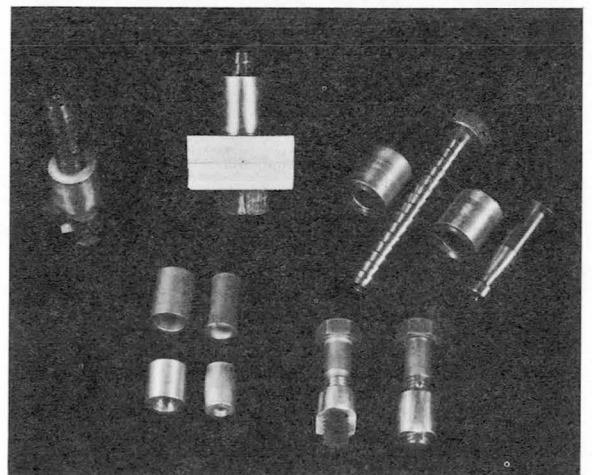


FIGURE 8.—Magnetomotive fasteners and concept.

Figure 11 shows a pair of typical 3-inch-diameter flares formed with a single magnetomotive impulse or shot. An exhaustive series of tests has been run to determine proper operating parameters for certain material

thicknesses of interest. This technique could conceivably eliminate much distortion, heat treatment, welding, and similar operations.

Figure 12 shows a 21-inch magnetomotively formed flare resting in the die. One pulse, or shot, was used to form the flare. The very large coil can be seen above the workpiece. More than 100 000 joules are required to form such a part.

A T-flare coil, workpiece, and die are shown in figure 13. By placing the coil inside the

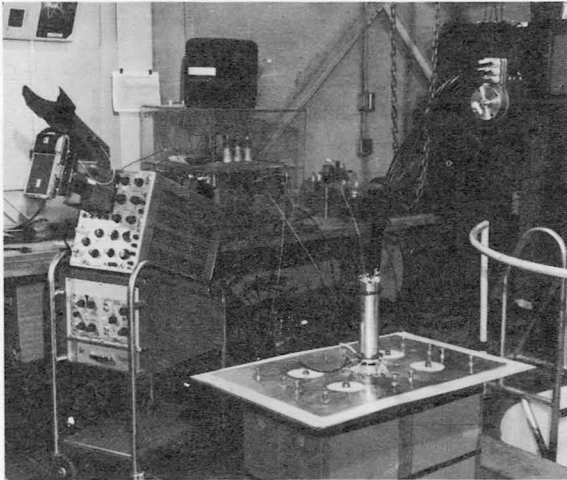


FIGURE 9.—MagneLok coil experiments.

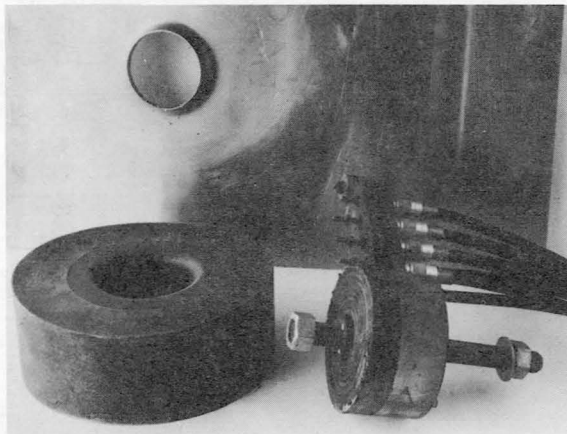


FIGURE 10.—One-shot magnetomotive flaring.

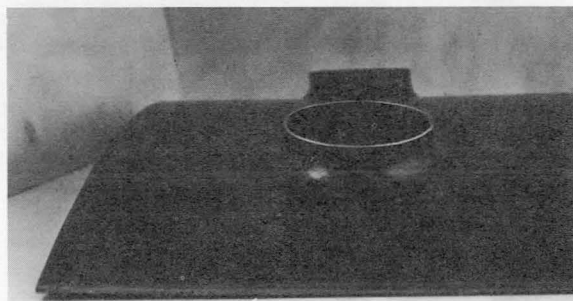


FIGURE 11.—Magnetomotively formed 3-inch diameter flare.



FIGURE 12.—21-inch flare magnetomotively formed.

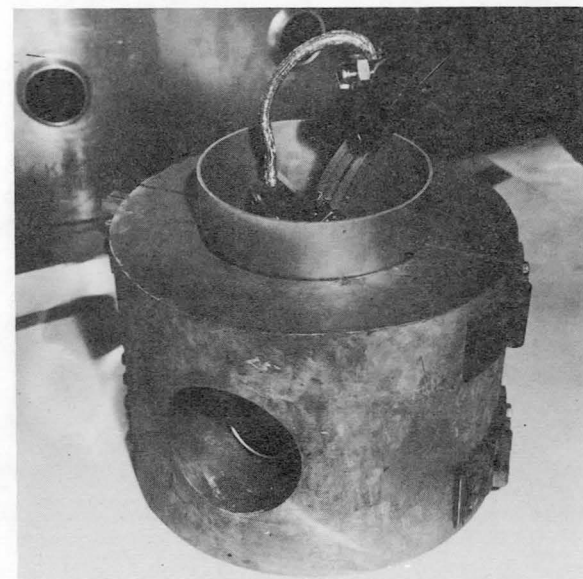


FIGURE 13.—T-flare coil, workpiece, and die.

workpiece, the central pilot hole expands outward into the die, creating a T-flared section as shown in figure 14. An early prototype of a T-flared opening formed into a thin-walled cylinder which was done with a single magnetomotive pulse is shown in this figure.

Figure 15 shows some typical equipment used in magnetomotive-forming diagnostics techniques. In developing this unique new family of tools, diagnostics techniques of quite sophisticated refinement are required. The illustration shows some typical measurements in progress. By similar techniques, metal velocities of 300 to 1000 ft/sec have been measured during forming, and strain rates in the range of thousands of inches per inch per second have been attained.

MAGNETOMOTIVE HAMMERS

One of the industrially attractive developments in the forming area has been the magnetomotive hammer. Figure 16 shows the early

experiments of a few years ago which were concerned with weld-bead sizing on an advanced vehicle experimental tank segment. Figure 17 illustrates a more sophisticated version, the pneumatically clamped improved magnetomotive hammer. This device was designed to produce intense pulses of force sufficient to size or

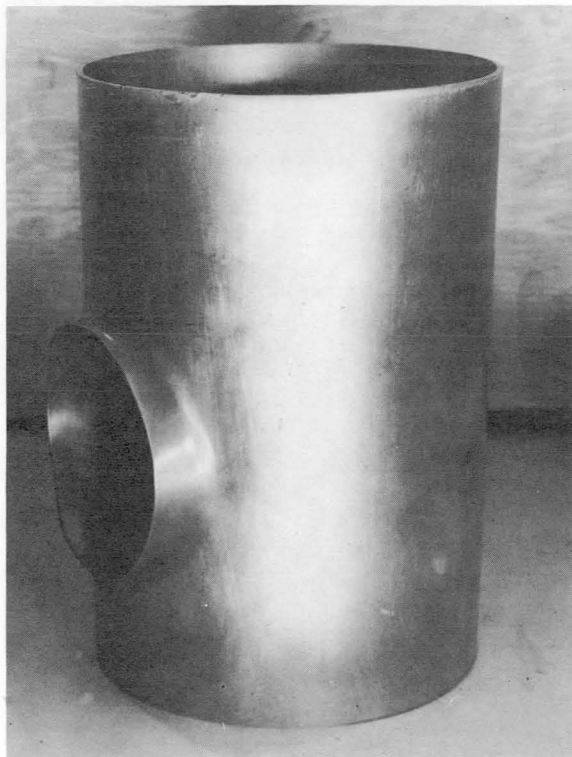


FIGURE 14.—*Experimental T-flare, magnetomotively formed.*

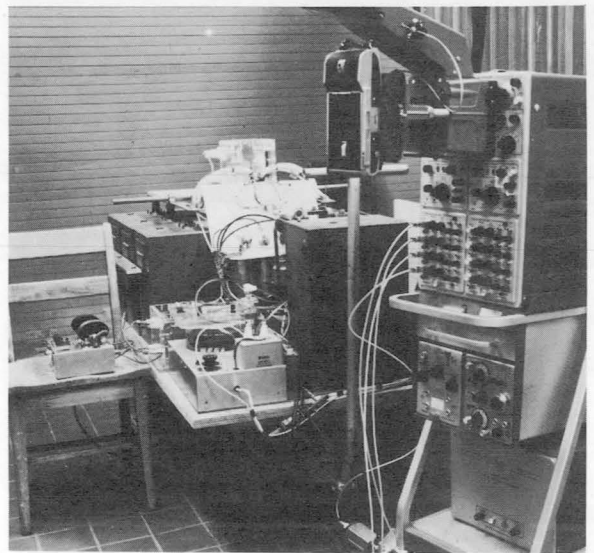


FIGURE 15.—*Typical magnetomotive forming diagnostics and apparatus development.*

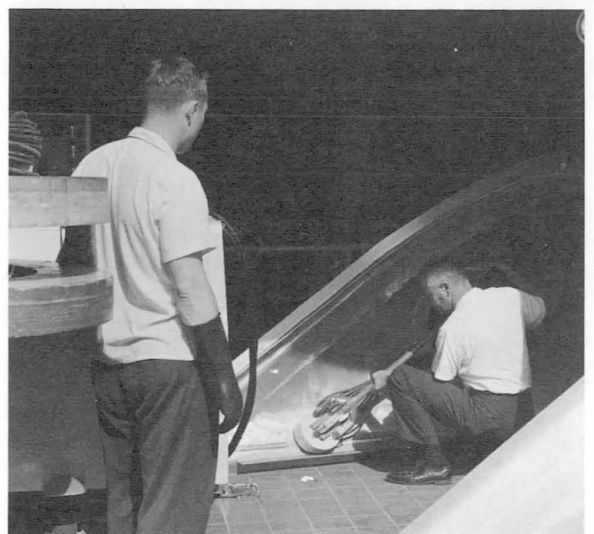


FIGURE 16.—*Early magnetomotive hammer experiment.*

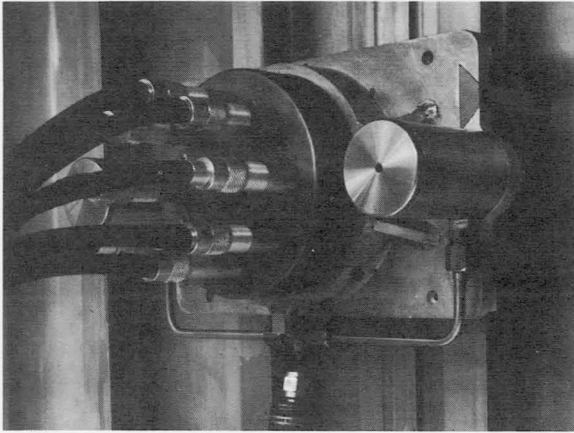


FIGURE 17.—Pneumatically clamped improved magnetomotive hammer.

stretch weld beads of one-half inch to three-quarter inch over the hammer face area. This illustration shows the device in position on a typical Saturn V skin. The small vertical cylinders at either end provide the pneumatic clamping force, while the coil proper occupies the central location.

Figure 18 shows a hand-held hammer removing distortion from a saturn bulkhead segment. This is a practical example of the magnetomotive hammer's usefulness. Saturn first-stage bulkheads are fabricated by welding huge orange-peel-like sections (gores) together to form a complete bulkhead or tank end. Very heavy fittings are welded into thinner material in the process, and considerable material distortion can result. A unique, specially designed, hand-



FIGURE 18.—Hand-held hammer.

held magnetomotive hammer proved to solve the problem. The 18 kilojoule pulse power unit is shown on the left, and the hammer unit held in position for precision-controlled distortion removal is shown on the right.

The hand-held hammer, shown closeup in figure 19, has the attractive feature of reasonably equitable fluidlike pressure distribution through the thickness of the material, while delivering the impulse. Strictly speaking, it is quite unlike a hammer in almost every respect, including the metallurgical aspects. In addition, no surface marring of the material results when the device is used. A sheet of Mylar is used under the coil proper to provide additional voltage breakdown protection.

An estimate of the effectiveness of the process can be seen in figures 20 and 21. Figure 20 shows an apparent hump in the gore segment before magnetomotive sizing. The hump is ac-



FIGURE 19.—Closeup of hand-held hammer.



FIGURE 20.—Distortion gore segments before magnetomotive sizing.

tually the result of considerable weld bead shrinkage between adjacent fittings in a gore segment. Figure 21 shows the segment after magnetomotive removal of distortion. Here it can be seen that the proper contour has been restored to the part. Some feel must be developed for this type operation since no backup dies are used, but any good machinist gets the idea rapidly, and one day's instruction has so far proved adequate.



FIGURE 21.—Gore segment after magnetomotive removal of distortion.

Figure 22 shows a completed Saturn bulkhead in which the magnetomotive hammer has been used to eliminate the distortion which occasionally occurs around the meridian welds approaching the apex of the dome. Figure 23 shows how this distortion is removed. An early prototype

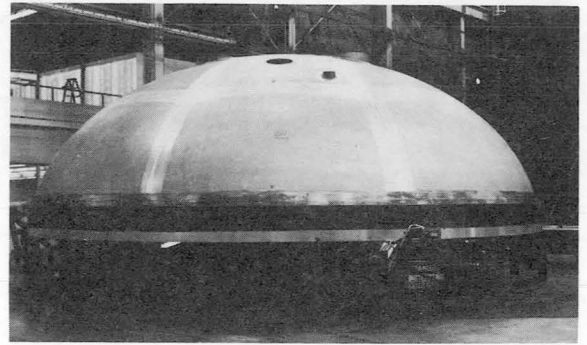


FIGURE 22.—Completed Saturn bulkhead, hammer unit in foreground.



FIGURE 23.—Distortion removal from finished Saturn bulkhead, or tank end.

pulse power unit can be seen in the foreground, while the hammer unit is at top center, being used in the overhead position by the operator. Here again, precision-controlled sizing was accomplished without the need of any backup dies. The ease with which electric charge and power can be controlled facilitates precision sizing.

Figure 24 shows some of the family of magnetic field tools under development at MSFC. A variety of applications is being studied, including precision sizing, stress relieving, coining, blanking, fastening, constricting, bulging, powder compaction, and other magnetic field manipulations of solid electrically conductive materials.

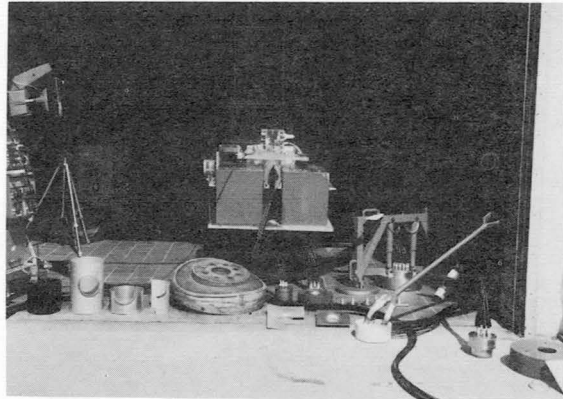
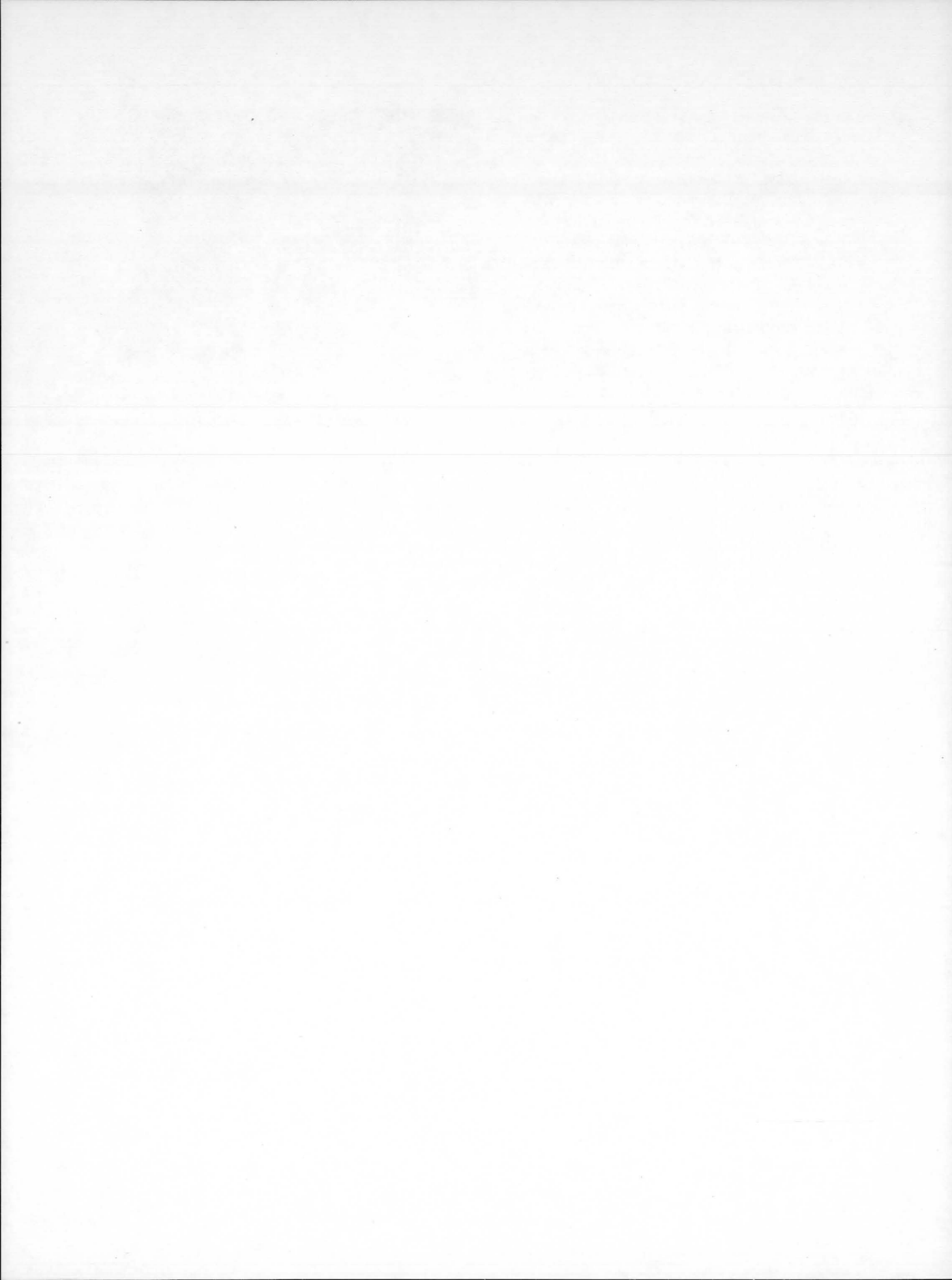


FIGURE 24.—*Portion of magnetic field tools under development at MSFC.*



7. Sculpturing, Forming, and Spinning of Large Components for Launch Vehicles

ETRIC L. STONE

*Manufacturing Development, Launch Systems Branch,
The Boeing Company*

At the beginning of the S-IC booster contract, it was evident that certain manufacturing techniques would have to be developed before the proposed design could be put into full production. Much of the development activity that has been accomplished was initiated because the size of booster components was greater than the capacities of available equipment. This paper describes some of the more significant methods that have evolved from this development activity, and which demonstrate how the capability to manufacture S-IC components such as bulkhead gore segments, tank skins, Y-rings, and lox tunnels, has been acquired.

The fabrication methods used to transform 2219 aluminum alloy plate into the large, sculptured, and contoured parts that make up the structural surfaces of the booster include hydraulic bulge forming, age forming, and adaptations of conventional skin milling and chemical milling processes. The importance of fixturing and the machining sequence related to fabrication of the Y-ring are pointed out. The shear-spinning process that is used to produce a seamless, one-piece lox tunnel 40 feet long from a cylindrical blank only 62 inches long is described.

The presentation is concluded with a synopsis of the current design changes that are being implemented to improve strength-to-weight ratios. A brief statement of possible future activity is included.

On May 25, 1961, President John F. Kennedy said, ". . . this nation should commit itself to achieving the goal, before this decade is out, of landing a man on the moon and returning him safely to earth." In effect, this statement was the go-ahead to science and industry for developing the capabilities of moving men and equipment into lunar orbit, for making moon landings, and for conducting deep space probes. As a consequence, there has evolved a spacecraft-booster combination of such size, weight, and complexity as to challenge the nation's manufacturing capability. Our answer to this challenge to manufacturing technology is represented by the three-stage Saturn V launch vehicle which will propel the manned Apollo spacecraft to the moon.

The first and largest stage of the Saturn V launch vehicle is the Saturn S-IC booster. A cutaway model of the S-IC booster is shown in figure 1. Proper perspective is gained by comparing the relative size of the booster with that of man. The first stage consists of two cylindrical propellant containers, a fuel tank, and a lox tank, connected in tandem by an intertank structure assembly, a thrust structure assembly to withstand and distribute engine thrust loads, and a forward skirt assembly to provide the interface connection between the first and second stages.

The gigantic size of the booster with its necessary strength-to-weight ratio has created the complexity of its parts. However, in spite of its size, the S-IC booster is being constructed

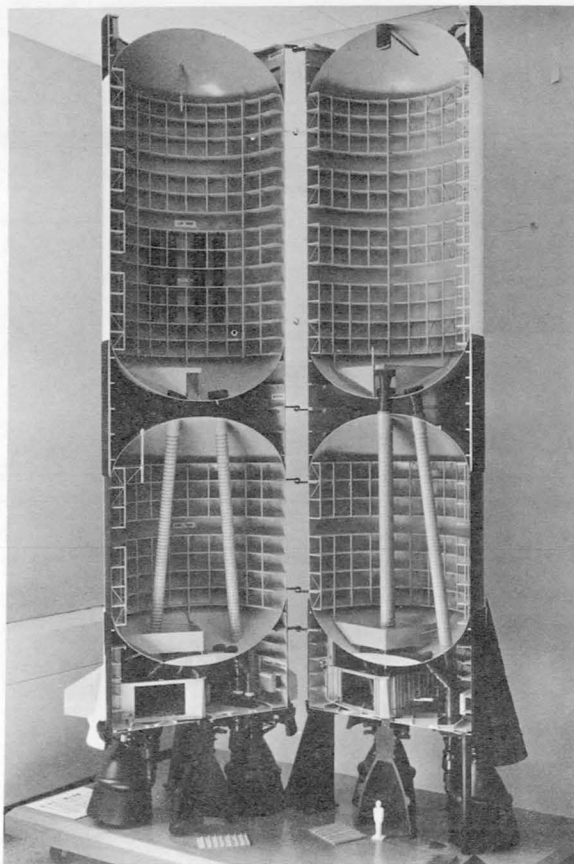


FIGURE 1.—Cutaway model of S-IC booster.

with the precision of a fine watch. Its 33-foot diameter will not vary more than 0.030 inch from nominal diameter.

This report presents four principal areas of manufacturing which required major development effort to meet the ever-increasing demands of the space industry. It also introduces some additional development efforts which will further advance manufacturing technology for the future.

MANUFACTURING TECHNOLOGY DEVELOPMENTS

The manufacture of an enormous product such as the S-IC has led to the development of new and unusual methods of fabrication as well as extending and refining of the more conventional, established methods. Throughout the numerous fabrication facilities required by the S-IC program will be found newly established methods, the older more conventional

methods, or a combination of the two for forming, machining, cleaning, and protective coating of large structural components. For example: at Michoud Operations in New Orleans, Louisiana, the new is contrasted with the old, not only by manufacturing techniques, but also by equipment. Chips fly from a huge aluminum alloy ring being machined in an environmentally controlled room on a 1914 vintage vertical boring mill whose 27-foot table has been extended to increase the turning capability to 42 feet. Less than 200 feet away, completed components and assemblies are thoroughly cleaned, rinsed, and protectively coated in the world's largest automatic dishwasher, a 40-foot square, ultramodern facility which cleans parts to hospital standards.

The technology gained thus far on the S-IC program by the Marshall Space Flight Center and The Boeing Company with its many subcontractors is being demonstrated in the successful manufacture of stage fuel and lox containers. Since the S-IC is a man-rated booster, precision weight control and reliability are paramount. The structural design requirements of the containers are stringent and call for materials such as the 2219 aluminum alloy developed by Alcoa. From the time of its earliest introduction to the aerospace industry in 1957, the characteristics of the 2219 aluminum alloy, together with its adaptability and limitations related to manufacturing processing, have been determined and utilized. The knowledge gained is now being extended for space application. Processes such as age forming and hydraulic bulge forming, using 2219 aluminum alloy sheet and plate in the largest obtainable dimensions, were developed for this program. Established processes such as machining, shear spinning, chemical milling, cleaning, and protective coatings were adapted to the unusual demands created by the configuration and usage environment of the various components.

SCULPTURING AND HYDRAULIC BULGE FORMING OF BULKHEAD GORE SEGMENTS

The fuel and lox tanks are cylindrical vessels with ellipsoidal bulkheads for end closures. The bulkheads consist of eight pie-shaped gores,

each of which is made up of an apex segment and a base segment (see fig. 2). Each segment is made from one piece of material measuring approximately 12 ft by 12 ft with thicknesses up to 1 in. Smaller and thinner gore segments are commonly stretch formed, but the limitation on existing stretch-press sizes and tonnages preclude stretch forming of the large compound-contoured gore segments for the S-IC. The fabrication of the S-IC gore segments is further restricted by design requirements. The central portion of each segment is relatively thin for weight control; the peripheral edges are thicker to provide proportional strength in the weld areas required for bulkhead assembly.

Conventional methods such as stretch-press forming, have not proved to be reliable for forming parts of nonuniform cross section because of excessive thin-out of material in the presculptured or membrane areas; therefore, the hydraulic bulge forming process was developed.

The concept of using hydraulic bulge forming for the S-IC gore segments was a result of a team effort between development engineers of the Manufacturing Engineering Laboratory of MSFC and development engineers of The Boeing Company in Huntsville, Alabama, early in 1962. The feasibility of the process was proved on a one-fifth scale presculptured and

bulge forming research program carried out by The Boeing Company at its Seattle, Washington, facility.

The principle that a confined fluid will transmit a uniform pressure over a surface has been well known and widely used in metal forming. The application of this principle requires the use of complex hydraulic presses, and since gore segments are larger than existing press capacities, their size has ruled out the use of a hydraulic press for forming. The idea of using the die halves to restrain the part blank with a peripheral seal to withstand the fluid pressure was conceived and has proved to be a practical solution in forming large, complex-contoured gore segments. The hydraulic fluid, in this case water, is analogous to the punch used on a hydraulic press and forces the part to take the shape of the die cavity.

Forming pressures will vary according to the thickness of the part. Pressure from 400 to 600 psi is used to form the thinnest parts; that is, those having sections as thin as 0.10 in. Other parts as thick as 0.835-in. will require pressures up to 1100 psi. Clamping pressure is adjusted to provide a predetermined amount of slippage based on forming tables developed by tests.

Design of the full-scale hydraulic bulge form tooling was done by The Boeing Company at Huntsville, Alabama, and New Orleans, Louisiana.

Fabrication of the tooling and final implementation of the process was accomplished at The Boeing Company Wichita facility. To date, nearly 900 gore segments have been successfully formed using the process.

The bulge form process has varied utilization and application. Not only is it feasible to presculpture the part in the flat by machine milling prior to forming, but is also possible to bulge-form a part having constant thickness and then sculpture it to the varying thickness requirements by chemical milling. At the present time, approximately 30 percent of the gore segments are presculptured in the flat by numerically controlled skin mills prior to forming; the balance are sculptured by chemical milling after constant-thickness forming.

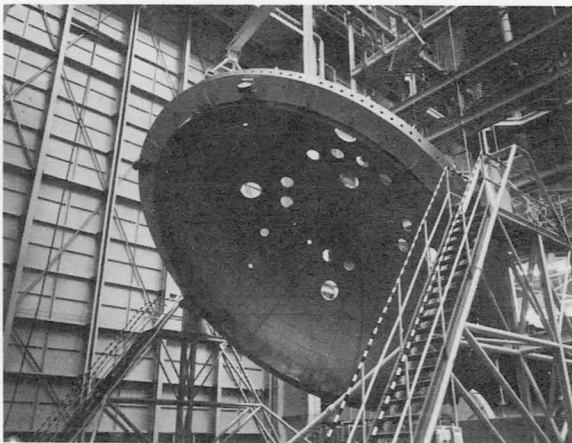


FIGURE 2.—Lower fuel tank bulkhead assembly.

The ultimate goal is to do all machine milling in the flat prior to hydraulic bulge forming. This method is more economical and will be possible as more skin-mill capacity becomes available. See figures 3 through 8.

SCULPTURING AND AGE FORMING OF CYLINDRICAL CONTAINER SKINS

Age forming of 2219 aluminum alloy skins is a process developed by The Boeing Company at its Wichita, Kansas, facility after many attempts to form skin panels using conventional methods proved unsuitable. Forming by press brake, forming rolls, and even creep forming, an early forming method using thermal en-

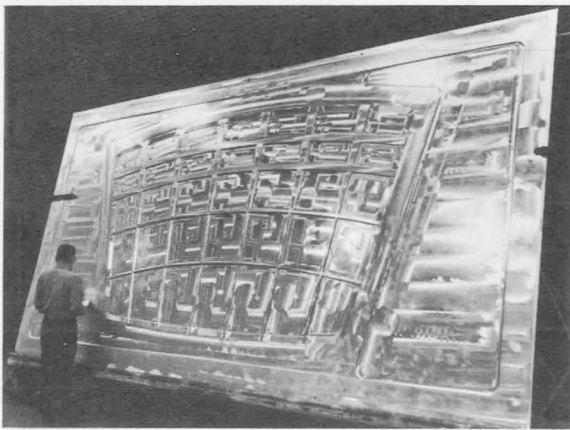


FIGURE 3.—Sculptured 2219 aluminum alloy gore base prior to forming.

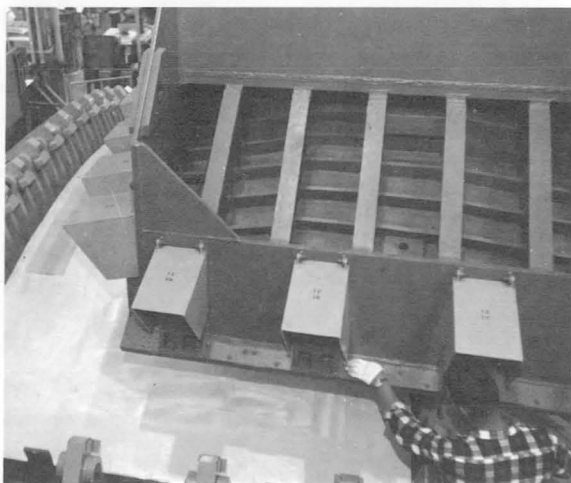


FIGURE 4.—Placing upper die half prior to forming a gore base.

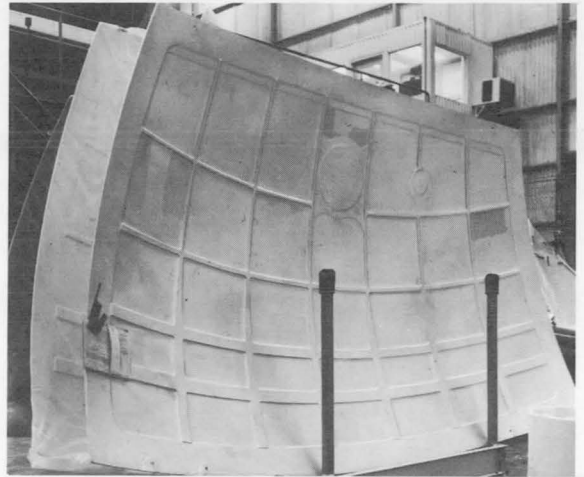


FIGURE 5.—Sculptured 2219 aluminum alloy gore base after forming.



FIGURE 6.—Thickness measurements being taken on sculptured 2219 aluminum alloy gore apex prior to forming.

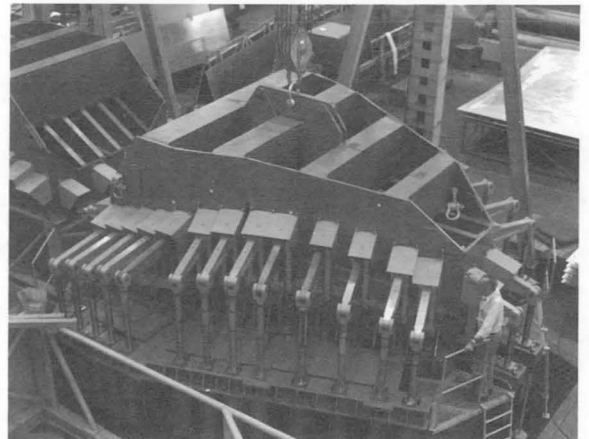


FIGURE 7.—Gore apex hydraulic bulge forming tool in operation.

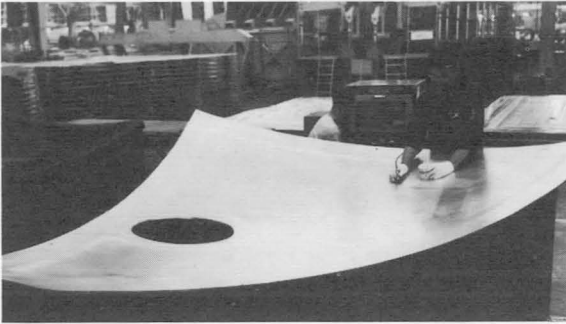


FIGURE 8.—2219 aluminum alloy gore apex after forming.

vironments, was tried. Nothing compared with the relatively inexpensive operation of aging and forming parts simultaneously.

The fabrication of large complex skin panels which form the walls of the Saturn S-IC cylindrical propellant tanks is done by skin mill sculpturing in the flat followed by age forming to the single-radius contour. Using a numerically controlled skin mill, each skin panel is sculptured from 2½-in. thick 2219-T37 aluminum alloy plate to produce an 11 by 26-ft. panel having integral stiffening ribs and sculptured lightening pockets. The machined parts are then clamped to a fixture having a predetermined radius of 148 in. (75 percent of the desired final radius) and then heated in a furnace to the aging temperature of 325° F. for a period of 24 hours. While the part is held at temperature, the material, through thermal relaxation, takes a permanent set to contour, is age hardened to the T87 condition, and reaches its maximum strength capability. Upon removal from the fixture, the age-formed skin panel springs back to the desired 198-in. radius.

Development effort currently is being directed toward expanding the potential of age forming to include large, compound-contoured parts (having more than one radius of curvature) in the range of 5 to 400-in. radii (see figs. 9 and 10).

MACHINING OF CONTAINER BULKHEAD-TO-SKIN TRANSITION SECTIONS (Y-RINGS)

In the construction of both the fuel tank and the lox tank, it is necessary to join the tank ends or bulkheads to the cylindrical skin section as well as to provide a means for connecting the



FIGURE 9.—Thickness measurements being taken on milled 2219 aluminum alloy cylindrical skin panel.

thrust structure, intertank structure, and forward skirt structure to the tanks. The Boeing Company, with design and fabrication method concurrence of MSFC, developed this transition section whose cross-section is shaped like the letter Y. This Y-ring eliminates lap joints and provides a pressure vessel of high structural integrity.

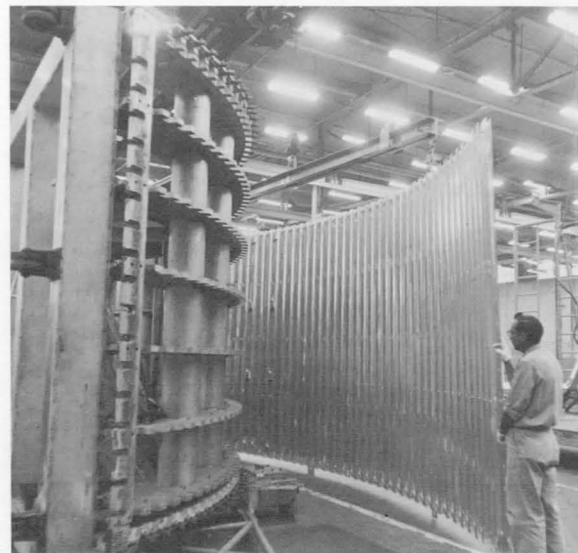


FIGURE 10.—Removing age-formed 2219 aluminum alloy cylindrical skin from age-forming fixture.

The fabrication of this ring involves rolling and machining of the largest aluminum alloy billets ever produced on a commercial basis. Flat billets weighing approximately 7000 pounds and measuring 5½-in. thick, 27 in. wide, and 36 ft in length are obtained from the aluminum supplier. The billets are roll formed and edge prepared for welding by Ingalls Ship Building Corporation, Pascagoula, Mississippi. Three of these segments are welded into a ring slightly larger than 33 ft in diameter and then machined to the Y-configuration. Approximately 14 500 pounds of material are removed during machining, leaving a finished Y-ring which weighs about 3500 pounds.

Joining the three ring segments by metal-inert-gas welding is accomplished at Michoud Operations by positioning the parts in a weld fixture and applying weld-filler metal alternately to each side of each of the three joints. By control of the amount of weld metal deposited and time phasing of each weld pass, the ring is maintained to a roundness of 0.250 in. Stress relieving of the weld joints is done by induction heating and requires heating each weld joint to 650° F for 15 minutes and air cooling to ambient temperature. Temperature gradients are measured and controlled at 24 points on the ring billet to prevent material property degradation.

Machining of the Y-ring at Michoud Operations is accomplished on a Niles Vertical Boring Mill having a 27-ft diameter table with extensions added to provide the capability of turning a 42-ft diameter. The ring is positioned in the turning fixture, clamped from the outside, and then rough cut to the inside diameter. The ring is then clamped from the inside and roughing cuts made on the outside diameter, top, and bottom surfaces of the ring. Clamping pressure on the part is released to permit residual stresses induced during roll forming to be relieved. The ring is then reclamped and the final machining of the outside diameter is accomplished. Following inspection of the outside diameter, the backup-ring segments of the fixture are positioned, clamps are secured, and the inside diameter further rough machined to a minimum of 0.125 in. from nominal finish di-

ameter. Following X-ray inspection of the weld areas, the inside diameter is machined to the finished dimension. The completed ring is subjected to final inspection, removed from the turning fixture, and cleaned. See figures 11 and 12. The ring is then prepared for joining to the tank bulkhead assembly.

SHEAR SPINNING OF LOX SUCTION LINE TUNNELS

Liquid oxygen is transmitted from the lox container through the fuel tank to each of the five agencies of the S-IC by means of lox suction lines. These are straight tubular assemblies consisting of two tubes, each approximately 40 ft long and assembled one inside the other. The inside tube, or lox suction line, is made of 321 stainless steel. It has an inside diameter of 20 in. with an 0.085-in. wall thickness. The lox tunnel, which encases the stainless steel suction line, is a one-piece seamless tube formed from 2219 aluminum alloy to an inside diameter of 25 in. with a 0.098-in. wall thickness for about 90 percent of its length, increasing to 0.224-in. thickness for the remainder. Each of these tubes is produced by the Parsons Corporation, Traverse City, Michigan.

In 1961, the Parsons Corporation established this spinning capability and began the development work to produce long, seamless, close-tolerance tubing for the aerospace industry. Some of their early problems were caused by inconsistencies in the composition of the raw material; however, tighter control of the material specification has resulted in improved grain structure and mechanical properties. Machining the inside and outside diameters of the workpiece prior to spinning removes any surface defects and provides a uniform wall thickness. Another major problem was growth experienced during aging. This has been resolved by completing the final tube reduction on an undersized mandrel.

The shear-forming or flow-turning process is widely used throughout the metal-working industry. When applied to thin-wall tubes 40 ft long squeezed from a 1-in.-thick cylindrical blank only 62-in. long, conventional methods must be modified to ensure distortion-free and



FIGURE 11.—Welded 2219 aluminum alloy Y-ring billet prior to machining.

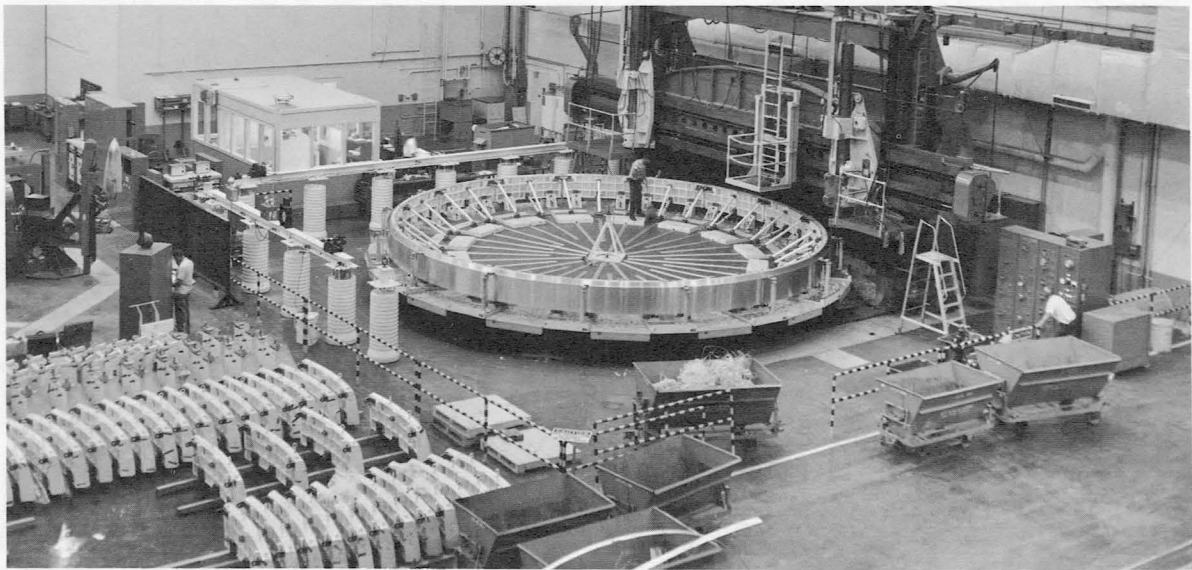


FIGURE 12.—Machining of Y-ring on 42-foot-diameter vertical boring mill.

properly sized parts. The Parsons Corporation accomplishes this in a series of passes which first reduces the annealed workpiece 75 percent of its wall thickness. It is then solution heat treated to the T42 condition and further reduced 50 percent of the remaining wall thickness. After the part is aged to the T8 condition, it exhibits an ultimate strength of 65 000 psi, a yield strength of 55 000 psi, and an average elongation of 9 percent, in a 2-in. gage length (fig. 13).

SCULPTURING AND HYDRAULIC BULGE FORMING OF BULKHEAD GORE SEGMENTS HAVING INTEGRAL FITTING OUTLETS

The Boeing Company, Wichita, Kansas, is currently developing techniques for bulge forming apex and base gore segments which have bulkhead fitting outlets presculptured in the part. Figure 14 shows a gore apex segment having integral fittings. This improved manufacturing method will eliminate welded fitting outlets which currently require bump press or electro-magnetic straightening of the welded gore assembly prior to aging. Presculpturing and bulge forming methods developed and used for previous part fabrication will be extended for this new requirement.

MACHINING AND SCULPTURING OF CONTAINER BULKHEAD-TO-SKIN TRANSITION SECTIONS (INTEGRAL TEE STIFFENED Y-RINGS)

A new design for the bulkhead-to-skin transition is being incorporated for weight reduction. This new design currently under process development will result in a weight reduction of



FIGURE 13.—Full length shear-formed 2219 aluminum lox suction line tunnel being measured for thickness; premachined billet and partially shear-formed part in foreground.

more than 5000 pounds per S-IC booster. Figure 15 shows a full-size section of the integral tee-stiffened Y-ring. Preliminary pocket milling on 1/4-scale test rings is complete, and full-size fabrication is feasible. Tests have also been completed on full-size straight sections for establishing cutter geometry, feed, speeds, and other procedures in preparation for fabrication of the first full-size part. Not only will this new configuration reduce weight, but it will also simplify weld assembly of the bulkhead to the cylindrical tank skin by reducing the weld-joint thickness from 0.90 in. to 0.50 in.

CONCLUDING REMARKS

This paper touched upon but a few of the more significant developments for sculpturing, forming, and spinning of large parts for launch vehicles. An attempt has been made to demonstrate how the size of booster components has influenced and further advanced manufacturing technology. Age forming and hydraulic bulge forming have been described as completely new processes developed as the result of demands made upon manufacturing capabilities. The application of other, time-proven and more conventional methods has been expanded to satisfy additional demands. Requirements for the future are expected to reflect the present trend of fabricating larger and more complex parts.

Size limitations imposed by existing equipment capacities will be considered less important than the search for ways to keep weight to a minimum. If the number of smaller parts that comprises a welded assembly can be reduced, or consolidated into a single one-piece unit, then weight can be saved through the elimination of weld seams. The seamless, one-piece lox tunnel is an example of this trend. It is also possible that the fabrication of large tank end closures from a single piece of material may become a reality in the not too distant future. These examples serve to illustrate the dynamic nature of the aerospace industry. As long as the demand for new techniques exists, the advancement of manufacturing technology will be a continuing process.

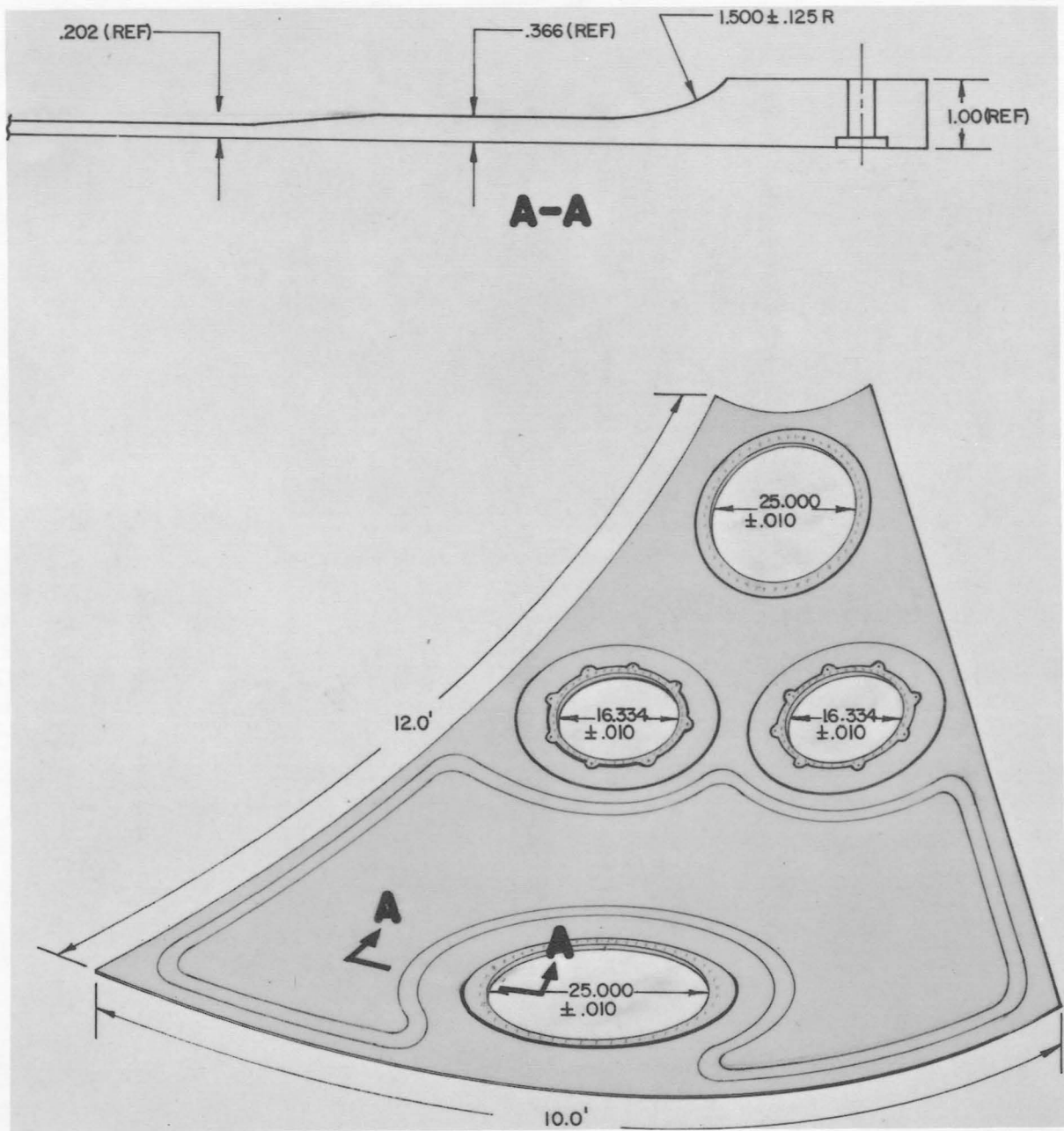


FIGURE 14.—Sketch of 2219 aluminum alloy gore apex showing integrally machined fitting outlets.

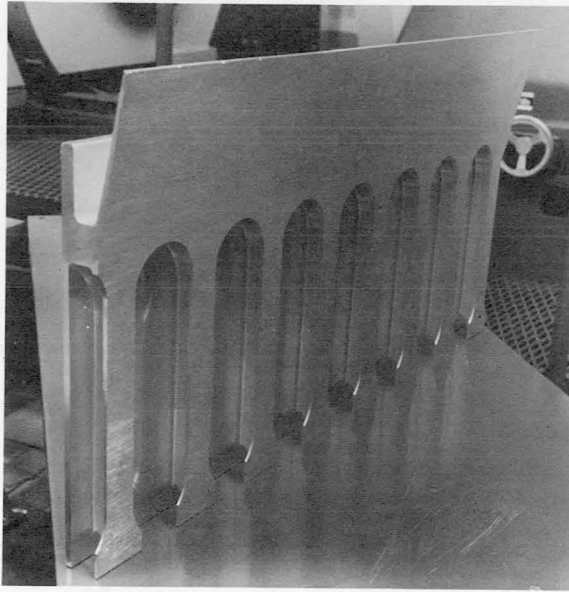


FIGURE 15.—*Tee-stiffened 2219 aluminum alloy
Y-ring segment.*

8. Orbital Tube Flare for Tubing Connectors

JAMES R. WILLIAMS

George C. Marshall Space Flight Center, NASA

Marshall engineering personnel have developed and are now refining a new and unique method of mechanically flaring tubing. The system eliminates the use of the conventional split backing die which is used with most tube-flaring equipment.

The Marshall-developed tool is adapted for use on standard Leonard 3-CP-HD flaring machines. The stationary split backing die is replaced in function with a die ring, whose i.d.-surface rolls or orbits around the o.d. of the tube flare zone. An i.d.-flaring cone moves axially and forces the metal against the rolling die to form the flare.

Major advantages of this system are the elimination of flash, or split die marks, on the back angle of the flare, and improved flare-surface finishes, permitting more uniform sealing characteristics and improvements of the total geometric configuration of the flare as required by the MSFC specification MC-146.

The Orbital Adapter system of tooling is currently being used to manufacture flared tube hardware for the Saturn V S-IC space launch vehicle at MSFC, for the Agena space launch vehicle (used for the Gemini project) at Lockheed, Sunnyvale, for LEM checkout equipment for Grumman, and for the Saturn S-IV-B space launch vehicle by Douglas Aircraft Company. Several other aerospace firms are evaluating the system for possible incorporation on their tube flaring requirements. Marshall engineers are now concentrating their efforts on refining and reducing the total cost of the overall system.

The theme of this symposium offers a rather large variety of subjects to be discussed. Today, we would like to review a method of tube flaring.

Tube flares can be produced by many different methods, such as mechanically, explosively, or hydraulically. In principle, tube flaring is not difficult and the complexity of any system is normally related to the quality of the flare required. Tube flares can be required for many reasons, but the major reason we need them at Marshall is to provide a leak-tight mechanical connection, which can be taken apart and reassembled on the pneumatic and hydraulic tube system on the Saturn space launch vehicle.

First, let us look at the location of the tube flare within the total flared tube connector. The tube flare connector under discussion is composed of the flared tube end, a sleeve, coupling nut, and coupling. The flare is conical in shape, and self-centering, and uses a wedge ac-

tion to increase sealing pressure as the mating parts of the connector are tightened (fig. 1).

Most automobiles have a connector similar to that illustrated on the hydraulic brake system. Such a system uses soft steel or copper tubing, and good sealing characteristics are obtained

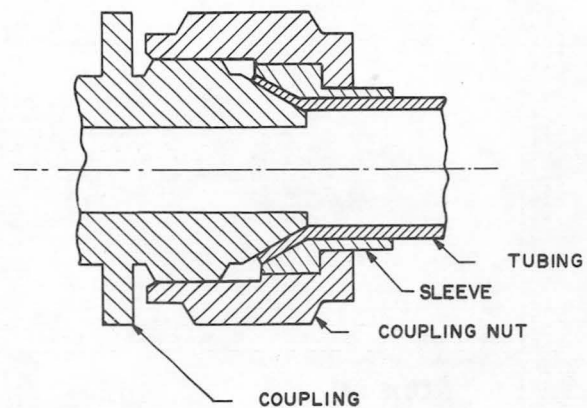


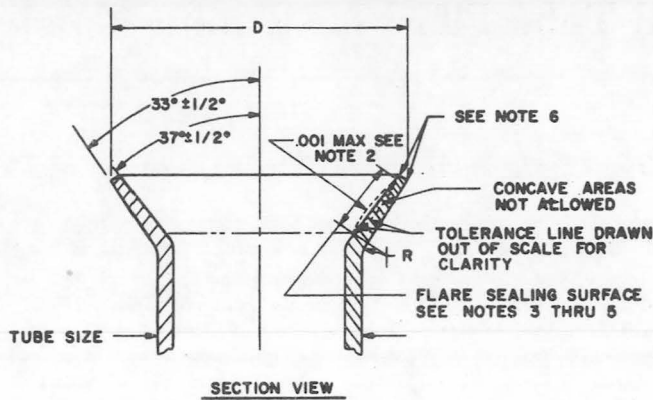
FIGURE 1.—Flared tube connector.



4730-239

FED SUP CLASS
NONE

NOTICE: When Gov't. designs, specs., or other data are used for any purpose other than in connection with a definitely related Gov't. procurement operation, the U. S. Gov't. thereby incurs no responsibility, nor does it warrant or represent that the Gov't. has furnished the said data for the purpose intended. The holder of this document may not reproduce it or otherwise use it in any manner without the prior written permission of the holder or any other person or corporation, or conveying any rights or permission to manufacture, use, or sell any patented invention that may in any way be related thereto.



©

TUBING OD	D DIA	D TOL	R RADIUS	R TOL.
1/8	.200			
3/16	.302			
1/4	.359		.032	
5/16	.421	+ .000		± .010
3/8	.484	- .010	.046	
1/2	.656		.062	
5/8	.781		.078	
3/4	.937		.093	
1	1.187	+ .000		
1 1/8	1.500	- .015		
1 1/4	1.721			
1 3/8	2.000			
1 1/2	2.375			
1 3/4	2.875			
2	3.375			
2 1/4	3.875			
3	4.375			

© SIZES 1 - 1/4 THRU 3 ARE INACTIVE FOR NEW DESIGN AFTER SEPTEMBER 1, 1964.

© NOTES:

1. THIS DESIGN STANDARD ESTABLISHES DIMENSIONS GOVERNING THE FORMING OF TUBE FLARES THAT ARE TO BE USED WITH STANDARD FLARED TUBE FITTINGS.
2. THE FLARE SEALING SURFACE SHALL NOT EXHIBIT CONCAVE AREAS BUT MAY HAVE A CONVEX CONFIGURATION OF A CONCENTRIC NATURE NOT TO EXCEED .001 AS INDICATED IN SECTION A-A.
3. FLARE SEALING SURFACE SHALL BE CONCENTRIC WITH OUTSIDE DIAMETER OF TUBE WITHIN .003 TIR PER MIL-STD-8 AND BE FREE FROM FLAWS AS DEFINED IN MIL-STD-10.
4. FLARE SEALING SURFACE ROUNDNESS TO BE WITHIN .0008 MAXIMUM DEVIATION AND NOT HAVE MORE THAN .0008 TOTAL ACCUMULATIVE INDICATOR CHANGE IN ANY 60° OF ARC.
5. THE SEALING SURFACE ROUGHNESS IN BOTH RADIAL AND TANGENTIAL DIRECTIONS SHALL NOT EXCEED 1/4 FOR STEEL TUBING OR 3/2 FOR AL ALLOY TUBING IN ACCORDANCE WITH MIL-STD-10.
6. DEBURR EDGES OF TUBING BEFORE FLARING; RADIUS OR CHAMFER AT EDGES MUST NOT EXCEED 20% OF THE TUBING WALL THICKNESS AND BE VOID OF CHATTER MARKS.
7. THERE SHALL BE NO RADIAL SCRATCHES ON THE FLARE.
8. DIMENSIONS ARE IN INCHES.
9. THIS DESIGN STANDARD IS NOT TO BE USED AS A PART NUMBER.

PROPOSED

CUSTODIAN		GEORGE C. MARSHALL SPACE FLIGHT CENTER Huntsville, Alabama	
PROCUREMENT SPECIFICATION	TITLE	DESIGN STANDARD	
NONE	© TUBING END, FLARED, STANDARD DIMENSION FOR	MC146	
COORDINATION STATUS		SHEET 1 OF 1	
MSFC <input type="checkbox"/>			

FORM 1 - Form 146-4 (Rev. 10-22-60)

APPROVED 1 JUN 61 REVISED (A) 26 JUL 61 (B) 7 MAR 63 (C) 30 JUL 64

FIGURE 2.—Flared tube design standard MC146.

with minimum torque, and pressure requirements are relatively low.

To review the requirements of the Marshall design standard for flared tubing which is identified by MC-146 specifications, see figure 2. The fine print defines the flare configuration requirements found necessary by experience and tests to provide a flare capable of providing the necessary sealing characteristics when internal pressures within the system range up to 4000 psi. The specification requires the flare angle to be $\pm 1\frac{1}{2}^\circ$, 0.0008-in. TIR on roundless and 0.003-in. concentric with the tube o.d. The i.d. flare surface can have no concavity and must be very smooth, that is, 16 microinches for steel and 32 microinches for aluminum.

The task for forming tube flares to MC-146 standards has been a difficult assignment for Marshall's manufacturing shops and the aerospace firms which are fabricating Saturn V high-pressure liquid and pneumatic systems.

The tube flaring tools which have been used in past years in most manufacturing shops basically consisted of an eccentric rolling center cone and a two-piece split backing die. Statistical records indicate that this system and its principle of forming produce flares which are borderline in geometric configuration when inspected against the Marshall MC-146 specification for flared tubing.

This paper describes a new mechanical system for flaring tubing now being introduced for use in the Marshall shops and at the Saturn V stage contractors. The process shows much promise of producing, on a high percentage basis, a flare as defined by the specification (fig. 3). For future reference in this paper, the tool will be referred to as an Orbital Flaring Adapter.

HISTORY OF FLARING TOOL DEVELOPMENT

The development of the system has an interesting history. The initial effort on the basic mechanical principle was started at Marshall in 1961. This principle uses roll-forming techniques for metal, where the material is reduced in thickness between opposed rolls. A prototype unit, known as the Saturn flaring machine,



FIGURE 3.—*Split die and orbital adapter. Left—Split die system; Fwd—Split-die tube clamp; Rear—Center flaring cone. Right—Orbital flaring adapter; Fwd—Iris tube chuck and spanner wrench; Rear—Orbital flaring head.*

was built and successfully produced tube flares to very close tolerances as required by MC-146.

Leak tests conducted with the flares produced on the Saturn machine were also at a tolerable low rate. The Saturn flaring machine, because of its complexity and prototype nature and its many modifications, did not lend itself to production requirements. The major problem was repetition of machine settings for a given flare requirement. The final results of the Saturn flaring machine project are described in a Manufacturing Engineering Laboratory Internal Note R-ME-IN-63-6.

ORBITAL ADAPTER DEVELOPMENT

In 1963, the ME laboratory initiated a new program to exploit some of the flaring principles of the Saturn flaring machine and develop a new tool applicable to fabrication shop needs.

A prototype orbital flaring adapter for 1-in. o.d. tubing was conceived, built, and successfully tried out in February 1964. Based on an

evaluation of this prototype tool, a production type of orbital adapter tool was designed, built, and is now being used here at Marshall to manufacture flight-quality flared tubing. Orbital adapters for 1/8-in., 1/4-in., 3/8-in., 1/2-in., 3/4-in., and 1-in. o.d. tubing are the sizes currently being used.

The basic design of the tool is applicable to any size or type of metal tubing requiring flaring and extends the normal elongation capability of most materials because of the opposed roll technique of forming the flare. The design of this orbital flaring tool has been adapted for use on the commercially available Leonard 3CP-HD flaring machines which are in major use here in the Manufacturing Engineering shops.

Orbital Adapter Components

The following items were designed and comprise the basic components of the orbital adapter flaring system now being used; figure 4 shows:

1. An eccentric rolling center cone with axial movement
2. An orbiting rolling backup ring
3. A self-centering chuck for holding the tubing.

Orbital Flaring Tool Design Considerations

Based on earlier work on the prototype tool, several design characteristics were established and incorporated into the configuration of the orbital adapter tools now in use:

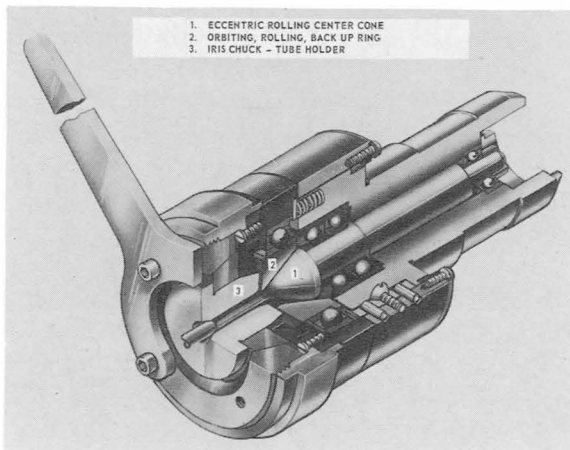


FIGURE 4.—Orbital flaring adapter.

1. The tooling was designed to be adaptable to the existing Leonard 3CP-HD machines in the Marshall shops, thus capitalizing on the use of commercially available equipment.
2. The basic adapter head does not require mechanical adjustment by the machine operator. This has been accomplished by manufacturing a separate orbital adapter for each required outside diameter of tubing, but each size of tool can accept any normal type of material or wall thickness of tubing.
3. Special efforts were made to design a rugged bearing system using low-cost ball bearings available at most bearing supply houses. The four SKF Catalog bearings required for the orbital adapter cost approximately \$16.00.
4. The problem of flare concentricity to tube o.d. was controlled by designing a variable-diameter gripping chuck which centers the tube o.d. in the correct position to the flaring mechanism. This relationship is locked in place during the actual flaring cycle by requiring the rotating head to revolve on the face and i.d. surface of the porous bronze wear-plate attached to the tube chuck.
5. The location of the tube, or the projected length of the tube to be flared, is critical within a few thousandths of an inch. The existing tube stop design did not provide a precision controllable adjustment. A micrometer-type adjustment has been incorporated into tube stop of the flaring machine.
6. The number of parts were kept to a minimum, and variations of material hardness were controlled to prevent galling of sliding surfaces. Where possible, close-tolerance parts were designed to permit the tool maker to produce critical surfaces from the same setup.
7. Special consideration was given to the center flaring cone to minimize shaft deflection under load. This was accomplished by increasing the flaring cone shaft diameter and controlling the loca-

tion of the bearings to minimize cantilever loading on the cone end of the shaft.

Operation of the Orbital Flaring System

Figure 5 illustrates the relative movement of the major components of the unit as viewed from the end and side. At the start of the flare cycle, the center cone moves axially and makes contact with the tube end. The rolling center cone is used to form the i.d. surface of the flare in a manner similar to the conventional split-die system. The flaring center is eccentric relative to the stationary tube, but is designed to move axially and to form the i.d. flare surface by an oscillating rolling movement. At 90°, the orbiting cone has moved forward and is beginning to rotate about its own centerline by frictional contact with the tube. The main drive spindle provides only the rotational movement to roll the eccentric cone around the tube i.d.

The axial movement also permits precision flares, to MC-146 standards, to be made on the 1/8 in. diameter tube as well as the larger sizes. Eccentricity of the center flaring cone increases as tube diameter increases, permitting a cone

section of adequate cross section to form the heavier gage material specified on some of the large diameter tubes. As the center cone continues to move forward and the flare begins to form, a second friction force is established and causes the orbiting die ring to roll around the o.d. of the tubing in a fixed plane. The backup ring and the center cone are keyed to remain in radial register, thus keeping the rolling surfaces which contact the flare diametrically opposed. The center hole in the orbiting ring is larger in diameter than the o.d. of the formed flare, thus permitting the enlarged end of the tube to be withdrawn through the hole in the die ring when flared. The i.d.-edge profile of the orbiting ring matches the o.d. profile of the flare. With each revolution of the cone and ring an additional quantity of flare will be formed. Normally, it takes approximately 10 revolutions to complete a flare.

Electronic Control Console

In addition to the orbital flaring adapter, it was recognized at the start of the program that it would be necessary to closely control the number of revolutions of work required to form a

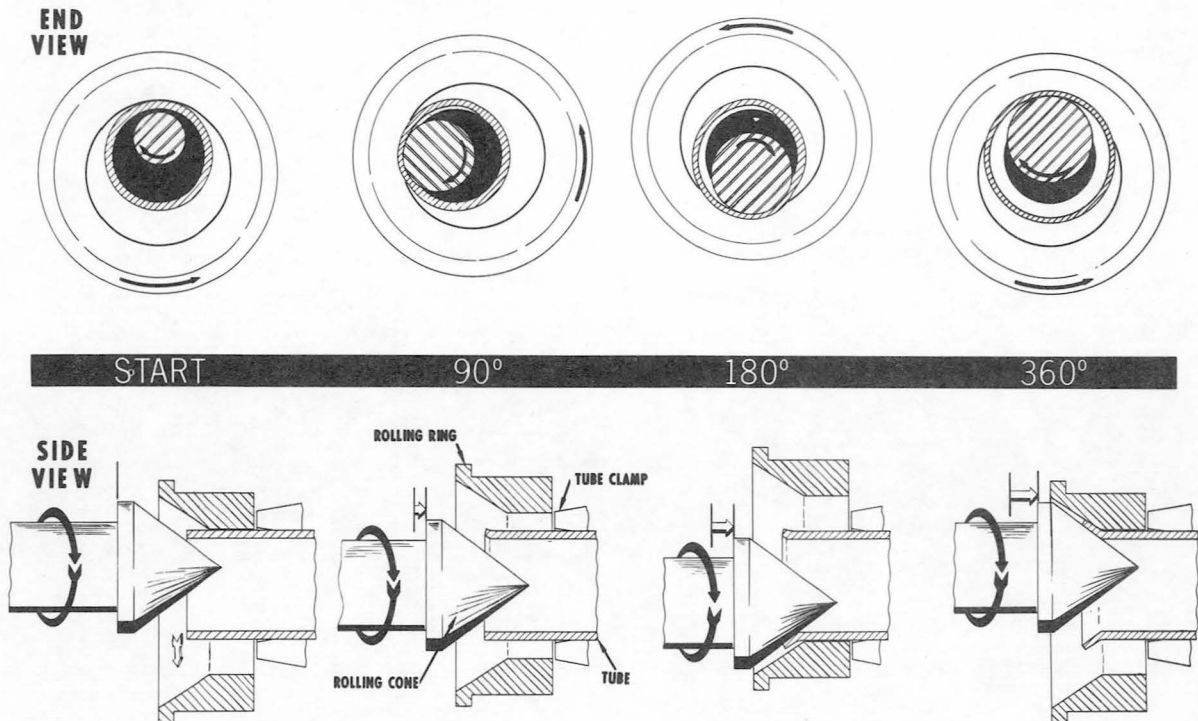


FIGURE 5.—Sequence of flare generation orbital adapter.

given flare configuration at a specific pressure and within a defined time frame. This required control is accomplished by use of a Marshall-designed and built electronic console (fig. 6) which is electrically wired to the flaring machine. It performs several functions. First, it is used to indicate the rpm of the drive spindle when adjusting or setting the flaring machine spindle speed; then, it is used to count and control the number of revolutions of the flaring head during the forming operation.

The unit also registers the applied pressure of the center flaring cone on the tube surface being flared. This was accomplished by strain-gaging the torque handle of the flaring machine and transferring the deflection values electrically into the console. Correct pressure values or settings, plus high and low limits, are empirically determined for each flaring requirement. The orbital flaring adapter and the control console, as described, provide the operator with a system of semi-automatic and precision control over all phases of the flaring operation.

Console Electrical Operation

Figure 7 illustrates a block electric diagram of the console. The unit is operated by a stand-

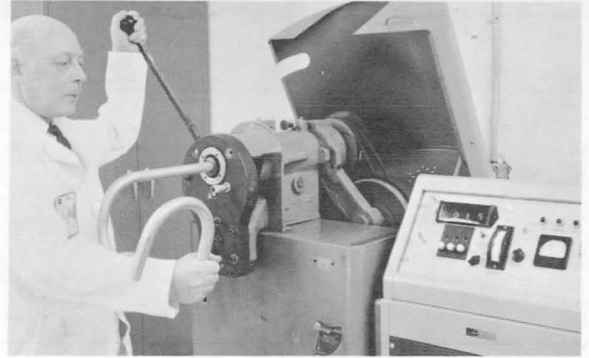


FIGURE 6.—Operator using total equipment. Left—Orbital flaring adapter inserted into a standard Leonard-3CP-HD tube-flaring machine. Right—Electronic control console. Attached accessories on machine are torque handle (operator's left hand) and timing wheel at rear of drive spindle.

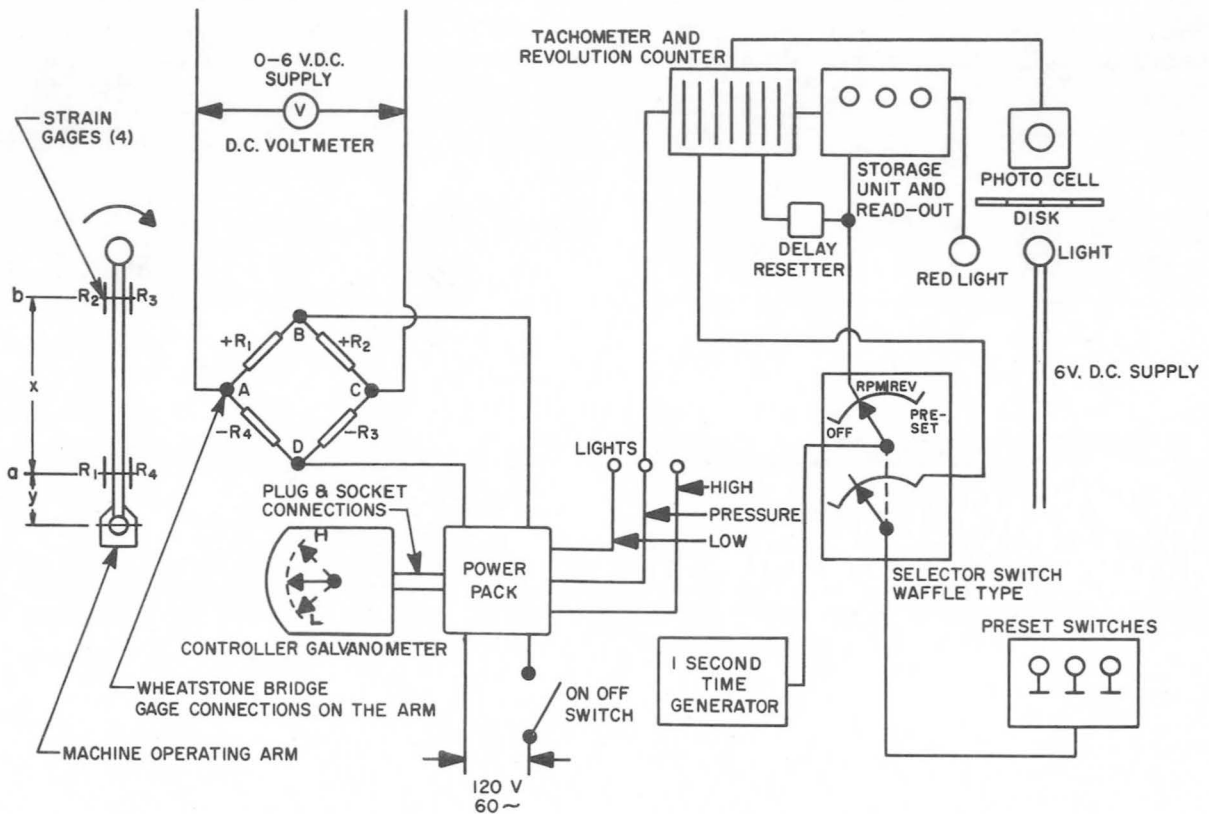


FIGURE 7.—Electric-block diagram of the console.

ard 120V 60-cycle power supply. The unit is partially controlled by a photo-cell receiving light impulses from a separate 6V d-c power source, and the output of 4 semiconductor active strain gages mounted on the torque handle. These gages are connected in a Wheatstone bridge circuit, as shown, and have a separate 6V d-c power supply.

The manually positioned controller-galvanometer has three settings for pressure or predetermined force to be applied to the operating arm: high, low, and correct.

The preset switches, as shown in the diagram are manually set for the established number of revolutions of work necessary to produce the MC-146 specification flare required.

The selector switch is positioned on the "Preset" point during the actual flare-forming process. To obtain the number or revolutions per minute, as previously determined for the particular specification flare under consideration, the selector switch is turned to the rpm pointer. The storage and read-out unit will then show in lighted digits the actual number of rpm at which the machine is operating. Necessary corrections to spindle speed are made by adjusting a variable speed pulley mounted on the drive spindle of the machine. The storage and read-out unit indicates the rpm speed by means of a photocell receiving light impulses through small diameter holes in a steel disc mounted on the spindle shaft of the machine. There are sixty evenly spaced holes in the disc, drilled on a common diameter circle. Therefore, the number of holes going past the light in one second is equal to the number of revolutions of the disc per minute. The time interval equal to one second is supplied to the counter through the selector switch by the 1-second time generator.

Due to the positioning of the strain gages on the operating arm and the method of their connection in a Wheatstone bridge circuit, the bridge output will be proportional to the difference between the bending moments taken at the gage locations on the operating arm with respect to the center of the torqued shaft. This holds true regardless of the point of application of the force producing the bending moments,

provided it is on the outside of the first pair of gages.

The strain gages have sufficiently high output to permit the pointer of the controller-galvanometer to close a mechanical contact and energize one of two relays in the power pack. Closing of a relay lights either the "high" or "low" pressure lamps, thus indicating whether the force on the operating arm should be increased or decreased.

When the operating arm pressure is correct, and the middle pressure lamp is lit the revolution counter starts to count the pulses it receives from the photocell and to transmit these pulses to the storage and read-out unit. When the number indicated by the lighted digits in the storage and read-out units becomes equal to the previously selected number on the preset switches, the counter stops transmitting the pulses to the read-out unit, and a red lamp lights. This light is an indication to the operator to release all pressure on the operating arm, because the flare-forming process is completed.

RESULTS OF ORBITAL ADAPTER FLARING TECHNIQUES

As of this date, we have formed several thousand flares using $\frac{1}{8}$ in. through 1 in. size adapters. No major difficulties have been encountered in producing a quality flare when the adapter head and components conform to the tool design drawings and are operated properly. We are currently producing flares, following the MC-146 specification on a very high percentage basis. The most encouraging aspect of the entire program is the consistently narrow band of values obtainable for each measured characteristic. We are now at a stage of establishing the optimum series of settings for each flare and material requirement. Minor electrical and mechanical refinements are also being incorporated into the flaring system which will bring the band of controlled values closer to MC-146 nominal requirements. Development efforts are now being directed toward automating the total flaring cycle based on values established with the use of the electronic control console. Emphasis will also be placed on developing an economical automation system.

Internal and External Angle

The item requiring the greatest amount of development in the orbital adapter tooling was the geometric definition of the tool surfaces which control the 33- and 37-degree angles. It was necessary to try several combinations of tooling angles with variations of forming pressures and the number of revolutions of work. Normally, the band of variation was narrow for a particular set of conditions. The problem then becomes one of balance where the angles, surface roughness, and flare o.d. are adjusted to bring the total flare configuration within tolerances as defined by MC-146. See figures 8 and 9.

Surface Roughness

The surface finish produced on the flare i.d. (fig. 10) usually fails in the 5- 10-microinch range. No polish operation is required after flaring.

Any nicks on the o.d. of tubes are usually rolled smooth during the flaring operation producing a finish which is usually equal to i.d. finishes. Although the current MC-146 specification does not fully control the backside characteristics of the flare, it is felt important to produce a smooth surface free from surface roughness, split-die flash, or configuration offset. The backside surface quality inherently produced by the roll-form technique becomes an advantage toward optimum sealing conditions.

Roundness of the Flare

The MC-146 specification requires the roundness of the flare to be within 0.0008 in. TIR. Flares produced by the three aerospace firms and Marshall using the split die system had results meeting specification approximately 80% of the time. Normally, flares produced with the orbital adapter system of flaring will

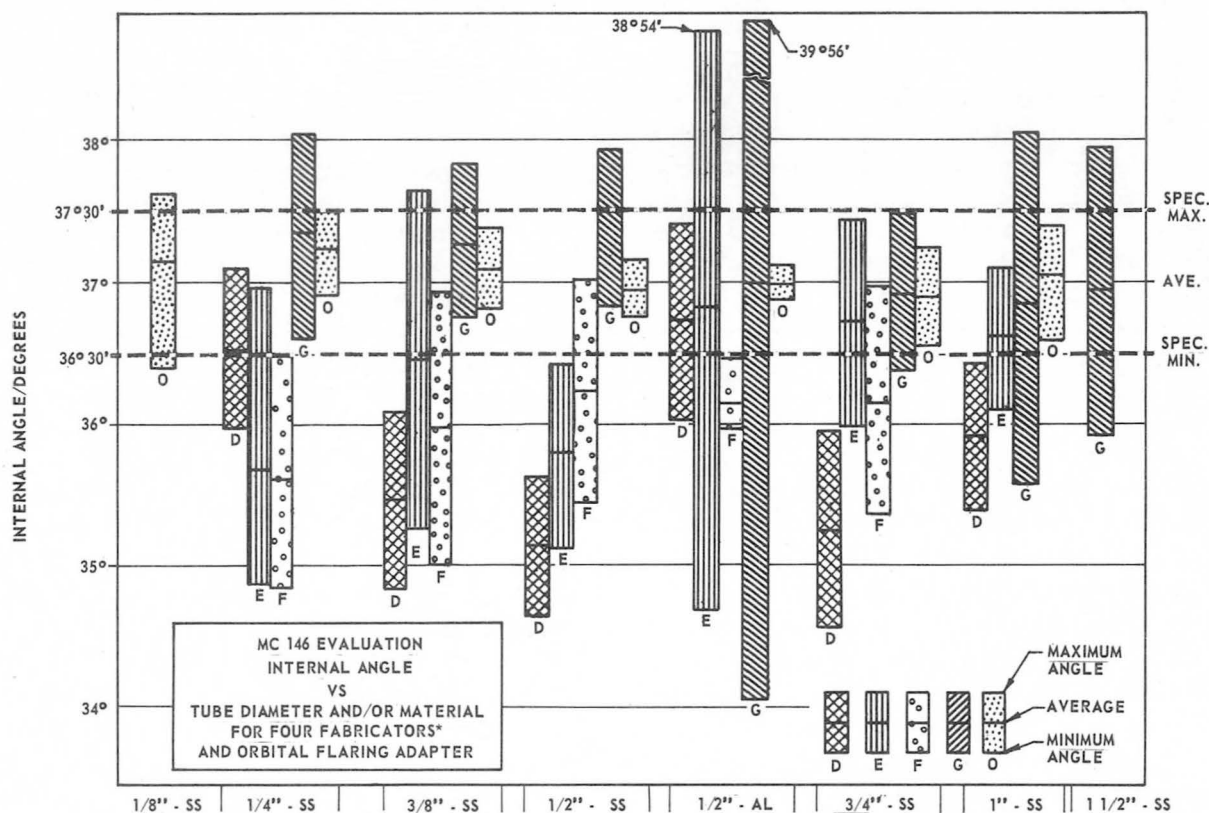


FIGURE 8.—Graphical illustration showing tube-flare internal angle measurements as obtained from statistical recordings. Asterisk indicates use of split-die tooling.

exceed this 80% level. Inherent in the roll-flaring process, roundness is produced because of the uniform circular geometric movement of both tool surfaces forming the material. Roundness of the backside of the flare will match the i.d. side within 0.0002 in. to 0.0003 in. We believe this uniform-flare wall thickness adds to the potential sealing capability of any flare.

Concavity and Convexity of Flare Surface

The i.d. surface of the flare formed with the orbital adapter normally possesses a slight convexity of 100 to 300 microinches (fig. 11). This provides a line or ring contact which improves the sealing characteristic of the joint.

In a control program to study causes of flare-surface concavity, a center flaring cone was

ground 0.003 in. eccentric to its shaft and then used to flare (30) 1/8 in. o.d. and (30) 3/4 in. o.d. tubes. Approximately 75% of the i.d. flare surfaces exhibited some measurement of concavity. The cones were reground to design requirements, and the convex surfaces were again obtained. This point has been made to stress the importance of closely controlling the dimensional quality of components comprising the orbital head. It is a precision tool and must be treated as one.

Concentricity

Concentricity as defined by MC-146 is the relationship between the i.d. of the flare and the o.d. of the tube (fig. 12). Normally, flares produced by the roll-form technique will meet this requirement. Exceptions to this have been

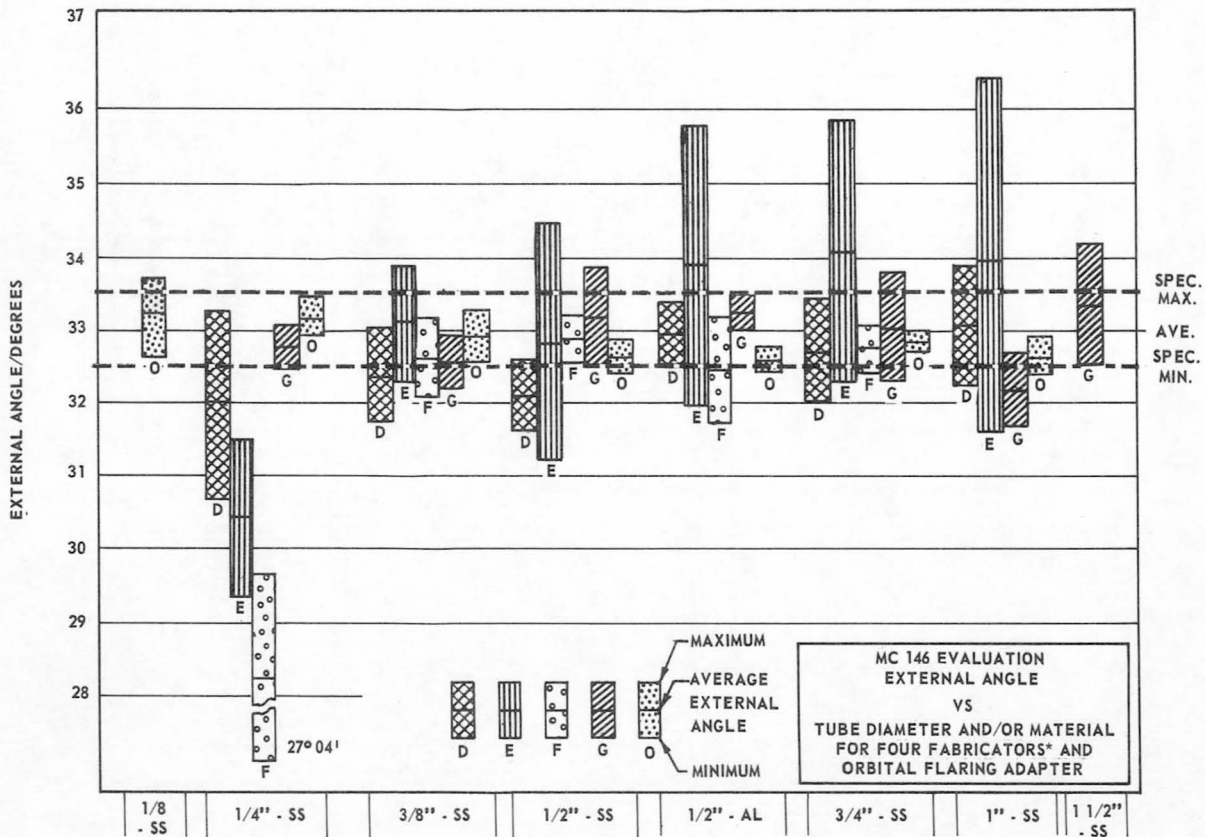


FIGURE 9.—Tube diameter and material—tube-flare external angle measurements as obtained from statistical recordings. Asterisk indicates use of split-die tooling.

traced to tool components which were out of design tolerance and allowed the tube to be positioned and held off of the rotational centerline of the flaring head. The backside of the flare is normally similar to the concentricity characteristic of the front side and adds to optimum sealing conditions.

Cracking of Material at Flare o.d.

The flare cracking problem that periodically occurs on $\frac{1}{8}$ in. and $\frac{1}{4}$ in. o.d. tube flared by the split-die technique is practically non-existent on flares produced with the orbital adapter. It is possible to roll-form flare surfaces 2 and 3 times their normal length before the material fails.

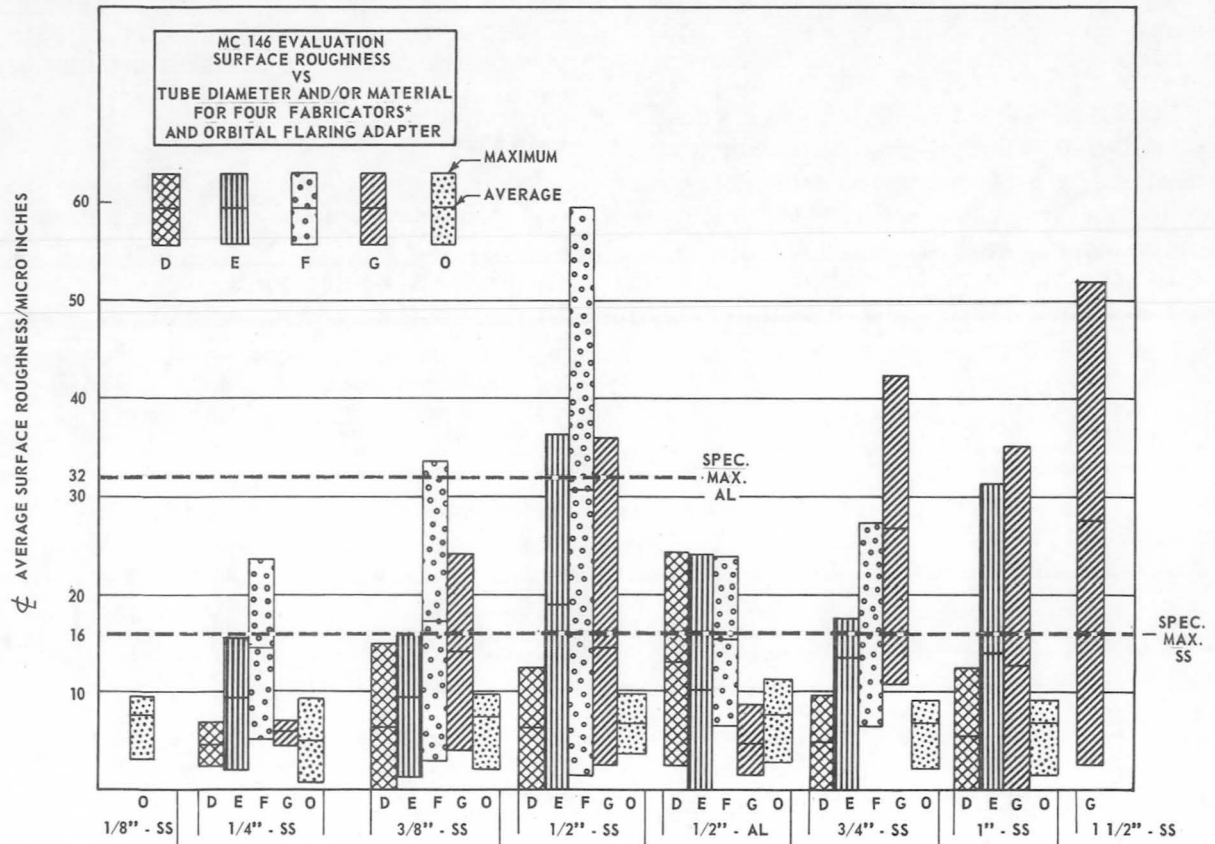


FIGURE 10.—Tube diameter and material—surface finish of tube flare measurements as obtained from statistical recordings. Asterisk indicates use of split-die tooling.

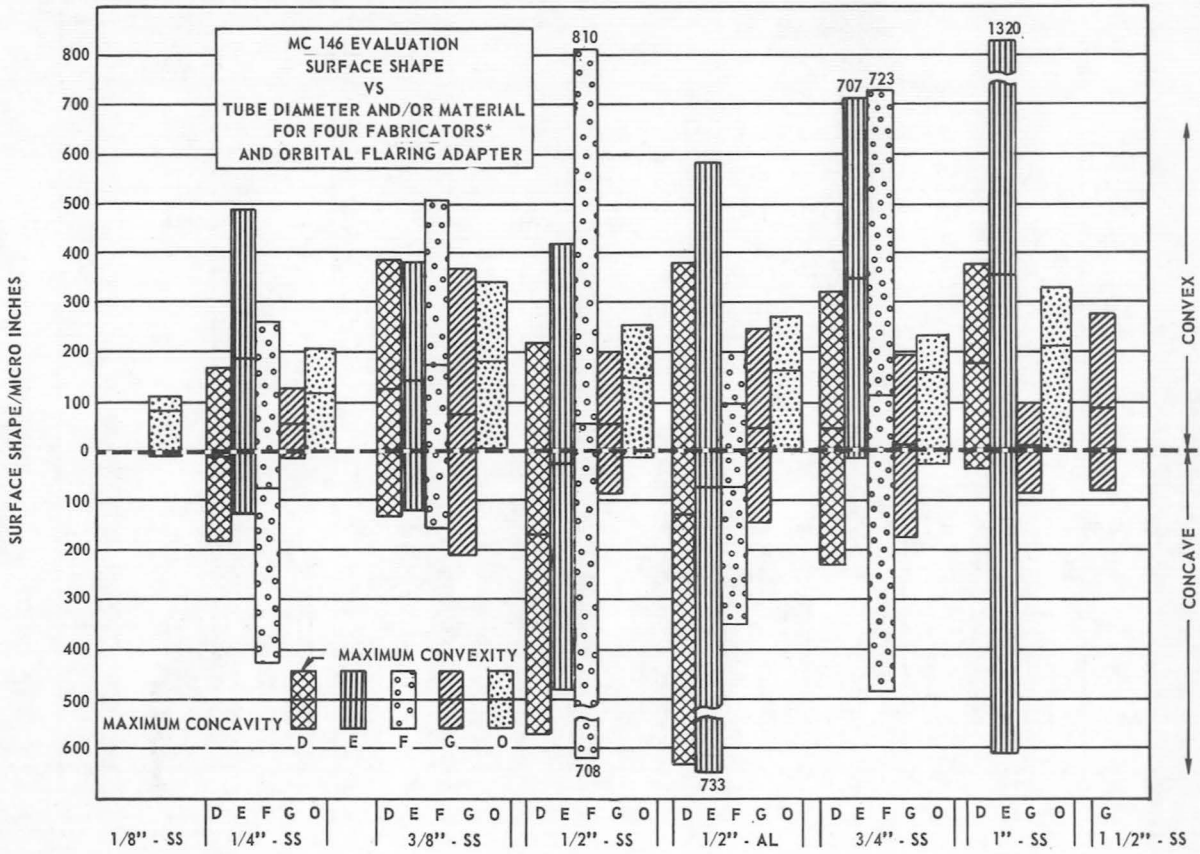


FIGURE 11.—Tube diameter and material—surface shape as obtained from statistical averages. Asterisk indicates use of split-die tooling.

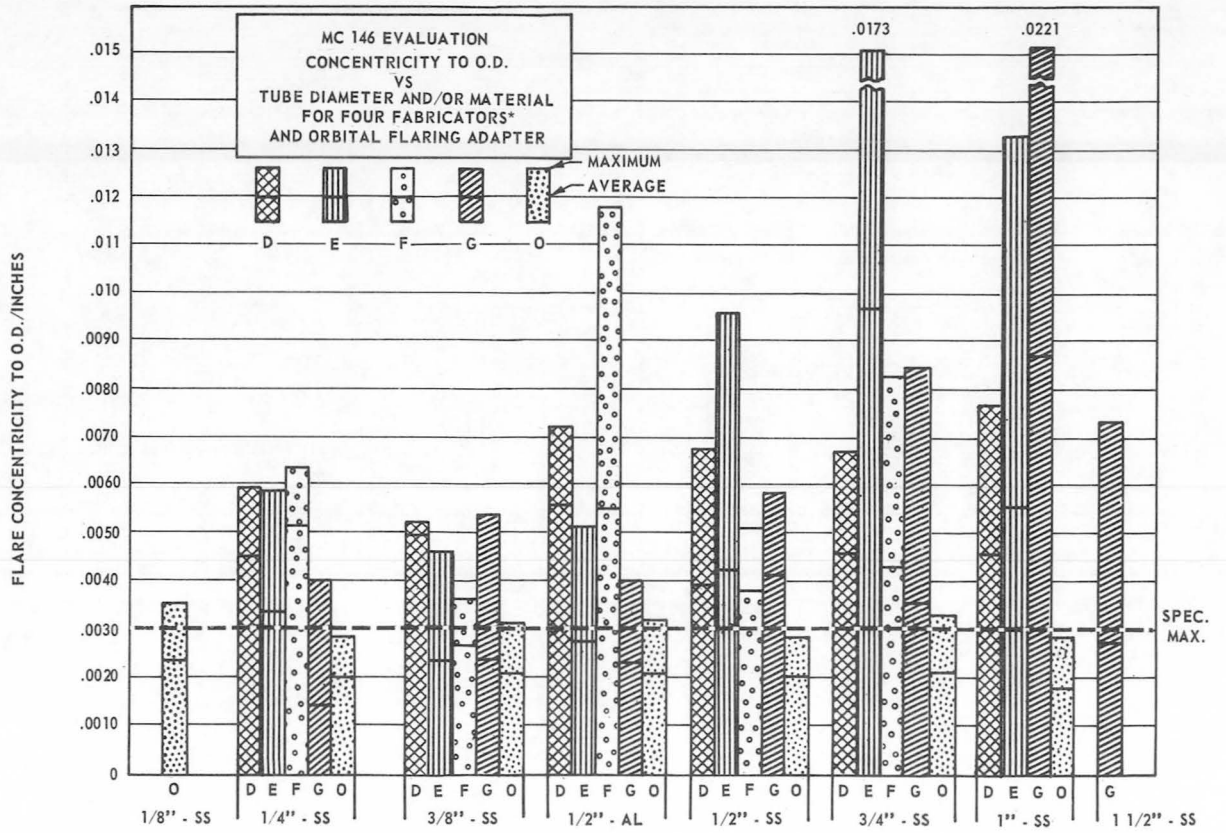


FIGURE 12.—Tube diameter and material—tube-flare concentricity to o.d. measurements as obtained from statistical records. Asterisk indicates use of split-die tooling.

9. Tooling Concepts for Assembly of Large Structures

R. HOPPE

George C. Marshall Space Flight Center, NASA

Manufacture of the S-IC stage of the Saturn V space vehicle has resulted in new concepts and innovations in the field of tooling. The structure size (35-ft diameter), the high reliability and accuracy requirements, and the low density or production quantity lead to a greater degree of simplicity, economy, and versatility in fabrication and assembly tooling. There are three specific concepts which should be applicable in industry, local jiggling for welding, rotation of structures in vertical assemblies, and the assembly of two structures.

The usual weld jiggling serves a two-fold purpose: (a) to support the molten weld puddle and (b) to force and maintain alinement of the parts being welded. The extension of this method to large-diameter tanks is expensive and difficult. An alternate procedure used at MSFC is to perform free-state welding and use local jiggling (strap-clamps) and intermittent tack welding.

Cylindrical structures can be accurately rotated for routing or welding on a simplified ring turntable. The tool consists of a ring of the structure diameter resting on rollers. Torque is nearly zero since the ring is rotated by friction rollers with the force being applied at the ring perimeter. Two such turntables are used at MSFC.

The horizontal mating of two large components, where controlled motions of small magnitude are necessary, can be easily done by positioning units equipped with air-bearings. Such bearings are usable on concrete of minimum surface preparation and require no special air pressure source. This concept is used in assembly of the two S-IC containers.

A brief history of the evolution of tooling philosophy at the MSFC will clarify the need and logic of present concepts for assembly of large structures and will perhaps help others avoid some of the pains in tooling-concept development.

The history starts with the Redstone and Jupiter missiles which have diameters of 70 and 105 inches, respectively. Structural and component assembly was done with the center axis of the cylindrical segments in the horizontal position. Welding was done in the conventional positions using round-out rings for sizing, jiggling, and supporting the weld. The tooling was successful and was neither bulky nor expensive. Moving to the 95-in.-diameter Jupiter was still considered practical with conventional tooling. The event of the S-IC vehicle, 33 feet in diameter and 4 times the size of the Jupiter,

stretched the practicality of unchanged tooling concepts. It became necessary to erect the container with its center axis in the vertical. Welding techniques had to be extended to horizontal and vertical modes seldom used in high-quality aluminum welding, but jiggling accuracy requirements did not lessen. Mating of parts, distortion control, and the like, were just as important in large vehicles as in small. Production density was too small to justify the cost of large, complex tooling patterned after the Redstone.

NEW CONCEPTS

New concepts that would provide simplicity, economy, and versatility were in order. A new philosophy was evolved which (1) placed greater responsibility on electronic and welding equipment, thus allowing less complex and ac-

curate tooling, (2) omitted superfluous tooling details not really pertinent to functional requirements, and (3) stimulated new or different tooling concepts. It is not the purpose of this paper to discuss the complete system in detail but to present some of the less abstract tooling concepts to industry.

Three specific concepts should be applicable in industry: (1) local jiggling for welding, (2) rotation of structures in vertical assembly, and (3) horizontal assembly of structures.

Local Jiggling for Welding

The weld jiggling most often used in industry consists of round-out rings (in the case of longitudinal joints, backing, and support bars) and rigid clamping members (fig. 1). Jiggling serves a two-fold purpose: (a) to support the molten weld puddle and control solidification,

and (b) to force and maintain alinement of the parts being welded. The extension of this method to large-diameter tanks is expensive, and it is difficult to accomplish the necessary degree of jiggling.

An alternate procedure (used at MSFC) is to perform free-state welding and use local jiggling (strap clamps) and intermittent tack welding.

Free-state welding, that is, welding without puddle support, became practical in materials as thin as $\frac{1}{8}$ in. through improved power sources and electronic controls. But removing the puddle support only insured more uniformity of solidification and did not lessen alinement of parts. The old principle of strap-clamps, not unknown in large tank construction, is effectively used to aline parts, as in figure 2. A number of these devices may be applied at

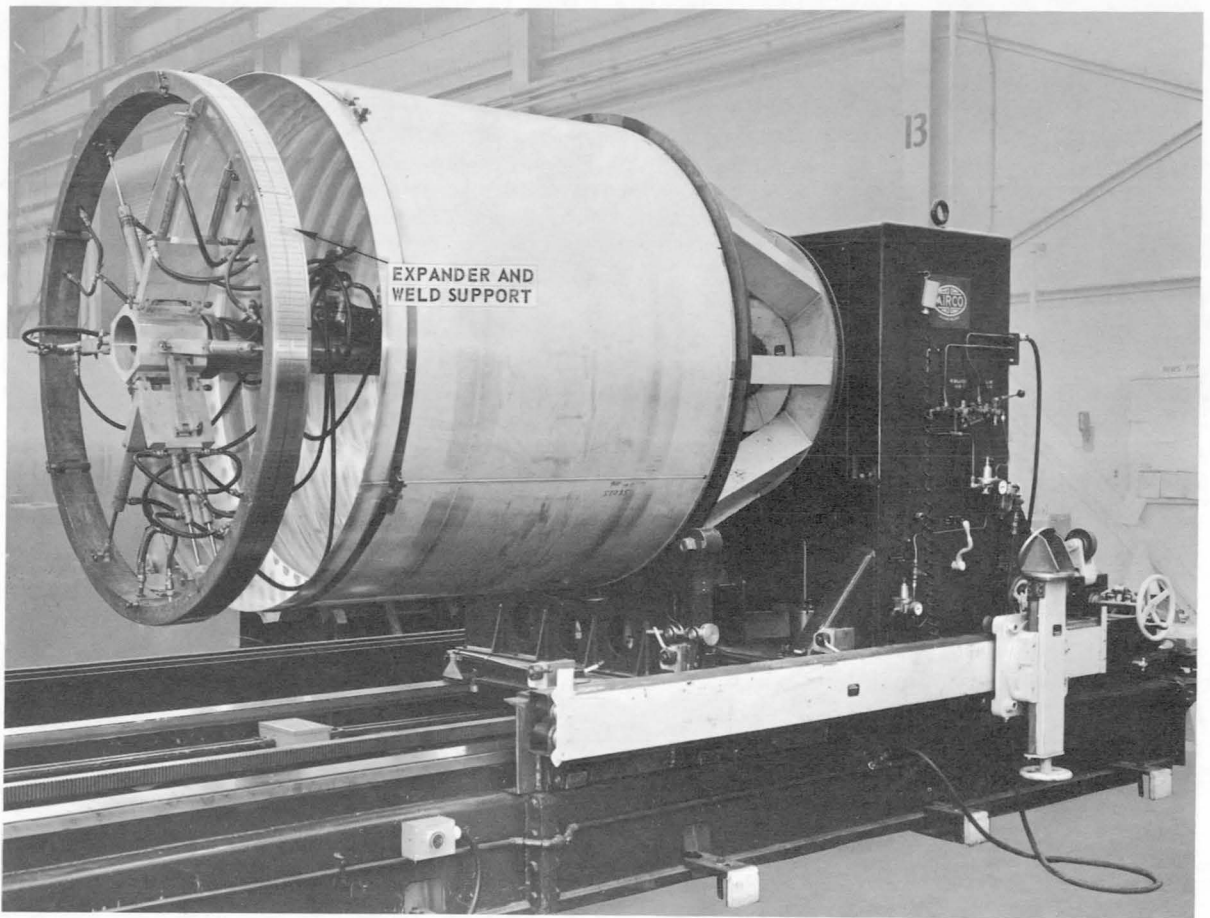


FIGURE 1.—*Conventional tooling concept.*

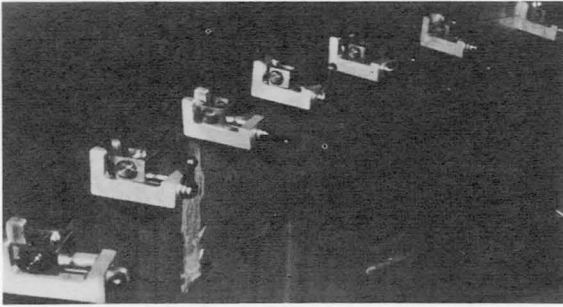


FIGURE 2.—Application of strap clamps.

intervals around the two cylinders to be joined, and are presently adjustable to material thicknesses up to $1\frac{1}{2}$ in. without change of operational procedures. Each tool consists of a retainer, a stainless steel band, and a screw housing as in figure 3.

The theory of operation is that of a simple compressive mechanical device, with the two basic parts located on opposite sides of a weld joint and drawn together by tightening the thin band until the workpieces are aligned, as in figure 4. A weld joint separation of about 0.010 in. is required to install and remove the clamps. The device has a built-in shear to effect removal from a weld joint. The tool weighs $2\frac{1}{2}$ pounds and is constructed of nonmagnetic materials. It is designed to insure continued reuse in various applications.

A third requirement in jiggling is to maintain alinement during welding. This has been done by tack welding before removing the strap

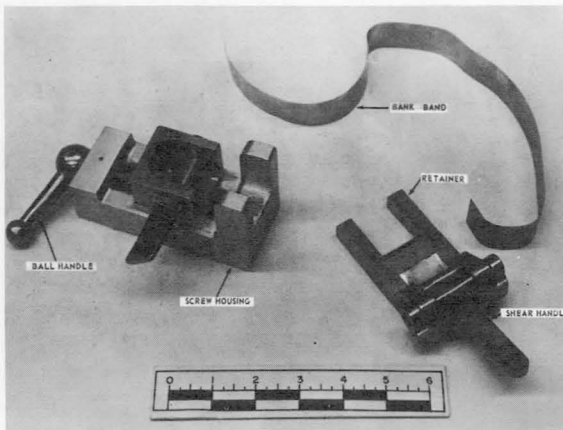


FIGURE 3.—Components and strap clamp.

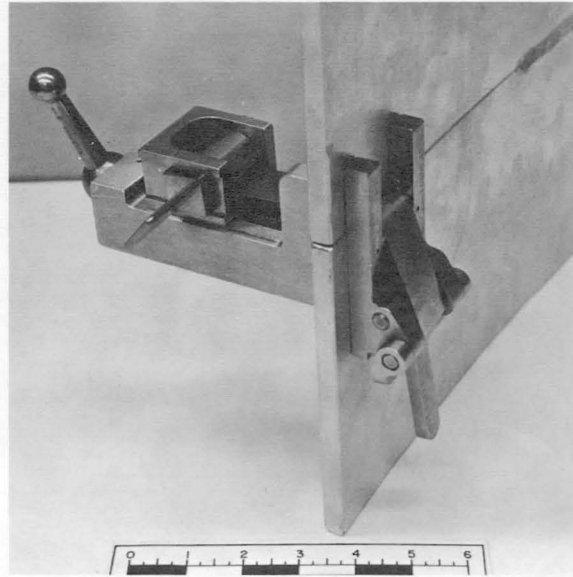


FIGURE 4.—Cross section of weld joint.

clamps (fig. 5). The combination of tack welds, strap clamps, and accurate weld equipment constitute a jiggling method that is economical, versatile, and accurate, and should be usable where tooling costs outrun production density or where component size exceeds normal tooling design.

Rotation of Structures in Vertical Assembly

The second tooling concept deals with the rotation of large structures, during the process of machining or welding. Such structures can be accurately rotated on a simplified ringturn table (fig. 6). The tool consists of a retaining-ring roller support, electrical drive motors, and associated controls. The independent support modules and motors can be repositioned for different diameter structures, requiring only the manufacture of corresponding retaining rings.

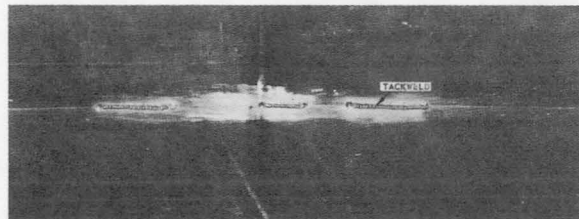


FIGURE 5.—DSCP-TIG tack welds.

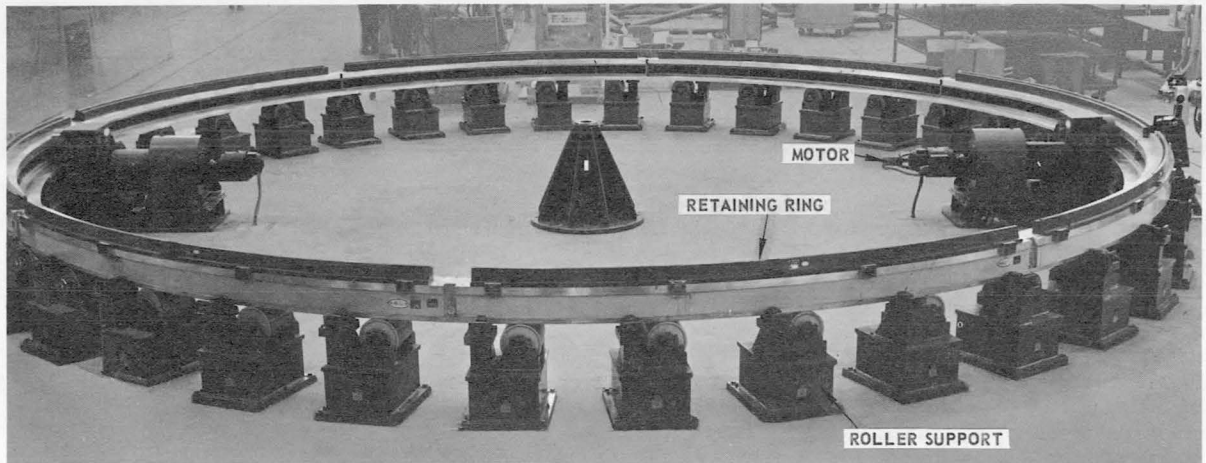


FIGURE 6.—Ring turntable.

Thus, the initial tool cost is reduced through simplicity, and the assembly is to a large degree versatile and independent of vehicle diameter.

The drive system consists of two Sciakydyne $\frac{1}{2}$ -hp motors and controls. The motors are wired in series. There are two pressure wheels per motor, one of which is driven. Approximate ring-travel speed range is from 2 to 60 ipm. The ring rotates in a plane within 0.002 inch. The routing and welding of bulkheads, Y-rings and cylinders of the S-IC stage have been accomplished on this tool. A similar tool is used for final assembly in the vertical assembly tower.

It is the tooling principle that is of major interest, namely, the use of independent tooling modules which can be re-arranged into several functional wholes, each whole serving a specific manufacturing task. Thus it is possible to conceive of tools for machining, welding, assembly and support, being formed from simple, basic modules, reducing cost and lead time in tool fabrication.

Horizontal Assembly of Two Structures

The third concept, applicable to the horizontal mating of many large structures, is that of air-bearing positioning units. Saturn V assembly tools are an example. The General Motors Defense Research Laboratories designed, fabricated, and tested the tools under contract to MSFC.

The following theory of operation is quoted from the operation handbook prepared by General Motors:

Hovair is a unique air-flotation device which combines the advantages of the standard air bearing (namely its ability to support large loads on low-pressure air and its low air-flow requirements) with the advantages of the air-cushion device, that is, its relative insensitivity to surface undulations and irregularities. Hovair's principal advantages over conventional means of support are its ability to provide omnidirectional, essentially frictionless motion in a plane normal to the load (hence, exceptional load maneuverability), its low load-support profile, and its lightening of the load to reduce surface-unit loading.

Figure 7a is a cross section through a simple air bearing, showing the lubricating air film. The air bearing supports large loads with small unit pressures. Its principal advantages are: low power requirements, low noise characteristics, and low surface disturbance (absence of dust and flying debris). An air source supplies a film of air between the support surface and the ground surface, but because this film is only a few thousandths of an inch thick, a very smooth-ground surface is required.

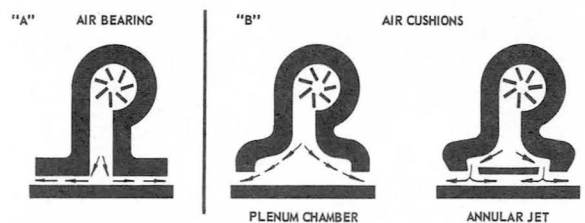


FIGURE 7.—Air-bearing and air-cushion devices.

Figure 7b is a cross section of two typical air-cushion devices that overcome the requirement for a very smooth-ground surface because of their higher operating clearances. The principal advantages of the air cushion are: relative insensitivity to irregularities and undulations in the ground surface and ability to negotiate large foreign objects in its path. However, its requirements for air flows are greater by orders of magnitude than those of the air bearing.

Figure 8 is a cross section of a Hovair pad depicting its ability to conform to surface undulations. It combines the advantages of the air bearing and the air cushion by employing a flexible diaphragm beneath the load-support surface. First, air fills the cavity between the diaphragm and the load-support surface and then escapes through the clearance between the undersurface of the diaphragm and the ground. The clearance between the diaphragm and the ground is only a few thousandths of an inch, but the distance between the load-support surface and the ground can be several inches.

Figure 9 compares the radial pressure distribution of the air bearing to that of the Hovair pad. Since the lifting force of both devices is determined by the product of the area and the integrated pressure, it

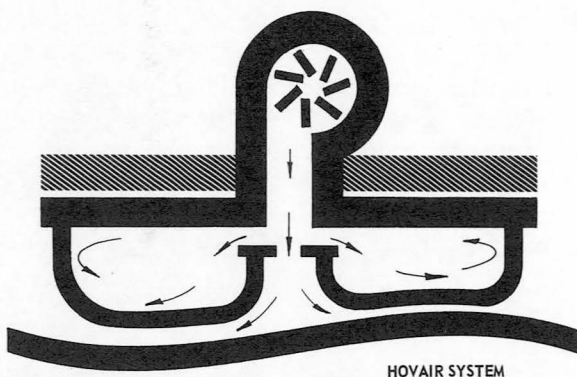


FIGURE 8.—Air-flotation device.

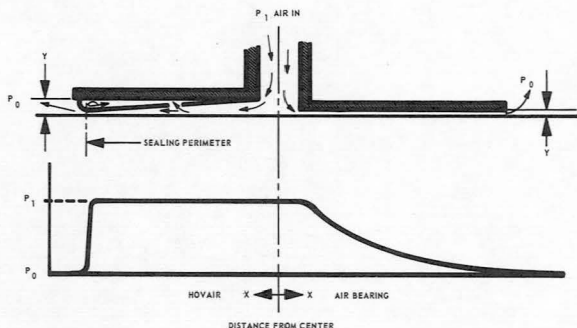


FIGURE 9.—Comparison of radial pressure distribution.

can be seen that the Hovair pad of equal size supplied with equal pressure will actually lift a much larger load than the air-bearing for the air clearances shown. It should be noted here that, while the air-bearing clearance is in the order of a few thousandths of an inch, that of the Hovair can be several inches from the ground to the rigid platform. Thus, it can operate satisfactorily over conventional factory-quality concrete floors.

General Motors has made an excellent structural application of this theory. Two separate tools provide 6 degrees of freedom for the final adjustment of the lox section and the thrust section of the S-IC stage of the Saturn vehicle (fig. 10). The air-bearing supports allow three degrees of adjustment in the horizontal plane (axial, transverse, and yaw): hydraulic jacks provide the remaining degrees of freedom of adjustment in the vertical plane (pitch, elevation, and roll).

The two elements of each Support Tool consist of:

- (1) A welded-steel structure with provisions for attachment of an interconnecting beam
- (2) An air-flotation system
- (3) A set of floor jacks, and
- (4) Hydraulic components, including hydraulic jacks for adjustment of the lox section.

The elements for both the tooling ring and the transporter support tools are typical except for the number of pad assemblies. There are four pad assemblies on the tooling ring support elements and six on the transporter support elements (see fig. 11).

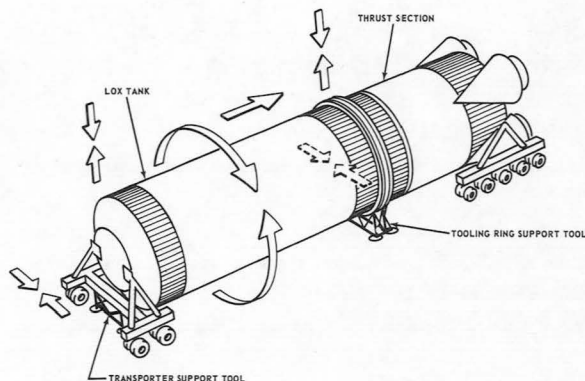


FIGURE 10.—Assembly adjustment.

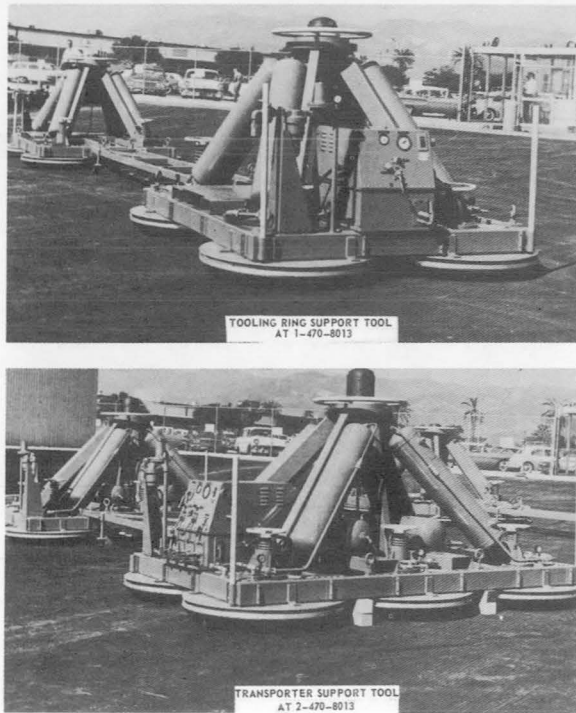


FIGURE 11.—*Transporter support tool.*

The welded-steel structure was designed to a specified load while supported by the pad assemblies during operation, or by the floor jacks during shutdown. A minimum safety factor of 2.5 (based upon yield strength) was used to compensate for possible uneven floor conditions. The interconnecting beams were designed to transmit the transverse forces exerted by the Saturn ground-location device to the support elements.

Each pad assembly is accompanied by a manual floor jack, whose function is to prevent a sudden settling of the lox section during the mating operation in the event of an inadvertent air-supply stoppage to the tool as a whole or from the failure of an individual pad.

There are two hydraulic jacks for each support tool to provide precise vertical positioning of the lox section during mating. The jacks are controlled from a control panel on the power pack for each tool. By selective operation of the four hydraulic jacks, pitch and roll motions are also provided.

Each of the two support elements in figure 12 contains a separate air-flotation system consist-

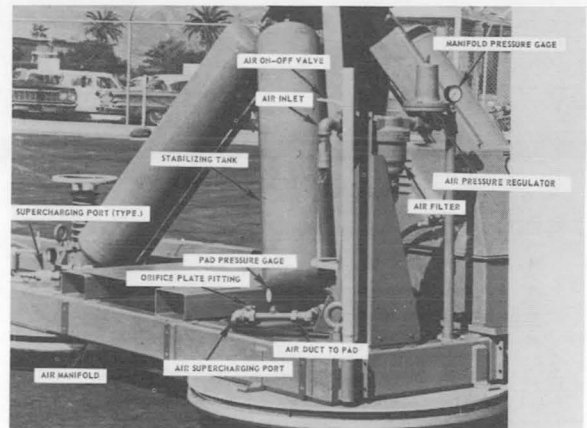


FIGURE 12.—*Pneumatic controls.*

ing of inlet plumbing with on-off valve, moisture trap or air filter, pressure regulator, flow-control orifices, pneumatic stabilizing tanks, provisions for supercharging individual pads, and the air-flotation pad assemblies.

A quick-disconnect fitting accepts an external air supply. Incoming air, at 65 psig and 15 scfm per pad, is dehydrated, and pressure is regulated to insure a constant manifold pressure of 45 psig. See figure 13. Operating pressure is a direct function of the load, resulting in pressures of approximately 6 psig for the tooling-ring support tool and 9 psig for the transporter support tool. The operating pressures will vary slightly among the pads due to an anticipated floor irregularities and manufacturing tolerances.

The pressure-regulated air is transmitted to the pads through an air-tight element-base structure manifold (the rectangular box beams

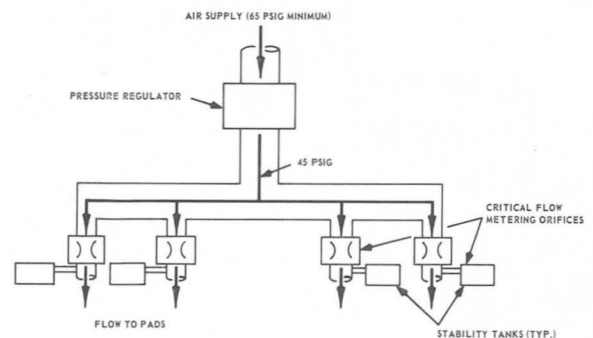


FIGURE 13.—*Air-control system.*

serve as air ducts) and through individual orifice plates. A stabilizing tank is vented to each pad air-supply line downstream from the orifice plate. The combination of a regulated manifold

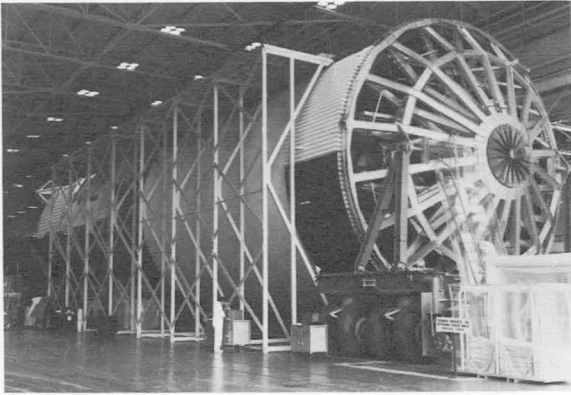


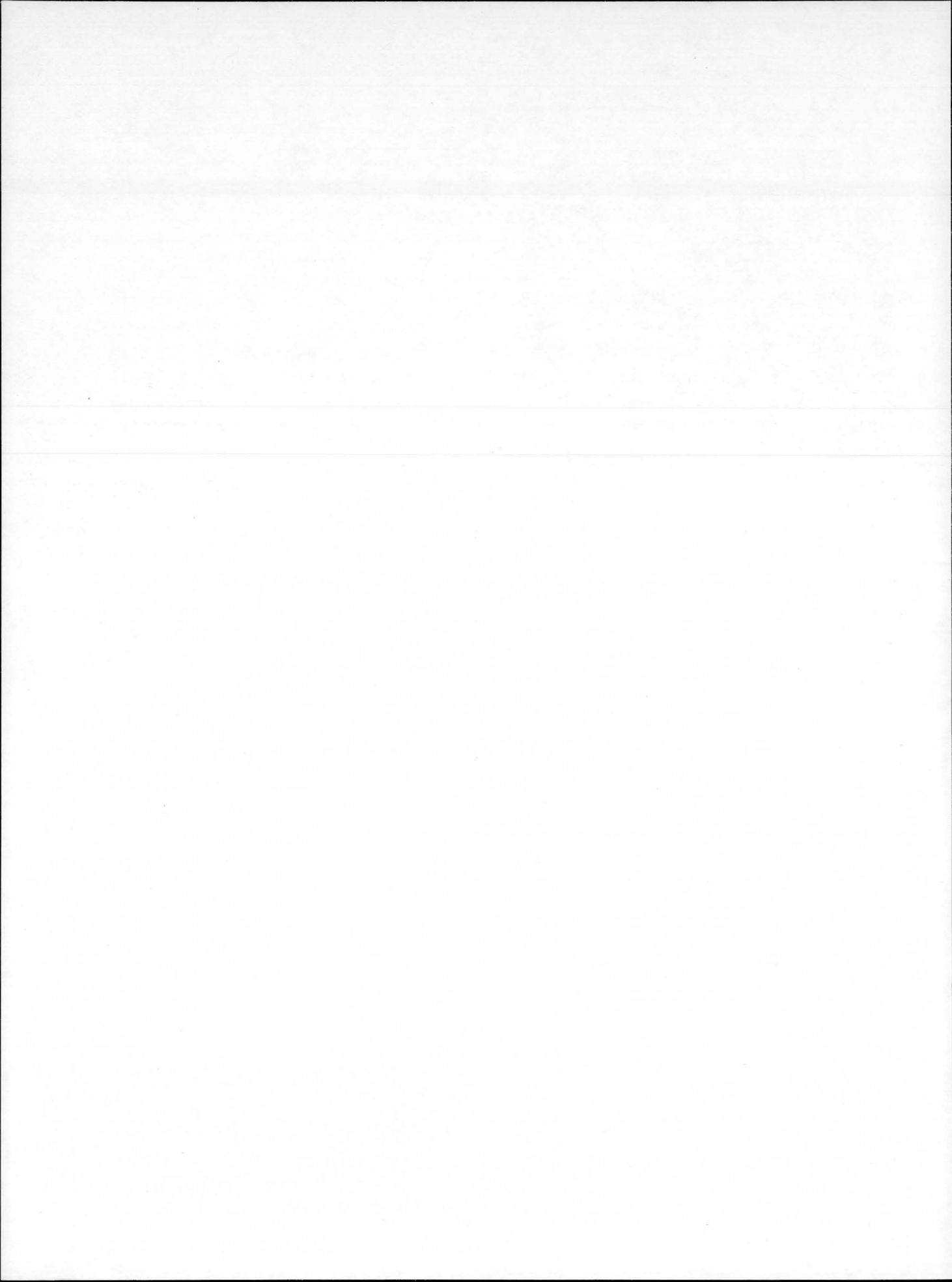
FIGURE 14.—*Lox section and thrust section assembly.*

pressure plus a critical-flow orifice and stabilizing tank assures essentially constant flow to each pad at all times. This arrangement makes the flow and pressure at each pad completely independent of the action of any other pad.

Figure 14 is a photograph of a lox and thrust-structure assembly. Some 25 000 pounds were supported by the air-bearing system. Yet the vehicle components were readily moved into assembly position, requiring less than 200-pounds horizontal force.

CONCLUDING REMARKS

The detailed procedure of the lox and thrust-structure assembly is well documented, and the pertinent point is that it is an example of applying the principle of air-bearing supports. By such tooling, large and heavy structures are easily maneuvered into precise assembly position.



10. Sliding Electrical Contact Materials

J. C. HORTON

George C. Marshall Space Flight Center, NASA

The results of research programs to develop sliding electrical contact materials, both brushes and slip rings, are discussed. Problems attendant to operating sliding contacts in a vacuum are defined; limitations of commercial materials in solving these problems are described, and special materials and surface finish conditions which have resulted in solutions to these problems are presented. Data from operational tests on the newly developed materials are compared with similar data obtained from materials now used as standards in consumer products. Possible commercial applications of the more efficient sliding contact materials are discussed briefly.

The majority of the work done on sliding electrical contacts has been directed toward obtaining a solution to a specific problem relating to space vehicle development. Much of the work has been done under conditions simulating the environment of space. Nevertheless, there are several areas of investigation which have potential commercial applications and should be of general interest. One of these is a program to develop materials for use as electrical brushes in motor-generator type apparatus operating under high vacuum. The second is the development of materials for low-noise, miniature slip rings for use in the vehicle-guidance system.

The electrical-brush development program has been entirely an inhouse effort. The miniature slip-ring program was conducted as a joint inhouse, contractor effort with the IIT Research Institute of the Illinois Institute of Technology in Chicago.

ELECTRICAL BRUSHES

Electrical brushes are used to transfer electrical current from the stationary frame to the rotating armature of an electric motor. They are mounted in holders attached to the frame of the motor and are spring loaded for a firm contact with the commutator portion of the

armature. The brushes must be capable of conducting an electric current and providing lubrication for the contact surfaces between the stationary brush and the rotating commutator.

The first motors and generators used brushes made of many small copper wires similar in configuration to a paint brush. This originated the term brush, and it is generally applied to any device which transfers current from a stationary to a rotating body. The brushes were not very efficient and had a short wear life. Fortunately for electric motor manufacturers in particular, and the industry in general, not long after the electric motor emerged from the laboratory, it was discovered that there was a material already in existence which was ideally suited for electrical brushes. Graphite, a form of carbon, possessed both electrical conductivity and excellent lubricating qualities and provided a long, trouble-free life. It was relatively inexpensive and could be easily formed into the proper shape. Almost from the inception of the d-c electric motor, graphite brushes performed so well that almost no effort was expended in developing other possible materials.

This bright picture clouded somewhat in 1940 when high altitude aircraft encountered premature failure of motors and generators due to short brush-life from rapid wear of the

brushes. The reasons for the short wear life can be understood by briefly examining the lubrication mechanism of graphite brushes. The lubricity of graphite is due to absorbed water vapor and oxygen, which effectively saturates the intercrystallite spaces, satisfies the interlaminar bonding-energy requirements, allows the individual crystallites to slide easily over one another, and produces the normal slippery feeling of graphite. The lubricating action of graphite is enhanced by the layer of copper oxide produced on the surface of the copper commutator by its contact with air, which presents a smooth, tough surface for the deposition of a graphite film by the brush.

As the aircraft industry progressed, the products achieved higher altitudes, and consequently lower atmospheric pressure, with less water vapor and oxygen content than at sea-level pressures. Because of this, some of the water vapor and oxygen is lost from the graphite, and is not replaced. The lubricating action of the brushes is destroyed, with a resulting high wear rate and short brush life.

Since this problem had military significance, considerable effort was expended to produce a brush with a useful wear life at these altitudes and pressures. Solutions to the problem were various additives designed to enable the utilization of the small amounts of water vapor and oxygen in the atmosphere at high altitude to restore the normal lubricating action of the graphite. These solutions were successful, and again the brush problem appeared to be solved.

The advent of satellites, space probes, and other vehicles designed to operate in the environment of space produced a new interest in electrical brush materials when it became apparent that even the so-called high-altitude brushes would not operate at the extreme low pressures found in space where there is no water vapor or oxygen. Table I shows a comparison of ordinary graphite and graphite with the high-altitude additives operated at atmospheric pressure and at a common orbital altitude of 500 000 feet. It is patently clear from this comparison that the high wear-rates and subsequent short wear life of graphite type brushes under

these conditions render them useless as electrical brushes.

For this reason, the aerospace industry generally chose to abandon the d-c type motor, which requires brushes for operation, and utilize a-c operated motors. This approach presents additional problems, since all spacecraft power sources are d-c. A method of converting d-c into a-c must be added to the motor system, increasing weight and expense and reducing reliability. This approach also ignores the many desirable features of the d-c motor, such as high starting torque, simplicity, and continuous speed control. The approach was to retain the inherent simplicity and flexibility of operation of the d-c motor by developing materials which could function properly as electrical brushes in vacuum. The requirements for the material were well known, based on experience with graphite, except that the material would have to continue operating properly at very low pressures. The requirements for material selection were established as shown in table I and used as criteria for the selection of candidate materials.

The initial material selected was molybdenum disulfide because its properties are well known, and it has a crystal structure strikingly similar to that of graphite. However, its sharp cleavage is due to a weak sulfur-sulfur bond, and its lubricating qualities are, therefore, independent of any absorbed gases or of its operating environment. The two primary difficulties in utilizing this material for electrical brushes was the fact that it normally exists as a dispersed powder and has a resistivity much too high to be an effective electrical conductor. These two problems were solved by forming the powder into a solid by compacting it under high pressure and temperature and adding metallic atoms substitutionally to the lattice to produce useful electrical conductivity. The resulting material was a firm solid with good lubricity and excellent electrical conductivity. The material may be cut or ground to any desired shape using standard techniques.

The material was evaluated as an electrical brush under conditions similar to the other tests described previously. The brushes have run for

TABLE I.—*Comparison of Graphite and Graphite With Additives*

Material	Pressure, mm Hg	Duration, Hours	Wear Rate, Inches/hour
Graphite.....	760 (sea level).....	-----	1×10^{-4}
Graphite.....	225 (30 000 ft).....	6	1×10^{-1}
Graphite plus halide additive.....	225 (30 000 ft).....	112	4×10^{-3}
Graphite plus MoS ₂ pockets.....	225 (30 000 ft).....	-----	3×10^{-4}
Graphite.....	1×10^{-6} (500 000 ft).....	0.5	1.2
Graphite plus halide additives.....	1×10^{-6} (500 000 ft).....	1.5	3.5×10^{-1}
Graphite plus MoS ₂ pockets.....	1×10^{-6} (500 000 ft).....	16	2×10^{-2}

A lubricating film on the commutator would be essential.

The lubricating film would have to be solid and inorganic, and adhere tenaciously but not interfere with proper electrical contact.

The brush material would have to be solid, inorganic, nonabrasive, durable, and a good electrical conductor.

periods up to 7000 hours with a brush-wear rate of one millionth of an inch per hour of operation. These results are not only a significant improvement over the performance of any other material operating at reduced pressure but actually indicate a lower wear rate than graphite brushes operating at atmospheric pressure. Several other materials of similar structure and of a general family have been produced by the same techniques and operated as electrical brushes in vacuum with equally good results. More complete and more detailed information on the general development of these materials and the specific techniques of producing them is available from the several reports which have been written and which are listed in the appendix.

There are a number of factors to be considered in the possible commercial or industrial applications for the brush materials. It is obvious, that for any motor operational environment involving reduced pressure or a sealed condition or a corrosive atmosphere, these brushes would be ideal. Many ordinary consumer products such as food mixers, washing machines, garbage disposals, automobile generators, power tools, and other items utilize brush type motors, and hence offer a wide range of possible applications.

The second and the third items follow logically, and these are the relative difficulty of producing the materials and their cost. We have produced the brush materials only in research quantities, small lots under carefully controlled

conditions. We do not have appreciable experience in mass production or in volume procurement of raw materials. Nevertheless, a fairly accurate estimate of both factors can be made from our experience. Production would not be a particularly troublesome process. Our laboratory procedures could readily be adapted to volume production. The cost of the brushes would be somewhat dependent on the quantity produced but is estimated to be about \$1.25 per brush.

MINIATURE SLIP RINGS

The miniature slip rings present an entirely different set of problems in the area of sliding electrical contacts. With the brushes, we were concerned with transfer of electrical power from a stationary frame to an armature rotating at high speed. With the miniature slip rings, we are interested in transferring small electrical signals from a stationary frame to a slip ring which is not rotating at all, but simply oscillating about one point, moving through less than one degree of arc. The situation is further complicated by the extremely small size of the slip ring assemblies. This can best be illustrated by looking at figure 1. The rings are of $\frac{1}{4}$ -in. diameter, and the rotor is $2\frac{1}{4}$ -in. long. The brushes are seven-thousandths of an inch in diameter and $\frac{1}{4}$ in. long. In a device the diameter of a cigarette, and only half as long, there are eighty complete and separate electrical circuits. The materials utilized were a filled plastic for

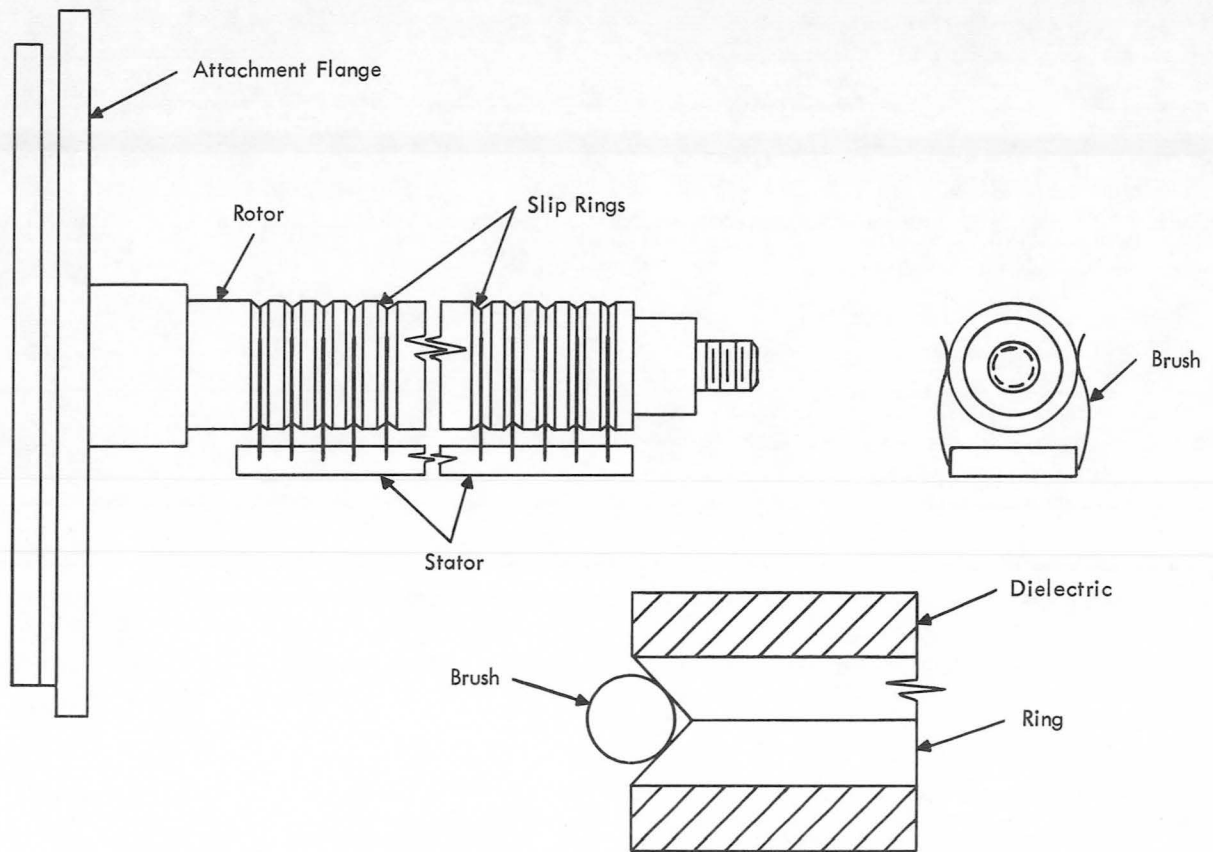


FIGURE 1.—*Miniature slip ring.*

the rotor body and the brush block, 24-kt gold for the rings, and a commercial gold alloy for the brushes.

The problem was to transmit the electrical information required by the guidance system without producing more than a few millionths of a volt extraneous electrical noise at the contacting surfaces and to maintain this condition for the duration of the guidance system operation. The difficulty lay in measuring the extremely small quantities involved and determining just what was occurring on a microscopic scale at the contacting surfaces, without causing a disturbance greater than the process being measured with the measuring apparatus.

Techniques were developed which would permit the measurement of the small quantities involved, and it was learned immediately that, in normal test procedures, electrical noise pro-

duced by external mechanical vibrations and stray electrical and magnetic fields was masking the intrinsic noise of the contacting materials. Special techniques had to be developed to permit accurate simulation of the operation of the slip rings without contributing electrical interference. The first system developed effectively used a vibrating column of gas to provide the oscillations and showed improvement but was still causing a disturbance. The methods finally utilized allowed the rings to oscillate freely after an initial deflection with a restoring force supplied by a small torsion rod. This system produced an intrinsic noise level of only 1 millionth volt.

Initial testing indicated that noise, as would be expected, was dependent on the frequency and amplitude of the oscillations. It was also evident that they exhibited a threshold effect,

being linearly dependent on the amplitude of the oscillations up to about 0.4-degree amplitude, with a higher, but constant noise level for amplitudes greater than 0.4 degree. An investigation of this apparent anomaly revealed that there was no sliding contact between the brush and the ring up to the transition point of about 0.4 degree, but only rolling contact. This was possible because the small diameter brushes could deflect or bend a small amount and still maintain contact with the ring surface.

This further complicated the problem, because with no sliding action the two contact materials would tend to mutually diffuse; then when a large excursion would be required, a portion of one of the materials might be torn loose and present a roughened surface to subsequent operation. This problem was effectively eliminated by flash coating the soft 24-kt. gold rings with a hard gold overlay.

An investigation was made on the influence of gases exuding from the plastic and being deposited on the rings or brushes to cause electrical noise. It was determined that deposition of contaminants on the contacting surface was unlikely in the expected operating temperature range. Possible contamination from the synthetic lubricant used on the rotor support bearings by liquid creep or vapor phase movement was investigated by deliberately introducing the oil onto the ring surfaces. No adverse effects were noted, and noise levels were reduced and remained low for several hundred hours of operation.

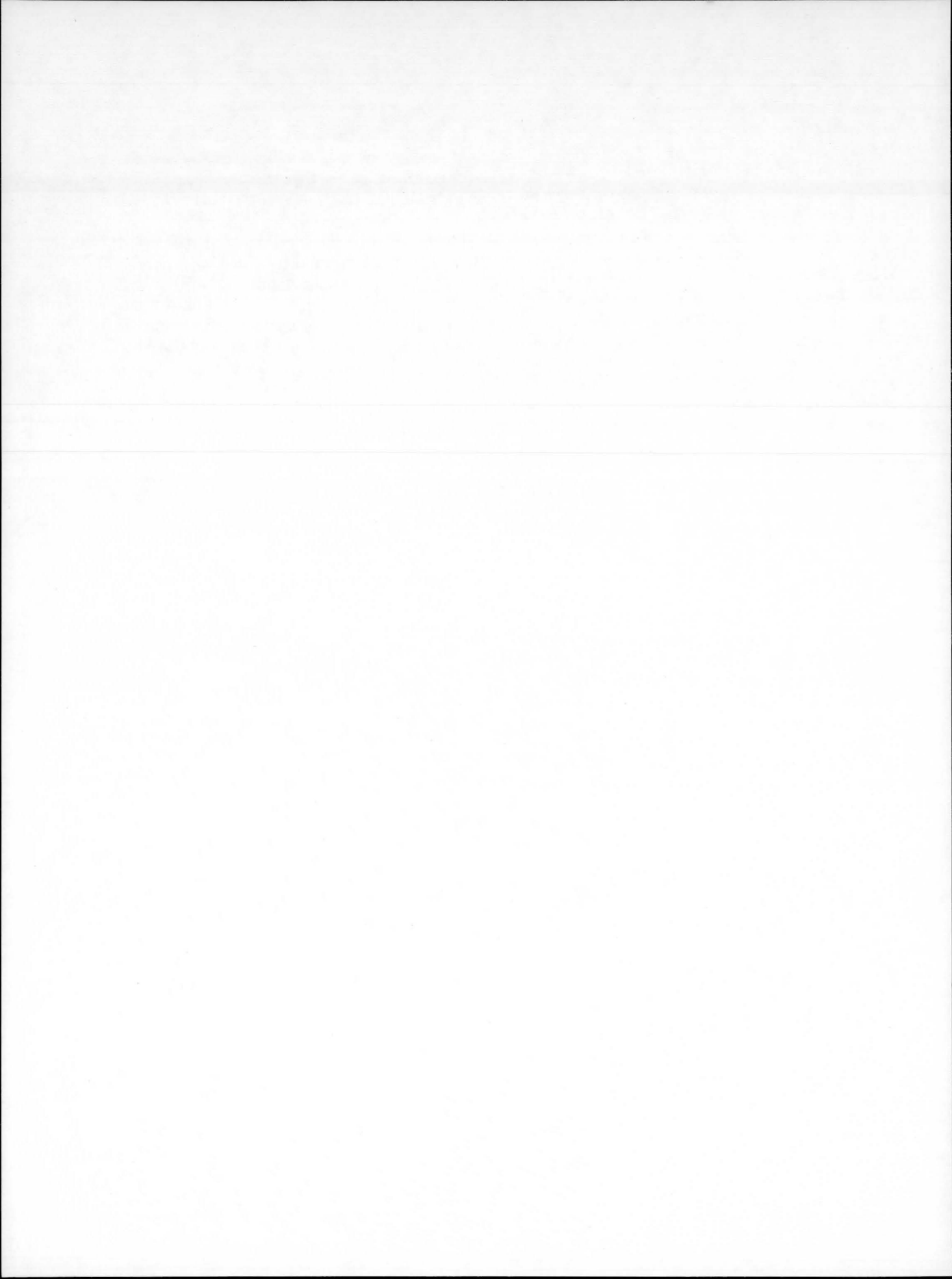
CONCLUDING REMARKS

In summary, the materials presently being used are intrinsically capable of sustained low-noise operation. Further information is available from the IIT technical report which is listed in the bibliography.

The techniques developed to allow the determination of the fundamental electrical properties of these materials could be useful in any application where the basic behavior of two electrically contacting surfaces are required. The equipment used is standard, and the techniques are neither involved nor tedious. Application of the slip ring assemblies would be limited, but where the precise measurement of extremely low noise levels is required for rotating or oscillating bodies, these rings are ideal. Cost will depend to some extent on the number of circuits required. An 80 circuit ring costs about \$2000.

REFERENCES

1. HORTON, J. C.: Electrical Contacts in Vacuum (A) Brushes—Status Report No. 1, MSFC TP-S&M-61-19, October 1961.
2. HORTON, J. C.: Electrical Contacts in Vacuum (A) Brushes—Status Report No. 2, MTP-P&VE-M-62-17, December 1962.
3. ULRICH, D. R., and KING, H. M.: The Kinetics of the Sintering of Hot Pressed Molybdenum Disulfide and Molybdenum Disulfide—Silver Compositions and the Effect on the Electrical Conduction Process, NASA TM X 53111, August 1964.
4. IIT RESEARCH INSTITUTE: Investigation of Slip Ring Assemblies, Final Report, Contract No. NAS8-5251, IITRI Project E-6000.



11. Dry Film Lubricants

J. E. KINGSBURY AND E. C. MCKANNAN

George C. Marshall Space Flight Center, NASA

The Space Age has necessitated accelerated development of many technologies which have direct application to commercial, earthbound hardware. One striking example is dry film lubrication. The stimulus for the development of dry film lubricants was provided by the unsatisfactory condition created when commercial liquid lubricants were exposed to the multiple environs of space. In the search for a satisfactory solution to lubrication in space, dry films were investigated. The dry film lubrication concept has proven most desirable for space, and a natural fallout is the potential shown by such films for consumer item application. On the acceptance that the coefficient of friction of dry films is not equivalent to that of a liquid lubricant under ideal conditions, this paper discusses how the ideal condition for liquid lubrication is rarely achieved in practical applications. Comparisons are made between the performance of dry film and liquid lubricants as a function of temperature, environmental pressure, and life. Furthermore, consideration is given to the comparative costs of liquid versus dry film lubricants to show the practicality and desirability of dry film lubrication to consumer items. Although no data on the performance of consumer items lubricated with dry films are presented, the comparisons clearly establish the potential of dry film lubricants in a competitive consumer market.

Centuries ago man invented the wheel. Not long thereafter he learned that animal fat was of great benefit in lubricating his wheel. Hundreds of millions of dollars have been spent since then in preparing better lubricants. With the advent of the space age, we found ourselves in a position comparable to that of our cave-man forefathers who invented the wheel; that is, although we knew about the benefits derived from lubrication, our most refined earthbound lubricants are known to be ineffective in space. To review our knowledge of lubrication as it applies to machinery used on earth, it is known that no matter what pressure is exerted on components required to function by movement, we cannot eliminate a finite layer of air. In addition to the air layer, if we introduce a material such as oil, we provide a surface condition which will aid in reducing the tendency of the components to gall. The theory of liquid lubrication is much more complex than this very simple explanation, but the explanation is ac-

curate and suitable for showing why such a concept is not applicable for space. In space there will be no air (or any other gas) layer. Furthermore, all natural and synthetic organic lubricants evaporate at the environmental pressure of space in addition to being seriously degraded by other components of the spatial environments, such as indigenous radiation and temperature. Limited efforts had been expended prior to the mid-1950's toward developing solid lubricants; that is, lubricants which in dry form are effective in reducing friction in moving parts. The efforts were limited, because there was no pressing need for such materials, and early work indicated that the coefficient of friction attained with dry film lubricants was at least an order of magnitude higher than with conventional liquid lubricants. The theory of liquid lubricants, that is, oils and greases, is well understood; however, in the mid-1950's the theory of dry film lubrication was understood only to the extent of know-

ing that it was different from liquid lubrication.

Three alternatives were available as solutions to the problem of lubrication in space. First, by providing the necessary radiation shielding of liquid lubricant reservoirs required for lubricant replenishing, unpressurized components could be lubricated. Second, by sealing all components to permit air pressurization, liquid lubrication techniques could be employed. Third, the development of the dry film lubrication theory could be undertaken which would permit optimized materials to be synthesized as dry film lubricants. The penalties of weight, cost and complexity involved in using liquid lubricants were unacceptable for long-range space flight plans; therefore, these approaches were discarded in favor of developing dry film lubrication techniques and materials. The urgency of the problem was such that initial designs for space vehicles included the cumbersome technique of liquid lubrication at a significant penalty. Because of the significant success in developing dry film lubricants, old designs are being revised to include dry film lubricants, and all new designs are employing dry film lubrication techniques.

DISCUSSION

It must be recognized that dry film lubricants, after approximately five years of development time, have not surpassed liquid lubricants in all areas of application. However, we have been successful in deriving a theory which explains how and why dry film lubrication works. Although our theory is directed toward lubrication in a vacuum environment, it is equally appropriate to the environment on earth; the major difference is the presence of a gas (air) layer in the lubrication system when applied to the earth environment. Basically, solid or dry film lubricants capitalize on the inherent mechanical capability of certain materials to readjust their lattice structures when subjected to shear force, that is, materials which can readjust to a shear environment without flaking. Materials which flake are undesirable because the flaking may cause particle concentrations which contribute to creating direct compressive forces, thus increasing the pressure exerted be-

tween the components being lubricated. Examples of materials which possess the desired properties for dry film lubricants include most refractory metal sulfides, the most widely known being molybdenum disulfide. By selectively compounding the refractory metal sulfides with other materials which complement the inherent capability of these sulfides, it has been demonstrated that low coefficients of friction can be achieved even under high bearing pressures. Note that the dry film lubricants referred to in this paper do not include materials such as graphite, which has lubricating properties that are dependent on the earth's atmosphere, but lubricants which have resulted from a planned program directed at implementing the basic theory previously outlined. These films function independently of any surrounding environment.

Figure 1 shows a comparison of the typical torque required to overcome friction using a typical synthetic, or natural liquid lubricant as well as the torque required to overcome friction with a selected dry film lubricant under similar bearing conditions at 1-atmosphere pressure. The torque using the liquid lubricant is approximately 20 percent of that of the dry film. The additional power required to overcome the friction of components lubricated with dry film, as opposed to liquids, is generally measured in terms of small fractions of 1-horsepower. Liquid lubrication systems are designed for a nominal operating temperature range, and operation beyond the limits of that range results in gross inefficiency of the lubricant. Dry film lubricants, on the other hand,

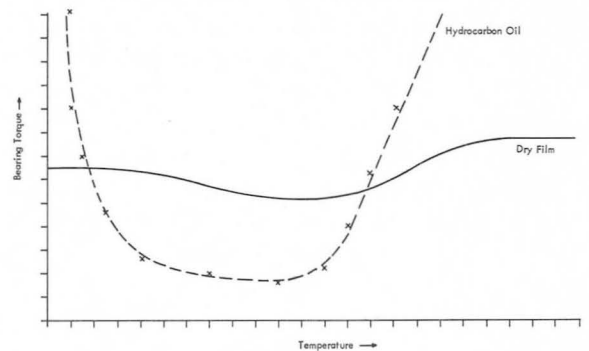


FIGURE 1.—Bearing-drag torque caused by lubricant.

are essentially insensitive to temperature; therefore, in selected applications where significant temperature cycling may be anticipated, dry film lubricants become superior to liquid lubricants. It is especially interesting to note that the coefficient of static friction, that is, the force necessary to initiate movement of a component, is often greater in liquid lubricants than in dry films simply because, at starting, the liquid lubricant temperature may be significantly outside of the operating temperature range. This is especially true for applications where the temperature of the components to be lubricated is governed by atmospheric conditions. Dry film lubricants can function effectively for years, but liquid lubricants can rarely go unreplenished for more than a few months. If we extrapolate these data to a period, for example, after six months of operation, the torque required for the liquid lubricant, if it has not been replenished, would become essentially that required to overcome the friction between the basic component materials; the liquid lubricant would have been either destroyed by heat or sufficiently contaminated to reduce its efficiency to essentially zero. If we increase the severity of the temperature environment (i.e., we create a cyclic temperature profile ranging between 0° F and 250° F), a marked increase in the torque is observed using the same liquid lubricants characterized in this figure; the coefficient of friction of the dry film lubricant is essentially unaffected. This situation makes the dry film lubricant much more attractive for applications where cyclic temperatures are anticipated, since it is impractical to consider using more than one liquid lubricant in a single component to account for temperature variations. As noted earlier, the primary motivating force for developing dry film lubricants was to overcome the deficiency of liquid lubricants when exposed to reduced pressures. Dry film lubricants are essentially unaffected by pressures as low as 10^{-10} millimeter of mercury (an altitude equivalent to approximately 400 miles) as demonstrated by test results. The physical characteristics of the constituents used in the dry film lubricants give no reason to indicate that these films will be affected by the

most extreme pressure conditions known to exist in deep space. There is no evidence to indicate that the dry film lubricants are affected by the electromagnetic radiation known to be present in space. One important fact is the cleanliness associated with dry film lubrication. It is well established that liquid lubricants have an affinity for attracting contamination. Situations are often experienced where dirt and sludge were collected because of overlubrication. This condition does not exist with dry film lubrication. The cleanliness consideration in lubrication may not be important in all applications for consumer items, but in some it is, for example, food processing machinery. All too often, no consideration is given to the effects of dirt clinging to lubricants. The great majority of bearing failures are caused by contamination of the lubricant. Rarely does an automobile wheel bearing fail because of lack of lubricant, but the failure is attributed to scoring of a bearing ball by a foreign particle entrapped in the bearing lubricant. This is not to say that the lubricant was not at fault in the failure but rather that the lubricant may have held the foreign object captive because of its physical properties. By using dry film, the lubricated component could be sealed permanently and thus preclude the occurrence of contamination. In summary, dry film lubricants exhibit higher friction coefficients at normal selected operating temperature ranges and pressure conditions than do commercial liquid lubricants, but the dry film lubricants are virtually insensitive to parameters such as elevated and reduced temperatures and reduced pressures, parameters which significantly degrade the operating characteristics of liquid lubricants. Dry film lubricants can be designed to function efficiently for periods of years without replacement; while liquid lubricants under the most optimum conditions require replenishing at maximum periods of a few months.

It is not suggested that dry film lubricants are a panacea for all lubrication problems. On the contrary, development has not progressed enough to provide a dry film lubricant for many applications. There is no evidence to show that dry film lubricants could not be used,

for example, in automobile engines, although there exists no data upon which to base selection of a dry film for this application. Similarly, dry film lubricants appear attractive for application in machine tools, household appliances, hand tools, food and textile machinery, heavy machinery, and a host of other applications. It is not the purpose of NASA or MSFC to evaluate dry films for these applications, but rather to suggest the potential of dry film and urge investigation of it for particular products.

A final factor in dry film lubricant application, which may be of some casual interest, is that of cost. The cost of dry film lubrication, once designed into a component, is of minor consequence. Many consumer items are now sold with a little tag attached to them saying, "Fill with oil before using." The cost of dry film lubrication to the manufacturer will obviously be more than the cost of liquid lubricants, since, as indicated by the little tags, the cost of liquid lubricants to the manufacturer is presently nonexistent. However, the per-unit cost of lubricating large quantities of components with dry film is negligible. The long-range savings in a permanently lubricated consumer item, not to mention the saving experienced if the item is not maintained as prescribed, resulting in a requirement for replacing worn parts, may well offset the slight increase in original cost of the item. The slight

increase is in the order of a fraction of 1 percent of the total market price of the item.

Reports on the development of dry film lubricants are listed in the bibliography. These reports are available through the Redstone Scientific Information Center or the MSFC Technology Utilization Office.

CONCLUDING REMARKS

Our work to date indicates a great potential for dry film lubricants in consumer items. It is believed that such investigations by individual manufacturers will result in application of dry film lubricants to items which will be available for personal lives in the near future.

BIBLIOGRAPHY

- DEMAREST, K. E. and MCKANNAN, E. C. : Evaluation of Dry Film Lubricants in Vacuum for Engine Gimbal Bearings, IN-P&VE-M-63-6, April 1963.
- DEMAREST, K. E. and MCKANNAN, E. C. : An Evaluation of the Centaur Gimbal in a Simulated Flight Environment, MPR-C-61-1, December 1961.
- MCKANNAN, E. C. and KINGSBURY, J. E. : A Survey of Vacuum Lubrication Developments, MTP-P&VE-M-63-17, December 1963.
- Research on Bearing Lubricants for Use in High Vacuum, Midwest Research Institute, Summary Report, February 1961 to March 1962. Contract NAs8-1540.
- Research on Bearing Lubricants for Use in High Vacuum, Midwest Research Institute, Summary Report, March 1962 to April 1963, Contract NAs8-1540.
- Research on Bearing Lubricants for Use in High Vacuum, Midwest Research Institute, Summary Report, April 1963 to May 1964, Contract NAs8-1540.

12. Insulation Materials

R. E. SHANNON

George C. Marshall Space Flight Center, NASA

Three insulation materials which have been developed by the George C. Marshall Space Flight Center are discussed in some detail. The first of these is a material which might find commercial application as an insulation for cryogenic fluid containers or transfer lines. The second is a ceramic-gold coating which might be useful as an infrared reflector or as decorative coatings. Finally, a ceramic material is discussed which can be used as an insulator against a thermal environment which is primarily radiative but also contains some convective heat load.

The development of the Saturn-class launch vehicles has presented many major materials-engineering problems. Among the most significant of these have been materials for thermal insulation. The insulation problems faced by MSFC have covered the temperature range of -423°F to 1800°F .

The two temperature extremes are represented by the requirement for materials to (1) insulate propellant tanks containing liquid hydrogen (at a temperature of -423°F) to prevent excessive boiloff, and (2) to protect components in the base region of the vehicle from heat induced by radiation from the engine plumes and convection from the recirculating exhaust gases.

Although several insulation materials will be touched upon in this paper, primary emphasis will be placed upon discussion of the two composite materials developed by MSFC to solve the two extreme requirements stated above. The first of these is a lightweight, self-evacuating, plastic-honeycomb, composite system called Dual Seal for external application to containers for cryogenic liquids.

CRYOGENIC INSULATION

The nation's space program is influenced to a significant extent by the availability of suitable material systems for insulating tanks con-

taining cryogenic propellants to prevent excessive boiloff. Such insulation systems should have high reliability, be light in weight, and low in thermal conductance. The demands for such insulation systems are pressing current technology. Many research and development programs are currently in progress throughout the country. The ultimate goals of such studies are to provide insulation systems for launch-vehicle short-duration flights as well as long-duration flights or missions for lunar exploration.

For approximately the past two years, this center has conducted in-house development on insulation systems for hydrogen tanks typical of those utilized in the Saturn V program as well as tankage configurations appropriate for long-duration missions. The program reported herein was initiated to reduce the weight and increase the reliability of the stages in the Saturn V program. Upon program initiation, the lightest weight insulation system proposed for one of the stages of the Saturn V was the system shown in figure 1, weighing 0.82 lb/ft^2 and having a thermal conductivity of $0.7\text{ Btu/in./hr/ft}^2/^{\circ}\text{F}$.

The relatively poor thermal performance of this insulation concept is attributed to a required helium purge of the insulation, establishing a system conductivity of approximately

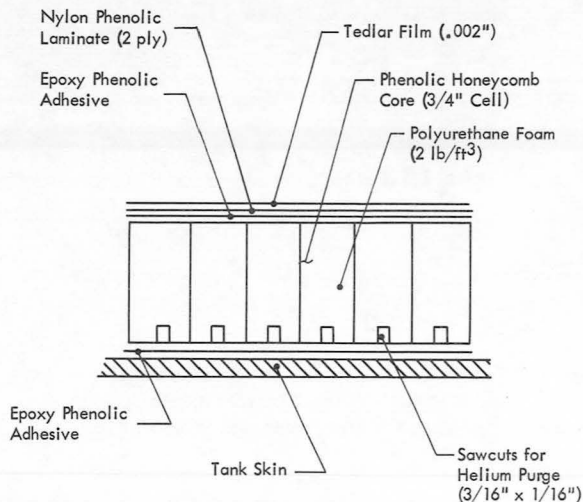


FIGURE 1.—*Helium-purged insulation (1.6 in.).*
 Weight = 0.82 lb/ft^2 ; thermal conductivity =
 $0.7 \text{ Btu/in./hr/ft}^2/\text{° F}$.

that of the helium gas. The helium purge is required on this insulation to prevent air cryopumping into the insulation (in the event of a damaged outer seal) and creating lox compatibility problems or additional weight penalty.

The cryogenic insulation system, dual seal, developed by MSFC, has an approximate weight of 0.4 lb/ft^2 and a thermal conductivity of $0.2 \text{ Btu/in./hr/ft}^2/\text{° F}$. This represents a reduction in weight of one-half and a three and one-half reduction in thermal conductivity.

The dual seal insulation (fig. 2) consists of an inner portion of sealed-cell mylar honeycomb and an outer helium-purge channel of fiberglass-reinforced phenolic honeycomb. By sealed cell, it is meant that each individual cell in the Mylar honeycomb is a hermetically sealed entity. Gases cannot permeate cell to cell.

The operating concept of this system is based upon the self-evacuation of the sealed cells. This is accomplished by the cryopumping or condensation of the entrapped gases when the back surface of the insulation reaches -423° F as the propellant tanks are filled with liquid hydrogen.

The honeycomb used in the helium-purge channel is perforated while being manufactured, resulting in a $1/16\text{-in.}$ -diameter hole in each side of the cell. These holes allow helium

to flow through the entire outer channel. The outer helium-purge channel is separated from the inner portion by a low-permeability aluminum film. In the event that both the outer and inner seals are punctured by a sharp object, helium under pressure will flow through the puncture in the outer seal, preventing air from entering the insulation. The helium gas will also enter the affected cell of the inner portion through the puncture in the inner seal. However, due to the individually sealed cell property of the inner portion, the helium will be confined to the affected cell. Thus, there is no degradation in thermal conductivity of large areas due to local damage. The concept thus retains all the reliability of the helium-purged insulation of figure 1, yet achieves thermal performance close to that of a cryopumped insulation.

In selecting the materials used in this insulation concept, weight was always a primary consideration. Strength factors, permeability, and cost were other factors considered.

This insulation is applied to the external surface of the propellant tanks. It is exposed to aerodynamic forces and ascent heating during the flight. This raises the temperature on the outside skin to approximately 400° F for a short time period. This particular application, therefore, presented the problem of having a temperature of -423° F on one surface and on another surface, 0.6 in. away a temperature of 400° F .

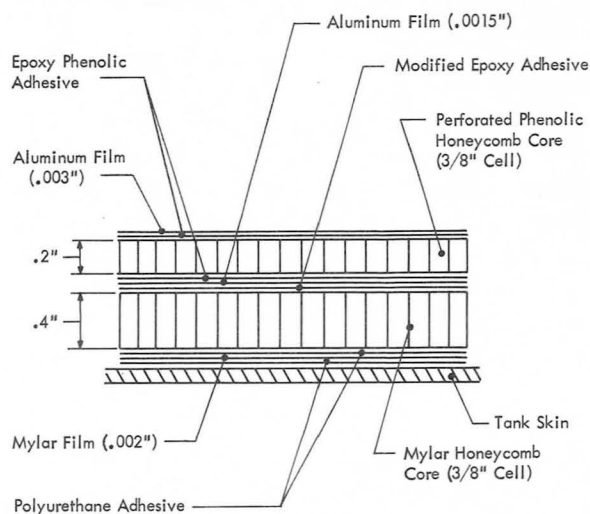


FIGURE 2.—*Double seal insulation.*

The cryopumped sealed-cell Mylar honeycomb is the part of the system which provides the cryogenic insulation. Unfortunately, the Mylar core softens at a little over 200° F. The sealed cell Mylar core had to be protected from aerodynamic heating. The heat-resistant phenolic-honeycomb core, or purge-channel portion, meets this need.

For the outer skin, a readily available aluminum film was selected. This material is lightweight, has low permeability, and has the desired structural properties over the range of expected operating temperatures. An epoxy phenolic adhesive was used to bond the outer skin to the phenolic core because of its good, high-temperature properties and its ability to form effective bonds between these materials.

An aluminum film was selected for the inner seal because of its low porosity and permeability and its bonding characteristics. The inner seal can be bonded either to the phenolic core, to the Mylar core, or to both. The latter method is generally employed to eliminate one bonding operation, although the preferred method would be to first bond the Mylar core to the inner seal. When the inner seal is bonded to the phenolic core first, a rippled surface is obtained which makes it difficult to obtain a uniform, completely sealed, bond to the Mylar core.

A modified epoxy film adhesive was used to bond the Mylar core to the inner aluminum seal. In this application the adhesive was required to have the following properties:

- (1) The adhesive must form an effective bond between the Mylar core and the inner seal. The bond must retain usable strength properties over a temperature range of approximately -250° F to 250° F.
- (2) The adhesive must form a relatively nonporous bond when used to join the inner seal to the Mylar core. The adhesive, therefore, must be low in volatile materials and must liberate a minimum of gases in the curing process.
- (3) The adhesive must not require a cure temperature above 225° F to 250° F when moderate pressure is used. Tests have indicated that crushing of the

Mylar core will result if cure temperatures of 275° F or higher and pressures of five pounds per square inch or more are used.

A Mylar film was bonded to the bottom side of the Mylar core to form the sealed cell lower insulation. This was done to insure that a sealed cell was obtained. The clear Mylar film makes a visual examination possible, insuring a good bond. The entire insulation panel can then be inspected ultrasonically by through-transmission techniques, to insure a perfect subassembly before bonding it on the tank. If a film close-out were not used, the sealed cell would have to be formed by bonding the Mylar core to the tank wall. Any appreciable mismatch or irregularities between the Mylar core and the tank wall would introduce sections in the insulation where there would be a sealed area but not a sealed-cell concept. A polyurethane adhesive was used for bonding the close-out film to the Mylar core due to its high strength and low permeability. Since this bond line was at a temperature of -423° F, the adhesive used was one developed under an MSFC contract and is the strongest and most flexible at this temperature of any known adhesive for use at room-temperature. For the same reasons this adhesive was also used to bond the insulation to the tank wall. This adhesive cures at room temperature and the insulation panels can be bonded to the tank at anytime in the vehicle manufacturing cycle without the use of heat.

Each material has a particular function to perform and was selected carefully to take maximum advantage of its best characteristics. The composite material achieves the capability to do a better job than any single material by itself. This is the appealing benefit which can be derived from composite materials.

The potential commercial applications of this or similar concepts are not yet certain. Any effective application would require the backface temperature to be low enough to condense or cryopump the gases entrapped in the sealed cells to create a vacuum. It has been found that by fabricating the sealed-cell portion in a carbon dioxide or Freon gas environment, this system could be utilized for insulating liquid nitrogen

or liquid oxygen containers. This material has been applied to surfaces with compound curvatures and around cryogenic transfer lines or pipes down to 1½ in. diameter.

HIGH TEMPERATURE INSULATIONS

As stated in the introduction, MSFC's insulation problems have encompassed both extremes of the temperature spectrum. Most of the high-temperature problems have arisen in the base region of the vehicles. The heat load derives from two sources: radiation from the engine plumes and convection from the recirculating exhaust gases. Nominally, 60 to 80 percent of the total heat is from radiation with the remainder resulting from convection. The Saturn I with its cluster of eight 188 000-lb thrust H-1 engines creates a total heat load of 3600 Btu/ft².

Since the major component of the total heat load results from radiation, attention was focused on developing a material with a high reflectance in the infrared region. The first such material evaluated was a ceramic-gold coating which had been developed for use on the Jupiter missile while this organization was under the cognizance of the U.S. Army Ballistic Missile Agency. Although this material was not selected for use on the Saturn family of vehicles, for reasons which will be stated later, it still might be of commercial interest and, therefore, will be described briefly.

In the Jupiter flame shield application, the highly reflective coating was applied to a stainless steel substrate. The process consisted of (1) preparation of the metal surface (degreasing and sandblasting), (2) base coat (ceramic enamel fired at 1650° F for 3½ min), and (3) surface coat (liquid gold-resinate solution fired at 1300° F for 30 min).

Several methods of metal-surface preparation were investigated. The best method was found to be vapor degreasing followed by a fine-sand wet blasting. This treatment produces a satin finish surface to which the porcelain enamel bonds well.

The formula for the porcelain enamel which is next applied and fired at 1650° F for 3½ min is shown in table I. The adherence between the enamel and the metal substrate is a

TABLE I.—*Batch Formula for Enamel Base Coat*

No. 5210 Solaramic Frit (Feno Corporation) ..	100 lb
Red Label Clay (Feno Corporation)	2 lb
Chromium Oxide (Cr ₂ O ₃)	1 lb
Nickel Oxide	8 oz
Lithium Metasilicate (Li ₂ O·SiO ₂)	12 oz
Bentonite	8 oz
Water	4 gal

combination of a mechanical and a chemical bond. The nickel and chromic oxides used in the enamel serve to improve the chemical bonding. This coating is sprayed onto the metal substrate.

The gold reflective coating is applied in a manner similar to the gold decoration of fine china and glassware. A solution of gold resinate is sprayed onto the porcelain surface and fired in a furnace at 1300° F to decompose the resinate and deposit elemental gold. Various ceramic type fluxes are incorporated in the resinate solution to improve the adhesion to the material being coated.

After considerable experimental work, Liquid Bright Gold RH (Hanovia Division of Engelhardt Industries) was selected on the basis of superior adhesion, reflectance, and ease of application. This solution contains approximately 11 percent (by weight) gold as received. A very light bloom results after firing, but this can be removed easily by a light buffing with magnesium oxide powder and water.

Heat resistance and reflectivity tests showed that this coating on a stainless steel substrate gave a 10° F per second rate of back surface temperature rise in a 20 Btu/sec/ft² environment and 33° F per second in a 60 Btu/sec/ft² heat flux.

Several comparisons were made between this ceramic-gold coating and an electrodeposited gold coating. It was found that the reflectivity of the ceramic-gold was slightly better, the adherence was better, and the heat resistance was better. The electrodeposited samples failed at 690° F while the ceramic-gold coatings did not break down until temperatures in excess of 1550° F were reached.

By use of both impact and bending tests, the ceramic-gold coating was found to possess excel-

lent adhesion to the base metal. Impact tests were conducted by use of a 1-inch-diameter steel ball which struck the surface at approximately 30-inch per pound force. Test samples withstood such impacts without appreciable spalling or cracking. In addition, pieces coated on both sides were bent around a 1/2-inch-diameter mandrel. Microscopic cracks appeared on the surface in tension, but no change was observed on the surface in compression.

Potential commercial applications of such a coating would be as infrared reflectors or decorative coatings. This coating might well be considered seriously as a replacement for any current applications of electrodeposited gold coatings. In addition to its considerably higher temperature resistance and its better adherence, the time required for application also is greatly reduced. In the case of the Jupiter missile application, the time required for coating a flame shield was reduced from the 1000 man-hours required for electrodeposition to 14 man-hours for the ceramic-gold coating.

This coating was considered for application in the Saturn family of launch vehicles. But, after much investigation, it was recognized that two conditions could render the ceramic-gold ineffective: (1) deposition of carbon at high altitudes which could not be burned off for lack of oxygen, and (2) a large convective component in the total heat flux. Consequently, ceramic-gold was eliminated as a candidate material. For convective heating, a heat sink or insulation type material was required. Because materials which act as a heat sink would impose a severe weight penalty, prime consideration was given to insulation materials. Concurrent with the evaluation of many proprietary commercial insulations, a program was initiated to develop a suitable insulation.

The development of an insulation had three primary requirements: (1) The material had to be capable of providing thermal protection for structural members of the vehicle (maximum allowable temperature for these structural members was 500° F); (2) it had to be non-burning since, for a portion of the vehicle flight time, convective cooling of the base will result if the air scooped into the base is not passed

through the flames caused by burning of the insulation; (3) it had to be applied easily and cured at relatively low temperatures since some of the areas to be protected can be insulated only after the vehicle is assembled. Oven curing of the components assembled on the vehicle cannot be accomplished because of size and because other components in the vehicle cannot stand exposure to the temperatures normally associated with thermosetting materials.

Based upon the above requirements, efforts were directed toward development of a low density, highly reflective inorganic insulation which would be resistant to and insulate against a radiant heat flux of approximately 40 Btu/ft²/sec and, at the same time, be resistant to the shock and vibration of testing and launch operations. After considerable investigation of many materials, it was concluded that fibrous potassium titanate, available commercially as Tipersul, was the most suitable material for this application. (Tipersul and Ludox HS are trade names of E. I. du Pont de Nemours and Company, Inc., Wilmington, Delaware.)

Tipersul was selected as the major constituent of the insulation on the basis of its low thermal conductivity, high reflectivity, low bulk density, and fibrous characteristics. Two forms of Tipersul were evaluated—block and loose fibers. The block form contains approximately 10 percent of another inorganic reinforcing fiber; whereas, the loose, fiber form is entirely fibrous potassium titanate. Specimens prepared from the block form displayed less drying shrinkage than specimens prepared from the loose, fiber form, and the form of Tipersul had no appreciable effect on the insulating capabilities of the coatings when exposed to a radiant heat flux of 24 Btu/ft²/sec. Consequently, the block form was considered the more attractive source of Tipersul.

Colloidal silica was selected as the binder for Tipersul because it provided the finished insulation with both structural stability and water resistance when cured at temperatures as low as 180° F. For this program, Ludox HS, a colloidal silica sol containing 30 percent silica was used as the binder.

To provide additional strength and minimize drying shrinkage, asbestos fibers were incorporated into the insulation. After investigating the effects of the asbestos fibers on both the strength and insulating ability of the coating, it was determined that a 10-percent addition was optimum.

The asbestos fibers and Tipersul block were blended into a uniform mix with a Patterson Foundary Thoroblender that was equipped with a disintegrator. The resultant mix and colloidal silica were combined in a kitchen aid mixer. Sufficient colloidal silica was added to give a matrix with a trowelable consistency. The final composition, designated as M-31 thermal insulation, is listed in table II.

TABLE II.—*Batch Composition of M-31 Thermal Insulation*

Material	Parts by weight
Tipersul block.....	90
Asbestos fibers.....	10
Ludox HS.....	420

To utilize the capabilities of M-31 as a thermal insulation for metal substrates, it was necessary to develop techniques by which a continuous coating of the material could be bonded to the substrates. A recent report by Skalrew, Hauch, and Levy (ref. 1) indicated that an expanded metal reinforcement improved the structural stability of a ceramic insulating layer. It provided an excellent mechanical interlock because its sides are not vertical but are set on an angle. For M-31 application, a 22-gauge AISI 302 stainless steel expanded metal was used for mechanically interlocking the insulation to the metal substrates. M-31 also has been applied successfully to stainless steel honeycomb sandwich substrates utilizing a crimped open-faced honeycomb reinforcement core for the mechanical bonding mechanism.

Drying M-31 applied to metal substrates is accomplished best by uniformly heating the specimens from the uncoated sides of the sub-

strate. A bank of infrared heat lamps was used as the heat source for this program. A typical drying curve and the related moisture content for a 1/4-inch-thick coating is shown in figure 3.

M-31 is an anisotropic material. Two factors contribute to its anisotropy: (1) its hard exterior and its soft interior caused by migration of the silica during drying, and (2) partial orientation of both the asbestos and potassium titanate fibers caused by troweling during application. The density gradient through a 1/4-inch thickness is shown in figure 4. The thermal conductivity of M-31 was determined in the two primary directions, that is, both normal and parallel to its plane of application. Figure 5 illustrates the result of these determinations. It shows that the thermal conductivity with the heat flowing in the direction parallel to the plane of application is essentially constant at 1.7 Btu/ft²/hr/°F/in. in the temperature range of 100° F to 1500° F. With the heat flowing in the direction normal to the plane of application, the thermal conductivity is 0.85 Btu/ft²/hr/°F/in at 100° F and increases to 1.3 Btu/ft²/hr/°F/in at 730° F.

To illustrate the effectiveness of M-31 in a radiant heating environment, a 0.040-in. thick sheet steel blank and 0.320-in. thick coating of M-31 were exposed to a radiant heat flux of 24 Btu/ft²/sec. The results of this test are illustrated in figure 6 which shows that the back-face temperature rise for the first eight seconds of the test was about 1° F for the M-31 compared to 400° F for the sheet steel blank. It

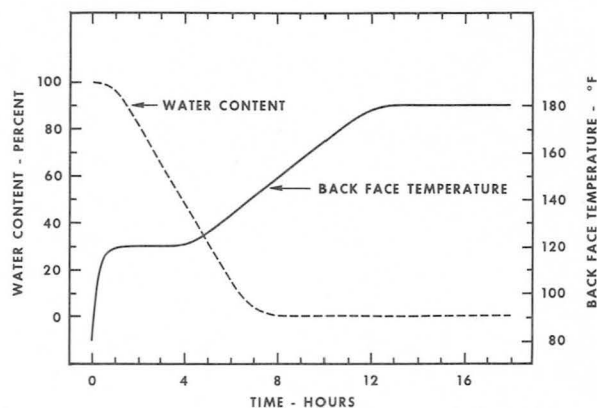


FIGURE 3.—*Drying curves for M-31.*

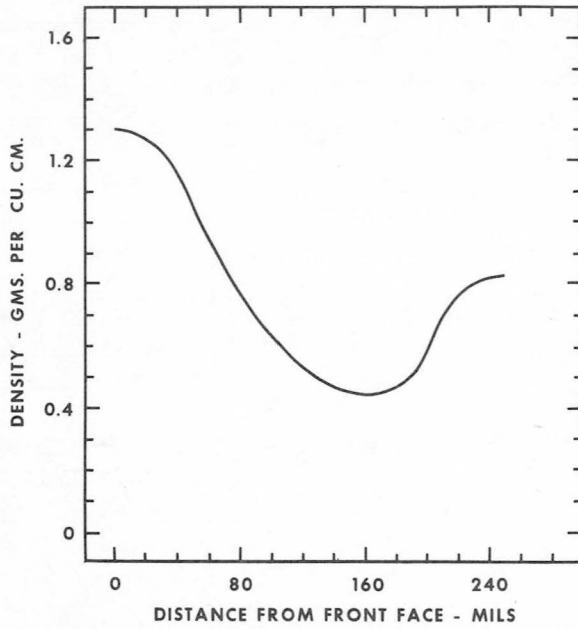


FIGURE 4.—Density gradient through 1/4-in. thick specimen of M-31.

also shows that the backface temperature rise of the M-31 was less than 300° F after 180 seconds of exposure.

Because the Saturn I heat shield must afford protection against the recirculating exhaust gases, an investigation of the effect of convective heating on M-31 was considered necessary. Sample for this study were prepared by applying the material to mild steel blanks

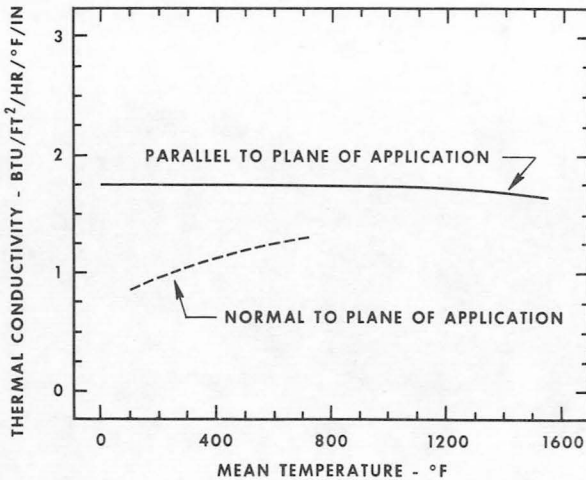


FIGURE 5.—Thermal conductivity of M-31.

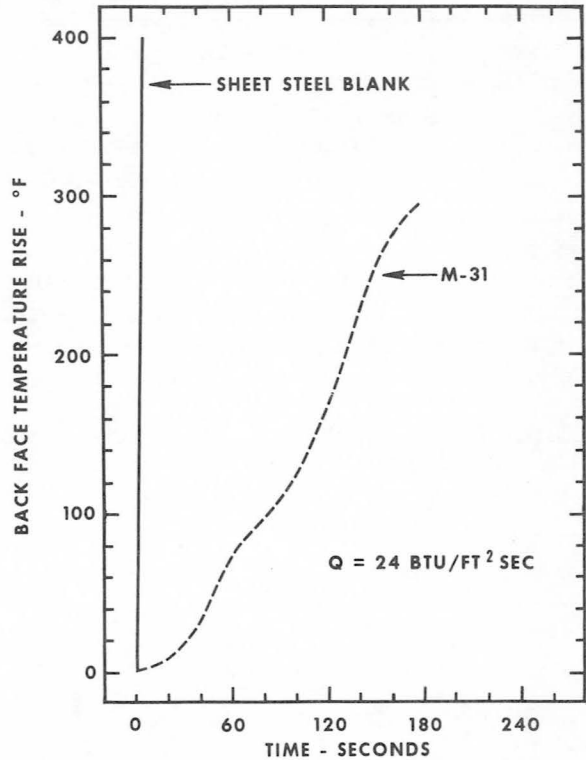


FIGURE 6.—Resistance of M-31 to radiant heating.

(0.038 in. by 4 in. by 6 in.) overlaid with expanded metal. Chromel-alumel thermocouples were attached to the backface of each sample to measure temperature rise. An oxygen-acetylene blast burner was used as the heat source. Table III shows the effects of convective heating on M-31.

The maximum radiant heat flux which the M-31 can withstand was determined by increas-

TABLE III.—Effects of Convective Heating on M-31

Thick-ness of M-31, in.	Heat flux Btu/ft²/sec	Temperature rise, °F		
		60 sec	120 sec	180 sec
0.310	10.5	97	251	372
0.540	10.5	62	88	101
0.310	30.4	193	505	690
0.540	45.0	120	378	630

ing the heat flux until a level was reached at which the material failed. To eliminate accumulated heating effects, a fresh set of samples was tested at each heat flux level. The results of these tests are illustrated in table IV which shows that the M-31 ($\frac{1}{2}$ in. thick) is an effective insulator in radiant heating environments of 70 Btu/ft²/sec or less. At a heat flux of 80 Btu/ft²/sec, the material fails rapidly. These results were indicated by the backface temperature rise after 180 seconds of exposure and by visual examination during and after testing.

TABLE IV.—*Limitations of M-31 in Radiant Heating Environments*

Heat flux, Btu/ft ² /sec	Exposure time, sec	Back-face temp. rise, °F	Remarks
37	180	125	Slight discoloration of surface.
50	180	235	Small amount of surface fusion on hot face.
70	180	330	Melting of surface started at 75 sec and continued throughout test.
80	180	750	Fusion started at 60 sec; large roll of glass formed along bottom half of samples; glass cream colored streaked with blue.

In addition to the application of M-31 to a stainless plate overlaid with expanded metal, a honeycomb sandwich substrate was investigated. The basic honeycomb sandwich construction selected for this study utilized 10-mil face sheets and a 1-in.-thick honeycomb core having $\frac{1}{4}$ -in. square cell openings and a wall thickness of 2-mils. The components were fabricated from a high-strength stainless steel and joined with a silver-brazing alloy. A 190-mil thick honeycomb-reinforcement core, having $\frac{1}{2}$ -in. square cell openings and a wall thickness of 2 mils, was brazed to one face of the basic

honeycomb structure to serve as a mechanical device for bonding the insulation. The basic honeycomb structure including the reinforcement core weighs approximately 1.6 pounds per square foot.

Since M-31 has to be mechanically interlocked to its substrate, it was necessary to devise a means of increasing the holding power of the reinforcement core. This was achieved by crushing or bending over approximately 45-mils of the upper portion of the core walls. A hydraulic press equipped with parallel platens was used for this purpose. Figure 7 shows the honeycomb construction before and after alteration of the reinforcement core. The effect of crushing the core walls on the adherence of M-31 was determined. Coatings, approximately 0.300 in. thick, were applied to both types of the honeycomb structure, both with and without the reinforcement core altered. All test specimens were 2-in. squares cut from larger panels so that edge effects would not be a factor. A flatwise tensile test was used to determine adherence. The stresses required to separate the M-31 from the honeycomb substrate with and without the reinforcement core altered were measured to be 12.5 and 0.25 lb/sq in., respectively. This shows that the reinforcement core has very little holding power unless it is modified to interlock the M-31 in place.

Evaluating brazed stainless steel honeycomb construction as a substrate for M-31 included subjecting the composite structure to radiant heating. Specimens 6-in. wide and 11-in. long

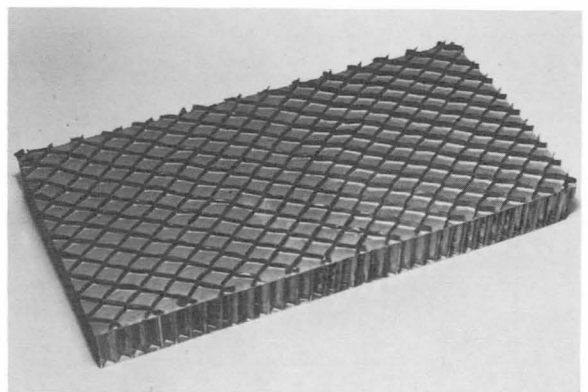


FIGURE 7.—*Honeycomb-sandwich construction with and without open-face core crushed.*

were coated with 0.300-, 0.380-, and 0.500-in. thicknesses of M-31 (fig. 8). Each specimen was exposed to a radiant heat flux of 24 Btu/ft²/sec for 180 seconds. The results are given in figure 9 which illustrates the backface temperature rise as a function of time.

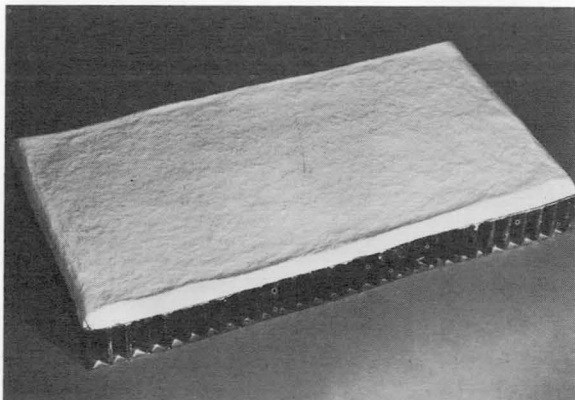


FIGURE 8.—Honeycomb-sandwich construction with M-31 insulation applied.

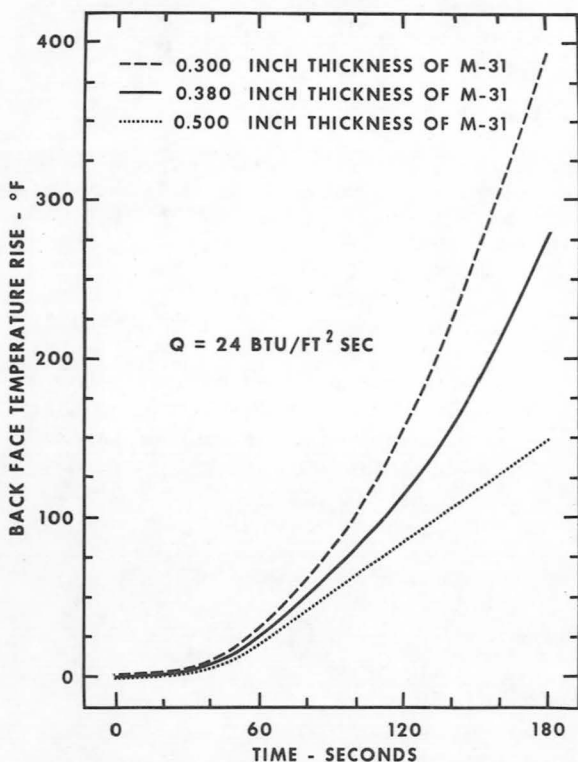


FIGURE 9.—Effect of coating thickness on performance of M-31 applied to stainless steel honeycomb.

Certain other properties of engineering interest also were determined, including (1) bulk density and water absorption, (2) water effect, (3) thermal-shock resistance, (4) thermal expansion, (5) reflectance, (6) emittance, (7) specific heat, and (8) mechanical strength. Reflectance and emittance results are shown in figures 10 and 11.

The material also has been demonstrated to be capable of withstanding the shock, vibration, and flexure loads associated with handling and launch operations. It also has excellent thermal shock resistance when water-quenched from 1600° F and below. Full details on physical properties and qualification tests are available in reference 2.

M-31 is a lightweight insulation that is capable of protecting the base region of the Saturn vehicle against heating from the engine exhaust and, at the same time, resists the shock and vibration of launch operations. The final composition contains fibrous potassium titanate to act

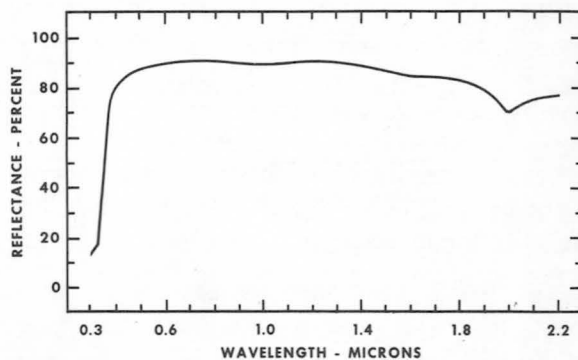


FIGURE 10.—Absolute spectral reflectance of M-31.

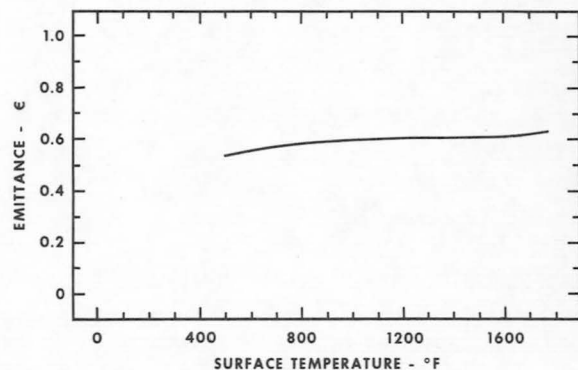


FIGURE 11.—Total normal emittance of M-31.

as an insulator and to provide the requisite reflectance asbestos fibers to provide structural stability and additional insulation and colloidal silica to serve as a binder. The resultant coating does not have to be cured at high temperatures; drying at a maximum temperature of 180° F imparts structural stability to the material and provides excellent water resistance. Further details may be found in reference 3.

The new coating has a dense exterior that is hard enough to resist ablation by the high velocity exhaust gases and a lightweight interior that is an excellent thermal insulator. The thermal conductivity of the material in the direction normal to its plane of application is between 0.85 and 1.3 Btu/ft²/hr/°F/in. in the 100° F to 730° F temperature range. It has excellent thermal shock resistance when water-quenched from 1600° F and below.

The greatest potential commercial use for this new coating is as an insulator for radiant heating environments. Coatings (1/2 in. thick) will withstand radiant heat fluxes up to 70 Btu/ft²/sec for short durations. Although it is most effective in radiant heating environments, it will also afford some protection against convective heat. A 0.310-in. thickness of the material was not affected when exposed to a convective heat flux of 10.5 Btu/ft²/sec for three minutes.

CONCLUDING REMARKS

Each of the three materials discussed was developed by MSFC to solve a particular insulation problem for which there was no existing solution. In each case, commercially available materials were combined into a composite system in such a manner as to take advantage of particular characteristics of each of the com-

ponents. The resulting composite materials possess properties and capabilities which are greatly different from those of the components which are incorporated. This characteristic of composite materials is what makes them so attractive for the solution of many problems.

It is believed that the most promising commercial application of the sealed cell or the Dual Seal concept would be as insulation for cryogenic liquid containers or cryogenic fluid transfer lines. The ceramic-gold coating is a good infrared reflector and also offers advantages over electrodeposited gold coatings for decorative applications. The M-31 material is an excellent insulator for applications where the heat load is made up of both radiative and convective components.

The potential commercial applications of the three insulation systems discussed are believed to be attractive. But just as MSFC has had to adapt commercial materials to uses for which they were not intended originally, industry will have to apply some ingenuity in finding the commercial usages of the three materials so developed.

REFERENCES

1. SKALREW, S.; HAUCH, C. A.; and LEVY, A. V.: Development and Evaluation of Insulating Type Ceramic Coatings, Part I, WADC TR 57-5777, August 1957.
2. SEITZINGER, V. F.: Further Development and Evaluation of M-31 Insulation for Radiant Heating Environments. NASA TMX-53267, 1965.
3. MIDDLETON, R. L.; and STUCKEY, J. M.; ET AL.: Development of a Lightweight External Insulation System for Liquid Hydrogen Stages of the Saturn V Vehicle, Proceedings of the 1964 Cryogenic Engineering Conference, University of Pennsylvania, August 18-21, 1964.

13. New Polymers for High Temperature Applications

ROBERT E. BURKS,

Southern Research Institute, Birmingham, Alabama

JAMES D. BYRD, AND JAMES E. CURRY

George C. Marshall Space Flight Center, NASA

The temperature extremes associated with the Saturn-class launch vehicles have created demands for new plastics and synthetic rubbers. Efforts are being made to provide for materials usable in these environments through several different approaches.

Polymers containing silicon-nitrogen bonds which show promise of satisfying some of these requirements have been studied. The chemistry of simple silicon-nitrogen compounds and their polymer-forming reactions is described. Data are presented which substantiate that certain silazane polymers are characterized by high thermal stability. Different modifications of these materials appear promising as coatings and as high-temperature rubbers.

Efforts to broaden this program by investigating other polymer-forming reactions of simple silazanes are described. One recent development in this area that appears particularly promising has led to the development of ordered phenylethersiloxane copolymers which are exceptionally stable at high temperatures. These materials may eventually be useful in many industrial applications when resistance to high temperatures is a requirement.

Polymeric materials, mainly in the form of synthetic rubbers, adhesives, and plastics, are used throughout the Saturn launch vehicle in a variety of applications. The complex piping associated with the engine system contains myriads of seals, gaskets, O-rings, diaphragms, and similar components. Organic resins or plastics reinforced with glass fibers or fabrics offer attractive structural advantages in many cases. There are instances where adhesive bonding is preferred over more conventional methods of joining parts. Plastic foams are used for insulation and structural rigidization. Plastics have achieved one milestone in the aerospace field that probably could not have been attained by any other type of material. The use of polymer-based composite materials as heat shields for the protection of structures reentering the earth's atmosphere from space is past history. Perhaps the importance of these

materials is emphasized by the national concern that developed during the final stages of Astronaut John Glenn's orbital flight when a false telemetry signal indicated that the heat shield of his spacecraft had loosened prematurely; fortunately, the fault was in the telemetry system and not the heat shield.

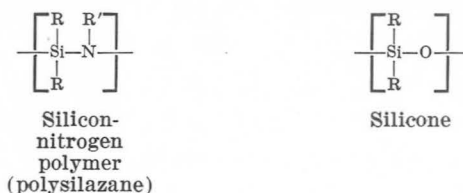
If a rational subdivision of the polymeric materials problem is possible, one might arbitrarily divide it into cryogenic and high temperature areas, as they apply to the George C. Marshall Space Flight Center (MSFC). Improved polymers are needed urgently and are being sought for a variety of functions at cryogenic temperatures down to the temperature of liquid hydrogen, -423° F. Other efforts are in progress to develop polymers that will be useful as adhesives, structural plastics, laminating resins, at elevated temperatures. It is this aspect of the total MSFC program that will be

emphasized in this paper. Most major programs now being carried out in this area are partnership ventures, with MSFC specialists working here on complementary phases of the overall experimental program in collaboration with scientists in various industrial and institutional research organizations.

SILICON-NITROGEN POLYMER STUDIES

One major area of research emphasis is the field of silicon-nitrogen chemistry. When a program was first initiated on this subject several years ago (ref. 1), there was no significant research activity underway that was oriented toward the development of polymers containing silicon-nitrogen bonds. During the time span of our program, many other investigators, including Breed and Elliott (ref. 2), Fessenden and Fessenden (ref. 3) and Rochow and co-workers (refs. 4 and 5), have made research contributions which indicate a growing interest in this field by the scientific community.

One of the first features of the silicon-nitrogen bond of interest to the chemist is the fact that it is isoelectronic with the silicon-oxygen bond, which is the backbone unit of the versatile silicones:

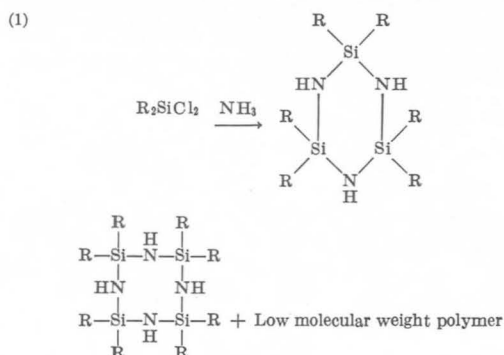


The isoelectronic relationship merely implies

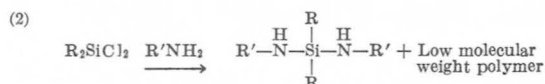
that the $\overset{\text{R}'}{\text{N}}$ group would be an electronically equivalent bridging group to the oxygen atom of the silicones. The estimated strength (ref. 6) of the silicon-nitrogen bond is only slightly less than that of the silicon-oxygen bond, which suggests that Si-N polymers should have attractive thermal stability. The nitrogen atom of the silazane linkage has a substituent (designated R' above) which can be varied with concurrent variations in polymer properties. There is also an electron pair associated with the silazane nitrogen which is available for coordination with suitable electron acceptors. There are points of similarity between the sila-

zanes and silicones and also subtle differences, which both suggest that the silazanes are materials worthy of further study.

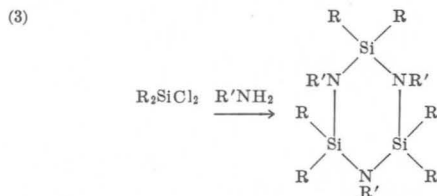
The most obvious route to silicon-nitrogen polymers is through the direct reaction of silicon dihalides with ammonia or amines. Possible products are silicon diamines, cyclic silazanes, or polysilazanes. When ammonia is the starting material, the product is a mixture of the latter two forms. Silicon diamine compounds are the major products when there is considerable steric bulk on the silicon (ref. 7). The ratio of cyclization to linear polymer formation that occurs with small substituents on the starting silicon dihalide is governed by several factors. Reactions involving ammonia usually give products containing large proportions of cyclic trimer and tetramer:



A primary amine tends to first form the corresponding silane diamine derivative:



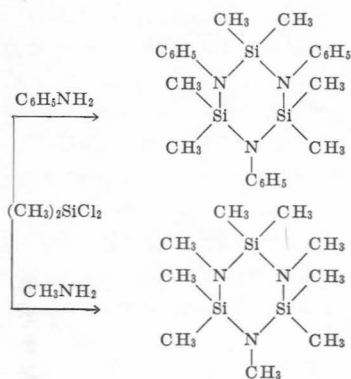
The resulting diamine compound may react further, especially under forcing reaction conditions, so that cyclization is sometimes observed with amine reactants:



Although a number of these cyclic and linear silazane compounds had been studied at the time this investigation began, there had been no published study of the conditions required to

favor the formation of polymers over other possible products. Consequently, the reactions normally leading to these cyclic products were studied in some detail. Hexamethylcyclotrisilazane and octamethylcyclotetrasilazane were prepared readily by applying reaction (1) to dimethyldichlorosilane. These materials were found experimentally to be more thermally stable than a corresponding cyclic silicone, octamethylcyclotetrasiloxane. Reaction (3) was utilized to prepare a number of N-substituted cyclic silazanes, as shown below:

(4)



Using cyclic silazanes prepared by these two methods which contained different distributions of various substituents between the silicon and nitrogen atoms, it was possible to carry out comparative hydrolytic stability measurements which established that the following effects favor hydrolytic stability:

- Attachment of phenyl groups to silicon or nitrogen atoms
- Replacement of hydrogen atoms on nitrogen atoms with phenyl, methyl, or isopropyl groups
- Cyclization or elimination of amine end groups
- Silylation of nitrogen atoms in cyclic silazanes.

None of these studies suggested any effective means of improving the yield of polymers associated with these cyclic products. It was only in occasional instances that enough polymer was formed to be recovered during subsequent laboratory purification of the crude reaction product.

The thermal behavior of cyclic silazanes is exemplified by hexaphenylcyclotrisilazane.

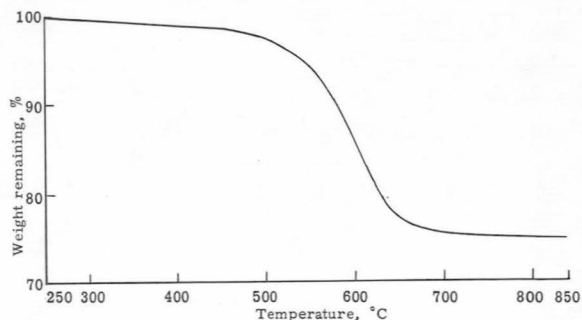


FIGURE 1.—*Thermogravimetric analysis of hexaphenylcyclotrisilazane condensation polymer in a nitrogen atmosphere (rate of temperature rise, 6° C per minute).*

Chemical analyses of the parent compound and its high temperature condensation products indicate that as the material is heated to progressively higher temperatures, a very stable polymer approaching the composition $(\text{C}_6\text{H}_5\text{SiN})$ is formed. Figures 1 and 2 show the results of thermogravimetric analysis applied to the polymer, and a differential thermal analysis over the relevant temperature range starting with the initial compound. Unfortunately, this solid product is very brittle and is obtained as a foam unless the parent compound is cured in very thin layers. The behavior of these phenyl-substituted silazanes seems to confirm the thermal stability one would predict from bond-energy considerations.

Some promising but complex chemistry has been brought to light during investigations of the polymeric products prepared from dihalosilanes and organic diamines. The reaction

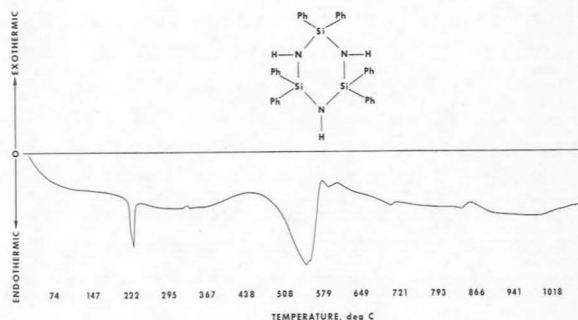
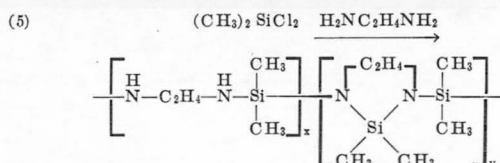
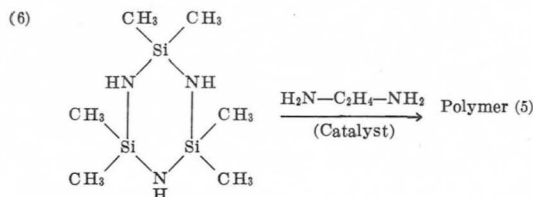


FIGURE 2.—*Differential thermal analysis hexaphenylcyclotrisilazane.*

product of dimethyldichlorosilane and ethylene diamine that has been investigated during our program also has been studied in some detail by three other groups (refs. 2, 4, and 8) :



Rochow and Minné (ref. 4) postulated a linear structure for the polymer and studied its coordination behavior with copper and beryllium. Henglein and Lienhard (ref. 8) in Germany obtained some evidence for the cyclic structure. Their work apparently has been confirmed by Breed and coworkers (ref. 2). All of this work indicates that the initial product is a random combination of the linear and cyclic forms. This appears to be true of the polymer when prepared by the direct dihalosilane-diamine route or when prepared by a catalyzed amine-exchange process from hexamethylcyclotrisilazane :



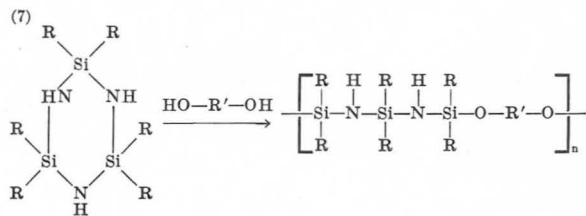
Variations of synthetic techniques can be utilized to produce a range of materials from elastomeric gums to viscous fluids. The properties of these polymers are not encouraging, but our work has shown that the polymer prepared by either (5) or (6) can be cured in air at 425° C to yield a spongy elastomeric solid which retains its resiliency after exposure to elevated temperatures that seriously embrittle the best known commercial high-temperature rubbers. The polymer loses a variable portion of its nitrogen content during this curing step, but apparently the portion that remains confers this high temperature behavior. In its present form, the elastomer has very poor tensile strength, but there are ways of improving this situation.

OTHER POLYMERS DERIVED FROM SILAZANES

This program was initiated with the knowledge that many early investigators had de-

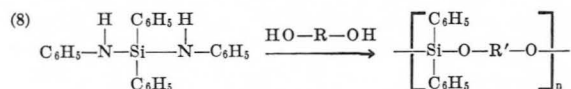
clared silazane polymers unlikely candidates for commercial success because of scattered observations which implied that they would have poor hydrolytic stability. Even if this statement were true without exception, it would only serve to justify exploring silazane chemistry for another reason. The very traits that could render silazanes, in some cases, susceptible to hydrolysis could also make them potentially reactive intermediates for the synthesis of other polymers. Consequently, this possibility is being studied in a parallel investigation. In their review article on silicon-nitrogen chemistry, Fessenden and Fessenden (ref. 3) mentioned several attractive approaches, including the cleavage of silicon-nitrogen bonds by alcohols and silanols. The work of Pike (ref. 9) suggests that these reactions would take place at reasonable rates.

Breed and coworkers (ref. 2) have studied the ring-opening, polymer-forming reactions of cyclic silazanes with organic diols :



Similar polymers have been prepared during this study which have attractive thermal stability, as shown in figure 3.

Curry and Byrd (ref. 10) have investigated the reactions of a simpler silazane, bis(anilino)-diphenylsilane, with stoichiometric quantities of a variety of organic diols :



This particular silazane was favored initially over other possibilities because it was believed that the bulky phenyl groups would render it less prone to undergo competing reactions.

Phenylether-silicone copolymers of this type had been sought earlier by MacFarlane and Yankura (ref. 11) who obtained similar materials with promising thermal stability by other synthetic approaches. However, the approach

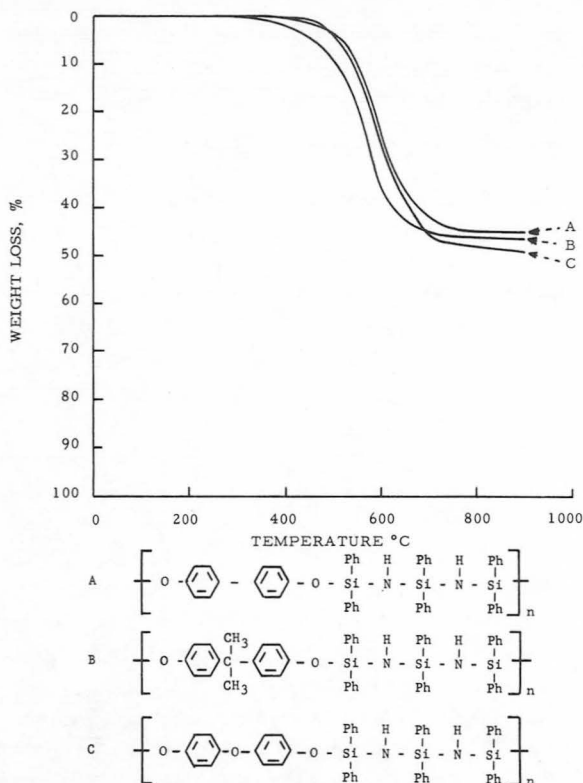
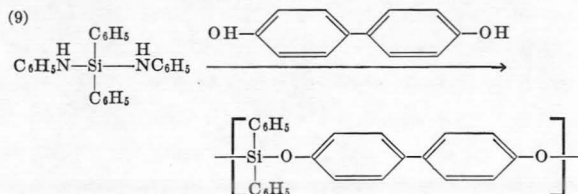


FIGURE 3.—*Thermogravimetric analysis. Ph represents a phenyl group in each case.*

shown in reaction (8) appears to promote the formation of higher molecular weights.

The reaction is conducted as a melt polymerization. Final heating of the polymer melt is conducted under vacuum at 300–325° C to insure complete removal of the byproduct aniline. The yield of polymer has exceeded 90 percent in every case so far. All polymers prepared from aromatic diols were tough, rigid solids; some of these did not soften appreciably at temperatures up to 250° C. Polymers derived from aliphatic diols have not been investigated as extensively.

The polymer prepared so far which seems to show the best potential balance of properties is derived from 4,4'-dihydroxybiphenyl:



The thermal stability of this polymer relative to three others prepared from other diols is indicated by the TGA data in figure 4. Molecular weights ranging up to 200 000 have been attained in some preparations, and the polymer is soluble in tetrahydrofuran, dimethylformamide, and dimethylsulfoxide. Fibers can be pulled readily from a melt of this polymer, and it adheres tenaciously to a wide variety of surfaces. Further work is in progress to evaluate the potential of this polymer on a larger scale. (ref. 12).

Burks and coworkers (ref. 1) have studied similar polymers based upon the reactions of phenylene-bridged silicon diols with silylamines. The diols required for this study are not commercially available, and several aspects of their preparation have been investigated.

One patented process (ref. 13) for the preparation of phenylene-bridged silicon compounds

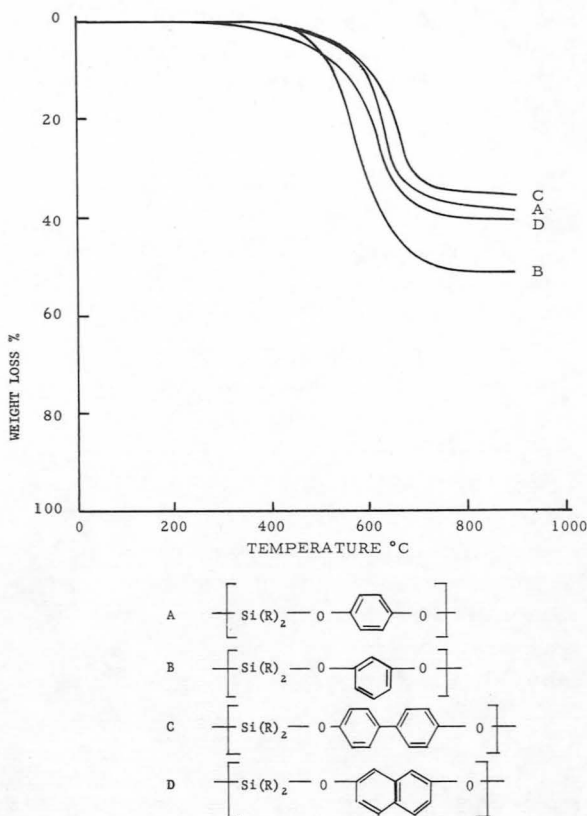
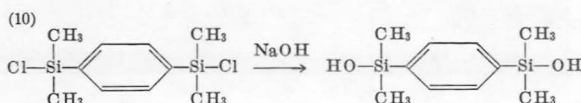
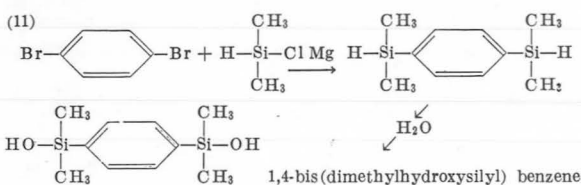


FIGURE 4.—*Thermogravimetric analysis of polymers. R represents a phenyl group.*

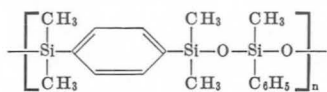
is based upon the hydrolysis of 1,4-bis(dimethylchlorosilyl) benzene.



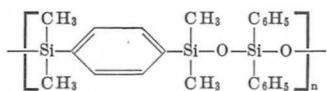
The preparation of the starting chlorine derivative required by this procedure is not easy, and during this hydrolysis step shown above, it is difficult to avoid partial condensation of the product with elimination of water. A modification of the following method published recently by Merker and Scott (ref. 14) has given better results.



The above silane diol has been polymerized with a number of silazane derivatives in a manner fully analogous to reaction (8). Two polymers with particularly outstanding properties that have been obtained by this route are shown below:



Poly (tetramethyl-p-silphenylenesiloxane) - (methylphenylsiloxane)



Poly (tetramethyl-p-silphenylenesiloxane) - diphenylsiloxane

Molecular weights up to 290 000 have been obtained, and it appears that as a class, these silphenylenediol-diaminosilane polymers deserve concentrated study in an effort to produce elastomers with high thermal stability. Benzoyl peroxide-cured specimens have been obtained in the form of elastomers which retain their resiliency after exposure to 400° C for over an hour. One silica-filled sample was cured for three hours at 300° C to a tough rubber. This material grew progressively harder and tougher during heating at 400° C, but after two hours exposure to this environment, it was embrittled only slightly and retained more

resiliency than has been detected in commercial high-temperature rubbers that have been subjected to the same treatment.

APPLICATION STUDIES

These materials must still be classed as developmental and several versions of the polymers described earlier are under evaluation. Several silazane-containing compositions have been given a preliminary screening at MSFC as components of heat-shield composites. This application was suggested by the tendency of silazanes to undergo high temperature condensation reactions which appear to be endothermic in nature. Considerable additional study will be required to establish their utility for this application.

Some of these materials have been considered for pigmented high-temperature coating applications by Butler (ref. 15) and coworkers during a study for the U.S. Air Force. Asilazane-polymer blend developed during our program that is comprised of a mixture of poly (diphenyl-silazane) and the polymeric product of reaction (5) was formulated into a pigmented coating that retained good integrity, adhesion, and color in thin films during 8-hour exposures in argon (1000° F) and air (800° F). A sample of the polymer shown in reaction (9) was evaluated and found to be stable and adherent in an inert atmosphere at 1000° F. Its lifetime in air at 800° F was proven to be substantially less due to oxidative instability. This oxidative stability problem must be solved if the full high-temperature potential of this material is ever to be realized in a normal environment.

The very recent discovery during this investigation of elastomeric materials incorporating the stable silphenylene moiety indicates that an exhaustive evaluation should be made of their properties. It is easy to foretell many possible uses both within and without the aerospace industry for synthetic rubbers whose high temperature properties overshadow those of materials now available.

One area where a step-up the thermal ladder would be welcomed is in the area of static and dynamic seals. Dynamic seals in particular

are being called upon to function at temperatures that are approaching the upper temperature limit of the best commercial high-temperature elastomers. Some hope is also justified for the development of high-temperature wire coatings which will allow a step beyond the increased electric motor operating temperatures that the silicones have permitted. Specialized industrial requirements for improved high-temperature coatings can also be visualized. Furnace hardware and tanks or process piping for hot fluids are two possible coating applications that come to mind. Virtually all materials studied during this program are characterized by good adhesion to a wide variety of substrates, a key requirement of coating resins.

The thermal stability of the alternating phenylether-silicone block copolymers prepared by reaction (7) is also believed to warrant further study, particularly with respect to improving their oxidative stability. The specific polymer formed by reaction (8) has looked particularly encouraging. Crude fibers pulled directly from melts of this material have been obtained with tenacities as high as 0.8 gram per denier. More optimized spinning conditions should certainly improve this value. Thermally pressed 15-mil films of the same polymer had a tensile strength of 3600 psi. When applied as a hot-melt adhesive to mild steel adherends, the tensile shear strength averaged 2900 pounds per square inch. Small samples have been compression molded, but the material's tendency to stick to a wide variety of substrates has created a mold-release problem.

CONCLUDING REMARKS

In conclusion, it seems very likely that new high temperature materials may be developed through either or both of the approaches described in this paper. The possibilities for new high temperature coating resins and synthetic rubbers are particularly impressive. There also are reasons to hope that new adhesives with improved properties at both low and high temperatures may be developed.

A study of polymers containing silicon-nitrogen bonds has resulted in the development of a number of new and interesting materials.

Silazane compounds and polymers having outstanding thermal stability have been developed. These show particular promise as high temperature coatings and elastomers which exhibit stability to temperatures in the range of 400 to 500° C.

Polymers prepared by the use of silazanes as monomers have resulted in tough materials with molecular weights as high as 280 000. These materials are also stable to about 500° C and may be used as coatings, fibers, films, elastomers and adhesives. These materials offer considerable potential in industrial applications where high thermal stability is required.

REFERENCES

1. BURKS, R. E.; and RAY, T. W. (Southern Research Institute, Birmingham, Alabama): First Annual Summary Report, U.S. Army Contract DA-01-009-506-ORD-829, December 1, 1959-January 31, 1961. (Subsequent reports were issued by the same investigators under NASA Contract NAS8-1510).
2. BREED, L. W.; and ELLIOTT, R. L. (Midwest Research Institute, Kansas City, Missouri): Technical Progress Reports prepared under U.S. Army Contract DA-23-072-ORD-1687, June 29, 1961-to date.
3. FESSENDEN, R.; and FESSENDEN, J. L.: *Chemical Reviews*, 61, 377, 1961.
4. ROCHOW, E. G.; and MINNÉ, R.: *Journal of the American Chemical Society*, 82, 1960, 5625, 5628.
5. KUMMER, D.; and ROCHOW, E. G. (Harvard University, Cambridge, Massachusetts): Unnumbered Technical Report, U.S. Navy Contract Nonr-1866 (13), December 1962. Additional reports have been prepared under this same contract by the following investigators: LIENHARD, K., September 4, 1963. KUMMER, D., January 1963. BARRANTE, J. R., August 1963. MASELLI, J. M., March 31, 1962. PFLEGER, H., September 1961. WEISS, R., September 1961. MINNÉ, R. N., May 1960.
6. STONE, F. G. A.; and GRAHAM, W. A. G., eds.: *Inorganic Polymers*, Academic Press, Incorporated, New York City, New York (1962), p. 244, table XI.
7. SOMMER, L. H.; and TYLER, L. J.: *Journal of the American Chemical Society*, 76, 1030, 1954.
8. HENGLEIN, F. A.; and LIENHARD: *Makromolekulare Chemie*, 32, 218, 1959.
9. PIKE, R. M.: *Journal of Polymer Science*, 50, 151, 1961, *Journal of Organic Chemistry*, 26, 232 1961.
10. CURRY, J. E.; and BYRD, J. D.: *Journal of Applied Polymer Science*, 9, 295, 1965.

11. MACFARLANE, R. S.; and YANKURA, E. S. (U. S. Rubber Company, Naugatuck, Connecticut): Terminal Report, U.S. Army Contract DA-19-020-ORD-5507, 1 July 1961-15 January 1964.
12. DUNNAVENT, W. R.; MARKLE, R. A.; BERRY, O. A.; and STICKNEY, P. B. (Battelle Memorial Institute, Columbus, Ohio): Technical Reports Prepared under NASA Contract NAS8-11837, January 14, 1965.
13. SVEDA, M.: U.S. Patent 2,561,469, Assigned to E. I. du Pont de Nemours and Company, Incorporated, July 24, 1951.
14. MERKER, R. L.; and SCOTT, M. J.: Journal of Polymer Science, A2, 15, 1964.
15. BUTLER, J. M.; HATHAWAY, C. E.; and ANDUZE, R. A. (Monsanto Research Corporation, Dayton, Ohio): Eighth Quarterly Progress Report, U.S. Air Force Contract AF 33(657)-8641, 1 February 1964-1 May 1964.

14. New Lightweight Alloys

C. E. CATALDO

George C. Marshall Space Flight Center, NASA

This paper describes three alloys that are under development for specific aerospace applications which show considerable promise for certain industrial applications. A new high-strength weldable aluminum plate alloy, an aluminum casting alloy, and a magnesium-lithium alloy of exceptional light weight are described. The aluminum plate material has a tensile strength 10-15% higher than existing commercial alloys used for welded aerospace structures. It has good low temperature strength, and notch sensitivity appears to be satisfactory. The aluminum casting alloy was developed to have high impact strength at cryogenic temperatures, but room temperature properties also exceed those of generally used aluminum casting alloys. Although magnesium-lithium alloys have already been used in some aerospace applications, additional properties of these alloys are presented, and a new alloy with improved strength is discussed.

One of the most important design criteria for space vehicles is that the structural materials should have the lightest weight possible within the service requirement envelope. The National Aeronautics and Space Administration (NASA) has undertaken, in many of its system development programs, to develop lightweight, high-strength alloys by either modifying existing alloys or developing completely new ones for specific structural requirements. Such research has been done both in-house and by various research organizations sponsored by the government. Only a small portion of materials-development work falls under a security classification; most of the work is reported and is available through general government publications. The government has supported many materials-research programs that could not be justified economically for self-support by industry. This has been particularly true where expensive and exotic materials are concerned and where critical aerospace or defense requirements are the only justifying factor. One good example is the Defense Department support of titanium development during the past few years. Today, industry is reaping considerable

benefits from many of these expensive early programs.

One important factor to consider is that, often a material developed for one purpose may, at some later time, find application for another purpose where its properties are found to be superior to alloys previously used. One recent example of this is the aluminum alloy 2219, an alloy developed by Alcoa for elevated-temperature service. A screening program conducted by Marshall Space Flight Center (MSFC) several years ago indicated that this alloy had excellent low-temperature properties at temperatures as low as that of liquid hydrogen. At the present time, 2219 is the major structural material for the Saturn V first-stage booster, which uses plate and forgings of this alloy ranging from 0.250 in. to 5.0 in. thick. Unanticipated applications of materials have been common occurrences in the aerospace industry; however, the modern materials engineer recognizes that there is much to be gained by the concentrated development of a material tailored for a specific application.

This report describes three alloys developed through MSFC-sponsored research for specific

applications. These include an aluminum plate alloy, an aluminum casting alloy, and a magnesium-lithium alloy of exceptionally light weight.

One of the three alloys discussed in this report is already being used in a wide variety of applications both in aerospace and other industries. The other two alloys are more recent developments and still require additional evaluation before release for general use.

DEVELOPMENT OF A HIGH-STRENGTH WELDABLE ALUMINUM ALLOY PLATE FOR CRYOGENIC APPLICATIONS

Basis for Development

The large liquid-propellant space boosters now being designed and built use weldable aluminum alloys having the highest possible strength/weight ratio characteristics consistent with good ductility and notch-insensitivity at temperatures down to that of liquid hydrogen (-423°F , -253°C). Currently, the predominant alloys used are the 2014 and 2219 alloys in various tempers that provide yield strengths in the 50 000 to 60 000 psi range and ultimate strengths in the 60 000 to 70 000 psi range. Neither of these alloys was initially developed to serve in this particular environment.

Alloys of the Al-Zn-Mg-Cu series which develop considerably higher strengths have been used extensively for aircraft and other structural applications in which no welding is involved, but their inferior weldability and rather poor notch toughness at cryogenic temperatures make them unsuitable for booster oxidizer and fuel tankage.

Recently developed alloys of the Al-Zn-Mg (Cu-free) type are readily weldable and develop potentially useful combinations of weld strengths, tensile properties, and cryogenic toughness, but do not meet the high strength requirements considered essential for the most advanced booster concepts. The need for aluminum alloys having higher strengths stimulated the support of a research program with Alcoa under MSFC Contract NAS8-5452.

Compositions of Experimental Alloys

The goal of this program was to develop an alloy with exceptionally high strength, good notch toughness, fabricability, weldability, and

resistance to corrosion. An alloy was desired that would have a tensile strength approaching 75 ksi, yield strength 65 ksi, elongation of 15%, and a notched/unnotched tensile ratio of 1.0 at room temperature. Three alloy types were initially considered: Al-Cu (2000 type), Al-Mg (5000 type), and Al-Zn-Mg (7000 type). Based on the experimental survey results, the Al-Mg alloys were discarded as incapable of meeting the requirements. A more intensive evaluation of the properties and optimization of thermal treatments was undertaken with the promising Al-Cu and Al-Zn-Mg compositions.

Two alloys emerged from this evaluation that were considered capable of approaching the initial program goals. These alloys, designated M825 (Al-Cu type) and M826 (Al-Zn-Mg type) were indicated to have good fabricability and weldability, although each has certain advantages and disadvantages. In initial work, both of these alloys developed strengths 10-15% higher than the highest strength weldable alloys now available commercially and exhibited good cryogenic toughness.

TABLE I.—*Chemical Composition of Experimental Alloys M825 and M826 (nominal)*

Alloying element	M825	M826
Cu.....	6.3	0.10
Mn.....	0.3	0.2
Mg.....	-----	1.8
Cr.....	-----	0.12
Zn.....	-----	6.5
Ti.....	0.06	-----
V.....	0.10	-----
Zr.....	0.18	0.12
Cd.....	0.15	-----
Sn.....	0.05	-----
Al.....	Remainder	Remainder

Table I shows the chemical composition of the M825 and M826 alloys. As indicated, M825 is basically the 2219 alloy with additions of copper and tin. It should be noted that these are nominal compositions. Determination of the optimum composition limits will be made in the second year's effort on this program which is currently underway.

TABLE II.—Comparison of Typical Mechanical Properties of Experimental Alloys With Commercial Alloys

Property	Testing Temp.	M825	M826 ^a	2219-T87	X7106-T6351	5456-H343	Goals
Tensile strength, ksi---	R.T.	75.4	79.5	67.6	65.6	56.1	75.0
	-320° F	89.8	92.3	85.0	86.8	72.1	-----
	-423° F	99.1	-----	99.4	102.5	74.8	-----
Yield strength, ksi----	R.T.	66.0	72.2	56.0	58.1	44.4	65.0
	-320° F	73.8	86.8	67.6	70.5	52.3	-----
	-423° F	82.8	-----	72.2	75.0	54.8	-----
Elongation, % in 2 in--	R.T.	9.0	12.2	10.5	12.8	10.2	^b 15.0
	-320° F	12.7	2.2	11.0	14.0	13.9	-----
	-423° F	10.0	-----	13.5	15.2	7.0	-----
Notched/unnotched tensile ratio ^c	R.T.	0.98	1.31	1.13	1.36	0.95	1.0
	-320° F	1.06	0.95	1.03	1.06	0.85	-----
	-423° F	1.03	0.95	0.94	0.94	0.88	0.9

^a-423° F Test data on M826 not complete.

^b Recently changed to 10%.

^c $K_t=10.0$.

Mechanical Properties of Experimental and Commercially Available Alloys

Table II shows typical mechanical properties obtained to date on plate thicknesses of M825 and M826. The program goals are included in this table, as well as typical properties of three commercially available alloys: 2219-T87 (Al-Cu type), 7106-T6351 (Al-Zn-Mg type), and 5456-H343 (Al-Mg type). Although test data at -423° F of the two plant-fabricated experimental alloys are not available at the present time, results of tests on laboratory-produced plates indicate that both alloys are capable of exceeding the -423° F notched/unnotched tensile ratio requirement of 0.90. Tests have also indicated that the notched/unnotched ratio of M825 is much less temperature sensitive than that of M826. Higher strengths can be obtained with the M826 alloy than those shown in table II by variations in thermal treatment; however, with the higher strength, the notch sensitivity of the alloy increases. The strengths shown in table II meet the minimum goal requirements, but, average strengths would have to be 6-7 ksi higher to meet the goals with a good level of confidence. The goal of 15 percent elongation is apparently outside the capa-

bilities of aluminum alloys having tensile and yield strengths of this level. Therefore, this goal has been revised downward to 10-percent minimum.

Suitability for Plate Thickness

Both M825 and M826 have been plant-fabricated in various plate thicknesses to 2.375 inches with no serious problems reported either in ingot casting or rolling. There is a problem with the 2.375-in. thick material in attaining the strength objectives, particularly with the M826 alloy, due to its greater quench sensitivity. Various thermal and mechanical treatments are being investigated to determine optimum treatments for all thicknesses.

Weldability of M825 and M826

The weldability of M825 and M826 alloys is still being studied. Based on weld cracking tests, M825 is rated very easy to weld, or having good commercial weldability, when 2319 or the base-metal composition is used as the filler alloy. Welding characteristic determinations made on the Al-Zn-Mg type alloy indicate that the amount of weld cracking is generally low when the filler metal contains Zr. It is antici-

pated that this alloy will be easy to weld, although not equal to the excellent weldability of the 2219/2319 or 5456/5556 combinations. The strength of 1/2-in. thick MIG-welded M825 plate, using 2319 filler, is similar to that of 2219 welded with 2319 filler, having an as-welded efficiency of about 60%. MIG-welded M826, using a base-metal filler alloy composition, resulted in a tensile strength of approximately 60 000 psi as-welded. Typical weld tensile properties for both alloys are shown in table III. Preliminary results in some recent tests show that one experimental filler alloy will increase the as-welded strength of M825 6000 to 8000 psi over that obtained with 2319-filler alloy. A thorough evaluation of welds of 1.0-in. thick plant-fabricated M825 and M826, including both MIG- and TIG-welds, is being made.

TABLE III.—Room Temperature Properties of M825 and M826 Welded Plate

[Material thickness—0.500 in.; Material tested as-welded]

Property	M825 (2319 filler)		M826 (M822 filler)	
	MIG	TIG	MIG	TIG
Tensile strength, ksi.....	42.4	42.8	59.0	54.0
Yield strength, ksi.....	37.6	33.2	52.5	46.0
Elong., % in 2 in.	1.1	1.4	1.1	2.0
Notched/un-notched ratio ^a	1.0	----	1.1	----

^a KT=10.0.

Stress Corrosion Resistance

Stress-corrosion tests are being conducted on both experimental alloys in industrial and sea-coast atmospheres, using alternate immersion tests. The comparative merits of the two alloys, with respect to resistance to stress-corrosion cracking, are not clearly defined at this time because of the inadequacy of test data. Results for M825 show some inconsistencies, but there are indications that a resistant temper can be achieved. Since resistance varies greatly with temper, an attempt to optimize the thermal

treatment for stress-corrosion resistance has been started. M826 has good stress-corrosion resistance in the longitudinal and long-transverse directions, but is susceptible in the short-transverse direction. However, it is still similar to that exhibited by lower strength alloys such as X7106 and 7039.

Industrial Applications

Although this program was undertaken primarily for the development of weldable, high-strength aluminum alloys for aerospace applications, the alloys could be potentially useful for commercial or military applications. They would probably be suitable for storage vessels for gases or cryogenics. They may also be satisfactory for some bridge structures where weldability is desirable. In a broader sense, the high strength may give strong impetus to the substitution of aluminum for other general construction materials over a wide range of industrial applications. Military usage could possibly include armor, engineering items, vehicles, and bridge applications.

Summary

In summary, two weldable alloys with room-temperature properties 10 to 15 percent higher than existing commercial alloys are under development. Results indicate that both will be readily weldable although an improvement in weld strength is desirable, particularly for the Al-Cu type (M825). Low temperature properties look good, as do the notch sensitivity characteristics of the alloys at room temperature and low temperatures. Although results are not conclusive at this time, stress corrosion resistance of the two alloys appears similar to that of commercial heat-treatable, high-strength alloys. Development of the alloys is continuing, and efforts are being expended to improve the properties by various techniques, such as modification of composition and improvements in thermal and mechanical processing. Efforts to improve weld strength are being made, particularly by utilization of a number of experimental filler alloys, and improvements in stress corrosion resistance are being sought by optimization of thermal treatment.

DEVELOPMENT OF A NEW HIGH-STRENGTH ALUMINUM
CASTING ALLOY (M-45)

Basis for Development

Forgings and welded structures, which are costly and usually require extensive machining, are used in many instances where a casting would be ideal if it were strong enough. Castings are of particular advantage where designs are rather complex and procurement times are generally much shorter. Suitable castings must have high strength and toughness and must be compatible with the adjoining structure, especially where welding is to be done. The heat-treatable aluminum casting alloy described in this report was developed to satisfy the requirements of high strength and toughness for cryogenic applications, and the initial development work was done by the Battelle Memorial Institute under Contract NAS 8-1689 with MSFC. The primary goal of the program was to develop a casting having exceptionally high impact strength at cryogenic temperatures down to the boiling point of liquid hydrogen (-423°F); however the resulting alloy has exceptional properties in other respects. The alloy has been tentatively designated M45, denoting the yield strength characteristics.

Chemical Composition

The chemical composition of this alloy is given in table IV. The compositions of other

commonly used high-strength alloys are shown for comparison. During the initial development program, a variety of compositions were investigated, and several demonstrated very good impact properties, better than currently available alloys. However, the 4.5Cu-0.1Cd-0.1Mg-0.5Ti alloy appeared to be the best alloy composition developed. In the initial study of the alloying effects of various metals, it appeared that in the presence of magnesium, cadmium is much less effective than usual in increasing strength. Instead, it resulted in significant improvements in impact properties and in ductility. A possible Mg-Cd interaction seems likely, but this has not yet been investigated in detail.

Mechanical and Physical Properties

Mechanical properties of M45, as compared to other commonly used casting alloys, are given in table V. A limited number of actual castings have been made to date, and it is expected that improved casting techniques will produce properties somewhat higher than those reported.

Heat treatment processes have not been thoroughly investigated with respect to optimum mechanical properties. However, even the lowest results obtained for an acceptable casting are remarkably good for an aluminum casting alloy. Impact strengths increase considerably with decreasing temperature and are

TABLE IV.—Chemical Composition of M-45 and Other High Strength Aluminum Casting Alloys

Alloying element	Nominal composition, ^a weight percent				
	M-45	A356	Tens-50	Almag 35 ^b	195
Cu.....	3.90-4.50	0.20	0.20	0.01	4.00-5.00
Cd.....	0.08-0.12	-----	-----	-----	-----
Mg.....	0.06-0.10	0.25-0.40	0.40-0.60	7.00	0.03
Ti.....	0.02-0.05	0.20	0.10-0.20	0.10	0.20
Si.....	0.017	-----	7.60-8.60	0.10	0.50-1.2
Fe.....	0.010	0.35	0.40	0.10	0.80
Cr.....	0.001	-----	0.20	-----	-----
Mn.....	-----	0.10	0.20	0.10	0.20
Zn.....	-----	0.10	0.20	-----	0.20
Be.....	-----	-----	0.10-0.30	-----	-----
Al.....	Bal	-----	Bal	Bal	Bal

^a Composition given is maximum permissible unless given as a range.

^b Typical.

TABLE V.—*Mechanical Properties of Aluminum Casting Alloys*

Alloy	Ultimate tensile strength, psi	Tensile yield strength, psi	Elongation, percent in 2 inches	Charpy impact, ft-lb
M-45.....	48 000	45 000	5	13
A 356.....	34 000	29 000	2	2
Tens-50.....	37 000	32 000	2	1
Almag 35.....	30 000	16 000	7	3
195.....	30 000	24 000	2	3

in excess of 15 ft-lb at -423° F. The alloy is significantly stronger and tougher than high purity 195 alloy.

Figure 1 gives the ultimate strength, yield strength, and percent elongation (percent in 2.0 in.) of M45 heat-treated to the -T6 condition in relation to the test temperature. Figure 2 shows the impact strengths of two heats of the alloy. Although there is considerable scatter in these values which indicates variations in casting procedures, all values are rather high for a cast alloy. Figure 3 shows a comparison of both yield strength and impact strength of M45 with Tens-50, A356, and Almag 35 casting alloy at -320° F.

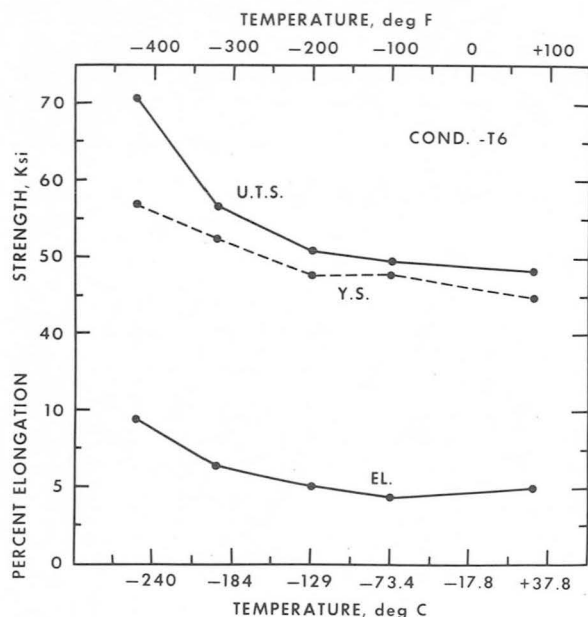


FIGURE 1.—*Low-temperature mechanical properties of a new aluminum alloy sand casting.*

The density of M45 is approximately 0.1. Although other physical properties are expected to be very similar to the 195 casting alloy, complete data are not yet available.

Microstructure

The M45 is characterized by a rather large grain size in castings made to date. Figure 4 shows the typical microstructure obtained, and a random distribution of CuAl_2 throughout the matrix and grain boundaries is evident. There appears to be no tendency for significant segregation of microconstituents. Along with the coarse grain, there is an absence of columnar or dendritic type structures.

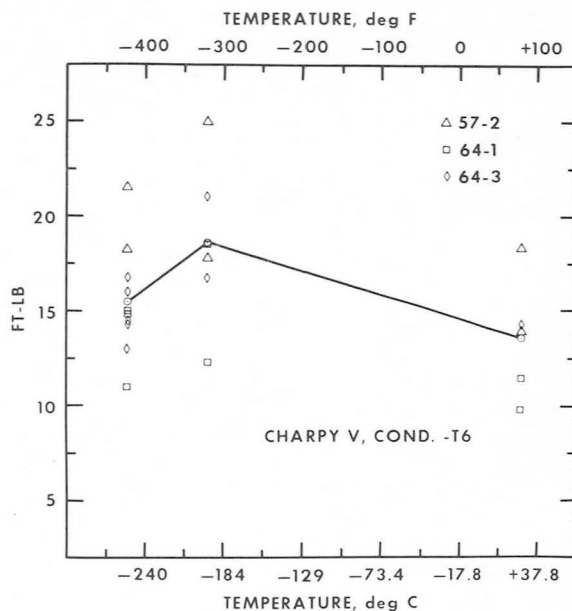


FIGURE 2.—*Impact energy of a new aluminum alloy sand casting.*

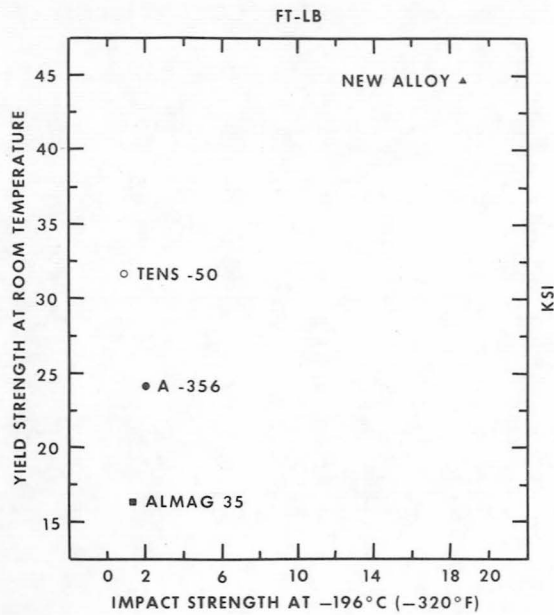


FIGURE 3.—Comparison of mechanical properties of several aluminum alloys, sand castings.

Castability

Castings of various configurations and sizes have been made and are shown in figures 5, 6, and 7. The latter two castings were cast from ingots prepared in a 1000-lb lot by a commercial supplier. No problem was encountered in preparing the ingots according to the specification composition limits. Some gas porosity and shrinkage were found in the three castings illustrated, but the castings shown in figures 6 and 7 were found to be acceptable for Saturn hardware as determined by radiographic inspection. Radiographic standards for Saturn hardware are very rigid; thus, these castings were of excellent quality. The first castings shown in figure 5 were rejected against flight standards, but the quality was such that they would be satisfactory for most commercial applications. Mechanical properties of these particular castings are shown in table VI.

Although these castings were made with usual foundry procedures, and no difficulty was experienced, it is believed that optimization through experience with production castings will result in more consistent strength properties and structural soundness. Laboratory tests have indicated that the alloy is comparable to 195 alloy

TABLE VI.—Mechanical Properties of Typical Saturn Configuration Castings Made From M45 Alloy

Casting	Temp., °F	Uts, ksi	Ys, ksi	% Elong., 4D
Figure 5	Room	48	45	5
	-432	71	57	9
Figures 6 and 7	Room	52	50	3
	-423	82	68	8

in castability and that it is slightly less easily cast into intricate shapes than A356.

Weldability

Limited tests have been made to determine the weldability of M45. Casting-to-casting weldments with 2319-filler material and manual TIG-welding have been made, as well as casting-to-2219 plate weldments with 2319-filler material and automatic TIG-welding.

Weld strengths of castings joined to castings by manual welds are shown in figure 8. The average strength was 25 700 psi in the as-welded condition. Reheat treatment of a welded test sample using the -T6 treatment almost doubled the strength.

Weld strengths of casting-to-2219-T87 plate ($\frac{3}{8}$ -in. thick) are shown in the same figure. The average strength of these automatic welds was 36 200 psi, considerably higher than the previous manual welds.

Industrial Applications

Although the casting alloy described shows particular promise in aerospace applications where high strength, coupled with light weight requirements and cryogenic temperature applications are important, the alloy has properties which also make it attractive for a variety of industrial applications, at both ambient and cryogenic temperatures.

Summary

Based on test results from a limited number of castings made from the M45 casting alloy, the alloy is extremely promising for applica-

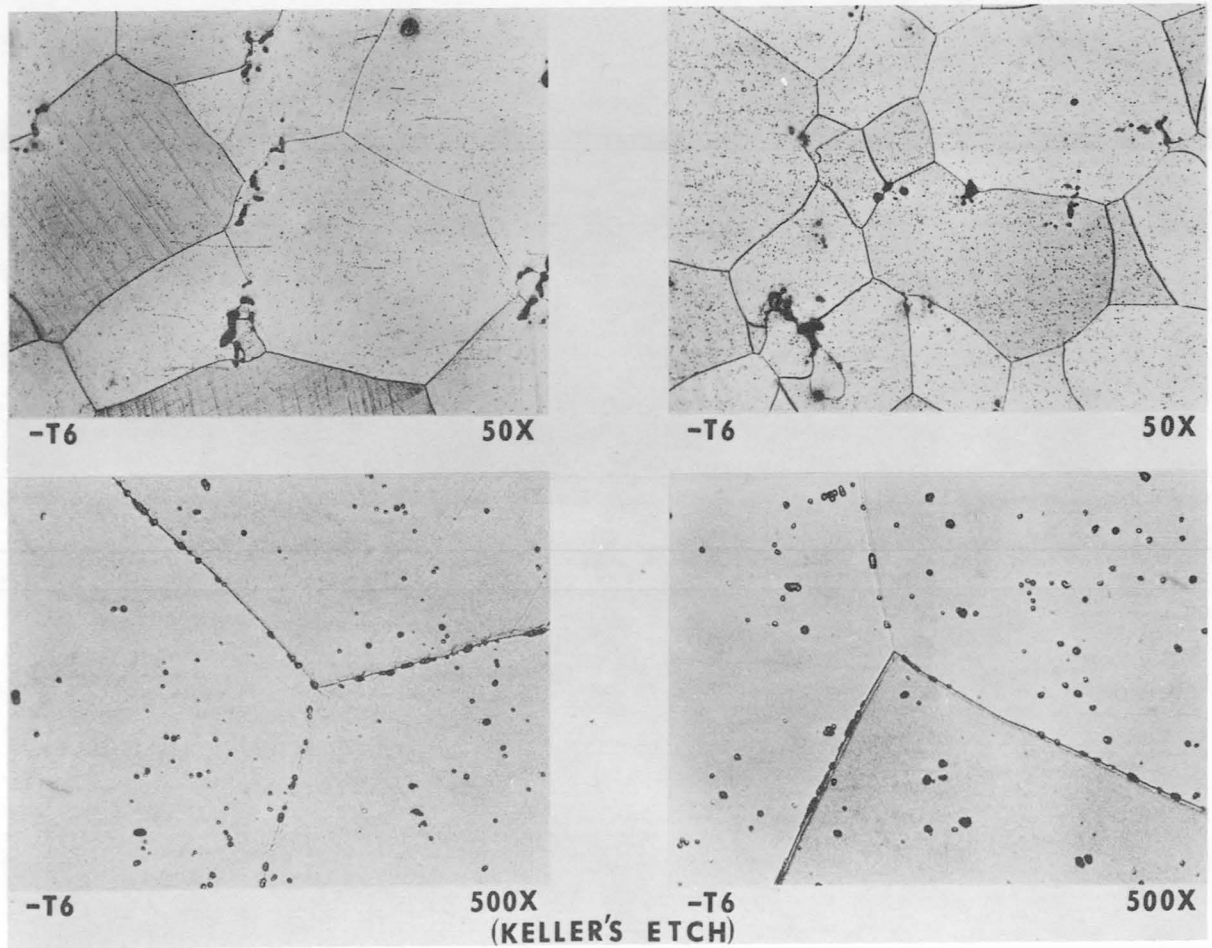


FIGURE 4.—*Typical microstructures of alloy M-45.*

tions where high resistance to failure under dynamic loads is needed. The alloy has considerably higher strength than other commonly used casting alloys such as Tens-50, A356, and Almag 35; it has excellent impact strength at cryogenic temperatures down to -423°F ; and it is heat treatable and weldable. Castability is similar to the commercially available 195 alloy. Ingots of the M45 are available on special order from ingot suppliers.

DEVELOPMENT OF MAGNESIUM-LITHIUM ALLOYS

Basis for Development

The magnesium-lithium alloys are not new as far as basic development is concerned, but only recently have specific requirements in the aerospace industry prompted an increased effort in

the development of this family of alloys. The Mg-Li alloys have found a position in fulfilling many requirements by virtue of their very low density and high elastic modulus-to-weight ratio. Particular emphasis on the potential of the Mg-Li alloys for missiles and space-vehicle applications dates back to 1957, when the Army Ballistic Missile Agency (ABMA) sponsored a research program with Battelle Memorial Institute.

Chronological Development of Mg-Li Alloys

A brief review of the chronological development of Mg-Li alloys is presented in table VII. As early as 1910, Masing and Tammann attempted to develop the Mg-Li phase diagram, although their work was hampered by tempera-

TABLE VII.—*Chronological Development of Mg-Li Alloys*

Year	Investigator	Program
1910	Masing & Tamman.	Mg-Li Diagram?
1934	Grube, von Zeppelin & Bumm.	Mg-Li Diagram.
1944	Battelle-Mathieson Chem.	Alloys.
1945	Humme-Rothery, et al.	Ternary Alloys.
1945	Battelle-Naval Bureau of Aeronautics & Mathieson.	Alloys.
1947	Dow Chem.-Corp of Eng.	Alloys, Portable landing field mats.
1950	Battelle-Naval Research Lab.	Mg-Li-Al, Mg-Li-Zn.
1957	Armour Research Found.-Frankford Arsenal.	Alloy for M-113 personnel carrier.
1957	Battelle-ABMA-----	Alloys for missile and space applications.
1962	Battelle-NASA-----	Development of alloys for structural applications.
1964	Frankford Arsenal-NASA.	Mg-Li casting.

ture measurement problems. Work continued on various phases of development for 37 years, until 1947, when the Dow Chemical Company, in conjunction with the Corps of Engineers, produced portable prototype landing-field mats. In 1957 Armour Research Foundation, funded by Frankford Arsenal, developed an alloy to be used in a prototype M-113 personnel carrier. In the same year, Battelle, under contract to the Army Ballistic Missile Agency (Contract DA-33-019-ORD-2593), began studies on the development of alloys for missiles and space applications. These studies were continued under Contract NAS8-5049 when the ABMA group became a part of NASA in 1960.

In the Battelle programs sponsored by ABMA and MSFC, two alloys of particular significance emerged. These two alloys and their current

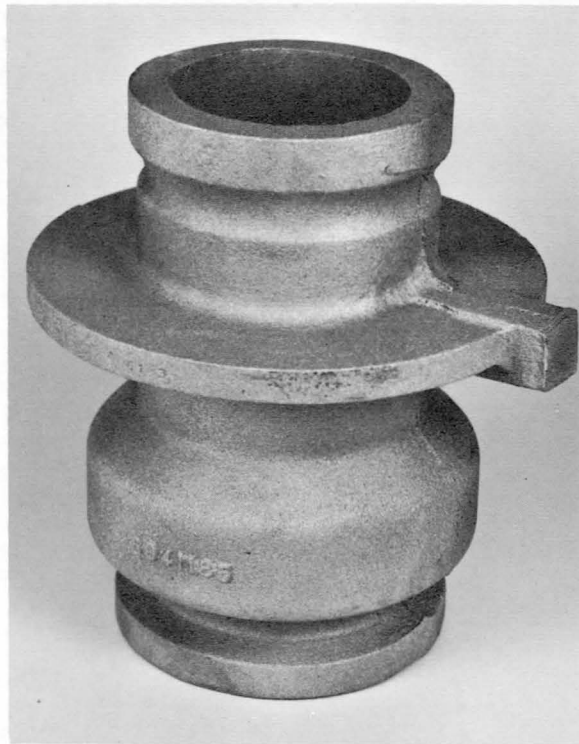


FIGURE 5.—Casting of alloy M-45.

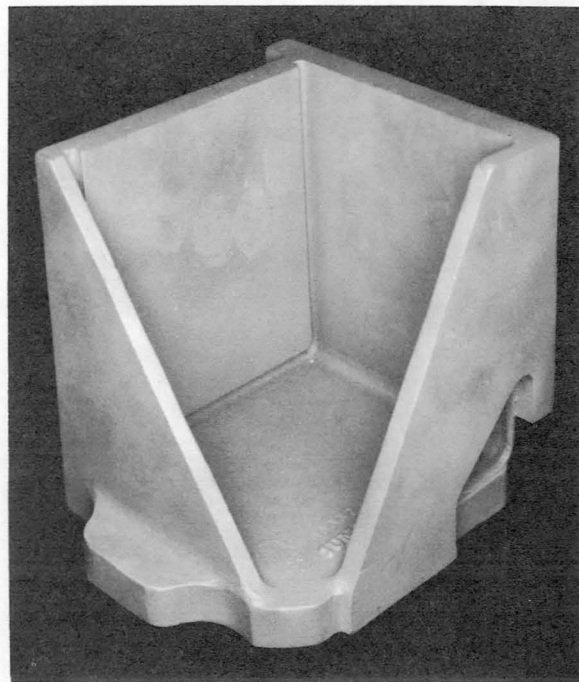


FIGURE 6.—Alloy M-45 casting for Saturn hardware.

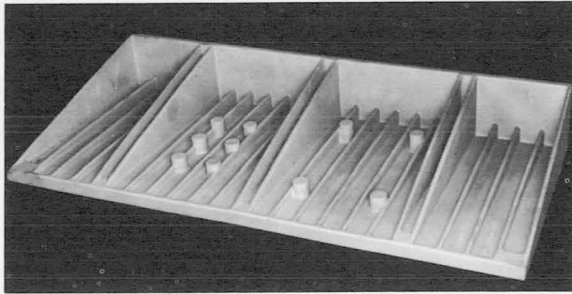


FIGURE 7.—Saturn casting from aluminum alloy M-45.

and potential applications are described in this report. In addition, several studies on these alloys conducted at MSFC, including mechanical property determinations, aging studies, corrosion studies, protective coatings, composites, fabrication, and weldability are discussed. A program is presently underway with Frankford Arsenal, under direction of MSFC (Contract G.O. H.-71508), to determine the feasibility of casting Mg-Li alloys into intricate shapes.

Alloy Designation

The alloys developed by Battelle have been designated according to procedures of the Mag-

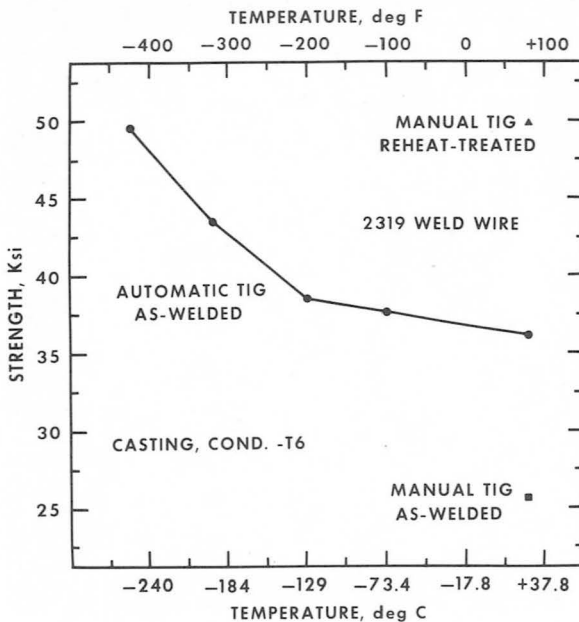


FIGURE 8.—Weld strengths of a new aluminum alloy sand casting.

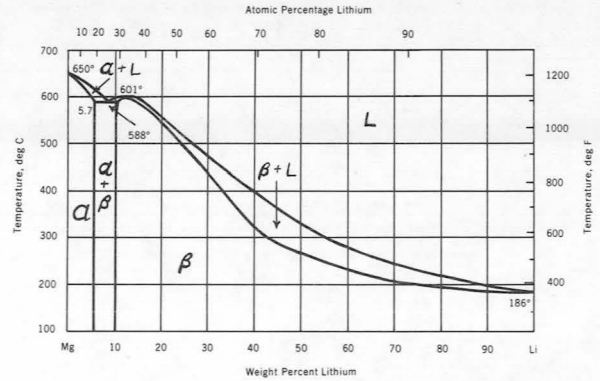


FIGURE 9.—Magnesium-lithium phase diagram.

TABLE VIII.—Alloy Designation

Alloy	Nominal composition, percent
LA-141.....	85 Mg-14Li-1Al.
LAZ-933.....	85 Mg-9 Li-3Al-3Zn.

nesium Association, as shown in table VIII. In the Mg-Li equilibrium diagram, shown in figure 9, the LA-141, although a ternary alloy, has a body-centered cubic structure, whereas the LAZ-933 is a body-centered cubic, plus close-packed, hexagonal structure ($\alpha + B$).

Physical and Mechanical Properties

Comparative densities of the Mg-Li alloys are shown in table IX. The LA-141 has a density less than one-half that of the aluminum alloys and is about 25% lighter than the standard commercial magnesium alloys.

TABLE IX.—Comparative Densities

Material	Density, gm/cm ³	Density, lb/in. ³
Lithium metal.....	0.534	0.019
Magnesium alloy LA-141..	1.349	0.049
Magnesium alloy LAZ-933..	1.560	0.056
Magnesium metal.....	1.738	0.063
Magnesium alloy HK-31...	1.799	0.065
Beryllium metal.....	1.848	0.067
Aluminum alloy 2219.....	2.823	0.102
Titanium alloy 6AL-4V....	4.429	0.160
Stainless steel 301.....	7.916	0.286

TABLE X.—Strength-to-Weight Ratios of Stabilized LA-141 and LAZ-933

Alloy	Ultimate tensile strength, psi	Measured density, lb/in. ³	Strength-to-weight ratios, in.
LA-141-----	20 000	0.0486	412 000
LAZ-933-----	30 000	0.0564	532 000

The strength-to-weight ratios of stabilized LA-141 and LAZ-933 are shown in table X. Note that the LA-933 shows a strength-to-weight advantage of over 22%. A 30% advantage is achieved when the solution-treated and aged condition of the LAZ-933 is used.

The LAZ-933 is a heat-treatable alloy, unlike LA-141, and shows promise of being very stable thermally. Table XI gives the properties of LAZ-933 as heat treated. It does not possess the overaging characteristic of LA-141 which loses about 30% of its as-rolled strength after heating for only a short time at 200° F. Only a very small loss of strength was noted in the LAZ-933 after aging 500 hours at 200° F.

Tensile and yield strengths of the two alloys down to liquid hydrogen temperature are shown in table XII. LAZ-933 is slightly more notch-sensitive than the LA-141, and LAZ-933 shows a sharper decrease of elongation with decreasing temperatures.

TABLE XI.—Mechanical Properties of Heat Treated LAZ-933 Alloy^a

	Rolled and aged 48 hours at 200° F	Rolled, solution ^b treated 800° F, 1 hour, cwq, aged 500 hours at 200° F
Ultimate tensile strength, psi--	30 000	33 000
Yield strength, psi-----	25 000	25 000
Elong., % in 2 in.-----	28.0	24.0

^a Longitudinal parent metal, 0.063 in. thickness

^b Solution heat treated in vacuum furnace

Fabricability and Formability

Battelle's research has shown that LA-141 can be extruded readily into thin-wall tubing and T-shapes can be warm-formed into typical aerospace parts requiring simultaneous shrink and stretch operations. The alloy was found to have machinability, in lathe tests, comparable to that of 2024-aluminum alloy at low feed rates, but much greater than the aluminum alloy at high feed rates.

Both LA-141 and LAZ-933 were found to be readily adaptable to metal removal by chemical

TABLE XII.—Stabilized Mechanical Properties

[LA-141 longitudinal parent metal, 0.090 in. thick; LAZ-933 longitudinal parent metal, 0.063 in. thick]

Alloy	Ultimate tensile strength, psi	Yield strength, psi	Notched tensile strength, psi	Elong., percent in 2 in.
LA-141:				
R.T.-----	20 000	18 000	21 000	24.0
-320° F.---	33 000	28 000	32 000	14.0
-423° F.---	43 000	39 000	38 000	14.0
LAZ-933:				
R.T.-----	30 000	25 000	32 000	29.0
-320° F.---	37 000	34 000	37 000	8.0
-423° F.---	53 000	45 000	42 000	6.0

milling. Phosphoric acid solutions appear to be suitable reagents in this respect.

Several prototype instrument boxes have been fabricated by cold forming and welding. Ribbed covers for these boxes were fabricated by machining and/or chemical milling.

Weldability

LA-141 may be readily fusion welded with an a-c or d-c power supply; the choice of the current depends primarily on the method used. The electrodes used may include pure tungsten as well as those alloyed with small percentages of thorium or zirconium. Backside shielding is required to reduce the extent of oxidation on the underside of the weld bead.

Several filler metals, including LA-141, EZ33, AZ92 or AZ61, may be used for welding LA-141 to itself. Filler metals used for welding LA-141 to other magnesium alloys include EZ33, AZ92, or AZ61.

The data in figure 10 show that almost 100% weld efficiency can be achieved with this alloy if correct procedures are used.

Although no mechanical strength data are available on welded LAZ-933, limited welding studies to date indicate that the alloy is readily weldable. Several small plates were welded without incident, and radiographs of the welds showed them to be free of cracks and porosity. This soundness of weld and weld-interface was borne out in subsequent metallographic examination. Two samples were tested for bend ductility. These limited data indicate a minimum bend radius of $\frac{1}{4}$ in. for 0.063-in. material at room temperature.

Corrosion Resistance and Surface Protection

Limited tests at Battelle with 100% humidity at 95° F showed the LAZ-933 alloy to be comparable to the LA-141 alloy in corrosion resistance; however, more extensive tests at MSFC have indicated that LA-141 is slightly superior. Considerable work was done at MSFC to determine the corrosion resistance of LA-141 in a 60% methanol-40% distilled water solution to be used as a coolant solution in the Saturn V Instrument Unit. This unit contains two large components fabricated from LA-141. Several corrosion inhibitors were investigated, but it

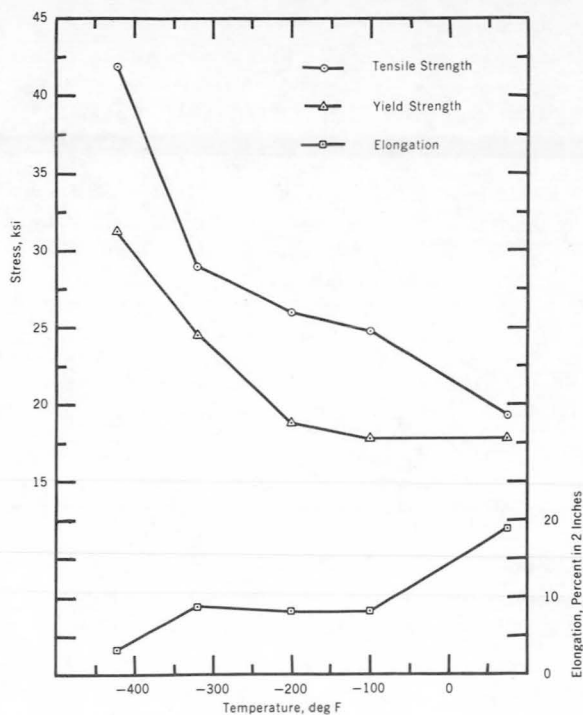


FIGURE 10.—Mechanical properties of magnesium-lithium alloy LA-141, sheet thickness 0.090 in transverse TIG-welds, longitudinal parent metal.

was found that the LA-141 showed satisfactory corrosion resistance in an uninhibited solution.

Coating studies have been made on the LA-141 alloy by using the Dow Stannate, Dow 17, and Fluoride-anodize processes. Comparative tests were run on the LAZ-933 with the Stannate and Dow 17 processes. The Dow Stannate afforded better protection on the LA-141 than the other processes and, in turn, the coated LA-141 was slightly superior to the coated LAZ-933 in all cases.

Limited electroplating work has been done on the magnesium-lithium alloys to date; however, several investigators recently began studies on such platings, since electronic containers fabricated from the material must be soldered for electrical connections and require rf-attenuation control.

Space Vehicle and Industrial Applications

The major uses to date for the magnesium-lithium alloys have been in the aerospace indus-

try. The Saturn V guidance computer, data adapter frames, and Q-ball angle of attack component cover are fabricated from LA-141 (fig. 11).

The Agena Booster Rocket and Satellites orbited by Agena contained magnesium-lithium components such as electronic boxes and covers; angles, channels, and Z's for structural supports; air-conditioning duct work; gyro mounts; heat shields; and pressure and dust panels.

Base and support structures for the manual data keyboard unit and several circuit module covers are used in the Gemini.

The accelerometer housing in the advanced Minuteman missiles' guidance system is fabricated from LA-141.

A large slip plate used on an electronic-component vibration table located in MSFC's Astrionics Laboratory was fabricated from 2-in. thick plate. Results obtained from this

plate were excellent and superior to results obtained on either a commercial magnesium or aluminum plate previously used. A more comprehensive listing of applications is provided in a technology summary report prepared for NASA by Battelle, entitled "Technical and Economic Status of Mg-Li Alloys, Part I," August 1964.

Summary

The magnesium-lithium alloys LA-141 and LAZ-933, by virtue of their low densities and high elastic modulus-to-weight ratios, certainly have drawn much interest in recent months for their potential use in light, rigid structural application in aerospace vehicles. This interest was largely generated by the initial work at Battelle.

Further development of the magnesium-lithium alloys has been continued in research programs sponsored by NASA, particularly in the areas of formability, machinability, chemical milling, and coating. The LAZ-933 alloy was developed in an endeavor to obtain a better combination of strength and stability.

The sponsored work at Battelle and the backup support from the MSFC laboratory, especially in the determination of mechanical properties at cryogenic temperatures and corrosion work, have been a great factor toward the acceptance of these alloys by industry.

The main research interest at present is directed toward developing better coatings, especially electroplated coatings. Upon completion of this work, the magnesium-lithium alloys will certainly be material candidates where low density and low load bearing requirements are needed for relatively low temperature applications.

CONCLUDING REMARKS

The three alloys described in this report are typical of those that are of interest to NASA. These materials represent an advancement in the state-of-the-art and all offer promise, through proper application, of effecting lighter weight and/or more reliable structures for space vehicles. Likewise, these alloys offer similar advantages for a variety of industrial applications.

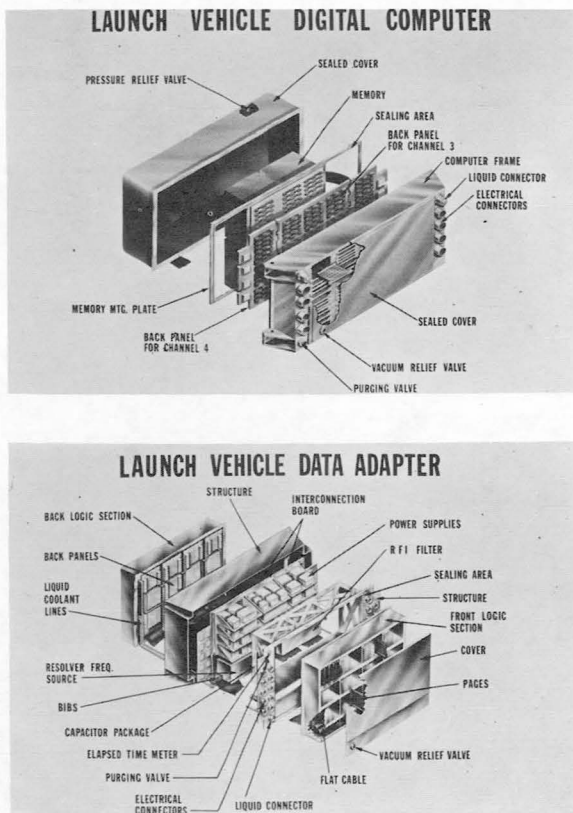
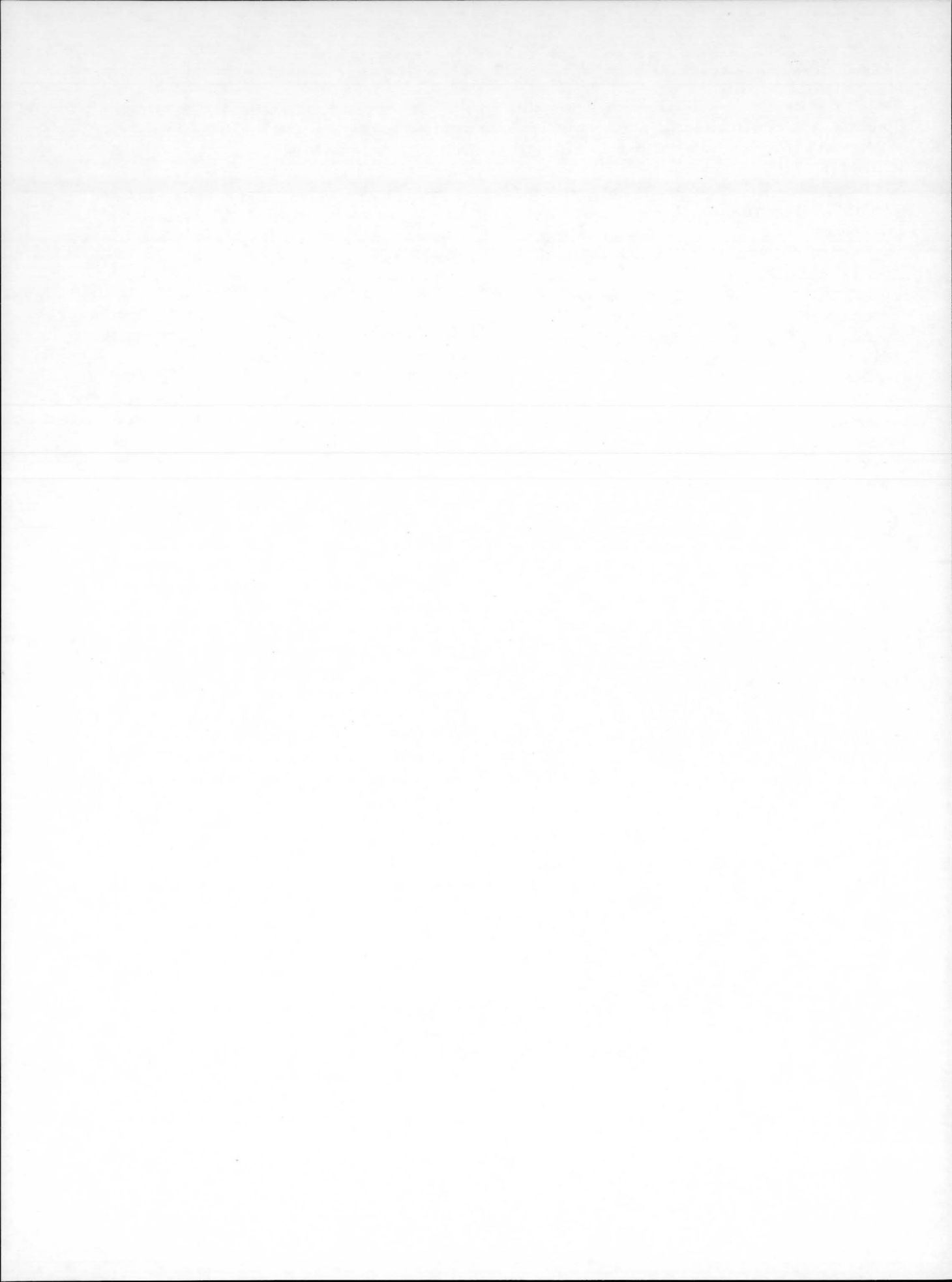


FIGURE 11.—Typical components fabricated from LA-141.



15. Effects of Aerospace Technology on Civilian Life Through Scientific Instrumentation

JOHN G. ATWOOD

Director of Research, Electro-Optical Division, The Perkin-Elmer Corporation

The development and production of scientific instruments for industrial, medical, and educational use is closely associated with, and affected by the national aerospace program. Part of the effect comes directly through the aerospace support of technology actually used in instruments, such as electro-optics. Part comes from requirements of the instrumentation industry to develop new instrument systems of extraordinary performance to meet special aerospace needs. This knowledge and technology becomes available to other users through commercial instrumentation which later embodies it.

The scientific instrument industry thus plays a major role in transferring to the civilian technology the benefits of advances in materials, components, and production techniques, spurred into development by the needs of the national aerospace program.

A realistic discussion of how this transfer comes about cannot be carried on only by recitation of individual examples, although many interesting ones exist. Rather, the larger scale economic factors are to be considered such as the effect which demands of the aerospace industries have on the technical capital equipment industry. Tracing these effects on the technical capital equipment available to civilian industry, education, and medicine completes the cycle. The depth to which familiar aspects of our daily lives have become dependent on a highly advanced and expanding civilian technology is revealed in this process.

There is good evidence that the national aerospace program is a major factor in the recent acceleration of our civilian technology. This may be a reason why the standard of living in the United States continues substantially higher than that of other advanced countries in the Western world which also have highly educated, highly industrialized producing and consuming populations, but which have not adopted large-scale national objectives of a highly technical nature.

THE ELECTRO-OPTIC INDUSTRY

One of the fastest growing segments of the industrial economy today is what has come to be called the electro-optic industry. It makes components and systems of which the following are only a few examples:

Heat-seeking guidance units for anti-aircraft missiles which "see" a target aircraft by the infrared, or heat rays it emits.

Ultra-high performance aerial reconnaissance cameras.

The special television cameras and recording systems used on space vehicles such as

Tiros and Nimbus, the weather satellites, or recently, and spectacularly, on the Ranger moon probes.

The precision tracking telescopes which monitor and photograph the details of every launch at Cape Kennedy.

Spectrophotometers used by scientists for chemical analysis of complex materials.

Xerographic office copying machines.

The first two examples are important to space systems, the next two are important to space exploration, while the last two examples are

principally of industrial significance. None of the examples is a consumer product. Things like ordinary cameras, projectors, binoculars, and eye glasses are not generally included in the definition. Only highly technical products qualify.

One result of this is that few laymen have any clear idea that the electro-optic industry exists at all. Fewer still have a clear idea how it affects them as individuals, beyond a suspicion that it raises their taxes slightly.

Nevertheless it exists, it is big, and is growing fast. It is hard to get good statistics on the electro-optic industry because the Standard Industrial Classification (SIC) system used by the Department of Commerce to report industrial statistics does not recognize the electro-optic industry, and buries fragments of it all the way from "stones, clay and glass products" through "communication equipment" and electronic components" to "professional and scientific instruments."

However, an excellent survey of the electro-optic industry by the trade journal *Missiles and Rockets* puts the size of the industry in 1964 at a little over one billion dollars, and growing at about 15% per year. Table I shows some of the trade journal's estimates of the breakdown of 1964 output between government and commercial business, and it predicted that the industry will double in size by 1970. These estimates are rough, but are plausible and good enough for our purpose. They include research, development, and production.

TABLE I.—*Estimates of Electro-Optic Industry*^a

	Millions of dollars	
	1964	Est. 1970
Scientific instruments, test instrumentation, and process control.....	\$125	\$200
Industrial and special photographic....	350	550
Total industrial and commercial^b	475	750
Aerospace	425	900
Other	125	175
Total government^b	550	1,075
Lasers (all applications).....	50	200
Total	1,075	2,025

^a Excerpted from *Missiles and Rockets*, June 1, 1964.

^b Excludes lasers.

Table I shows several interesting things. First, there is at present a roughly equal split between government and commercial parts of the industry. Second, the aerospace segment accounts for nearly all the government's share.

At present, the total electro-optic industry represents about 1/600 of the Gross National Product, comparable in size to the commercial TV broadcasting industry. However, the commercial and industrial segment of the electro-optical industry is almost entirely a *capital equipment* industry. That is, its products are permanent hardware purchased as capital equipment by other industries as tools for control of production and for new product development.

The commercial part of the electro-optic industry should really be compared with total *business expenditure for new plant and equipment*. This was \$43 billion in 1964. Commercial electro-optics is a respectable 1% of this total.

Finally, let us analyze "business expenditure on new plant and equipment" in a little more detail. Let us cast out of it all that is bricks and mortar and steel "I" beams. Then cast out automobiles, office furniture, and the like. Finally, we get down to the *technical capital equipment*, the uniquely essential means of production in many industries. Then, the commercial part of the electro-optic industry, especially its industrial and scientific instrumentation branch, is a tangible fraction of the total, perhaps as much as 5%, depending on how the difference between technical capital equipment and other kinds is defined.

A matter of great interest is how this commercial sector of the electro-optic industry is affected by its booming government-supported other half. Let us examine what is taking place on the other side of the fence.

THE AEROSPACE HALF

It is impossible in a short time to mention each of the aerospace programs which are generating major demands upon the government half of the electro-optic industry. The number of them is in the hundreds in NASA alone. However, some important trends in the technology is illustrated by specific programs.

Astronomy

One of the most significant trends is the pursuit of optical astronomy in space with large telescopes of unprecedented performance. There are several good reasons why astronomers desire to have observatories in space. One is that the turbulence of our atmosphere, which causes stars to twinkle, also prevents astronomers from seeing or photographing them clearly at high magnification. In addition, the atmosphere is opaque to much light in the infrared and ultraviolet regions of the spectrum.

Stratoscope II

One of the first astronomical telescopes designed to penetrate the turbulence and absorption barrier is Stratoscope II (fig. 1) jointly supported by ONR, NSF and NASA. The instrument, which weighs 3 tons, is carried aloft

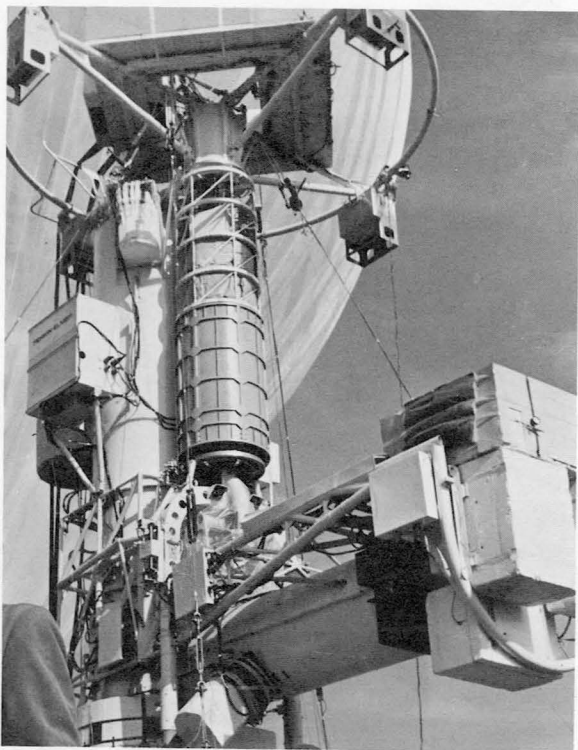


FIGURE 1.—The 36-in.-aperture three-story-high Stratoscope II, a balloon-borne telescope that flies at 80 000 ft to make observations of planets, stars, and other night sky objects. In the background, a balloon is being inflated for a Stratoscope flight.

to 80 000 feet on a giant unmanned balloon. There above most of the atmosphere, it is capable of obtaining photographs of planets and stars with 0.1 arc second resolution. This is three to five times better than has ever been obtained from the surface.

The system embodies some remarkable technology. First, in order to fully exploit the freedom from atmospheric disturbance, the fused-silica primary mirror, which is 36 inches in diameter, was required to be made accurate to $\frac{1}{50}$ of a wavelength of light, or $\frac{1}{2}$ 500 000 inch over its entire surface. This is unprecedented accuracy even in the field of optics for an optical element this large by at least a factor of five. Final working of the mirror took two years to accomplish. Most of this time was spent devising entirely new testing methods which could see the incredibly small errors which had to be removed.

Orbiting Astronomical Observatory

Another group of large astronomical systems is NASA's Orbiting Astronomical Observatory (OAO) series. These instruments will principally exploit the complete freedom of spectral region available to the telescope in orbit.

Figure 2 shows components for the payload of one of the experiments. It is a 32-inch-diameter telescope designed to operate in the vacuum ultraviolet spectral region. In this spectral region, the light is so energetic that it decomposes molecules of air and is extinguished in the process. This OAO experiment will map and spectrographically analyze the vacuum ultraviolet radiation which abounds in space. To build it, it was necessary to develop a method of making mirrors reflect efficiently in this forbidding spectral region and then apply the technique to a very large mirror.

Giant Space Observatories

The future of large telescopes in space is now being planned by NASA. Eventually, it is likely that a huge instrument will be orbited. It will be bigger than the 100-inch reflector at Mount Wilson, perhaps even as large as the 200-inch telescope at Palomar. It will have more than 10 times the acuity of any earthbound sys-

tem. It may even see to the edge of the universe, and gain answers to some of the most basic questions of science.

But to build such a telescope many scientists believe we will first require the development of entirely new technology in optics, that of a self-correcting optical system. Only with a system that continually measures and corrects its own departures from perfect alignment can the necessary accuracy be achieved in the hostile environment of space.

Image Transducers

Another field of electro-optic activity which is receiving a substantial share of NASA's research and development effort is electro-optic image transducers. These are high resolution precision television pickup tubes, image dissectors, and image intensifiers. They are needed, of course, for all kinds of unmanned space probes. They are a way of putting our eyes into environments otherwise forbidden to us.

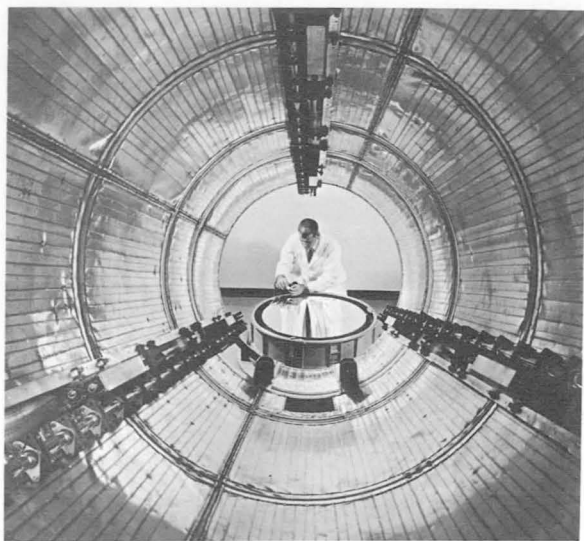


FIGURE 2.—*Lightweight optical components of the Orbiting Astronomical Observatory to study interstellar gas and dust clouds from which stars are formed. View through lightweight aluminum telescope tube shows three slender quartz rods at top and sides which will maintain optical system spacing in the cold operating environment of outer space.*

The importance of these image transducers, and their successors, in the technology of the future is connected with the revolution we see going on in computer technology. Digital computers are now becoming powerful enough to deal with information in two dimensional or graphic form. To receive graphic information, however, computers need the electronic equivalent of eyes. The combination of improved electronic eyes with the electronic brains we foresee in the future will bring a revolution in how humans deal with information.

Lasers

Another electro-optic field being greatly advanced by the aerospace industry is that of lasers. These new sources of intense, directional, spectrally pure light are now about 4 years of age. They have already started to establish themselves as having bona fide value in many applications of light. Hardly any of these applications are the same as predicted by the sensationalists. Most are entirely new and highly technical and have required extensive development of laser performance levels and of other technology as well. This is why they have been slow in coming.

One of the promising applications of lasers in space technology is in communication from interplanetary distances—sending pictures back from Mars, for example. This is possible, because a laser beam transmitted from a perfect optical system diverges so little with distance that, if sent from Mars by a 32-inch diameter transmitter, all of it would land on the Earth within a circle 100 miles in diameter and could be detected by present techniques. NASA is studying plans of an experimental optical technology satellite to explore this application. One of the main problems of such a system is the need to point the narrow transmitter beam toward the receiver on Earth with incredible accuracy.

These and many other aerospace projects, many of which are of military origin are causing a great growth of activity in the government-funded side of the electro-optic industry. Virtually all this activity comes under one of two categories:

Research and development work which establishes new knowledge and advanced technology in the field

Production of systems so advanced that new methods, new skills and advanced capital equipment are required.

How this activity relates to the civilian economy, and ultimately to our daily lives is explored in the next paragraph.

RELATION TO CIVILIAN TECHNOLOGY

Let us set aside the question of whether there are things of technological or economic value to be learned by the actual exploration of space. Let us focus our attention only on the question of what price we are paying for the decision to explore space. This price should be measured in terms of other personal and national objectives which remain unmet because of the assignment of some of our national resources to space exploration. Finally, I would like to restrict the discussion to electro-optics and scientific instrumentation in general. In this narrower framework, the question becomes more detailed—"what is the effect of the aerospace-supported electro-optics industry on the civilian technology and the related economy?"

We can dispose of some possibilities right away. First, it is not true that Federal R and D funds pay directly for a significant amount of commercial product development in the electro-optic industry. Most federally supported R and D is done on cost plus fixed-fee contracts, and there is close auditing of expenses.

Another way direct support might happen would be for an aerospace-supported development to coincide directly with an item which would also be a good commercial product. Although it does happen for developments of materials, or very basic components, it very rarely happens for electro-optic systems, instruments or assemblies of parts. The main reason, of course, is that aerospace items and competitive commercial products usually differ very markedly in function, design for environmental stress, cost in relation to performance, weight, compatibility with other equipment, power requirements—in short all the things that determine an electro-optic system design.

The exception, when it happens, is usually in an area of important new and fast-moving technological development, where both the aerospace and commercial customer will tolerate departure from ideal specifications and lowest cost in the interest of getting the item quickly. This leads to short-lived markets for anything that works, often at high prices. As the field matures, however, aerospace and commercial specifications for more advanced products diverge as usual, and the normal relationship returns. One of the best recent examples of this kind in the electro-optic industry took place in the early years of the market for lasers.

Such coincidences of aerospace and commercial goals for complete systems or assemblies at the development level are economically small in scope, but they are sometimes important technologically because they cause bursts of acceleration in the civilian technology which would not normally occur without aerospace money to power them. Nevertheless they are rare events and hence of minor effect in the overall picture.

The results seems to be that the only outputs of aerospace-supported technology which are easily available for use in commercial technology in the electro-optic industry are:

The knowledge and ideas gained from basic and applied research. Example: understanding of the uses of lasers in spectroscopy

New or improved materials and basic components developed on aerospace supported projects. Example: laser optical glass and improved solid state photo-detectors

Advanced capital equipment acquired by industrial firms to do aerospace-supported research, development and production jobs. Examples: special polishing machines for making optical elements with non-spherical surfaces

Human skills and experience developed on Federally funded jobs. Examples: technicians who have learned to make interferometric test lenses. Project engineers with years of advanced technical project management experience. Executives who have

gained experience as corporate officers because they were promoted to vice presidencies of aerospace-supported corporate divisions.

These things happen every day on almost every aerospace-supported project. They represent the major assets remaining in the economy from an aerospace program after the rocket is launched, or the project is completed. The number of people involved is as large or larger than the number engaged in the civilian part of the electro-optic industry. The amount of equipment is also comparable to that in the commercial segment of the business. And because of the more basic knowledge that the aerospace programs demand, the amount of new knowledge generated by the aerospace half of the business is greater per annum, probably several times greater than that generated by the commercial half.

Do these assets actually enter into the civilian technology? Do they actually benefit us individually and collectively as civilians? I believe so, but for three very simple reasons it is hard for the average person to see how.

One reason is that the process takes place slowly. It takes 5 to 10 years, typically for the full effect of aerospace-gained knowledge to be felt in civilian technology. An excellent example is the chronology from the start of an aerospace-supported project at Hughes Research Laboratories, when there was the first attempt at making a laser in 1958, until the actual shipment of the first commercial spectroscopic instrument employing a laser light source by the Perkin-Elmer Corporation in 1965.

The second reason why it is hard for the layman to see how aerospace knowledge benefits civilian technology is that the direct part of the process takes place in the technical capital equipment industry. No consumer products are directly involved at all, and the effect is intangible to the layman.

The third reason is that the final outcome which eventually benefits the civilian market is generally extremely indirect. It usually takes the form of lower prices, better quality, and wider variety available to us as consumers in materials, foods, drugs, transportation, medical

care, and other goods and services. These benefits occur because of the improved technical capital equipment at their point of production, but by now the relation to aerospace-supported technology, though real, is very indirect.

In summary, we can not comprehend the true effect of aerospace technology upon the civilian technology merely by reciting a number of specific direct examples. This would be as fruitless as trying to understand the effect of smoking on the nation's health by listing which of our friends are smokers, and when they last were in the hospital. To fully understand why this indirect effect is real and large, we need to look at the extent to which civilian life in the United States today is based on advanced technology.

DEPENDENCE OF CIVILIAN LIFE ON UNSEEN TECHNOLOGY

Technology has become so identified with space and defense and special research efforts, that people generally do not begin to realize how great a role it plays in their daily lives. Before you leave your home on an average morning, you have already come in contact with the products of dozens of different industries. Each one of these industries is heavily dependent upon many technologies in some form to process its product and get it to the consumer at an accustomed quality and price.

For an example molecular spectroscopy is an extremely important modern technology. It forms the basis of the scientific-instrumentation branch of the commercial electro-optic industry that the layman scarcely knows to exist. He may only have heard that the FBI catches hit-and-run drivers by spectroscopic analysis of paint chips.

Molecular spectroscopy works by "pinging" atoms and molecules of a sample with different frequencies of light and recording the frequencies at which their parts vibrate. This record tells what an unknown material is made of and permits chemists to analyze its composition and purity. It helps chemists determine the structure of the molecules they make. As a result it is of crucial importance in the synthesis of new chemicals, the quality control of chemicals in production, and the detection and analysis of chemicals everywhere.

Spectroscopy was a kind of pure, "long-hair" research subject prior to 1940. Then under stimulus of the war effort, a number of small firms began to make instruments which would make molecular spectroscopy available to chemists. In 1943 the structure of the then new penicillin molecule was identified by infrared spectroscopy. Development of synthetic rubber manufacture during the war, and of fluorinated compounds on the Manhattan Project were examples of federally supported efforts which boosted the technology of spectroscopy in those times.

After the war the commercial spectroscopic instrument business began to take off. Instruments became better and far lower in cost. This was in part because they all used difficult non-spherical optics and evaporated film technology. Equipment, skill, and knowledge paid for by military programs of the 50's greatly reduced the cost of this type of optical technology.

As the cost of getting a good infrared spectrum became lower and lower, the technique spread more and more widely into industry and academic chemical research. Four-fold cost reduction of infrared spectrophotometers was important in this expansion of use. Where early instruments cost \$15 000 each, new cost instruments at \$3 500 each became common. Wider use of spectroscopy went hand in hand with the spectacular explosion of chemical, pharmaceutical, and materials technology in the 1950's which is mainly responsible for the remarkable standard of living today.

Since the early days, more than 10 000 infrared and 30 000 ultraviolet spectrometers have been sold. We estimate that more than \$200 million worth of spectrometers are in active use today as technical capital equipment. They are being increased at the rate of \$25 million per year in new advanced equipment.

When an inquiry is made in the chemical and pharmaceutical industries to find out what it would be like if the technology of spectroscopy were set back to that of the prewar days, the picture is hard to imagine. A consensus of views suggests that the products which would exist now only in rudimentary forms would be

most pharmaceuticals, most insecticides, and most products of polymer synthetic fiber and plastics industries. The petroleum industry would exist, but it would still be in an antiquated state. As a result, transportation would be more expensive and less effective than it is today.

Therefore when we get up in the morning, alive and free of disease because of wonder drugs we have recently taken, and eat cheap plentiful food which was checked for safety by a Food and Drug Administration spectroscopic test for insecticide residues, and get into a car with an engine that requires high test gas, we are benefiting in the most intimate personal way from technology that was accelerated by funds spent on national objectives of a technical nature 15 to 20 years ago. We can reasonably expect, then, that aerospace technology and skill being developed now will have a similar major, but indirect effect on our lives 5 to 15 years from now.

WOULD IT HAPPEN ANYWAY?

Probably most of the developments of civilian technology would happen eventually even without the spurring effect of federally supported effort toward national goals of a technical nature. This would normally happen as a step-by-step development of improved technology in the technical capital equipment industry. But it would take a much longer time to happen, as much as two to three times longer for each step.

One reason is that only one-half or one-third the people would be working on advanced technology. Also, those working on it would have much less equipment on the average because technical capital equipment would cost more. Most such equipment, even today is sold at volume levels where increased production brings substantial cost reduction. Cut the volume by a factor of two, and some important capital items would not be economically feasible at all. There is no doubt that aerospace demands make advanced technical capital equipment more freely available by paying indirectly for its development.

Some people believe that the aerospace program slows down the march of civilian technology because it competes for manpower and facilities with industrial pursuit of advanced technology. This is not necessarily true. In the first place, there is today a plentiful supply of engineers, scientists, and technical managers *because of* Federal support of technology in past years. Thus, industrial needs for skilled men are being met out of a better educated and more experienced labor pool which is roughly twice as large as would now exist without Federal support.

If there were less Federal support of national, technical objectives, would not engineers' and scientists' salaries decrease? Would not this spur industrial research and development? I am quite sure that technical salaries would be lower, but not by half, for many people would leave the field, and many others would never have entered it. In any case, it would have very little effect on the amount of industrial research and development in the scientific instrument industry.

In our commercial business, it costs about 100 to 500 thousand dollars to develop a new instrument from research breadboard to production prototype. Only about one-third of this is technical labor cost. Most is overhead and equipment. In any case, even if industrial R and D cost less, there are other factors which would limit the amount that can be done. One is simply that manufacturing departments, our sales staffs, and indeed customers can absorb only a limited number of new products each year. To double or triple R and D output would be to waste part of it bumping into new product introduction delays.

Then why not spend more industrial money on basic research instead of development? Because, in small companies which are characteristic of the instrument industry, basic research is very inefficient from the point of view of return on assets employed. This is not only because large research groups are more productive than small ones, but also because the exact nature of basic research output can not be predicted. The fewer the types of business a company engages in, the less chance it can exploit a

given research breakthrough originating in its laboratories. Competition prevents passing the cost of this inefficiency on to the customer.

CONCLUDING REMARKS

In summary, the main effect of current aerospace programs is seen as causing a general stimulation of the technical capital equipment area and generating new knowledge. The commercial scientific instrument industry is packaging this advanced technology as fast as markets for it develop and disseminating it widely in all fields which employ technology. This is how aerospace research in electro-optics benefits improbable fields ranging from agriculture to medical research.

The process takes a decade to mature, but it has been a leading cause of the explosive advance of the health and wealth of the people of this country since 1946. It should become an even more efficient process as part of the wasteful aspect of obsolescence of military production items is replaced by more space and atomic energy research projects.

I believe that the price we pay is no price at all, because we have made unexpected gains in spite of the diversion of national resources, and in part because of it. In the next decade our industry can look forward to at least the following exciting developments:

A new revolution in spectroscopy and other scientific and technical use of light as the laser field develops. We will gain new understanding, and new materials ranging from antibiotics to textiles. The technology of precision measurement will also be changed by laser light which will become a working standard of length measurement in industry. This will occur through interferometric monitoring of numerically controlled machine tools.

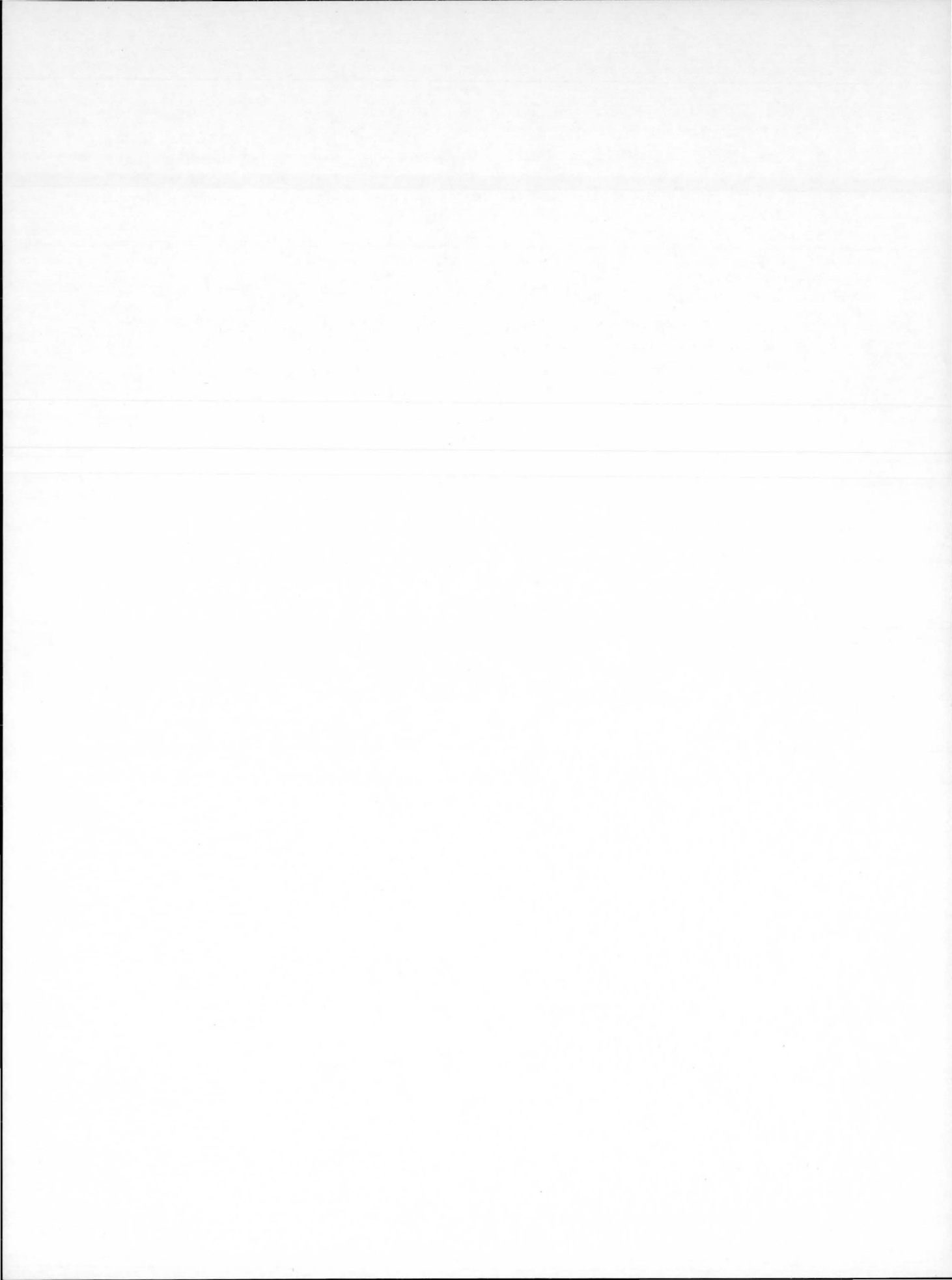
A revolution in uses of computers coupled with electro-optic image transducers to permit computers to deal with graphic and pictorial information. This will permit the freeing of humans from the drudgery of performing countless tasks in which men are used purely as visual perception machines. Examples are read-

ing merely to transcribe, steering vehicles, operating machines, preparing and reading mechanical drawings, assembling parts, analyzing charts and graphical data, performing numerous counting and visual inspection operations.

In medicine, for example, automatic computer performance of pathology tests on microscope slides of tissues and smears may within a decade make it economically feasible to do mass screening for malignancies.

I work at an American company which has factories, laboratories, affiliates, and scientific consultants in many foreign countries. I see the way the process I have described here goes, or doesn't go, in the technical capital equipment

industry of these countries. All of these countries have highly educated, highly industrialized producing and consuming populations. When I compare what I see happening abroad with what is happening at home in our industry, I conclude that I am looking at some experimental evidence in a gigantic social experiment. What the evidence seems to show is this: the continued advance of the standard of living in the United States over that in many other countries is at least in part due to the character of our national goals over the past 20 years. We have had forced upon us, first by the Cold War, then by the challenge of space, the need to pursue expensive, large-scale national goals of a highly technical nature.



16. Computer-Aided Design for Civil Engineering Structures

L. A. HARRIS, J. C. MITCHELL, AND G. W. MORGAN

Structural Sciences Department, Aerospace Sciences, North American Aviation, Inc.

Described in this paper is the development by North American Aviation, Inc., of techniques for automating the design process. Computers have been used predominantly in the past to perform analysis. This coincides with the designer's historic position of designing by successful analytical iteration. Techniques are described by which the design iteration process is systematically programmed for solution on a high-speed digital computer. The result is that more realistic design decisions relative to structural performance, cost, and schedule can be made. Computer-aided design would allow the civil engineer to improve design decisions by having available a larger mass of trade-off data and automatically produced drawings. The engineer inputs the design requirements and makes systematic variations in structural concept, materials, and design detail. The output is a set of designs which meet the performance requirements and design criteria. An example of the application to a multi-stage launch vehicle is described in the text. The text then illustrates how these same techniques could be used for civil engineering structures.

Until recently, scientific and engineering uses of the computer have been restricted almost exclusively to the task of analysis. This is true in civil engineering structures as well as in aeronautical structural engineering. Historically, by virtue of education and practice, engineers have generally conducted a large portion of the design process by analytical investigations. That is, for a given structure, the engineer can determine the stresses under the applied loads and compare them to some allowable criteria. The criteria are usually defined by applicable civil engineering and/or building codes. Thus, the design process as used in most fields of engineering is basically one of design by successive iteration rather than design by the direct solution of some closed form equation that expresses the primary design problem. It is unlikely that this process will change in the near future because of difficulties encountered

in expressing the design problem parameters in their required form. Therefore, in order to efficiently use the computer as a design tool, one must find techniques for analysis which permit rapid synthesis by iteration. A concept for such a process has been developed as part of the Independent Research and Development Program at the Space and Information Systems Division of North American Aviation and Civil Engineering; applications of the technique are discussed in this paper.

Engineers have progressed rapidly in the transition from the desk calculator to the modern high-speed electronic digital computer. In the process, the types of problems that can be solved have become increasingly complex. Perhaps one of the best examples of this is the current capability to solve with relative ease large numbers of simultaneous equations in the order of 300 to 500. Whereas, only about a

decade ago, the solution of such a problem involved a large amount of desk-calculator computation, and the size of the problem was severely limited to a sixth- or eighth-order matrix. As a consequence, it is now possible to solve a large class of problems which previously were not capable of solution. However, the utilization of the computer for this class of problems is not the subject of this paper. Rather, the subject of this paper is the utilization of computer capabilities for the generation of data that aid the engineer in making design decisions.

In the aerospace industry, design decisions are generally based upon considerations of performance, schedule, and cost. It is necessary, therefore, in the design process to obtain as much data as possible on alternate design possibilities in order to make a knowledgeable selection. One of the principal measures of performance in the aerospace industry is weight. It is desired in most cases to provide the greatest payload attainable for a given system. A consequence of this is that weight is a key item of study in aerospace vehicles. Recently, computer techniques have been developed for the preliminary-design weight synthesis of vehicle systems which answer some of the performance questions and can be useful in the development of data regarding cost and schedule. The example which is considered in this paper is the vertical-launch vehicle. As will be seen, it is possible to mathematically describe the analysis of such a vehicle in a preliminary design sense and to make systematic variations of conditions allowing the decision-making process to be based upon a much larger volume of calculated data. In the past, designers sometimes had the solution to a limited number of discrete designs, whereas today it appears possible to provide a much greater knowledge in the form of preliminary designs and applicable parametric trends in the design areas of interest.

The single premise upon which computer-aided design becomes feasible in the above sense is that key decisions may be more efficiently made if design advantages and disadvan-

tages of alternate solutions are made apparent to the engineer.

DESIGN

Design is the process by which a configuration is evolved to perform a set of specified functional purposes. This can be shown graphically in figure 1. The design process begins with a performance requirement for a structure and ends with drawings and specifications. In the aerospace industry the design process is initiated by a mission statement, performance specifications and applicable criteria. If the structure is very simple, it may be directly solved in terms of the design parameters, in which case the requirements are directly input to the computer to obtain the desired solution of the design problem. For instance, if the problem is to design a circular cross section as an elastic column to withstand a given load with a given length so that the structure will be of minimum weight, then it is possible to solve this particular design problem explicitly. In practice, however, most structures cannot be designed in this explicit fashion.

Because of the complexity of most structures, a direct closed form solution to the design problem is not practical. The design process is therefore based upon an iterative method in which the designer selects a configuration,

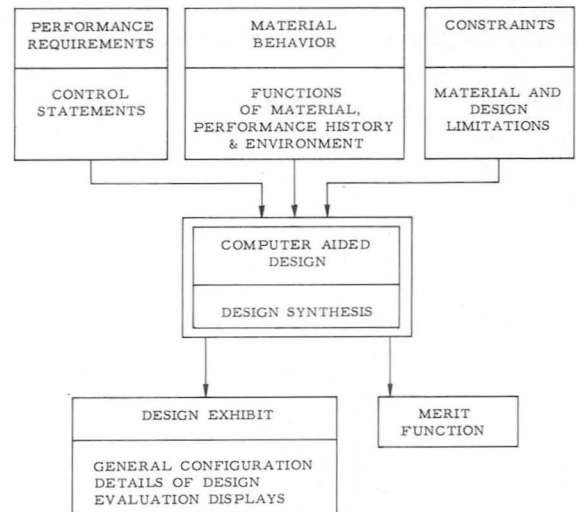


FIGURE 1.—General logic flow of computer-aided solution.

analyzes it; selects another, analyzes it, a third, a fourth, and so on. The cost schedule, and performance implications of the alternate structures are then evaluated. In the case of the aerospace industry, the interrelationships of the various dependent functions are extremely complex and the calculations become mammoth. However, in a preliminary design sense, many simplifications can be made, and it is possible to conceive of techniques which permit the computer to generate a great deal more data than the engineer generated formerly, and to display them in the form of drawings, specifications, bills of materials, and parts lists.

To further indicate the distinction between analysis and the design process, consider again the case of the column. In the case of analysis, the total geometry is known, the load conditions are known, the material is given and it is necessary only to analyze for the stress, deflection, and/or buckling under the given-load conditions. In the design process, the geometry of the column is not initially known. The performance requirements of the column are given and the design problem is the generation of a feasible structural design which must meet some cost and schedule requirements. In the case of aerospace structures, the number of variables is so great that it is inconceivable to provide a complete solution for the preliminary design portion of the program. As a consequence, approximate analytical techniques are frequently used. For example, in the case of stresses in a plate element of an aerodynamic surface, approximate equations may be used and solved explicitly for the preliminary design problem, whereas once the configuration is frozen, very accurate detail analyses are conducted.

DESIGN OF AN AEROSPACE LAUNCH VEHICLE

As an example of the design process in the aerospace industry, consider the specific example of the vertically launched booster. The problem is to design a booster with a maximum payload consistent with currently available rocket engines. In this example, the designer is given wide latitude regarding the geometrical configuration of the overall vehicle, as well as many other aspects of the structure. Figure 2

is a representative sketch of such a vehicle, and defines the principal geometry of a multistage launch vehicle. Figure 3 presents the principal steps in the design process for such an aerospace vehicle. The designer starts with a statement of the mission requirement which includes specific performance specifications. In the case

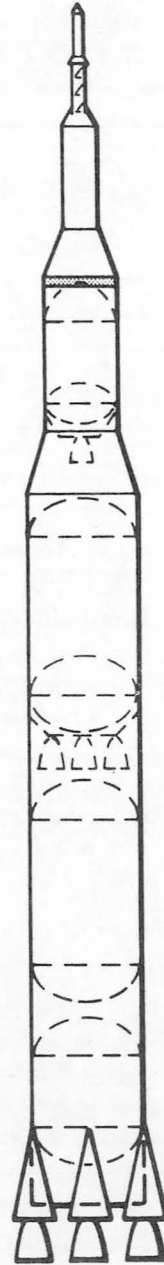


FIGURE 2.—Representative sketch of launch vehicle.

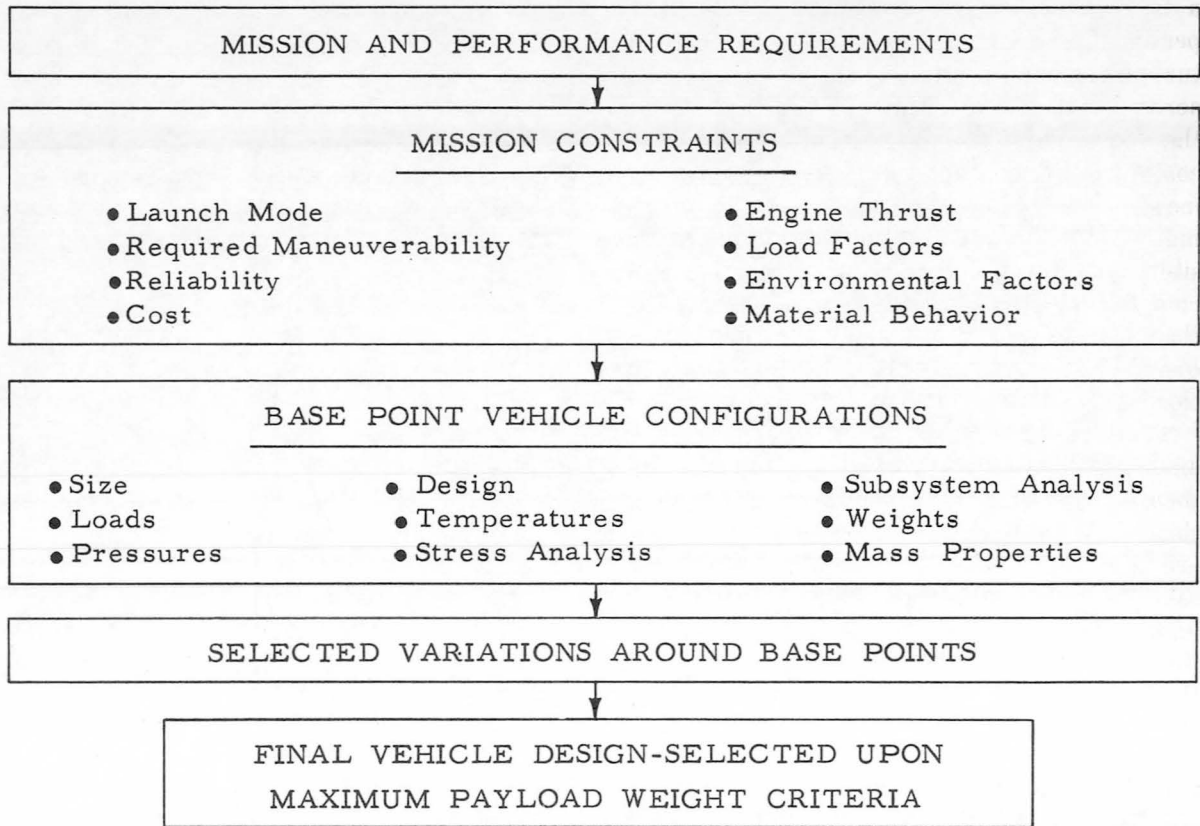


FIGURE 3.—Principal steps in aerospace vehicle design process.

of a launch vehicle, the performance specification may require the placement of a specified weight into a given orbit oriented specifically with respect to the Earth. There also may be specific requirements relating to load factors, maneuverability, and reliability factors. Environmental exposure factors must also be specified. In addition, other data are generally specified for the launch vehicle, such as the vehicle launch mode and engine thrust. The launch site is usually specified, as well as the desired orbital characteristics. These reduce the number of considerations the designer must evaluate. With these given design conditions, preliminary analyses are made to establish the approximate size of the vehicle. Preliminary design drawings are produced, and a preliminary structural analysis is performed to determine whether or not the vehicle as shown satisfies the requirements of the mission specifications and design criteria. If not, the design

is varied about the preliminary configuration until a vehicle results which satisfies the design requirements. Actually, a true maximum payload vehicle is seldom found by conventional design methods because of the limited number of cases that can be treated by hand and the small number of vehicle configurations that can be evaluated.

Most often, in the initial phases of a major design effort, a small group of key, senior personnel will apply their combined capabilities and intuitive judgement in the development and assessment of a number of candidate configurations. They are often restricted in their considerations by time limitations and incomplete parametric trend data. Once the general configuration has been selected, however, it is then possible to accomplish the preliminary sizing, the loads analysis and the preliminary design-stress analysis for all components of the vehicle. This effort will result in the definition of a total

vehicle from which the weight can be determined. In most design practices, it is possible to investigate only a limited number of individual cases during this preliminary-design period.

The concept of computer-aided design presented in this paper utilizes the same flow of data but allows the designer to consider hundreds of cases in the same time that he previously investigated a very limited number, perhaps less than half a dozen. The analytical techniques used in computer-aided design can be stated concisely in mathematical form and coded for efficient solution by high-speed digital computers. By so doing, the designer is no longer restricted to some half-dozen configurations for evaluation, but may look at hundreds of alternate solutions during the same time period. As a consequence, he is more likely to design a higher payload vehicle to meet the balance of performance requirements, as well as a vehicle that can be fabricated on schedule for the desired cost.

VEHICLE SYNTHESIS PROGRAM

An example of the computer-aided design concept is the NAA Launch Vehicle Weight Synthesis Program, which was developed for the preliminary design-weight synthesis of multistage launch vehicles. The program is initiated with computer inputs relating to performance, specifications, and design criteria. The program computes the weight of individual structural components, tank pressurization systems, propellant systems, and insulation systems for each stage of the vehicle configuration. Other system weights, such as propulsion, flight control, guidance, electronics and instrumentation packages, are handled as input numbers. The program provides a rapid means of optimizing structural weight, including associated geometry weight penalties.

The program is illustrated by block diagram in figure 4, and consists basically of a sizing subroutine, a loads-analysis subroutine, a tank-pressure subroutine, various stress-analysis subroutines, and a detailed weight-analysis subroutine which includes system analyses. In addition, subroutines are included which inter-

relate the various analyses and accomplish the optimization of the stage-mass fractions and print-out calculated numbers, as well as provide profile drawings of the vehicle. The key to successful weight optimization is the establishment of an iteration loop that will control all design structural and system data within the program. Because in weight minimization the stage-mass fraction includes all system and component weights, this is a logical parameter upon which to iterate. The stage mass fraction is defined as the usable propellant weight of the stage divided by the gross weight of the stage. Figure 4 illustrates the iteration loop used in this program. Iteration in the program is accomplished by stages. Since the sizing subroutine starts with the first stage and works to the final payload of the vehicle, the stage-mass fraction is iterated on the first stage which results in a change in load capability above the first stage. When requirements have been met, the program then jumps to the second stage, iterates on the mass fraction of the second stage, revising the capability above the second stage and continues up the entire vehicle until the final-payload weight has been determined. By using this method of iteration, design numbers and design equations for each individual component in a stage are cycled to a minimum weight.

The input to the sizing subroutine consists of total stage thrust values, stage thrust-overweight ratios, estimated tank diameters, desired length-over-diameter ratios, useful propellant ratio of the stage (which is associated with the trajectory information), estimated stage-mass fraction, bulkhead geometries, propellant densities, ullage factors, the position of the oxidizer (whether it is in the forward or aft tank), engine weights and thrusts, engine centers of gravity and inertias, and the type of final payload that is being analyzed. The vehicle payload may be a ballistic-type, a winged-vehicle, or an Apollo-type payload. The output of the preliminary sizing subroutine consists of a tabulation of the complete vehicle geometry and includes stage length and estimated weights, centers of gravity, and inertia of all components and systems. These numbers are preliminary

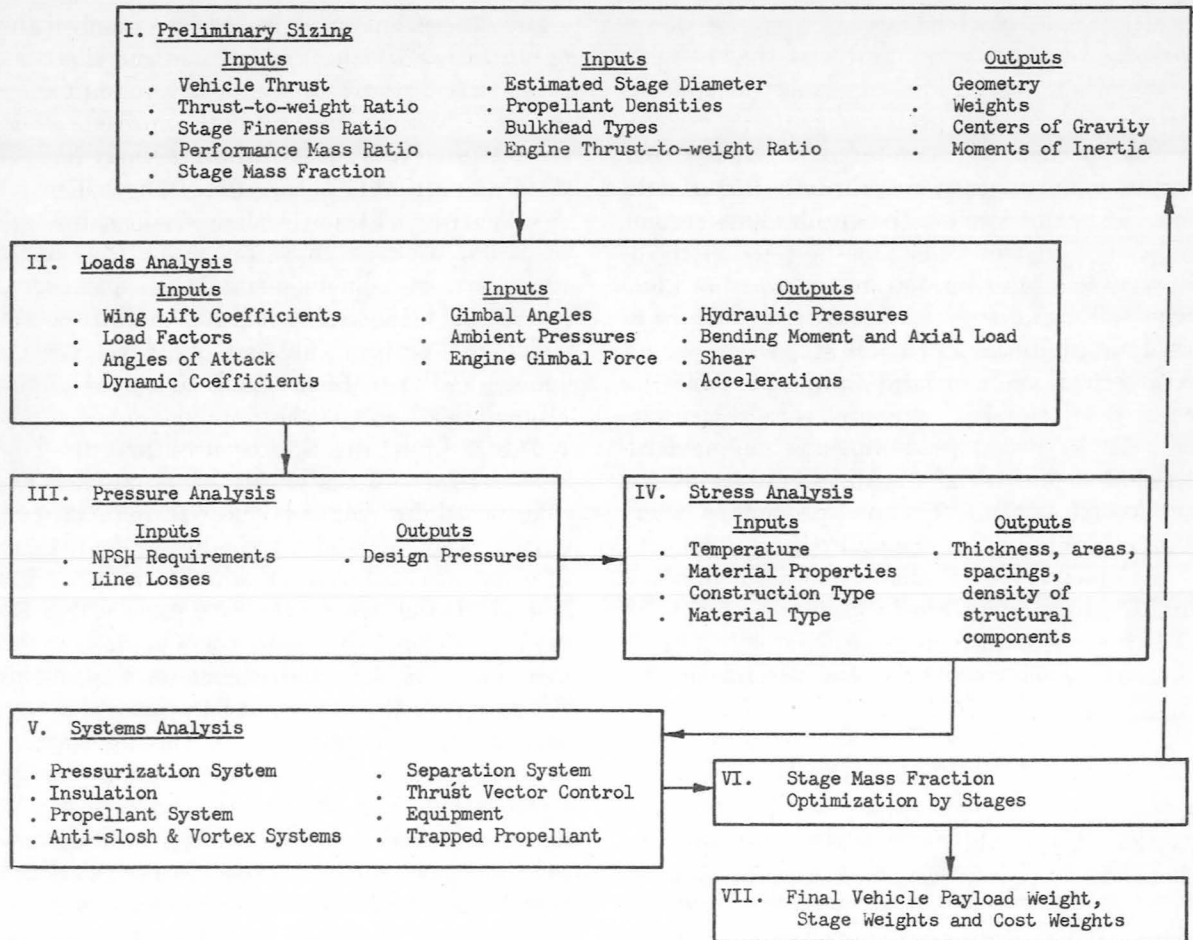


FIGURE 4.—Vehicle synthesis program.

Estimates and serve to initiate the cycling of the program.

The loads-analysis subroutine computes hydraulic heads, bending moments, axial loads, shear values, acceleration numbers, and inertia and center of gravity check numbers for all the load stations and for every point considered in the trajectory. Inputs required for this subroutine include the output of the sizing subroutine, winglift coefficients for the payload, drag coefficients, load factors, angles of attack at mid-boost and end-boost, gimbal angle requirements, ambient pressures, engine-actuator forces and moment arm of the actuators. The hydraulic pressures from the loads analysis subroutine are used in the tank-pressure subroutine along with net-positive suction head requirements on the engines, estimated line losses, ambient pressures and acceleration

forces. The tank-pressure subroutine then computes vapor pressures, ullage pressures and ullage plus hydraulic-head pressures for all required design points in the stages.

In the stress analysis subroutines, the material properties are selected for the input estimated temperature that is associated with the point being considered in the trajectory. Other inputs are pressures, geometry numbers, axial loads, bending moments, shear values, accelerations, construction indicators, material indicators and the particular subroutine indicators. Methods of construction include monocoque, stiffened, sandwich, waffle and filament-wound shells. Typical outputs of the stress-analysis subroutines consist of stringer and frame areas, stringer and frame spacing, facing sheet and skin thickness, core cell size, core thickness, core

density, waffle equivalent thickness and frame areas.

Pressurization system analysis utilizes the pressures from the pressure subroutine in determining the system weights. This design also considers the effect of stage length in determining weights of the associated plumbing system. Insulation analysis uses areas derived from the sizing subroutine and input temperature numbers to determine parametrically the weight of required insulation of various stage components. Fuel-system analysis determines propellant flow rates from burning time, and based on design allowables, design pressures, and engine feed-line diameters, weighs out a minimum weight propellant system. Trapped propellant is calculated for the stage using NPSH requirements, stage geometry, propellant line diameters and bulkhead aspect ratios.

The program provides automatic print-outs of weight, mass property, and design data including a profile drawing of the configuration. Figure 5 presents a typical automated drawing. Weight data is also automatically provided in cost analysis formats.

This program provides a means of analyzing all load conditions in a trajectory and can select minimum component design weights. A complete definition is provided automatically of the minimum-weight vehicle system that can be designed within the input parameters. In addition, the stiffened-shell sections of the structures are described by print-outs which define the material used, skin gage, areas of stiffeners, and stiffener spacing in both the longitudinal and circumferential directions. The efficiency of this procedure is illustrated by the fact that it is possible to synthesize a four-stage launch vehicle system by this process in ten minutes of computer time. The same problem done by hand would take many man-months of detailed effort.

UTILIZATION OF COMPUTER-AIDED DESIGN TECHNIQUES FOR CIVIL ENGINEERING STRUCTURES

Bridge Design

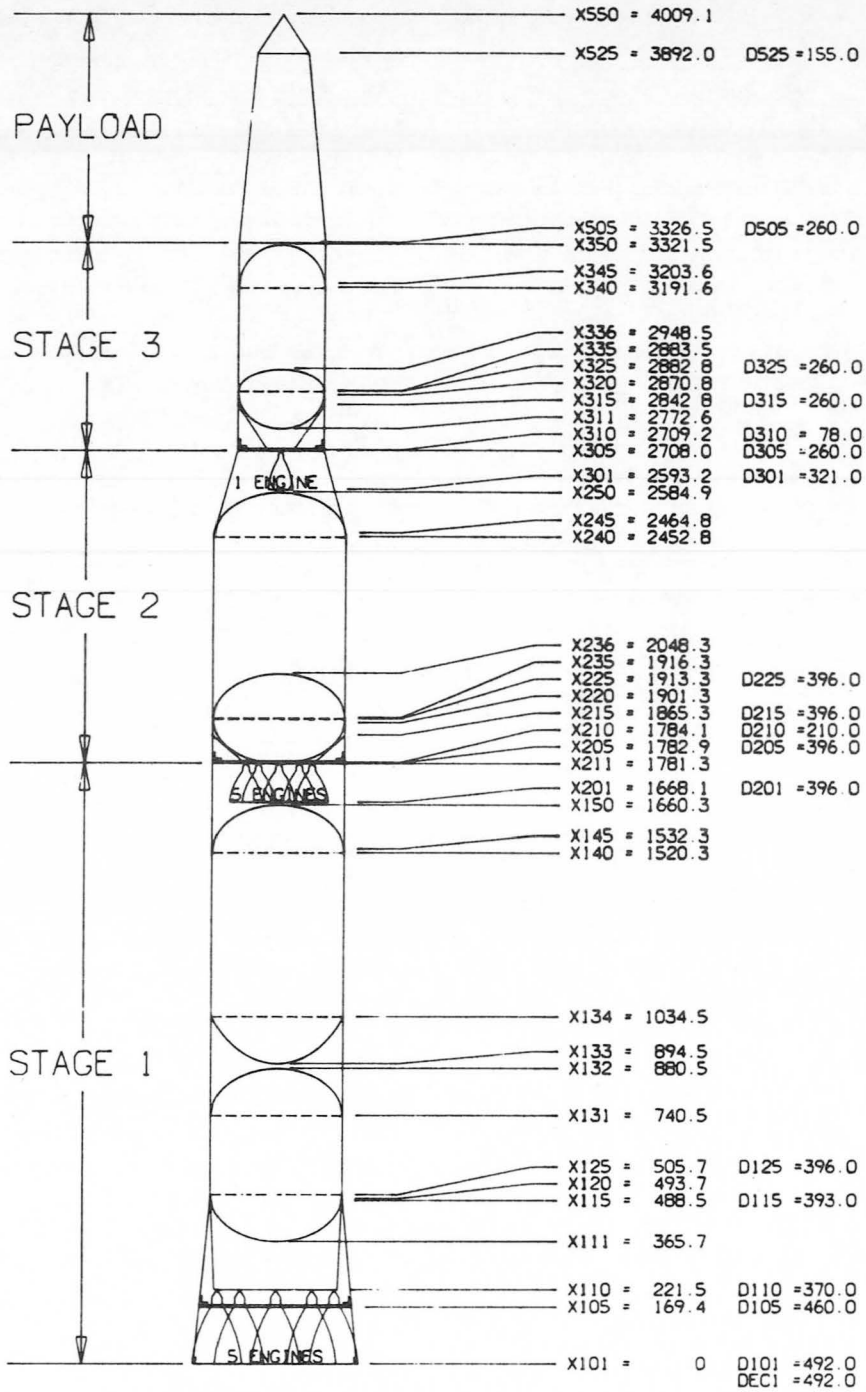
Consider the case of a bridge to span a given distance and to provide a given traffic-flow capability. Before the design can be initiated, all applicable criteria must be established and the design constraints defined. The perform-

ance requirements may include the number and width of traffic lanes, magnitude and distribution of all imposed loads (static, dynamic, aerodynamic, seismic), and arterial-approach geometry. Material behavior properties may include yield and ultimate properties, strength/density relationships, elastic/density relationships and corrosive-resistant characteristics. Constraint functions may include minimum clearances below the bridge, maximum allowable profile gradients and applicable specifications, for instance, the American Association of State Highway Officials' Code.

The scope of the investigation may first include a review of the general configurations applicable to the particular service regime, span length, and foundation conditions. Outlines of general bridge concepts are shown in figure 6 and are based upon various types and combinations of types of trusses, such as deck pratt, through pratt, deck warren, and inclined chord trusses. Within each configuration investigation, the preliminary review should consider the effects of variation in principal design parameters. The investigation of each candidate configuration, for example, should include principal variations in truss-framing geometry, pier locations, deck-framing concepts, foundation concepts, approach ramp effects, material usage, maintenance concepts and related problems.

The display of design data may include a graphic centerline profile of each bridge investigated, with cross sections at specified stations. Gradients and elevations may be printed out at all significant points, including grade transitions, superelevations, drainage requirements and curb requirements. Dimensions and positions of all structural members may be automatically tabulated. Horizontal, vertical and torsional rigidity properties of the bridge may be tabulated for all significant design positions. Bills of materials, weight statements, excavation cubages, foundation cubages and other related data could be approximately tabulated. From these data, material costs, excavation costs, fabrication and erection costs, and maintenance and operation costs can be calculated.

Based upon the above data, an overall merit function can then be expressed for each candi-



APOLLO PAYLOAD

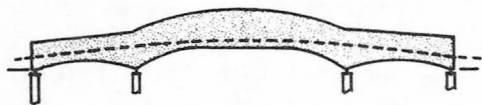
FIGURE 5.—Typical automated drawings.



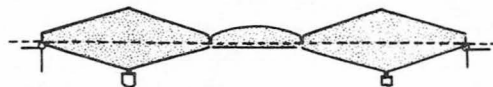
(A) CONTINUOUS TRUSS



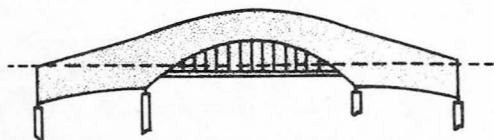
(B) SUSPENSION



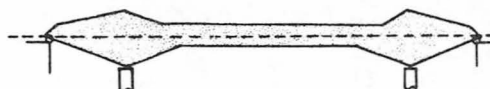
(C) CONTINUOUS TRUSS



(D) ARCHED CANTILEVER



(E) CONTINUOUS TRUSS, CENTER SPAN SUSPENDED



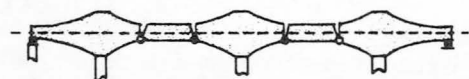
(F) CANTILEVER



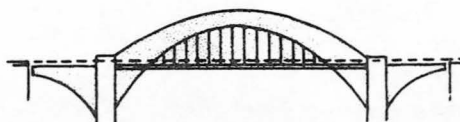
(G) CANTILEVER



(H) CANTILEVER



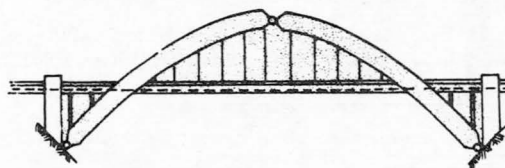
(I) CANTILEVER



(J) TIED ARCH BRIDGE



(K) CANTILEVER



(L) THREE-HINGED ARCH BRIDGE

FIGURE 6.—Representative bridge configurations available for evaluation.

date design. One such merit function is a figure which expresses the total cost of ownership and operation per year in terms of vehicle-ton capacity per year. Such an expression must include all items which are functions of candidate design change.

Using this general design approach, the engineer may input data one day for several hundred alternate bridge designs. In some cases, instructions to the computer may be written which enforce step-by-step changes in significant parameters, provided the merit function is correspondingly improved. The next day he would receive from the computer the solutions to the design problems for those several hundred bridge configurations. The engineer then would be in a position to make a rather complete study of the various configurations available for the design solution.

Design of Freeway Interchanges

Use of computer-aided design techniques should also provide economic insight to the study of complex freeway interchanges. Properties of standard highway bridge constructions, as functions of load and span, could first be input to the computer. The specific interchange boundary conditions and performance requirements may then be input. Various candidate geometries of highway-centerline intersection conditions and their corresponding limitations are also specified to the computer. The limitations would include minimum and maximum horizontal-curve properties, maximum centerline profile gradients, and minimum clearances. The design investigations may then result in displays of the interchange plan, centerline profiles, cross sections, and quantity takeoffs. If all required unit costs are input, such as engineering, right-of-way acquisition, site preparation, construction and materials, the candidate concepts of the interchange can be expressed as merit functions based upon complete cost-in-place of a specified traffic-handling capability.

Design of Domelike Space Frames

Another example of a design problem with a great number of variables is the space frame that conforms to a surface of revolution or to some nonsymmetrical configuration. Design requirements may sometimes define a structure

other than the much-used spherical surface or ellipsoid. Common variations in domelike surfaces are shown in figure 7.

Given a certain volume of requirement, a specified range of height-to-radius ratios, and a statement of environment and load conditions, the computer-aided design investigation can be initiated. One of the most sensitive parameters in this type of study is the geometrical relationships of the space-frame configuration. Trade-off trends are affected greatly by length of framing members, total number of joints, members intersecting at a single joint, relationship of member orientation to load direction, standardization of member details, distance between upper and lower chords, roof-purlin arrangement and type of roof decking.

The use of computer-aided design techniques permits the study of wind-load distributions, effects of perimeter discontinuities, thermal stresses and irregular load and support conditions. The determination of the most economical framing geometry, when combined with non-standard performance or support conditions, often constitutes a sizeable problem. Computer techniques have been developed which analyze space frames of this general type by use of the principle of minimum-strain energy. In addition to the geometry and wind-load inputs, structural parameters such as moments of inertia, cross-sectional areas of members, and connection rigidities are coded into the program in such a manner that they may be easily revised for design optimization. These programs sum the total internal-strain energy of the structure, case-by-case, together with all the interaction products, thus making possible the computation of structural deflections and influence coefficients as required. When using this type of analysis, the geometrical configurations and member types can be iterated to obtain an overall minimum cost structure. A typical geometrical configuration for a space-frame dome, resulting from a computer-aided design study, is shown in figure 8.

The base radius and dome height are input data. Load magnitudes and distributions were specified. Various geometries were assigned for investigation. The merit function used in this case was defined as "cost-in-place" expressed in

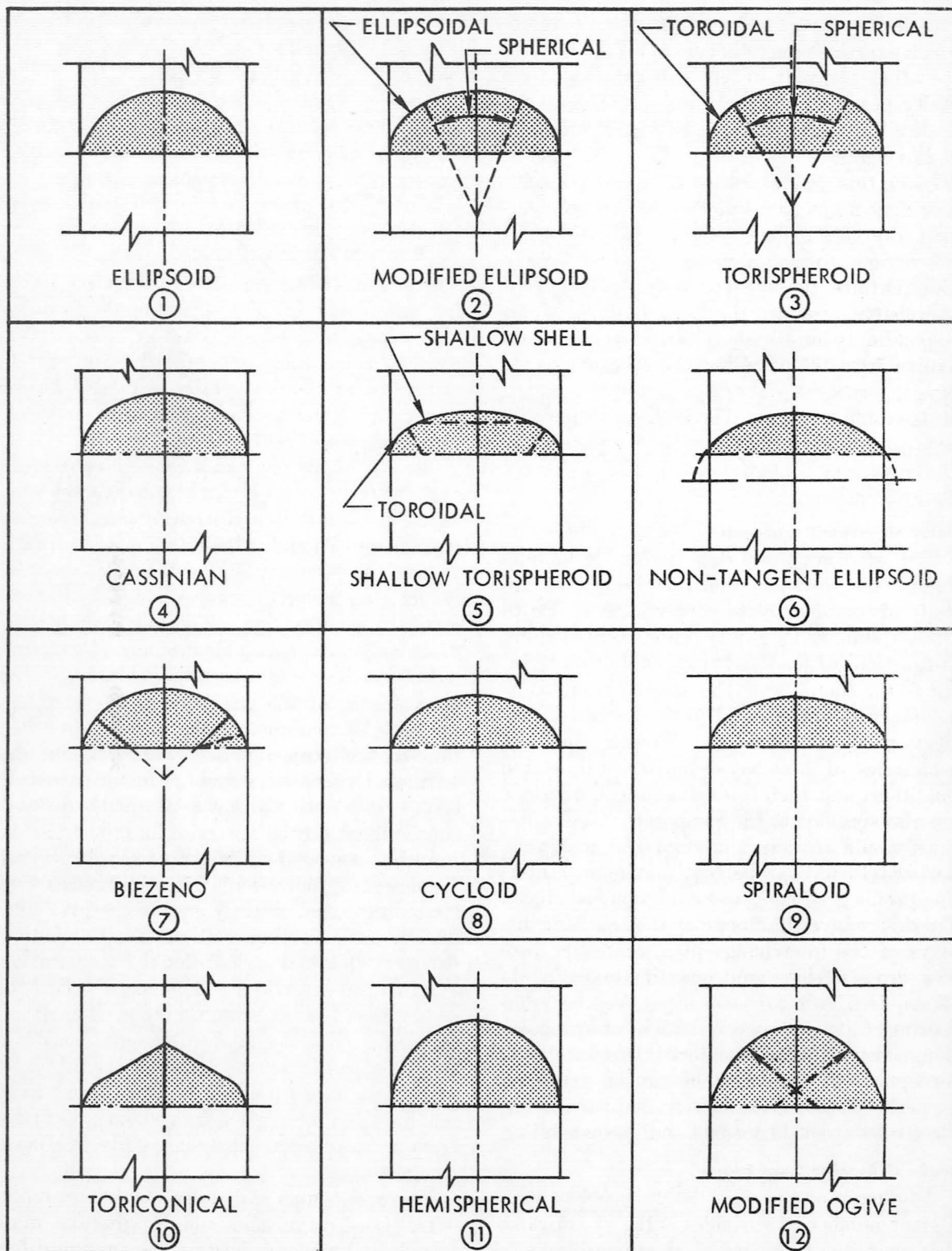


FIGURE 7.—General categories of surfaces of revolution analyzed by computer subroutines.

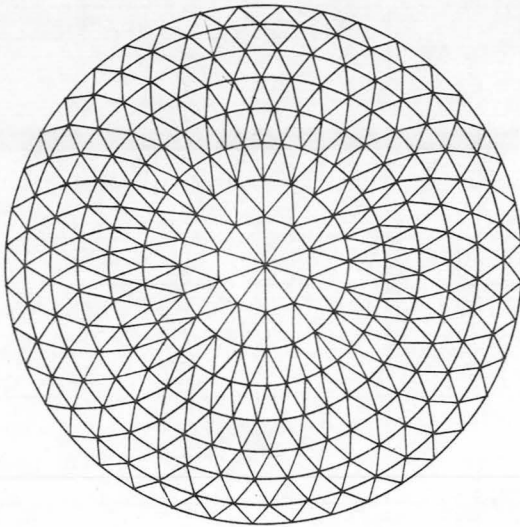


FIGURE 8.—Dome-framing plan developed by computer-aided design techniques.

terms of enclosed volume. A significant fabrication and erection saving resulted from a high repetition of member cross section, length, and end-attachment detail. In the configuration shown, approximately 60 percent of the framing members were identical in fabrication.

The configuration shown in figure 8 resulted from a study conducted at North American Aviation, Inc., relating to the application of computer techniques to civil structures. The general category of space-frame construction represented by this configuration has been identified by NAA as Geolatic framing. The term Geolatic refers to framing systems in which a considerable amount of framing members lie in parallels of latitude. Space-frame radomes have also been designed by this computer-aided technique. Figure 9 illustrates a typical geometry selected for certain types of radome structures. The irregular geometry shown in figure 9 resulted from the geometrical pattern capability to permit passage of electromagnetic waves with minimum distortion. Regular geometric framing patterns exerted a disturbing influence on the directional properties of the electromagnetic wave. In addition, the framing members in this design were required to develop an absolute minimum "shadow" for the antenna aperture. Figure 9 also shows the relationship of the framing geometry to a basic icosahedron, and further illustrates the repet-

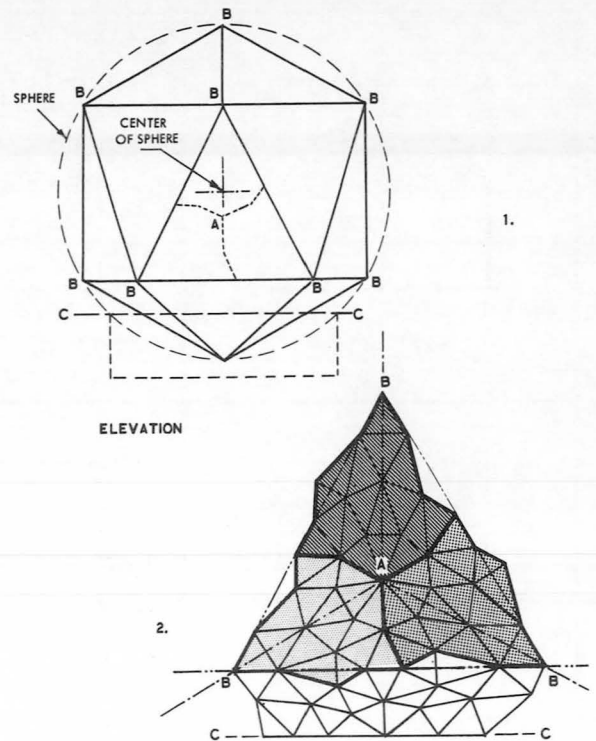


FIGURE 9.—Irregular geometry for radome space frame.

itive nature of the irregularly arranged triangles. The merit function in this case was minimum electromagnetic directional disturbance and minimum shadow associated with a specific structure which was adequate to resist the imposed loads.

In civil engineering problems of these types, cost tradeoff studies include the investigation of many types of framing geometries; framing member length/cost penalties versus framing joint costs; various curvature possibilities for the enclosing surface; weight/cost relationships; air-conditioning systems costs versus insulation and exterior cover-costs; and foundation-type costs versus dome-framing costs.

Computer-aided design can be used to generate a large number of design concepts which meet the service requirements. Selection of the final configuration can then be made on the basis of detailed cost studies, schedule, and architectural considerations.

COMPARISON OF DESIGN PROCEDURES

Table I summarizes and compares the design procedures required for a selected launch vehi-

cle, a bridge structure, and a specific type of dome structure.

The similarity of the general approach is illustrated by the related categories of design items. In all design problems, the engineer is generally provided with a specific set of performance requirements upon which are imposed certain design constraints. The engineer then specifies the material properties to be used in the investigation and defines the merit function by which he will evaluate the candidate designs.

By use of computer-aided techniques the

engineer may evaluate the many candidate solutions provided by the computer. The engineer's decision-making process is therefore strengthened by the additional designs available for his evaluation.

A study of table I will indicate that the number of variables in the design of suspension bridges and domical structures may be somewhat comparable to those relating to launch vehicles. Since computer-aided design techniques have proven to be of practical value for launch vehicles, it is suggested that the tech-

TABLE I.—*Comparison of Computer-Aided Design Procedures*

	Launch vehicle	Bridges	Dome-like structures
Performance requirements	Velocity requirements. Specified payload weight in specific (orbital) mode. Type of mission (scientific vs. military; manned vs. unmanned).	Number of traffic lanes. Magnitude and distribution of loads. Clearance height for vehicles. Topographical conditions. Subsurface conditions. Arterial approach requirements.	Specified enclosed volume of surface area. Specified maintained environment in the enclosed volume. Specified esthetic requirements. Structural provisions to resist specified type, magnitude and distribution of loads.
Material behavior properties.	Strength/density relationships. Elastic/density relationships. Chemical compatibility factors.	Strength/density relationships. Elastic/density relationships. Corrosion-resistant properties.	Strength/density relationships. Elastic/density relationships. Absorptivity/emissivity properties. Thermal insulation/weight relationships. Acoustic insulation/weight relationships.
Constraint functions.	Acceleration limits. Feasible stage diameters and fineness ratios. Time element for design (i.e., 1965 vs. 1970 type structure-systems). Manufacturing-procurement feasibility of components. Least cost components. Manufacturing, R&D time scheduling. Launch environment. Recovery problems. Minimum gage restrictions.	Feasible geometric proportions. Navigation clearance. Minimum traffic lane width. Applicable specifications of the American Association of State Highway Officials. Gradient limitations. Dynamic response. Aerodynamic response. Fabrication limitations. Construction period limitations (time and environment). Construction time period. Depreciation method.	Minimum height as a function of distance from dome perimeter. Upper and lower bounds on temperature and humidity. Upper and lower bounds on acoustic characteristics. Fabrication limitations. Maximum construction time. Construction time period. Amortization method.

TABLE I.—*Comparison of Computer-Aided Design Procedures—Continued*

	Launch vehicle	Bridges	Domelike structures
Scope of design investigation.	Vehicle geometric models (configurations). Construction concepts (components). Variations in strength-density of materials. Effects of loadings induced by various trajectories. Pressure and temperature variations due to flight loadings, trajectories, and system changes. Performance weight partials Cost analysis (R&D plus Operational).	Variations in deck width as function of number of traffic lanes. Deck stacking concepts. Variations in span lengths. Variations in support concepts. Variations in profile gradients. Variations in anchorage configurations. Variations in strength/density ratios of principal structural materials. Variations in ramp concepts. Cost effects upon adjacent land areas.	Variations in aspect ratios (height/radius at base). Variations in meridian curvature properties. Variations in framing geometry. Variations in framing material. Variations in support concepts.
Design exhibit.	Profile drawings. Design sketches. Component detail sketches. Master dimensions. Parts lists. Cost analysis weight statements. Detailed weight statements. Performance weight statements. Detailed geometry of components. Design conditions (loads, pressures, temperatures). Evaluation logic in selection of candidate vehicle evaluation curves).	Drawings of bridge profile, cross-sections, and elevation. Detailed geometry of components. Horizontal, vertical and torsional rigidities of bridge sections. Dynamic response properties. Aerodynamic response properties. Parts list. Excavation and foundation costs. Material costs. Fabrication costs. Erection costs. Maintenance costs. Operational costs. Total construction time.	Drawing of dome cross-section. Three-dimensional coordinate values of all space frame joints and other significant positions. Internal loads and stresses in all members. Load deflection of all significant joints. Aerodynamic response properties. Excavation and foundation costs. Material costs. Fabrication costs. Erection costs. Maintenance costs. Operational costs. Total construction time.
Merit function.	Cost per pound payload in specified earth orbit or space trajectory as a function of number of launches within particular time period.	Cost per year of operation per vehicle ton capacity.	Cost per year of operation per usable unit enclosed, operating in the specified environmental condition.

nique may also be useful for civil engineering structures.

CONCLUSION

This paper illustrates the application of the computer to solving the design problem in the

aerospace industry. It is believed by the authors that similar techniques can be used for the design of sizable engineering structures such as bridges and domes. The use of such techniques should result in the development of more efficient structures at lower costs.

17. Lenticular Stereoscopic Television

CHARLES WHITE

Human Factors Laboratory, SPACO, Incorporated

An old optical technique utilizing cylindrical lenses has been adapted to dynamic displays, with particular reference to television. The techniques also apply to motion picture photography and projection. Two cameras and an electronic switch are required to produce the television picture. The television display itself is a flat-faced cathode ray tube, but the effect of the lenses in front of the display is to cause each eye to view only those portions of the picture that were derived from the appropriate TV camera. Thus the viewer sees what he would see if he were looking at a three dimensional presentation, and his brain therefore visualizes the presentation as being truly three dimensional. The limitation of the original concept, and later concepts which do not have these limitations, are presented.

On examining the various existing types of two-dimensional displays that gave the sensation of being three-dimensional, a striking similarity is noticed between lenticular presentation and standard TV practice.

Lenticular means "lens-like" and a lenticular screen consists of many lenses parallel and adjacent to each other.

The picture for lenticular presentation consists of many vertical strips, with strips alternating across the screen, left to right, and belonging to the view to be seen by a particular eye. Television pictures consist of many nearly horizontal lines; with alternate lines belonging to a particular field.

The field of a TV system consists of every other line. Two interlaced fields constitute a frame or picture. Each field possesses a vertical-synchronization pulse, ambiguously called a frame sync pulse.

A stereoscopic television presentation can be made by making the television picture consist of vertical lines, alternating the fields from two TV cameras, and placing a lenticular screen in front of the viewing picture tube. The lenticular screen consists of vertical-axis cylindrical

lenses, (fig. 1) to each pair of strips. Due to left-to-right reversal by the lenses, each strip pair must be reversed left-to-right on the picture. The position of the lenses is such that the image plane is at or near the focal length. This condition is called collimation. Thus,

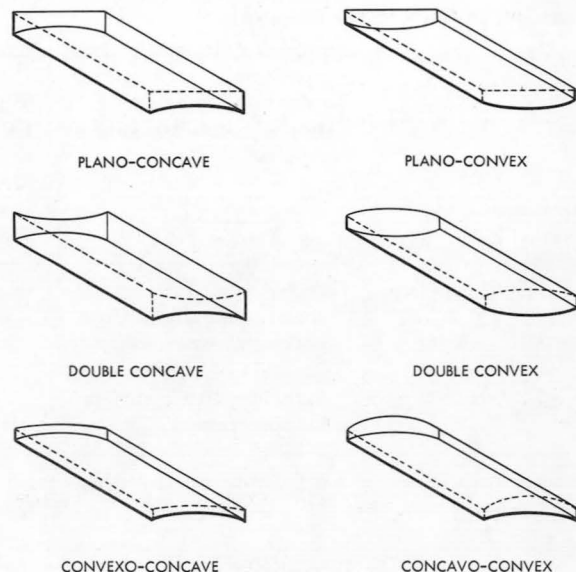


FIGURE 1.—Cylindrical lens configurations.

which picture is seen depends upon the angle at which the picture is viewed (fig. 2). Resolution increases as the number of vertical strips and associated lenses increases.

LENTICULAR STEREO PRESENTATION

There is one basic premise to stereoscopic presentation: the two eyes must not see identical pictures. A vertical lenticular screen, consisting of vertical-axis cylindrical lenses, when used with an image plane at or near the focal plane of the screen, will cause one eye to see only certain vertical strips of the image plane, and the other eye to see the other vertical strips. If the image plane consists of alternate strips from two pictures (fig. 3), and the strips are properly aligned with the lenses, each eye will see only portions of one of the pictures. If the pictures were of the same general view, but one was taken with lateral displacement from the other, the viewer's mental processing will tell him that he is viewing a three-dimensional picture.

There are a number of ways of producing a lenticular stereoscopic television presentation. These will be discussed below in the order in which they were conceived. All require a minimum of either special viewing optics on a camera, or a pair of cameras to generate signals derived from two viewing positions.

Lenticular Stereoscopic Television—Type I

The simple approach to lenticular stereoscopic television is to use a vertical-line raster. The raster is the pattern of lines that makes up

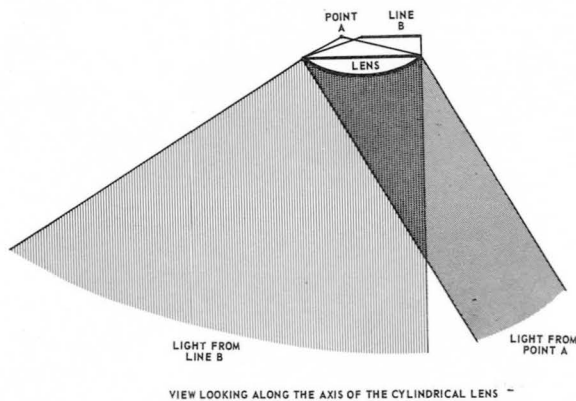


FIGURE 2.—Light patterns produced by point and line sources, with a collimated lens.

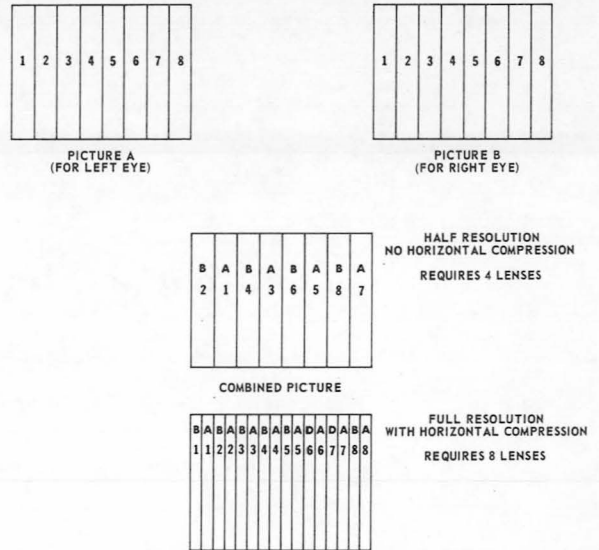


FIGURE 3.—Simplified lenticular-presentation picture generation.

a television picture. The lenticular screen consists of one vertical-axis cylindrical lens for each pair of lines in the raster. The standard television practice of two fields per frame must be used. An electronic switch toggled by the frame synchronization (sync) pulse combines the outputs of two cameras into a combined picture. Toggling is the changing back and forth between two conditions or inputs upon receipt of a stimulus. The result is that each eye will view alternate frames on one screen.

Note that both the cameras and the picture-reproducing device must use the vertical-line raster and are therefore incompatible with National Television Standards Committee TV equipment.

There must be one lens in the lenticular screen for each pair of vertical-scan lines. Therefore, the horizontal resolution is limited to approximately 121 lines when the NTSC standard-raster format of 485 usable lines is used.

Lenticular Stereoscopic Television—Type IA

One of the deficiencies of the Type I system is that the picture image remains fixed in relation to the viewer, that is, if he moves within the area of good stereoscopic viewing, he gets the impression that the items pictured are rotating

about a common axis in the center of the viewing screen as he moves. Since this does not happen in real life, this effect will tend to break the 3D illusion momentarily. When he stops moving, he again obtains the stereoscopic illusion.

A remedy to this situation is to present, not a pair of strips behind each lens, but a continuum behind each lens. A continuum can be produced by shaping the spot that produces the line on the TV screen. While simply spreading the spot horizontally would tend to produce this effect, the best way is probably to introduce a high frequency horizontal signal which would allow selective brightness across the scanned area (fig. 4). A signal inverter turned on and off by the frame sync signal would allow a simple way of inverting the spot-shaping modulation from the first to the second field *ad infinitum*.

Lenticular Stereoscopic Television—Type II

The incompatibility of the Type I picture with a standard TV picture (due primarily to the vertical-line raster) is a major obstacle to its wide use. A compatible system, although more complex, can be made using a horizontal raster, standard TV cameras, and a vertical-lens screen as before. An electronic switch changes from one camera output to the other camera output as the picture spot passes behind the lenses in the viewing screen.

If the width of the lenses is the vertical distance from the center of one scan line to the center of the next scan line, this system produces equal resolution vertically and horizontally.

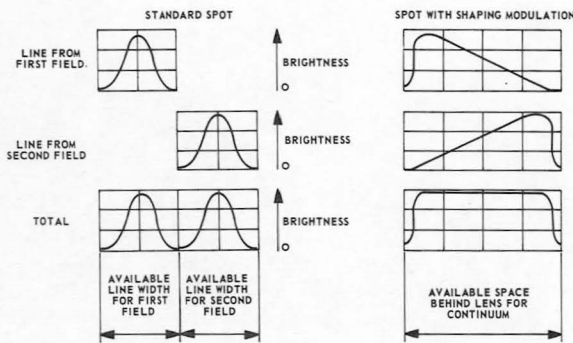


FIGURE 4.—Production of a continuum from a pair of lines by spot shaping.

While there is no particular limit to the number of lenses that can be used, the alinement problem and electronic switch design become more severe as the number of lenses increases. However, the incompatibility of the picture becomes better as the number of lines increases.

If the electronic switch were to blend from the right signal to the left camera signal, and then switch to the right camera again continually, a continuum would be produced which would have the advantages of the Type IA system.

Lenticular Stereoscopic Television—Type III

The problem of alignment of the lenticular surface with the picture to be displayed behind it can be overcome by using front projectors that project through the lenticular screen onto a conventional reflective screen. Since the combined picture behind the screen is produced by the same screen with which it is viewed, there is no alinement problem. However, it would be necessary to use two or more projection units, each receiving a picture from a separate camera. There is, however, no requirement for synchronization between the cameras or projectors for the Type III system.

The production of a continuum on the reflective screen can be accomplished by slightly defocusing the lenticular screen. The continuum might be particularly smooth if the reflective surface were to have some depth to it for better melding of the pictures.

Lenticular Stereoscopic Television—Type IV

There is another solution to the alinement problem of Types I, IA, and II, but this approach applies only to cathode ray tube (CRT) displays. A two-gun CRT, whose guns are horizontally displaced, with each gun driven by a separate camera would produce a 3D picture. The area of the screen's phosphor that each gun can stimulate would be limited to the appropriate strips behind and in registration with the lenticular surface, which might be an integral part of the CRT. If the two guns use a common deflection system, the two TV cameras must be synchronized. If the guns use separate deflection circuitry, then each gun can use any raster, any resolution, and any scan rate desired.

Advantages and Disadvantages

There are many practical problems involved in implementing all of these concepts. There are two main problems in particular that require careful consideration:

- (1) Picture-to-lenticular screen alinement.
- (2) Mounting of the lenticular screen at the proper distance from the image plane.

Picture-to-lenticular screen alinement is a problem only to Types I, IA, and II. An obvious way to achieve permanent alinement is to use photocells on the screen periphery to monitor the line locations and to provide feedback to correct any misalignment. A system without a servo loop must be accurate and stable to within about 0.1%, that is, half a line at 525 lines/frame. To date, this is well beyond current TV requirements and practice.

Mounting of the lenticular screen at the proper distance from the image plane turns out

to be a problem for conventional cathode-ray tubes. This CRT would be required to have a very thin, flat face to get the lenticular screen close enough. The first unit built (a Type I) used a solid-fiber optics bundle for a faceplate on the CRT. Naturally, this is an expensive approach. A simpler CRT could be constructed with a flat phosphor screen and an attached lenticular screen mounted within a CRT envelope. But this design would prohibit adjusting the lenticular screen to aline with the picture. There is no particular problem in mounting a stiff lenticular screen over a stiff rear-projection screen for projection TV.

The resolution for Types I and IA is not as good as in standard television practice because a standard raster is used, and because each eye views only half of the information on the screen. These systems also employ a 4:3 aspect ratio as opposed to the standard 3:4 ratio and therefore, the picture format is less de-

TABLE I.—3D TV System Comparison

	Standard black and white	Type I	Type IA	Type II	Type III	Type IV
Camera requirements:						
Number	One	Two	Two	Two	Two+	Two
Modification	No	Yes	Yes	No	No	No
Processed signal: Compatible with NTSC...	Yes	No	No	Yes	Yes	Yes
Characteristics: Number of signals required	One	One	One	One	Two+	Two
Picture characteristics:						
Compatible with NTSC	Yes	No	No	Yes	Yes	Yes
Aspect ratio (W/H)	3:4	4:3	4:3	3:4	3:4	3:4
Horizontal line resolution	242	323	323	242	242	242
Vertical line resolution	323 ^a	121	121	323 ^b	323	323
Relative horizontal-vertical resolution...	1.0	0.5	0.5	1.0	1.0	1.1
Projection:						
Suitable for projection TV	Yes	Yes	Yes	Yes	Yes	No
Number of projectors required	One	One	One	One	Two+	-----
Type of projection	Front or rear	Rear	Rear	Rear	Front	-----
Cathode ray tube:						
Suitable for CRT	Yes	Yes	Yes	Yes	No	Yes
Number of guns required	One	One	One	One	-----	Two
Difficulty of alinement	-----	Difficult	Difficult	Severe	Easy	Easy
Viewing angle	Wide	Very nar- row	Narrow	Narrow	Wide	Narrow

^a Based upon equal vertical and horizontal resolution.

^b Assuming that the lenticular screen consists of at least 646.

sirable. If the picture (and camera scan) width were increased to achieve a 3:4 aspect ratio without increasing the number of lines the Relative Horizontal-Vertical Resolution factor (table I) would change from 0.5 to 0.28. Since information theory specifies that 1.0 is optimum, a better approach would be to use more lines to increase the width. This would deviate from standard raster and standard video signal practice, but there are several semi-standard rasters containing more lines. A nominal 1000-line raster would provide a Relative Horizontal-Vertical Resolution of about 1.0. The Type II system has a standard aspect ratio, but again the horizontal resolution is half the vertical resolution. Increasing the signal bandwidth would increase the horizontal resolution if the number of lenses was also increased. This would make picture-lens alinement more difficult. Since Type III and Type IV use a full raster for each eye, they are standard resolution systems and use the standard aspect ratio.

The Type III system is not limited to television usage. It works equally well for film slides and motion pictures. The principal disadvantages to this system are the need for wide separation of the projectors, and the need for good anti-reflective coatings on the lenticular screen. If three or four projectors were used (each with its own camera) it would be possible to move around in front of the screen and look behind objects in the picture foreground.

Applications

The most obvious applications are those where the data to be displayed is three dimensional to begin with.

Air traffic control is a three-dimensional problem. Using lenticular stereoscopic television as a display device, the air traffic controller could directly perceive the flight paths and altitudes of the airplanes within his control zone. The naturalness of the display would lessen the training requirements and reduce the fatigue-causing elements for the controller.

Ground Controlled Approach for aircraft is virtually the same problem that exists for the air traffic controller. At present, GCA must

monitor two displays and mentally conceive the three-dimensional picture. An interesting system here might include a ground radar-derived computer-generated display in the aircraft cockpit. The ground-based system would generate the signal which would be transmitted to the airplane and displayed without processing. If the CRT were mounted vertically behind the plane's instrument panel, and an angled, partially silvered mirror were mounted above it, the pilot would see the display precisely as he would see the runway. With such a system, there would be virtually no transition problem from the display to ground reference at the moment of getting below the overcast.

Deep-sea salvage and mining is daily becoming more practical. Most systems now envisaged use a remotely controlled machine. The use of lenticular stereoscopic television as the display medium, as opposed to ordinary television, would greatly enhance the naturalness of operation and the speed and efficiency of the remote control.

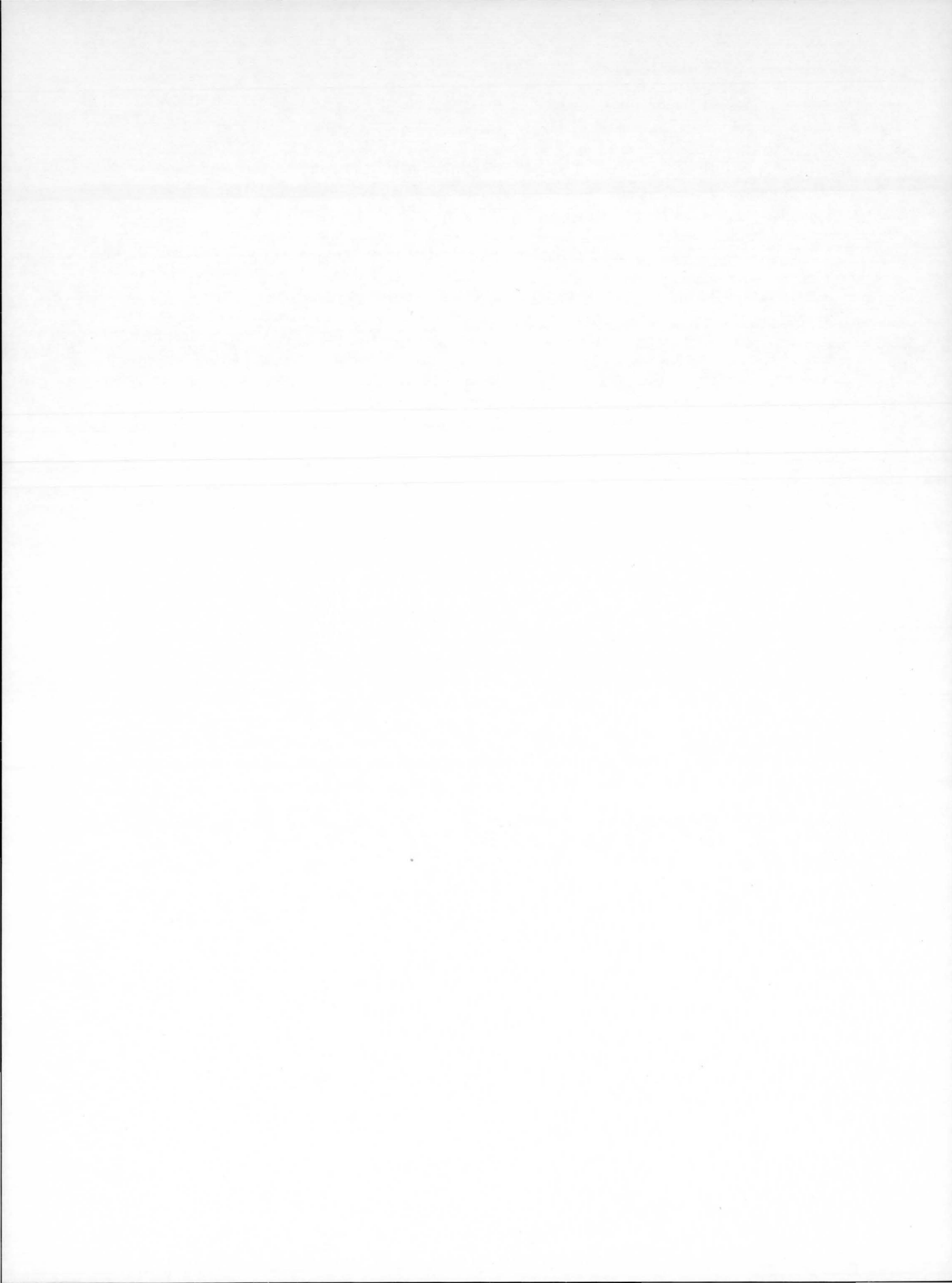
Vector electrocardiography, a two-dimensional plot of the electrical activity of the heart, could be made more useful by plotting in three dimensions. The same technique might be useful in electroencephalography, the study of the electrical activity of the brain.

Commercial television could use Type II. There is no inherent practical reason why color lenticular stereoscopic television could not be built, other than financial reasons.

Any three related parameters could be displayed in three-dimensional format. Since two two-dimensional pictures are much easier to generate than a three-dimensional picture, these display systems are well suited for computer-generated display.

CONCLUSION

There is a need for three-dimensional presentations. The lenticular stereoscopic television systems is believed to present the most feasible and economical way of filling that need. The principles are simple, and their execution is now possible with aerospace-electronics techniques.



18. Use of Space Vehicle Television Developments for Commercial and Industrial Use

C. T. HUGGINS

George C. Marshall Space Flight Center, NASA

The application of a technique developed by MSFC for space vehicles for expanding the capacity of a transmission system is discussed as it could apply to commercial and industrial situations. A short history of the development and theory of operation is given using slides and film clips for illustration.

The system is basically a specialized method of time-sharing the output of a number of cameras to create an interleaved-information stream which can be sent over conventional television transmission links such as a long-line cable or microwave links. The composite stream of information is separated at the receiving terminal into a number of channels equal to the channels at the transmitting terminal. Each channel may be viewed on a monitor as though it were being transmitted continuously.

Uses of the capacity-expansion portion of the system is described as it is related to industrial and commercial applications. Examples of these are multipoint surveillance within two or more plants and multicamera coverage of sports or news events. Also briefly discussed are the new developments which compliment both the transmission and reception ends of the above system.

HISTORY

This paper will describe a technique for transmission of a number of channels of unrelated video and, if desired, audio information over a common-carrier medium and allow them to retain their individual identity.

A generalized explanation of the sections and operation of a complete transmission and reception system, of which this is a part, will be covered. A detailed description of the subsystems required for this technique will be given.

Brief discussions are given of the devices developed in support of this technique which are not a direct part but can be used with the system. This applies to both the receiving and transmitting terminal equipment.

Some educational, commercial, and industrial applications of the technique combined with

various portions of the peripheral equipment designed with the system are given.

During growth of Redstone, Jupiter, and Pershing vehicle development, there were many times when normal measuring instruments and methods failed to give the development engineer a reasonably certain answer to a problem he had with the operation of some part of the vehicle while it was in flight. The measuring instruments used gave such indications as temperature, pressure, acceleration, vibration, shock, and humidity. A single picture in some of these areas would have given the answer.

It was decided in early 1959 to begin design-development work on an instrumentation TV system for Saturn research vehicles, for the Astrionics Division of MSFC. Since that time this organizational segment has been engaged in evolving TV systems for use between space vehicles and earth to gain information useful in the development phase of the Saturn systems

and to provide real-time operational data from the post-development vehicles while engaged in the navigation of space. A continuous study was made of the various instrumentation problems as they were presented in the course of the development of the Redstone, Jupiter, and Pershing missiles, both as they were related to vehicle systems development, and to space navigation as they were inferred.

In the early programs, flight times and operational ranges were relatively short. The application of vehicle TV systems then meant that a high picture rate was required with good resolution for the acquisition of as much information as could reasonably be recovered during the short times involved. Commercially available TV subsystems were then providing a capability of 30 pictures per second with the desired resolution. On this and other considerations the decision was made to concentrate, at least in the beginning, on a small extremely rugged camera capable of withstanding environmental extremes expected during powered flight and free-space coasting of the test vehicles.

The first complete system assembled included an entire flight system consisting of wideband transmitter, using FM modulation and a miniaturized camera chain capable of withstanding the least favorable launch environment expected, which was at that time the Redstone booster. The ground system consisted of a laboratory-fabricated receiver, a broadband amplifier and a specially built kinescope recorder. The in-house-assembled ground station was operated by laboratory personnel because of their familiarity with the laboratory arrangement of the apparatus.

This system was the first to transmit real-time high-resolution TV at 30 pictures per second compatible with commercial TV systems from a ballistic missile operating outside the earth's atmosphere. It operated satisfactorily from lift-off to the optical horizon, a distance of more than 320 kilometers on the famed flight of the monkey "Ham" on the Mercury Redstone vehicle, January 31, 1961.

The multiple-camera, single-transmitter system concept was evolved in late 1959 and early 1960 and tested. A proposal including a sys-

tem description along with details of the test and evaluation of the test results was subsequently submitted to Wernher von Braun in 1960. Extensive tests of the new camera and fighting concepts for application both on the test stand and in flight, continued until the fall of 1961, at which time it was considered operational for the 1.5-million-pound thrust environment of the Saturn booster. It was then included as part of the test program as an instrumentation device for the Saturn system.

Pictures received from this system may be displayed on any standard television system such as the local commercial broadcast television stations or any of the major television networks, which must conform to the Federal Communication Commission's standards for the generation of synchronization signals.

Recent single-camera, real-time pictures made of such things as the deployment of the Echo I balloon and the deployment of the Pegasus payload as well as flights and separation of the stages of the Saturn series vehicles demonstrate the results that can be obtained from flight television systems. The pictures from Echo I, the Saturn series, and the Pegasus were shown over the major commercial television networks.

DESCRIPTION OF EXISTING SYSTEM

The Saturn television system provides real time display and permanent storage of pictures televised from the vehicle during flight. The system antedates all known research-rocket television systems with inherent commercial television systems compatibility, high picture resolution, and display-analysis features. The Saturn TV system is considered applicable to many other research projects where environments comparable to that of the Saturn are expected. The system is modular in form and, consequently, highly adapted to a wide variety of layout schemes. It is divided into two categories, which are referred to as transmitting and receiving terminal equipment.

Figure 1 shows a simple block diagram of a two-camera flight system, employing all of the components mentioned in the transmitting terminal equipment.

Figure 2 shows a simplified block diagram of a ground receiving terminal from the para-

metric amplifier, which is normally a portion of the antenna system through the monitor and recording system at the other end.

The ground-terminal equipment consists of an appropriate receiver connected to a unit called a decoder which separates the combined pictures. This allows the picture originating from each individual camera to be routed to its own individual monitor. The viewing unit is essentially a device employed to store single frames of high rate information and play them continuously to a given monitor so that the picture presented will be at a 30-picture-per-second rate, while the information received from the vehicle will be at a rate lower than this, dependent upon the number of cameras in the system. Information is recorded from the receiver on a video tape recorder and a special kinescope recorder simultaneously with the display on the monitors. A part of the system allows the output from the receiver or the playback from the video tape to be fed into a decoder unit, which automatically separates the

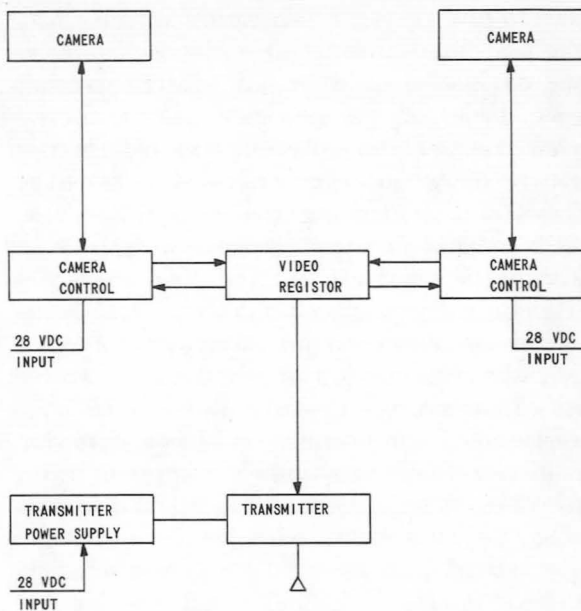


FIGURE 1.—Inflight equipment.

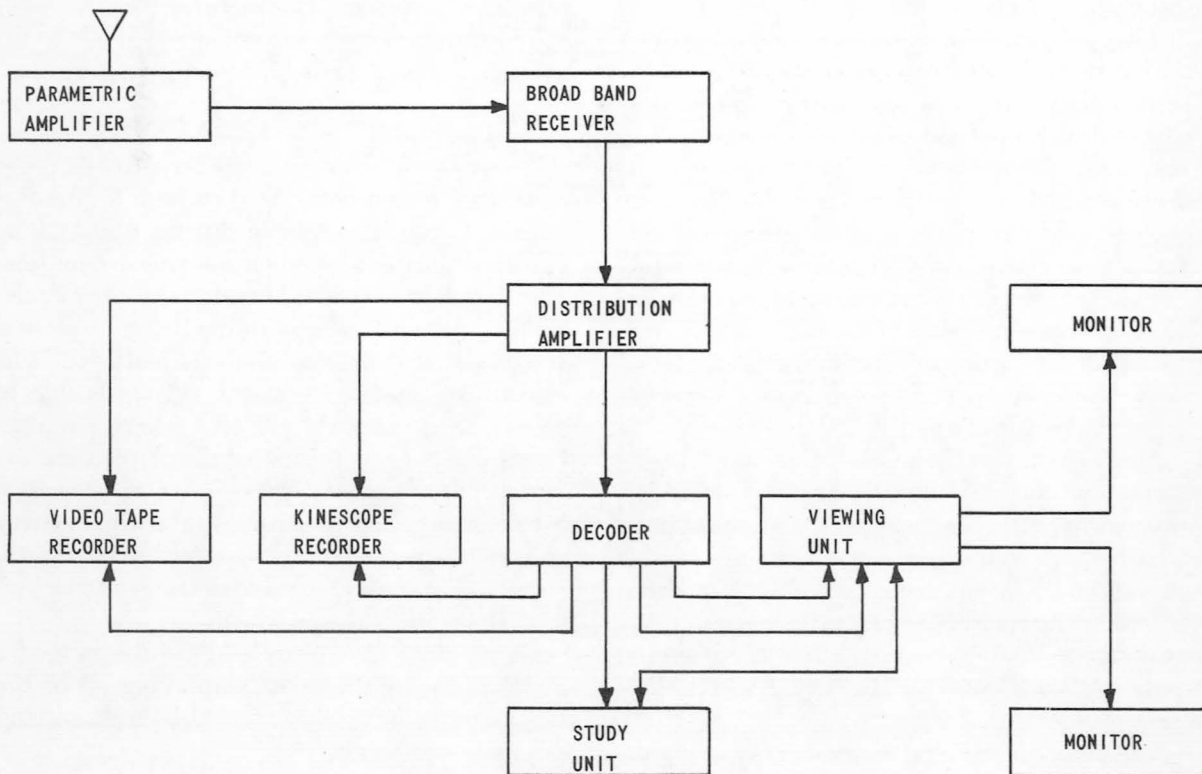


FIGURE 2.—Ground receiving station.

two frames from each camera into two channels. The two frames from camera one are fed to output one and the two frames from camera two are fed to output two.

In the first system models the information coming out of these two channels needed to be displayed. If this were fed to a simple television monitor it would produce two frames, or pictures, of information and then omit two frames of information resulting in a 15-cycle-per-second flicker which occurred every two frames for a duration of two frames. To the eye of the average observer, this was very objectionable. However, it was decided that a device which had the ability to store this information for a short period of time could be used to bridge this two-frame gap when no information was being transmitted to the monitor from its own channel. Methods to achieve this will be discussed in later paragraphs.

Figure 3 shows a diagram of the essential parts of both ends of this system. The point of

interest for this discussion is the use of the portion of the system lying within the dotted lines. This portion actually changes the capacity of the link joining the two ends of the system. The original concept for the system was to get the maximum amount of information for a given RF bandwidth. Therefore, the first system tried was one which alternated transmission from two cameras on a two-frame basis. That is, the end referred to as the video register allowed the output of one camera to pass into the transmitter for two complete pictures, and then, during the interval between the second and third picture, the input to the video-register unit was transferred to the second camera, and two complete pictures from this camera were allowed to pass into the transmitter. The video register would return to the original position and allow two more pictures from the first camera to pass into the transmitter. This back-and-forth cycling of the pictorial information was received on the ground and video taped. At the

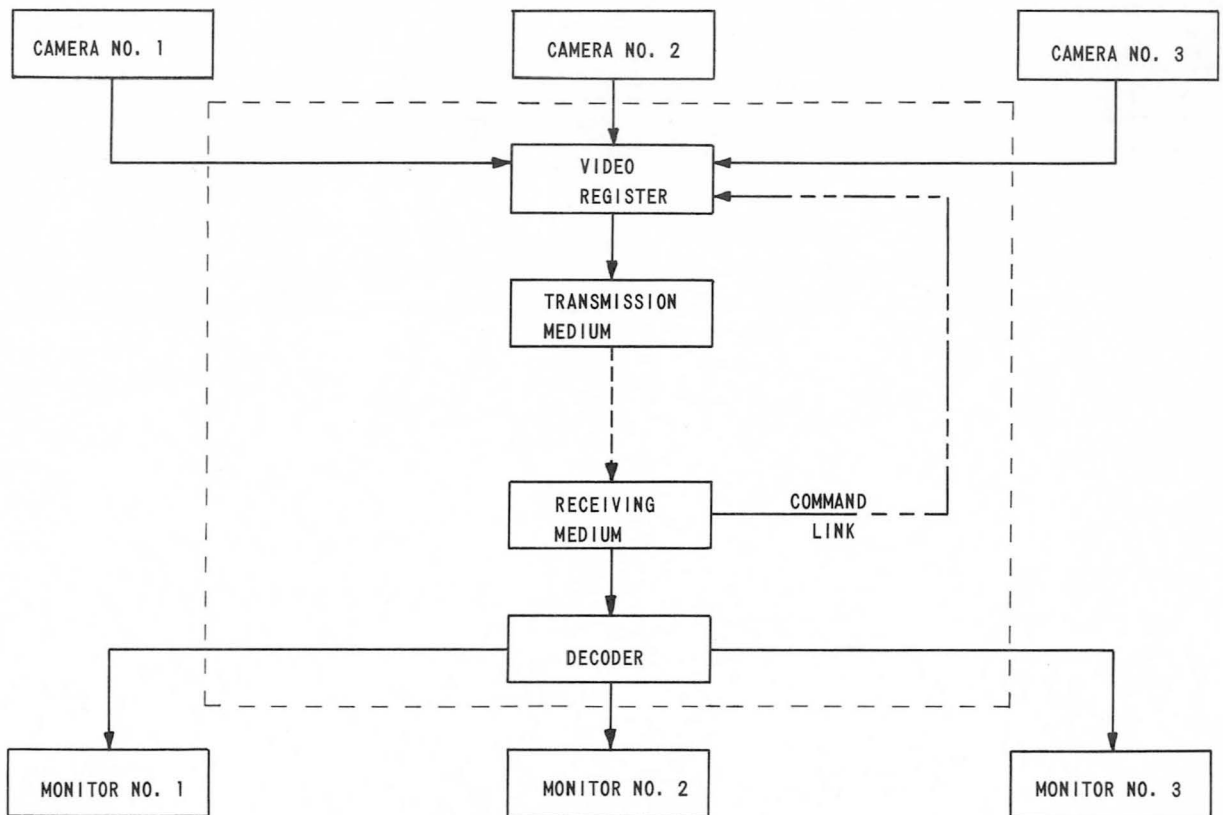


FIGURE 3.—Total TV system block diagram.

same time, a kinescope recording was made. These films would be viewed as individual frames, as any other single frame pictorial information is used without regard to the fact that the information was interleaved on a two-frame basis.

Since each picture was now viewed once every $\frac{1}{15}$ second, the next step in this process was to eliminate the second frame and transmit only one frame from each camera per switching interval. This meant that the motion continuity could be increased and objects having a motion rate twice that capable of being viewed by the first system could be accepted by the new system.

Originally, each picture was viewed $3\frac{1}{4}$ times per second for a series of four cameras. Now each camera output would be viewed for $7\frac{1}{2}$ times per second. Motion studies made of the moving parts of the Redstone, Jupiter, and the Pershing missiles indicated that the usual moving parts such as actuators, separation rates between vehicle parts, etc., normally did not exceed a rate which could be viewed at an information renewal time of $7\frac{1}{2}$ times per second. Therefore, this frame switching system was selected as the first version of the information conservation transmission program and used on the SA-6 developmental flight as a two-camera system on a two-frame per camera switching basis. The results of this were very good. Switching showed perfect matched registry with no displaced frames or disassociated fields throughout the entire recorded flight.

Since that time, other methods of switching have been employed in the laboratory and have proved feasible. Among these are (1) switching from camera to camera every field, and (2) switching from camera to camera every line. The switching from camera to camera every line imposes motion limitations which increase in severity as the number of cameras go up. However, so long as only two cameras are used, most slow motion is not objectional. The field switching system appears to be from this standpoint perhaps the most feasible on the basis of two cameras.

On the basis of four cameras, field switching could be used; however, again there is the prob-

lem of motion continuity between consecutive fields for a given camera and frame switching is best because of the recording of complete pictures from each camera.

DETAILED BREAKDOWN OF SPECIAL SECTIONS OF TRANSMITTING AND RECEIVING TERMINAL EQUIPMENT

A Description of the Video Register Unit

For purposes of this discussion it will be assumed that four cameras or video signals are being used for transmission over this system. The heart of this system is a four-stage ring counter (fig. 4) which is designed to rotate one position every frame or every two fields of video information. The video register contains, as the basic timing system, a crystal-controlled oscillator running at twice the horizontal line rate, followed by a binary counter which derives the necessary timing information to control all of the functions of the video register. The signals coming from the timer are used to control the vertical-drive signal, the vertical sync, the horizontal sync, the horizontal drive, the sync mixer, the blanking mixer, and the reset or burst generator.

Operation of the device is now given. Video is accepted from one to four sources at commercial frame and line rates. The register unit switches on the single frame or two-field basis from one input to the other in rotation. The output from these switches is fed to a video amplifier where the reset or burst generator input is introduced. This shall be discussed later. The video amplifier sends its signal then to the blanking mixer, then to the sync mixer, to the video buffer, and out of the register unit to the transmitter. In order to keep everything in exact synchronization, the cameras are provided with horizontal and vertical drive signals so that their inputs will be exactly in step with the switcher accepting the composite video from each camera. In order to provide some reference point for the decoder, a reset signal is supplied by a video frequency oscillator issuing a single frequency burst of a narrow width. This burst occupies slightly less than one horizontal line at the top of the picture and is not seen on the receiving monitor. This burst is injected into the video amplifier as mentioned above only

during the beginning of the first picture from the camera which is arbitrarily chosen as camera No. 1. The ground decoding equipment is able to find this burst and use it as a reclocking pulse to insure that the decoder is continuously locked in step with the video register unit. Figure 5 shows a flight version for shape and size comparison.

A Description of the Video Decoder

The video decoder (fig. 6) is a device previously mentioned which separates the individual cameras into separate channels displaying them on separate monitors at the receiving terminal of the system. There are two basic parts making up the video decoder: a four-stage ring counter and a sync generator or clock. The four outputs of the ring counter operate four video switches. These switches are opened in numerical sequence. The incoming information from either a receiver or a coaxial cable is fed simul-

taneously to the input of each of these four video switches. It is also fed to a unit called a sync stripper which eliminates the video information from its output leaving only the synchronization information. The output of the sync stripper is fed into the other main portion of the video decoder, the sync generator. This sync generator provides standard output timing and sends pulses to the four-stage ring counter at the vertical-frame rate, so that the ring counter will rotate one position for each frame pulse delivered to it by the sync generator. Thus the video switches are commanded open one at a time. The video switch 1 opens first sending one frame of video information to a display monitor 1. This switch then closes and video switch number 2 opens. The information from camera 2 is now coming in and is passed through this switch to monitor 2 to be displayed for one frame. Then switch 2 is closed, and the same procedure is followed with switches 3 and 4 in

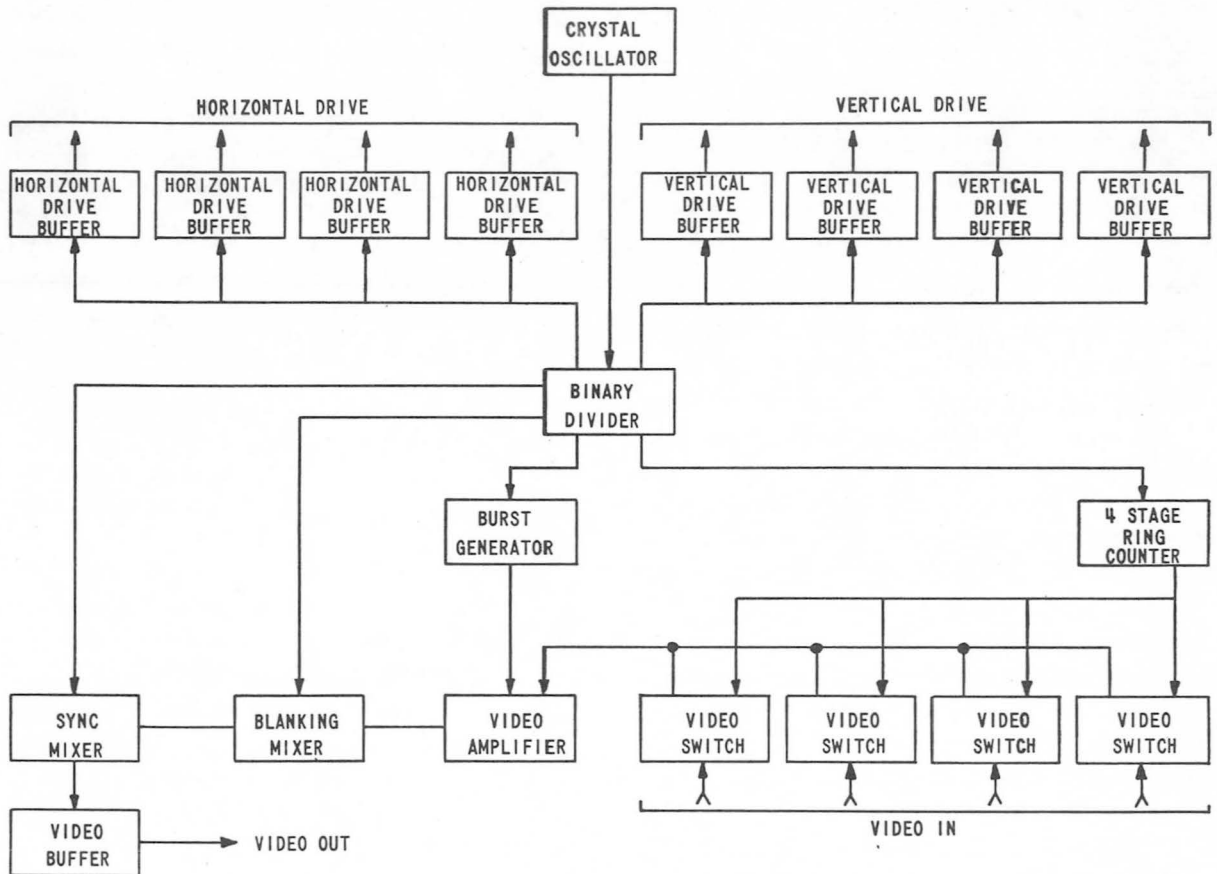


FIGURE 4.—Video register block diagram.

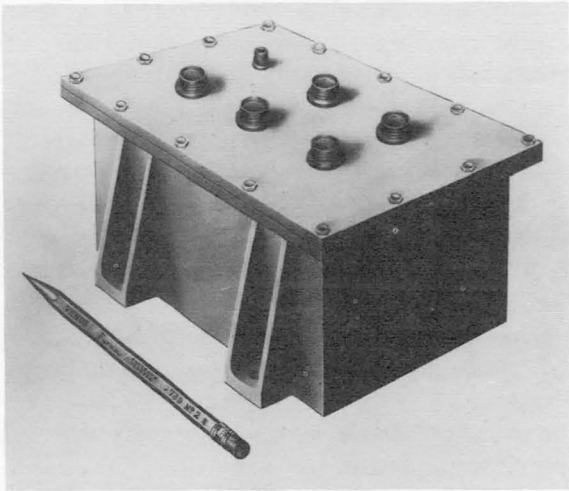


FIGURE 5.—Video register.

turn allowing one frame corresponding to the numbered camera at the other end of the transmission medium to pass through each switch. The sync-stripper signal keeps the synchronizing generator locked or in phase with the syn-

chronizing generator employed in the video register unit at the transmitting terminal.

There is one other necessary item to insure proper operation of this system without which the position of the counter in the decoder would not stay in phase with the position of the counter in the transmission equipment. If this condition existed the information from the cameras could be displayed on the wrong monitors. To prevent this, as was described previously in the video register section, a burst generator applies a burst frequency at the beginning of the first line of the first field of camera 1. This burst is filtered out by the burst-generator filter in the video decoder and appears as a pulse whose width corresponds to the originating pulse or slightly less than one line in duration. This pulse, referred to as the reset pulse, is applied to position one of the ring counter such that if the ring counter is in any other position than number 1 at the beginning of the first picture originating from camera 1, it will immediately shift to position 1 so that

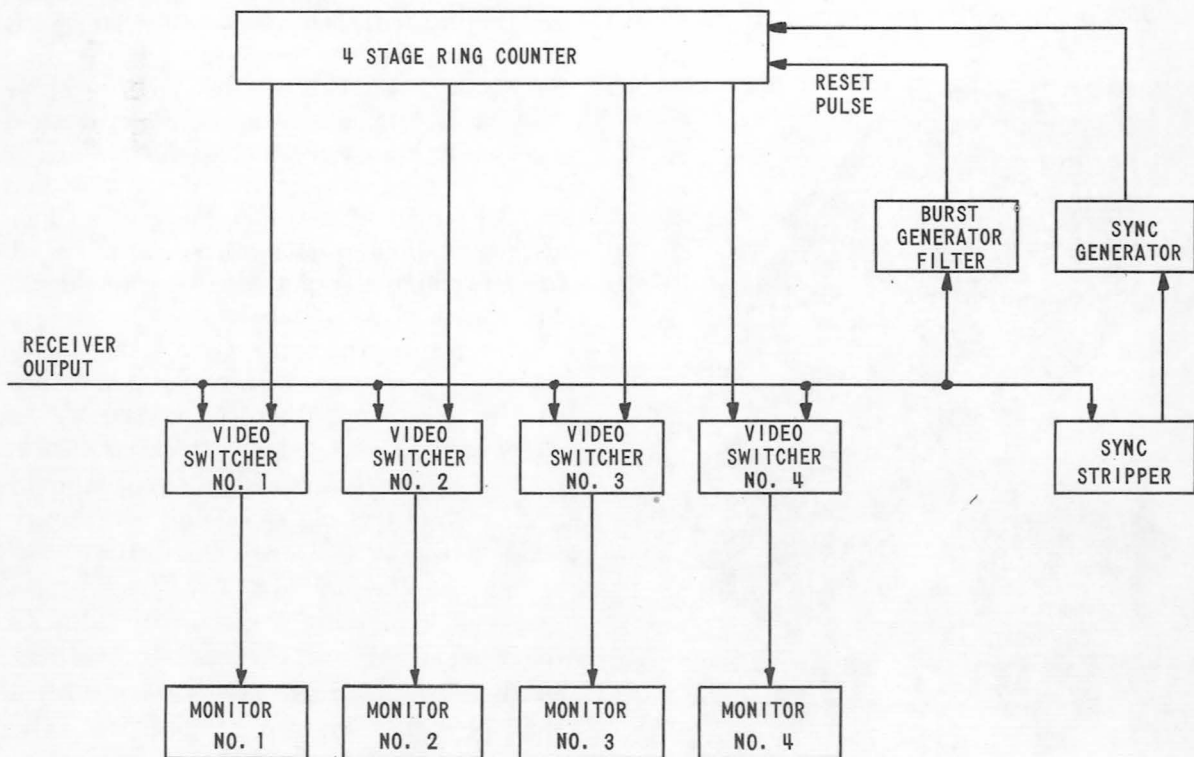


FIGURE 6.—Video decoder.

the remaining portion of this frame will pass through switcher 1 and on to monitor 1. This is called restoration of frame registry. This insures that each monitor receives the information from its corresponding camera and should it get out of step for any reason during one rotation of the ring counter it will be reset at the beginning of the next rotation. The maximum time that any one monitor could be supplied the wrong information is one frame or in the case of four cameras approximately $\frac{1}{8}$ second. Figure 7 shows an operational unit designed for rack mounting.

OTHER EQUIPMENT PRODUCED AS A RESULT OF THE SYSTEM

As has been explained, the information derived from the video decoder is fed out to a monitor for each camera of the originating system at the transmission terminal. These monitors could be high-persistence monitors so that the retention of the image could be held for $\frac{1}{8}$ second without any appreciable smear so long as the viewed image had very low motion rate—examples being plant surveillance, or slowly moving machinery. However, in those cases

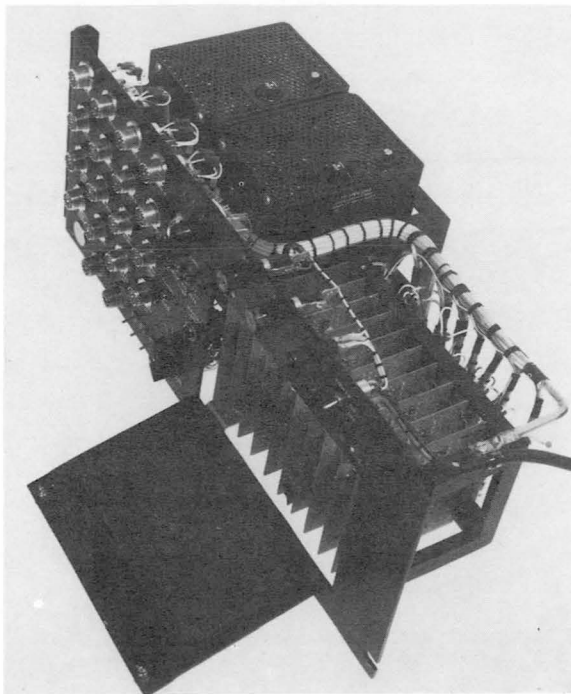


FIGURE 7.—Video decoder.

where the information could move at low rate, a high-persistence screen is undesirable. It would be more convenient to supply a conventional monitor displaying 30 pictures per second as is normally done with standard closed-circuit TV. If it is desired to view continuously 7.5- or 15-frame per second information, it is a necessity to have a long-storage-time tube and feed it a standard 30 frames per second as in conventional closed-circuit television. There are a number of ways this could be accomplished.

A system first tried and proved successful was one using a storage tube between the decoder and the monitor. This storage tube was another special development by this center. It was a requirement that the storage tube have the capability of being able to write in or store one single frame of information in a period of $\frac{1}{30}$ second, be able to retain this frame of information for a period approaching 1 minute, and then be able to completely erase the picture stored in the tube in less than one vertical interval which is a period of approximately 1100 microseconds.

At the time of the need for this device, no such tube existed; therefore, the tube having the nearest qualifications was chosen as the most likely candidate. This tube had an erased time of about 2500 microseconds and was reworked to reduce its erase time to 1100 microseconds or less. The storage capability of the tube was good for periods of 10 to 20 seconds where erasure was required at 1100 microseconds. Each channel coming out of the decoder would employ one of these storage tubes similar to a monitor picture tube. As each frame of information came out of the decoder it would be fed into a storage tube corresponding to the originating camera in the system. The next frame of information would be switched to the second storage tube corresponding to the originating camera two. During the vertical interval following the picture received from camera number 4, the storage tube associated with camera number 1 would be completely erased, and the next picture from camera number 1 would be written into this storage tube. Observing these tubes visually, one could see a small picture approximately 3 by 4 inches which

would be similar to the one displayed on the conventional monitor. The resolution of the picture was better than commercial standards, but the shades of gray were not quite as good.

In order to translate this information to a conventional monitor, a small high-resolution camera was placed in front of this tube and scanned at 30 frames per second. Its output was fed in turn to a conventional monitor; therefore, as the storage tube retained its information, the secondary camera continued to deliver to the monitor 30 frames per second. This system was a good beginning.

The second generation of this approach was tried eliminating the optical readout so that the information was read into the tube electrically and read out of the tube electrically. The storage surface in this particular tube was not visible. This approach, though reasonable and accurate with respect to each individual section of the tube, did not prove out realistically when combined. However, it is thought the basic concept is sound and the idea has not been abandoned.

Another method of translation from the decoder to the standard monitor is by the use of a magnetic drum. The magnetic drum has the capability of storing one frame of information per track per revolution; therefore, one frame of information may be stored upon command and then read out of the drum as long as desired up to about an hour if necessary—the signal-noise ratio reduction being the limit on time. The drums examined to date show that there is a capability of handling two or three times the number of channels of video information per drum compared to the description of this initial system. In one version, the drum itself and all its associated drive equipment can be mounted in one standard 19-inch rack, along with a monitor and waveform monitor for observing the various channels as they are read into or out of the rotating drum. Another version is much smaller but will not accommodate as many channels of information. It does not have as high a signal-to-noise ratio or as wide a bandwidth, but for a number of practical commercial applications would be quite desirable. The life of these machines runs in the order of

2000 hours before there is any replacement required.

At the transmitting end of the system, the state-of-the-art of cameras is going along very well. The size of cameras and the complexity is being reduced as the resolution capabilities of the cameras is slowly increasing. There is always the question of how much resolution is required or how much is the user willing to pay for a particular job. In connection with this subject, this center has been engaged in the development of ruggedized cameras for some years as evidenced by those now in use onboard the Saturn vehicle. A special type of tube had to be developed to survive in these environments. Continuation of this development has produced a tube which is a half-inch vidicon able to survive the Saturn operational conditions.

Now in the final stages of assembly and testing is a camera utilizing integrated circuitry of the micromodular concept for the peripheral equipment associated with the imaging tube which is made from ceramic rather than glass, and is much smaller than any other known tube of the conventional vidicon type made today. This tube has the advantages of low mass, high vibration resistance, the ability to maintain good resolution and withstand considerably higher temperatures than any other tubes currently available. Figure 8 shows an artist's conception of the complete camera package as it might appear ready to be installed. This includes all associated circuitry necessary to produce standard composite video picture. Work is still being carried on in the area of the critical portion of the camera which is the imaging tube. It is felt that the technology of micro-miniaturization and photosensitive devices can ultimately provide us with a sensor capable of producing television type pictures but having no electron-scanning beam, and therefore, no electron gun to withstand the shock and vibration imposed by launch and maneuvering of space vehicles. This would leave only the temperature and humidity problem which now exist to be overcome as the growth of the art continues.



FIGURE 8.—*Miniature TV camera.*

APPLICATIONS OF A COMMERCIAL AND INDUSTRIAL NATURE

Now let us apply this technique to some applications other than our space program. A few hypothetical cases will demonstrate the versatile use of this system. Suppose a company has a number of plants or buildings situated relatively near to each other. Perhaps now they employ roving night watchmen or they may have installed TV cameras in a central monitoring point in each building to monitor the various areas of the plant during operational or off-duty hours. Using the system described here, the camera located in the plant could be combined using this time-sharing technique because the information usually desired in this case is that of the presence of undesired motion rather than observance of a fast motion rate. These cameras could be combined and transmitted over a single transmission cable to another point where they could be viewed by a single man. Let us suppose that three buildings are employed. The output from each building could be sent, using this technique, over a cable to a central observation point, where one or two men could be employed to observe the entire three-plant facility. Now, it is true that if the number of monitors is in-

creased there are created some problems with a symptom comparable to road hypnosis. This may be eliminated by the use of standard redundancy elimination techniques whereby all monitors would have no display as long as there was no moving object in the picture. The minute an object moved in the picture it would appear on a screen. This in itself would be a much more practical approach to psychologically efficient use of the observers.

The current video register unit could be programmed externally over any kind of audio lines available from the observation point to a particular plant to cause the sampling circuitry to stop on a particular camera, thereby allowing continuing observance of a particular view, if it were felt necessary by the observer.

The transmission of this information from the plant to the viewing point could be accomplished by conventional coaxial cable and line boosters. For a remote plant it could be done by microwave link if the remote observation warranted the expense of a low-cost microwave link, since the bandwidths required are those in commercial use. The use of this technique of observance over a relatively short period of time would pay for the equipment in the saving of roving guards, or night watchmen, or an individual observer for each installation.

In the area of commercial entertainment this technique could again be employed in a somewhat similar manner. In the case of covering sports events of any type where multiple cameras are set up for point observances, the information is usually relayed to some central point by cable or microwave where someone selects the view to be used to feed the network. With this technique the person selecting the view to be fed to the network would not necessarily have to be located at the sight of the event. The information could be transmitted over a microwave link to some remote point where other facilities required for the integrated operation of such a program were also available.

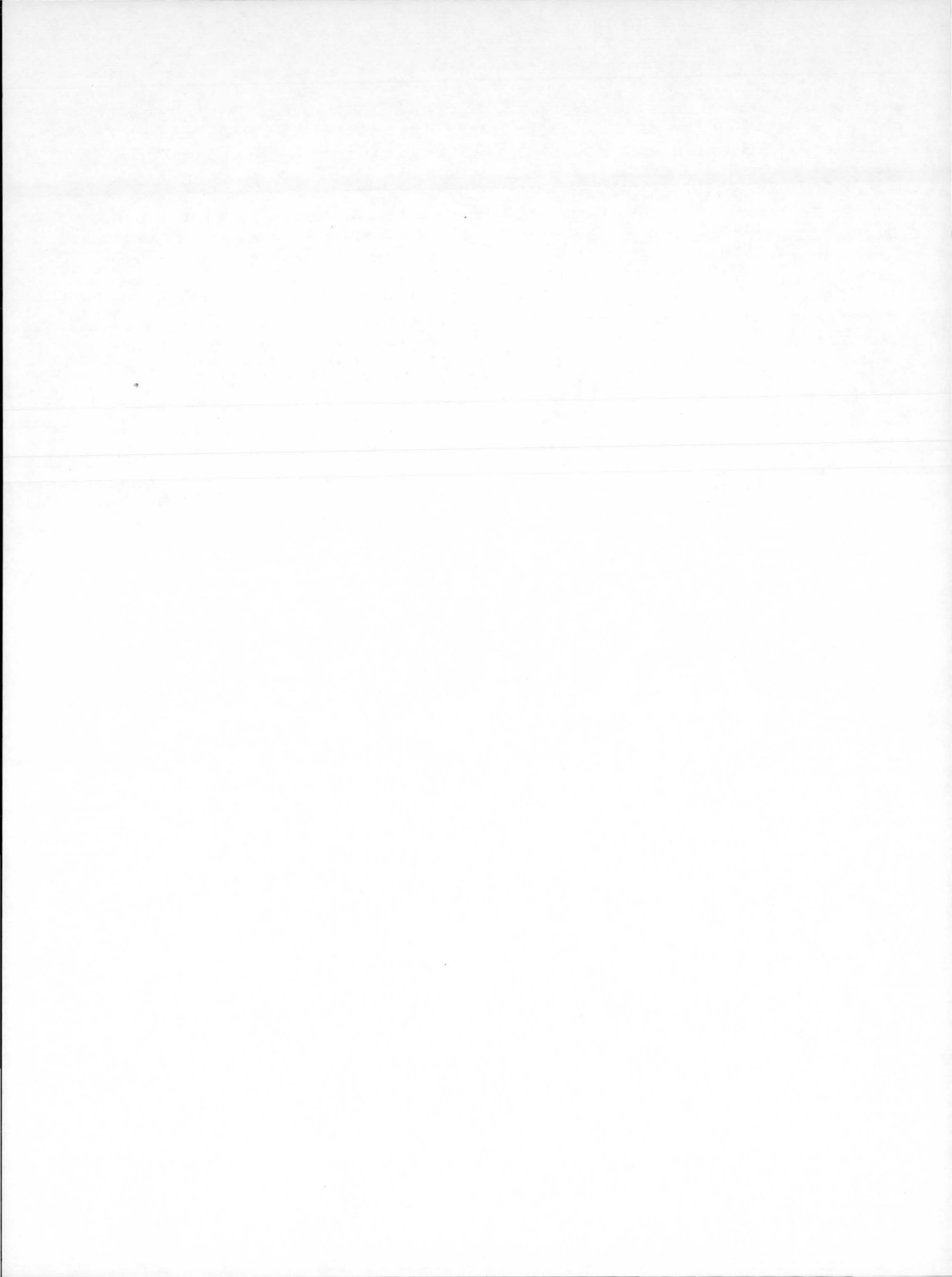
For a particular camera to be transmitted it would simply be necessary for the selector to send a command by means of any hardwire line such as telephone to the central transmission

site where the particular camera selected would be held continuously on the feeder line to the network. The feeder line could be at the point of the sports event. The operator or selector referred to above could continue observance of all the other cameras by the above means, and at any time change from one camera to another. The motion continuity problem would not be serious since the general content of the picture could be observed for each camera and only one transmission line or RF link would be needed to accomplish this.

One application of this system which has already been considered in our own area is a link between the MSFC launch facility and Houston Control Center. This system would allow a motion continuity of 30 frames per second, but would have lower resolution, if it did not use storage techniques described earlier in this paper. This will allow Houston to observe many areas essentially simultaneously where motion is either nonexistent or relatively low.

Another use entirely removed from this is for educational television. A system is now in existence which could be used over any TV station or community TV system without interfering with regular programming. This system would allow the teacher to present lecture material on a given subject and then actually provide self-test facilities in the home for the home student. At intervals during the presentation, questions would be shown on the screen which has been divided into four parts, each

offering a different possible answer to the question. The student at home could indicate his selection of an answer by activating one of four buttons on a small unit connected to a special FM receiver. This receiver could be associated with the FM section of the TV set. Activation of this button would cause the TV set to become a decoder and select only one of the four possible solutions and display it on the screen of the TV set. At the same time the audio recording corresponding to this is selected by the decoder so that if the student is correct he gets acknowledgment plus additional reasoning for his answer and additional information. If he has picked the wrong answer the picture and the voice associated tell him where his reasoning went astray. This system would derive its information from a four track tape which would be multiplexed similarly to the system already discussed along with a multiplexed audio, and fed into a conventional TV transmitter as video and audio. This multiplex signal could not be intercepted by a standard AM or FM receiver. This could be a great boon to the educational network throughout our country. The sampling rate of the information would be at $7\frac{1}{2}$ times per picture per second repeated continuously. Information could be renewed at $7\frac{1}{2}$ times per second. The multiplexed audio would be sampled at an ultrasonic frequency such that no loss in intelligibility would be lost or be detectable by the ear.



19. Commercial Applications of NASA Research in Semiconductors and Microelectronics

A. M. HOLLADAY

George C. Marshall Space Flight Center NASA

The success of the aerospace effort depends greatly upon electronics. Telemetry, guidance and control, and related earth-based electronics require increasingly reliable, fast, miniature, and economical solid-state devices for successful space missions. Reliance upon the vacuum tube without the modern transistor and microcircuits would have made recent space feats practically unachievable.

The third era of electronics has dawned. First came the vacuum tube, second the transistor, and third the microcircuit. It now appears that the microcircuit will offer as many advantages over the transistor in appropriate applications as did the transistor over the tube.

This paper will briefly present the status of microcircuits and will then give a smorgasbord of commercial applications resulting from semiconductor research with emphasis on microcircuits. Fields of application include medicine, industry, transportation, communication, entertainment, and education. Areas of carryover to commercial applications will include materials, techniques, instruments, and related areas.

Specific topics to be included are: hearing aids, integrated audioamplifiers, miniscopes (for electrocardiography), pacemakers, automobile ignition systems, miniature computers, solid-state watches, microminiature information control, solid-state inverters, ultrachemical analysis, light dimmers, and miniature radios and television.

HISTORICAL PERSPECTIVE

On Thursday morning, July 1, 1948, a news release came from the Bell Telephone Laboratories which was destined to revolutionize the future of electronics progress. It began as follows:

An amazingly simple device, capable of performing efficiently nearly all the functions of an ordinary vacuum tube, was demonstrated for the first time yesterday at Bell Telephone Laboratories where it was invented.

Known as the Transistor, the device works on an entirely new physical principle discovered by the Laboratories in the course of fundamental research into the electrical properties of solids. Although the device is still in the laboratory stage, Bell scientists and engineers expect it may have far-reaching significance in electronics and electrical communication.

The whole apparatus is housed in a tiny cylinder less than an inch long. It will serve as an amplifier or an oscillator—yet it bears almost no resemblance

to the vacuum tube now used to do these basic jobs. It has no vacuum, no glass envelope, no grid, no plate, no cathode and therefore no warm-up delay.

Two hair-thin wires touching a pinhead of a solid semi-conductive material soldered to a metal base, are the principal parts of the Transistor. These are enclosed in a simple, metal cylinder not much larger than a shoelace tip. More than a hundred of them can easily be held in the palm of the hand.

Since the device is still in the experimental stage, no data on cost are available. Its essential simplicity, however, indicates the possibility of widespread use, with resultant mass-production economies. When fully developed, the Transistor is also expected to find new applications in electronics where vacuum tubes have not proved suitable.

Tests have shown that the Transistor will amplify at least 100 times (20 decibels). Some test models have been operated as amplifiers at frequencies up to ten million cycles per second. Because of the basically simple structure of the new units, stability and long life are expected.

From the vantage point of history we can now see that this announcement was very modest in its understatement. For the writers of the history of science will undoubtedly say that electronics was one of the outstanding achievements in human progress in the twentieth century and that the transistor was a chief contributor. Today, well past the midpoint of the century, we are in the third era of electronic advancement. First the vacuum tube came near the turn of the century, a remarkable invention itself, born of the genius of Edison, de Forest, and Fleming. Just as the Space Age was dawning came the second era, the transistor, without which, we can now safely state in retrospect, the rapid advances in space explorations would have been practically impossible.

Then, when the transistor had hardly begun to come of age at about the time NASA was created in 1958, and when the Space Age was still in its infancy, a series of exciting developments in electronics came which caused this third era to burst upon us with unprecedented speed and promise. This era has been labeled "microelectronics." This new field is offering so many vast possibilities for research, development, and application, and is providing so many fresh insights into the behavior of matter and electricity, that, despite many formidable problems it is imposing upon us, it is receiving such effort and support that we can say even now in 1965, it has already passed through adolescence and is beginning to mature rapidly. The growth rate in electronics thus appears to be exponential. NASA has had, and will continue to have, a significant influence upon the speed and direction of this growth.

A typical integrated circuit is comparable in size with a single transistor. A 5-watt circuit is made by Westinghouse and is used as an audio amplifier for such uses as phonographs. The flat pack is $\frac{1}{4} \times \frac{1}{4}$ inch. This is built on a single silicon slab 0.085×0.112 inch and contains 18 transistors, 7 diodes, and 13 resistors, a total of 38 components. The efficiency of this 35 volt circuit is 55% and it can operate to 50 kc, and can be used in temperatures from -55 to 125° C. The connections of the "outside

world" are made by tiny gold wires 0.001 inch in diameter. Compare the size of this amplifier and an audio tube amplifier.

A thin film circuit is another type of miniaturization. In this case small conductors and resistors are laid down, and transistors can be added in the form of small silicon plates.

IMPACT OF ELECTRONICS ON AMERICAN LIVING

James M. Bridges, Director of Electronics R and E for DOD, recently stated: "Microelectronics will have a greater impact economically and technologically than any previous innovation in military electronics. It offers improved system performance, reliability, and life, and reduced size, weight, cost, and power consumption."

The same can be said for the commercial applications of this fast-moving field. It is difficult to discuss electronic developments and their impact on American living during the past 15 years, without appearing to be dramatic and indulging in superlatives. Popular acceptance of electronics in the fields of entertainment, support for space exploration and defense by the military and NASA, and industrial requirements, especially in the processing and computer fields, have jointly contributed to push developments in the solid state devices at an unprecedented rate. From the now commonplace portable radios to the breathtaking feats in space flights, the American public has witnessed an unending array of electronic innovations, until it now begins to appear that a veritable Pandora's box has been opened. We begin to accept as reality the imagination of science fiction, and see little doubt that Dick Tracy's wrist radio and TV are feasible, if not near. When we visit the doctor's office we expect to have an awe-inspiring array of electronic analytical tools used on us to assist the doctor in measuring such things as brain impulses, heart functioning, and respiratory activity. The hearing aid typifies the revolutionary transition from the large to the small. Thanks to the transistor and microcircuit, in a few decades it has changed from the unwieldy and inefficient horn to the device so tiny as to be almost unnoticed.

Our automobiles, symbols of the modern era, increasingly utilize the transistor in its radio, ignition systems, electronic-eye light dimmers, and other electronic controls hardly dreamed of ten short years ago. In our homes we enjoy the intercoms, the accutron wristwatches, color TV, automatic comfort controls, and a host of other electronic gadgetry on which the American housewife increasingly relies for relieving the tedium of her chores.

In business we use portable transistorized voice recorders, we fly computerized planes, talk over microwave long distance, program shipments with computers, and even automatize production lines electronically, so that the electron with which Franklin toyed so amateurishly on the kite string has now been tamed to give us all a promise of a fuller and richer life, and more leisure time. But, in all frankness, we think the best is yet to come.

OBJECTIVES OF NASA RESEARCH AND DEVELOPMENT

Before detailing results of NASA R and D which may have commercial application, it is pertinent to emphasize the chief objectives of this research effort. These objectives are the same in all three eras of electronics discussed, and differ only in emphases. They are:

1. Greater reliability,
2. Smaller size and less weight,
3. Wider application,
4. More economy.

Of these four items, reliability is of course paramount, and it may well prove to be true that NASA's greatest contribution to commercial electronics will be its influence on improved reliability. NASA's field of operation is the infinity of the oceans of space, with all its facts and mysteries. It is redundant perhaps to re-emphasize the absolute need for maximum reliability, but we must do this repeatedly in view of more, longer, and increasingly complex space flights.

It is gratifying to report that in contrast to the consistently low yields and poor quality of transistors a few years ago, some transistors are being made with such fantastically low failure rates as 0.0007% per 1000 hours. This is

equivalent to a mean time to failure of 15 000 years!

It is most encouraging to note that a properly designed and well made integrated circuit on a silicon chip approximately 60 mils square, and containing 30 equivalent components such as diodes, transistors, and resistors, now approaches the reliability of a single transistor. By 1966 we expect intrinsic integrated circuits to have a mean time before failure of a billion hours, which is approximately 100 000 years! By that time we rather expect that the package will have disintegrated, or new and better designs will make present ones obsolete. It goes without saying that vacuum tubes simply cannot be used in the present sophisticated, reliable electronics needed in space exploration.

The Saturn vehicle contains over 160 000 electronic components, including 22 000 diodes and 16 000 transistors. Each of these components must be extremely reliable if the system is to be successfully launched and flown. Remember that the total reliability is the product, not the sum, of each component reliability. Marshall Space Flight Center is now engaged in converting as many transistorized circuits over to the integrated form as possible. Probably as many as 70% of the present components can be converted to microcircuits. These circuits are even now considered so reliable that a computer being designed to provide navigation and guidance controls for the Apollo moon probe will not have redundancy, and the designers are making no provision for midflight repairs.

It needs scarcely to be said that more reliable solid state devices resulting from NASA and other research will find ready use in countless commercial applications, from complex computers to programed washers and dryers in the home.

Integrated circuits have had a dramatic influence on packing density. The cordwood assembly is not good either for reliability or size. Note that integrated circuits now can be packed to represent the equivalent of 100 000 000 components per cubic foot. The human brain has a capacity of a million times this, or 100 billion components per cubic foot.

While the enormous thrust of Saturn engines makes it generally less imperative that we here at Marshall be concerned with the ultimate in miniaturization, some NASA programs do have these requirements. In these cases appropriate NASA research is under way. This should result in double dividends—one for space effort and the other for earthbound applications. For example, for each pound of weight saved in a typical space vehicle, 300–500 pounds less fuel are required to put it into orbit. The value of saving a pound for a typical deep-space system may be as high as \$20 000. Each pound of weight saved in a modern commercial airplane is literally worth more than its weight in gold (presently \$420 per pound) because of the added cargo it can carry during the millions of miles it is expected to fly in service. For ground-based electronics, except that to be carried by persons, the savings is less, and may be as low as 5 cents per pound.

At present microcircuits are being produced in quantity in which silicon chips measuring approximately 100 mils square contain in the neighborhood of 200 components. One firm is ready to manufacture circuits on silicon chips measuring one-quarter inch square and containing 500 components. With the growth of silicon in strips one can begin to visualize whole computers being printed on one piece of silicon in somewhat the same way postage stamps are printed.

Work now under way using electron beams promises to make incredibly small circuits. Stanford Research Institute, Westinghouse, IBM, Hamilton Standard Division of United Aircraft, and others are carrying on research, supported in part by NASA, which indicates that transistors may be made as small as one (1) micron, or about 0.00004 inch. The new line will be called "IST's," incredibly small transistors. In addition, work is being done on high-density arrays of integrated circuits in which subsystems will be produced on a single slice of silicon the size of a quarter.

One recent report indicates it may be possible now to pack as many as 172 trillion transistors per cubic foot. This beats the brain capacity by at least an order of magnitude. Of practical

significance is the announcement by IBM of a data recording system with a reading and writing speed of a million bits per second, and a density of a million bits per square centimeter. Another firm is planning to make a data processor that will contain 100 billion thin film components per cubic inch and which will call up 10 billion bits of data per second. It is predicted that within ten years billion-word memories and self-organizing computers with as many as 100 trillion components per cubic foot will be developed. NASA expects to continue its interest in such developments.

The wider application of the microcircuit will lead to better performance. In broad terms this means research in producing circuits with higher speeds, increasing stability over a wider spread of temperature and radiation, and providing for lower noise, higher power, and greater efficiency. Of particular interest are the temperature problems. Heat is the biggest single enemy of component reliability. The temperature of the moon is thought to range from -300 to 250° F. By earth standards this is not too hospitable. In view of this, we can begin to understand the electronic problems facing the Apollo mission to the moon, and can imagine the problems faced by NASA and industry in developing a lunar, portable TV camera for the astronaut landing party in 1969. Similar problems are met in developing the guidance computer for the lunar excursion module, which will use 20 to 30 computers, each of which will involve over 1000 microcircuits.

Successful exploration of Mars and Venus will require electronic components for even more rigorous environments. Ways must be found to protect these circuits against temperature and radiation hazards of space, or build them so that they can tolerate these hazards.

NASA sponsored research is in progress to permit the safe operation of electronic circuits from -55° to 500° C, and to withstand neutron dosage of approximately 10^{13} nvt greater than 0.1 MV, and gamma radiation to 10^5 roentgens from a Cobalt-60 source. When these circuits are perfected, they should find wide terrestrial application in commercial electronics.

There is an impressive decrease in cost per equivalent component in an integrated circuit compared with that of discrete components. There is no reason why we cannot have greater reliability at less cost—that we cannot have our cake and eat it too?

During the current year the cost of integrated circuits will be on a par with that of discrete components, and will then outstrip them. The integrated circuit business is now geared for high production, and production yields are beginning to be more profitable. In 1964 sales of integrated and hybrid circuits totaled \$48.5 million. In 1965 this will jump to \$90 million, and in 1968 to \$210 million. Of the \$17.2 billion spent in the nation for electronics in 1964, NASA spent \$1.6 billion (9.4%) for its space program of probes and manned flights.

That the investment in microelectronics research and production techniques is paying off is obvious. In 1965, for the first time, civilian applications of microcircuits will represent a bigger market than will the military. In most cases, the reason for the switch to microcircuits from discrete components is the economy brought about by the fact that the circuitry lends itself to automation of manufacture. Some digital circuits now used in computers are half the price of discrete components. Hence, the commercial upsurge in microelectronics has been so far largely in the computer field, and every major computer manufacturer is designing the computer around microcircuits. Commercial transistors, now literally being sold by the barrel, are being packaged in plastic and sold for as little as 25 cents each. So automated have our lives become, that we now witness the strange sight of seeing transistors shipped to Japan. General Electric is selling a six-transistor radio for less than \$10.00.

By comparison, a logic block containing six to eight components may sell for \$5.00 and larger blocks (up to a size) may sell for more, but the cost per component may be quite low. Motorola predicts that transistors in an integrated circuit will be selling for less than 1 cent each before 1970.

This whole electronic picture not only appeals to NASA in its space program but indicates

strongly that commercial electronics can safely plan on more reliable, smaller, and more economical circuits in the future. Federal funds have been the chief impetus to the rapid development of microcircuits due to the early recognition by the military and space groups of their inherent advantages. It is gratifying to see these developments, and to note that they offer so much promise for commercial use.

COMMERCIAL APPLICATIONS IN ELECTRONIC DEVICES AND MICROCIRCUITS

Light Dimmer

The Marshall Space Flight Center has sponsored research on a number of devices which can have commercial use. Typical of these is a silicon-controlled rectifier, the purpose of which is to convert ac to dc. This rugged device can now be obtained with ratings as high as 200 amperes continuously, and approaching 1000 volts. Aside from use in regular circuits and power supplies, these rectifiers are being used in smaller sizes in automobile ignition systems to replace the coil-distributor approach used so long. Transistors have found some use here, but the rectifier performs better, and is reported to give better gasoline mileage, smoother engine performance, and spark plug life up to 100 000 miles.

In addition, these rectifiers are beginning to be used as a low-cost lamp dimmer in homes, schools, and industries. The rectifier phase-control circuit has made incandescent lamp dimmers compact enough to fit conventional wall receptacles, and inexpensive enough to be attractive for home use. The circuit can be arranged to provide continuous control from zero to full brilliance. It is used on regular 60-cycle line, and is recommended for loads up to 500 watts at 25° C when mounted in a wall switch box, or up to 1300 watts when adequate heat sinking is used.

Power Transistors

Because power requirements on Saturn are large, MSFC has sponsored several studies on power transistors. One of these led to the development of a reliable 30-ampere, 200-volt transistor. Another study, now underway, is designed to develop a 100-ampere, 150-volt

transistor for use as a power switch. It will have a dc amplification factor of at least 10, a turn-on time of one (1) microsecond, and a turn-off time of three (3) microseconds. When d-c power from fuel cells, solar energy, or atomic reactors become available, these transistors can be used to switch it or convert it to ac by use of inverters. At present, ac can be switched by ordinary relays.

TV Cameras

Two small TV cameras are being developed for use in the Appollo lunar mission, under the direction of the Manned Spacecraft Center. They will contain over 80% microcircuits for reliability and miniaturization. One of the cameras for capsule or earth use weighs 4.2 pounds. The other one weighs about 7 pounds, and is designed to be carried on to the moon's surface by the astronauts and operate from -300 to 250° F. in a hard vacuum. The extra weight necessary insulation. This camera operates on 6 watts of power, and measures approximately 15 inches in length.

It is of interest to note that the intensity of sunlight varies so much from the lunar night to the lunar day that the light input to the camera lens varies from 0.007 to 12 600 foot candles, which requires an optical and electronic system with very wide dynamic control. A special vidicon image sensor has been developed, based on secondary emission conduction, which, in conjunction with appropriate electronic circuits, provides the necessary controls to produce good TV pictures under these wide variations of light intensity. All of these techniques should prove useful to commercial TV, especially in areas of extreme temperatures or light often encountered in industry, or when remote pickup of TV programs makes a portable camera easier to transport to the scene of action.

Static Inverter

Space vehicles may derive their electrical power from batteries, solar cells, fuel cells, or nuclear reactors. Usually, this is in the form of direct current. Since alternating current is needed in flight, some means must be found to convert the dc to a-c. Generators are not always the best way to do this. Research on this

problem at MSFC in connection with the sizable a-c power requirements for Saturn has shown the desirability of using static inverters in place of generators, since the inverters have no moving parts, are smaller, lighter, more reliable, and easier to maintain.

The inverter developed at MSFC, and which has performed well on the last several Saturn flights, operates from the unregulated 28 V d-c battery supply on board. The a-c output is 115 Volt, three-phase, 400 cycle. The voltage is \pm Vac at any load from zero to full, and with inputs from 25 to 30 V d-c.

The inverter has of course been fully transistorized and at present a microelectronic pre-amplifier is being developed by Westinghouse for added reliability and smaller size. Its d-c supply is 28 volts, and an output of 10 amperes is required for a 1-ampere drive. Turn-on time is 6 microseconds, and storage plus fall time must be less than 20 microseconds. Operating temperature is -55 to 150° C. This inverter should find commercial use wherever it is desirable to convert dc to a-c in an efficient and reliable manner.

Miniature Communication Equipment

So much research is being done in this field which directly involves microcircuits that only scant mention can be made of some of it. For example, for MSFC a microminiaturized radar altimeter is being developed by Westinghouse, a control signal processor by Martin, and a switch selector by Fairchild. An analog-to-digital converter is being developed for the Goddard Space Flight Center by CBS, using low-power microelectronic techniques. Motorola is developing digital decoding circuits of the command receiver for Appollo, also using microcircuits. Honeywell is working on the stabilization and control systems, while Giannini Controls is developing the fuel-gaging system.

A three-phase space power supply is being studied by Westinghouse for JPL. A number of integrated circuits count down from a crystal oscillator to provide the timing for the three-phase output. NAND logic is employed, and the plan is to reduce the number of interconnects by putting all the 46 logic elements on two chips.

Of special interest is a miniature communication system being developed for the moon program. Astronauts landing on the moon cannot converse with each other since there is no atmosphere. Due to this fact, as well as the need to provide telemetry of various data, a miniature, battery-powered communications system is under development. The first model used discrete components and weighed 5 pounds. A more recent model using miniature components stacked in cordwood fashion was reduced to 1.6 pounds. The latest version, almost completely microcircuit, will weigh only 9 ounces. This model will contain two transmitters and two receivers, allowing simultaneous voice transmission and seven telemetry channels at 300 mc, and voice only at 260 mc.

This miniature system should find many commercial uses. Perhaps toys will soon incorporate many of these features; the football coach may well direct his quarterback who has a tiny receiver tucked under his helmet.

Electrical Instruments

Other developments in miniaturized instruments include a new three-digit nixie readout digital capacitance bridge with a range of 0-100 microfarads, dissipation factor of 0-20%, 0-200 d-c volts bias, and frequency range of 120 or 1000 cps.

A new five-pound, compact, battery operated, solid-state electrical thermometer measures -100° to 500° C in seven ranges, to an accuracy of 0.75° C.

Another small instrument is a pH meter measuring approximately $4 \times 7 \times 8$ inches, and weighing 4 pounds. Battery operated, and covering the normal range of 0-14 pH, it is accurate to 0.02 pH units, and can be used over a temperature range of 0- 100° C.

In general it can be said that a revolution is underway in making instruments smaller and more reliable.

Computers

No report on NASA and commercial electronics would be complete without including the vast, fast growing field of computers. Computer makers are already important users of integrated circuits. Texas Instruments is work-

ing on an ultrafast circuit with only a 2 to 3 nanosecond delay. It is reported that Signetics Corporation is putting 25% of its R and D effort into the commercial computer market. Honeywell's Electronic Data Processing Division announces that integrated circuits will be standard in virtually all new equipment to be made in 1965. IBM generally uses hybrid circuits because of their speed and power, while RCA uses monolithic silicon integrated circuits on the upper end of the line and hybrids on the lower end. Integrated circuits at present do not have the power required for use in memory and input-output circuits, but are used in the logic sections of the computers. For memory driving, discrete components or hybrid circuits are now used; for input and output circuits, which have to drive electromechanical equipment such as printout systems and tape recorders, discrete components such as transistors are used.

A typical commercial application is a new digital, in-line blending system which keeps all product components at correct ratios, regardless of a reduction in flow. This system is expected to be used to process foods, chemicals, and petroleum, and to manufacture fertilizers. Featuring a new automatic-pacing, digital controller, the system blends either liquids or solids, and is particularly useful for short runs involving relatively small quantities. The advanced system is based on pace setting, that is, allowing the lagging component to set the pace for the other streams. With the system in operation, a master demand module paces the blend, sending a pulse signal, whose frequency is proportional to the total blend rate, to the digital controllers. One controller is on each component line. If a component falls behind, due to start-up or to strainer clog, the controller takes over and slows all feeds in proportion to the lagging one. Computers are already under development to expedite the educational process, control traffic systems, make weighted decisions, and carry on many other useful activities.

COMMERCIAL APPLICATION IN MATERIALS

High Purity Materials

Many areas of scientific endeavors are requiring purer materials, and better control over im-

purities purposely introduced. Semiconductors probably represent the ultimate in this regard. To demonstrate the critical nature of impurities in semiconductors, the purest silicon obtainable has a resistivity of 230 000 ohms per cm. By introducing only one part per million of some dopant such as phosphorus, boron, or arsenic, the resistivity is reduced to less than 10 ohms per cm. Just a trace of gold in silicon greatly influences the speed with which the transistors operate. Small amounts of an element such as lithium, which has a small atomic diameter, may diffuse rapidly, even at room temperature, through a silicon crystal and cause harmful effects at the p-n junction. It may cause equally deleterious effects in the silicon dioxide layer used to passivate the silicon surface.

It is more and more necessary to think in terms of parts per billion rather than parts per million. Old tried-and-true technique such as emission spectrometry are not sufficiently sensitive to measure the purities needed. Mass spectrometry, both gaseous and spark gap for solids using electron multipliers, is being improved to meet these needs. The residual resistance ratio method of measuring purity at 4.2° K (liquid helium) is being investigated and is based on the fact that, at this cryogenic temperature, the increase in resistance of metals is approximately proportional to the purity of the metal. The resistance ratio is taken as the resistance at room temperature divided by the resistance of 4.2° K. It now begins to appear that the characteristics of semiconductors themselves may become the most sensitive measure of their purity.

In view of numerous reliability problems of semiconductors associated with impurities, MSFC is sponsoring research to determine the limits of present chemical analysis and then to determine what new technique of ultra-analysis may be developed. This will include areas such as neutron activation analysis, mass spectrometry, nuclear magnetic resonance, electron spin resonance, and the like. When this work is completed, there should be many uses in the fields of study on the effects of minute concentrations on surface conditions, as in catalysis for chemical reactions, the influence of

trace elements on rate of corrosion, on physiological reactions, the properties of superpure metals, and the effects of trace alloying on their properties.

The problem of corrosion representing annual losses in this country of billions of dollars, should be emphasized. Up to now our knowledge of crystal structures, defects, and impurities revealed in solid state physics has been almost neglected in metal applications. This field is worthy of detailed exploration.

Crystals (Epitaxy)

One of the greatest boons to crystallography has been the semiconductor business. This is a complex subject, but NASA research is helping to provide a better understanding of crystal structure and use. Crystals are nature's most perfect creation, and we rely upon them in countless ways in our daily living.

One area of crystal work now under particular study at MSFC (with Westinghouse and Texas Instruments) is the process known as epitaxy. In this process, a layer of crystals may be deposited in a controlled manner on another crystal. Pure or doped silicon may be deposited onto a silicon crystal by reducing a gas such as SiH_4 , Silane, with hydrogen in a quartz tube heated to 1100 to 1200° C. It has been found that specks of dust or other foreign particles greatly influence the number of imperfections in the grown crystal. Improved crystal growing techniques can be used to commercial advantage not only in electronics but in lasers, optics, metallurgy, and related fields. We should have a new toll in understanding better the basic structure of matter.

Surfaces

Closely related to high purity materials are several studies sponsored by MSFC on surfaces, with emphasis on silicon dioxide and silicon. This is one of the major areas of interest and support at present. The stability of this oxide is of paramount importance since it is used to (a) passivate the silicon devices, (b) serve as a masking agent during diffusion, and (c) to serve as a capacitor dielectric for certain microcircuits. Under conditions of radiation, temperature, and voltage, the oxide becomes unstable and, therefore causes the circuit to drift

in its characteristics. Few microcircuit problems today are receiving more research effort than this one. NASA and the electronics industry in general can benefit greatly by a solution to this problem.

Research on this involves several approaches:

1. Measuring capacitance to four significant figures.
2. Using ellipsometer, X-ray diffraction, electron diffraction, and related equipment to determine structure of silicon dioxide.
3. Determining the effect of trace amounts of highly dipolar molecules such as water on the properties of the silicon dioxide dielectric.
4. Finding ways to measure pinholes and other imperfections (such as hot chlorine) in the film.

Research on surfaces has revealed some interesting phenomena. One foreign atom on a clean glass surface may serve as a nucleus which can influence the deposition of 10 000 other atoms. We are beginning to understand that very thin films of a metal on an insulator behave in peculiar ways. Over a period of time, the metal may coalesce into little islands and therefore become a resistor instead of a conductor. We have learned to count the rate of deposition of atoms in a vacuum accurately. At 10^{-6} mm pressure we can normally expect a layer of atoms one atom thick to deposit each second. Those of you interested in making highly polished mirrors for instruments and the like can now be assured of a well-nigh perfectly controlled process for a variety of metals and alloys on any choice of a substrate.

The subject of surfaces is a vast one. Many of the analytical tools and techniques developed or improved in the electronic programs should prove extremely useful in several commercial fields. One is in the area of understanding and improving surface catalysis, used so much in such chemical processes as petroleum cracking and synthesis; producing fertilizer by the synthesis of ammonia from nitrogen and hydrogen; and the oxidation of ammonia to form nitric acid and nitrates. The poisoning of surface catalysts is a perennial problem.

Electroplaters should benefit by a deeper understanding of these surface conditions. Tiny pits or holes may be spots for corrosion of automobile bumpers, especially in contact with salt used on icy roads. Oxides find wide use in industry as the passivation of surfaces, such as aluminum ware. Industry too little understands why some metals, such as nickel and chromium, remain shiny while others readily corrode. The research underway in silicon and silicon dioxide should provide clues to a fuller comprehension of these surface phenomena. This includes the area of surface etching on which MSFC is doing research on both an in-house and out-of-house basis.

APPLICATIONS IN PROCESS TECHNIQUES

Fly's Eye Camera

A multiple lens camera has been developed jointly by the Electromechanical Engineering Branch and the Applied Research Branch of the Astrionics Laboratory at MSFC for making masks for producing transistors and integrated circuits. This first version of the camera contains nine two-element achromatic (color corrected) lenses in a 3×3 array. Each lens has a diameter of 4 mm and a focal length of 10.6 mm. A line-width resolution of 1 micron, about $\frac{1}{25}$ mil, has been achieved with this device.

This camera makes it possible to lay down nine identical patterns for diffusion on a silicon wafer from a single piece of art work, thus avoiding the tedious step-and-repeat operation. The main advantage of this technique over the step-and-repeat process is the simplicity of operation and the inherent overlay capability. It is possible to utilize more than nine lenses. This camera can find use in any commercial photography in which numerous identical patterns need to be photographed onto a single plate or film.

Diffusion

Another area of process study (with Research Triangle Institute) is in the form of determining optimum conditions for diffusing phosphorus into silicon in a one-step process, using phosphine as a gaseous source, rather than a two-step process used in industry. The approach has been to develop a statistical model

in which the chief variables of process control (time, temperature, and concentration of dopant, and resistivity, lifetime and dislocation of wafers) are correlated with intermediate process parameters (junction depth, sheet resistivity, oxide thickness, and base width), which in turn are correlated with device characteristics (breakdown voltage, reverse current, dc current gain, and gain-bandwidth product). If this process proves successful, it may then be possible to establish circuit and even system performance in terms of material and process controls.

The chief direct benefit of this study is in electronics. However, the approach can be used not only for diffusion, but for other critical steps such as crystal growth, epitaxy, photoresist, and interconnects. The degree to which this is done determines how far the art or black magic so prevalent in electronics fabrication today can become a science, and thus give higher yields of more reliable semiconductors. At present, over 3000 transistors can be produced from a single silicon wafer the size of a quarter, but the industry depends too much on testing and sorting to make these devices.

Statistical modeling has been used successfully in other industries. If it can be used advantageously in these intricate solid state processes, then the experience should add a new level of sophistication to process controls in industry in general.

Other techniques under NASA study which will have wide application are microwelding, electron beam technology, leak detectors, microscan-microscope techniques, microprobe analysis, and related areas.

MEDICAL APPLICATIONS

Sterilization

Important byproducts from NASA research in semiconductors may occur in indirect ways. It is generally known that probes designed to land on Mars and Venus will be sterilized to avoid contaminating these planets with earthly microbes. Research is in progress to guarantee that space vehicles do not become the unwitting agents of artificial panspermia (seeding of life on planets by means of space travel through

interplanetary space). To permit implantation of foreign life onto other planets would confuse future attempts to determine the existence of extraterrestrial life. Americans and Russians have already demonstrated that biological material such as vegetative bacteria, bacterial spores, algae, tissue cultures, and the like, are remarkably immune to the vacuum, radiation, and weightless conditions of orbiting in space.

It is necessary to conduct experiments on earth to determine the ability of micro-organisms to survive low temperature, high vacuum, ionizing radiation, and high ultraviolet fluxes, and then to find ways to destroy the microbes on the vehicle prior to launch. One of the difficult problems encountered in this work (at JPL, MSFC, and other NASA Centers) has been to sterilize the electronic circuits and components without harming them. There is little advantage in making the spacecraft sterile but inoperative due to sterilization damage. Typically sterilization is achieved by using chemicals and/or heat at 135° C (275° F) for 24 hours. This is believed to offer a probability of a complete kill of bacteria of greater than 10 000, a figure generally agreed to be satisfactory. Electronic components are screened at 145° C for three 36-hour periods on a non-operating basis.

During attempts to minimize the time-temperature stress on these components, very extensive research has been carried out on the effects of sterilizing agents on micro-organisms; efficiency of clean rooms; optimum lethal conditions such as pH, humidity, temperature, and time. This work should greatly assist medical authorities in the design and use of surgical rooms. It should give a deeper understanding of the kinetics of death of the microbes, and enable us to derive a more scientific death-rate relationship. The food industry—certainly the canning factories—should find this information very useful. It is to be noted that death of organisms during sterilization is based on probability, and that in general industry depends on moist heat as a weapon. In dealing with such lethal organisms as *clostridium botulinum* it is necessary to have a high degree of confidence that the logarithmic rate of destruction based on time is a safe approach.

Instruments

A number of medical instruments utilizing microelectronics in one form or another have been developed by NASA particularly in biophysical research in connection with the astronauts and their flight equipment. One of these is an analog circuit for calculating blood volume in liters per minute by computing the area under a curve representing blood volume as a function of time. This technique can be used on data obtained by either an indicator dilution method (densitometer) or by the radioactive surface counting method. From a typical time curve, a cardiac output can be calculated.

The analog circuit is a simple, automatic method for calculating the area under the curve, thereby eliminating laborious manual computing. It is used to make cardiac studies of astronauts under clinical conditions in a faster and simpler fashion than previously possible. The contractor who developed the device for the Manned Spacecraft Center has estimated its commercial value at \$5 000 000, based on \$5000 per unit including counter, precordial scintillation detector, and high voltage power supply, as well as associated radioisotope equipment.

Another medical device developed for the Manned Spacecraft Center is a transistorized digital pneumotachometer which is capable of determining the respiration rate on a breath-to-breath basis by measuring the time interval between breaths. It is used to monitor respiration rates of astronauts during checkout of the ground systems Apollo suit. This information has been monitored on every manned orbital flight. The device provides a numerical display of breaths per minute on a breath-to-breath basis. The electronics is based on a digital logic system. This device can be useful as a research tool, or as an educational aid when teaching physiological principles to students of medicine, health, or physical education.

Still another device, known as a digital cardiometer, has been developed for NASA which can find wide medical application. It computes an astronaut's heart rate (ventricular depolarization) and displays this information in beats per minute. This, too, is a logic circuit built around either transistors or integrated circuits.

The input to the device is the EKG waveform from either an electrocardiogram amplifier or a ground telemetry station. The circuit converts the waveform into a short negative pulse, which resets a counting circuit called the pulse multiplier. This multiplier allows four pulses to be counted for each heartbeat. The output is read on nixie tubes (tubes with lighted numbers) and is updated every 10 or 15 seconds, depending on the position of the update switch. The last reading on the bulbs stays on until a new reading is computed.

Typical of an indirect spin-off of NASA-supported research in solid state is the recent development of a new, high-power hearing aid announced by Zenith Radio Corp. This device is 30 to 40 times more powerful than conventional devices on the market. Employing six transistors and three diodes, it will help persons suffering from certain hearing losses as high as 96 decibels. Research is now underway to place most of these circuits on an integrated silicon wafer, making them smaller and even more efficient.

Another recent commercial innovation in miniaturized, transistorized medical instruments is a portable oscilloscope used to visually record electrical output of the heart. Developed by Westinghouse, and weighing only 3 pounds, the Miniscope is powered by four flashlight batteries. Prior to this instrument, heart activity was measured by an electrocardiograph machine, which records the electrical impulses on a strip of paper, or by a standard-size oscilloscope, where activity appears as a visible wave on a fluorescent screen. Oscilloscopes are generally found in hospitals and laboratories, while EKG machines are used in the doctor's office. Portable versions of these instruments up to now have weighed 50 pounds or more, are costly, and require an electrical outlet.

Use of the Miniscope is simple. The two suction cups are fastened to the palms of the hands of the patient, and in 6 to 8 seconds the heart signal is magnified on the small screen. In emergency heart cases, the Miniscope can mean the difference between life and death. In cases of drowning, electrical shock, adverse reaction

to drugs or anesthetics, and similar emergencies, the Miniscope can be used to advantage, even out of the physician's office.

The heart has three types of activity: normal beating, complete stoppage, or ventricular fibrillation, which is an uncoordinated quivering of the heart muscle. Ventricular fibrillation may be fatal without prompt attention. The Miniscope becomes an important diagnostic tool to determine if a defibrillator unit, which uses an electrical shock to restore the heart to normal rhythmic beat, should be used; thus precious time may be saved under emergency conditions. Anesthetists should find it very helpful. The Miniscope measures only 7 by 5 by 2 inches, and can operate 4½ hours on one set of the rechargeable batteries. Designed for single operation, the unit has only two control knobs, one

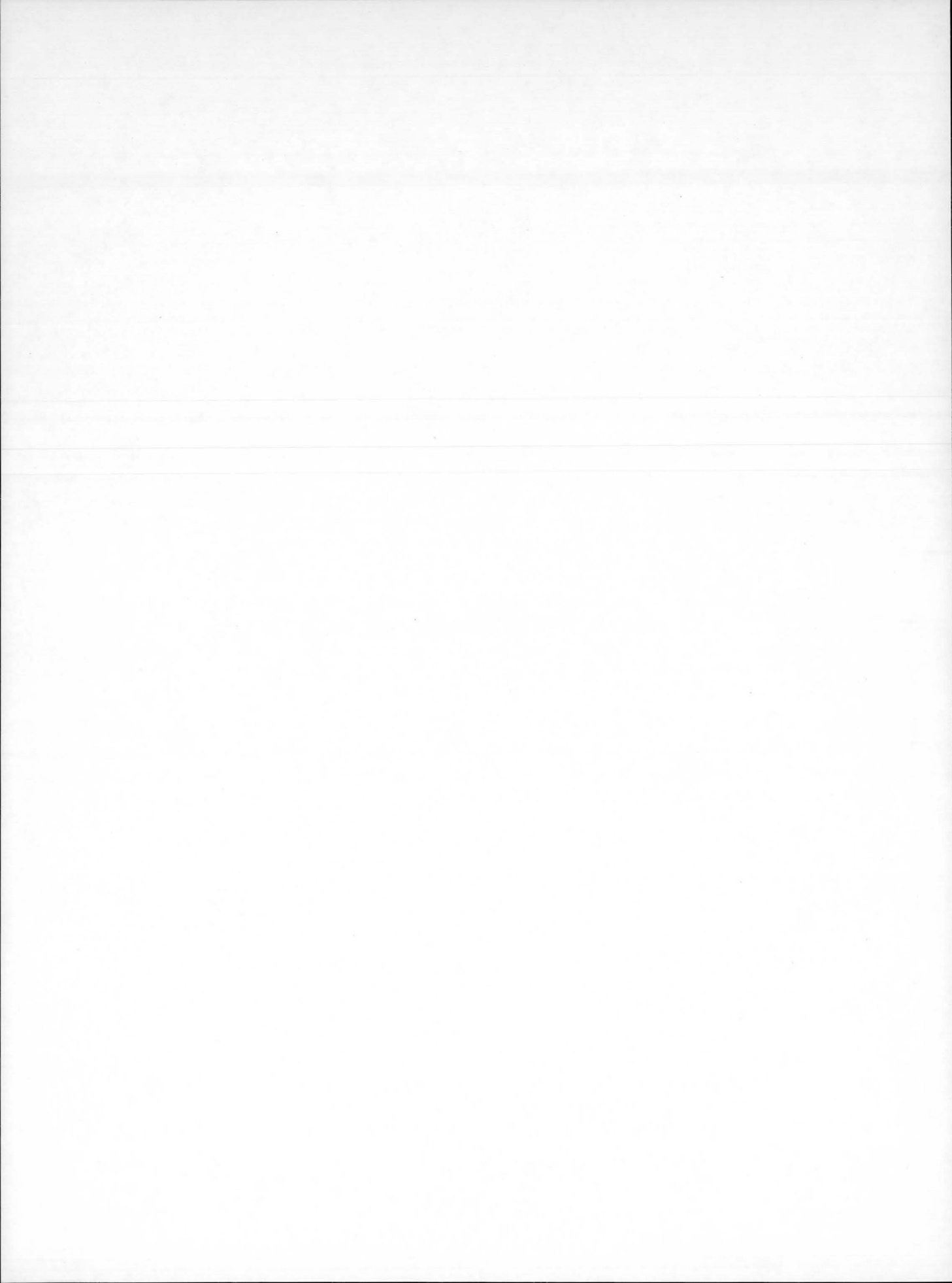
for vertical amplification and the other for centering.

Closely related to these instruments, and already commercially available, is the publicized Pacemaker, which is a tiny two-transistor electronic pulser. When embedded under the skin in a human chest, and connected to the heart, the pacemaker helps the ailing heart patient by controlling the rate of heartbeat. Already about 300 persons, who have arrhythmia due to faulty functioning of the nerve bundle in the heart which controls its contraction, are using this device.

It can be confidently expected that the medical profession will see a steady stream of more reliable, miniature electronic instruments being made available to it. NASA is happy to have been contributing to these achievements.

Additional Papers

The following papers were not a part of the presentations of this symposium, but are included in this document to further enhance the objective of information exchange.



20. The Parametric Amplification of D-C Currents

THOMAS L. GREENWOOD

George C. Marshall Space Flight Center, NASA

A new amplifying element has been developed using the fundamental principles of the parametron. It was found that the "flux pumping" effect in a second harmonic parametron circuit provided large amplification factors when the core drive was extended far into the non-linear region. The phase of the output signal may be controlled by an input signal as low as 5×10^{-15} watts. The device may find application as a memory element in logic circuits as an ultra-sensitive relay, or in a very low-noise d-c amplifier.

One of the classical problems of physics and engineering is the detection of weak d-c currents. In almost every branch of engineering and data handling, measurements are made and information transmitted at some point in terms of low-level d-c voltages and currents.

Unfortunately, the very nature of amplifying devices has made it difficult to raise the level of these signals without the use of a substantial amount of apparatus. In addition, some of the apparatus has serious practical limitations. Among the most successful detectors of low-voltage d-c are the mechanical chopper, the transistor switch, and the magnetic amplifier. The basic reason that these devices or their equivalent are needed is that in the case of direct-coupled amplifiers, zero offsets arising from temperature variation and other factors are so large that they can mask weak signals.

The simplest in concept is the chopper, which may be thought of as a high-speed relay capable of interrupting and switching d-c current. There are two basic problems with choppers. The first is that the device has an inherent noise level which, depending on the design, speed, and life may be either very high or moderately low, but is seldom below the microvolt level. The life of the chopper and the effect of the overloads on the life is such that these devices are not used unless necessary. The size and weight

are another factor, although substantial progress has been made in this regard.

The transistor switch has a much longer potential life, and is certainly more reliable than the mechanical chopper. Its principal disadvantage is that in the region of microvolts, zero offsets may become quite significant (50 microvolts typical), and the devices usually have a substantial temperature coefficient, even at moderate temperatures.

Magnetic amplifiers offer the possibility of detecting weak d-c voltages, but they tend to be relatively insensitive in terms of power input required to make the measurement, and the gain bandwidth product is strictly limited so that the performance of the device in a stable feedback amplifying system leaves much to be desired.

During 1963, Hans Klemperer, while working on NASA contract, NAS8-5439, discovered a mode of amplification in which a d-c flux resulting from the current to be detected, was amplified parametrically until it was of such large value that it resulted in volts output of the detecting device. However, the device had the property, that once having detected the d-c, it would no longer respond to a change in polarity unless the drive signal was modulated. Means of accomplishing this were devised, and a system providing control with a magneto-

motive force as weak as 10-microampere turns was demonstrated. Current as low as 30×10^{-9} amperes would therefore control the output of the sensor. This corresponded to a control power of 5×10^{-15} watts.

The name Paractor (trade name of Trans-Sonics, Inc., Burlington, Mass.) has been given to a family of devices which employ this type of parametric amplification (fig. 1). One circuit of the Paractor is shown in figure 2. The cores are miniature permalloy structures that are usually driven with high frequency current, a typical value being 50 kc. When the circuit is driven, sinusoidal oscillations of twice the drive frequency will appear at the output terminals. These oscillations can have either of two phases, 0° or 180° .

The amplitude of the output signal depends on the drive current and does not vary significantly with the d-c signal being detected. However, the phase of the output oscillation is determined by the direction of the d-c current at the time that the driver amplitude reaches a critical value called the reversal point. By modulating the drive current as will be described in later paragraphs, it is possible to cause the phase to periodically indicate the direction of d-c current in the control coil.

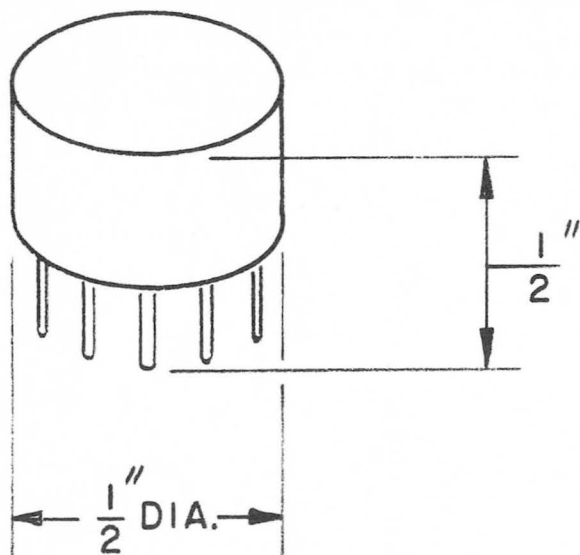


FIGURE 1.—View of the paractor.

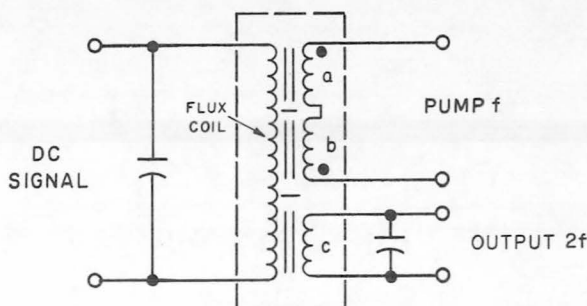


FIGURE 2.—Paractor circuit.

DESIGN AND CIRCUIT

External appearance and internal circuit of the Paractor are shown in figure 1 and figure 2. The two drive or pump cores, *a* and *b*, are wound in opposing directions. Preferably, the pump cores are magnetically matched. The third core carries the output winding which is externally tuned to double pump frequency ($2f$). The d-c signal or flux winding passes through all three cores.

The three-core assembly is shielded from external magnetic fields by a soft magnetic enclosure. The flux coil is shortcircuited for ac by an external bypass capacitor, effecting the superposition of pump and output frequencies ($f+2f$) which is responsible for the remarkable d-c sensitivity and other characteristic features of the Paractor.

Cores *a* and *b* are driven, for example, from a modulated 50-kc source. A sinusoidal voltage of frequency $2f$ (100 kc) is observed at the output terminals. The amplitude of this voltage depends largely on the drive current. The phase of the output signal $2f$ is found to have one of two values $+\frac{\pi}{2}$ and $-\frac{\pi}{2}$. The phase of the oscillation is determined by the direction of the d-c signal current at the time when the drive current is near its maximum.

FLUX PUMPING

The sensitivity of the Paractor to weak d-c signals is caused by internal d-c flux amplification or flux pumping which may be described as follows:

As the Paractor is energized, a small error voltage appears across the two opposing pump

coils which is transferred by means of the flux coil to the tuned output circuit. The responding $2f$ oscillation of the output circuit is coupled by the flux coil into the pump cores. The pump cores are therefore magnetized by the superimposed $f+2f$ frequencies. The f and $2f$ currents are substantially sine wave, and the resulting mmf in the individual pump cores has no d-c component. In each pump core, however, though the areas under the $f+2f$ current half-waves are alike, they differ in shape. This peculiarity occurs when even harmonics are added to the fundamental frequency. Therefore, though $\int_0^{2\pi f} H dt=0$, the curvature of the

magnetizing curve causes $\int_0^{2\pi f} B dt=\Delta F$; the positive flux is unlike the negative flux. The difference ΔF is the flux component. The d-c flux rises with the pump current, causing an increase of the second harmonic which is fed back into the output which aids the d-c flux signal. This, in turn, increases the second harmonic in the output circuit. Depending on pump power, this flux pumping goes on until core saturation sets the limit.

The phenomenon of d-c flux pumping is responsible for the difference in performance between the Paractor and the magnetic amplifier. Firstly, due to the internal d-c amplification caused by flux pumping, the sensitivity of the Paractor is 100 to 1000 times greater than that of the magnetic amplifier. The Paractor responds to signals down to 10-microampere turns. Secondly, while the magnetic amplifier responds to the d-c signal with a more or less proportional change in amplitude, the response of the Paractor is digital. The $2f$ -output frequency appears at the $+\frac{\pi}{2}$ or $-\frac{\pi}{2}$ phase corresponding to + or - d-c signals respectively. Changes in amplitude are incidental and not usable for measurement. The phase alone counts; it is transmitted to the Paractor control circuitry where it directs an integrator to generate high level feedback signals which are

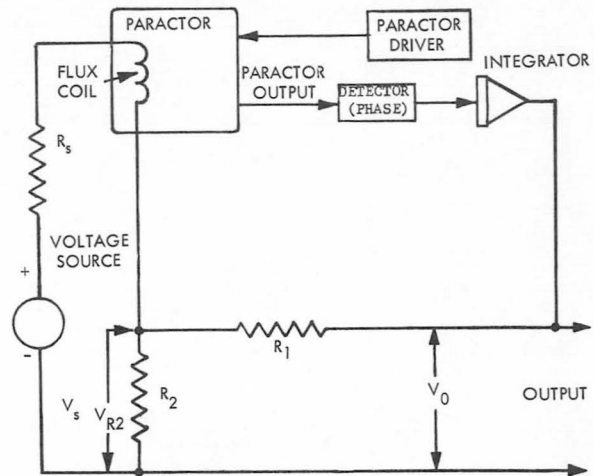


FIGURE 3.—d-c voltage amplifier.

accurately proportional to the unknown signal and used for the measurement of the d-c input signal (fig. 3).

PERFORMANCE

The performance of the Paractor is described with reference to figure 4 which shows in Curve 1, the $2f$ -output voltage in mV per turn vs pump ampere turns. The output-voltage curve indicates the effectiveness of flux pumping. The output voltage rises with pump current and reaches a typical maximum of 1 volt. Beyond that maximum, the fourth harmonic appears in the output, and the output amplitude decreases rapidly as flux pumping is limited by saturation of the cores (see fig. 5, oscillogram I for output wave shapes and corresponding pump currents).

Curve 2 of figure 4 shows, as a function of pump current, the mA turns of a d-c signal necessary to reverse the output phase. Curve 2 is typical; it shows the dependence of output stability on pump current; the amplitudes shown vary considerably with the magnetic status of the pump cores. Phase stability is very high when the pump is weak. Without a d-c signal, the Paractor always starts oscillating at the phase of its last operation. With increasing pump ampere turns, output stability decreases. At a particular point which is close to saturation of the pump cores, flux pumping ceases completely and the output phase can be

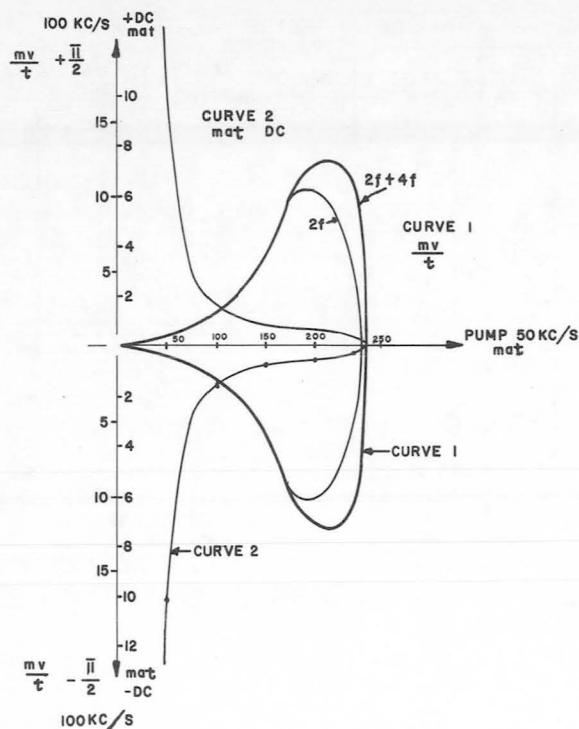


FIGURE 4.—Paractor output (1) and stability curves (2).

set by a minute d-c signal. This is called the Phase Reversal Point.

At this point, the phase of the Paractor is set by a minute d-c current (see fig. 6, oscillogram II for wave shapes below, at, and beyond

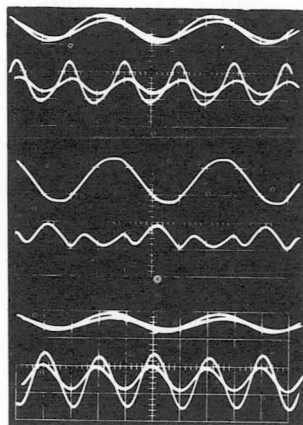
Reversal Point). As the pump power is reduced below the reversal point, flux pumping starts rapidly and the established phase is retained until changed during the next sweep through the reversal point. In the absence of a d-c signal, the phase, after sweeping through the reversal point, is random. In order to combine d-c sensitivity and phase stability, the Paractor is normally driven with an amplitude-modulated pump current.

The modulated pump sweeps back and forth, between phase reversal and a convenient reading amplitude. In some cases, it may be more practical to use a fixed pump amplitude with a superimposed modulated low frequency (400 cps). (See Oscillogram III, fig. 7.) The Paractor can also be operated with a constant pump current, preferably at points nearer the reversal point where relatively small d-c signals suffice to reverse the phase. This mode of operation does not exhibit the high sensitivity and gain obtainable with the modulated pump.

CIRCUIT APPLICATION OF THE PARACTOR

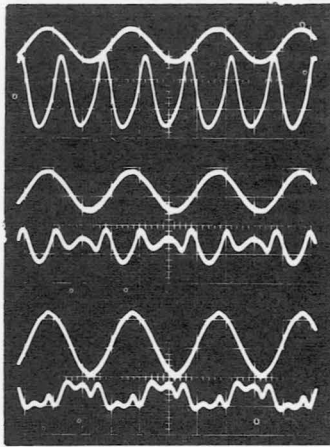
As a result of the Paractor's ability to detect small currents with a good zero stability, it is ideally suited for potentiometric measurement of low-level d-c voltage. In this typical application, the Paractor flux-coil terminals are connected between the voltage source to be measured and an electrically controlled voltage

Upper Traces: Output Voltage 100 kc/s
Lower Traces: Pump Current, 50 kc/s



Pump (f)	Signal (DC) Phase set by -DC	Output (2f)
a. 62.5 & 125 mA	+50 μ At	0.05V/cm
b. 250 mA Phase Reversal	+50 μ At	0.05V/cm
c. 125 & 200 mA	+50 μ At	0.2V/cm Phase re-versed

FIGURE 5.—Oscillogram I, phase reversal.



Upper Traces: Output Voltage 100 kc/s
 Lower Traces: Pump Current, 50 kc/s

Pump (f)	Signal (DC) Phase set by -DC	Output (2)
a. 375 mA Saturated	50 μ At	0.05V/cm
b. 250 mA Phase Reversal	50 μ At	0.05V/cm
c. 200 mA Min. Output	50 μ At	0.01V/cm

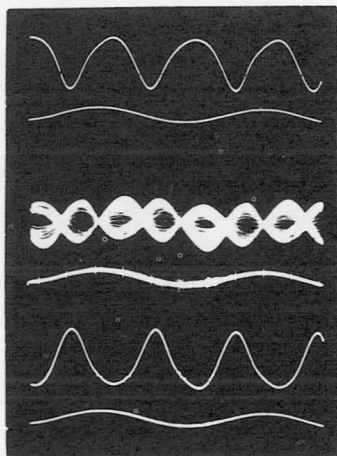
FIGURE 6.—Oscillogram II, a-c saturation.

that will track the source voltage. An accurate voltage divider determines the amount of voltage amplification (fig. 3).

The Paractor output is phase-detected, and the resulting d-c programs an integrator circuit of the Miller type. The phase detector is arranged so that if VR2 is smaller than Vs, the phase detector output will cause the integrator to increase its output, hence VR2.

Once balance is established between Vs and VR2, a negligible current flows through the flux coil. The gain of such an amplifier circuit is

determined by the ratio $\frac{R2+R1}{R2}$. The "negligible" loading of the voltage source at balance also guarantees the accuracy of the gain as set by the resistive divider since the potentiometric voltage VR2 is also "negligibly" loaded. As an example, an output voltage of 5 volts for a source voltage of 10 millivolts and an accuracy of 0.05 percent calls for an input resolution of 5 microvolts or better. The maximum current flowing through the flux coil is $\frac{5}{R3 + RL + R2}$



Upper Traces: Output Voltage, 100 kc/s
 Lower Traces: Pump Current

Pump (f)	Signal (DC) Phased by -DC	Output (2f)
a. 200 mA	+50 μ At	0.1V/cm
b. 200 mA at 65 kc/s +100 mA at 400 c/s	+50 μ At	0.1V/cm
c. 200 mA	+50 μ At	0.1V/cm Phase re-versed

FIGURE 7.—Oscillogram III, phase reversing with superimposed modulated 400-cps frequency.

microamperes at balance. (RL is the resistance of the flux coil.) This current must be sufficient to yield a Paractor output capable of programming the integrator after phase detection. The crudest integrator circuit will require a relatively small input even at full output.

As a result, the difference between the feedback voltage and the signal is made negligibly small, and the circuit gain is dependent only on the quality of the feedback resistance divider. It will be seen that this circuit operates in a manner similar to a self-balancing potentiometer. The integrator runs until the error voltage as fed back equals the input signal. This method has the inherent advantage that the electronic circuit need not be linear or have precise gain.

The speed of response from zero to full scale is determined by the integrator-circuit time constant and the phase-detector output voltage. The modulation frequency determines the speed of response of the Paractor, and therefore the ultimate frequency response of the system.

CONCLUSION

A new approach to the problem of detecting dc currents has been reviewed. Parametric pumping of a d-c flux that controls the output is the reason for the high gain and sensitivity. The device described may be thought of as having three general classes of application:

1. As an ultra-sensitive relay.

An existing commercial application has been in the detection of the binary output of a transducer having parallel d-c outputs. The device is used aboard the TFX-F111 airplane where it detects the presence or absence of d-c voltages from an oil tank gage.

2. As a d-c amplifier.

In this application, the Paractor may be used in a circuit similar to that described earlier in this paper, and appears to offer a level of performance which may be considerably higher than previously available. It has been noted

that the Paractor will operate at very low temperatures and has therefore made available an intercomparison device which has virtually no zero shift as a function of temperature. This, along with its high gain, should make the device of great use in cryogenic applications.

3. As a memory element.

A property of the device which has not been explored commercially, but which may have important implications, is the use of the Paractor as a memory element. Referring to figure 4, if the drive amplitude is less than the amplitude at the reversal point, the phase of oscillation of the Paractor remains constant and is determined by the direction of the dc flowing in the flux coil when the Paractor was last operated at the reversal point.

The device possesses the unique property that it is able to remember the phase of the a-c voltage (with respect to a similar device) even after the power has been turned off, and the phase may be recovered at any time; for example, several days after a power interruption. It is the first device, so far as I know, which has an a-c output and is capable of remembering an inserted state following power interruption.

The Paractor used as a memory unit has another property which may be of importance in the future; its output is a continuous stream of oscillations, and it has a definite and continuous output indicating whether a one or a zero has been stored. Most magnetic memories have the property of being one shot, and of having a limited amount of total energy available to indicate the quantity stored. The energy available from the Paractor is dependent only on the length of time that the Paractor is observed, and the longer the observation period, the larger the total energy. This may open up the possibility of using the Paractor as memory elements aboard satellites where they could be interrogated after a long period of time, and the output read-out over a substantial period, as might be required by certain communication systems.

21. Flat Conductor Wiring Systems for Federal and Commercial Applications

WILHELM ANGELE

George C. Marshall Space Flight Center, NASA

This article gives general information on cable types, materials, design standardization, manufacturing, installation, performance, advantages, and present limitations. Savings in weight and cost are mentioned, and a tentative estimate is suggested for the business volume in the near future.

HISTORY

The first printed-and-etched flat cable was designed and manufactured in 1957 to replace a 40-inch long, 40-wire, gimbal-transfer cable for a 3-axis gyroscope platform. The previously used round-wire cable was stiff and heavy and required a servoloop to compensate for the cable torque, while the new flat cable was a tape of only 10-mil thickness and therefore very flexible. Though the new flat cable demonstrated excellent properties and filled all the requirements, it was not used. Still it was the first representative of an entirely new cabling technology. Meanwhile, the flat-conductor cable has found numerous applications in instrumentation and packaging. New industries have developed which are specializing in etched, flat-conductor, flexible circuitry and cabling.

Soon after the first printed cable was made, it was thought that flat cable should be produced in great length by using the laminating rather than the etching principle (fig. 1). While conducting patent research, an attorney made a surprising discovery. The flat-conductor cable was not new at all. Mr. C. T. Jackson of New York was granted a patent in 1884 for his invention to laminate parallel flat copper conductors between two strips of high-voltage paper. The Jackson cable was intended for house wiring; yet it was never accepted for that purpose. After considerable

efforts during recent years, the etched printed cable as well as the laminated flat-conductor cable is making its entry into the electrical market. Several industrial organizations are producing flat cables, and more are preparing themselves for this field.

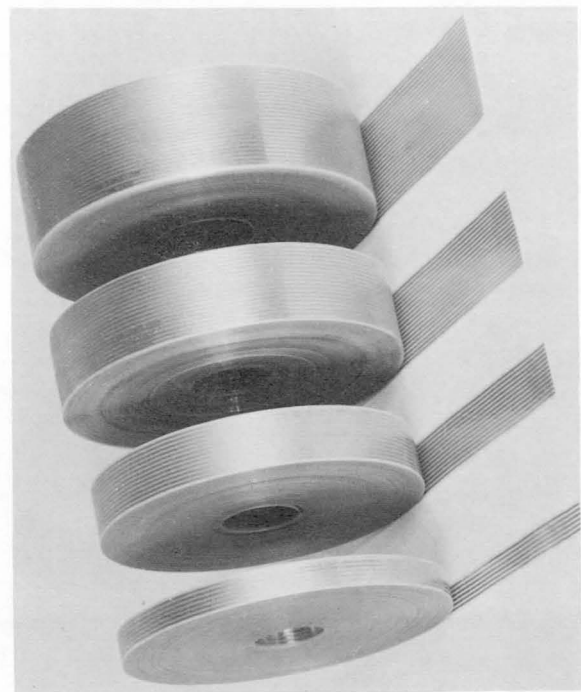


FIGURE 1.—*Flat-conductor cables of various widths.*

FLAT CONDUCTOR CABLE TYPES AND MANUFACTURING

Printed Cables

As mentioned before, the flexible printed cable is basically a printed circuit on a thin plastic carrier. It is manufactured similar to printed circuits by printing and etching. If large quantities of a pattern are needed, for example, wiring for the Prince Telephone or the Polaroid Camera, then a copper-clad plastic tape is printed and etched in a continuous process. If needed, a cover layer for circuit protection can be added.

This printed and etched cable system is very adaptable to the various needs of diagram configurations, conductor widths, and termination designs. It is somewhat limited in conductor thickness. Heavy conductors pose an etching problem when small center spacing is required. Also, etching time is directly proportional to copper thickness, and flexibility is much reduced with increased thickness. Fortunately, these extremes are exemptions. The bulk of the wiring needs for electronics and communication equipment can well be fulfilled by etched

wiring. When long runs of parallel conductors are needed, the lamination manufacturing method is mostly used.

Laminated Cables

Flat conductors parallel and precisely spaced are sandwiched between plastic films of suitable electrical and mechanical properties. Special machines were developed to handle the various parameters important in laminating of plastics and adhesives. Such variables are: temperature, pressure, and speed. Other important factors are: adjustable conductor guides for precise center spacing, consideration of shrinkage of cable width during quenching, preheating of tapes and wires, sensitive tension-control devices for tapes and conductors, proper guidance for the tapes and the cable throughout the machine. The production speed is a thermodynamic problem. Newer flat-cable laminating machines produce cables 12 inches wide. The wide cable can be slitted to the desired width of individual cables (fig. 2).

The manufacture of shielded cables is still more or less in the development status. At the

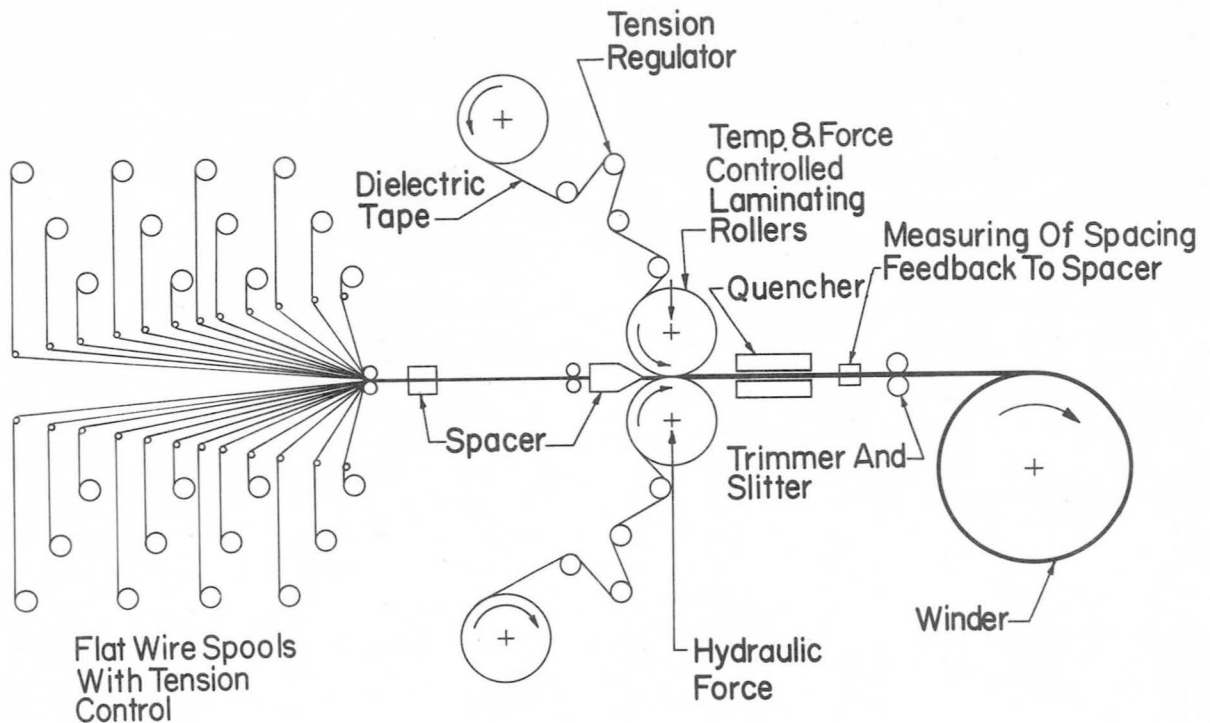


FIGURE 2.—Cable-laminating machine schematic.

present time, it seems to be more practical to add the shielding foil to the cable in a second pass through the laminating machine when needed. The adhesive used for laminating must have enough bonding strength to prevent delamination and minimize wrinkling when the cable is flexed or folded.

Other Cable Designs

Besides the two cable designs and manufacturing methods mentioned above are combinations of etching and lamination procedures used. Conformal coating of the etched surface is an accepted way of making flexible flat cables. Still another system is the extruded cable. The latest type is the high-density, flat-conductor cable. Preinsulated flat conductors are cemented together edgewise and sandwiched between strong plastic films. This cable type permits the smallest spacing between conductors because of the seamless insulation (fig. 3).

MATERIALS

The electrical conductors of the cable will in most cases be high-conductivity copper. Copper alloys to improve the tensile strength of the cable are not necessary because the strength of all conductors combined with a strong dielectric film makes the cable strong enough for all practical purposes. The dielectric materials must meet the electrical requirements of high-dielectric strength and low-dielectric loss. In some cases the cable must withstand high tem-

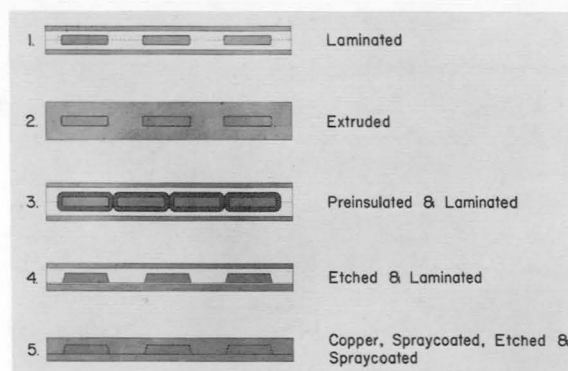


FIGURE 3.—Various ways of manufacturing flat cables.

peratures. Table I is a chart of plastic materials mostly used for making flat conductor cables.

The advantage of Mylar and H-film over polyvinyl chloride and Teflon lies in their tensile strength and dielectric strength. Teflon has a low dielectric constant. Therefore, a combination of Teflon FEP as internal bond and insulator and H-film for mechanical strength is the best combination. In addition, Teflon can stand temperatures up to 200° C. For applications not requiring over 85° C operating temperature and no special mechanical strength, Polyvinyl chloride is the most economical choice. Next higher in quality and price is Kel F, Teflon, and Mylar. The best overall material and the highest in price is the combination of FEP Teflon plus H-film.

TABLE I.—Properties of Some Flat-Cable Plastics

Properties	Unit	Mylar	Teflon-FEP fiberglass	"H" film	PVC
Dielectric strength.....	V/Mil.....	6000	1000.....	6000.....	800.
Dielectric constant.....	10 ³ Hz.....	3.2	2.5 to 5.0*.....	3.2 to 3.5.....	3 to 4.
Tensile strength.....	kg/cm ²	1270	400 to 1000*.....	1200.....	200.
Maximum service temperature.	°C.....	125	250.....	500+.....	85.
Gamma radiation endurance.	REP.....	10 ⁸	10 ⁵	5x10 ⁹	10 ⁷

*Depending on amount of fiberglass.

FLAT CABLE PERFORMANCE DATA

Mechanical Qualities

As described in the previous chapter, Mylar, Teflon, and H-film have outstanding possibilities and are very useful for flat cables. The application and installation of flat cables require mechanical flexibility, foldability without showing cracks, high-fatigue strength at high-vibration levels, and the cable must fill the electrical requirements over a wide temperature range. Mylar cables have proven acceptable in a range from -60°C to $+100^{\circ}\text{C}$. H-film cable bonded with FEP Teflon can successfully be used from -60°C to $+200^{\circ}\text{C}$. Strong efforts are under way to replace the FEP adhesive by a new material which can stand higher temperatures to make use of the full temperature range of H-film. Figure 4 shows how the flat cable can be folded to change routing direction and to fulfill the placing requirements of installation conditions. Figure 5 illustrates a flex test setup as required in MSFC-SPEC-220.

H-film and Mylar having a very high modulus of elasticity, as compared to PVC and Teflon, cannot be used for round-wire cable without paying the penalty for stiffness. Abrasion tests (pull tests over a $\frac{1}{8}$ -inch-diameter steel pin) show the superiority of flat cable over a round-wire cable by a factor of 3 to 10. This is easily understandable by looking at the contact pressures of round and flat conductors when pulled over an edge.

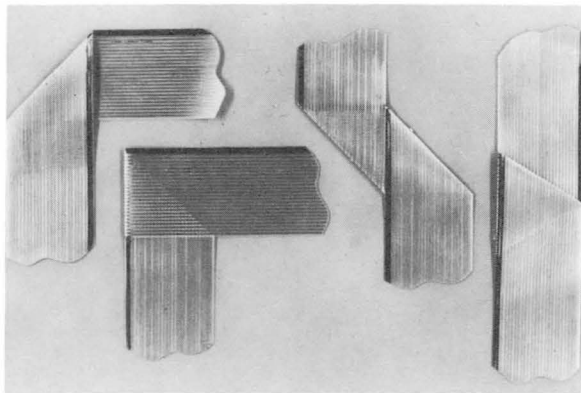


FIGURE 4.—Flat-cable folding techniques.

SYMPOSIUM ON TECHNOLOGY STATUS AND TRENDS

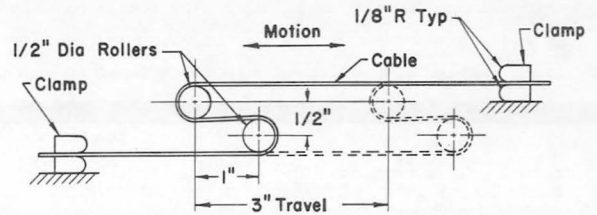


FIGURE 5.—Flex test. Stainless steel rollers, 32 finish on o.d. supported by low-friction pivot bearings (free moving at 75°C).

The installation of flat conductor cables to the surface of a liquid oxygen tank by adhesives also reveals remarkable properties. The adhesive-bond strength of the flat cable to the tank wall and the shear strength of the adhesive is high enough to stretch and upset the flat cable by the same amount that the tank grows and shrinks as temperatures change when the tank is being filled or emptied. Figure 6 shows a 10-foot flat cable installed on a lox tank in a rocket motor test area.

Electrical Data

From the very large number of tests and data available, only a few of the more important and typical ones are presented. The electrical-load capability of flat cables as a function of temperature is shown in figure 7. The flat-conductor cable can handle more current at the same temperature than round-wire cables when the same amount of copper cross sections are used;

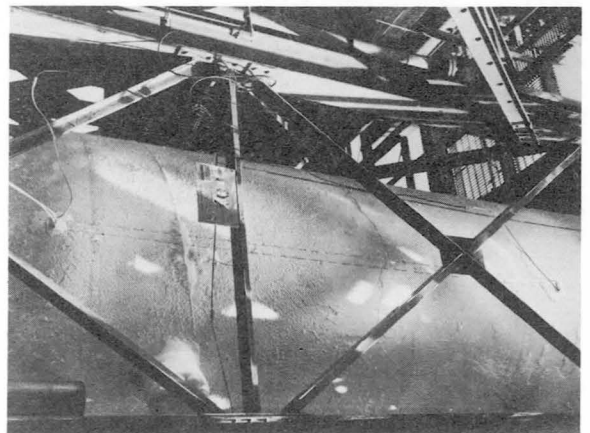


FIGURE 6.—Adhesive test on a liquid oxygen tank.

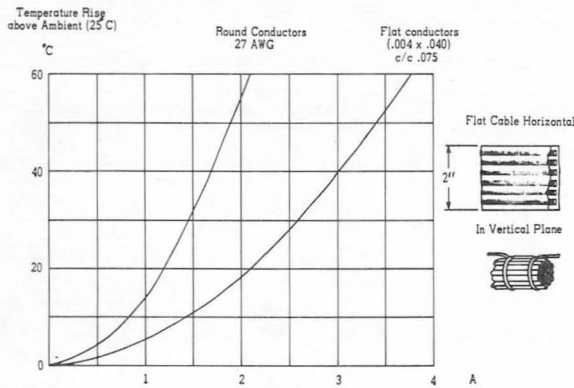
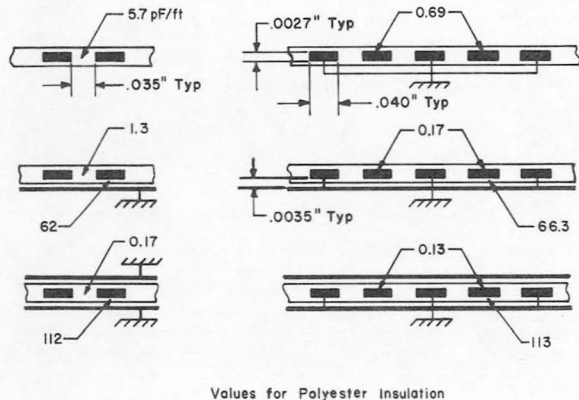


FIGURE 7.—Cable temperature rise versus current. Laced round wire cables (PVC) and flat conductor cables (Mylar) 25 conductors 1 m long, in series, horizontal position.

the copper cross section in communication and signal cables is usually of no electrical significance. Often the size of the copper cross section is controlled by the mechanical handling requirements. The flat cable offers good advantages here because of the structure. Flat cables for high power are feasible and practical in isolated cases where heavy round-wire cables pose an installation problem. For instance, on the surface of a spacecraft or large rocket, wide, thin copper strips can be mounted by using adhesive and eliminating fasteners, thus saving weight and labor. The contact mounting of cable also has considerable heat-sink benefits, which in turn reduces the temperature and resistance growth, and consequently the R-I losses.



Values for Polyester Insulation

FIGURE 8.—Typical flat-cable capacity figures.

Cable Impedance

Figure 8 shows some dielectric capacity figures in pF/ft on various conductor configurations. The electrical capacity between adjacent conductors is very small (5.7 pF/ft) because they face each other with a small surface area. The conductor-to-ground capacity (6.2 pF/ft) is relatively high if the dielectric material is thin. In cases where high capacity is detrimental to the circuit functioning, the conductors should be separated, or extremely small copper cross sections should be used.

Figure 9 shows 8 cases of pickup voltage caused by disturbing signals in neighboring lines. The influence of separation and shielding is clearly demonstrated.

Figures 10, 11, and 12 are demonstrating the voltage pickup as a function of frequency shielding and positioning.

CABLE TERMINATIONS

By the nature of their geometry flat-conductor cables of any kind call for a type of termination and connector much different from the connector used for conventional, round-wire cables. The pin and socket design is no longer the best approach, because it is much more expensive than the design which uses the flat conductor itself as contact surface. The commercial use of flat cables demands simpler and less expensive terminations, and the improved reliability inherent in a simpler design is also very desirable. Weight saving is another welcome advantage.

The termination of tailormade etched cables is mostly handled by soldering eyelets on the conductor ends to a set of pins. Other etched-cable terminations are also feasible. The nearly direct approach of using the conductor as contact element is applicable to both etched and laminated type cables. The following paragraphs describe the NASA-Marshall termination and connector design.

Cable Plug

Figure 13 shows a typical section of a flat cable plug which is molded to a cable end. Before molding can take place the cable end must be stripped of its insulation. Figure 14 shows the three steps of termination: (1) the cable is

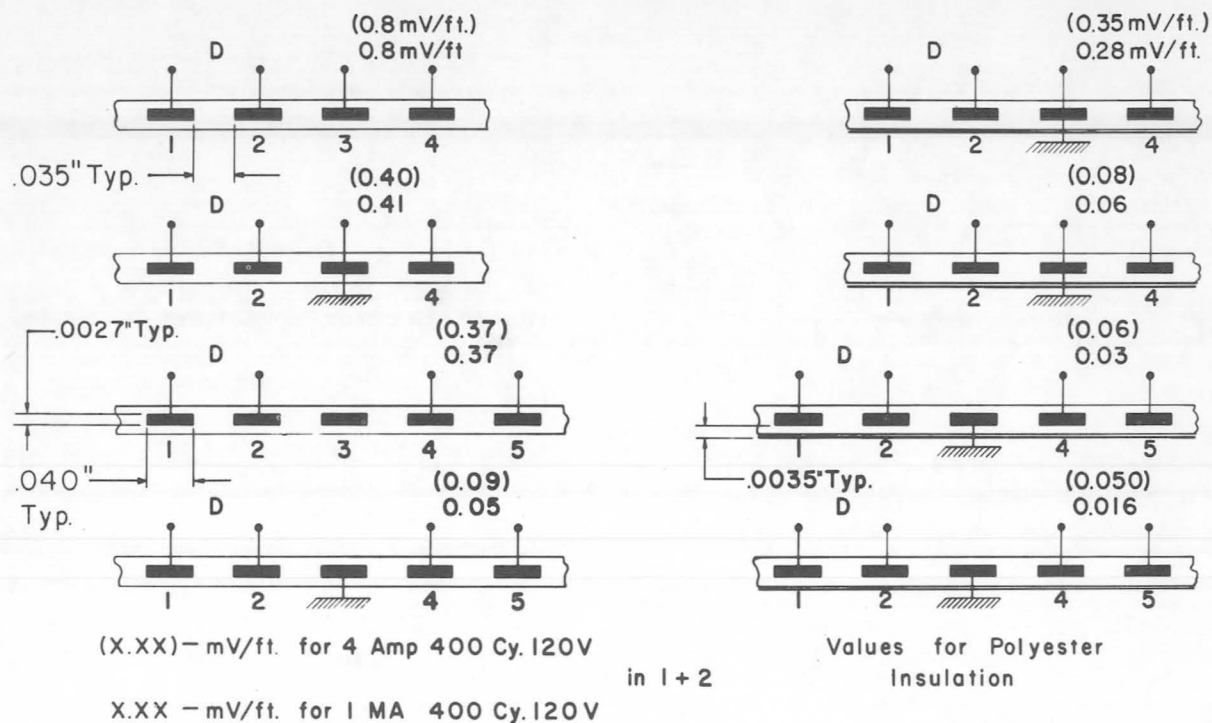


FIGURE 9.—Typical single-cable crosstalk figures at 400 Hz.

stripped, (2) a spacer is inserted to place all conductors properly, and (3) the plug is molded. Figure 15 shows a schematic of a stripping tool designed for FEP Teflon-bonded H-film cables. The cable end is inserted into a simple hand tool and clamped in place by flipping a lever. A knife-edge is then used to pull the insulation off. The entire stripping operation of a cable up to 3 inches wide takes but a few seconds. Figure 16 shows this stripper in operation.

For cables built of thermoplastic materials, a stripper with a heated blade can be used. The cable end to be stripped is placed between a rubber roller and the heated blade. After insertion of the cable end, the blade is pressed against cable and roller and then pulled slowly out while the blade takes the insulation off one side of the cable. A second pass with the cable reversed removes the plastic from the other side. A paper strip removes the molten insulation from the cable and blade. This procedure takes about 30 seconds.

Another stripper, which is still in development, uses a fast-rotating felt wheel. This abrasive stripper seems to work well with thermoplastic materials.

The next step in cable end preparation is the insertion of the contact spacer. Two small, premolded parts with precisely spaced recesses serve for the proper placing of the stripped conductors. The spacer is held by forming the conductors. The last phase is molding. Injection, transfer, or compression molding, depending on the material selected, can be used. In most cases a protective coating of the conductors will be needed; 100-microinch nickel can be used as a sealcoat against copper corrosion, and 50-microinch hardgold electroplating have produced excellent contact quality and wear resistance. Adding the proper rubber seals completes the cable plug. For cable applications without moisture protection and with infrequent insertion requirements more inexpensive designs may be used. Flat-cable manufacturers, users, and firms of the connector indus-

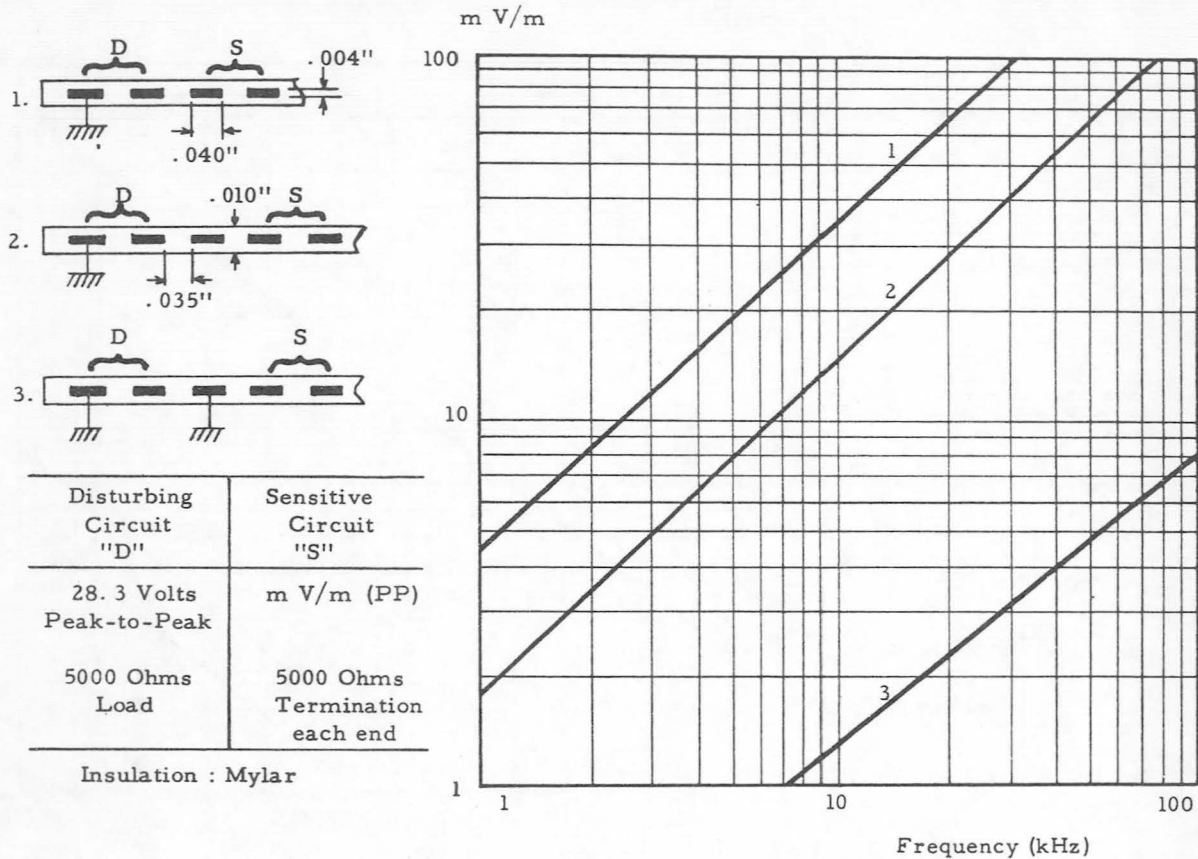


FIGURE 10.—Crosstalk voltage versus frequency, no shield.

try have proposed and designed a variety of flat-cable terminations.

Receptacle

In many cases a standard printed circuit card receptacle will suffice. When protection against moisture, vibration, or a gas seal is requested, a more sophisticated design is needed. The NASA-Marshall connector receptacle fills all these requirements. A sufficient number have been manufactured and tested, and accepted and qualified for spacecraft launch vehicle use. Figure 17 shows five sizes for flat conductor cables of 1- to 3-inch widths in half inch increments. Figure 18 illustrates a typical section with some design details. The contact spring is formed of beryllium-copper wire of a rectangular profile with one rounded side. One side is for making contact with the cable plug. The roundness is important for wearlife and defined

contact data, such as contact area at a given force, contact resistance, and the like. The contact spring hardened after forming, also nickel and hardgold plated, is mounted with pre-tension. Figure 18 shows 130g-preload and 200-g contact force after 0.84 mm deflection when the plug is inserted. This indicates a high contact force at a low spring rate (soft spring) allowing reasonable manufacturing tolerances for the molded connector parts. Methods for applying the contact-spring system to various types with 5 sizes each have been developed: a connector housing for mounting to the inside and one for the outside of an instrument box, connectors with solder pins on one side for soldering the eyelets of etched flat cables, and the third type, a cable coupling. All types have protection against moisture and air leakage. They are vibration and shockproof and can

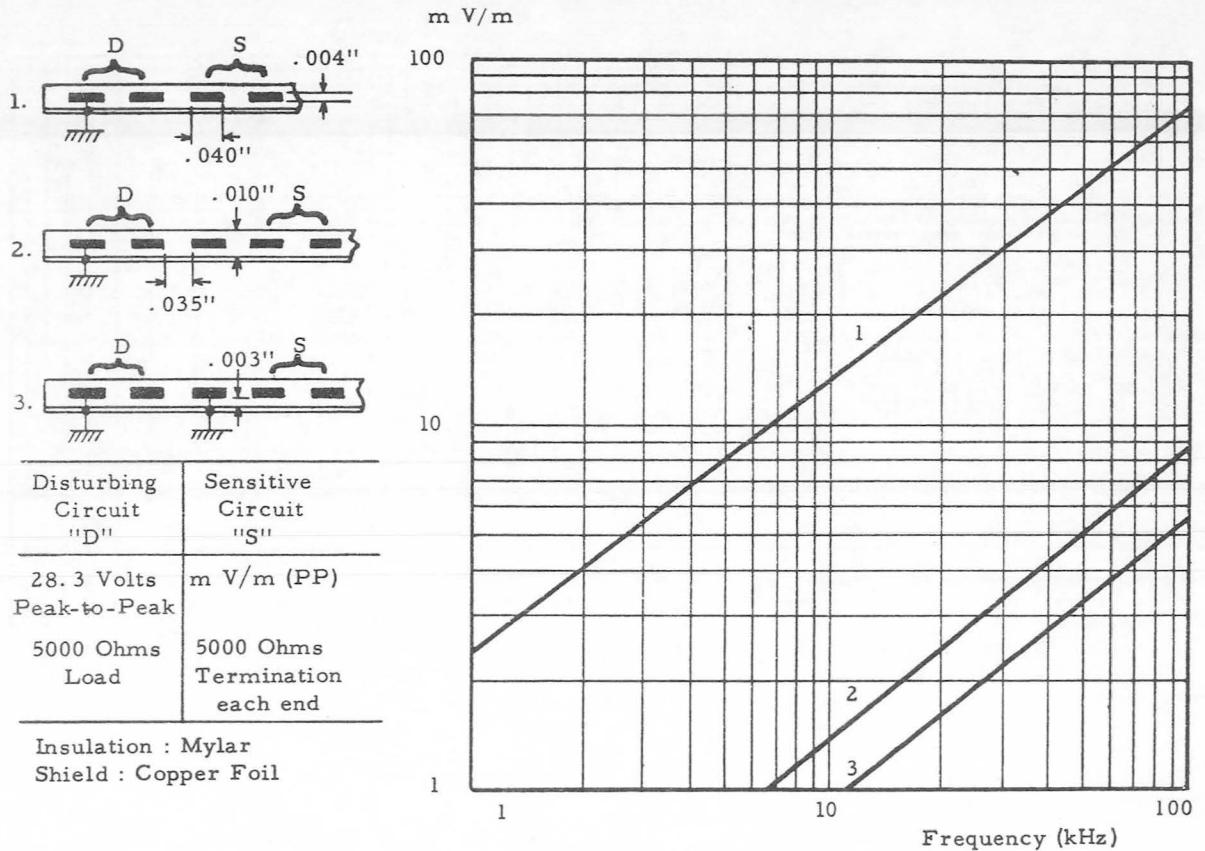


FIGURE 11.—Crosstalk voltage versus frequency, one shield.

stand some abuse in handling. The plugs are keyed to the receptacles and retained in place by snap springs; safety wiring can be applied.

STANDARDIZATION

The introduction of an entirely new cable concept offers the best opportunity for standardization. Even American Wire Gages are clumsy in comparison with the millimeter or square mm dimensions which signify diameter or cross-sectional area of conductors, and are used in all metric countries (all countries except the United States, Canada, England, and Australia). The writer proposed the metric system for expressing flat-cable dimensions, but United States industry was not ready to accept it.

Standardization Details and Goals

The copper dimensions of flat-conductor cables are given in mils (0.001 inch). The

cross-sectional area is given in square mils; for example, a 4×40 conductor has 160 square mils. The conductor center spacing has been fixed to 50, 75, 100, and 150 mils. The number of conductors per cable depends on the cable widths, which are accepted by all major manufacturers to be increments of $\frac{1}{2}$ inch. NASA, IPC, and AIA have established cable dimensions up to 3-inch width. This is reflected in NAS 729 and NASA-MSFC-SPEC-220.

The benefit of cable standardization and limitation of the number of cable sizes (6 so far, including $\frac{1}{2}$ in.) will become prominent when looking at the connector inventory. Hundreds of round wire connectors of various types and styles and sizes will be replaced by not more than 6 types with 6 sizes each including the shielded types. A very optimistic goal is a standardization of connectors so that the plugs

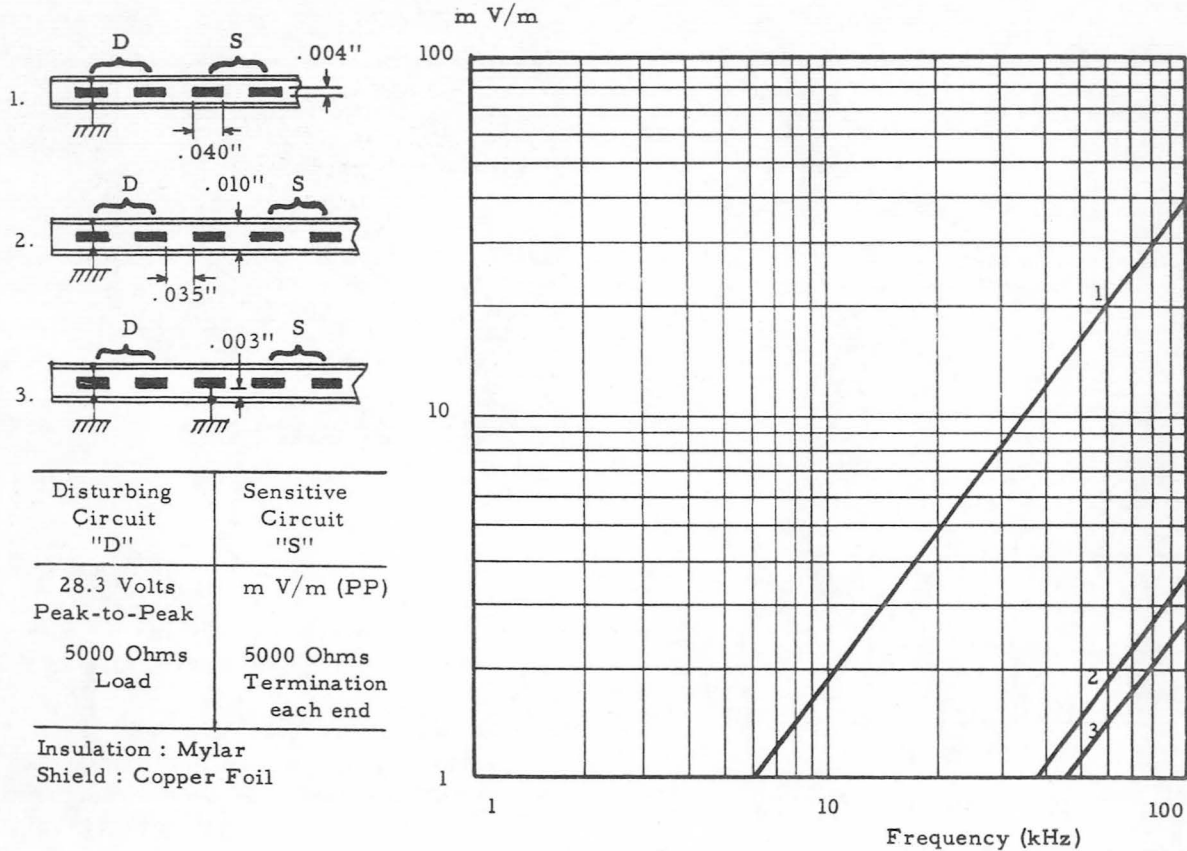


FIGURE 12.—Crosstalk voltage versus frequency, two shields.

of one company will fit receptacles manufactured by another company.

FLAT CABLE HARNESS DESIGN

The wiring of military rockets and of huge NASA spacecraft involves very large and com-

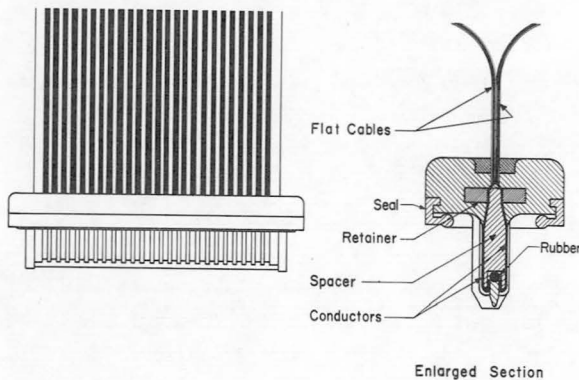


FIGURE 13.—Plug for two cables, section.

plicated cabling systems. Yet these cumbersome, heavy, and expensive long-lead-time items are generally not planned for or designed. It is left to the shop personnel to adopt the cables to existing missile systems. The flat-cable system demands an entirely new manufacturing approach to make full use of its inherent benefits. The word "cable harness" of former days no longer fits, because the flat-cable system mainly consists of individual single cables not interconnected nor branched into many arms. This simplification brings short manufacturing time, and in turn, short lead time. The cost for this is coordination of all interconnection requirements. The equipment designers must coordinate the pin functions of the boxes to be interconnected, since the flat cable cannot be used as switch gear for wiring diagrams and changes, which has occurred so frequently in the past during cable harness manufacturing

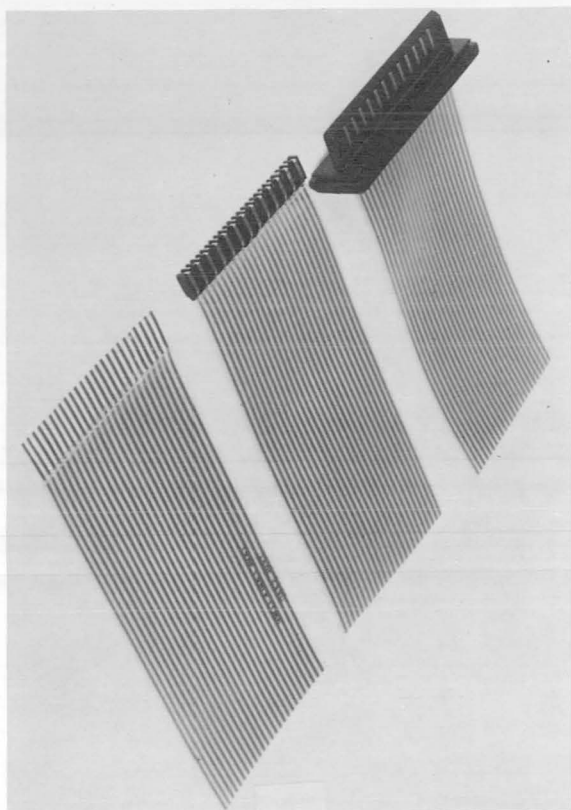


FIGURE 14.—Cable termination in three steps.

phases. The short lead time allows more time for changes before cable manufacturing starts.

The principle of straight cable runs (cables without branches) may necessitate more connectors than in the past when round wire harnesses were used.

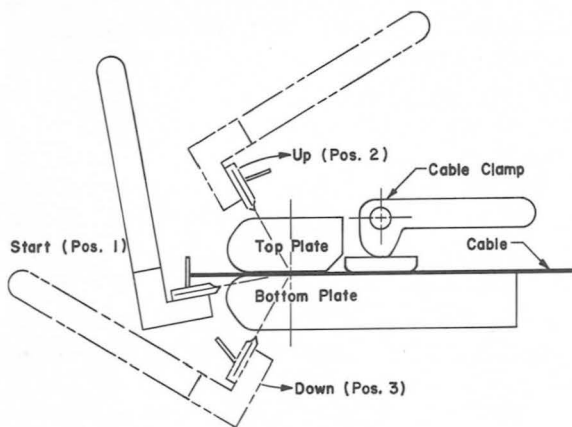


FIGURE 15.—H-film stripper, schematic.

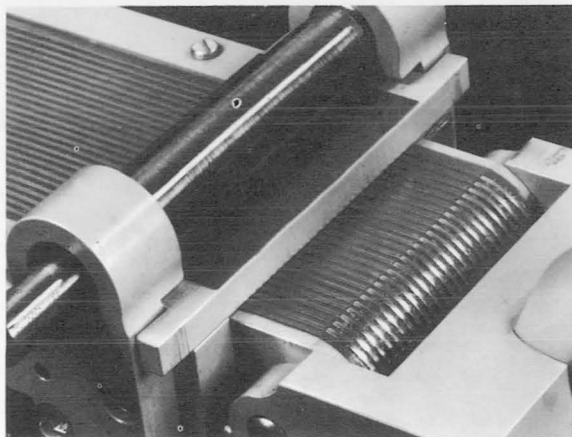


FIGURE 16.—H-film stripper, photograph.

The straight runs also offer advantages when changes are needed or when a cable has to be repaired. Such repairs can be made by cutting off the plugs of the damaged cable, leaving the cable in place when inaccessible, or taking it out and replacing it with a new one.

In certain applications branching is unavoidable; for instance where a group of strain gages, temperature, or vibration measurements must be carried to a signal conditioner and telemeter. This necessitates a Christmas-tree-like cable with end organs at the branch ends and a single connector at the trunk end. In other words, the cables have to be slit, folded, and routed to the proper points of measurement. Cables with sufficient space between conductors to facilitate slitting should be used.

DATA FOR FIVE RECEPTACLES

CABLE WIDTH INCHES	NUMBER OF CONTACTS	MOUNTING AREA SQ. INCHES	WEIGHT OF PLUG AND RECEPTACLE GRAMS
3	76	2.87	57
2.5	64	2.51	50
2	50	1.85	39
1.5	36	1.51	32
1	24	1.23	25

FIGURE 17.—Connectors, data for 5 sizes.

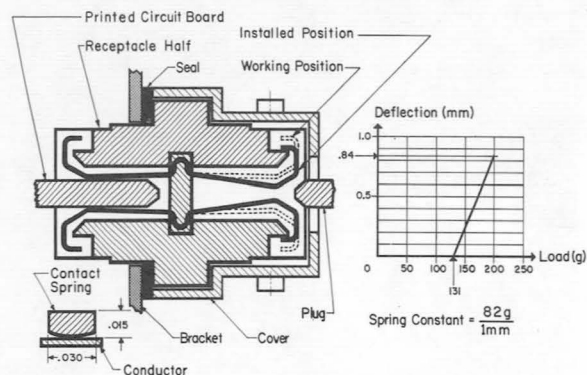


FIGURE 18.—Receptacle section and spring diagram.

The designer should always use the minimum copper conductor size controlled by the permissible voltage drop and the nearest standard size. It is recommended to use uniform conductor sizes and spacing in one cable to conform to standard connector designs. When one conductor cannot handle the current load, two or more conductors should be used in parallel. In extreme cases, a power cable with 0.150 mil center spacing or solid copper tapes should be used. The flat cables have a marking along one edge or margin for polarization purposes. Plugs and receptacles have keys to avoid wrong insertion.

FIELDS OF APPLICATION FOR FLAT-CONDUCTOR CABLES

This question is difficult to discuss because the potential use of flat cables is almost universal. It might be easier to point out the few areas where the flat cable offers little or no advantages. Insulated heavy power conductors are an example. Voltage drop is of primary interest, and permanent terminations rather than plug-in connectors are used. Since weight savings are of little interest here, flat cable will offer no advantage. However, power lines installed at the outer surfaces of space boosters can well be flat cables. Wide insulated copper strips cemented to the skin, eliminating mounting and protection hardware, will save weight and manufacturing time. Flat cable mounting with adhesives even on lox tanks has proven technically feasible. Another field where flat cables have no place is the transmission of high frequencies by waveguide plumbing.

The bulk of flat cable will be used for measuring, signal, and control cables, especially where reliability, light weight, and low overall cost are essential.

It may be of interest that General Motors is using flat cables in passenger car wiring, and other automobile producers are believed to be seriously considering the flat cable. Plans are being developed by major airplane companies to apply flat conductor wiring. The computer industry has been using flat conductor flexible cables in high-density packaging for some time.

FLAT CONDUCTOR CABLE INSTALLATION

The installation technique for flat cables is relatively simple. The exact routing should be determined after the equipment to be connected is installed. A dummy cable is made from a strong paper tape cut to the final cable width and coated with pressure-sensitive adhesive; the dummy cable is used to develop the needed folds and proper length. The exact location can be marked by paint spraying. Dummy cable and final cable should be identified by numbering. Figure 4 shows typical folds to change direction and/or polarity. Unshielded cable can stand sharp creases; shielded cables may be folded over a 1/8-inch diameter pin as a form tool to avoid damage to the outer-shield foil. Slitting and branching should be used only when no other practical way exists. Figure 19 illustrates a cable-slitting tool. The table guiding the

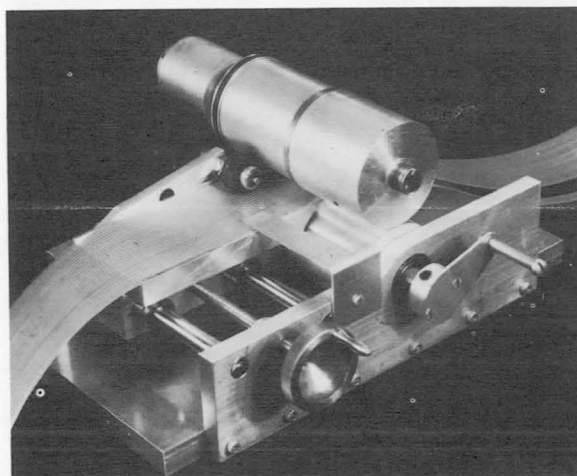


FIGURE 19.—Slitting tool for cable branching.

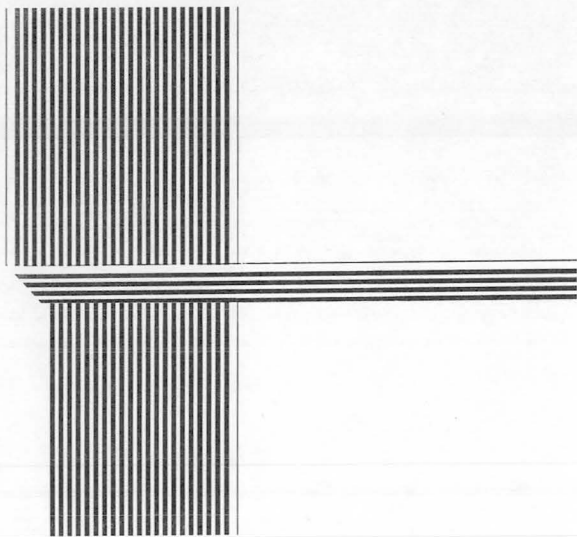


FIGURE 20.—Flat-cable typical branch out.

cable to the rotating cutter is adjustable sideways to permit cutting at any desired location. When slitting is needed, it is advisable to use cables with sufficient space between the conductors (0.035 inch, or better 0.050 inch) to provide enough insulation. Figure 20 gives information how to branch out after slitting. The fold should be made over the cable and the branch safely taped to prevent further slitting or tearing at the end of the cut. Figure 21 is a demonstration of typical strain-gage cable. Eight strain gages are connected to a single connector. The final installation of the cables can be accomplished with pressure-sensitive adhesives rather than using clamps, nuts, and bolts.

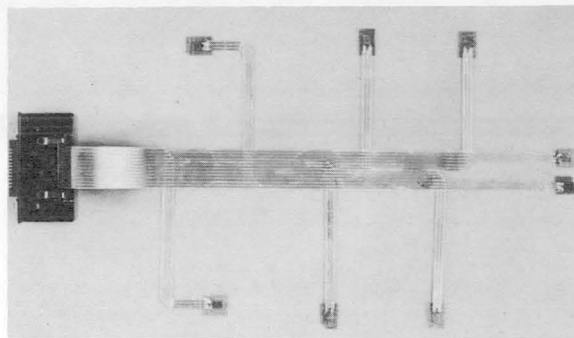


FIGURE 21.—Flat cables for strain gage application.

Table II gives some information on 3 adhesive materials successfully used in cable mounting. The bond strength was tested by pulling 90° to the substrate at a speed of 30 cm/min. Good results have been obtained by the use of a nitrophenolic resin for mounting H-film cable to aluminum.

One cable with EC 1099 and another cable with Fasson tape were cemented to an aluminum sheet $\frac{1}{16}$ inch by 6 inches by 48 inches and exposed to a weathering test at the south side of the laboratory building starting in August 1963. The outer H-film cable layer delaminated after ten months, but the FEP-bonded conductors stayed together. The H-film and the core of the cable cemented to the aluminum substrate are still in place.

Another test was performed with a Mylar cable using the same adhesives and substrate. The bond is still in good shape after over 1 year

TABLE II.—Adhesives for Flat Cable Installation

Designation	EC1099	Silastic 140	5277
Mfg source.....	3M.....	Dow Corning.....	Fasson.
Type.....	Nitrophenolic.....	Silicon.....	Polyester.
Condition.....	Liquid.....	Paste.....	Film.
Application.....	Brush.....	Trowel.....	Hand.
Mat. bonded.....	Mylar, H-film.....	Mylar.....	Mylar, H-film.
Temp. range, °C.....	-160 to +120.....	-160 to +100.....	-25 to +100.
Cure temp.....	Room temp.....	Room temp.....	Room temp.
Cure time, hr.....	24.....	24.....	24.
Bond strength, lb/in.....	15.....	12.....	10.

of exposure to the weather. The temperature ranged from minus 10° C to plus 50° C, and the humidity cycled from dry weather to rain.

Other bonding tests were made at cryogenic temperatures by cementing flat cables to a painted liquid oxygen tank (fig. 6). The cables were Mylar and H-film, each 10 feet long, and EC 1099 was used to bond the cable to the tank. This test was continued over several months. The lox tank was filled every Monday and emptied during the week, as rocket engines under test used the lox. Temperatures of the tank skin ranged from minus 160° C to plus 30° C. Neither icing nor changes in cable length due to expansion and contraction broke the bond. These tests indicate the practicality of adhesive bonding. Testing is presently being continued to improve handling technique and increase initial tack of the bonding agent. Samples of flat-cable installation are shown in figures 22.

ADVANTAGES AND LIMITATIONS

The printed cable, as it was called in the beginning, was designed for use in a gyroscope

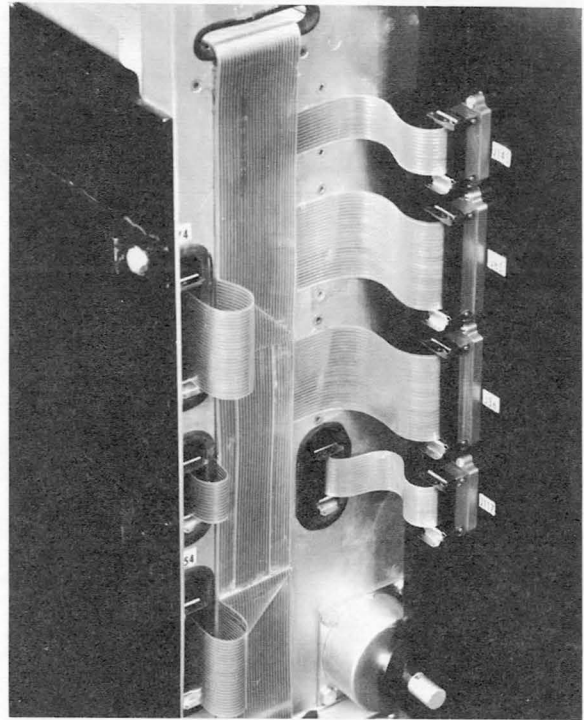


FIGURE 22.—Continued.

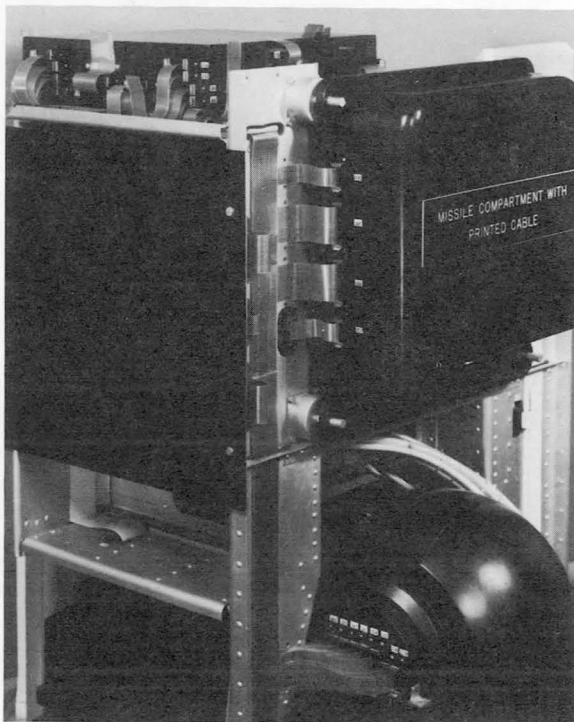


FIGURE 22.—Typical flat-cable installation.

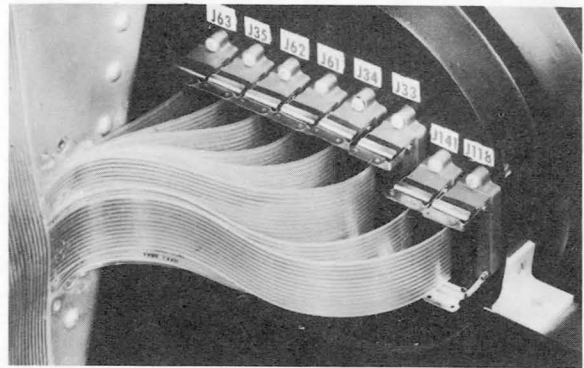


FIGURE 22.—Continued.

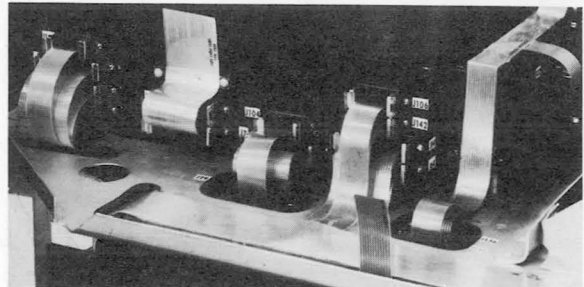


FIGURE 22.—Concluded.

TABLE III.—*Weight-Saving Comparison Data, Unshielded Insulated Wire*

Flat conductor wire (Mylar insulation)			Stranded round wire (PVC insulation)			Weight savings
Size, mils	Area, 10^{-6} in. ²	Weight, g/m	Size, AWG #	Area, 10^{-6} in. ²	Weight, g/m	Weight, %
2×25	50	0.51	32	50	0.82	38
3×40	120	1.04	28	126	1.53	32
5×65	325	2.38	24	320	3.10	23
4×115	460	3.25	22	510	4.38	26

and started in an effort to save weight and gain mechanical flexibility. By further development, application studies, and tests it was learned that the reliability was very high. As an unexpected byproduct, a very substantial time saving in manufacturing and installation was noted.

Table III shows some area and weight-saving figures. In most hand-laced cable harnesses AWG 22 was the smallest wire gage, yet electrically, a much thinner wire would have been sufficient. Comparing a round AWG 24 wire with a flat wire AWG 28 would reduce the weight from 3.10 g/m to 1.04 g/m, which is a reduction by a factor of 3 or a saving of 66%. The MSFC flat-cable connector demonstrates similar percentages. Table IV compares a 50-pin flat connector with a 61-pin standard round connector and shows a weight saving per pin of 75%. Weight saving of well over 50% makes

TABLE IV.—*Weight-Saving Data on Connectors*

	Standard conn. round wire	NASA "M2" flat wire	Weight saving
	26 pins	25 pins	
Total weight, g---	74	39	-----
Weight per pin, g-	2.84	1.56	45%
	61 pins	50 pins	-----
Total weight, g---	195	40	-----
Weight per pin, g-	3.2	0.8	75%

the flat cable very attractive. Yet the biggest savings appear to be the cost savings. Table V explains in some detail the cost of a 5-foot long cable including connectors. While material costs reduction from \$33 to \$22 in favor of the flat cable is moderate, the labor costs are reduced drastically. The key is the almost complete machine termination of flat cables as compared to the hand operation of round-wire termination. The present limitations of flat-conductor cables are mainly due to lack of experience by the potential.

ECONOMIC IMPACT

According to information from the Institute of Printed Circuits, in the United States the sales of printed circuit boards (etched and

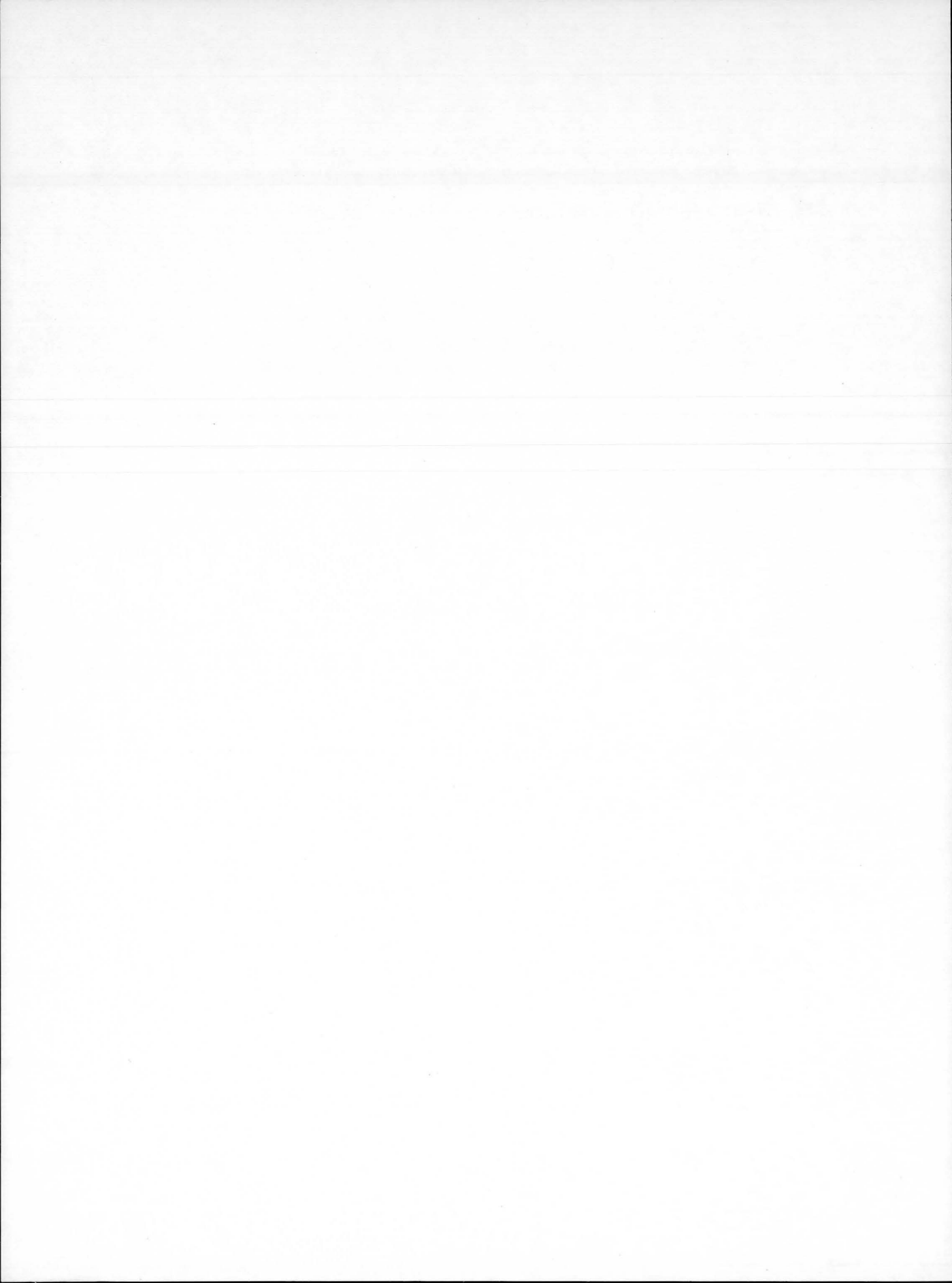
TABLE V.—*Cost Saving Data on Cable Harness*

[Cables, 25 conductors, 5 foot length, including plugs and sockets]

	Round wire cable (soldered & potted)		Flat cond. cable (injection molded)	
	Material	Labor	Material	Labor
2 Sockets----	16.00	36.00	16.00	
2 Plugs-----	16.00	36.00	1.00	1.00
5 ft cable----	1.00	12.00	5.00	1.00
Total---	33.00	84.00	22.00	2.00
TOTAL	117.00		24.00	
Saving--	-----		80%	

drilled only without components) was at least \$85 million in 1964. The estimate of sales in flat cables for 1965 is \$10 million. The use potential is \$100 million per year at present. These figures do not include sales volume of connectors. It can be expected that the sales figures

of round-cable connectors will shrink as the figures for flat-cable connectors grow, and that with the drastic reduction of labor cost for flat cable termination, the cost of a completed flat-conductor cable harness will be half as much as the cost of a round-wire harness.



22. Nondestructive Testing—The Road to Quality

J. E. KINGSBURY AND W. N. CLOTFELTER

George C. Marshall Space Flight Center, NASA

The demand for perfection in the manned space program has been responsible for major studies in the techniques of non-destructively evaluating materials and structures. Verification of the integrity of the complex systems and subsystems without damaging the components under investigation is a major requirement for space age hardware. The paper recounts the development of ultrasonic, eddy-current, and infrared techniques as applied to space programs, giving advantages and limitations of these systems. Particular attention is placed on the sensitivity of the techniques discussed. Examples of non-destructive techniques applied in both simple and complex materials and components are shown to demonstrate the versatility of the tools. Because of the widespread use of radiography and the general familiarity with radiographic techniques, only a limited discussion of these is included in the paper.

Man's never-ending search for quality has received its most significant stimulus from the National Aeronautics and Space Administration's program to explore our lunar satellite; in this program, the life of man is at stake. When the monstrous Saturn V launch vehicle lifts itself and its precious manned cargo ponderously from the earth, probably the greatest single scientific achievement in all human history will occur. Certainly, those responsible for the Apollo program are not necessarily more intelligent than people who build washing machines, TV sets, or numerous other consumer items. What, then, makes this Saturn vehicle different—so different, in fact, that we are confident that the mission will be a success? There are several things, but high on any list of items that might be suggested is the quality of the vehicle. Recognize, if you will, that in this lunar explorer weight is of utmost importance; therefore, design safety factors cannot be large enough to account for design and manufacturing inefficiencies. To assure maximum reliability from minimum weight in the structural, propulsion, and guidance systems, some method had to be conceived which would give assurance

that those items which fly, not similar ones, would function efficiently and precisely. The concept of testing to working conditions has certain major limitations (all of which have not been surmounted, thus requiring this concept to still be used selectively) which cause serious concern as to its appropriateness. For example, let us assume that we test a transistor to specified conditions 1000 times. This in no way assures that on the 1001 test it will not fail. As a matter of fact, unless we know the life expectancy of the unit under test (something we can only learn on that unit by testing it to failure), we may well have increased the probability of failure of the unit by simply wearing it out. The answer to assured quality of in-flight hardware lies in non-destructive testing.

By far, the greatest utilization of non-destructive techniques is in the vehicle structure. To point out the development pace of non-destructive techniques, a short 10 years ago, virtually no non-destructive inspection procedures were utilized in the structural assembly of the largest ballistic missile then under development in the United States, the Redstone. During the flight test of an early Redstone missile, a propellant-

tank pressure drop occurred, causing the flight to be aborted. Investigations revealed that the pressure drop experienced during that flight could have occurred only by a major structural weldment failure. This incident can be recounted now as the turning point in attention to the reliability of missile and launch vehicle structures, because investigation of sister tanks to that which failed revealed serious weldment deficiencies. X-ray was the tool used for the investigation. Subsequent to that abortive flight, the Marshall Space Flight Center and its predecessor organization, the Army Ballistic Missile Agency, have utilized 100-percent non-destructive inspection of all primary and secondary structural fusion weldments. Interestingly enough, no structural failure has been experienced in any vehicle developed by this organization since the initiation of the non-destructive evaluation procedures. These vehicles include the Redstone missile, the Jupiter C (which was the free world's first satellite launcher), the Juno series of satellite launchers, the Jupiter weapons system, and the Saturn I. X-ray inspection techniques have been developed and used for these systems over the range of applications encompassed by aluminum sheet thickness of 0.015 inch to solid graphite blocks 16 inches thick. In the latter case, the technique involved moving the graphite at a predetermined speed through a collimated beam of X-rays with a total exposure time of 2½ hours required for one complete radiograph. Time consuming as this may appear, vehicle success or failure was hinged on the functioning of the graphite component, and subsequent to the utilization of this inspection technique, no component failures were experienced. As to cost, the price tag on the inspection technique for four vehicle components was approximately \$400.00. Failure of one such component during flight would have cost several hundred thousand dollars.

The assets and liabilities of radiographic techniques, however, are well established. Although it is not the purpose of this paper to repeat them, it is important to show how some of the liabilities associated with radiographic techniques provided the stimulus for the develop-

ment of new non-destructive techniques. Foremost among these liabilities is safety. Safety considerations require massive areas which must be shielded at tremendous costs. There are, however, technical liabilities such as insensitivity and, in fact, ineffectiveness of radiographic techniques for many of today's needs. All of these liabilities and others not noted were sufficient to initiate the search for new and more efficient non-destructive evaluation tools.

One of the major dangers encountered in presenting data on non-destructive evaluation techniques is that the reader may be given the impression that this or that technique is a panacea for all problem solutions. Let it be clear that each of the techniques to be discussed has application to certain requirements, but no one technique universally obviates the needs for any of the others. The most efficient evaluation system may include all known non-destructive techniques; however, until appropriate techniques for all applications have been developed, no system of evaluation can be completely efficient.

Probably the three most popular non-destructive systems in development today are ultrasonic, electromagnetic (eddy current), and infrared techniques. We can state with certainty that the full potential of these systems has not been realized today. However, let us review what we know of these systems and show examples of how they are being applied.

ULTRASONICS

The use of ultrasonic energy as a tool for non-destructively evaluating structural components has received widespread attention. "Ultrasonic" is a term which defines high frequency sound beyond the audible range. The term is fast becoming a misnomer, because much is now being done with sound in the audible range; however, for purposes of clarity in this paper, we shall refer to all sound energy techniques as ultrasonic. Ultrasonic techniques are not new. If you have ever tapped a china bowl with a half-dollar to determine if it were cracked, or gently knocked on a wall to locate a stud behind the surface, you have used an ultrasonic technique. Today's techniques are somewhat more

refined than these examples, but only because they use measured quantities of sound input to determine the precise degree of quality or lack of it. The basic laws of physics demonstrate clearly that sound travels in straight lines. Similarly, we know that sound can be refracted, reflected, and absorbed in many different, but well-known ways. Furthermore, by using the analogy of throwing a stone into a lake, we can show that energy waves are propagated in two directions; that is, along the surface of the lake, and in the direction of the stone's path in the lake. Whether these waves are created by a stone thrown into a lake or by a pulse of sound introduced into a material is irrelevant to the laws of physics. Therefore, we have two very useful means of utilizing ultrasonic waves induced into a material, since the induced energy can be carefully controlled as to quantity. We know from the study of acoustics that certain materials are more sound absorbent than others; as a general rule, soft materials are better absorbers than hard ones. Finally, we know that sound is dispersed rapidly in air; therefore, if we are to have accurate accounting of the sound energy introduced into a material, we must preclude exposing the energy to air.

With our basic knowledge of sound, how can we apply this knowledge to useful, non-destructive techniques of evaluation? Figure 1 shows an application of an ultrasonic technique for evaluating fusion weldments. The ultrasonic energy introduced in such a manner that the energy beam is reflected in a sawtooth pattern within the materials, passing through the weldment, and then is picked up by a receiver. Since metal is by far a better conductor of sound than air, the ultrasonic energy follows the path of least resistance and stays within the metal rather than being dissipated in air

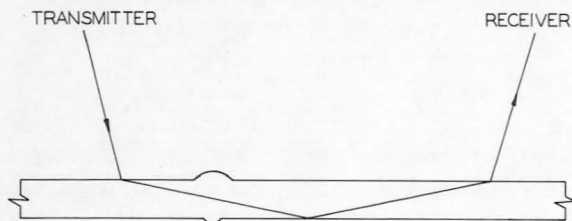


FIGURE 1.—Transmission of sound through a good weldment.

at the reflection points. By knowing the quantity of energy introduced and measuring the quantity received, we get a very accurate record of the condition of the weld. This is true because any energy lost can be attributed only to a weld defect which has reflected the energy beam out of the path into which it was directed originally. This is shown pictorially in figure 2. This technique, although not new today, is widely overlooked. The technique can be adjusted to be sensitive enough to depict metal grain boundaries or insensitive enough to permit defects of almost any size to go unobserved. There is no practical limit to the application of this technique; however, note in figure 1 that both crown and penetration, top and bottom, of the weld are not exposed to the ultrasonic beam since, if the beam does enter these protrusions, it is reflected out of the primary path and lost to the receiver. One can postulate that a weld crack being in the plane of the beam would also go unnoticed; however, this is not true. The corner effects of the crack, however small, will cause complex disturbances to the beam, effecting major energy losses. The theory of this phenomenon is too complex for this paper; it is sufficient to say that air-flow theories apply almost directly to this situation. It is accepted that no finite thickness can go unnoticed by a jet of high stream air, that is, without creating some turbulence in the air stream.

A second use for ultrasonic-energy techniques is the inspection of plate or complex surfaces. As shown in figure 3, the ultrasonic beam can be controlled immediately under the surface of any shape by careful insertion. The importance of surface scratches or other discontinuities in highly stressed components can be shown by stress analyses and patterns which

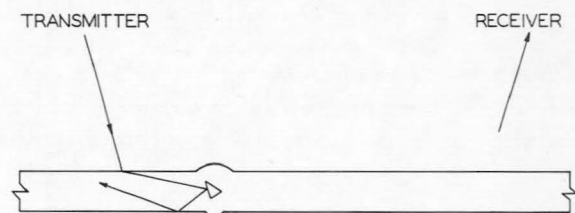


FIGURE 2.—Sound reflection from weldment defect.

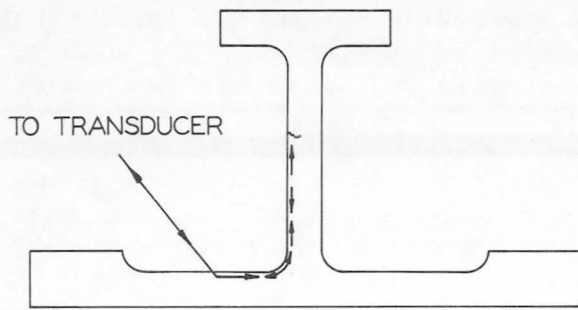


FIGURE 3.—The inspection of complex specimens with surface waves.

are easily calculated. Studies have proven that even minute scratches in a surface can cause catastrophic results. It is important in many applications to know not only that surface defects exist (often visible with the unaided eye) but the depth of the defect in order to determine the seriousness of the defect to the component. As shown, the depth can be measured accurately, permitting a reliable analysis of the reduction in structural integrity incurred by the defect.

One of the newest uses of ultrasonic techniques is in evaluating adhesively bonded honeycomb materials. Let us use the example shown in figure 4. As shown here, there are eight interfaces in a cross section of this composite material. The problem here is to be able to evaluate all eight interface conditions accurately. It is not enough to know, for example, that the adhesive is present at each interface, but we must determine if it is adhering to each component being joined.

Before proceeding with a discussion of one applicable technique, it is necessary to define the material shown in figure 4. The face sheets, A and B, and the vapor barrier, C, are aluminum. The honeycomb, D, is a resin-impregnated fiberglass, and honeycomb, E, is a plastic. The remaining sheets, designated F, are adhesive layers used to join the various components. Although there are several approaches which could be utilized in developing a technique for evaluating this complex material non-destructively, only one approach is described here. In this particular approach, advantage was taken of our ability to measure the time taken for an

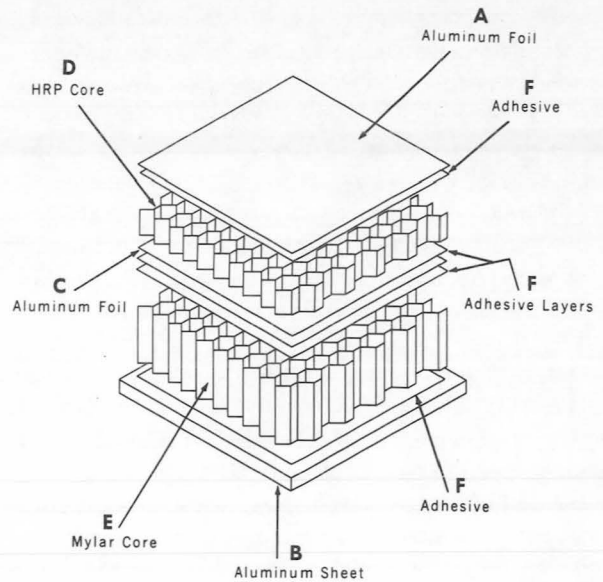


FIGURE 4.—Design of dual-seal insulation.

echo to travel over the finite distances involved. Ultrasonic energy is introduced at one outer surface and reflections from this energy are recorded on a time scale. Since we can calculate the time required for the energy to travel from the point of introduction to the various interfaces and return, the existence of defects at the various adhesive interfaces can be recorded. If the top joint is bad, there is no way of evaluating the subsequent joints until that one has been repaired. However, with most other techniques, it is impossible to establish which of the eight joints causes the indication of fault. Admittedly, this technique was not as simple to develop as may be indicated in this discussion, nor is it necessarily the optimum technique for this application. However, this example has been used to show the potential of ultrasonic techniques for non-destructively evaluating extremely complex structures made with more advanced materials today.

These are but three examples of how ultrasonic techniques can and are being applied in the aerospace industry. Note that each technique is utilized from one side of the component being evaluated, which is a major advantage in these and many other applications. Furthermore, it is important to mention that the evaluation results can be plotted in two

planes with each of these techniques, thus presenting a record which can be interpreted readily by technicians. Finally, by proper use of precalibration standards, the fallibility of human interpretation can be essentially eliminated.

EDDY CURRENT

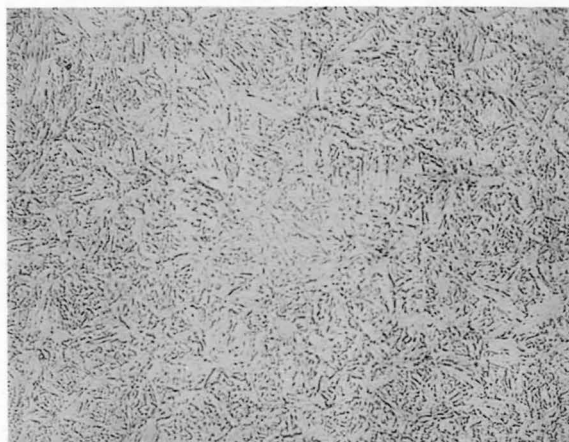
A second non-destructive tool receiving major attention today involves electromagnetic or eddy-current techniques. By exposing electrical conducting materials to a strong magnetic field, eddy currents are created within these materials. These eddy currents then establish a magnetic field. Of course, if defects exist in the material, no eddy currents will be created, thus at defect locations there will be no magnetic field. By measuring the magnetic field caused by the eddy currents, it is a relatively simple matter to define the existence of defects.

To demonstrate how eddy current techniques may be applied, we can again use the problem mentioned earlier in describing the application of ultrasonic techniques to determine surface defects or immediate-subsurface defects. Using an eddy-current technique, large areas can be scanned rapidly, although with less sensitivity than with ultrasonic techniques. For example, a plate measuring eight by fifteen feet can be scanned by eddy current techniques, with proper tooling, in approximately three minutes; whereas, the same task with ultrasonics takes approximately fifteen minutes. This suggests that rapid scanning by eddy-current techniques, complemented by detailed scanning of only defective areas by ultrasonic techniques, would yield the most efficient results in terms of time which is, of course, money.

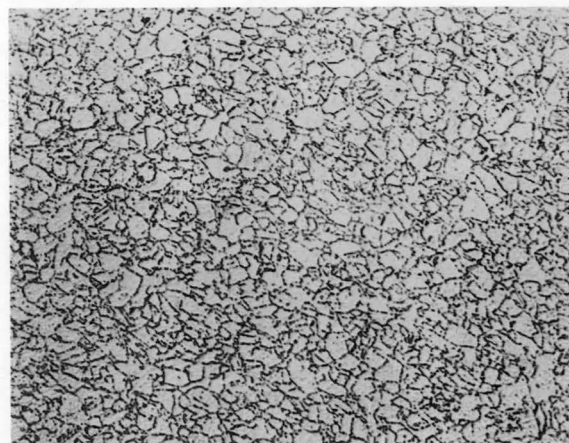
A second application of eddy current techniques is the determination of the metallurgical structure of a component. As shown in figure 5, these two structures are representative of what can be experienced in a given precipitation hardening or heat-treatable material. The first illustration is completely undesirable because it is highly susceptible to stress corrosion because of the heavy precipitate formed along the grain boundaries. For maximum stress-corrosion resistance, the second illustration is the more

desirable because the precipitate does not form a continuous network but has been dispersed into solution and is contained in the metal grains. By using eddy-current techniques, these differences can be demonstrated clearly. Similarly, degree of tempering in precipitation hardening alloys can be measured. As shown in figure 6, plotting the results of an eddy-current evaluation of the degree of precipitation hardening which has occurred in a given component is clear and dramatic as to the point where the material has been overheated.

Although lagging ultrasonic techniques in development, eddy-current techniques are



GOOD AM 355



BAD AM 355

FIGURE 5.—Types of microstructure.

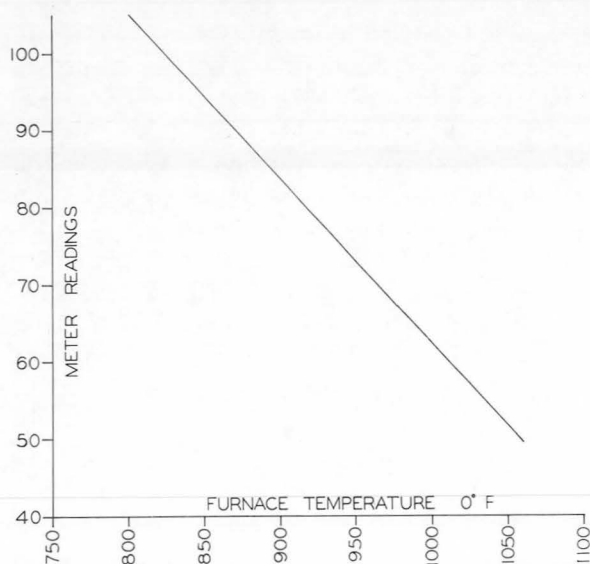


FIGURE 6.—*Eddy current evaluation of precipitation hardening.*

quickly finding a necessary place in the non-destructive evaluation of metallic materials. For obvious reasons, eddy current techniques are not applicable to nonmetallic materials.

INFRARED

A third, non-destructive technique that only recently began to receive attention utilizes infrared energy. Like the techniques discussed previously, infrared techniques are not new. They have been used in chemical analyses for many years; however, application of infrared techniques to verify component integrity is new. In simple form, infrared techniques capitalize on the fact that heat is either generated by or can be induced into anything. The capability of sensors to measure the heat has resulted in the interest in infrared techniques since measurement of the infrared energy given off, regardless of the quantity, is not only practical but has been demonstrated. Calibrated in temperature, infrared sensors have measured temperature differences in given structures of less than 1° F. Interpreting the meaning of this temperature differential requires a knowledge of the basic material thermal properties; data which, in many cases, is available in numerous handbooks. Therefore, only the problem of

applying infrared techniques needs to be solved to utilize these. This is not to say such problems are minor. Since the measured media is heat, such things as local drafts can become critical problems of application. However, the simplicity of the technique, once applied, is sufficiently desirable to prompt development of implementation methods. In the case of a structure, either a homogeneous structure or one of well defined inhomogeneity can be expected to conduct heat in a uniform or mathematically definable pattern. Any variations in the pattern are caused by inherent structural defects. Therefore, the introduction of a known heat pulse into a metallic or nonmetallic material will result in a mathematically defined heat pattern if the thermal constants of the material are known. By using infrared sensors, the actual heat pattern in the material can be established and compared to the mathematically defined pattern. A typical material which may be appropriate for infrared analysis would be a honeycomb as described earlier. The failure of adhesives to adhere to the materials to be joined would cause a significant change in the heat pattern produced in a honeycomb material when compared to that produced in a structurally sound honeycomb material.

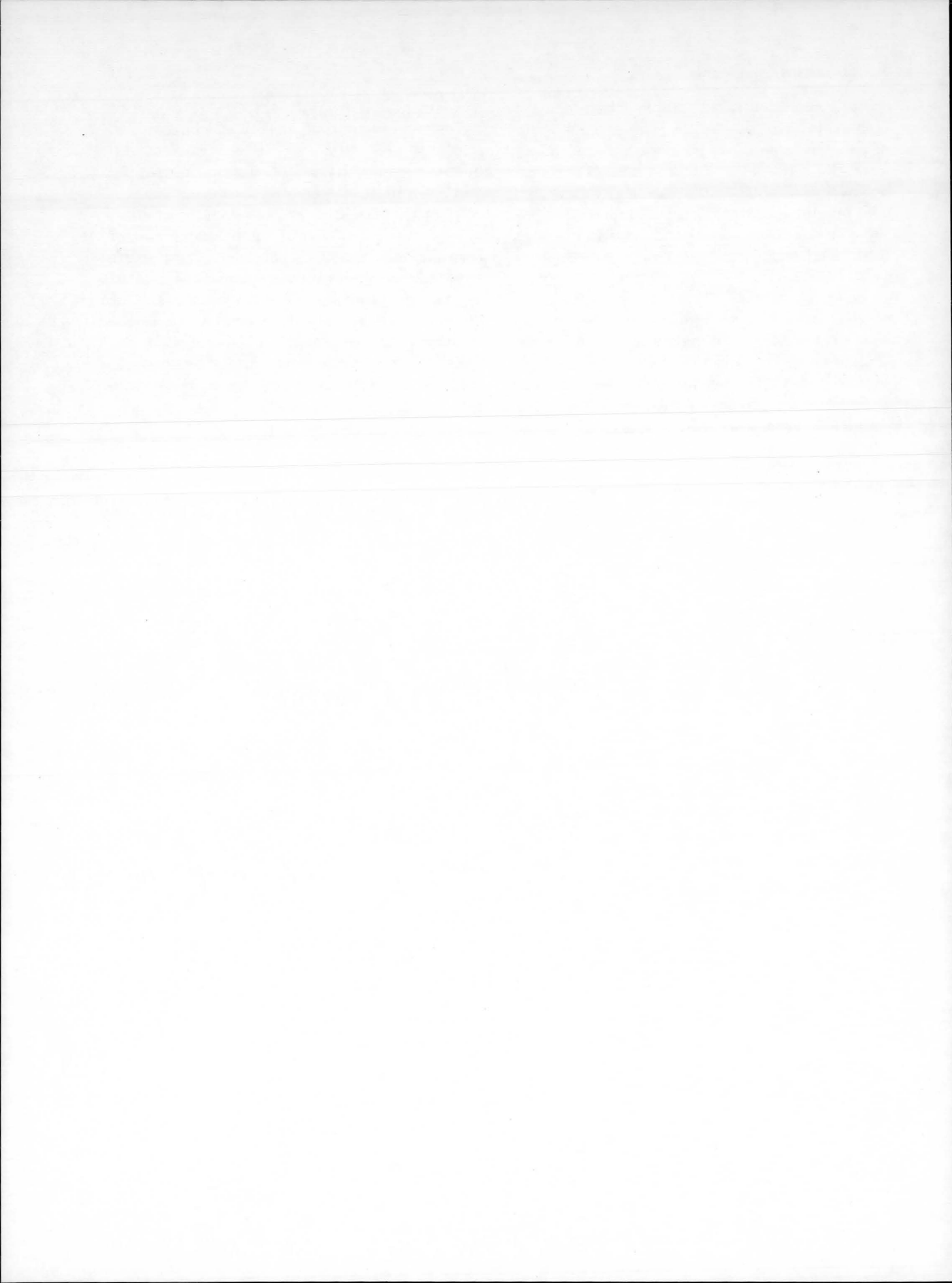
A more interesting use for infrared techniques appears to be in evaluating the condition of electrical and electronic components. It is well known that soldered electrical contacts, for example, follow a well defined trend of increasing resistance with time until failure occurs. The sensitivity of infrared sensors is such that the heat generated by the contact can be measured accurately. Therefore, by knowing the heat generated by a sound, efficient contact, one can predict the life expectancy of any similar contact simply by measuring the heat generated from the contact being evaluated. In this manner, it may be possible to accurately establish the life expectancy of electrical contacts without affecting the contact. The advantages of such a technique over the old method of testing several times to prove integrity is clear. The problem of testing X times may result in failure on test $X + 1$, the time when human life may be at stake.

The fact that infrared technique development is in its infancy should not limit consideration of these techniques for current application, because the potential of infrared sensors for non-destructive evaluations is essentially limitless. The practicability of these techniques provides the boundary, not the capability of the sensors to detect heat.

CONCLUSION

Non-destructive techniques for the evaluation of manufactured hardware need not be limited to items used in the national space program. Indeed, few people today have not experienced some problem in their daily life which could have been averted by proper non-destructive

evaluation techniques. In our world of increasing automation, quality and integrity of hardware is mandatory. No longer can the industrial community use the excuse that proper and appropriate methods of determining integrity are not available. In fact, even the problem of cost is not excessive if the principal cost of necessary equipment is prorated over the life expectancy of the equipment and if the number of manufactured-item failures which can be averted by the use of non-destructive technique evaluation is considered. In this day of emphasis on quality in everything from toys to space ships, it is incumbent upon industry to take advantage of the potential offered by non-destructive techniques.



23. An Improved Wind Sensor for Measuring Vertical Wind Velocity Profiles and Some Possible Commercial Uses

JAMES R. SCOGGINS

George C. Marshall Space Flight Center, NASA

The approach to the development of an accurate and aerodynamically stable spherical-balloon wind sensor (Jimsphere) is discussed. A comparison of wind profiles measured by the Rawinsonde and FPS-16 radar/Jimsphere methods is presented. Some of the possible commercial uses of the Jimsphere are discussed.

When a space vehicle is launched, it experiences changes in the wind field while rising vertically through the atmosphere. Wind measured as a function of altitude at a given location on the earth is called a vertical wind velocity profile. Vertical wind velocity profiles are normally measured by tracking a helium- or hydrogen-filled neoprene or rubber balloon by theodolites to obtain space position data from which wind profile data are calculated. Most of the data measured in this way are averaged over an altitude layer of approximately 600 m (2000 ft). The wind speed may vary considerably over this altitude interval, but it is not possible to measure these variations because of the large averaging interval. The small-scale motions which are omitted by averaging are important in the design and operation of space vehicles.

In order to measure the small-scale motions accurately an aerodynamically stable wind sensor is required. Leviton (1962) proposed that a superpressure Mylar constant-volume sphere be used for this purpose and tracked by an FPS-16 radar (Getler, 1962). The balloon originally proposed by Leviton was aerodynamically unstable and did not follow the winds accurately. The instability arises from a phenomenon called vortex shedding which causes

the balloon to experience highly erratic lateral motions even in a calm atmosphere. These motions have been studied by Scoggins (1964, 1965).

A program was begun early in 1963 at the Marshall Space Flight Center to design an aerodynamically stable wind sensor which could be used to obtain highly accurate and detailed wind velocity profile measurements to an altitude of approximately 20 km. The approach was to modify the sensor proposed by Leviton. A series of experiments were conducted at MSFC and at Cape Kennedy using various balloon configurations to assess the influence of surface roughness, weight, size, ascent rate, and mass distribution on the stability of the balloon. As a result of this program, an accurate spherical-balloon wind sensor has been developed and is currently being used for obtaining detailed and accurate wind velocity profiles.

THE DEVELOPMENT AND USE OF AN ACCURATE WIND SENSOR

The Aerodynamic Problem and Its Solution

The motion of a fluid, such as air, around a sphere is characterized by well organized motion on the forward portion, and generally chaotic motion on the rear portion. The fluid becomes chaotic at the point where it separates

from the balloon. The point of separation on a sphere is a function of the Reynolds number which is defined as

$$Re = \frac{\rho V D}{\mu}$$

where ρ is the density of the air V the flow relative to the sphere, D the diameter of the sphere, and μ the coefficient of viscosity. The drag force which is produced by flow around the sphere is given by

$$F = \frac{1}{2} \rho V^2 C_D A$$

where ρ and V are as defined above, C_D the drag coefficient, and A the cross-sectional area of the sphere. It has been stated by Schlichting (1960) and others, that the drag coefficient is a function of the Reynolds number. For a sphere at high Reynolds numbers (supercritical) the drag coefficient is small. As the Reynolds number decreases, the drag coefficient goes through a sharp increase in value (critical Reynolds number) and reaches a rather large value at small Reynolds numbers (subcritical) (MacCready and Jex, 1964). The nature of the flow-separation process is quite different at supercritical and subcritical Reynolds numbers. Characteristics of the flow-separation process influence the forces which act on the balloon and, therefore, also the induced motions. At subcritical Reynolds numbers, flow separation takes place further up-stream on the sphere resulting in a smaller variation in the forces. Therefore at subcritical Reynolds numbers the spherical balloon is more stable and gives a better indication of the true wind conditions.

The nature of the flow separation process can be altered by the addition of surface roughness elements on the sphere. The size, shape, number, and distribution of the roughness elements which are required to provide the desired type of separation and wake characteristics behind the balloon were determined experimentally. A 2-meter diameter, 1/2-mil, aluminized Mylar superpressure balloon was used as the basic sphere. Roughness elements of various sizes and numbers ranging from approximately 200 to 500 with heights between approximately 1.5 and 3 inches were molded into the balloon. The rough configuration is now called "Jimsphere". The optimum configuration was selected on the

basis of experimental data. Wind profile data obtained by photographing visual smoke trails (Henry, et al., 1961) were used for comparison. During the course of the program it was found that a small weight attached at a point on the sphere was required to prevent the sphere from rotating and developing undesirable forces which caused lateral oscillations of the balloon.

Description of the Jimsphere Balloon

Figure 1 is a photograph of the wind sensor developed as a result of the experimental program at the Marshall Space Flight Center and Kennedy Space Center. The balloon is superpressurized so that it maintains its shape during ascent. A spring-loaded valve maintains a pressure inside the balloon of approximately 6 millibars in excess of the ambient pressure. As the balloon ascends in the atmosphere the ambient pressure decreases and the valve allows gas to escape, but the pressure difference is maintained. There are 398 conical roughness elements which are 3 inches in diameter at the base, 3 inches high, and spaced randomly on the surface of the sphere. A 100-gram mass of lead shot is sewed into the load patch (handle

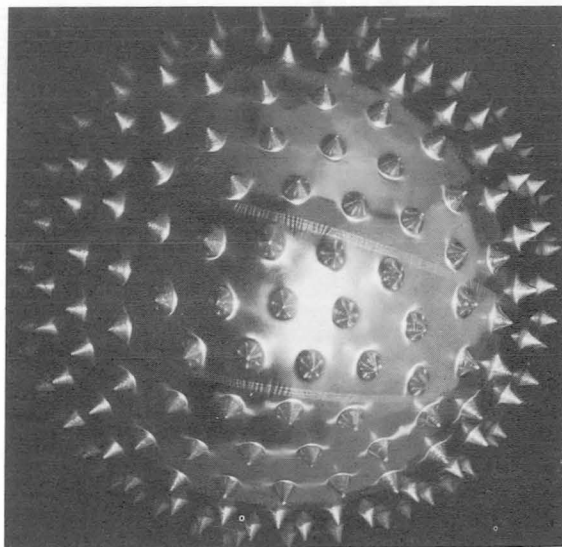


FIGURE 1.—The Jimsphere configuration. The sphere (not including the cones) is 2 meters (6.52 ft) in diameter; there are 398 full cones which are 3 inches in diameter and 3 inches high, randomly spaced on the sphere.

for holding the balloon) which prevents the balloon from rotating during flight. The combination of surface-roughness elements with the spacing and dimensions as given above, and the lead shot to provide attitude stabilization, produce the desired separation and wake characteristics for an aerodynamically stable spherical-balloon wind sensor.

Examples of Wind Profile Measurements

Figure 2 shows a comparison of wind profiles measured by the rawinsonde (GMD) and the FPS-16 radar/Jimsphere methods on the day the Saturn SA-9 was launched, February 16, 1965. Four profiles are presented in the figure; two for wind speed and two for wind direction. The wind speed and wind direction profiles measured by the two methods are shown on the same graph over a limited altitude range. The crosses represent the rawinsonde data, and the dots the FPS-16 radar/Jimsphere data. The profiles were not measured at exactly the same time and may be slightly different for this reason; however, the capability of the improved wind-measuring system is demonstrated. Much more detail is presented in the FPS-16/Jimsphere data than in the rawinsonde data. Features appear on the Jimsphere wind speed profile between 10 and 11 km which do not appear on the GMD wind profile. On days

when the atmosphere is unstable there may be pronounced differences in the profiles as measured by the two methods. The detail motions as measured by the improved system are important in designing and operating space vehicles.

SOME POSSIBLE COMMERCIAL USES OF THE JIMSPHERE

Improved Wind Profile Measurements In Aircraft Design

Improved wind profile and turbulence measurements are needed for use in the design of aircraft in much the same way as they are needed for the design of space vehicles. Turbulence which an aircraft experiences in flight is due to small-scale motions for the most part. Anyone who has flown through a turbulent region is aware that the aircraft responds to changes in the wind field, and that in doing so it experiences stresses and strains that are not ordinarily experienced in smooth air. The aircraft must be designed to withstand forces resulting from all scales of motion regardless of where or when they are encountered. Atmospheric turbulence is produced and influenced by processes which vary in space and time and which are not well understood. If detailed and accurate wind-profile measurements were made at several places in the United States, for example, and if vertical motions could be measured, it would provide data which would possibly be useful

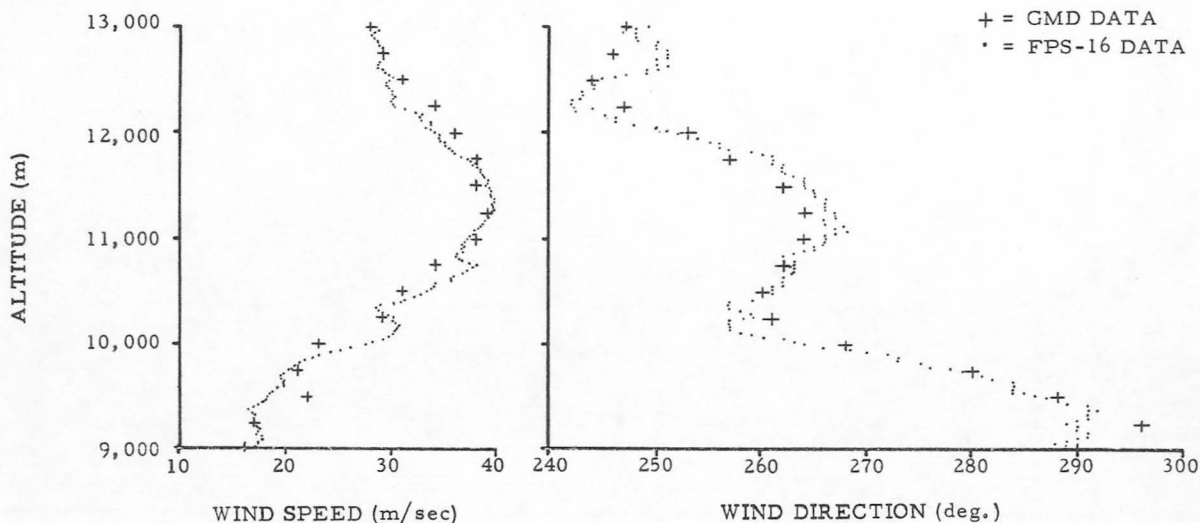


FIGURE 2.—Wind speed and wind direction profiles measured by the FPS-16 Radar/Jimsphere and Rawinsonde (GMD) methods at Cape Kennedy, February 16, 1965. The FPS-16 measurements began at 0525Z and the Rawinsonde at 0613Z.

for improving the design of aircraft. These profile measurements might be of particular value in the design and operation of supersonic aircraft which might have steep climb and descent paths.

Weather Forecasting Improvements

Weather forecasts are based on wind data as measured by the rawinsonde system. Within the United States there are approximately 100 rawinsonde stations which make wind-velocity profile measurements twice daily. Many meteorologists believe that weather forecasts for a given locality could be improved if better wind data were available. The data could also be used for determining and predicting atmospheric pollution conditions over cities, the propagation of sound through the atmosphere which might result, for example, from static firings of large space boosters, and to acquire a better understanding of the atmosphere and the physical laws governing its behavior.

Measurement of the Level of Turbulence in Wind Tunnels

Wind-tunnel tests are frequently conducted using scaled models of aircraft, space vehicles, or other aerodynamic bodies. The results obtained are usually influenced by the degree of turbulence present in the tunnel during the tests. Smooth spheres have been used to determine the degree of turbulence present. This is done by measuring variations in the drag force. It is now known that these variations may be due to the nature of the vortex shedding and separation phenomena rather than turbulence. A rough sphere could be used for obtaining accurate information on the turbulence level in tunnels. Figure 3 shows a drag curve measured in a wind tunnel using a scaled model of the Jimsphere, and a comparison with a drag curve using a smooth sphere. The drag curve obtained from the rough sphere shows little scatter at the higher Reynolds numbers, and shows only a slight decrease in the drag coefficient as the Reynolds number is decreased. For the smooth sphere, considerable scatter is noticed and the

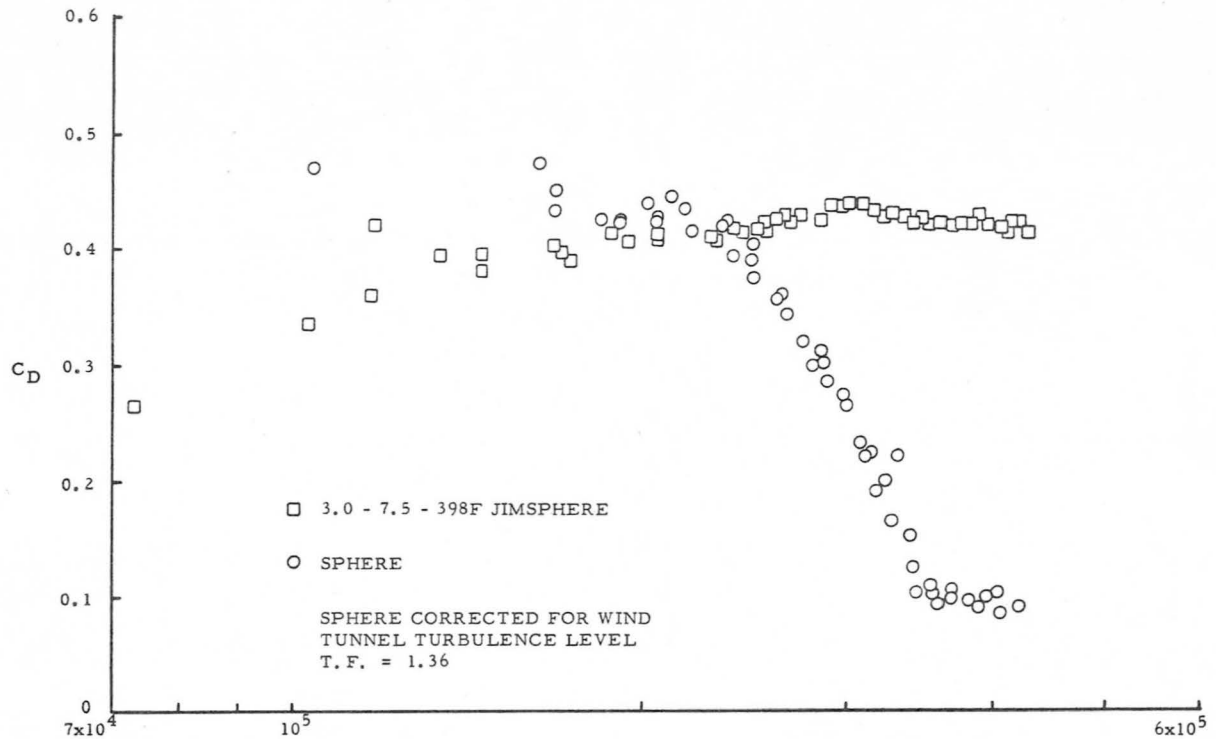


FIGURE 3.—Drag coefficient versus Reynolds-number curves for the Jimsphere and a smooth sphere.

curve undergoes a sharp transition in going from high to low Reynolds numbers.

Better Understanding of Flow Separation Problems

The flow-separation characteristics around blunt bodies is not well understood. For example, a space vehicle erected on the launch pad ready for flight may be excited and caused to oscillate by the vortex-shedding phenomena which results in the presence of a wind. The techniques employed to develop an aerodynamically stable spherical-balloon wind sensor may find some application in solving such problems.

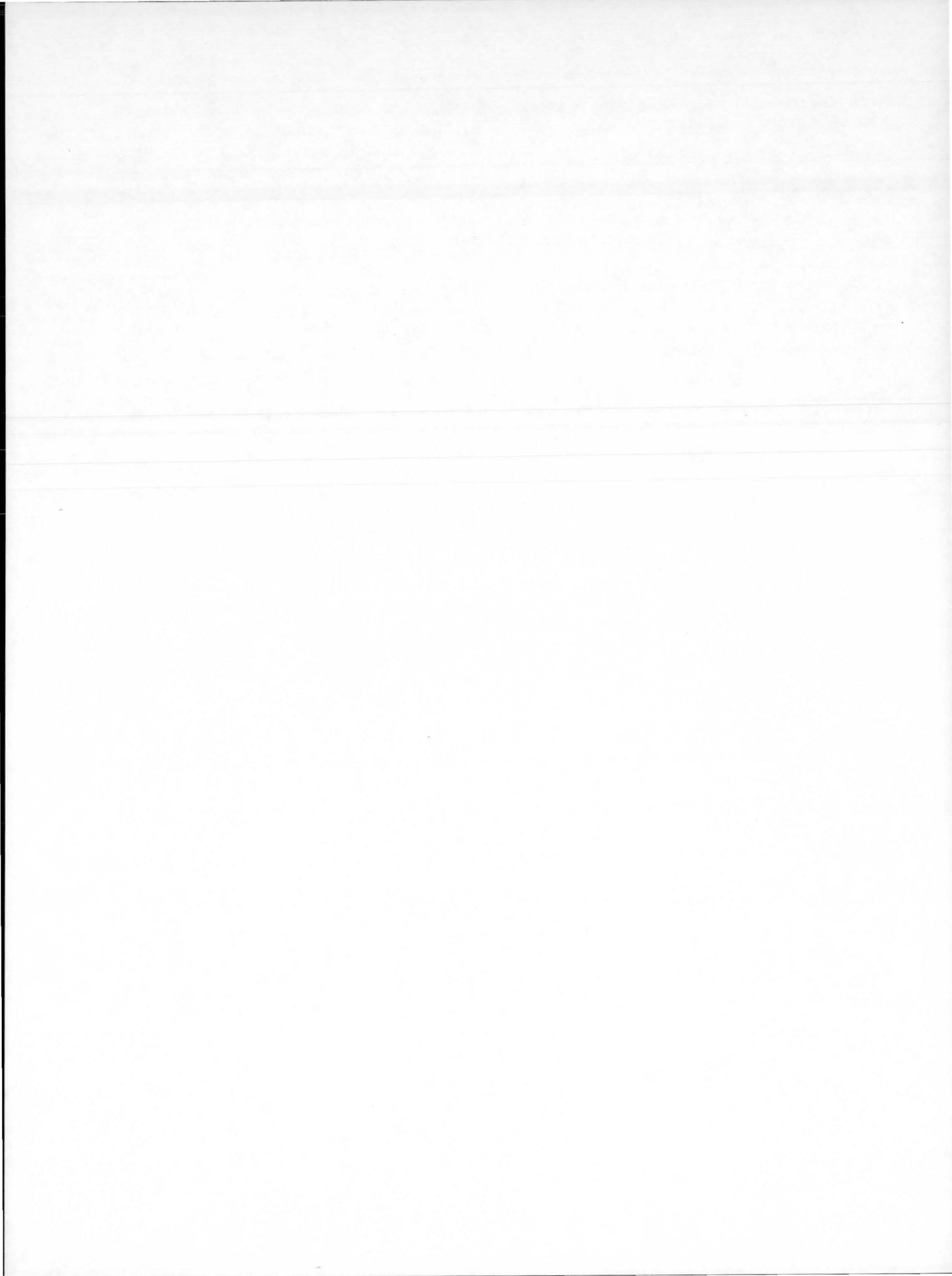
CONCLUSION

The development of the Jimsphere has demonstrated that the forces acting on a free-lifting or falling blunt body while moving through a fluid may be altered considerably. Roughness elements apparently create a turbulent flow and induce separation at a point on the body which is nearly independent of the Reynolds number. The experimental test data show that as the surface roughness of a sphere increases at supercritical Reynolds numbers, the drag force becomes more stable and larger in magnitude, and the aerodynamically induced horizontal motions are reduced.

Only a few possible uses of the improved wind sensor are mentioned in this report. There are no doubt many specialized problems which may be solved by the proper application of the knowledge gained and the concepts employed in developing the Jimsphere.

REFERENCES

- HENRY, ROBERT M. ; ET AL. : The Smoke-Trail Method for Obtaining Detailed Measurements of the Vertical Wind Profile for Application to Missile-Dynamic-Response Problems. NASA TN D-976, 1961.
- LEVITON, R. : A Detailed Wind Profile Sounding Technique, Proceedings of the National Symposium on Winds for Aerospace Vehicle Design, Air Force Surveys in Geophysics, 1(140), Geophysics Research Directorate, Bedford, Massachusetts, 1962.
- MACCREADY, PAUL B. ; and JEX, HENRY R. : Study of Sphere Motion and Balloon Wind Sensors. NASA TM X-53089, 1964.
- SCHLICHTING, HERMANN : Boundary Layer Theory. McGraw-Hill Book Company, New York, 1960.
- SCOGGINS, JAMES R. : Aerodynamics of Spherical Balloon Wind Sensors. Journal of Geophysical Research, 60(4), February 15, 1964.
- SCOGGINS, JAMES R. : Spherical Balloon Wind Sensor Behavior. Journal of Applied Meteorology, 1965.



24. Digital Events Evaluator

E. F. BULLINGTON

George C. Marshall Space Flight Center, NASA

When a vehicle is being tested, any function that causes a discrete voltage change is defined as a "digital event". For example, a relay closure may cause the voltage on a line to change abruptly from zero volts to +28 volts. The nomenclature that has been adopted would express this change as; the status of the given line has changed from "off" to "on".

In vehicle checkout, the changes that take place on the discrete lines can provide the test conductor with valuable information. However, it is imperative that this information be available on some form of record within a short time after occurrence of the event. This allows an evaluation of the record to be made periodically during checkout and results in malfunctions being detected at the earliest possible time.

The scientific data systems digital events evaluator is the latest effort in this field, and is presently in use on the Saturn I, Saturn IB, and Saturn V Programs.

SYSTEM DESCRIPTION

The DEE-3 is physically composed of an SDS-910 solid state, core memory, digital computer, and associated circuitry. This associated circuitry is used to implement the scanning capabilities of the DEE-3 system, giving it a capability of monitoring up to 768 input lines and evaluating digital events that occur on any of the input lines. This evaluation, to a great degree, depends upon test requirements, but can include such things as: total "on" time on each line, total number of on/off cycles on each line, sequences of groups of events, program step number, and the like.

Input/output capabilities of the DEE-3 system are implemented by an International Business Machines Selectric Typewriter, a Tally Paper Tape Punch, and a Rheem Paper Tape Reader. The paper tape punch is capable of outputting at the rate of 60 characters per second and is mounted in the main racks of the system. The Rheem Paper Tape Reader, also mounted in the main racks, is capable of reading paper tape at the rate of 300 characters per second. The input/output typewriter, which is mounted on a table immediately adjacent to the main racks, is capable of accepting input or output information at the rate of 15 characters

per second. The DEE-3A input/output capabilities differ from the DEE-3 in that the IBM Selectric Typewriter has been replaced by the Teletype Model 35 Typewriter, which has a speed of 10 characters per second. The capability of feeding the Teletype Typewriter and the Tally Paper Tape Punch with the same data has been incorporated into the DEE-3A system. This feature permits the simultaneous output to two recording devices, thus decreasing the possibility of losing data because of an output device failure.

External connections for the system are required only for the input lines which are to be monitored, and for the input operating power to the system. Input power requirements are 110 volts, single phase, 60 cycles per second. The input power is received through two receptacles which should be protected with circuit breakers of 30-ampere capacity.

The input lines to the system are terminated at a bulkhead and distributed to the input filters by means of module terminated cables. Any of the input modules may be replaced by a special test module, which is connected to a test panel and allows any of the input lines to be checked manually.

SYSTEM OPERATION

A block diagram of the DEE-3 system is shown in figure 1. It should be noted that the component blocks in this diagram are composed, in part, of actual hardware circuits and portions of the core memory reserved for the DEE-3 program. The input circuitry, the comparator chassis, and the control chassis are all system electrical components. The previous scan cycle memory and the output buffer are programmed tables set up in the core memory to facilitate processing of information concerning the digital inputs to the system.

The system design requires that the operation procedures follow through three basis cycles: (1) scanning cycle, (2) alarm recording cycle, and (3) output cycle.

Scanning Cycle

The input lines which the DEE-3 is to monitor are divided into 32 groups of 24 input lines each. The system begins scanning with group 1 and proceeds through each group of 24 input lines until all 32 groups have been scanned. While any group of input lines is be-

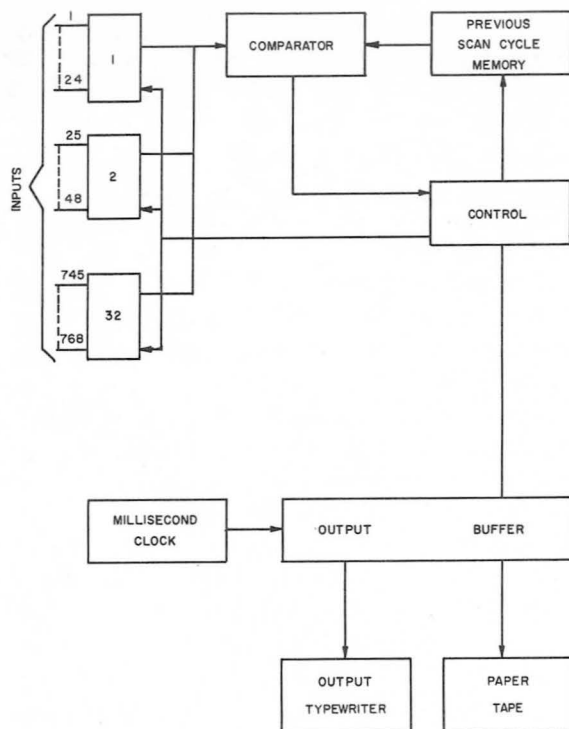


FIGURE 1.—*Dec-3* block diagram.

ing presented to the comparator circuitry, the computer program is presenting the status of the same group of lines during the previous scan cycle to the opposite side of the comparator. This information has been retrieved from the previous scan cycle memory portion of the computer memory. Each input line is normally scanned every 4 milliseconds. If the present status of each input line within the group being tested compares with the status of the same line during the previous cycle, no action is required, and the scan then advances to the next group. However, if the status of any line in a group has changed since the previous scan cycle, a digital event has occurred, and action is required by the system in order to properly evaluate the event. This action is discussed in the following paragraph.

Alarm Recording Cycle

If a digital event has occurred on any input line in the group being tested, a signal is sent from the comparator chassis, through the SKS (skip if signal not set) control lines to the computer. This signal will force the computer into a program whereby it will store four computer words, each containing information about the digital event, into a portion of the core memory called the change buffer. These four words are: (1) the time of detection of the event, (2) an index number defining which group did not compare, (3) the present status of the 24 inputs to the group, and (4) the previous status of the 24 inputs to the group. In addition, the present status of the group will be used to update the previous scan cycle memory and as a basis of comparison for the group during the next scan cycle.

If no digital events are detected during a scan cycle, the time required to scan all 32 groups is 1.2 milliseconds. However, this time period is extended 300 microseconds for each group of inputs in which an event occurs.

After all 32 input groups have been scanned, there will usually be some time remaining before the start of the next scan cycle. This time, which will be a maximum of 2.8 milliseconds, is used for processing the information in the change buffer and transferring it to the output buffer. Where there have been changes, up to

six groups may be processed for output during the remaining 2.8 milliseconds of the initial 4-millisecond period allotted for scanning and processing. If the total time allowed for processing events is not used, the output cycle program has an opportunity to function. This cycle is discussed in the following step.

Output Cycle

In the output cycle, data stored in the output buffer during the alarm recording cycle is converted to a format where it can be presented to a selected output device. Since the output devices are relatively slow as compared to computer speed, the output cycle need operate only once every few milliseconds.

In addition to the normal output, typewritten record or punched paper tape record, the DEE-3 is capable of performing special output functions. If at any time during a scanning cycle, the operator wishes to know the status of all input lines, he exercises the On Demand Print option. When this command is given, the numbers of the lines that are at +28-volt level will be typed out. However, previously detected events already in process will be printed out before the demand print is started. When demand-print information is received by the operator, even though it may be delayed by other printouts, it will contain line-status information detected when the operator initially exercised his key option. Immediately following the alarm recording cycle of the On Demand Print sequence, the DEE-3 will return to normal scan operation and continue to operate during demand printout.

If the events in a given test are expected to occur in a certain sequence, the operator may elect to use the Sequence Scan Option. This option allows for a table of expected sequence to be stored in the core memory and to be used in comparing the information on the table with each event as it occurs. There are two sub-options to the Sequence Scan Option. The first being, every event that takes place may be printed out, with the out-of-sequence events indicated by asterisks. The second sub-option allows for only out-of-sequence events to be typed out.

The formats for the various printout options are given in figure 2. For normal scan Alarm Printouts, the format consists of a line identification number, on-off column giving the line status, and the detection time of the event. For sequence scans, the detection time will be followed by an asterisk to indicate that the event was out of its expected sequence.

		22:
011	OFF	23.010
113	ON	23.742
156	OFF	24.136
192	ON	27.110

(a) Alarm printout format.

	ON	23:30.004
036		
119		
237		
436		
682		

(b) On demand print.

FIGURE 2.—Formats.

The On Demand Print contains the word "on," followed by the time the command was given. All lines that are in the "on" status when the command is given will then be printed out.

TECHNICAL DESCRIPTION

A simplified schematic diagram of the DEE-3 system input and comparator network is shown in figure 3. Input lines are brought into the system through a filter network implemented by special modules, ZX-30 and ZX-31. Voltage on the input lines may vary from -50 volts to $+50$ volts without damage to the input circuits components. In order to insure that random noise on the input lines is not recorded as an event, input filters are used to reject pulses of less than 0.5-millisecond duration. However, any pulse greater than 2-millisecond duration will be passed by the input filter circuit and presented to the comparator.

From the input filter circuit, input status is applied to an "And" gate (gate A in fig. 3) along with a strobe signal from the computer portion of the system. This And function, which selects the group of lines being tested, is applied to And gate B of figure 3, along with a signal from the computer C register. The computer C register output represents the previous status of the line being tested. If the two signals compare, either both "on" or both "off," then a logical "one" is applied to And gate C in figure 3, where it is Anded with 23

other signals from lines being tested within the group. If none of the lines in the group have changed in status since the last scan, all the inputs to gate C on figure 3 will be logical ones, and the output will also be a one. This signal, which is the SKS (skip if signal not set) line of the computer, allows the computer to proceed with testing the next group of inputs. However, if there have been any changes in the group under test, one or more of the inputs to gate C will be logical zero. This will cause the gate C output to be a logical zero and the computer will skip into a subroutine bringing both the old and new status of the entire 24 input lines in the group, along with the detection time of the changes, into the computer Change Buffer. This input subroutine requires 300 microseconds for execution before allowing the computer to proceed to the next group to be tested. The information that was stored in the Change Buffer is held for processing until the end of the scan cycle.

There are two program interrupt channels used with the DEE-3/3A system, in addition to the standard interrupts used with the SDS-910 computer. Interrupt channel 30 is used to initiate the basic scan of the input lines, normally every 4 milliseconds. The interrupt pulse is obtained by counting down the output from a 1 kc oscillator. Interrupt channel 32 is activated by special switch on the input/output typewriter console which causes the computer to go into an input subroutine, whereby the opera-

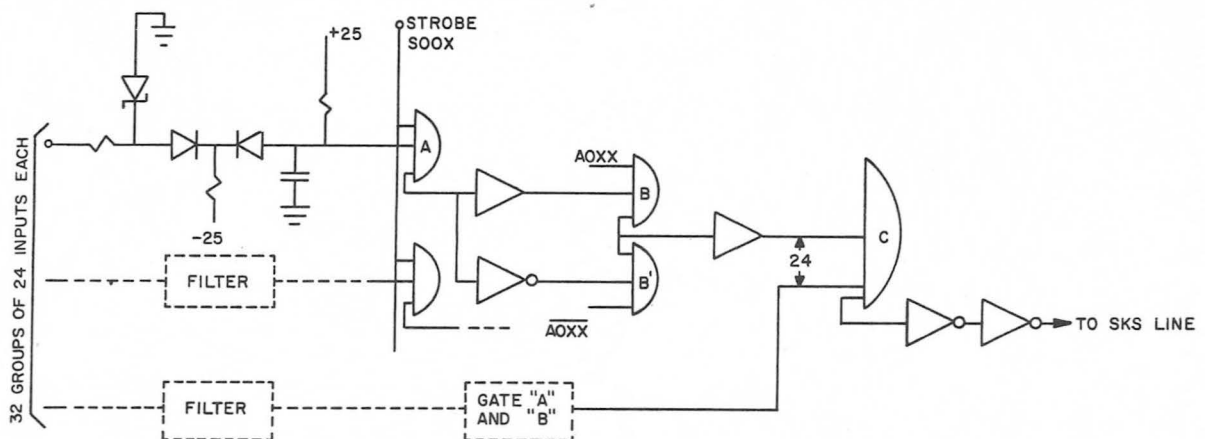


FIGURE 3.—Simplified schematic diagram of input and comparator network.

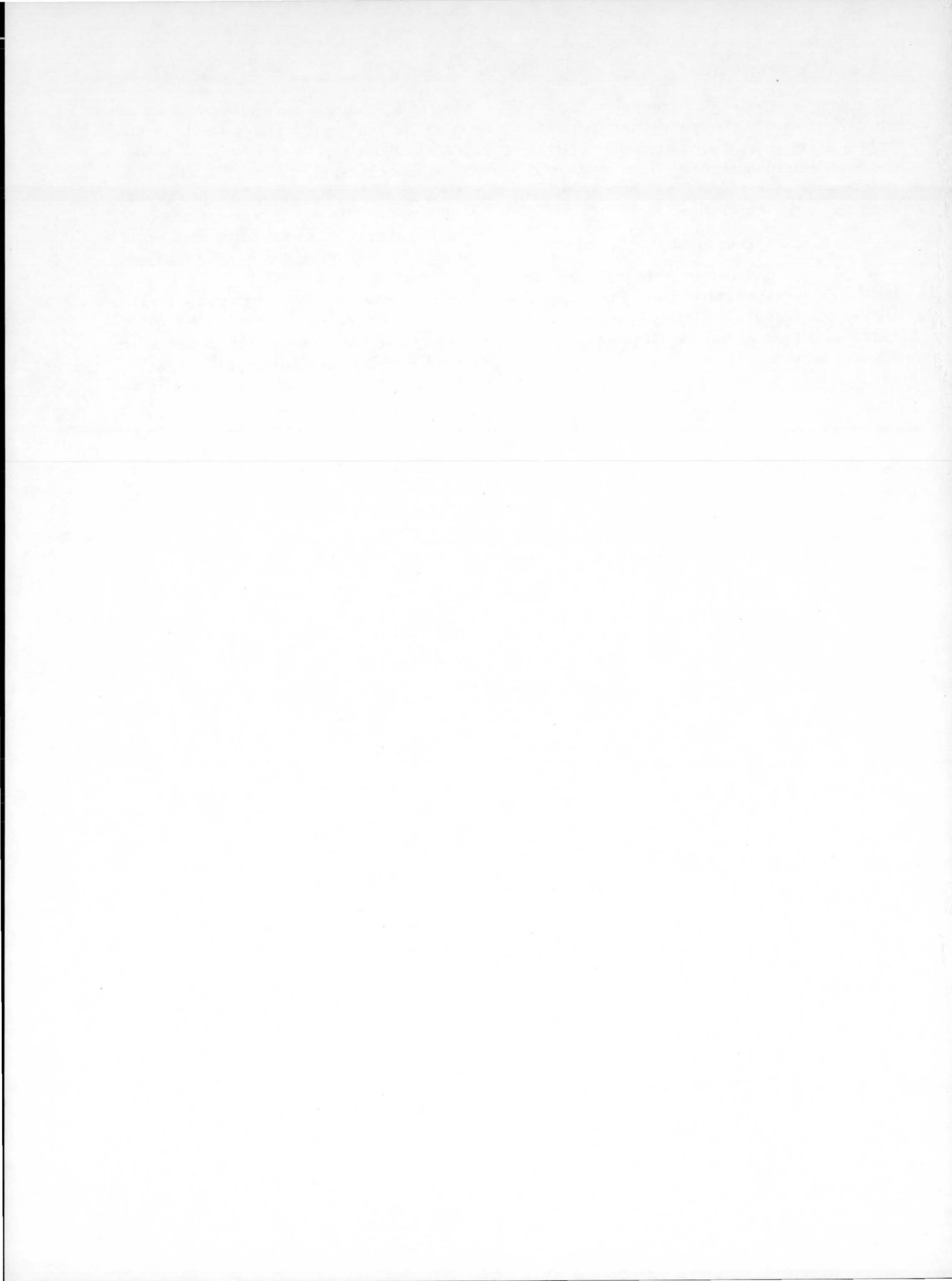
tor may input special commands into the system. For example, the operator may request a print of all on lines, or he may wish to exercise the Sequence Scan Option. This is the normal method of man/machine communication during a checkout operation.

CONCLUSION

While the input/output hardware for the DEE-3A varies slightly from that of the DEE-3, the scanning capability is implemented in the same manner and for all practical purposes is identical.

The DEE-3/3A systems originally depended upon an internal oscillator for the interrupt pulses, which initiated the scan cycles. A modification now exists, however, which will allow the DEE-3/3A to be operated from an external timing source. This results in better time resolution and also, gives an automatic changeover capability to the internal oscillator in the event the external timing source fails.

These systems have been thoroughly proven in factory checkout of the Saturn S-I Stage and also have been used in the launch of a Saturn I vehicle at Kennedy Space Center.



25. The New Micro-Flowmeter

FRED WELLS

George C. Marshall Space Flight Center, NASA

The accurate measurement of small flow rates has always been a difficult task. Measuring systems for precise measurements of very small flows are generally complex and usually require extensive observations, considerable setup time, are not readily portable, and must be separately calibrated for each different gas.

Although flow-measurement techniques have been developed extensively, utilizing many different concepts, there is still difficulty in measuring very small gas flows (less than 1 standard cubic inch) with less than 2-percent error. This problem is compounded if it is desired to have a meter that is independent of the physical characteristics of the gas to be measured, capable of direct calibration, free of subtle error, and readily moved.

The constant increase in reliability demands and the continual refinement of checkout methods as used in the space industry have generated a requirement for convenient precision measurements of gas flow rates below 1 standard cubic inch per minute (1 scim).

Several excellent devices that are readily transported and easily operated have been developed for this purpose. Most of these new devices are based on a thermoelectric phenomena and depend on electronic circuitry for readout. The Hastings Flowmeter which utilizes the hot-wire principle, is typical of this group. (The term "hot wire" means change in resistance or thermocouple output as a function of heat removal by the gas being metered.)

The primary problem with these flowmeters is maintaining the calibration in the face of electronic component ageing and interpreting the readings obtained when measuring a gas different than that for which the device was calibrated. (The term "ageing" means a change in the property of a substance with time.) These problems exist because the devices usually depend on a comparative calibration and are affected by one or more of the physical characteristics of the gas such as density, specific heat, and viscosity. "Comparative calibration" means a direct comparison with a standard.)

The need for periodic calibration checks and the conversion problems involved in measuring various gases has in turn generated a need for a convenient standard meter for calibration of the working meters. Ideally, this meter would have an inherent calibration and not be dependent on electronic circuitry nor be affected by the physical characteristics of the gas, nor add or remove anything from the gas.

A new concept of measuring extremely small gas flow rates, in the order of 0.4 scim or less, has been implemented in the construction of a model flowmeter (fig. 1). This flowmeter incorporates a positive displacement principle; thus the theoretical lower limit is zero. In addition, this new flowmeter features an inherent calibration system and, after calibration, can be used to measure flow rates of most gases.

Test results have proven that the Micro-flowmeter is more accurate than existing flow-measuring devices and that the Micro-flowmeter is simply calibrated from linear measurements, independent of gas characteristics.

DISCUSSION

The present devices used as laboratory standards to check working meters are one of three types: roto meters, orifice meters, and water-dependent devices. The roto meters are limited in the lower limit (approximately 0.5 scim), have a calibration dependent on comparison with another standard, and are dependent on the physical characteristics of the gas. Orifice meters or other restriction types are also dependent on the physical characteristics of the gas. Water displacement and soap-bubble methods are frequently troubled by gas solubility and saturation problems.

The new device, the Micro-flowmeter, is a positive displacement device[®] independent of gas composition and features an inherent calibration derived from measurable dimensions.

The upper limit of the useful range of the present version is about 0.5 scim. The lower limit is a function of time and flow stability; a 2-minute cycle yields a measured flow of 0.015 scim.

The Micro-flowmeter (figs. 1 and 2) consists of an inlet, a mercury reservoir, a metering dispenser, and equilibrium chamber, a metering tube, a mercury-gas separator, an outlet, a mercury return, and two bench marks.

The flow for the gas to be measured is admitted at the inlet port, passes through the equilibrium chamber, the metering tube, the mercury-gas separator, and is vented at the outlet port. The gas continuously flows through this path whether a measurement is being performed or not.

To initiate operation, the metering dispenser is rotated one revolution. The rotation passes a precise quantity of mercury from the mercury reservoir to the equilibrium chamber.

The amount of Hg slug dispensed is determined by the porting of the metering dispenser and is chosen so that its length is approximately equivalent to the diameter of the metering tube. Because of the high surface tension of mercury, the dispensed Hg slug completely fills the inside diameter of the equilibrium tube, sealing the passage.

This Hg slug seals the tube and isolates the gas in front from the gas behind. The slug

is forced through the meter by the flow of gas and through the metering tube until it reaches the separator. At this point the Hg slug separates and returns via the mercury return to the mercury reservoir for re-use. The gas flows continuously from the outlet.

The measuring function is performed by measuring the time required for the Hg slug to pass from the lower bench mark to the upper bench mark. The previously measured cross-sectional area of the measuring tube and the measured distance from the lower to the upper bench mark is used to find the volume. The time of passage is measured. Flow equals volume divided by time.

The range of the instrument is determined by the bore size of the metering tube, and convenient time limits for Hg slug passage.

Test Results

The 2-mm Micro-flowmeter model was subjected to several tests. Tests showed that the upper limit was approximately 0.4 scim. This

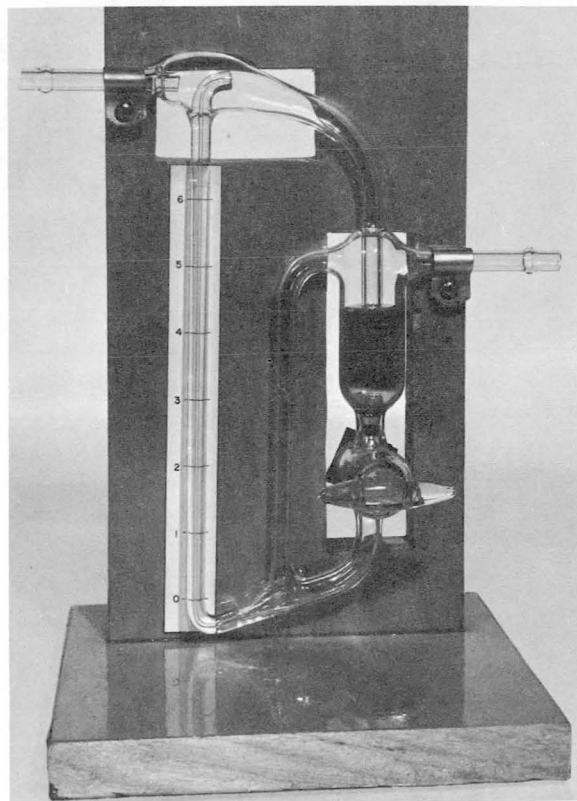


FIGURE 1.—Micro-flowmeter.

limit was imposed by the accuracy of measuring the time of Hg slug passage between bench marks. This measurement was made with visual observation and manual start and stop of a time. (An automatic timer would eliminate human errors and increase the accuracy of the time measurement, but would not extend the range. At higher velocities the Hg slug movement would become erratic.)

The lower limit is dictated by the stability of the flow to be measured and the patience of the operator. The meter itself has no lower limit, since it is a positive-displacement device with mercury sealing the metered quantity. A typical useful lower limit might be a 120-second cycle or a flow of 0.015 scim.

Accuracy

The fundamental accuracy of the Micro-flowmeter is a function of bore diameter accuracy, bench mark dimensional accuracy, and timing accuracy. The dimensions can be determined within ± 0.02 percent. Timing accuracy is ± 1 percent when measured by a skilled operator. This accuracy can easily be improved by a factor of 10 by using photo cells or other electronic bench marks.

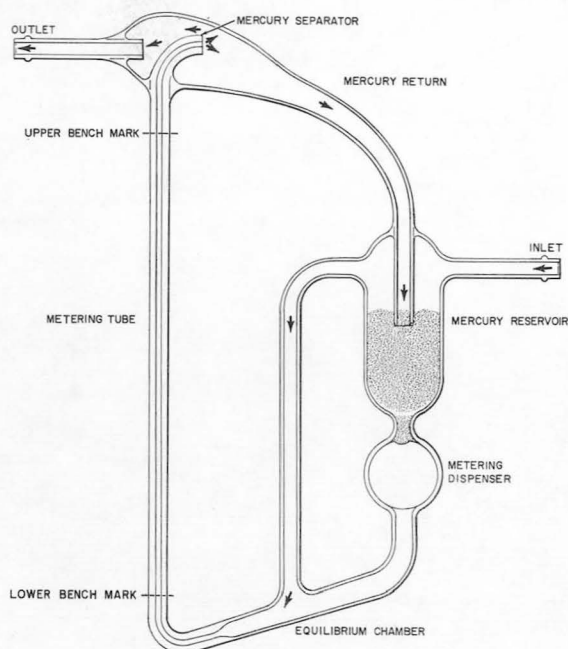


FIGURE 2.—Micro-flowmeter pictorial diagram.

The working accuracy of the meter is further affected by the use or absence of a correction for the actual absolute pressure and temperature of the gas in the Micro-flowmeter. The pressure correction, which can approach 5 percent, must include a true-barometer reading plus the back pressure imposed by the Hg slug in the meter. The back pressure is estimated by observing the height of the mercury column in the mercury return tube as compared to the reservoir level. The back pressure tends to compensate for a barometric pressure of less than 760 mm. The temperature correction, which seldom exceeds 2 percent, is obtained by observing ambient temperature in the work area. The mass flow through the meter is so low that it can be assumed to be the same temperature as room ambient.

Computation of Flow

Each meter has a volume between bench marks that can be computed from a measured diameter and length.

Flow can be computed as follows:

$$\text{Flow rate} = \frac{V}{T} \times \frac{P_m}{P_s} \times \frac{T_s}{T_m}$$

where

- V = Volume between bench marks
- T = Time of Hg slug passage between bench marks
- P_m = Pressure in meter (absolute)
- P_s = Standard pressure (absolute)
- T_m = Temperature in meter (absolute)
- T_s = Standard temperature (absolute)

Accuracy when using this formula is dependent on the quality of the measurements. Under normal laboratory practice, this accuracy will be ± 5.0 percent of the reading.

Dirt in the metering tube or contamination in the mercury can cause erratic behavior. Anytime the Hg slug moves in an erratic or jumpy manner, and the flow is known to be stable, the meter should be thoroughly cleaned by normal laboratory glass cleaning methods (such as a dichromate flush) and refilled with clean mercury.

Long lines or a large connected volume between the meter and the source of flow should

be avoided. This causes an annoying time delay between dropping the Hg slug and the start of the actual measured time. Extremely large volumes can amplify certain phenomena and introduce errors of unknown magnitude.

CONCLUSION

The Micro-flowmeter was built and tested and proved the most accurate of present devices for measuring small flow rates. The meter is

primarily intended as an end item meter to be used for calibrating working meters. The Micro-flowmeter is already being used at MSFC.

The upper limit of the range of the 2-mm Micro-flowmeter is about 0.4 scim. Accuracy without corrections for standard conditions is better than ± 5.0 percent of the reading. With corrections for standard conditions, error will be less than ± 0.5 percent of the reading.

26. Bellows Joints, Gimbals, and Clamps

C. M. DANIELS

Rocketdyne Division, North American Aviation, Inc.

As an outgrowth of the F-1 and J-2 liquid-propellant rocket engine programs, there have been advancements in the state of the art of many areas of technology which may have utilization in other industries. As a typical example, the area of bellows joints, gimbals, and clamps has been selected for discussion. Four examples of unique bellows restraints, two thrust-vector attitude-control gimbal devices, and one tube clamp are described.

GENERAL INTRODUCTION TO BELLOW JOINTS

A liquid-propellant rocket engine has many requirements for ducting. Ducting in this case can be described as an enclosed leak-tight passage, usually circular in cross section, which is capable of containing and conveying a fluid under pressure from one location to another. On an engine, ducts are required for conveying the propellants from their storage tanks to the pump inlets, and from the pump outlets to the thrust chamber. They are also required to feed propellants to the gas generator, convey the gas generator exhaust gases to the turbine inlet, and carry these gases from the turbine outlet through the turbine exhaust duct.

Flexibility must be designed into rocket engine ducting for several reasons. Thermal expansion or contraction must be considered to prevent overstressing of the ducting or its attachment points. Deflection resulting from operational loading conditions must be accommodated for the same reasons. Flexibility should be allowed for duct interchangeability, installation, and engine or vehicle maintenance.

One way of providing this duct flexibility is with metal bellows. The design of linkages for these bellows provides an interesting and difficult challenge for the designer. Several unique designs developed by Rocketdyne are described in this paper.

A UNIQUE UNIVERSAL RESTRAINER AND GIMBAL

Flexible bellows joints for duct application have the capability of universal freedom of movement while being restrained against axial separation, and have classically been required to include ties of a generally heavy and bulky nature, usually including gimbal rings and tension ties. When such joints are adapted to aircraft or aerospace vehicle hardware, the weight and size of these components achieve major significance and therefore receive careful design consideration; compactness of the overall systems to which these joints are applied is adversely affected, as is the total vehicle weight.

In an effort to make a significant advancement in the state of the art of bellows tie-linkages, Rocketdyne has developed a universal joint design generally comprised of a pair of pivotally mounted beams, known as "swinging beams," positioned upon each end of a flexible duct (fig. 1). Each pair of beams is pivoted about an axis common to the beams, and the axis through the beams on opposite ends is mutually perpendicular. Each swinging beam has a mechanical tie movably connected to each of its ends; each tie essentially extends axially through the flexible duct and into universal connection with an end of one of the swinging-beam members on the opposite end of the flexible duct. Thus, each pair of ties connected to a single swinging beam on one end of the joint

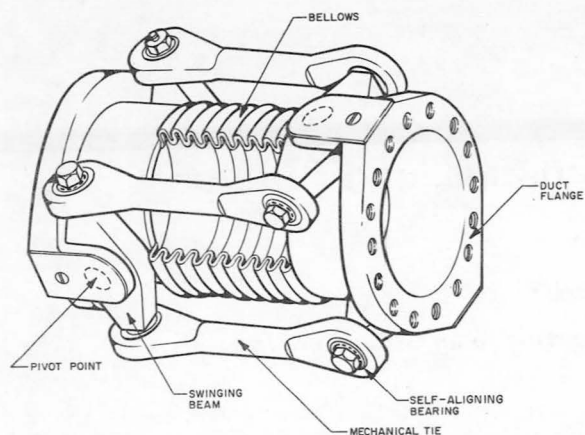


FIGURE 1.—Universal restrainer and joint.

is connected to one end of each swinging beam on the opposite end. It is this interconnection method which imparts to the design the ability of achieving all aspects of universal motion.

This novel linkage has application not only as a duct-bellows tie, but also as a gimbal linkage for thrust-attitude control motion in a rocket engine thrust chamber (fig. 2). This type of bellows restraint was utilized in the pump discharge ducts of early F-1 engines (fig. 3 and 4). In this particular application, the linkage was tied across two individual bellows sections which were connected with an intermediate spool piece, although each bellows can be tied as a separate integral unit.

The use of tied-bellows joints in piping and ducting has wide general use, not only in the

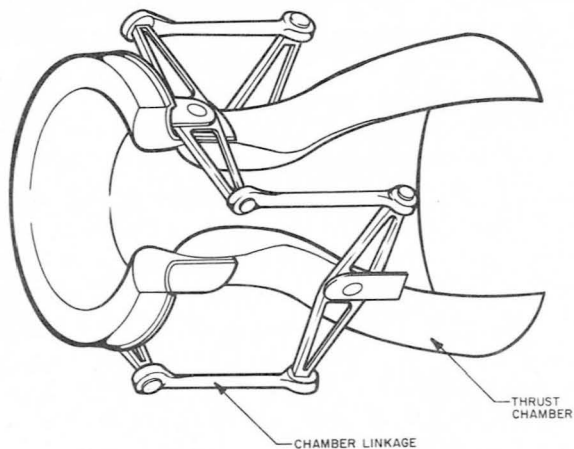


FIGURE 2.—Gimbal linkage for TVC.

aerospace and aircraft field, but in the petroleum, chemical, and heating fields. The use of a device, such as the linkage described, with its simplicity of construction and versatility of application, would undoubtedly be considered by designers in these fields if it were known to them.

FOLDED GIMBAL RING BELLOWS JOINT

A common problem with bellows restraints, both gimbal and hinge types, is that the bellows pressure-separating load produces a reaction in highly localized areas. In closely coupled ducts, it is sometimes necessary to locate the flex joints very near to the end-connecting bolted flanges of the duct. This nearness of the load-reaction point to the flange does not afford sufficient duct length to allow the concentrated load to redistribute itself circumferentially into the walls of the duct. Consequently, localized loads are applied to the bolted flange which can overload the bolts in the load area or cause de-

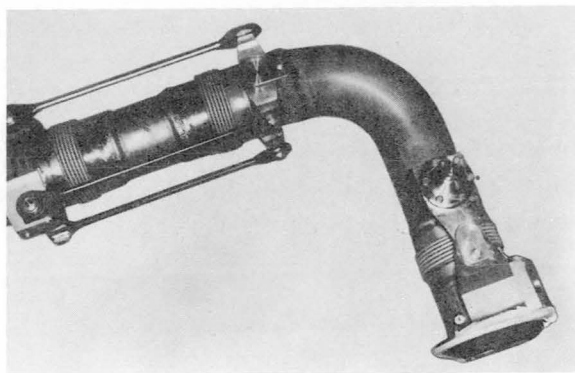


FIGURE 3.—Swinging beam joint on pump discharge ducts of early F-1 engines.

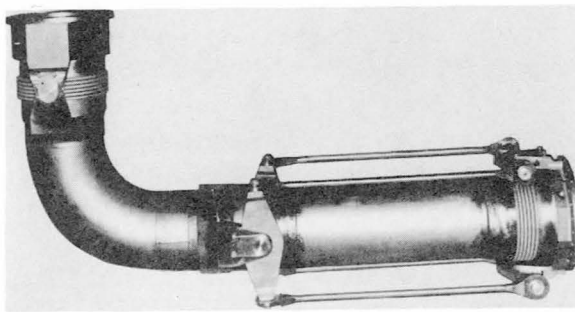


FIGURE 4.—Swinging beam joint on pump discharge ducts of early F-1 engines.

flection in the flange, possibly allowing static-seal leakage. One method for alleviating this condition is the artificial creation of sufficient duct length by the design described.

The highly concentrated loads of conventional bellows restraints, as mentioned in the introduction, would be allowed to redistribute themselves circumferentially into the duct walls, providing the duct was of sufficient length. A method for achieving the effect of the desired length in an actual short length is to collapse or fold the duct wall in concentric rings (fig. 5). Loads concentrated in a point on a member are distributed across the cross section of the member, as described by a 30- to 45-degree half angle. This means that to distribute a load applied at two points on a simple cylindrical shell, the length of the shell must be a minimum of π times half the radius. The same effect is achieved by folding or telescoping the shell on itself so that the total length of the individual rings is the same, but the actual length is considerably reduced, depending only on the diameter limitations. The folding process is feasible because the loads are distributed at approximately the same angle whether the part is in compression or tension.

This concept was put into practice in the lox pump suction duct for test stand use with the F-1 engine (fig. 6). The inside diameter of the duct is 16.75 inches, and it must withstand a proof pressure of 400 psig. Because of avail-

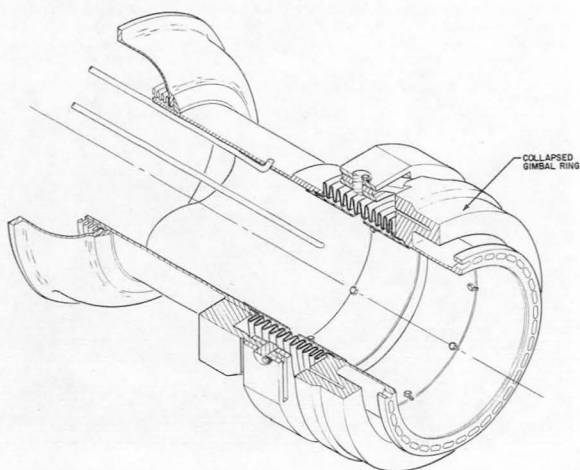


FIGURE 5.—Cross-sectional perspective, collapsed gimbal ring.

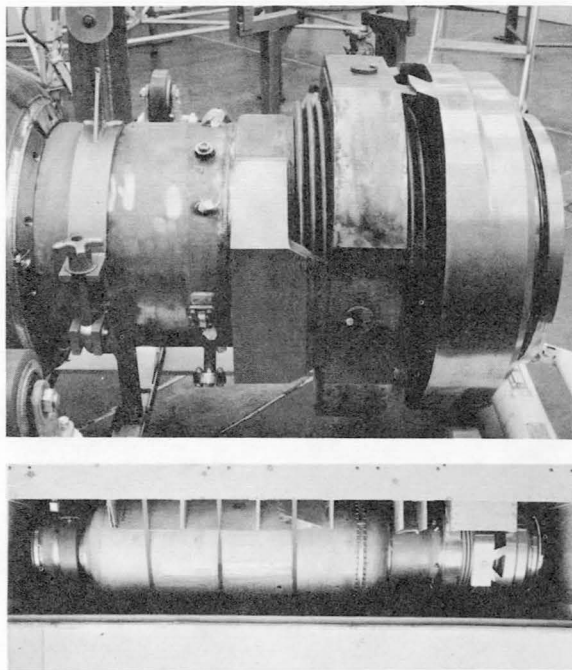


FIGURE 6.—Cam gimbal integrated into large advanced engine assembly.

able-length limitations and gimbal angular-deflection requirements, the bellows joint utilizing this restraint has to be located immediately on the pump-inlet flange. An uneven, circumferential loading of the pump flange could not be structurally tolerated by the pump. The folded gimbal-ring design offered a design capable of providing gimbal restraint and motion, while applying a uniform circumferential load into the pump flange. This design concept should have practical application in any industry in which piping or ducting flexibility is required.

HINGED BELLOWS RESTRAINT

As in the case of the gimbal bellows restraint, conventional bellows linkages for single-plane angulation applications have been heavy and cumbersome with the pressure-separating load of the bellows taken out in highly localized areas at the hinge pins. The hinged restraint described herein provides improvements in the deficient areas of classical hinged restraints, namely reduction of bulkiness and weight and increased load-carrying ability (fig. 7).

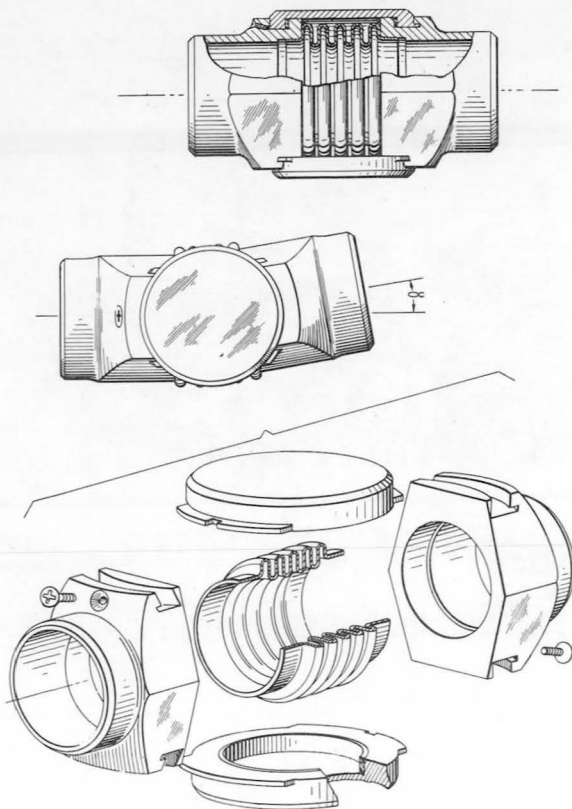


FIGURE 7.—Hinged bellows restraint.

The transmitted load is distributed over a relatively large structural area even though the structure itself is not excessive in size. Both the continuous annular character of the cap flanges in providing hoop strength, and the bearing relation of the cap surfaces to the surfaces of the annular grooves give the assembly good load-transmitting capability and structural integrity, despite its comparatively small size.

The hinged bellows restraint is comprised of a pair of retainers adapted for connection within a duct, a bellows which forms a flexible pressure carrier between the retainers, and restraining caps engaged within grooves appropriately provided in the retainers. A flanged portion of the restrainer cap can slide within at least one of the retainer grooves so as to prevent axial movement of the retainers while still allowing relative angular movement. A lubricant, such as molybdenum disulfide or Fabroid (fiberglass and Teflon cloth), can be used on the

bearing areas to reduce friction and increase wear life. This design has been reduced to practice in the gas-generator propellant feed ducts of early F-1 engines. Figure 8 shows a duct assembly which utilizes both the hinged joint and the universal joint. The hinge-joint design could be utilized in any flexible piping system where compactness, light weight, and relatively low cost are governing factors in selection of a given design.

J-2 INLET DUCTS, A BELLOWS FOR TWISTING APPLICATION

The pump-inlet ducts for the J-2 engine provided an extremely challenging design problem. The overall length allotted for these ducts was very short, considering the deflections they were asked to accommodate. The pumps for the J-2 engine are mounted diametrically opposite each other on the thrust chamber. Because of this position, and the fact that thrust attitude control is achieved by gimbaling the engine, the inlet ducts are required to accommodate ± 4.5 inches of axial travel and ± 10 degrees of angular travel plus over 2 degrees of torsional rotation. The design feature that accommodates the torsional deflection is described in the next paragraph.

In flexible-duct design, torsional loading (rotation about the duct axial centerline) is frequently induced because of duct routing and

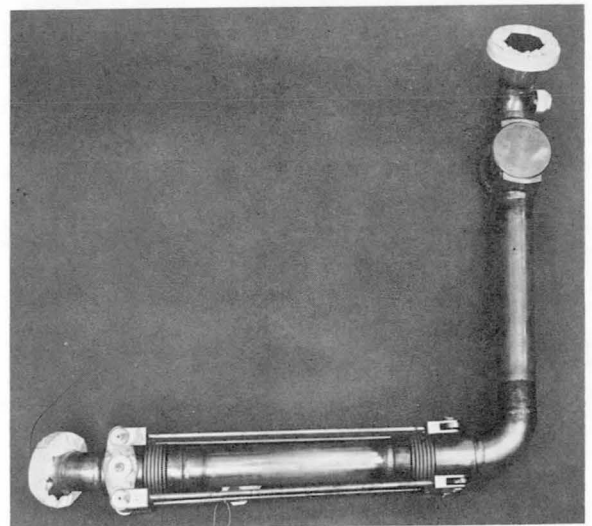


FIGURE 8.—F-1 gas generator feed line with hinged bellows restraint.

induced deflections. Bellows are very rigid and therefore unable to deflect and relieve these loads. To allow torsional deflection, ducts are usually arranged in a dog-leg configuration with a bellows joint in each half of the leg. Torsional loading in either half is absorbed by angular deflections of the bellows in the opposite half. In the case of the J-2 inlet duct, application of this design concept was not possible because of the short length available and the straight-in approach of the ducts. A unique bellows device was then developed to resolve the problem.

This problem was uniquely resolved by fabricating a long, thin-walled bellows, compressed into a short length, which was confined by a flanged linkage to take the pressure-separating load and limit the motion so that the bellows could absorb torsional deflections only (fig. 9). In theory, a long, thin-walled tube compressed into a short bellows can absorb the same amount of torsional deflection as the same tube in its full-length condition. The bolts holding the two flanges of the torsional bellows are loosely torqued so as to take the pressure-separating load, and allow relative torsional deflection between the two. The bolt holes in the flanges are slotted to allow freedom of rotation, and the flange faces are lubricated with a dry lubricant to further ease rotation. The torsional bellows has a lower torsional spring rate than any of the other bellows in the duct assembly and therefore absorbs the bulk of the duct torsional deflections, thus leaving the other bellows of the duct assembly free to take care of the axial and angular deflections.

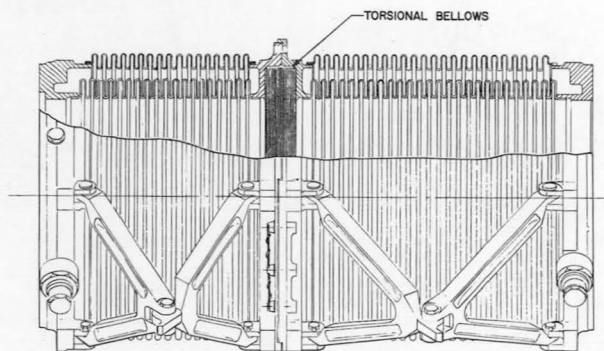


FIGURE 9.—Cross-sectional view of J-2 suction duct.

The scissors-like linkages tying across the other bellows of the assembly are, contrary to their appearance, not torsional-load carrying members, but are anti-buckling devices for the abnormally long primary bellows of the assembly.

Piping and ducting designers for commercial applications, instead of avoiding torsional deflections, now have a design tool that they can use to reduce duct complexity, cost, and space. This should be especially true in atomic energy and shipboard applications, where available space is at a premium.

PRESSURE-VOLUME COMPENSATING BELLOWS JOINT

The finger-compensator bellows joint is an example of a specialized design created to solve a specific ducting problem. In this case, a straight run of ducting was required to take axial and angulation travel without imposing excessive reactions on the attached flanges. The pressure volume compensating joint that resulted (fig. 10) has proved adequate for the requirements while being used in the pump discharge ducts of the J-2 engine.

As is common practice with pressure-volume compensating joints, this design utilizes a pressure (i.e., axial thrust) balancing chamber installed external to and concentric with the main duct bellows. This chamber is vented to internal-duct pressure and, since the annular area (A_1) is equal to the main duct bellows

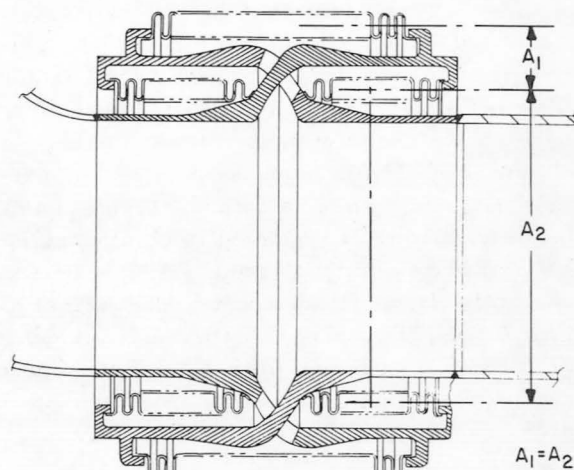


FIGURE 10.—J-2 finger compensator.

area (A_2), an axial force equal and opposite to the pressure-separating force of the main duct bellows is thus created. The entire joint is prevented from separating axially by the overlapping fingers alternately tying across the joint from each free end. Sufficient clearance is allowed between fingers to allow required axial and angular motion.

There are many variations of this theme. The primary use of the compensating joint is to retain a tension-type duct system in areas where limited space exists and axial travel cannot be absorbed by angulation. By proper selection of the cross-sectional area, the thrust force may be under, fully, or overly compensated so that a compressive balancing or tensile load is imposed on the system.

Pressure-volume compensating joints are commonly used in any industry where flexibility in ducting or piping systems is a requirement. This design is a novel one, and is more compact in an axial direction than any of the classical designs presently in use, which should therefore make it attractive to piping designers in general.

CAM RING GIMBAL

Future rocket engines with thrust chambers which utilize an expansion-deflection gas-flow principle (reverse flow, horizontal flow, annular, or spike) will be characterized by a relatively squat appearance, as compared to the conventional bell-shaped thrust chamber engines. Since the introduction of these advanced thrust chamber concepts, Rocketdyne has continually conducted analytical and design studies relative to methods for obtaining thrust-vector control, that is, TVC. Results of these studies have shown that the most efficient method of obtaining TVC for large boosters and upper-stage engines is one in which the thrust chamber is mechanically gimballed to obtain the desired thrust-vector attitude. Because of the relatively large diameters of the advanced thrust chambers, and the thrust load being uniformly distributed over this diameter, a need exists for an advanced gimbal mechanism different from the conventional bell-chamber designs.

The annular shape of advanced thrust-chamber concepts, usually involving allotment of the

entire central volume of the engine to turbo-pump and valving installation, eliminates a sound structural location for conventional bell-chamber, centrally located, gimbal block position. Obviously the most efficient thrust structure for this type of engine is a cylindrical unit located immediately forward of the thrust-developing section of the engine. These two factors logically led to the cam-ring gimbal concept.

A gimbal mechanism that can accommodate this unique requirement is shown integrated into a typical large advanced engine assembly in figure 11. This design, known as a cam-ring gimbal, provides an efficient load path to transmit thrust loads from the advanced chamber uniformly into the vehicle structure. Comparison of the cam-ring gimbal to a conventional bell chamber gimbal, as shown in figure 12, shows the obvious advantages of efficient load transmission and reduction in overall length.

Under an Air Force contract, Rocketdyne designed, fabricated, and delivered a 48-inch-diameter cam-ring gimbal with a 200,000-pound thrust rating. Photographs of this unit are shown in figures 13, 14, and 15.

The cam-ring gimbal is a mechanical device which supplies the desired thrust-vector-angle attitude by rotation of two axially aligned, large-diameter, wedge-shaped cylinders. When these cylinders (or rings) are rotated relative to each other, the angle (described by the top and bottom surfaces of the two adjacent cylinders) can change from zero to the desired vector angle in any direction. When the cylinders are in the

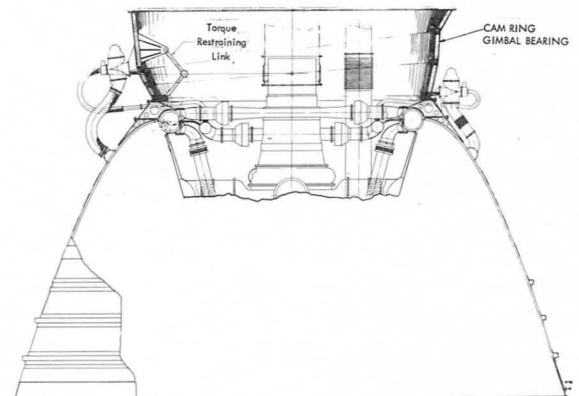


FIGURE 11.—Gimbal mechanism integrated into typical large advanced engine assembly.

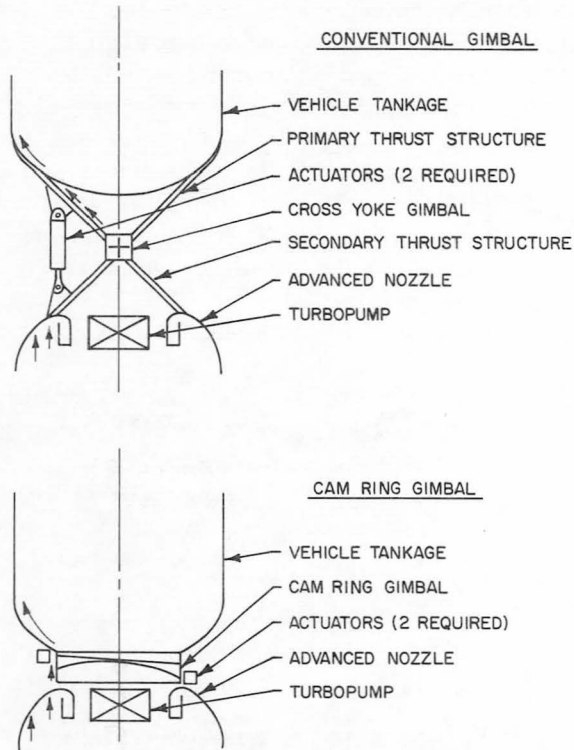


FIGURE 12.—Schematic comparison of conventional gimbal with a cam-ring gimbal.

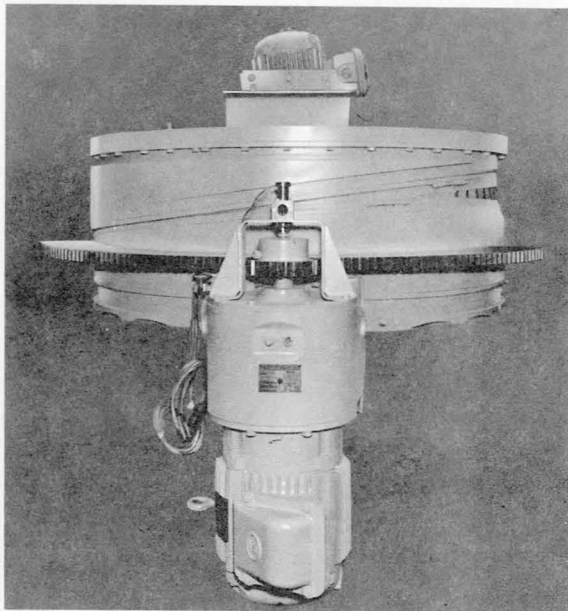


FIGURE 13.—Cam-ring gimbal.

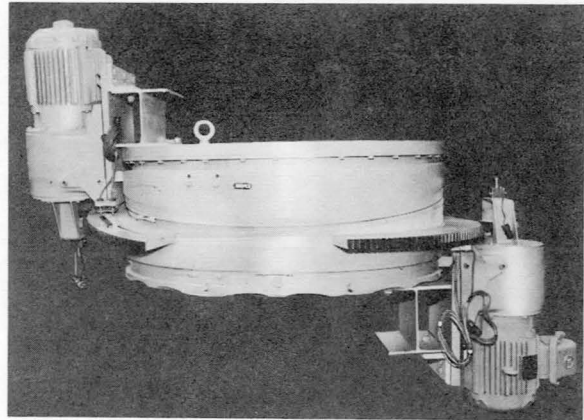


FIGURE 14.—Cam-ring gimbal.

neutral position (with parallel faces), motion of the thrust vector away from the neutral axis can occur in only one direction. This limitation can be overcome by rotating the entire gimbal-mount assembly to a new direction, but this requires a time lag during which no control is possible.

To overcome this limitation, the entire assembly is mounted at an angle to the vehicle axis somewhat greater than the maximum thrust-vector angle required. Vector movement within the required region thus can be accomplished without the two cylinders becoming parallel (fig. 16).

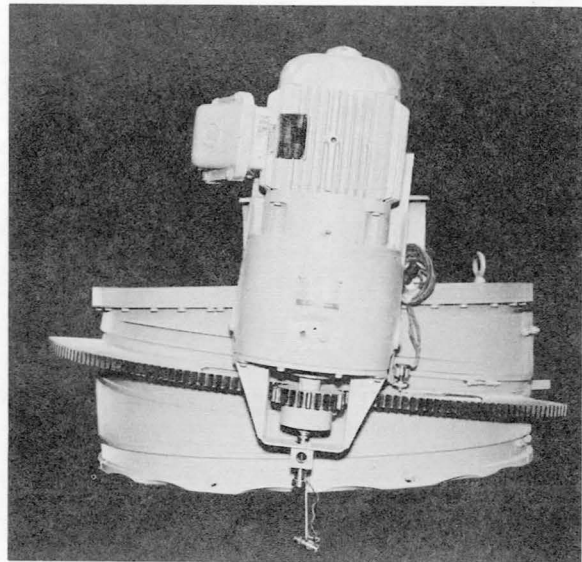


FIGURE 15.—Cam-ring gimbal.

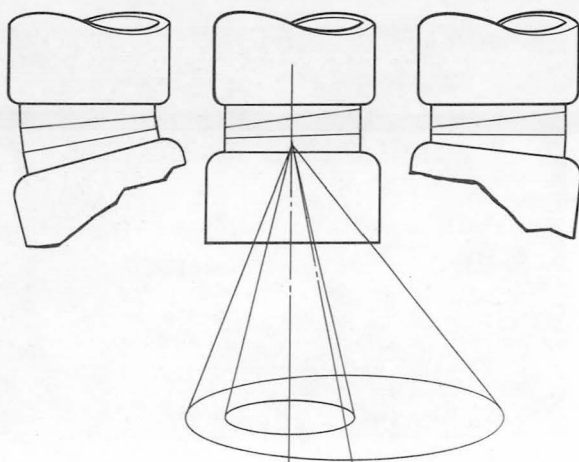


FIGURE 16.—Four stacked cylinders comprising cam-ring gimbal.

Actuation is accomplished by hydraulic motors. The motors are geared to the cylinders through gear segments. The motors are controlled by a computer which translates linear pitch and yaw signals into angular positions of the cylinders.

The complete cam-ring gimbal assembly is composed of four stacked cylinders (or rings). The low cylinder is of constant section height and constitutes the mounting for the engine or engine cluster. The lower cylinder could be an integral part of a thrust chamber if desired. The two wedge-shaped rotatable cylinders are placed above the lower mounting cylinder. Differential rotation of these rings causes the lower ring to tilt to the required gimbal-vector angle and direction. The top (fourth) ring is also made a wedge, since the three wedges in series accomplish the required total field of gimbaling with a minimum of rotating-wedge travel. The top ring is fixed to the vehicle or could be an integral part of the vehicle.

To develop a ± 5 -degree gimbal motor field, the wedge angle is 7 degrees for the upper wedge and 6 degrees for the two rotating wedges. The gimbal-angle vertex is approximately at half the height of the gimbal.

Drive mechanism for the rotating wedges involves a sector gear attached directly to each movable wedge ring. The units are driven by the pinion gears of electric actuators, which are

in turn mounted to the nonrotating top and bottom rings. A ball-socket-connected scissor linkage is attached between the top and bottom rings on the inside diameters of the rings. This linkage prevents relative rotation between the top and bottom rings (vehicle and engine), while also permitting full tilting action of the gimbal assembly. The electric actuators and switch gear can be standard industrial-type motor-gear reducer units.

Other possible applications for this concept include:

1. A base for scanning radar antenna which must traverse in both azimuth and angulation simultaneously
2. A base for large telescopes which also must traverse in two angular directions
3. A gun-stabilizing base for shipboard or military tanks
4. A means for keeping any device level as it moves over rough terrain; for example, in the use of a crane on a hillside.

A NEW RUBBERIZED WIRE-MESH CLAMP

Rubber-cushioned clamps used for supporting and maintaining separation of tube assemblies have been discontinued on the F-1 and J-2 engines of the Saturn vehicle because of their susceptibility to fire damage. The clamps were originally replaced with wire-mesh-cushioned clamps which met the requirement of providing a "fireproof clamp." Their lack of resiliency resulted in a loosely clamped joint, however, and vibration damping characteristics of the wire-mesh clamps became nullified. This situation led to the development of a rubber-impregnated wire-mesh clamp which is now in general use.

To provide better clamping characteristics while retaining the fireproof properties required, wire-mesh clamps were modified by impregnating the wire-mesh cushions with a high-temperature ablative silicone rubber similar to that used in the fabrication of armored electrical harness (fig. 17). The effect of the rubber is to restore the resiliency required for effective clamping.

Measurements of torsional resistance was made on 1-inch clamps so that quantitative comparisons might be made between the bare wire-

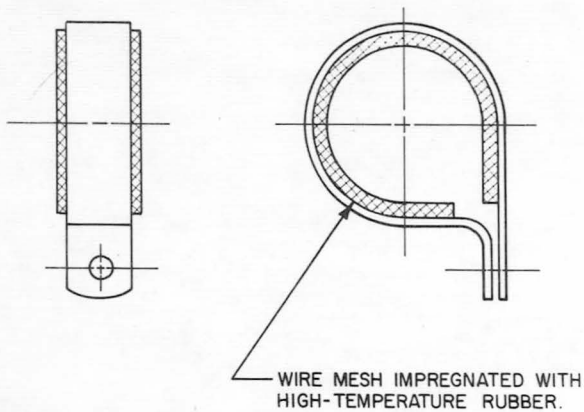


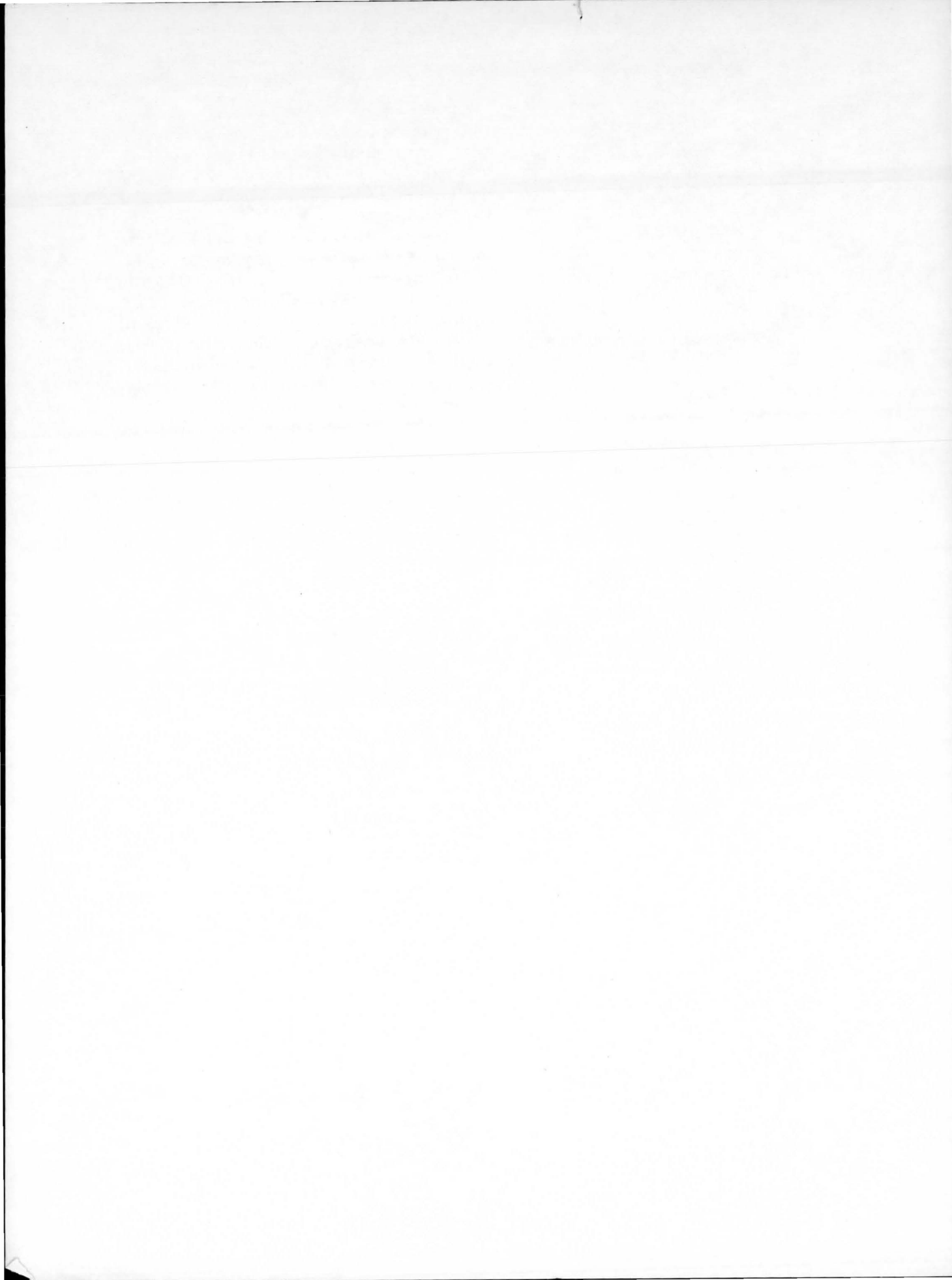
FIGURE 17.—*Wire-mesh clamp.*

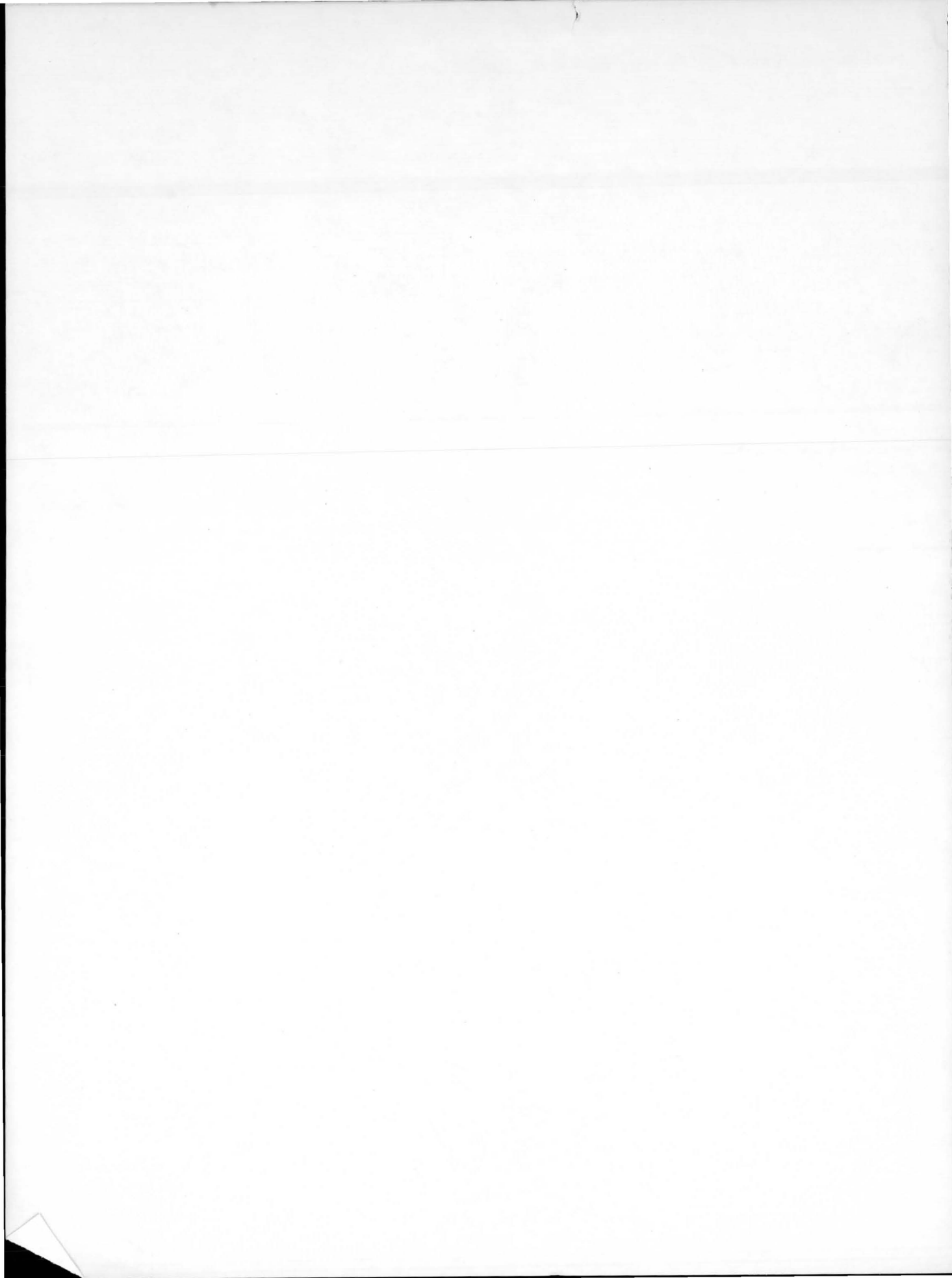
mesh clamps and the rubber-impregnated clamps. Tests were made at both room temperature and at -320° F. Results indicate that the rubber-impregnated clamp has significantly better clamping characteristics than those of the bare wire-mesh clamp.

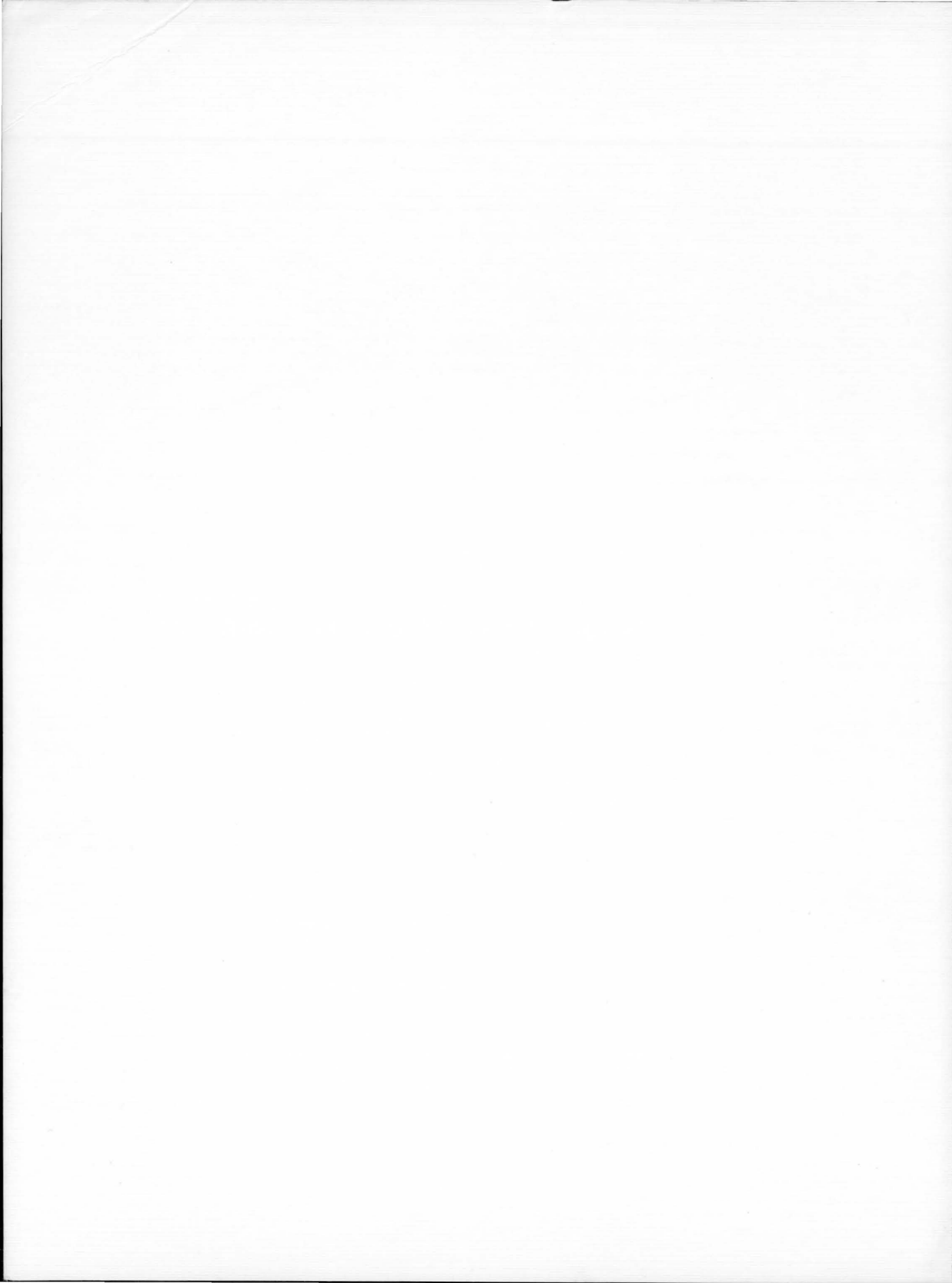
Engine history has shown that standard wire-mesh-cushioned clamps permanently deform during installation and engine operation, thus reducing their effectiveness as a supporting member and making them ineffective as vibration dampers.

Engine and laboratory tests also show that the wire-mesh-cushioned clamp can be significantly improved by impregnating the wire mesh with an ablative silicone rubber (RTV 560), while still retaining all the advantages of the bare wire-mesh clamp. The additional costs involved can be partially absorbed by the reusability characteristics of the rubber-impregnated clamp.

This clamp has utilization potential in any application which has a high-temperature and vibration environment. It is also resistant to corrosion and zone effects. Some applications in this area include shipboard applications, and those in atomic energy power plants and supersonic aircraft.







"The aeronautical and space activities of the United States shall be conducted so as to contribute . . . to the expansion of human knowledge of phenomena in the atmosphere and space. The Administration shall provide for the widest practicable and appropriate dissemination of information concerning its activities and the results thereof."

—NATIONAL AERONAUTICS AND SPACE ACT OF 1958

NASA TECHNOLOGY UTILIZATION PUBLICATIONS

These describe science or technology derived from NASA's activities that may be of particular interest in commercial and other nonaerospace applications. Publications include:

TECH BRIEFS: Single-page descriptions of individual innovations, devices, methods, or concepts.

TECHNOLOGY SURVEYS: Selected surveys of NASA contributions to entire areas of technology.

OTHER TU PUBLICATIONS: These include handbooks, reports, notes, conference proceedings, special studies, and selected bibliographies.

Details on the availability of these publications may be obtained from:

National Aeronautics and Space Administration
Code ATU
Washington, D.C. 20546

Technology Utilization publications are part of NASA's formal series of scientific and technical publications. Others include Technical Reports, Technical Notes, Technical Memorandums, Contractor Reports, Technical Translations, and Special Publications.

Details on their availability may be obtained from:

National Aeronautics and Space Administration
Code ATS
Washington, D.C. 20546

NATIONAL AERONAUTICS AND SPACE ADMINISTRATION
Washington, D.C. 20546